frontiers | Research Topics

Therapeutic mechanism of osteosarcoma

Edited by
Yang Wang, Tong-Chuan He and Yang-Fan Lv

Published in
Frontiers in Molecular Biosciences

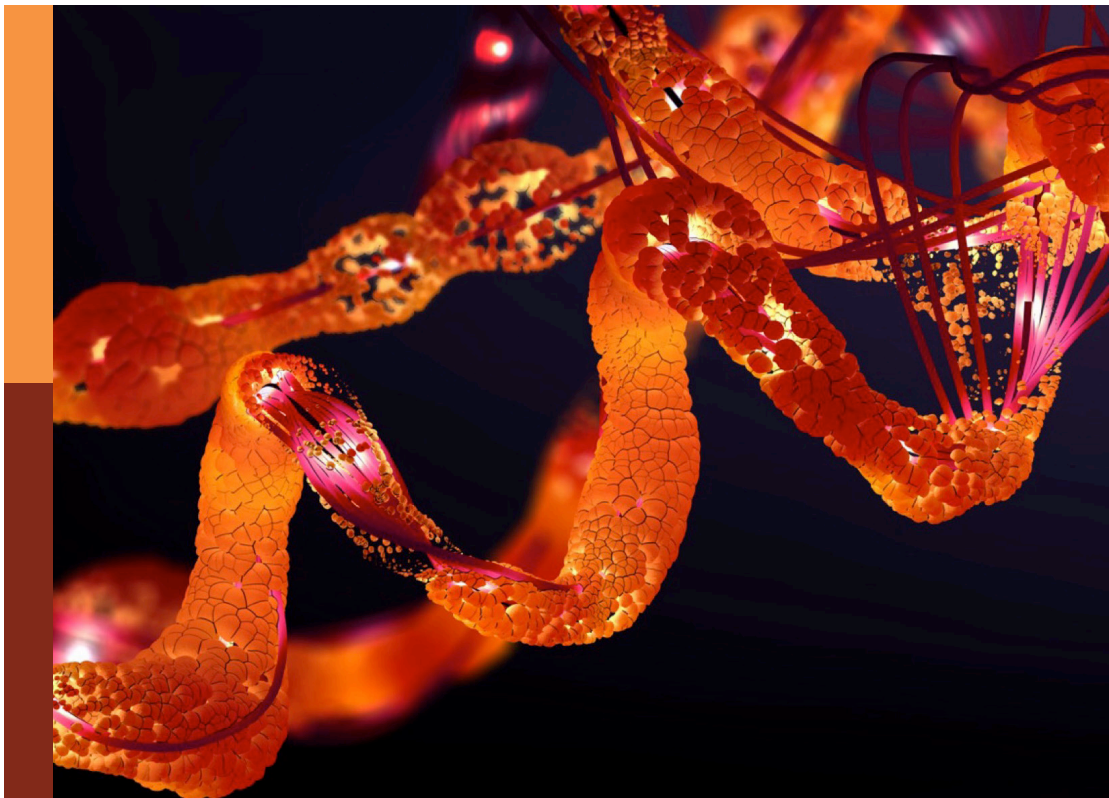

ISSN 1664-8714
ISBN 978-2-8325-6272-7
DOI 10.3389/978-2-8325-6272-7

About Frontiers

Frontiers is more than just an open access publisher of scholarly articles: it is a pioneering approach to the world of academia, radically improving the way scholarly research is managed. The grand vision of Frontiers is a world where all people have an equal opportunity to seek, share and generate knowledge. Frontiers provides immediate and permanent online open access to all its publications, but this alone is not enough to realize our grand goals.

Frontiers journal series

The Frontiers journal series is a multi-tier and interdisciplinary set of open-access, online journals, promising a paradigm shift from the current review, selection and dissemination processes in academic publishing. All Frontiers journals are driven by researchers for researchers; therefore, they constitute a service to the scholarly community. At the same time, the *Frontiers journal series* operates on a revolutionary invention, the tiered publishing system, initially addressing specific communities of scholars, and gradually climbing up to broader public understanding, thus serving the interests of the lay society, too.

Dedication to quality

Each Frontiers article is a landmark of the highest quality, thanks to genuinely collaborative interactions between authors and review editors, who include some of the world's best academicians. Research must be certified by peers before entering a stream of knowledge that may eventually reach the public - and shape society; therefore, Frontiers only applies the most rigorous and unbiased reviews. Frontiers revolutionizes research publishing by freely delivering the most outstanding research, evaluated with no bias from both the academic and social point of view. By applying the most advanced information technologies, Frontiers is catapulting scholarly publishing into a new generation.

What are Frontiers Research Topics?

Frontiers Research Topics are very popular trademarks of the *Frontiers journals series*: they are collections of at least ten articles, all centered on a particular subject. With their unique mix of varied contributions from Original Research to Review Articles, Frontiers Research Topics unify the most influential researchers, the latest key findings and historical advances in a hot research area.

Find out more on how to host your own Frontiers Research Topic or contribute to one as an author by contacting the Frontiers editorial office: frontiersin.org/about/contact

Therapeutic mechanism of osteosarcoma

Topic editors

Yang Wang — Sichuan Academy of Medical Sciences and Sichuan Provincial People's Hospital, China

Tong-Chuan He — University of Chicago Medicine, United States

Yang-Fan Lv — Army Medical University, China

Citation

Wang, Y., He, T.-C., Lv, Y.-F., eds. (2025). *Therapeutic mechanism of osteosarcoma*. Lausanne: Frontiers Media SA. doi: 10.3389/978-2-8325-6272-7

Table of contents

frontiers | Frontiers in Molecular Biosciences

TYPE Editorial
PUBLISHED 08 April 2025
DOI 10.3389/fmolb.2025.1597144

OPEN ACCESS

EDITED AND REVIEWED BY
Matteo Becatti,
University of Firenze, Italy

*CORRESPONDENCE
Yang Wang,
young0416@163.com

RECEIVED 20 March 2025
ACCEPTED 27 March 2025
PUBLISHED 08 April 2025

CITATION
Chen S and Wang Y (2025) Editorial: Therapeutic mechanism of osteosarcoma. *Front. Mol. Biosci.* 12:1597144. doi: 10.3389/fmolb.2025.1597144

Editorial: Therapeutic mechanism of osteosarcoma

Siyi Chen and Yang Wang*

Department of Emergency Medicine Center, Sichuan Provincial People's Hospital, University of Electronic Science and Technology of China, Chengdu, China

KEYWORDS

osteosarcoma, immunotherapy, Wnt/β-catenin signaling, tumor microenvironment, CAR-T cell therapy, metabolic reprogramming

Editorial on the Research Topic
Therapeutic mechanism of osteosarcoma

Osteosarcoma (OS) is a highly aggressive primary bone cancer with a particularly poor prognosis in metastatic cases, and treatment continues to face significant challenges due to tumor heterogeneity, immune resistance, and an unfavorable tumor microenvironment (TME) (Sabit et al., 2025). Despite important advancements in molecular biology, immunotherapy, and metabolic interventions, the treatment of OS remains difficult, requiring further research to optimize targeted therapies and improve immunotherapy and metabolic strategies. This review aims to explore the latest advancements in OS research, focusing on molecular targets, immunotherapy, metabolic reprogramming, and clinical trial strategies. Studies have shown that key signaling pathways, such as Wnt/β-catenin and mesenchymal-epithelial transition (MET), play crucial roles in OS progression, particularly in the activation at the tumor-stroma interface and the overexpression of the MET receptor. Emerging biomarkers like apo-transcobalamin-II (APO-TCN2) and death receptor 5 (DR5) have been identified, offering potential prognostic value. Additionally, chimeric antigen receptor T-cell (CAR-T) therapy and combination immunotherapies show promise in overcoming immune evasion mechanisms. Metabolic reprogramming, particularly through long non-coding RNA regulation (lncRNA) of glycolysis, provides new therapeutic targets for OS. Clinical research also highlights the importance of global participation in clinical trials, with the EuroSarcoma Network's RECOGNIZE study demonstrating the feasibility and necessity of global participation to improve accessibility to new treatments. Despite these advancements, the treatment of OS remains challenging, and future research should continue to focus on optimizing targeted therapies, refining immunotherapeutic and metabolic interventions, improving early detection methods, integrating precision medicine, and innovating clinical trial designs to effectively translate research findings into better outcomes, ultimately improving the prognosis and quality of life for OS patients.

A recent focus of research has been on the Wnt/β-catenin signaling pathway, which plays a significant role in OS progression. Its activation at the tumor-stroma interface has been shown to facilitate tumor development (Ding and Chen). Additionally, MET, a receptor for hepatocyte growth factor (HGF), is overexpressed in OS and associated with poor prognosis (Zeng et al.). Targeting MET has shown therapeutic potential, and ongoing studies aim to explore combination therapies targeting both MET and other key

pathways. Furthermore, novel biomarkers such as APO-TCN2 (Lacinski et al.) and DR5 (Gamie et al.) have been identified, with proteomic and transcriptomic studies indicating their correlation with improved overall survival in OS and other sarcomas. Research should focus on further exploring the interactions between Wnt/β-catenin and other signaling pathways, validating APO-TCN2 and DR5 as biomarkers for early detection, developing more specific MET inhibitors, and investigating combination therapies that could improve treatment outcomes in OS. Moreover, understanding the crosstalk between these pathways and their influence on immune cell recruitment presents new opportunities for therapeutic interventions. Recent advances in single-cell RNA sequencing (scRNA-seq) have enabled a more detailed exploration of TME, providing insights into how immune cells interact with tumor cells and surrounding stromal components, which can help identify novel therapeutic targets (Zou et al., 2022). Additionally, combining CRISPR-Cas9 gene editing technology with nanoparticle drug delivery systems allows for precise manipulation of immune responses and targeted gene editing of immune evasion mechanisms, presenting new avenues for treatment. By modulating immune cell recruitment and activation within the TME, these strategies aim to enhance the efficacy of immunotherapies and offer potential improvements in the treatment of OS and other cancers (Xu et al., 2021). These approaches hold promise for personalized therapy tailored to the unique immune landscape of each patient.

In recent years, immunotherapy has shown promise in treating various cancers, but its efficacy in OS remains limited due to the complexity of the TME. Immune evasion mechanisms, such as the inactivation of phosphatase and tensin homolog deleted on chromosome 10 (PTEN), lead to hyperactivation of the PI3K-AKT pathway, which significantly reduces the effectiveness of immunotherapies (Piro et al., 2019). The tumor cells in OS employ multiple mechanisms to evade immune detection, making single-agent therapies ineffective. Therefore, combination therapies aimed at overcoming tumor heterogeneity and immune evasion mechanisms are being actively researched. Fourth-generation CAR-T cell therapies, which utilize co-expression of CXC chemokine receptor 5 (CXCR5) and interleukin (IL)-7, have demonstrated preclinical efficacy (Xu et al., 2021). One study showed that the co-expression of CXCR5 and IL-7 significantly enhanced CAR-T cell effectiveness by improving tumor penetration, persistence, and cytotoxicity (Hui et al.). Additionally, a bibliometric analysis of immunotherapy research for OS highlights China's role as a leader in this field, with significant trends pointing toward increasing interest in the TME, immune checkpoint inhibitors, and CAR-T cell therapy (Hui et al.).

The TME plays an integral role in OS metastasis. Recent studies have shown that neutrophil plasticity influences tumor progression, with the N1 subset exhibiting tumoricidal effects and the N2 subset supporting premetastatic niche formation (Yu and Yao, 2024). Targeting these neutrophil subsets could offer a novel strategy to prevent metastasis (Xia et al.). Moreover, metabolic reprogramming, particularly the enhancement of the Warburg effect in OS tumor cells, presents new therapeutic opportunities. Modulating metabolic pathways to inhibit OS cell growth and migration has become an area of intense research (Zeng et al.). lncRNAC1QTNF1-AS1 has been shown to regulate glycolysis through miR-34a-5p, promoting tumor growth and metastasis (Zhang et al.). Targeting these metabolic pathways, especially glycolysis, may provide new therapeutic strategies to treat OS.

One of the major challenges in OS research is the limited representation of pediatric populations in clinical trials. Efforts to establish decentralized clinical trial networks, such as the EuroSarcoma Network's RECOGNIZE study, have proven that global participation is not only feasible but also critical for ensuring equitable access to new therapies. These efforts can serve as a model for future trials aiming to enhance diversity and ensure that all patient populations benefit from treatment advancements (Hu et al.). In addition, a clinical case report describes a rare occurrence of costal chondrosarcoma secondary to multiple hereditary exostoses (HME), which compressed the right ventricle. The patient underwent intralesional resection followed by adjuvant radiotherapy, with no recurrence observed during the one-year follow-up. This case highlights the importance of early imaging screening and multidisciplinary management in patients with HME to improve diagnostic accuracy, optimize treatment strategies, and reduce the risk of recurrence (Yang et al.).

As research in molecular biology and immunology progresses,OS treatment is entering an innovative phase. Future studies should prioritize precision medicine and individualized treatment plans, with a particular focus on integrating immunotherapy and metabolic interventions. Further exploration of lncRNA-miRNA interactions in OS is essential to identify new therapeutic targets, particularly those involving glycolytic enzymes (Zhang et al.). A review of competing endogenous RNA (ceRNA) mechanisms in cancer underscores the importance of ceRNA interactions in cancer biology, which could open new avenues for targeted therapy (Cont et al., 2021). Additionally, addressing immune resistance mechanisms and tumor resistance will be crucial in advancing OS treatment. Enhancing early screening methods for detecting malignant transformations in HME and refining treatment protocols for rare conditions such as costal chondrosarcoma will also be essential. The focus should be on translating these innovations into clinical practice to improve patient outcomes and inform personalized therapeutic approaches. By fostering interdisciplinary collaboration and embracing novel strategies, OS treatment outcomes can be significantly improved, ultimately offering patients better prognoses and quality of life. Integrating multi-omics data—such as genomics, proteomics, and metabolomics—provides a deeper understanding of tumor heterogeneity and the molecular basis of osteosarcoma, facilitating the development of precision medicine strategies tailored to individual patients (Zou et al., 2022). These omics-guided approaches can reveal actionable mutations, dysregulated signaling pathways, and metabolic vulnerabilities, enabling clinicians to select therapies that are more likely to be effective while minimizing unnecessary toxicity. This systems-level approach holds transformative potential for OS management (Sabit et al., 2025; Chadha and Huang, 2022).

This Research Topic underscores the importance of innovative, interdisciplinary approaches in overcoming the current limitations of OS treatment. The integration of novel therapeutic strategies, including targeted metabolic interventions, advances in immunotherapy, and TME modulation, offers new hope for improving patient outcomes. Moreover, addressing structural

barriers to clinical trial design—particularly by enhancing global participation and equity—is crucial for ensuring these innovations benefit all affected populations.

Author contributions

SC: Writing – original draft, Writing – review and editing. YW: Writing – original draft, Writing – review and editing.

Funding

The author(s) declare that financial support was received for the research and/or publication of this article. This work was supported by grants from the National Natural Science Foundation of China (82303712), Sichuan Science and Technology Program (2024NSFSC0751), China Postdoctoral Science Foundation (2023M740520,2024T170099), and the Health Commission of Sichuan Province Medical Science and Technology Program (24QNMP097).

Acknowledgments

We thank Tong-Chuan He from the University of Chicago Medicine, Chicago, United States, and Yang-Fan Lv from the Army Medical University, Chongqing, China, for their invaluable contributions and support to our research. We also express gratitude to Guosheng Zhao from Chongqing Medical University for his insightful guidance. Additionally, we appreciate the support and collaboration from Professor Chuan-Zhu Lv from the Department of Emergency Medicine Center, Sichuan Provincial People's Hospital, University of Electronic Science and Technology of China.

Conflict of interest

The authors declare that the research was conducted in the absence of any commercial or financial relationships that could be construed as a potential conflict of interest.

Generative AI statement

The author(s) declare that no Generative AI was used in the creation of this manuscript.

Publisher's note

References

Chadha, M., and Huang, P. H. (2022). Proteomic and metabolomic profiling in soft tissue sarcomas. *Curr. Treat. Options Oncol.* 23, 78–88. doi:10.1007/s11864-022-00947-3

Conte, F., Fiscon, G., Sibilio, P., Licursi, V., and Paci, P. (2021). An overview of the computational models dealing with the regulatory ceRNA mechanism and ceRNA deregulation in cancer. *Methods Mol. Biol.* 2324, 149–164. doi:10.1007/978-1-0716-1503-4_10

Piro, G., Carbone, C., Carbognin, L., Pilotto, S., Ciccarese, C., Iacovelli, R., et al. (2019). Revising PTEN in the era of immunotherapy: new perspectives for an old story. *Cancers* 11, 1525. doi:10.3390/cancers11101525

Sabit, H., Arneth, B., Pawlik, T. M., Abdel-Ghany, S., Ghazy, A., Abdelazeem, R. M., et al. (2025). Leveraging single-cell multi-omics to decode tumor microenvironment diversity and therapeutic resistance. *Pharm. (Basel)* 18, 75. doi:10.3390/ph18010075

Xu, X., Liu, C., Wang, Y., Koivisto, O., Zhou, J., Shu, Y., et al. (2021). Nanotechnology-based delivery of CRISPR/Cas9 for cancer treatment. *Adv. Drug Deliv. Rev.* 176, 113891. doi:10.1016/j.addr.2021.113891

Yu, S., and Yao, X. (2024). Advances on immunotherapy for osteosarcoma. *Mol. Cancer* 23, 192. doi:10.1186/s12943-024-02105-9

Zou, Z., Sun, W., Xu, Y., Liu, W., Zhong, J., Lin, X., et al. (2022). Application of multi-omics approach in sarcomas: a tool for studying mechanism, biomarkers, and therapeutic targets. *Front. Oncol.* 12, 946022. doi:10.3389/fonc.2022.946022

frontiers | Frontiers in Molecular Biosciences

TYPE Review
PUBLISHED 26 March 2024
DOI 10.3389/fmolb.2024.1367331

OPEN ACCESS

EDITED BY
Yang Wang,
Sichuan Academy of Medical Sciences and Sichuan Provincial People's Hospital, China

REVIEWED BY
Sowmya Ramesh,
Johns Hopkins University, United States
Nahid Arghiani,
Stockholm University, Sweden

*CORRESPONDENCE
Jie Wen,
cashwj@qq.com
Sisi Wang,
wangsisi@csu.edu.cn

†These authors have contributed equally to this work and share first authorship

RECEIVED 08 January 2024
ACCEPTED 08 March 2024
PUBLISHED 26 March 2024

CITATION
Zeng M, Liu C, Gong H, Tang Z, Wen J, Wang S and Xiao S (2024), Therapeutic potential of tyrosine-protein kinase MET in osteosarcoma. *Front. Mol. Biosci.* 11:1367331.
doi: 10.3389/fmolb.2024.1367331

Therapeutic potential of tyrosine-protein kinase MET in osteosarcoma

Ming Zeng[1†], Can Liu[2†], Haoli Gong[1], Zhongwen Tang[1], Jie Wen[1,2*], Sisi Wang[3*] and Sheng Xiao[1]

[1]Department of Pediatric Orthopedics, Hunan Provincial People's Hospital, The First Affiliated Hospital of Hunan Normal University, Changsha, Hunan, China, [2]Department of Anatomy, Hunan Normal University School of Medicine, Changsha, Hunan, China, [3]Department of Oncology, The Second Xiangya Hospital of Central South University, Changsha, Hunan, China

Osteosarcoma, the most prevalent primary bone tumor in children and young adults, can often be successfully treated with standard chemotherapy and surgery when diagnosed at an early stage. However, patients presenting with metastases face significant challenges in achieving a cure. Despite advancements in classical therapies over the past few decades, clinical outcomes for osteosarcoma have not substantially improved. Recently, there has been increased understanding of the biology of osteosarcoma, leading to the identification of new therapeutic targets. One such target is MET, a tyrosine kinase receptor for Hepatocyte Growth Factor (HGF) encoded by the MET gene. *In vitro* and *in vivo* studies have demonstrated that the HGF/MET pathway plays a crucial role in cancer growth, invasion, metastasis, and drug resistance across various cancers. Clinical trials targeting this pathway are already underway for lung cancer and hepatocellular carcinoma. Moreover, MET has also been implicated in promoting osteosarcoma progression. This review summarizes 3 decades' worth of research on MET's involvement in osteosarcoma and further explores its potential as a therapeutic target for patients with this disease.

KEYWORDS

osteosarcoma, tyrosine-protein kinase, met, targeted therapy, therapeutic potential

Introduction

Osteosarcoma (OS) mainly affects children and is characterized by abnormal formation of bone tissue and spindle cells. It originates from primitive bone-forming cells in the mesenchyme. Typically, the tumor forms near the growth plate in the long bones of the limbs, such as the shinbone, upper arm bone, and thigh bone. Occasionally, it may occur in the pelvis, jaw, or skull. Histologically, OS comprises malignant osteoblasts that produce immature bone and osteoid tissue. It can be classified into different subtypes including conventional, low-grade central periosteal, chondroblastic, parosteal, telangiectatic, and small cell varieties. Osteosarcomas are highly aggressive, often leading to symptoms such as severe pain, noticeable swelling, and frequent fractures (Rossi and Del Fattore, 2023). The current treatment involves a combination of surgery, chemotherapy before surgery, and chemotherapy after surgery (Yang et al., 2022). The introduction of chemotherapy has improved the 5-year survival rate of OS patients to 60%–75%. However, more than a third of patients experience relapse and/or metastasis to the lungs, resulting in a significantly worse prognosis, with a 5-year survival rate dropping to 20% (Wu et al., 2009; Allison et al., 2012).

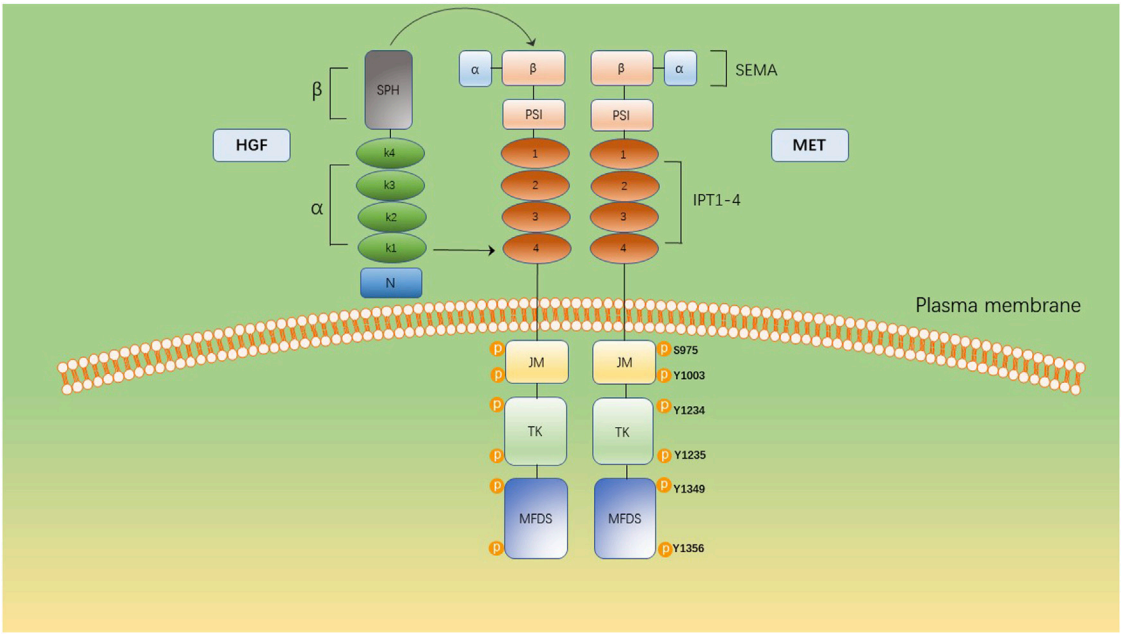

FIGURE 1
The multidomain structure of MET and its ligand, HGF. The extracellular domain comprises a SEMA domain, a plexin, semaphorin, and integrin (PSI) domain and four immunoglobulin-like IPT (IPT1–4). The intracellular domain constitutes a juxtamembrane domain (JM), containing Ser975 and Y1003 and a tyrosine kinase (TK) domain, containing Y1234 and Y1235. The C-terminal multifunctional docking site (MFDS) facilitates the recruitment of cytoplasmic signaling molecules and adaptor proteins through Y1349 and Y1356.

As there has been no significant increase in the survival rate of patients with metastatic disease over recent decades (Ning et al., 2023), numerous studies have focused on understanding the molecular mechanisms underlying tumorigenesis and drug resistance in osteosarcoma. Targeted therapy, which includes immune system targets, drug delivery systems, as well as intercellular and extracellular signaling pathways of metabolism, has advanced rapidly in recent years (Shaikh et al., 2016). The discovery of MET has opened a new avenue for research and treatment of osteosarcoma. The receptor-tyrosine kinase (RTK) MET, encoded by the MET proto-oncogene, is activated solely by its high-affinity ligand HGF (also known as scatter factor). Initially identified as a product of chromosomal rearrangement induced by carcinogens in the human osteosarcoma cell line HOS, MET was formed through fusion between the translocated promoter region (TPR) locus on chromosome one and the MET sequence on chromosome 7. Consequently, this encodes a constitutively active TPR-MET protein with a molecular weight of 65 kDa.

Abnormal HGF/MET signaling is implicated in the development and metastasis of various malignant tumors, including sarcomas. While MET mutations are rare in sarcomas, overexpression of MET is common and associated with poor clinical outcomes in patients with this disease. Both wild-type and persistently activated MET overexpression have been shown to induce human primary osteoblasts into osteosarcoma (Patane et al., 2006). Molecular pathology and cancer biology data suggest that HGF/MET signaling plays a crucial role in the survival, growth, proliferation, metastasis, and drug resistance of osteosarcoma (Coltella et al., 2003; Wang et al., 2012; Kunii et al., 2015).

These findings highlight the significance of dysregulated MET signaling in sarcomas. Various strategies, including tyrosine kinase inhibitors and monoclonal antibodies targeting MET activation, are currently being developed, with some already in advanced stages of clinical trials. In this review, we explore the current biological evidence regarding MET in osteosarcoma and discuss its potential as a therapeutic target for osteosarcoma patients.

HGF/MET signaling

HGF/MET signaling begins with the MET proto-oncogene, located on human chromosome 7q31, encoding a single 1,390 amino-acid precursor protein (Giordano et al., 1989). This precursor protein undergoes cleavage to form a mature receptor consisting of disulfide-bound α- and β-subunits (see Figure 1). The α-subunit, located extracellularly, shares homology with proteins from the semaphorin superfamily. The β-subunit comprises an extracellular domain responsible for ligand binding and an intracellular domain accountable for kinase activity and signal transduction (Gherardi et al., 2003). HGF, the sole known ligand of MET, is primarily secreted by stromal cells and activates MET on neighboring epithelial cells (Chan et al., 1991; Lokker et al., 1992; Goetsch et al., 2013). HGF binds to MET through two distinct affinity sites: the high-affinity site located in the N-terminal and first kringle regions, interacting with IPT3 and IPT4 domains in MET; and the low-affinity site situated in the serine protease homology domain, interacting with the semaphorin domain in MET (Gherardi et al., 2006; Holmes et al., 2007). Upon binding to MET, HGF induces dimerization of MET and phosphorylation of tyrosine

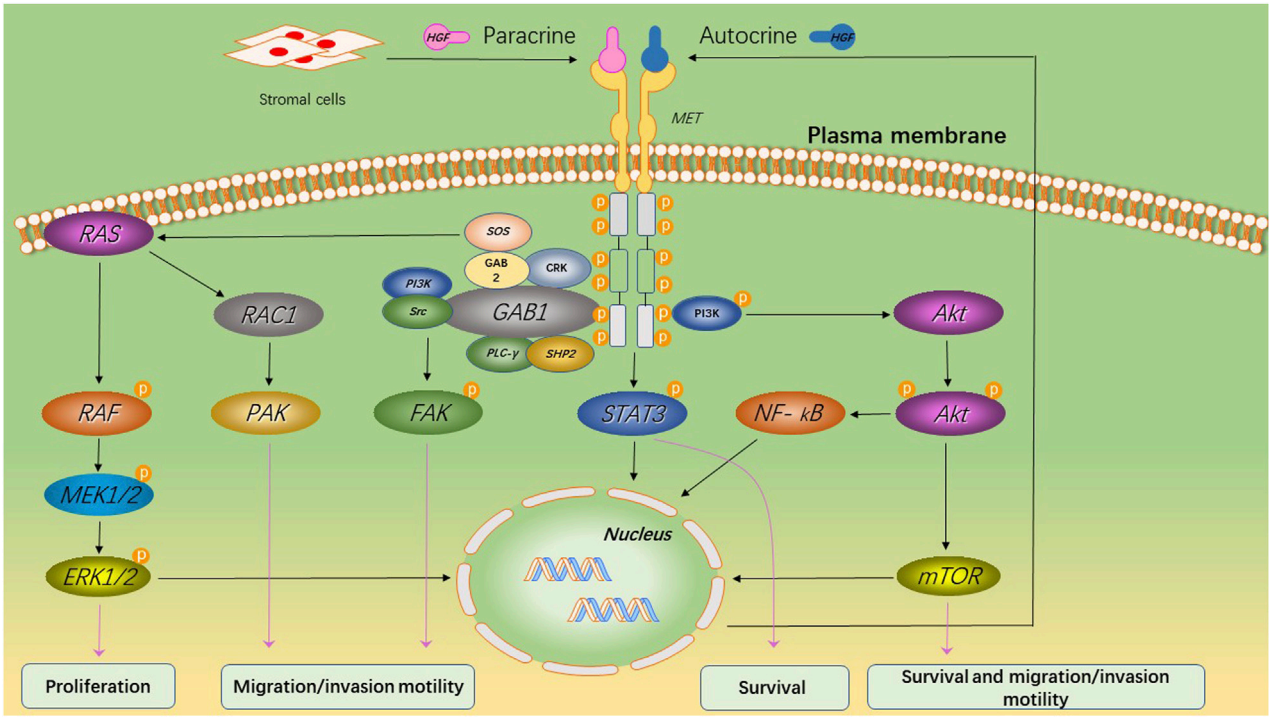

FIGURE 2
MET-induced signaling pathways and its primary biological effects. Upon binding of HGF to MET, the tyrosine kinase domain of MET initiates a cascade of phosphorylation events that lead to the activation of multiple key cell signaling pathways. This activation promotes cell survival and proliferation, while also enhancing cellular motility and invasive capacity.

residues Y1003, Y1234, and Y1235. It further phosphorylates tyrosine residues Y1349 and Y1356 within the multi-docking site at the C-terminus tail of the receptor (Giordano et al., 1989; Birchmeier et al., 2003). Phosphorylation of Y1349/1,356 is critical for activating downstream signaling pathways by recruiting intracellular adaptor proteins and signaling molecules that rely on src homology two domain-mediated interactions. These include SRC, phospholipase C γ (PLCγ), Shc protein (Shc), CRK adapter protein (CRK), growth-factor receptor-bound protein 2 (GRB2), GRB2-associated binding protein 1 (GAB1), as well as the p85 subunit of phosphatidylinositol three kinase (PI3K) and signal transducer activator transcription factor 3 (STAT3) (see Figure 2) (Pelicci et al., 1995; Fixman et al., 1996; Zhang et al., 2002). This interaction with the mentioned factors activates the STAT3, PI3K/Akt pathway, along with extracellular signal-regulated kinase 1/2 (JNKs)/p38 MAPK cascades, leading to nuclear factor κB(NF κB) pathway activation associated with survival, migration, and invasion processes (Rahimi et al., 1998; Maroun et al., 1999; Sipeki et al., 1999; Royal et al., 2000; Saxton et al., 2000; Kumari et al., 2005).

Molecular alterations of HGF/MET in human OS

Several investigations have aimed to understand the genetic and functional changes of the HGF/MET pathway in human osteosarcoma, considering its crucial role in regulating cell proliferation and apoptosis in the liver (Table 1). As mentioned earlier, MET activation in human tumors can result from gene-activating mutations, amplification, or overexpression.

In recent years, several studies have assessed the expression of MET and HGF in osteosarcoma. One study examined frozen samples from 87 primary bone and soft tissue tumors and found that osteosarcoma exhibited the highest levels of MET/HGF expression. Among 46 human osteosarcoma cases analyzed, p145MET was overexpressed in all primary tumors, local recurrences, and the majority of metastases.

Moreover, remarkably high levels of MET/HGF receptor expression were observed in primary tumors and recurrences. However, no evidence of amplification was found when measuring the intensity of DNA bands obtained from osteosarcomas that overexpressed the MET/HGF receptor. The consistent detection of MET proto-oncogene overexpression in both primary and recurrent lesions, as well as in the majority of metastases, is significant for understanding the pathogenesis of osteosarcoma. Immunohistochemical analysis revealed MET overexpression in primary (95%), local recurrences (100%), and metastases (82%) of osteosarcomas (Scotlandi et al., 1996). Sing Rong et al. conducted a study using confocal laser scan microscopy to examine paraffin-embedded human osteosarcoma sections stained for MET and HGF/SF. The results demonstrated significant staining of MET and HGF/SF in osteosarcomas (Rong et al., 1993). Ferracini R et al. investigated MET overexpression in up to 60% of the examined osteosarcomas (Ferracini et al., 1995). In 12 osteosarcoma cell lines, the MET/HGF receptor exhibited

TABLE 1 MET alterations in osteosarcoma.

Author	Year	MET alterations	Findings
Ferracini et al. (1995)	1995	MET overexpression	MET was overexpressed in 60% of the osteosarcomas and 12 osteosarcoma cell lines
Scotlandi et al. (1996)	1996	MET overexpression	MET was overexpressed in the all primary (100%), local recurrences (100%), and most metastases (71%) osteosarcomas. (Western blotting)
			MET was overexpressed in the primary (95%), local recurrences (100%), and most metastases (82%) osteosarcomas. (Immunohistochemical analysis)
Rong et al. (1993)	1993	MET overexpression	osteosarcomas showed significant Met and HGF staining by confocal laser scan microscopy
Oda et al. (2000)	2000	MET overexpression	MET was express positive in 5 of 25 in the primary site *versus* 12 of 24 in the metastatic site (Immunohistochemical analysis)
Arihiro and Inai (2001)	2001	MET overexpression	MET was overexpressed in 71% osteosarcoma. (Immunohistochemical analysis)
Entz-Werle et al. (2007)	2007	*MET* gene amplification and deletion	quantitative polymerase chain reaction (QPCR) targeting *MET* indicate *MET* was amplified in 9% (8 of 88) and deleted in 41% (36 of 88)
Kawano et al. (2023)	2023	MET overexpression	MET was overexpressed in osteosarcoma cell (HOS, SaOS, and MG-63)

overexpression, phosphorylation upon HGF stimulation, and full functionality. HGF was detected in two out of seven clinical specimens of osteosarcomas. Co-expression of the ligand and the receptor was observed in two clonal osteosarcoma cell lines. Constitutive phosphorylation of the MET/HGF receptor occurred in these cell lines; however, this phosphorylation could be suppressed by suramin treatment, a well-known blocker of autocrine loops. These findings suggest that activation of the MET/HGF receptor through either paracrine or autocrine mechanisms may contribute to the particularly aggressive behavior observed in osteosarcoma. The role of the MET oncogene product between primary and metastatic sites in osteosarcoma has remained controversial. Another study showed that all osteosarcoma cell lines had elevated MET expression in the cDNA array. The findings of this study confirm that the heat shock protein inhibitor 17-DMAG effectively inhibits the proliferation of osteosarcoma cells and induces apoptosis by targeting MET (Kawano et al., 2023).

In small groups comprising 25 patients, seven cases (28%) that showed negative MET reaction at the primary site exhibited immunoreactivity for MET at the metastatic site, indicating a higher incidence of MET expression compared to the primary site. Among all tumors, those positive for MET displayed significantly elevated MIB-1 LI compared to those negative for MET (negative: 20.99; positive: 27.65; p = .0292). The positive correlation between MET expression and proliferative activity also suggests a potential significant role played by MET expression in tumor progression (Oda et al., 2000). Another immunohistochemical study found that plasma membrane and cytoplasmic staining for MET/HGF receptor were positive in 71% of osteosarcoma cases (Arihiro and Inai, 2001).

A distinct approach was taken by Natacha Entz-Werle and colleagues (Entz-Werle et al., 2007) to investigate the role of MET activation in osteosarcoma. Since osteosarcomas are histologically characterized by malignant osteoblasts producing an osteoid component, this research team examined the genomic status of MET, TWIST, and APC genes involved in ossification processes in pediatric osteosarcomas treated with the OS94 protocol. The analysis included allelotyping, real-time quantitative polymerase chain reaction (qPCR), gene sequencing, and protein polymorphism study for MET in 91 osteosarcoma cases. No microsatellite instability was observed, but allelic imbalance was found in 52% of cases at locus 7q31 containing MET. By qPCR analysis alone, it was determined that the MET gene was normal in 50% (44 out of 88) of cases, amplified in 9% (8 out of 88), and deleted in 41% (36 out of 88). Notably, significant statistical associations were identified between relapsed tumors and abnormalities involving MET (70%, predominantly deleted; p = .004) as well as TWIST abnormalities (69%, predominantly deleted; p = .03). When comparing molecular profiles between deceased children and surviving patients, statistically significant trends indicated a higher frequency of deletions for both MET (p = .03) and TWIST genes (p = .01), along with a more frequent rearrangement involving APC gene (p = .03). Furthermore, aberrations related to MET serve as significant indicators for poor event-free survival, particularly when amplification is present (p = .015), suggesting that tumors with amplified levels perform worse than those with deletions.

The involvement of the MET/HGF receptor in OS proliferation and invasive behavior

The involvement of the MET/HGF receptor in OS proliferation and invasive behavior has been extensively studied. Activation of the HGF/MET axis in OS cell lines has been shown to trigger downstream signaling pathways contributing to motility, mitogenesis, and morphogenesis in a cell type-specific manner. Nadia Coltella et al. investigated the impact of MET receptor activation on human OS cell lines by assessing HGF-dependent MAPK and PKB/AKT activation levels as biochemical indicators of mitogenic and invasive responses, respectively. Stimulation with HGF led to ERK1/2 phosphorylation in U-2OS, Saos-2, IOR/OS9, and IOR/OS10 OS cell lines. Phosphorylation of specific residues on ERK1/2 facilitated its translocation to the nucleus and increased

enzymatic activity, evidenced by phosphorylation of its physiological substrate, the Elk-1 transcription factor at Ser 383 (Coltella et al., 2003). In U-2OS and Saos-2 cells, HGF consistently induced PKB/AKT phosphorylation, leading to subsequent enzymatic activation of its physiological substrate GSK-3α/β. A modest AKT response to HGF was also observed in MG-63 and IOR/OS10 cells. Cell cultures treated with 100 ng/mL HGF demonstrated a proliferative response dependent on HGF stimulation for all cell lines except MG-63, where the MAPK cascade was not activated.

The cell lines U-2OS and Saos-2, which exhibited HGF-induced activation of PKB/AKT, displayed migratory capability through the micropore filter of a Transwell chamber in response to recombinant HGF. Both HGF-dependent responses were reversed by the specific MET inhibitor K252a. The activation of the MET receptor by HGF is implicated in OS progression, as it confers functions facilitating metastatic diffusion and invasion of both local and peripheral tissues. Metastasis is a complex process involving multiple steps, with motility and invasion through the basement membrane being crucial stages. This study has demonstrated that HGF stimulates motility in OS cell lines where MET activation also triggers AKT activation. Furthermore, OS cells can invade collagen matrix in an HGF-dependent manner if they exhibit an AKT response to HGF.

Another study investigated the signal transduction and downregulation of MET in HGF-stimulated low and highly metastatic human OS cells (Husmann et al., 2015). The mRNA and protein expression levels of these molecules, as well as HGF-stimulated signaling and downregulation of MET, were compared between the parental low metastatic HOS and MG63 cell lines, their respective highly metastatic MNNG-HOS and 143B cell lines, along with the MG63-M6 and MG63-M8 sublines. TPR-MET expression resulting from a chromosomal rearrangement induced by treatment with the carcinogen N-methyl-N′-nitronitrosoguanidine was only observed in MNNG-HOS cells (Dean et al., 1987). Akt and Erk1/2 phosphorylation were stimulated by HGF in all examined cell lines; however, phospho-Stat3 levels remained basal. Downregulation of HGF-stimulated Akt and Erk1/2 phosphorylation occurred more rapidly in the HGF-expressing MG63-M8 cells compared to HOS cells. Degradation of activated MET primarily occurred through the proteasomal pathway, with a lesser contribution from the lysosomal pathway in these cell lines. Therefore, targeting HGF-stimulated Akt and Erk1/2 signaling pathways as well as proteasomal degradation of activated MET could be potential therapeutic strategies for OS. In both normal and tumor cells, Akt, Erk1/2, and Stat3 are known targets of MET signaling (Goetsch et al., 2013). However, only Akt and Erk1/2 were found to be phosphorylated upon HGF treatment in the examined OS cell lines. The absence of HGF-induced Stat3 phosphorylation suggests that Stat3 is not activated by MET specifically in these cell lines (Yan et al., 2015). This observation further supports the notion that the activation of signaling pathways by MET is contingent upon the specific cellular context.

The MET inhibitor effectively suppressed colony formation in all tested cell lines and specifically attenuated the motility of the MNNG cell line (Messerschmitt et al., 2008), which is consistent with the known expression of the TPR-MET oncogene. Furthermore, it was observed that the MET inhibitor not only impacted the MNNG cell line expressing TPR-MET but also inhibited colony formation in TE85 and 143B cell lines lacking TPR-MET expression (Peschard and Park, 2007). Therefore, incorporating a MET inhibitor into a chemotherapeutic regimen could potentially offer benefits for OS patients, irrespective of TPR-MET expression.

MET as a prognostic marker in OS

Abnormal activation of MET has emerged as a crucial factor in the advancement and growth of OS. Traditionally, the tissue response to chemotherapy before surgery has been seen as the primary factor predicting the outcome of primary OS. Yet, recent studies have explored the link between MET activation and treatment effectiveness in OS. N Entz Werle et al. carried out research involving 54 patients under 20 years old with primary OS who underwent treatment as per the French Society of Pediatric Oncology OS 94 plan (Entz-Werle et al., 2003). They collected paired normal and biopsy samples, and surgical specimens were obtained from 13 cases post preoperative chemotherapy. Genomic DNA was extracted, followed by an analysis targeting microsatellites linked to chromosome 7q31 regions. The findings at the 7q31 locus and the region involving APC show a significant involvement of these areas in OS cancer development, despite the relatively low occurrence of changes at this locus (34%). However, among patients with partial remissions, relapses, or fatalities, the frequency of this allelic imbalance rose to 80%, indicating a strong link with this unfavorable prognosis subgroup ($p = 0.04$). Thus, these results have pinpointed a new area implicated in OS prognosis. The noteworthy connection between changes in chromosome 7q31 and worse prognosis underscores its prognostic importance.

These findings are consistent with prior research on MET and suggest its potential involvement in aggressive osteosarcoma forms (Ferracini et al., 1995; Oda et al., 2000). Understanding allelic imbalances at this locus could be crucial for predicting relapse in patients achieving partial or complete remission and may spur future use of kinase inhibitors in osteosarcoma therapy.

As previously mentioned, Natacha Entz-Werle et al. (Entz-Werle et al., 2007) conducted a study on the genomic status of various genes implicated in the ossification process in 91 pediatric osteosarcoma patients using the OS94 protocol. MET abnormalities, particularly MET amplification, are significant markers of poor event-free survival (EFS) and are often linked with inferior overall survival (OS). Tumors with MET amplification have a worse prognosis compared to those with deletions. Specifically, patients with MET-amplified tumors exhibit a 5-year EFS rate of only 28% and a 5-year OS rate of 53%. Additionally, the identification of MET abnormalities can further stratify the overall poor outcome group and pinpoint the subset of patients with the most adverse prognosis.

The activation patterns of receptor tyrosine kinases (RTKs) were also investigated in chemonaive fresh frozen tissues from osteosarcoma patients using a multiplex immunoassay (Chaiyawat et al., 2017). This analysis unveiled distinct RTK tyrosine phosphorylation patterns in osteosarcoma cases. Unsupervised hierarchical clustering, utilizing the Pearson uncentered correlation coefficient, classified RTKs into two groups: Group A (MET, c-Kit, VEGFR2, and HER2) and Group

B (FGFR1 and PDGFRα), based on their tyrosine phosphorylation profiles. The study found that patients with inactive Group A-RTKs tended to have shorter overall survival compared to those with at least one active Group A-RTK. Additionally, the percentage of tumor necrosis emerged as a significant adverse prognostic factor in this investigation.

In summary, a notable correlation was observed between rearrangements at 7q31 and a poorer prognosis. MET has demonstrated its efficacy as a diagnostic marker in osteosarcoma.

The relationship between MET activation and chemosensitivity

An analysis of survival indicated that OS patients with inactive MET tended to have a worse prognosis. Consequently, a further investigation delved into the link between MET activation status and both resistance to chemotherapy and metastasis (Chaiyawat et al., 2017). Among patients who underwent the same chemotherapy regimen consisting of doxorubicin and cisplatin (n = 10), a skilled pathologist assessed their tumor necrosis levels post-treatment. The results revealed that OS patients with active MET displayed higher sensitivity to chemotherapy compared to those in the inactive group, as evidenced by significantly reduced levels of tumor necrosis in the latter. However, no association was observed between MET activation status and metastasis.

Furthermore, primary osteosarcoma cells were exposed to varying concentrations of doxorubicin or cisplatin, followed by evaluation of cell viability using the MTT assay. The findings indicated that most primary OS cells expressing active MET exhibited heightened sensitivity to both doxorubicin and cisplatin treatments compared to those lacking MET activation. Additionally, a positive correlation was noted between the number of activated MET and increased sensitivity to doxorubicin and cisplatin in primary OS cells.

The HGF/MET axis as a therapeutic target in OS

The occurrence and progression of malignant osteosarcoma are influenced by genetic factors and pathological changes. Angiogenesis plays a crucial role in the proliferation, migration, invasion, and metastasis of OS. Mounting evidence suggests that inhibiting angiogenesis could be a viable approach for OS treatment (Peng et al., 2016; Wang et al., 2017). Various angiogenesis inhibitors, such as sorafenib, sunitinib, and cediranib, have been employed to manage advanced OS (Coventon, 2017). However, recent studies indicate that these inhibitors may induce tumor adaptation and disease progression, fostering the development of highly invasive and metastatic tumors (Ebos et al., 2009; Paez-Ribes et al., 2009). Consequently, novel agents capable of concurrently inhibiting the VEGF signaling pathway along with other pathways involved in tumor invasion and metastasis hold promise as effective therapies for OS patients.

Anlotinib is an orally available, highly potent, multi-targeted tyrosine kinase inhibitor (TKI) that effectively impedes the phosphorylation of VEGFR2 and demonstrates activity against MET, platelet-derived growth factor receptors α/β (PDGFR α/β), c-Kit, Aurora-B, Ret, c-FMS, and discoidin domain receptor 1 (DDR1) (Sun et al., 2016; Wang et al., 2016). The results from phase II and III clinical trials have showcased the promising clinical efficacy of anlotinib in various solid tumors, including non-small cell lung cancer, hepatocellular carcinoma, renal carcinoma, gastric cancer, and soft tissue sarcoma. Anlotinib garnered approval from the CFDA for treating NSCLC in 2018.

Moreover, ongoing phase II trials have revealed significant activity of anlotinib against a broad spectrum of soft tissue sarcomas. The anti-tumor activity and underlying mechanism of anlotinib in osteosarcoma were explored (Wang et al., 2019). Various *in vitro* and *in vivo* models were employed to evaluate the effectiveness of anlotinib in terms of anti-proliferative, anti-angiogenic, and anti-metastatic properties. Anlotinib effectively suppresses tumor growth, enhances chemo-sensitivity, and inhibits migration and invasion in OS cells. Additionally, the molecular mechanism underlying its anti-tumor effects was elucidated using phospho-RTK antibody arrays, confirming its ability to inhibit the phosphorylation of MET and VEGFR2 along with activation of downstream signaling pathways. Furthermore, it was observed that anlotinib blocks HGF-induced cell migration and invasion, as well as VEGF-induced angiogenesis (Sun et al., 2016). Notably, in the 143B-Luc orthotopic OS model, treatment with anlotinib exhibited significant inhibition of tumor growth and lung metastasis. These preclinical findings collectively underscore the potential clinical utility of anlotinib as a novel inhibitor targeting MET and VEGFR2 to suppress tumorigenesis in OS.

The compound PHA-665752 is a powerful, selective, and ATP-competitive inhibitor of MET. In 2003, Christensen et al. found that PHA-665752 effectively stops the MET-dependent behavior in lab settings and shows anti-cancer activity in live subjects (Christensen et al., 2003). Later, Ma et al. showed that PHA-665752 works together with rapamycin to stop the growth of non-small cell lung cancer cells (Ma et al., 2005). Additionally, Puri et al. noted that PHA-665752 significantly reduces the growth of lung cancer tumors in mice and the formation of new blood vessels by more than 85% (Puri et al., 2007). This compound has demonstrated its ability to hinder the progression of OS, encourage cell death, and slow down the multiplication of human OS cells (Chen et al., 2021). Furthermore, the ERK1/2 pathway plays a critical role in mediating the anti-cancer effects of PHA-665752 in OS. This was reinforced by the discovery that LY3214996, a highly selective inhibitor of the ERK1/2 pathway, counteracted the effects of PHA-665752 in OS. Moreover, PHA-665752 effectively reduced tumor growth in a mouse model with transplanted tumors (Chen et al., 2021). Overall, MET presents a target for OS treatment, and PHA-665752 emerges as a promising option for fighting OS.

Cabozantinib (XL184) is a special inhibitor of VEGFR2 tyrosine kinase, which also effectively inhibits the MET receptor (Uitdehaag et al., 2014). It has shown anti-tumor effectiveness both in laboratory settings and in live subjects in different models of osteosarcoma and Ewing sarcoma (Houghton et al., 2015).

In collaboration with the Cancer Therapy Evaluation Program of the National Cancer Institute, the French Sarcoma

Group conducted a clinical study (CABONE) comprising two phase II trials to explore the potential of cabozantinib in patients with advanced Ewing sarcomas and advanced OSs respectively. One of the trials focused on evaluating the efficacy and safety of cabozantinib in patients with advanced OS (Italiano et al., 2020). The primary eligibility criteria included age ≥12 years, ECOG Performance status ≤1, metastatic or unresectable locally advanced disease, and documented disease progression (according to RECIST v1.1) prior to study enrollment. There were no restrictions on the number of previous lines of treatment. Patients received daily oral doses of cabozantinib (60 mg for adults and 40 mg/m2 for children) until disease progression or unacceptable toxicity occurred. The primary endpoint was a combined objective response and non-progression at 6 months for overall survival (OS). A total of 90 patients were enrolled in the study (Ewing sarcoma: 45; OS: 45). The median follow-up duration for OSs was determined to be 31.1 months (95%CI: [24.4–31.7]). Among the evaluated OS cases after histological and radiological review, 42 patients (93.3%) demonstrated efficacy response, with seven patients (16.7%) showing partial response and fourteen patients (33.3%) exhibiting stable disease status. Additionally, fourteen patients with osteosarcoma (33.3%) remained free from disease progression 6 months after initiating treatment. The treatment was generally well tolerated; however, mild to moderate fatigue, diarrhea, mucositis, and liver transaminitis were commonly observed adverse events graded as grade 1 or grade 2 in severity among the participants. Among the more severe adverse events graded as grade 3 or grade 4 in severity were hypophosphatemia experienced by eight individuals (8.9%), an increase in aspartate aminotransferase levels reported by five individuals (5.6%), palmo-plantar syndrome observed in five individuals (5.6%), pneumothorax encountered by five individuals (=5), and neutropenia recorded among five individuals as well (5%). Furthermore, it is worth noting that at least one serious adverse event was reported among sixty-one participants accounting for approximately 67.8% of the total patient population. The efficacy of cabozantinib in patients with advanced osteosarcoma was significantly demonstrated, suggesting its potential as a novel therapeutic option in this clinical context.

Abnormal activation of MET is commonly observed in osteosarcoma patients, and MET inhibitors are acknowledged for their potential to suppress tumors. However, OS often becomes resistant to MET inhibitors, which poses a significant challenge that needs addressing.

The small-molecule inhibitor crizotinib, also known as PF02341066, has shown strong selectivity as an ATP-competitive inhibitor of MET kinase in various human tumors. It has undergone phase II/III clinical trials for treating non-small-cell lung cancer (De Mello et al., 2020). *In vitro* studies have demonstrated that specific inhibition of highly phosphorylated MET-expressing OS cells by PF02341066 effectively triggers cell death. However, the inhibitory effectiveness of PF02341066 is compromised *in vivo* due to interference from the vascular niche. A study revealed that crizotinib displayed concentration-dependent inhibition of OS cell line proliferation. Additionally, it significantly induced apoptosis. Furthermore, crizotinib caused an increase in G0/G1 phase cells and a decrease in S phase cells compared to the control group. Moreover, crizotinib effectively suppressed migration and invasion of osteosarcoma cells while decreasing the expression of MET/Gab1/STAT5 (Jia et al., 2023). OS cells located near microvessels or exhibiting vascular mimicry suppress both MET expression and phosphorylation.

Furthermore, acquired drug resistance in OS cells is linked to the activation of VEGFR2 (vascular endothelial growth factor receptor 2). Dual targeting of both MET and VEGFR2 has proven effective in reducing tumor size in a xenograft model. Combining targeted therapy against MET with VEGFR2 inhibition may offer significant benefits towards achieving an optimal therapeutic outcome for patients with OS (Tang et al., 2022). Together, these findings underscore the critical role played by tumor heterogeneity and the microenvironment in determining drug response while uncovering the molecular mechanisms behind acquired drug resistance to targeted therapy against MET.

Conclusion

In conclusion, MET is commonly overexpressed in OS tissue and is often linked with a poor prognosis. Current *in vitro* experiments have verified that MET activation can boost the proliferation and invasion abilities of OS cells. Numerous MET inhibitors have shown notable efficacy in inhibiting tumor growth in both preclinical and clinical settings. Interestingly, patients with elevated MET expression levels tend to display heightened sensitivity to chemotherapy drugs. Histological and genomic investigations have identified MET as a promising target for assessing the prognosis and treatment of OS. However, further characterization is necessary to delve into the therapeutic implications of inhibiting MET in OS, utilizing more pertinent preclinical models and specifically tailored clinical trials.

Author contributions

MZ: Conceptualization, Writing–original draft. CL: Conceptualization, Writing–original draft. HG: Investigation, Writing–original draft. ZT: Investigation, Writing–original draft. JW: Supervision, Writing–review and editing. SW: Software, Writing–review and editing. SX: Resources, Writing–review and editing.

Funding

The author(s) declare financial support was received for the research, authorship, and/or publication of this article. This study was supported by Doctor Science project of Hunan Provincial Peoples' Hospital, No. BSJJ202119.

Conflict of interest

The authors declare that the research was conducted in the absence of any commercial or financial relationships that could be construed as a potential conflict of interest.

Publisher's note

References

Allison, D. C., Carney, S. C., Ahlmann, E. R., Hendifar, A., Chawla, S., Fedenko, A., et al. (2012). A meta-analysis of osteosarcoma outcomes in the modern medical era. *Sarcoma* 2012, 704872. doi:10.1155/2012/704872

Arihiro, K., and Inai, K. (2001). Expression of CD31, Met/hepatocyte growth factor receptor and bone morphogenetic protein in bone metastasis of osteosarcoma. *Pathol. Int.* 51 (2), 100–106. doi:10.1046/j.1440-1827.2001.01164.x

Birchmeier, C., Birchmeier, W., Gherardi, E., and Vande Woude, G. F. (2003). Met, metastasis, motility and more. *Nat. Rev. Mol. Cell Biol.* 4 (12), 915–925. doi:10.1038/nrm1261

Chaiyawat, P., Klangjorhor, J., Settakorn, J., Champattanachai, V., Phanphaisarn, A., Teeyakasem, P., et al. (2017). Activation status of receptor tyrosine kinases as an early predictive marker of response to chemotherapy in osteosarcoma. *Transl. Oncol.* 10 (5), 846–853. doi:10.1016/j.tranon.2017.08.005

Chan, A. M., Rubin, J. S., Bottaro, D. P., Hirschfield, D. W., Chedid, M., and Aaronson, S. A. (1991). Identification of a competitive HGF antagonist encoded by an alternative transcript. *Science* 254 (5036), 1382–1385. doi:10.1126/science.1720571

Chen, W., Wu, S., Huang, Y., Zhang, T., Dong, H., Zheng, X., et al. (2021). A c-met inhibitor suppresses osteosarcoma progression via the ERK1/2 pathway in human osteosarcoma cells. *Onco Targets Ther.* 14, 4791–4804. doi:10.2147/OTT.S317122

Christensen, J. G., Schreck, R., Burrows, J., Kuruganti, P., Chan, E., Le, P., et al. (2003). A selective small molecule inhibitor of c-Met kinase inhibits c-Met-dependent phenotypes *in vitro* and exhibits cytoreductive antitumor activity *in vivo*. *Cancer Res.* 63 (21), 7345–7355.

Coltella, N., Manara, M. C., Cerisano, V., Trusolino, L., Di Renzo, M. F., Scotlandi, K., et al. (2003). Role of the MET/HGF receptor in proliferation and invasive behavior of osteosarcoma. *FASEB J.* 17 (9), 1162–1164. doi:10.1096/fj.02-0576fje

Coventon, J. (2017). A review of the mechanism of action and clinical applications of sorafenib in advanced osteosarcoma. *J. Bone Oncol.* 8, 4–7. doi:10.1016/j.jbo.2017.07.001

Dean, M., Park, M., and Vande Woude, G. F. (1987). Characterization of the rearranged tpr-met oncogene breakpoint. *Mol. Cell Biol.* 7 (2), 921–924. doi:10.1128/mcb.7.2.921

De Mello, R. A., Neves, N. M., Amaral, G. A., Lippo, E. G., Castelo-Branco, P., Pozza, D. H., et al. (2020). The role of MET inhibitor therapies in the treatment of advanced non-small cell lung cancer. *J. Clin. Med.* 9 (6), 1918. doi:10.3390/jcm9061918

Ebos, J. M., Lee, C. R., Cruz-Munoz, W., Bjarnason, G. A., Christensen, J. G., and Kerbel, R. S. (2009). Accelerated metastasis after short-term treatment with a potent inhibitor of tumor angiogenesis. *Cancer Cell* 15 (3), 232–239. doi:10.1016/j.ccr.2009.01.021

Entz-Werle, N., Lavaux, T., Metzger, N., Stoetzel, C., Lasthaus, C., Marec, P., et al. (2007). Involvement of MET/TWIST/APC combination or the potential role of ossification factors in pediatric high-grade osteosarcoma oncogenesis. *Neoplasia* 9 (8), 678–688. doi:10.1593/neo.07367

Entz-Werle, N., Schneider, A., Kalifa, C., Voegeli, A. C., Tabone, M. D., Marec-Berard, P., et al. (2003). Genetic alterations in primary osteosarcoma from 54 children and adolescents by targeted allelotyping. *Br. J. Cancer* 88 (12), 1925–1931. doi:10.1038/sj.bjc.6600968

Ferracini, R., Di Renzo, M. F., Scotlandi, K., Baldini, N., Olivero, M., Lollini, P., et al. (1995). The Met/HGF receptor is over-expressed in human osteosarcomas and is activated by either a paracrine or an autocrine circuit. *Oncogene* 10 (4), 739–749.

Fixman, E. D., Fournier, T. M., Kamikura, D. M., Naujokas, M. A., and Park, M. (1996). Pathways downstream of Shc and Grb2 are required for cell transformation by the tpr-Met oncoprotein. *J. Biol. Chem.* 271 (22), 13116–13122. doi:10.1074/jbc.271.22.13116

Gherardi, E., Sandin, S., Petoukhov, M. V., Finch, J., Youles, M. E., Ofverstedt, L. G., et al. (2006). Structural basis of hepatocyte growth factor/scatter factor and MET signalling. *Proc. Natl. Acad. Sci. U. S. A.* 103 (11), 4046–4051. doi:10.1073/pnas.0509040103

Gherardi, E., Youles, M. E., Miguel, R. N., Blundell, T. L., Iamele, L., Gough, J., et al. (2003). Functional map and domain structure of MET, the product of the c-met protooncogene and receptor for hepatocyte growth factor/scatter factor. *Proc. Natl. Acad. Sci. U. S. A.* 100 (21), 12039–12044. doi:10.1073/pnas.2034936100

Giordano, S., Di Renzo, M. F., Narsimhan, R. P., Cooper, C. S., Rosa, C., and Comoglio, P. M. (1989). Biosynthesis of the protein encoded by the c-met proto-oncogene. *Oncogene* 4 (11), 1383–1388.

Goetsch, L., Caussanel, V., and Corvaia, N. (2013). Biological significance and targeting of c-Met tyrosine kinase receptor in cancer. *Front. Biosci. Landmark Ed.* 18, 454–473. doi:10.2741/4114

Holmes, O., Pillozzi, S., Deakin, J. A., Carafoli, F., Kemp, L., Butler, P. J. G., et al. (2007). Insights into the structure/function of hepatocyte growth factor/scatter factor from studies with individual domains. *J. Mol. Biol.* 367 (2), 395–408. doi:10.1016/j.jmb.2006.12.061

Houghton, P. J., Kurmasheva, R. T., Kolb, E. A., Gorlick, R., Maris, J. M., Wu, J., et al. (2015). Initial testing (stage 1) of the tubulin binding agent nanoparticle albumin-bound (nab) paclitaxel (Abraxane(®)) by the Pediatric Preclinical Testing Program (PPTP). *Pediatr. Blood Cancer* 62 (7), 1214–1221. doi:10.1002/pbc.25474

Husmann, K., Ducommun, P., Sabile, A. A., Pedersen, E. M., Born, W., and Fuchs, B. (2015). Signal transduction and downregulation of C-MET in HGF stimulated low and highly metastatic human osteosarcoma cells. *Biochem. Biophys. Res. Commun.* 464 (4), 1222–1227. doi:10.1016/j.bbrc.2015.07.108

Italiano, A., Mir, O., Mathoulin-Pelissier, S., Penel, N., Piperno-Neumann, S., Bompas, E., et al. (2020). Cabozantinib in patients with advanced Ewing sarcoma or osteosarcoma (CABONE): a multicentre, single-arm, phase 2 trial. *Lancet Oncol.* 21 (3), 446–455. doi:10.1016/S1470-2045(19)30825-3

Jia, T., Cai, M., Wang, Z., and Chen, T. (2023). Anticancer effect of crizotinib on osteosarcoma cells by targeting c-Met signaling pathway. *Cell Mol. Biol. (Noisy-le-grand)* 69 (5), 174–178. doi:10.14715/cmb/2023.69.5.27

Kawano, M., Tanaka, K., Itonaga, I., Iwasaki, T., Kubota, Y., and Tsumura, H. (2023). The anti-oncogenic effect of 17-DMAG via the inactivation of HSP90 and MET pathway in osteosarcoma cells. *Oncol. Res.* 31 (5), 631–643. doi:10.32604/or.2023.029745

Kumari, A. L., Ali, A. M., Das, S., Pardhasaradhi, B. V. V., Varalakshmi, C., and Khar, A. (2005). Role of STAT3 and NFkappaB signaling in the serum factor-induced apoptosis in AK-5 cells. *Biochem. Biophys. Res. Commun.* 336 (3), 860–867. doi:10.1016/j.bbrc.2005.08.185

Kunii, E., Ozasa, H., Oguri, T., Maeno, K., Fukuda, S., Uemura, T., et al. (2015). Reversal of c-MET-mediated resistance to cytotoxic anticancer drugs by a novel c-MET inhibitor TAS-115. *Anticancer Res.* 35 (10), 5241–5247.

Lokker, N. A., Mark, M. R., Luis, E. A., Bennett, G. L., Robbins, K. A., Baker, J. B., et al. (1992). Structure-function analysis of hepatocyte growth factor: identification of variants that lack mitogenic activity yet retain high affinity receptor binding. *EMBO J.* 11 (7), 2503–2510. doi:10.1002/j.1460-2075.1992.tb05315.x

Ma, P. C., Schaefer, E., Christensen, J. G., and Salgia, R. (2005). A selective small molecule c-MET Inhibitor, PHA665752, cooperates with rapamycin. *Clin. Cancer Res.* 11 (6), 2312–2319. doi:10.1158/1078-0432.CCR-04-1708

Maroun, C. R., Holgado-Madruga, M., Royal, I., Naujokas, M. A., Fournier, T. M., Wong, A. J., et al. (1999). The Gab1 PH domain is required for localization of Gab1 at sites of cell-cell contact and epithelial morphogenesis downstream from the met receptor tyrosine kinase. *Mol. Cell Biol.* 19 (3), 1784–1799. doi:10.1128/mcb.19.3.1784

Messerschmitt, P. J., Rettew, A. N., Brookover, R. E., Garcia, R. M., Getty, P. J., and Greenfield, E. M. (2008). Specific tyrosine kinase inhibitors regulate human osteosarcoma cells *in vitro*. *Clin. Orthop. Relat. Res.* 466 (9), 2168–2175. doi:10.1007/s11999-008-0338-9

Ning, B., Liu, Y., Huang, T., and Wei, Y. (2023). Autophagy and its role in osteosarcoma. *Cancer Med.* 12 (5), 5676–5687. doi:10.1002/cam4.5407

Oda, Y., Naka, T., Takeshita, M., Iwamoto, Y., and Tsuneyoshi, M. (2000). Comparison of histological changes and changes in nm23 and c-MET expression between primary and metastatic sites in osteosarcoma: a clinicopathologic and immunohistochemical study. *Hum. Pathol.* 31 (6), 709–716. doi:10.1053/hupa.2000.8230

Paez-Ribes, M., Allen, E., Hudock, J., Takeda, T., Okuyama, H., Viñals, F., et al. (2009). Antiangiogenic therapy elicits malignant progression of tumors to increased local invasion and distant metastasis. *Cancer Cell* 15 (3), 220–231. doi:10.1016/j.ccr.2009.01.027

Patane, S., Avnet, S., Coltella, N., Costa, B., Sponza, S., Olivero, M., et al. (2006). MET overexpression turns human primary osteoblasts into osteosarcomas. *Cancer Res.* 66 (9), 4750–4757. doi:10.1158/0008-5472.CAN-05-4422

Pelicci, G., Giordano, S., Zhen, Z., Salcini, A. E., Lanfrancone, L., Bardelli, A., et al. (1995). The motogenic and mitogenic responses to HGF are amplified by the Shc adaptor protein. *Oncogene* 10 (8), 1631–1638.

Peng, N., Gao, S., Guo, X., Wang, G., Cheng, C., Li, M., et al. (2016). Silencing of VEGF inhibits human osteosarcoma angiogenesis and promotes cell apoptosis via VEGF/PI3K/AKT signaling pathway. *Am. J. Transl. Res.* 8 (2), 1005–1015.

Peschard, P., and Park, M. (2007). From Tpr-Met to Met, tumorigenesis and tubes. *Oncogene* 26 (9), 1276–1285. doi:10.1038/sj.onc.1210201

Puri, N., Khramtsov, A., Ahmed, S., Nallasura, V., Hetzel, J. T., Jagadeeswaran, R., et al. (2007). A selective small molecule inhibitor of c-Met, PHA665752, inhibits tumorigenicity and angiogenesis in mouse lung cancer xenografts. *Cancer Res.* 67 (8), 3529–3534. doi:10.1158/0008-5472.CAN-06-4416

Rahimi, N., Hung, W., Tremblay, E., Saulnier, R., and Elliott, B. (1998). c-Src kinase activity is required for hepatocyte growth factor-induced motility and anchorage-independent growth of mammary carcinoma cells. *J. Biol. Chem.* 273 (50), 33714–33721. doi:10.1074/jbc.273.50.33714

Rong, S., Jeffers, M., Resau, J. H., Tsarfaty, I., Oskarsson, M., and Vande Woude, G. F. (1993). Met expression and sarcoma tumorigenicity. *Cancer Res.* 53 (22), 5355–5360.

Rossi, M., and Del Fattore, A. (2023). Molecular and translational research on bone tumors. *Int. J. Mol. Sci.* 24 (3), 1946. doi:10.3390/ijms24031946

Royal, I., Lamarche-Vane, N., Lamorte, L., Kaibuchi, K., and Park, M. (2000). Activation of cdc42, rac, PAK, and rho-kinase in response to hepatocyte growth factor differentially regulates epithelial cell colony spreading and dissociation. *Mol. Biol. Cell* 11 (5), 1709–1725. doi:10.1091/mbc.11.5.1709

Saxton, T. M., Ciruna, B. G., Holmyard, D., Kulkarni, S., Harpal, K., Rossant, J., et al. (2000). The SH2 tyrosine phosphatase shp2 is required for mammalian limb development. *Nat. Genet.* 24 (4), 420–423. doi:10.1038/74279

Scotlandi, K., Baldini, N., Oliviero, M., Di Renzo, M. F., Martano, M., Serra, M., et al. (1996). Expression of Met/hepatocyte growth factor receptor gene and malignant behavior of musculoskeletal tumors. *Am. J. Pathol.* 149 (4), 1209–1219.

Shaikh, A. B., Li, F., Li, M., He, B., He, X., Chen, G., et al. (2016). Present advances and future perspectives of molecular targeted therapy for osteosarcoma. *Int. J. Mol. Sci.* 17 (4), 506. doi:10.3390/ijms17040506

Sipeki, S., Bander, E., Buday, L., Farkas, G., Bácsy, E., Ways, D. K., et al. (1999). Phosphatidylinositol 3-kinase contributes to Erk1/Erk2 MAP kinase activation associated with hepatocyte growth factor-induced cell scattering. *Cell Signal* 11 (12), 885–890. doi:10.1016/s0898-6568(99)00060-1

Sun, Y., Niu, W., Du, F., Du, C., and Wang, J. (2016). Safety, pharmacokinetics, and antitumor properties of anlotinib, an oral multi-target tyrosine kinase inhibitor, in patients with advanced refractory solid tumors. *J. Hematol. Oncol.* 9 (1), 105. doi:10.1186/s13045-016-0332-8

Tang, W., Zhang, Y., Zhang, H., and Zhang, Y. (2022). Vascular niche facilitates acquired drug resistance to c-met inhibitor in originally sensitive osteosarcoma cells. *Cancers (Basel)* 14 (24), 6201. doi:10.3390/cancers14246201

Uitdehaag, J. C., de Roos, J. A. D. M., van Doornmalen, A. M., Prinsen, M. B. W., de Man, J., Tanizawa, Y., et al. (2014). Comparison of the cancer gene targeting and biochemical selectivities of all targeted kinase inhibitors approved for clinical use. *PLoS One* 9 (3), e92146. doi:10.1371/journal.pone.0092146

Wang, C., Chen, J., Cao, W., Sun, L., Sun, H., and Liu, Y. (2016). Aurora-B and HDAC synergistically regulate survival and proliferation of lymphoma cell via AKT, mTOR and Notch pathways. *Eur. J. Pharmacol.* 779, 1–7. doi:10.1016/j.ejphar.2015.11.049

Wang, G., Sun, M., Jiang, Y., Zhang, T., Sun, W., Wang, H., et al. (2019). Anlotinib, a novel small molecular tyrosine kinase inhibitor, suppresses growth and metastasis via dual blockade of VEGFR2 and MET in osteosarcoma. *Int. J. Cancer* 145 (4), 979–993. doi:10.1002/ijc.32180

Wang, K., Zhuang, Y., Liu, C., and Li, Y. (2012). Inhibition of c-Met activation sensitizes osteosarcoma cells to cisplatin via suppression of the PI3K-Akt signaling. *Arch. Biochem. Biophys.* 526 (1), 38–43. doi:10.1016/j.abb.2012.07.003

Wang, L. H., Tsai, H. C., Cheng, Y. C., Lin, C. Y., Huang, Y. L., Tsai, C. H., et al. (2017). CTGF promotes osteosarcoma angiogenesis by regulating miR-543/angiopoietin 2 signaling. *Cancer Lett.* 391, 28–37. doi:10.1016/j.canlet.2017.01.013

Wu, P. K., Chen, W. M., Chen, C. F., Lee, O. K., Haung, C. K., and Chen, T. H. (2009). Primary osteogenic sarcoma with pulmonary metastasis: clinical results and prognostic factors in 91 patients. *Jpn. J. Clin. Oncol.* 39 (8), 514–522. doi:10.1093/jjco/hyp057

Yan, J., Wang, Q., Zou, K., Wang, L., Schwartz, E. B., Fuchs, J. R., et al. (2015). Inhibition of the JAK2/STAT3 signaling pathway exerts a therapeutic effect on osteosarcoma. *Mol. Med. Rep.* 12 (1), 498–502. doi:10.3892/mmr.2015.3439

Yang, Q., Liu, J., Wu, B., Wang, X., Jiang, Y., and Zhu, D. (2022). Role of extracellular vesicles in osteosarcoma. *Int. J. Med. Sci.* 19 (8), 1216–1226. doi:10.7150/ijms.74137

Zhang, Y. W., Wang, L. M., Jove, R., and Vande Woude, G. F. (2002). Requirement of Stat3 signaling for HGF/SF-Met mediated tumorigenesis. *Oncogene* 21 (2), 217–226. doi:10.1038/sj.onc.1205004

frontiers | Frontiers in Molecular Biosciences

TYPE Review
PUBLISHED 02 September 2024
DOI 10.3389/fmolb.2024.1384795

OPEN ACCESS

EDITED BY
Tong-Chuan He,
University of Chicago Medicine, United States

REVIEWED BY
Donald Rao,
Gradalis, Inc., United States
Guo-sheng Zhao,
Chongqing Medical University, China

*CORRESPONDENCE
Zakareya Gamie,
zakareya.gamie@newcastle.ac.uk

RECEIVED 10 February 2024
ACCEPTED 14 August 2024
PUBLISHED 02 September 2024

CITATION
Gamie Z, Krippner-Heidenreich A, Gerrand C and Rankin KS (2024) Targeting Death Receptor 5 (DR5) for the imaging and treatment of primary bone and soft tissue tumors: an update of the literature. *Front. Mol. Biosci.* 11:1384795. doi: 10.3389/fmolb.2024.1384795

Targeting Death Receptor 5 (DR5) for the imaging and treatment of primary bone and soft tissue tumors: an update of the literature

Zakareya Gamie[1]*, Anja Krippner-Heidenreich[2], Craig Gerrand[3] and Kenneth Samora Rankin[1]

[1]Translational and Clinical Research Institute, Newcastle University, Newcastle upon Tyne, United Kingdom, [2]Princess Maxima Center of Pediatric Oncology, Utrecht, Netherlands, [3]Department of Orthopaedic Oncology, Royal National Orthopaedic Hospital NHS Trust, Stanmore, United Kingdom

Background: Death Receptor 5 (DR5) is expressed on the surface of primary bone and soft tissue sarcoma cells, and its activation induces cell death primarily through apoptosis. The combination of DR5 agonists and commonly used chemotherapeutic agents, such as doxorubicin, can promote cell death. Currently, clinical trials are investigating the effectiveness of DR5 activation using new biological agents, such as bi-specific or tetravalent antibodies, in improving the survival of patients with relapsed or refractory cancers. Furthermore, investigations continue into the use of novel combination therapies to enhance DR5 response, for example, with inhibitor of apoptosis protein (IAP) antagonist agents [such as the second mitochondria-derived activator of caspase (SMAC) mimetics] and with immune checkpoint inhibitor anti-programmed death-ligand 1 (anti-PD-L1) or anti-programmed cell death-1 (anti-PD-1) antibodies. Other therapies include nanoparticle-mediated delivery of TRAIL plasmid DNA or TRAIL mRNA and stem cells as a vehicle for the targeted delivery of anti-cancer agents, such as TRAIL, to the tumor.

Methods: Scoping review of the literature from November 2017 to March 2024, utilizing PubMed and Google Scholar.

Results: New agents under investigation include nanoTRAIL, anti-Kv10.1, multimeric IgM, and humanized tetravalent antibodies. Developments have been made to test novel agents, and imaging has been used to detect DR5 in preclinical models and patients. The models include 3D spheroids, genetically modified mouse models, a novel jaw osteosarcoma model, and patient-derived xenograft (PDX) animal models. There are currently two ongoing clinical trials focusing on the activation of DR5, namely, IGM-8444 and INBRX-109, which have progressed to phase 2. Further modifications of TRAIL delivery with fusion to single-chain variable fragments (scFv-TRAIL), directed against tumor-associated antigens (TAAs), and in the use of stem cells focus on targeted TRAIL delivery to cancer cells using bi-functional strategies.

Conclusion: *In vitro*, *in vivo*, and clinical trials, as well as advances in imaging and theranostics, indicate that targeting DR5 remains a valid strategy in the treatment of some relapsed and refractory cancers.

KEYWORDS

death, receptor, TRAIL, agonist, imaging, apoptosis, bone, sarcoma

Introduction

Connective tissue malignancies such as sarcoma are rare but can affect patients of all ages, have a variable but often poor prognosis, and have limited chemotherapeutic options (Bacon et al., 2023; Ducimetiere et al., 2011). They typically occur in the extremities but can also occur in a wide range of other anatomical locations, including the head and neck (e.g., maxillary and mandibular osteosarcoma). Patients, therefore, face esthetic and functional challenges that can significantly reduce their quality of life (Baumhoer et al., 2014; Cirstoiu et al., 2019). Bone and soft tissue sarcomas, in addition to some hematopoietic malignancies, such as multiple myeloma, are susceptible to TRAIL-induced apoptosis and therapy in combination with or without other chemotherapeutic options (Snajdauf et al., 2021; Subbiah et al., 2023; van der Horst et al., 2021; Trivedi and Mishra, 2015). The current understanding is that TRAIL binds to DR5/TRAILR2 more efficiently than it does to DR4/TRAILR1 through a stepwise binding mechanism (Kelley et al., 2005). However, many cancer cells are sensitive to apoptosis through both DR4 and DR5 activation (Pimentel et al., 2023a). Despite the lack of progression from phase 2 to phase 3 clinical trials of the early DR5 agonistic antibodies, TRAIL therapy remains a promising therapeutic approach, particularly as part of combination therapy (Montinaro and Walczak, 2023; Di Cristofano et al., 2023).

The mechanism of TRAIL-induced apoptosis, the transcriptional regulation, and modulation of the localization of the receptors (Min et al., 2019), and also TRAIL-mediated non-apoptotic signaling have been reviewed extensively (Gamie et al., 2017). There are promising TRAIL derivatives, such as the fusion of single-chain variable fragments (scFv-TRAIL), directed against a tumor-associated antigen (TAA) (Hutt et al., 2018). This allows for better target specificity and can be combined with other biological entities, such as immune checkpoint blockade, which is itself a potential treatment for bone and soft tissue sarcomas (Thanindratarn et al., 2019; Fazel et al., 2023). In mixed T-cell and cancer-cell culture experiments, the scFv-PD-L1:TRAIL derivative enhanced the cytotoxicity of TRAIL by exhibiting a multi-fold therapeutic effect, which includes reactivating T-cells and stimulating IFNγ production, thereby upregulating programmed death-ligand 1 (PD-L1) and sensitizing cancer cells to apoptosis by TRAIL (Hendriks et al., 2016). However, more recent experiments have shown that the knockdown or knockout of PD-L1 may sensitize certain cancer cells to TRAIL via a non-canonical mechanism (Pimentel et al., 2023b).

Improving the effectiveness of novel TRAIL agonists and derivatives and combining TRAIL with current chemotherapeutics require evidence of the protein expression of death receptors (DRs) and target antigens, immune-based stratification, and clinical trials to assess efficacy. The purpose of the current scoping review of the literature is, therefore, to provide a general overview and update on the effectiveness of therapies developed to activate DR5 for connective tissue malignancies such as sarcoma, modes of action, and models developed to test them, ongoing clinical trials, and effectiveness. A scoping review search strategy was used to assess a body of literature, clarify concepts, and identify areas for further investigation. This was performed using the following article subheadings, keywords, and index terms: Death; Receptor; TRAIL; Target; Imaging; Apoptosis; Bone; Sarcoma; Malignancy; Stem; Cell; *In vitro*; *In vivo*; Clinical; and Trial. One database (PubMed and Google Scholar) and one concept at a time were searched. Inclusion criteria were studies from 2017 to 2024; any *in vitro*, *in vivo*, or clinical studies in the English language investigating DR5 as a target for imaging or as an agonist to induce apoptosis in primary bone and soft tissue tumors; and published and unpublished work (gray literature), supplements, proceedings of meetings, or conference abstracts. There was an initial screening of titles and abstracts, followed by full manuscript reviews.

DR5 structural features and signal transduction

DR5 receptors are expressed on the cell surface, and like other members of the TNF receptor superfamily, TRAIL receptors pre-oligomerize in the absence of a ligand via their pre-ligand-binding domain (PLAD) (Chan et al., 2000). The stoichiometry of TRAIL receptor homotypic oligomerization is not fully clarified yet; however, homodimers, homotrimers, and even heterodimers of the tumor necrosis factor receptor (TNFR), including DR4 and DR5, have been described (Chan et al., 2000; Neumann et al., 2014; Richter et al., 2012). The natural ligands of DR5 are homotrimeric membrane-bound TRAIL and soluble TRAIL, the shed form of membrane-bound TRAIL (Wang Y. et al., 2021). Receptor clustering is a precisely controlled process, and its triggering has been described to involve the formation of hexagonal patterns (Scott et al., 2009). The dimerization of DR5 trimers resulting in the hexagonal structure has been previously hypothesized by studies investigating DR5 clusters on the surface of apoptotic cells (Scott et al., 2009; Martin et al., 2005; Pan et al., 2019). More recently, it has been shown that the ligand-induced dimerization/trimerization of the transmembrane domain of DR5 and other members of the TNFR superfamily, such as OX40 and TNFR2, drive higher-order ligand/receptor oligomerization and downstream signaling (Pan et al., 2019).

Unique to DRs, including TNFR1, DR3, DR4, DR5, DR6, and ectodysplasin A receptor (EDAR) and a nerve growth factor receptor

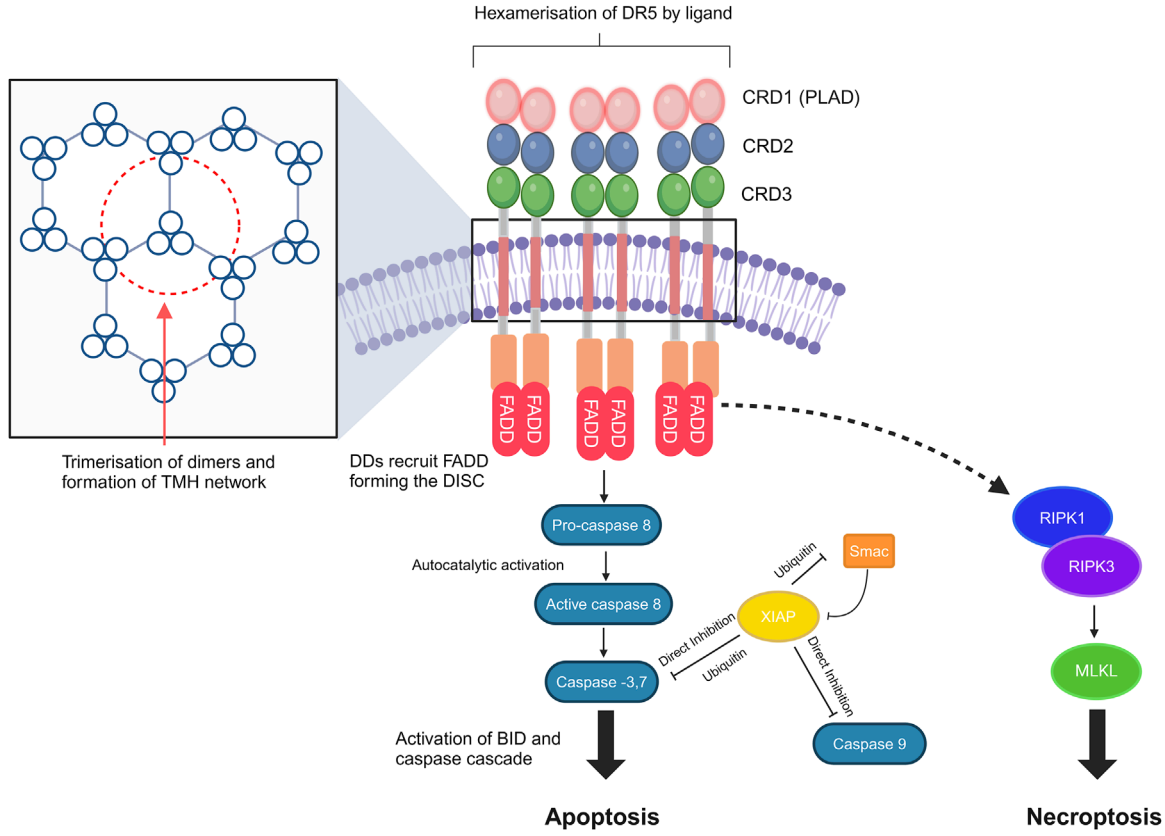

FIGURE 1
DR5 structure, clustering, and signal transduction. DR signaling leads to caspase-8 activation and cleavage of BID, resulting in mitochondrial outer-membrane permeabilization (MOMP). Transmembrane helix (THM) clustering induced by the targeted agents is required for DR5 signaling. Non-apoptotic pathways may also be activated, which result in the formation of secondary complexes and activation of necroptosis via the ripoptosome [core components are receptor-interacting serine/threonine-protein kinase 1 (RIPK1) and receptor-interacting serine/threonine-protein kinase 3 (RIPK3)]. DDs, death domains; FADD, Fas-associated death domain; DISC, death-inducing signaling complex; PLAD, pre-ligand association domain; BID, BH3-interacting-domain death agonist; XIAP, X-linked inhibitor of apoptosis protein; MLKL, mixed lineage kinase domain-like pseudokinase. The figure was created with BioRender (https://biorender.com/).

(NGFR), are the names given to the intra-cellular death domain (DD) (Green, 2022; Horiuchi et al., 2010). DDs bind to different DD-containing adapter proteins in the next step of the signaling pathway, such as the Fas-associated death domain (FADD), forming the death-inducing signaling complex (DISC), which binds to and dimerizes caspase 8, thereby activating it and cleaving BID, giving rise to mitochondrial outer-membrane permeabilization (MOMP), resulting in apoptosis (Green, 2022). Non-apoptotic pathways can also be activated, resulting in the formation of secondary complexes and activation of necroptosis via the ripoptosome and protumoral, survival, motility, and inflammatory effects via NF-kB activation (Guerrache and Micheau, 2024) (Figure 1).

DR5 expression and cancer-associated mutations of DR5

For a cell to be susceptible to apoptosis, at least one type of the two DD-containing TRAIL receptors must be expressed on the cell surface. DR4 and DR5 have been found in bone sarcomas (Ewing's sarcoma, osteosarcoma, and chondrosarcoma) and hematopoietic tumors such as myeloma, with the DR5 receptor being the most frequently expressed (Subbiah et al., 2023; Picarda et al., 2010; Surget et al., 2012; Chen et al., 2013). Further investigations are needed to better understand the expression levels and somatic mutations found in DRs and investigate how they influence signaling. In non-small-cell lung and breast cancer, most of the mutations identified to date affect the intracellular domain of DR5 (Bin et al., 2007) or heterodimerization (Neumann et al., 2014). Allelic loss has been found on chromosomes 8p21–22, where DR5 is located, in head and neck squamous cell cancer (Fisher et al., 2001) and non-Hodgkin's lymphoma (Lee et al., 2001). There may also be a dominant-negative effect where mutant DR5 can inhibit the activation of DR4 via competition for ligand binding (Bin et al., 2007). Other important mutations occur in the extracellular PLAD, which can prevent ligand binding by interfering with homotypic pre-ligand receptor oligomerization (Bin et al., 2007). Uncertainties exist in the knowledge of the prevalence and effects of these mutations in different cancer types, including bone and soft tissue tumors such as sarcomas; however, common similar mutations have been found repeatedly, resulting in an inability to properly recruit

TABLE 1 Novel DR5-targeting therapeutics developed.

DR5-activating construct	Structure/mode of action
Anti-Kv10.1 nanobody	Anti-Kv10.1 nanobody fused to single-chain TRAIL (scTRAIL). Dual-epitope targeting and enhanced hexamerization
DS-8273a	Humanized monoclonal agnostic antibody (super agonist) binding specifically to DR5 capable of receptor-enhanced multimerization
Zapadcine-1	Fully humanized antibody agonist of DR5 (zaptuzumab) linked to a toxic inhibitor of tubulin (MMAD) monomethyl auristatin D
INBRX-109	Humanized tetravalent antibody targeting DR5
ABBV-621(eftozanermin)	Hexavalent TRAIL-Fc fusion protein that activates both DR4 and DR5
IGM-8444 (aplitabart)	Multivalent IgM antibody agent targeting DR5
HexaBody-DR5/DR5	Two noncompeting DR5-specific immunoglobulin G1 (IgG1) antibodies, each carrying an E430G mutation in the Fc domain enhancing Fc–Fc interactions and hexamerization
Circularly permuted TRAIL (CPT)	A recombinant mutant of human TRAIL, which has a circularly permuted extracellular sequence of native TRAIL

the FADD (Bin et al., 2007). A study investigating osteosarcoma tumor samples and cell lines revealed mutations mainly in the DR4 gene that affect both the ligand binding and death domain regions and may be implicated in osteosarcoma pathogenesis (Dechant et al., 2004).

New biologics that target DR5

New drugs have been developed that target and achieve better activation of DR5 signaling in the last few years, following our previous review (Gamie et al., 2017). A challenge for TRAIL-based therapies is the ability to distribute and deliver TRAIL to the tumor, and combinations with nanoparticles (NPs) have also been developed to help enable this (Sadeghnezhad et al., 2019). The therapeutics are summarized in Table 1 and discussed in more detail below. Previous studies have utilized TRAIL agonists or recombinant TRAIL with mixed results in terms of progression-free survival and overall survival, which may be due to the inclusion of unselected patients (Gampa et al., 2023). Table 2 summarizes current ongoing clinical trials targeting DR4 and DR5 in orthopedic-related tumors.

Novel anti-Kv10.1 nanobody

Kv10.1 is a voltage-gated potassium channel overexpressed in cancer cells. It is considered to be a TAA, and, therefore, an anti-Kv10.1 nanobody has been produced and fused to a single-chain TRAIL (scTRAIL), named VHH-D9-scTRAIL, a development in the concept of scTNF and scTRAIL (Krippner-Heidenreich et al., 2008; Schneider et al., 2010). VHH-D9-scTRAIL has demonstrated enhanced apoptosis *in vitro* in human prostate cancer cells (DU-145), using live cell imaging and caspase assays (Hartung et al., 2020). VHH-D9-scTRAIL is based on the single-chain variant of TRAIL first described by Krippner-Heidenreich et al. (2008), with the advantage of including nanobodies to induce a strong and rapid apoptotic response in different tumor models, such as 2D culture and spheroids, involving a human prostate cancer cell line (DU-145) and a pancreatic cancer cell line (Caplan-1) and is more potent than the ScFv version. In the 3D culture model, the spheroids were monitored in the Incucyte system, and the change in size was determined by the degree of the surface occupied by green fluorescence, which was monitored as a measure of growth (Hartung et al., 2020).

DR5 agonist, DS-8273a

DS-8273a is a new generation of DR5 super-agonists capable of receptor-enhanced multimerization. Four of these multivalent targeting agents are being investigated in clinical trials studying malignant solid tumors, including sarcomas, i.e., ABBV-621, GEN 1029, INBX-109, and BI 905711. A number of these are undergoing first-in-human studies (Wang B. T. et al., 2021). The first-in-human study of the monoclonal antibody DR5 agonist DS-8273a is ongoing in patients with advanced solid tumors. DS-8273a can induce apoptosis in myeloid-derived suppressor cells (MDSCs) *ex vivo* and reduce peripheral blood numbers to levels found in healthy volunteers. Treatment is inversely correlated with the length of progression-free survival (Dominguez et al., 2017). This agent has also been investigated in combination with nivolumab (an anti-PD-1 antibody) for treating unresectable stage 3 or 4 melanoma in phase 1 clinical trials, completed in March 2024 (ClinicalTrials.gov Identifier: NCT02983006).

Zapadcine-1

Following on from the significant *in vitro* and *in vivo* efficacy of a humanized monoclonal antibody zaptuzumab in lung carcinoma, the same group demonstrated that a novel anti-DR5 antibody-drug conjugate, Zapadcine-1, possesses a high-potential therapeutic efficacy against leukemia and solid tumors (Zhang et al., 2019; Zheng et al., 2023). It is a fully-humanized agonist of DR5 (zaptuzumab) linked to a toxic inhibitor of tubulin, monomethyl auristatin D (MMAD). Zapadcine-1 was able to eliminate cancer cells in cell-derived xenografts and patient-derived xenograft (PDX) models of human lymphocytic leukemia in a dose-dependent manner and in a mouse model of lung cancer. Zapadcine-1 has an acceptable safety profile in rat and cynomolgus monkey models (Zhang et al., 2019; Zheng et al., 2023).

10.3389/fmolb.2024.1384795

TABLE 2 Clinical trials investigating DR-targeting therapeutics for primary bone tumors.

rTRAIL			DR4 targeting			DR5 targeting			DR5 targeting		
ABBV-621(eftozanermin)–hexavalent TRAIL-Fc fusion protein			Mapatumumab			INBRX-109			IGM-8444		
Cancer type	Clinical trial registration number	Phase	Cancer type	Clinical trial registration number	Phase	Cancer type	Clinical trial registration number	Phase	Cancer type	Clinical trial registration number	Phase
Advanced solid tumors and hematological malignancies	NCT03082209	Phase 1—completed	Multiple myeloma	NCT00315757	Phase 2 – completed	Solid tumors, malignant pleural mesothelioma, gastric, colorectal, sarcoma (Ewing and chondrosarcoma), and pancreatic cancer	NCT03715933	Phase 1—recruiting	Solid tumors, colorectal cancer, lymphoma (non-Hodgkin's and small lymphocytic), sarcoma (chondrosarcoma), and leukemia (chronic lymphocytic and acute)	NCT04553692	Phase 1a/1b—recruiting
Multiple myeloma	NCT04570631 - With IV or subcutaneous (SC) bortezomib and oral dexamethasone	Phase 2 - active, not recruiting				Chondrosarcoma	NCT04950075	Phase 2—recruiting			

INBRX-109

Another agent known as INBRX-109, a humanized tetravalent antibody targeting DR5, is being studied in a randomized, placebo-controlled phase 2 study in patients with unresectable and/or metastatic conventional chondrosarcoma (ClinicalTrials.gov Identifier: NCT04950075). Participants with radiological evidence of progression in the trial can be unblinded and offered crossover to the INBRX-109 agent if they have been receiving a placebo. The drug has been granted orphan drug designation. Trials were initially paused due to concerns about liver toxicity but were resumed to exclude high-risk patients. The primary endpoint is progression-free survival for over 3 years (Newton, 2023).

ABBV-621 (eftozanermin)

ABBV-621 (eftozanermin) is an engineered second-generation TRAIL agonist containing IgG1-Fc linked to a single-chain trimer of TRAIL subunits that was tested in phase 1 clinical trials (ClinicalTrials.gov Identifier: NCT03082209) in patients with previously treated solid tumors or hematological malignancies. This hexavalent TRAIL-Fc fusion protein activates both DR4 and DR5 with nanomolar affinity, inducing cell death in the COLO-205 cell line at concentrations ranging from 1 to 10 nmol/L (Phillips et al., 2021). It has been well tolerated in the first-in-human study, achieving tumor regression in colorectal cancer (LoRusso et al., 2022). However, there was a requirement for the evaluation of the expression of DR4/DR5 in fresh biopsies and the clinical response to this agent. Regarding bone tumors, it has been investigated in cell line models that have included multiple myeloma, and in combination with bortezomib, it has resulted in greater anti-tumor activity (Smith, 2020). A clinical trial on relapsed/refractory multiple myeloma patients is planned (Smith, 2020). Investigations have also demonstrated effectiveness in solid tumor colorectal cancer PDX models (Phillips et al., 2021).

IGM-8444 (aplitabart)

IGM-8444 (aplitabart) is an IgM antibody agent targeting DR5 and is a potent inducer of apoptosis, particularly when combined with a Bcl-2 inhibitor. This has been demonstrated in colorectal and lung cancer xenograft models and a gastric GXF251 PDX model without concern for hepatotoxicity (Wang B. T. et al., 2021). This agent has 10 binding sites to DR5, inducing effective multimerization (Wang B. T. et al., 2021). It can be administered i.v. and is being studied alone or in combination with relapsed, refractory, and newly diagnosed cancer patients in a randomized trial of 430 participants (ClinicalTrials.gov identifier: NCT04553692), which is still recruiting. This includes treatment in combination with birinapant [a second mitochondria-derived activator of caspase (SMAC) mimetic, which is an antagonist of the inhibitor of apoptosis (IAP) proteins] in sarcoma and venetoclax (a Bcl-2 inhibitor) in chondrosarcoma. Multimeric IGM-844 can also synergize with ABT199, a Bcl-2 inhibitor. It exhibited enhanced cytotoxicity and *in vivo,* efficacy in PDX tumor models, and no concern for increased hepatotoxicity in an investigation was noted using primary human hepatocytes. In addition, in cynomolgus monkeys, repeated IGM-844 dosing did not show a significant increase in liver enzymes compared to control (Wang B. T. et al., 2021).

HexaBody-DR5/DR5

There has been a development in dual-epitope targeting and enhanced hexamerization by DR5 antibodies as a novel approach to induce potent antitumor activity through the DR5 agonist. HexaBody-DR5/DR5 (GEN1029) has demonstrated enhanced hexamerization through the binding of two different DR5 epitopes on the cell surface (van der Horst et al., 2021). These multimeric IgM antibodies have also demonstrated effectiveness through efficient receptor clustering in gastric, skin, and squamous cell carcinomas. It has demonstrated little or no human hepatocyte cytotoxicity (Sinclair, 2021). It has been shown to work synergistically with birinapant in multiple cancer cell lines *in vitro*, including HT1080, HCT116, and NSCLC cells, and in studies of colorectal, sarcoma, and head and neck cancers (Sinclair, 2021).

HexaBody-DR5/DR5 has undergone clinical trials in solid cancers, which have been open-labeled and multi-centered. HexaBody-DR5/DR5 was developed for relapsed or refractory multiple myeloma and can induce significant cytotoxicity in primary multiple myeloma cells. It has shown potent antitumor activity in a variety of PDX models (gastric, urothelial, and colorectal cancers) in a preclinical proof-of-concept study (Overdijk et al., 2019). Recently, however, the phase 1 and expansion phase 2a studies in solid tumors were terminated due to safety concerns for unspecified reasons (NCT03576131) (Di Cristofano et al., 2023; Carter and Rajpal, 2022).

Circularly permuted TRAIL

Another therapeutic is circularly permuted TRAIL (CPT), a recombinant mutant of human TRAIL, which has a circularly permuted extracellular sequence of native TRAIL (Fang et al., 2005). It has better stability, a longer half-life, and less toxicity toward normal cells than wild-type TRAIL, and when combined with thalidomide and dexamethasone, it can prolong survival in relapsed/refractory multiple myeloma patients. It has progressed from phase 2 (Leng et al., 2017) to phase 3 clinical trials (Chen et al., 2021).

Nanoparticle-mediated delivery of TRAIL

Nanoparticle-mediated delivery of TRAIL genetic material has been utilized as a form of TRAIL gene therapy, e.g., using PEG-grafted chitosan to deliver TRAIL plasmid DNA to glioblastoma tumor cells (Wang et al., 2015). The uptake of the TRAIL plasmid-loaded nanoparticles enables the expression and liberation of TRAIL in the tumor microenvironment, thereby inducing apoptosis (Wang et al., 2015). A publication this year also detailed how TRAIL mRNA can be delivered using lipid NPs. It consists of intratumoral injection in an *in vivo* COLO-205 tumor cell study, resulting in

enhanced apoptosis and necrosis (da Silva et al., 2024). However, dosing and long-term effects require further investigation and studies in other cancer types, such as bone and soft tissue tumors.

Measures to avoid hepatotoxicity

Hepatotoxicity has been an ongoing concern regarding the use of TRAIL-related therapeutics (Gores and Kaufmann, 2001; Papadopoulos et al., 2015). There have been certain measures implemented to help reduce hepatotoxicity; for example, when using TRAIL in combination with the proteasome inhibitor bortezomib, the use of a lower concentration of bortezomib-induced apoptosis in treatment-resistant cancer cell lines (hepatoma, pancreatic, and colon) but not in primary hepatocytes by working within a specific therapeutic window (Koschny et al., 2007; Yuan et al., 2018; Diaz and Haisma, 2021). Developments have also been made to DR5 agonists using IgM antibodies, such as the multivalent agonistic antibody IGM-8444, which has demonstrated reduced cytotoxicity in primary human hepatocytes *in vitro* (Carter and Rajpal, 2022) and in cynomolgus monkeys (Wang B. T. et al., 2021). HexaBody DR5/DR5 has also demonstrated reduced human hepatocyte cytotoxicity compared to COLO-205 cells in 24-h *in vitro* cytotoxicity assays. INBRX-109 was engineered to limit hepatotoxicity by limiting its valency from 6 (hexavalent) to 4 (tetravalent) (Di Cristofano et al., 2023). It has also demonstrated reduced hepatotoxicity in preclinical studies *in vitro* and xenograft models and demonstrated favorable safety profiles in patients with unresectable/metastatic chondrosarcoma (Subbiah et al., 2023).

Animal model development

There has been a need to develop animal models to more accurately understand the progression of sarcoma and test new therapeutics. There have been cell line xenograft models, PDX models, and genetically modified mouse models produced (Yagolovich et al., 2020; Guijarro et al., 2014) with new developments, such as a dedifferentiated chondrosarcoma orthotopic mouse model (Pringle et al., 2022). In particular, for DR5 activation, a colon cancer xenograft model has been developed to assess the efficacy and pharmacokinetic profile of a DR5 ligand, a genetically modified DR5-B variant selective for DR5 (Gasparian et al., 2009), revealing dual pro-tumoral and antitumoral effects related to the concentration and mode of administration (Yagolovich et al., 2020).

For personalized therapy in sarcoma, a number of publications detailed the production of PDX models using surgical orthotopic implantation (biopsy or surgical specimen, which is frequently implanted subcutaneously) to mimic the clinical disease and be used to assess agents for treating drug-resistant osteosarcoma as monotherapy or combination therapy (Higuchi et al., 2021; Meohas et al., 2018). There have been developments in the creation of models for use in studying new therapeutics, mainly for the treatment of osteosarcoma. PDX models can be used to reproduce recurrent or recalcitrant disease and can help in studying experimental agents and drug combinations. More investigations are required using chondrosarcoma tissue to produce patient-derived chondrosarcoma models. Subcutaneous engraftment of patient tissue can fail, as reported. This is potentially due to the low aggressiveness of the tumor or a small sample size from the core biopsy (Meohas et al., 2018). This is in contrast to osteosarcoma and Ewing's sarcoma, which appear to be faithful and stable preclinical models (Guijarro et al., 2014; Nanni et al., 2019).

Osteosarcoma of the mandible has a reported 5-year survival rate of 84% with adjuvant chemotherapy (Nissanka et al., 2007). Treatment methods include wide radical resection, adjuvant chemotherapy, and radiotherapy (Bertin et al., 2020). An animal model has been developed, which can, in the future, help investigate the effectiveness of novel agents for jaw osteosarcoma (Bertin et al., 2019). It, however, requires comparative studies with models using long bones to study differences in the bone microenvironment and behavior. The cell lines engrafted were K7M2, POS-1, and MOS-J from mouse osteosarcoma, primary patient, and C57BL/6J mouse osteosarcoma origins, respectively (Bertin et al., 2019). Osteolytic lesions can be induced using these cell lines similar to those in previous paratibial models (Bertin et al., 2019). PDX models can be challenging due to the requirement of a sufficient amount of fresh tissue, and it can be challenging to achieve successful engraftment. However, they may be valuable for personalized therapies and for the small number of patients with rare cancers who are eligible for experimental therapies (Fujii et al., 2020). The benefit of genetically engineered models of osteosarcoma is the appearance of the tumor in easily accessible sites, such as long bones, compared to other models of cancer, such as abdominal tumors. A challenge has been developing models of tumor heterogeneity, spontaneous osteosarcoma, and micrometastases and monitoring their development in these models (Fujii et al., 2020). Therefore, there has been growing interest in the development of *in vivo* imaging of tumor cells, which includes bioluminescence, micro-CT, and positron emission tomography (PET) scanning (de Jong et al., 2014).

In vitro model system development

Disadvantages of animal models include cost, labor required, and prediction of drug safety (Van Norman, 2019). There has been increasing use of spheroids, organoids, and 3D cell cultures, terms used interchangeably, to try to replicate malignant tissues and microtumors (Bialkowska et al., 2020; Gunti et al., 2021). A number of methods have been described to generate them, such as the hanging drop method, which can exist as co-cultures with or without stromal cells and an extracellular matrix and better mimic tumor structure than 2D cell culture (Bialkowska et al., 2020; Gunti et al., 2021; Jensen and Teng, 2020). They have played a role in studying the chondrosarcoma microenvironment and factors such as hypoxia and pH, resistance to drug therapy, and the question of what the effect of 3D microenvironments is on susceptibility to apoptosis (Bialkowska et al., 2020). Stohr et al. (2020) found that there can be TRAIL-resistant subpopulations in spheroids generated by using HCT116 and NCI-H460 cells seeded in Terasaki multi-well plates and placed in humid chambers in the incubator (Stohr et al., 2020). They lacked DR4 and DR5 at the interface of proliferating and quiescent cells, which protect the TRAIL-sensitive cells residing in

the inner spheroid layers. This highlights the importance of studying and comparing the results from 3D as well as 2D models. This study also found that the COX-2 inhibitor, celecoxib, could upregulate DR4 and DR5 through increased ER stress (Stohr et al., 2020).

Imaging to detect DR5 cell surface levels and apoptosis induction

Imaging of solid tumors that relies on size-based criteria may be limited in assessing response; furthermore, bone scans for cancer may be limited in their sensitivity and specificity for treatment response (Cook and Goh, 2020). Imaging modalities such as PET and single-photon emission computed tomography (SPECT) can improve the diagnosis and treatment response. There have been tools developed to monitor the response to DR5 therapy, for example, *in vivo* by using fluorescence-labeled anti-DR5 with the reporter construct C-Luc-DEVD-N-Luc. Light is emitted upon the caspase-mediated cleavage of this construct and subsequent dimerization of C-Luc and N-Luc in the presence of externally supplied luciferin (Weber et al., 2014; Weber et al., 2013). In addition to DR5 being utilized as a potential imaging marker (Wang S. et al., 2021), PET has been used in combination with F18-duramycin to assess the response to DR5 agonists and early apoptosis in humans. Duramycin is a 19-amino acid peptide that can detect apoptosis by targeting and binding to phosphatidylethanolamine (PE) and phosphatidylserine (PS), which are expressed in the early stages of apoptosis (Cook and Goh, 2020; Li et al., 2019; Zhao et al., 2008). In preliminary data, using micro-PET and micro-CT scanning, the colorectal cancer cell line COLO-205 was injected into the shoulder of mice and found to be more drug-sensitive when using bioluminescence imaging (BLI), i.e., it was targeted more efficiently by duramycin, indicating greater apoptosis induction by the DR5 agonist agent AMG655 (Zhang et al., 2019; Kim et al., 2012).

The 177Lu or 89Zr radio-labeled anti-DR5 antibody CTB006 (89Zr-CTB006) PET/CT has been useful for screening cancers with DR5 overexpression, such as gastrointestinal cancer (Wang S. et al., 2021). Similar studies are required for bone and soft tissue tumors. Reduced DR5 expression may explain the poor response to DR5 agonists in clinical trials. Using this technology can help identify patients who may benefit from DR5 agonist therapy in a non-invasive manner. The inability to achieve the endpoint in previous trials may be due to the inability to accurately quantify the degree of DR5 expression in immunohistochemistry (IHC). DR5 expression was lower than that previously reported and requires further investigation. 89Zr-CTB006 PET/CT has also been able to detect DR5 levels in PDX mouse models with RNAscope scores of 3 and 4, which is a method to detect specific gene expression that is more sensitive and specific than IHC methods (Wang S. et al., 2021).

Furthermore, 89Zr-DS-8273a is being investigated as a theranostic agent for anti-DR5 cancer therapy (Burvenich et al., 2016). A theranostic agent is one that is both diagnostic and therapeutic; for example, the agent can bind to DR5-expressing cells in COLO cell line xenografts and is a novel PET imaging reagent in human bioimaging (Burvenich et al., 2016). Therefore, it can monitor both the response to therapies and doses required (Burvenich et al., 2016) (Figure 2).

Combination therapy using IAP antagonists

IAP antagonists can inhibit the caspase-inhibitory function of XIAP and also the cellular IAPs, cIAP1, and cIAP2, thereby enhancing apoptosis (Fulda, 2008). In solid tumor xenograft models using, for example, the breast cancer cell lines MDA-MB-231 and 2LMP TNBC, anti-tumor activity was demonstrated when the DR5 monoclonal antibody, CTB-006, was used together with the IAP antagonist APG-1387 (Li et al., 2021). Phase 1 dose-escalation studies have demonstrated the tolerability of IAP antagonists in the treatment of advanced solid tumors, such as breast cancer and lymphoma, in combination with pembrolizumab (Rasco et al., 2020). Phase I/II clinical trials for head and neck cancers have shown promising results (Kansal et al., 2023). Strong anti-tumor activity has been demonstrated with the combination of anti-DR5 agonist IGM-8444 with the SMAC mimetic, birinapant, in preclinical models using a range of cell lines and PDX models, including sarcoma; for example, 7/9 animals were tumor-free in a model using the HT1080 cell line (Wang et al., 2022), which has also been used to model dedifferentiated chondrosarcoma (Pringle et al., 2022). The same combination of anti-DR5 agonist IGM-8444 with birinapant is taking place for relapsed, refractory, or newly diagnosed cancers, which include soft tissue sarcoma and chondrosarcoma, in a phase 1a/1b study (ClinicalTrials.gov identifier: NCT04553692) and is still recruiting.

Stem cells expressing TRAIL for cancer treatment

The use of stem cells that can migrate to tumors and deliver therapeutic agents has expanded the options available for cancer therapy and skeletal tissue regeneration (Fakiruddin et al., 2018; Gamie et al., 2012; Kamalabadi-Farahani et al., 2018). They can also be genetically engineered to overexpress the TRAIL ligand (Stamatopoulos et al., 2019). The metastatic tumor burden has been found to decrease with the administration of human mesenchymal stem cells (MSCs) expressing TRAIL in a pulmonary metastasis model (Loebinger et al., 2009). Since these early findings, developments have been made in terms of how stem cells can be used to express TRAIL to induce apoptosis in cancer. Human bone marrow-derived MSCs (BMMSCs) have been used previously to deliver membrane-bound TRAIL (either genetically or via TNF-α pre-activation) to breast cancer cells in an animal model and successfully induce apoptosis and reduce the tumor signal. The use of BMMSCs as a mode of delivery for therapeutic agents has been decreasing (Patrick et al., 2020), and other stem cell types have been utilized, such as those easier to obtain, such as umbilical cord-derived stem cells and human placenta-derived MSCs (Aldoghachi et al., 2023). More recently, human placenta-derived MSCs with curcumin-loaded chitosan particles have been utilized as a tumor-tropic therapy (Xu et al., 2019). Curcumin is reported to be a chemopreventive agent for oral squamous cell cancer (Maulina et al., 2019). MSCs expressing TRAIL have been studied *in vitro* and in mouse models of breast cancer with promising effects (Loebinger et al., 2009). MSCs have the ability to reside or engraft preferentially in tumors and their micrometastases and are

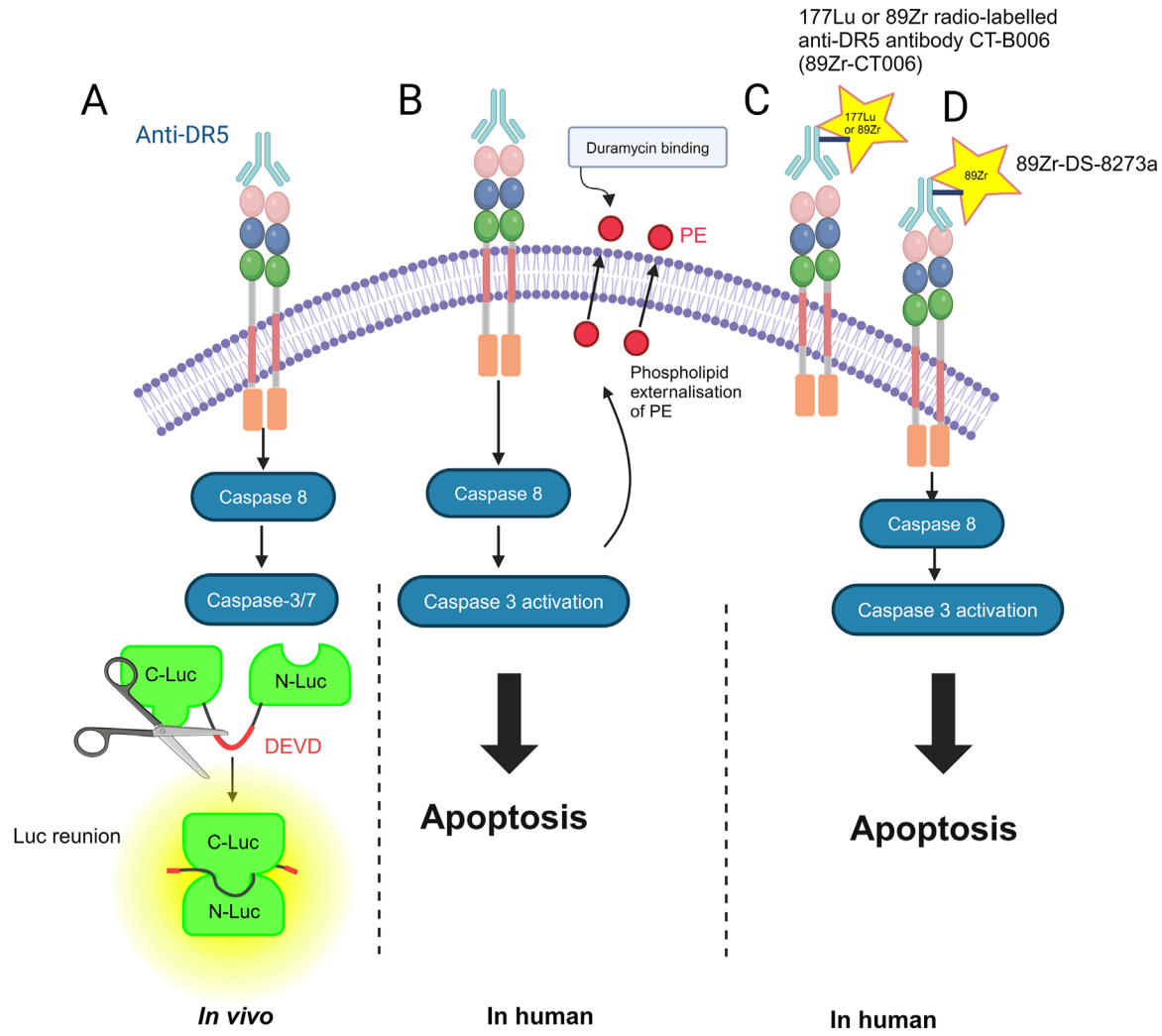

FIGURE 2
Methods for imaging DR5 and its cell death-inducing activity: **(A)** *in vivo* by using fluorescence-labeled anti-DR5 with the reporter construct C-Luc-DEVD-N-Luc. N-terminal (N-Luc) and C-terminal (C-Luc) (Weber et al., 2013). **(B)** In humans, duramycin, a 19-amino acid peptide that can detect apoptosis by targeting and binding to phosphatidylethanolamine (PE) (Li et al., 2019). **(C)** 177Lu or 89Zr radio-labeled anti-DR5 antibody CTB006 (89Zr-CTB006) (Wang S. et al., 2021). **(D)** 89Zr-DS-8273a is also being investigated as a theranostic for anti-DR5 cancer therapy (Burvenich et al., 2016). The figure was created with BioRender (https://biorender.com/).

an ideal candidate to deliver antineoplastic agents to the tumor site (Loebinger et al., 2009). Another agent investigated that upregulates DR5 is chrysanthemulide A (CA), which has been shown to induce apoptosis in osteosarcoma cells via JNK-mediated autophagosome accumulation (Zhuo et al., 2019).

MSCs can kill cancer cells *in vitro* and *in vivo,* and with sensitizing agents such as small-molecule inhibitors, TRAIL alone, or delivered with MSCs, the vehicle sensitizing agent can be enhanced (Fakiruddin et al., 2018). Stem cells engineered to express TRAIL can kill glioblastoma cells or hepatocellular carcinoma cells *in vitro*. Studies are ongoing utilizing this approach for the treatment of lung cancer (Patrick et al., 2020). The lung delivery of these umbilical cord-derived MSCs can be visualized using PET-CT in a novel study that uses 89Zr-oxine labeling to help evaluate the biodistribution of the MSCs and the amount migrating to the lungs (Patrick et al., 2020).

An ongoing trial known as TACTICAL is a multi-centered, randomized, double-blinded trial assessing the efficacy of MSC-TRAIL for lung adenocarcinoma, which combines the first-line standard-of-care chemotherapeutic agents, including pembrolizumab, with MSC-TRAIL, generated by transducing MSCs with a lentiviral vector to express TRAIL (ClinicalTrials.gov Identifier: NCT03298763) (Davies et al., 2019). It contains a first-in-man ^{89}Zr-oxine cell-labeling arm to help obtain a better understanding of cell-based therapies. It is currently still recruiting patients, with an estimated study completion time of 1 September 2025 (Davies et al., 2019). If the trial is successful, it will add further confidence to the use of allogenic stem cell therapy for cancer.

Further modifications of TRAIL delivery and the use of stem cells to enhance the efficacy of MSC-TRAIL have involved modifications to target TRAIL delivery to cancer cells expressing

specific antigens as part of a bi-functional strategy. TRAIL has been combined with a truncated anti-GD2 chimeric antigen receptor (GD2 tCAR) and delivered by MSCs in a novel strategy against metastatic Ewing's sarcoma, demonstrating affinity and killing of lesions in the lung but not in the liver (Golinelli et al., 2022).

Research also continues into the pre-activation of stem cells using TNF-α to stimulate the expression of TRAIL in a bioactive membrane-bound form on the surface of the cell. Recently, it has been shown that dental tissues such as the periodontal ligament contain stem cells that have the main properties of MSCs, which can be expanded *ex vivo* (Di et al., 2023) and were found to express TRAIL at the protein and RNA levels when pre-activated using TNF-α. The stem cells migrated toward cancer cells when co-cultured with primary head and neck squamous cell carcinoma cells and induced apoptosis (Di et al., 2023). Further studies will require the comparison of different stem cell sources for TNF-α pre-activation and induction of apoptosis, biodistribution, and appropriate delivery of sufficient amounts to tumor sites (Ohara et al., 2024).

Conclusions and future directions

Targeting DR5 remains a promising approach to help induce cell death by apoptosis or necroptosis (in combination with agents such as the SMAC mimetic birinapant) in the cancer cells of difficult-to-treat malignancies such as sarcoma. TRAIL therapeutics have had limited therapeutic efficacy and progress to phase 2 trials; however, the development of novel drugs and combination therapies allows for progress and advancements to phase 3 trials (Schneider et al., 2010). The remaining challenges include identifying patients with high levels of expression of DR5 and further study in 3D models, such as organoids, where resistant cells may limit the killing capabilities of the agent. Further investigation into the development of PDX mouse models that can help replicate tumor growth, local invasion, and metastatic potential, is needed. Ongoing phase 2 trials will demonstrate whether the strategies used in promising *in vivo* studies, utilizing antibodies that have superseded the early agonistic antibodies that had a weak ability to induce receptor multimerization, can be replicated in patients. Advancements in nanotechnology and nanoparticle-mediated TRAIL delivery, as well as MSC-mediated TRAIL delivery, have also proved to be successful *in vitro* and in preclinical animal models (Sadeghnezhad et al., 2019; Gampa et al., 2023; Aldoghachi et al., 2023). The progress in imaging strategies for the detection of DR5 levels and the potential to combine this with enhanced triggering of DR5 activity warrant further investigation as a strategy with standard-of-care chemotherapeutic agents, in particular in the difficult-to-treat malignancies, to enhance cytotoxicity and improve survival.

Author contributions

ZG: conceptualization, writing–original draft, and writing–review and editing. AK-H: formal analysis, investigation, methodology, supervision, validation, and writing–review and editing. CG: formal analysis, investigation, supervision, validation, and writing–review and editing. KR: formal analysis, investigation, methodology, supervision, validation, and writing–review and editing.

Funding

The author(s) declare that no financial support was received for the research, authorship, and/or publication of this article.

Acknowledgments

The authors thank Emane Gamie for creating the figures using BioRender software (https://biorender.com/).

Conflict of interest

The authors declare that the research was conducted in the absence of any commercial or financial relationships that could be construed as a potential conflict of interest.

Publisher's note

References

Aldoghachi, A. F., Chong, Z. X., Yeap, S. K., Cheong, S. K., Ho, W. Y., and Ong, A. H. K. (2023). Stem cells for cancer therapy: translating the uncertainties and possibilities of stem cell properties into opportunities for effective cancer therapy. *Int. J. Mol. Sci.* 24, 1012. doi:10.3390/ijms24021012

Bacon, A., Wong, K., Fernando, M. S., Rous, B., Hill, R. J. W., Collins, S. D., et al. (2023). Incidence and survival of soft tissue sarcoma in england between 2013 and 2017, an analysis from the national cancer registration and analysis service. *Int. J. Cancer* 152, 1789–1803. doi:10.1002/ijc.34409

Baumhoer, D., Brunner, P., Eppenberger-Castori, S., Smida, J., Nathrath, M., and Jundt, G. (2014). Osteosarcomas of the jaws differ from their peripheral counterparts and require a distinct treatment approach. Experiences from the DOESAK Registry. *Oral Oncol.* 50, 147–153. doi:10.1016/j.oraloncology.2013.10.017

Bertin, H., Gomez-Brouchet, A., and Redini, F. (2020). Osteosarcoma of the jaws: an overview of the pathophysiological mechanisms. *Crit. Rev. Oncol. Hematol.* 156, 103126. doi:10.1016/j.critrevonc.2020.103126

Bertin, H., Guilho, R., Brion, R., Amiaud, J., Battaglia, S., Moreau, A., et al. (2019). Jaw osteosarcoma models in mice: first description. *J. Transl. Med.* 17, 56. doi:10.1186/s12967-019-1807-5

Bialkowska, K., Komorowski, P., Bryszewska, M., and Milowska, K. (2020). Spheroids as a type of three-dimensional cell cultures-examples of methods of preparation and the most important application. *Int. J. Mol. Sci.* 21, 6225. doi:10.3390/ijms21176225

Bin, L., Thorburn, J., Thomas, L. R., Clark, P. E., Humphreys, R., and Thorburn, A. (2007). Tumor-derived mutations in the TRAIL receptor DR5 inhibit TRAIL signaling

through the DR4 receptor by competing for ligand binding. *J. Biol. Chem.* 282, 28189–28194. doi:10.1074/jbc.M704210200

Burvenich, I. J., Lee, F. T., Guo, N., Gan, H. K., Rigopoulos, A., Parslow, A. C., et al. (2016). *In vitro* and *in vivo* evaluation of (89)Zr-DS-8273a as a theranostic for anti-death receptor 5 therapy. *Theranostics* 6, 2225–2234. doi:10.7150/thno.16260

Carter, P. J., and Rajpal, A. (2022). Designing antibodies as therapeutics. *Cell* 185, 2789–2805. doi:10.1016/j.cell.2022.05.029

Chan, F. K., Chun, H. J., Zheng, L., Siegel, R. M., Bui, K. L., and Lenardo, M. J. (2000). A domain in TNF receptors that mediates ligand-independent receptor assembly and signaling. *Science* 288, 2351–2354. doi:10.1126/science.288.5475.2351

Chen, J. J., Mikelis, C. M., Zhang, Y., Gutkind, J. S., and Zhang, B. (2013). TRAIL induces apoptosis in oral squamous carcinoma cells–a crosstalk with oncogenic Ras regulated cell surface expression of death receptor 5. *Oncotarget* 4, 206–217. doi:10.18632/oncotarget.813

Chen, W., Xia, Z., Fang, B., Fu, C., Li, W., Yang, L., et al. (2021). P-192: Circularly permuted TRAIL (CPT) combined with Thalidomide and Dexamethasone in patients with relapsed/refractory Multiple Myeloma: a randomized, double-blind, placebo-controlled phase 3 study. *Clin. Lymphoma Myeloma Leukemia* 21, S143. doi:10.1016/s2152-2650(21)02319-3

Cilinical Trials.gov (2018). Available at: https://classic.clinicaltrials.gov/ct2/show/NCT02983006

Cirstoiu, C., Cretu, B., Serban, B., Panti, Z., and Nica, M. (2019). Current review of surgical management options for extremity bone sarcomas. *EFORT Open Rev.* 4, 174–182. doi:10.1302/2058-5241.4.180048

Cook, G. J. R., and Goh, V. (2020). Molecular imaging of bone metastases and their response to therapy. *J. Nucl. Med.* 61, 799–806. doi:10.2967/jnumed.119.234260

da Silva, W. N., Carvalho Costa, P. A., Scalzo Junior, S. R. A., Ferreira, H. A. S., Prazeres, P., Campos, C. L. V., et al. (2024). Ionizable lipid nanoparticle-mediated TRAIL mRNA delivery in the tumor microenvironment to inhibit colon cancer progression. *Int. J. Nanomedicine* 19, 2655–2673. doi:10.2147/IJN.S452896

Davies, A., Sage, B., Kolluri, K., Alrifai, D., Graham, R., Weil, B., et al. (2019). TACTICAL: a phase I/II trial to assess the safety and efficacy of MSCTRAIL in the treatment of metastatic lung adenocarcinoma. *TACTICAL A phase I/II trial assess Saf. efficacy MSCTRAIL Treat. metastatic lung adenocarcinoma* 37, TPS9116. doi:10.1200/JCO.2019.37.15_suppl.TPS9116

Dechant, M. J., Fellenberg, J., Scheuerpflug, C. G., Ewerbeck, V., and Debatin, K. M. (2004). Mutation analysis of the apoptotic "death-receptors" and the adaptors TRADD and FADD/MORT-1 in osteosarcoma tumor samples and osteosarcoma cell lines. *Int. J. Cancer* 109, 661–667. doi:10.1002/ijc.20008

de Jong, M., Essers, J., and van Weerden, W. M. (2014). Imaging preclinical tumour models: improving translational power. *Nat. Rev. Cancer* 14, 481–493. doi:10.1038/nrc3751

Di, V. A., Bria, J., Antonelli, A., Mesuraca, M., Barni, T., Giudice, A., et al. (2023). A review of novel strategies for human periodontal ligament stem cell *ex vivo* expansion: are they an evidence-based promise for regenerative periodontal therapy? *Int. J. Mol. Sci.* 24, 7798. doi:10.3390/ijms24097798

Diaz, A. O. A., and Haisma, H. J. (2021). Apoptosis-inducing TNF superfamily ligands for cancer therapy. *Cancers (Basel)* 13, 1543. doi:10.3390/cancers13071543

Di Cristofano, F., George, A., Tajiknia, V., Ghandali, M., Wu, L., Zhang, Y., et al. (2023). Therapeutic targeting of TRAIL death receptors. *Biochem. Soc. Trans.* 51, 57–70. doi:10.1042/BST20220098

Dominguez, G. A., Condamine, T., Mony, S., Hashimoto, A., Wang, F., Liu, Q., et al. (2017). Selective targeting of myeloid-derived suppressor cells in cancer patients using DS-8273a, an agonistic TRAIL-R2 antibody. *Clin. Cancer Res.* 23, 2942–2950. doi:10.1158/1078-0432.CCR-16-1784

Ducimetiere, F., Lurkin, A., Ranchere-Vince, D., Decouvelaere, A. V., Peoc'h, M., Istier, L., et al. (2011). Incidence of sarcoma histotypes and molecular subtypes in a prospective epidemiological study with central pathology review and molecular testing. *PLoS One* 6, e20294. doi:10.1371/journal.pone.0020294

Fakiruddin, K. S., Ghazalli, N., Lim, M. N., Zakaria, Z., and Abdullah, S. (2018). Mesenchymal stem cell expressing TRAIL as targeted therapy against sensitised tumour. *Int. J. Mol. Sci.* 19, 2188. doi:10.3390/ijms19082188

Fang, F., Wang, A. P., and Yang, S. F. (2005). Antitumor activity of a novel recombinant mutant human tumor necrosis factor-related apoptosis-inducing ligand. *Acta Pharmacol. Sin.* 26, 1373–1381. doi:10.1111/j.1745-7254.2005.00206.x

Fazel, M., Dufresne, A., Vanacker, H., Waissi, W., Blay, J. Y., and Brahmi, M. (2023). Immunotherapy for soft tissue sarcomas: anti-PD1/PDL1 and beyond. *Cancers (Basel)* 15, 1643. doi:10.3390/cancers15061643

Fisher, M. J., Virmani, A. K., Wu, L., Aplenc, R., Harper, J. C., Powell, S. M., et al. (2001). Nucleotide substitution in the ectodomain of trail receptor DR4 is associated with lung cancer and head and neck cancer. *Clin. Cancer Res.* 7, 1688–1697.

Fujii, E., Kato, A., and Suzuki, M. (2020). Patient-derived xenograft (PDX) models: characteristics and points to consider for the process of establishment. *J. Toxicol. Pathol.* 33, 153–160. doi:10.1293/tox.2020-0007

Fulda, S. (2008). Targeting inhibitor of apoptosis proteins (IAPs) for cancer therapy. *Anticancer Agents Med. Chem.* 8, 533–539. doi:10.2174/187152008784533107

Gamie, Z., Kapriniotis, K., Papanikolaou, D., Haagensen, E., Da Conceicao Ribeiro, R., Dalgarno, K., et al. (2017). TNF-related apoptosis-inducing ligand (TRAIL) for bone sarcoma treatment: pre-clinical and clinical data. *Cancer Lett.* 409, 66–80. doi:10.1016/j.canlet.2017.08.036

Gamie, Z., Tran, G. T., Vyzas, G., Korres, N., Heliotis, M., Mantalaris, A., et al. (2012). Stem cells combined with bone graft substitutes in skeletal tissue engineering. *Expert Opin. Biol. Ther.* 12, 713–729. doi:10.1517/14712598.2012.679652

Gampa, S. C., Garimella, S. V., and Pandrangi, S. (2023). Nano-TRAIL: a promising path to cancer therapy. *Cancer Drug Resist* 6, 78–102. doi:10.20517/cdr.2022.82

Gasparian, M. E., Chernyak, B. V., Dolgikh, D. A., Yagolovich, A. V., Popova, E. N., Sycheva, A. M., et al. (2009). Generation of new TRAIL mutants DR5-A and DR5-B with improved selectivity to death receptor 5. *Apoptosis* 14, 778–787. doi:10.1007/s10495-009-0349-3

Golinelli, G., Grisendi, G., Dall'Ora, M., Casari, G., Spano, C., Talami, R., et al. (2022). Anti-GD2 CAR MSCs against metastatic Ewing's sarcoma. *Transl. Oncol.* 15, 101240. doi:10.1016/j.tranon.2021.101240

Gores, G. J., and Kaufmann, S. H. (2001). Is TRAIL hepatotoxic? *Hepatology* 34, 3–6. doi:10.1053/jhep.2001.25173

Green, D. R. (2022). The death receptor pathway of apoptosis. *Cold Spring Harb. Perspect. Biol.* 14, a041053. doi:10.1101/cshperspect.a041053

Guerrache, A., and Micheau, O. (2024). TNF-related apoptosis-inducing ligand: non-apoptotic signalling. *Cells* 13, 521. doi:10.3390/cells13060521

Guijarro, M. V., Ghivizzani, S. C., and Gibbs, C. P. (2014). Animal models in osteosarcoma. *Front. Oncol.* 4, 189. doi:10.3389/fonc.2014.00189

Gunti, S., Hoke, A. T. K., Vu, K. P., and London, N. R., Jr. (2021). Organoid and spheroid tumor models: techniques and applications. *Cancers (Basel)* 13, 874. doi:10.3390/cancers13040874

Hartung, F., Kruwel, T., Shi, X., Pfizenmaier, K., Kontermann, R., Chames, P., et al. (2020). A novel anti-kv10.1 nanobody fused to single-chain TRAIL enhances apoptosis induction in cancer cells. *Front. Pharmacol.* 11, 686. doi:10.3389/fphar.2020.00686

Hendriks, D., He, Y., Koopmans, I., Wiersma, V. R., van Ginkel, R. J., Samplonius, D. F., et al. (2016). Programmed Death Ligand 1 (PD-L1)-targeted TRAIL combines PD-L1-mediated checkpoint inhibition with TRAIL-mediated apoptosis induction. *Oncoimmunology* 5, e1202390. doi:10.1080/2162402X.2016.1202390

Higuchi, T., Igarashi, K., Yamamoto, N., Hayashi, K., Kimura, H., Miwa, S., et al. (2021). Osteosarcoma patient-derived orthotopic xenograft (pdox) models used to identify novel and effective therapeutics: a review. *Anticancer Res.* 41, 5865–5871. doi:10.21873/anticanres.15406

Horiuchi, T., Mitoma, H., Harashima, S., Tsukamoto, H., and Shimoda, T. (2010). Transmembrane TNF-alpha: structure, function and interaction with anti-TNF agents. *Rheumatol. Oxf.* 49, 1215–1228. doi:10.1093/rheumatology/keq031

Hutt, M., Fellermeier-Kopf, S., Seifert, O., Schmitt, L. C., Pfizenmaier, K., and Kontermann, R. E. (2018). Targeting scFv-Fc-scTRAIL fusion proteins to tumor cells. *Oncotarget* 9, 11322–11335. doi:10.18632/oncotarget.24379

Jensen, C., and Teng, Y. (2020). Is it time to start transitioning from 2D to 3D cell culture? *Front. Mol. Biosci.* 7, 33. doi:10.3389/fmolb.2020.00033

Kamalabadi-Farahani, M., Vasei, M., Ahmadbeigi, N., Ebrahimi-Barough, S., Soleimani, M., and Roozafzoon, R. (2018). Anti-tumour effects of TRAIL-expressing human placental derived mesenchymal stem cells with curcumin-loaded chitosan nanoparticles in a mice model of triple negative breast cancer. *Artif. Cells Nanomed Biotechnol.* 46, S1011-S1021–S1021. doi:10.1080/21691401.2018.1527345

Kansal, V., Kinney, B. L. C., Uppada, S., Saba, N. F., Stokes, W. A., Buchwald, Z. S., et al. (2023). The expanding role of IAP antagonists for the treatment of head and neck cancer. *Cancer Med.* 12, 13958–13965. doi:10.1002/cam4.6011

Kelley, R. F., Totpal, K., Lindstrom, S. H., Mathieu, M., Billeci, K., Deforge, L., et al. (2005). Receptor-selective mutants of apoptosis-inducing ligand 2/tumor necrosis factor-related apoptosis-inducing ligand reveal a greater contribution of death receptor (DR) 5 than DR4 to apoptosis signaling. *J. Biol. Chem.* 280, 2205–2212. doi:10.1074/jbc.M410660200

Kim, H., Zhai, G., Samuel, S. L., Rigell, C. J., Umphrey, H. R., Rana, S., et al. (2012). Dual combination therapy targeting DR5 and EMMPRIN in pancreatic adenocarcinoma. *Mol. Cancer Ther.* 11, 405–415. doi:10.1158/1535-7163.MCT-11-0581

Koschny, R., Ganten, T. M., Sykora, J., Haas, T. L., Sprick, M. R., Kolb, A., et al. (2007). TRAIL/bortezomib cotreatment is potentially hepatotoxic but induces cancer-specific apoptosis within a therapeutic window. *Hepatology* 45, 649–658. doi:10.1002/hep.21555

Krippner-Heidenreich, A., Grunwald, I., Zimmermann, G., Kuhnle, M., Gerspach, J., Sterns, T., et al. (2008). Single-chain TNF, a TNF derivative with enhanced stability and antitumoral activity. *J. Immunol.* 180, 8176–8183. doi:10.4049/jimmunol.180.12.8176

Lee, S. H., Shin, M. S., Kim, H. S., Lee, H. K., Park, W. S., Kim, S. Y., et al. (2001). Somatic mutations of TRAIL-receptor 1 and TRAIL-receptor 2 genes in non-Hodgkin's lymphoma. *Oncogene* 20, 399–403. doi:10.1038/sj.onc.1204103

Leng, Y., Hou, J., Jin, J., Zhang, M., Ke, X., Jiang, B., et al. (2017). Circularly permuted TRAIL plus thalidomide and dexamethasone versus thalidomide and dexamethasone for relapsed/refractory multiple myeloma: a phase 2 study. *Cancer Chemother. Pharmacol.* 79, 1141–1149. doi:10.1007/s00280-017-3310-0

Li, J., Gray, B. D., Pak, K. Y., and Ng, C. K. (2019). Targeting phosphatidylethanolamine and phosphatidylserine for imaging apoptosis in cancer. *Nucl. Med. Biol.* 78-79, 23–30. doi:10.1016/j.nucmedbio.2019.10.002

Li, Q., Fang, D. D., Li, Z., Yang, D., Cao, F., and Zhai, Y. (2021). Abstract 1924: therapeutic potential of inhibitor of apoptosis protein (IAP) inhibitor APG-1387 combined with DR5 agonist monoclonal antibody (mAb) CTB-006 in preclinical models of solid tumors. *Cancer Res.* 81, 1924. doi:10.1158/1538-7445.AM2021-1924

Loebinger, M. R., Eddaoudi, A., Davies, D., and Janes, S. M. (2009). Mesenchymal stem cell delivery of TRAIL can eliminate metastatic cancer. *Cancer Res.* 69, 4134–4142. doi:10.1158/0008-5472.CAN-08-4698

LoRusso, P., Ratain, M. J., Doi, T., Rasco, D. W., de Jonge, M. J. A., Moreno, V., et al. (2022). Eftozanermin alfa (ABBV-621) monotherapy in patients with previously treated solid tumors: findings of a phase 1, first-in-human study. *Invest New Drugs* 40, 762–772. doi:10.1007/s10637-022-01247-1

Martin, S., Phillips, D. C., Szekely-Szucs, K., Elghazi, L., Desmots, F., and Houghton, J. A. (2005). Cyclooxygenase-2 inhibition sensitizes human colon carcinoma cells to TRAIL-induced apoptosis through clustering of DR5 and concentrating death-inducing signaling complex components into ceramide-enriched caveolae. *Cancer Res.* 65, 11447–11458. doi:10.1158/0008-5472.CAN-05-1494

Maulina, T., Widayanti, R., Hardianto, A., Sjamsudin, E., Pontjo, B., and Yusuf, H. Y. (2019). The usage of curcumin as chemopreventive agent for oral squamous cell carcinoma: an experimental study on sprague-dawley rat. *Integr. Cancer Ther.* 18, 1534735418822094. doi:10.1177/1534735418822094

Meohas, W., Granato, R. A., Guimaraes, J. A. M., Dias, R. B., Fortuna-Costa, A., and Duarte, M. E. L. (2018). Patient-derived xenografts as a preclinical model for bone sarcomas. *Acta Ortop. Bras.* 26, 98–102. doi:10.1590/1413-785220182602186998

Min, K. J., Woo, S. M., Shahriyar, S. A., and Kwon, T. K. (2019). Elucidation for modulation of death receptor (DR) 5 to strengthen apoptotic signals in cancer cells. *Arch. Pharm. Res.* 42, 88–100. doi:10.1007/s12272-018-01103-y

Montinaro, A., and Walczak, H. (2023). Harnessing TRAIL-induced cell death for cancer therapy: a long walk with thrilling discoveries. *Cell Death Differ.* 30, 237–249. doi:10.1038/s41418-022-01059-z

Nanni, P., Landuzzi, L., Manara, M. C., Righi, A., Nicoletti, G., Cristalli, C., et al. (2019). Bone sarcoma patient-derived xenografts are faithful and stable preclinical models for molecular and therapeutic investigations. *Sci. Rep.* 9, 12174. doi:10.1038/s41598-019-48634-y

Neumann, S., Hasenauer, J., Pollak, N., and Scheurich, P. (2014). Dominant negative effects of tumor necrosis factor (TNF)-related apoptosis-inducing ligand (TRAIL) receptor 4 on TRAIL receptor 1 signaling by formation of heteromeric complexes. *J. Biol. Chem.* 289, 16576–16587. doi:10.1074/jbc.M114.559468

Newton, W. (2023). Available at: https://www.clinicaltrialsarena.com/news/news-inhbirx-fda-lifts-partial-hold-chondrosarcoma/.

Nissanka, E. H., Amaratunge, E. A., and Tilakaratne, W. M. (2007). Clinicopathological analysis of osteosarcoma of jaw bones. *Oral Dis.* 13, 82–87. doi:10.1111/j.1601-0825.2006.01251.x

Ohara, G., Okabe, K., Toyama, N., Ohta, Y., Song, X., Tsuboi, M., et al. (2024). Stem cell therapy based on human periodontal ligament stem cells preactivated with TNF-α as for human head and neck squamous cell carcinoma. *J. Oral Maxillofac. Surg. Med. Pathology* 36, 217–226. doi:10.1016/j.ajoms.2023.08.006

Overdijk, M. B., Cecchini, M., Strumane, K., Brandhorst, M., Lingnau, A., Parren, P. W. H. I., et al. (2019). Abstract C025: HexaBody-DR5/DR5 (GEN1029) shows potent preclinical antitumor activity in a variety of patient-derived xenograft (PDX) tumor models. *Mol. Cancer Ther.* 18, C025. doi:10.1158/1535-7163.TARG-19-C025

Pan, L., Fu, T. M., Zhao, W., Zhao, L., Chen, W., Qiu, C., et al. (2019). Higher-order clustering of the transmembrane anchor of DR5 drives signaling. *Cell* 176, 1477–1489. doi:10.1016/j.cell.2019.02.001

Papadopoulos, K. P., Isaacs, R., Bilic, S., Kentsch, K., Huet, H. A., Hofmann, M., et al. (2015). Unexpected hepatotoxicity in a phase I study of TAS266, a novel tetravalent agonistic Nanobody®targeting the DR5 receptor. *Cancer Chemother. Pharmacol.* 75, 887–895. doi:10.1007/s00280-015-2712-0

Patrick, P. S., Kolluri, K. K., Zaw, T. M., Edwards, A., Sage, E. K., Sanderson, T., et al. (2020). Lung delivery of MSCs expressing anti-cancer protein TRAIL visualised with (89)Zr-oxine PET-CT. *Stem Cell Res. Ther.* 11, 256. doi:10.1186/s13287-020-01770-z

Phillips, D. C., Buchanan, F. G., Cheng, D., Solomon, L. R., Xiao, Y., Xue, J., et al. (2021). Hexavalent TRAIL fusion protein eftozanermin alfa optimally clusters apoptosis-inducing TRAIL receptors to induce on-target antitumor activity in solid tumors. *Cancer Res.* 81, 3402–3414. doi:10.1158/0008-5472.CAN-20-2178

Picarda, G., Lamoureux, F., Geffroy, L., Delepine, P., Montier, T., Laud, K., et al. (2010). Preclinical evidence that use of TRAIL in Ewing's sarcoma and osteosarcoma therapy inhibits tumor growth, prevents osteolysis, and increases animal survival. *Clin. Cancer Res.* 16, 2363–2374. doi:10.1158/1078-0432.CCR-09-1779

Pimentel, J. M., Zhou, J. Y., and Wu, G. S. (2023a). The role of TRAIL in apoptosis and immunosurveillance in cancer. *Cancers (Basel)* 15, 2752. doi:10.3390/cancers15102752

Pimentel, J. M., Zhou, J. Y., and Wu, G. S. (2023b). Regulation of programmed death ligand 1 (PD-L1) expression by TNF-related apoptosis-inducing ligand (TRAIL) in triple-negative breast cancer cells. *Mol. Carcinog.* 62, 135–144. doi:10.1002/mc.23471

Pringle, T. A., Chan, C. D., Luli, S., Blair, H. J., Rankin, K. S., and Knight, J. C. (2022). Synthesis and *in vivo* evaluation of a site-specifically labeled radioimmunoconjugate for dual-modal (PET/NIRF) imaging of MT1-MMP in sarcomas. *Bioconjug Chem.* 33, 1564–1573. doi:10.1021/acs.bioconjchem.2c00306

Rasco, D. W., Lakhani, N. J., Tang, Y., Wang, H., Ji, J., Chen, J., et al. (2020). Phase Ib study of a novel bivalent IAP antagonist APG-1387 in combination of pembrolizumab for patients with advanced solid tumors. *JCO* 38, 3508. doi:10.1200/JCO.2020.38.15_suppl.3508

Richter, C., Messerschmidt, S., Holeiter, G., Tepperink, J., Osswald, S., Zappe, A., et al. (2012). The tumor necrosis factor receptor stalk regions define responsiveness to soluble versus membrane-bound ligand. *Mol. Cell Biol.* 32, 2515–2529. doi:10.1128/MCB.06458-11

Sadeghnezhad, G., Romao, E., Bernedo-Navarro, R., Massa, S., Khajeh, K., Muyldermans, S., et al. (2019). Identification of new DR5 agonistic nanobodies and generation of multivalent nanobody constructs for cancer treatment. *Int. J. Mol. Sci.* 20, 4818. doi:10.3390/ijms20194818

Schneider, B., Munkel, S., Krippner-Heidenreich, A., Grunwald, I., Wels, W. S., Wajant, H., et al. (2010). Potent antitumoral activity of TRAIL through generation of tumor-targeted single-chain fusion proteins. *Cell Death Dis.* 1, e68. doi:10.1038/cddis.2010.45

Scott, F. L., Stec, B., Pop, C., Dobaczewska, M. K., Lee, J. J., Monosov, E., et al. (2009). The Fas-FADD death domain complex structure unravels signalling by receptor clustering. *Nature* 457, 1019–1022. doi:10.1038/nature07606

Sinclair, A. M., (2021). Available at: https://igmbio.com/wp-content/uploads/2021/12/MCT-20-1132_rp_final-approved.pdf

Smith, M. L. S. J., Chen, D., Haichao, Z., Huska, J., Widomski, D., Bontcheva, V., et al. (2020). The combinatorial activity of eftozanermin (ABBV-621), a novel and potent TRAIL receptor agonist fusion protein, in pre-clinical models of hematologic malignancies. *Blood* 136, 41. doi:10.1182/blood-2020-136155

Snajdauf, M., Havlova, K., Vachtenheim, J., Jr., Ozaniak, A., Lischke, R., Bartunkova, J., et al. (2021). The TRAIL in the treatment of human cancer: an update on clinical trials. *Front. Mol. Biosci.* 8, 628332. doi:10.3389/fmolb.2021.628332

Stamatopoulos, A., Stamatopoulos, T., Gamie, Z., Kenanidis, E., Ribeiro, R. D. C., Rankin, K. S., et al. (2019). Mesenchymal stromal cells for bone sarcoma treatment: roadmap to clinical practice. *J. Bone Oncol.* 16, 100231. doi:10.1016/j.jbo.2019.100231

Stohr, D., Schmid, J. O., Beigl, T. B., Mack, A., Maichl, D. S., Cao, K., et al. (2020). Stress-induced TRAILR2 expression overcomes TRAIL resistance in cancer cell spheroids. *Cell Death Differ.* 27, 3037–3052. doi:10.1038/s41418-020-0559-3

Subbiah, V., Chawla, S. P., Conley, A. P., Wilky, B. A., Tolcher, A., Lakhani, N. J., et al. (2023). Preclinical characterization and phase I trial results of INBRX-109, A third-generation, recombinant, humanized, death receptor 5 agonist antibody, in chondrosarcoma. *Clin. Cancer Res.* 29, 2988–3003. doi:10.1158/1078-0432.CCR-23-0974

Surget, S., Chiron, D., Gomez-Bougie, P., Descamps, G., Menoret, E., Bataille, R., et al. (2012). Cell death via DR5, but not DR4, is regulated by p53 in myeloma cells. *Cancer Res.* 72, 4562–4573. doi:10.1158/0008-5472.CAN-12-0487

Thanindratarn, P., Dean, D. C., Nelson, S. D., Hornicek, F. J., and Duan, Z. (2019). Advances in immune checkpoint inhibitors for bone sarcoma therapy. *J. Bone Oncol.* 15, 100221. doi:10.1016/j.jbo.2019.100221

Trivedi, R., and Mishra, D. P. (2015). Trailing TRAIL resistance: novel targets for TRAIL sensitization in cancer cells. *Front. Oncol.* 5, 69. doi:10.3389/fonc.2015.00069

van der Horst, H. J., Gelderloos, A. T., Chamuleau, M. E. D., Breij, E. C. W., Zweegman, S., Nijhof, I. S., et al. (2021). Potent preclinical activity of HexaBody-DR5/DR5 in relapsed and/or refractory multiple myeloma. *Blood Adv.* 5, 2165–2172. doi:10.1182/bloodadvances.2020003731

Van Norman, G. A. (2019). Limitations of animal studies for predicting toxicity in clinical trials: is it time to rethink our current approach? *JACC Basic Transl. Sci.* 4, 845–854. doi:10.1016/j.jacbts.2019.10.008

Wang, B. T., Desbois, M., Calhoun, S. E., Matthew, T. J., Yakkundi, P., Wang, L., et al. (2022). Abstract 1068: anti-DR5 agonist IgM antibody IGM-8444 combined with SMAC mimetic birinapant induces strong synergistic tumor cytotoxicity. *Cancer Res.* 82, 1068. doi:10.1158/1538-7445.AM2022-1068

Wang, B. T., Kothambawala, T., Wang, L., Matthew, T. J., Calhoun, S. E., Saini, A. K., et al. (2021b). Multimeric anti-DR5 IgM agonist antibody IGM-8444 is a potent inducer of cancer cell apoptosis and synergizes with chemotherapy and BCL-2 inhibitor ABT-199. *Mol. Cancer Ther.* 20, 2483–2494. doi:10.1158/1535-7163.MCT-20-1132

Wang, K., Kievit, F. M., Jeon, M., Silber, J. R., Ellenbogen, R. G., and Zhang, M. (2015). Nanoparticle-mediated target delivery of TRAIL as gene therapy for glioblastoma. *Adv. Healthc. Mater* 4, 2719–2726. doi:10.1002/adhm.201500563

Wang, S., Zhu, H., Li, Y., Ding, J., Wang, F., Ding, L., et al. (2021c). First-in-human DR5 PET reveals insufficient DR5 expression in patients with gastrointestinal cancer. *J. Immunother. Cancer* 9, e002926. doi:10.1136/jitc-2021-002926

Wang, Y., Baars, I., Fordos, F., and Hogberg, B. (2021a). Clustering of death receptor for apoptosis using nanoscale patterns of peptides. *ACS Nano* 15, 9614–9626. doi:10.1021/acsnano.0c10104

Weber, T. G., Osl, F., Renner, A., Poschinger, T., Galban, S., Rehemtulla, A., et al. (2014). Apoptosis imaging for monitoring DR5 antibody accumulation and pharmacodynamics in brain tumors noninvasively. *Cancer Res.* 74, 1913–1923. doi:10.1158/0008-5472.CAN-13-3001

Weber, T. G., Poschinger, T., Galban, S., Rehemtulla, A., and Scheuer, W. (2013). Noninvasive monitoring of pharmacodynamics and kinetics of a death receptor 5 antibody and its enhanced apoptosis induction in sequential application with doxorubicin. *Neoplasia* 15, 863–874. doi:10.1593/neo.13932

Xu, M., Asghar, S., Dai, S., Wang, Y., Feng, S., Jin, L., et al. (2019). Mesenchymal stem cells-curcumin loaded chitosan nanoparticles hybrid vectors for tumor-tropic therapy. *Int. J. Biol. Macromol.* 134, 1002–1012. doi:10.1016/j.ijbiomac.2019.04.201

Yagolovich, A. V., Artykov, A. A., Karmakova, T. A., Vorontsova, M. S., Pankratov, A. A., Andreev-Andrievsky, A. A., et al. (2020). Genetically modified DR5-specific TRAIL variant DR5-B revealed dual antitumor and protumoral effect in colon cancer xenografts and an improved pharmacokinetic profile. *Transl. Oncol.* 13, 100762. doi:10.1016/j.tranon.2020.100762

Yuan, X., Gajan, A., Chu, Q., Xiong, H., Wu, K., and Wu, G. S. (2018). Developing TRAIL/TRAIL death receptor-based cancer therapies. *Cancer Metastasis Rev.* 37, 733–748. doi:10.1007/s10555-018-9728-y

Zhang, S., Zheng, C., Zhu, W., Xiong, P., Zhou, D., Huang, C., et al. (2019). A novel anti-DR5 antibody-drug conjugate possesses a high-potential therapeutic efficacy for leukemia and solid tumors. *Theranostics* 9, 5412–5423. doi:10.7150/thno.33598

Zhao, M., Li, Z., and Bugenhagen, S. (2008). 99mTc-labeled duramycin as a novel phosphatidylethanolamine-binding molecular probe. *J. Nucl. Med.* 49, 1345–1352. doi:10.2967/jnumed.107.048603

Zheng, C., Zhou, D., Li, W., Duan, Y., Xu, M., Liu, J., et al. (2023). Therapeutic efficacy of a MMAE-based anti-DR5 drug conjugate Oba01 in preclinical models of pancreatic cancer. *Cell Death Dis.* 14, 295. doi:10.1038/s41419-023-05820-1

Zhuo, F. F., Zhang, C., Zhang, H., Xia, Y., Xue, G. M., Yang, L., et al. (2019). Chrysanthemulide A induces apoptosis through DR5 upregulation via JNK-mediated autophagosome accumulation in human osteosarcoma cells. *J. Cell Physiol.* 234, 13191–13208. doi:10.1002/jcp.27991

frontiers | Frontiers in Immunology

TYPE Original Research
PUBLISHED 10 October 2024
DOI 10.3389/fimmu.2024.1462076

OPEN ACCESS

EDITED BY
Yang Wang,
Sichuan Academy of Medical Sciences and Sichuan Provincial People's Hospital, China

REVIEWED BY
Malik Ihsan,
University of Lahore, Pakistan
Bikesh Kumar Nirala,
Emory University, United States

*CORRESPONDENCE
Wenzheng Jiang
wzjiang@bio.ecnu.edu.cn

†These authors have contributed equally to this work

RECEIVED 17 July 2024
ACCEPTED 17 September 2024
PUBLISHED 10 October 2024

CITATION
Hui X, Farooq MA, Chen Y, Ajmal I, Ren Y, Xue M, Ji Y, Du B, Wu S and Jiang W (2024) A novel strategy of co-expressing CXCR5 and IL-7 enhances CAR-T cell effectiveness in osteosarcoma. *Front. Immunol.* 15:1462076. doi: 10.3389/fimmu.2024.1462076

A novel strategy of co-expressing CXCR5 and IL-7 enhances CAR-T cell effectiveness in osteosarcoma

Xinhui Hui[1†], Muhammad Asad Farooq[1,2†], Yiran Chen[1], Iqra Ajmal[1,2], Yaojun Ren[1,3], Min Xue[1], Yuzhou Ji[1], Bingtan Du[1], Shijia Wu[1] and Wenzheng Jiang[1*]

[1]Shanghai Key Laboratory of Regulatory Biology, School of Life Sciences, East China Normal University, Shanghai, China, [2]The First Dongguan Affiliated Hospital, Guangdong Provincial Key Laboratory of Medical Immunology and Molecular Diagnostics, Guangdong Medical University, Dongguan, China, [3]College of Life Science, Xinjiang Normal University, Urumqi, China

Background: Solid tumors are characterized by a low blood supply, complex stromal architecture, and immunosuppressive milieu, which inhibit CAR-T cell entry and survival. CXCR5 has previously been employed to increase CAR-T cell infiltration into CXCL13+ cancers. On the other hand, IL-7 improves the survival and persistence of T cells inside a solid tumor milieu.

Methods: We constructed a novel NKG2D-based CAR (C5/IL7-CAR) that co-expressed CXCR5 and IL-7. The human osteosarcoma cell lines U-2 OS, 143B, and Mg63 highly expressed MICA/B and CXCL13, thus presenting a perfect avenue for the present study.

Results: Novel CAR-T cells are superior in their activation, degranulation, and cytokine release competence, hence lysing more target cells than conventional CAR. Furthermore, CXCR5 and IL-7 co-expression decreased the expression of PD-1, TIM-3, and TIGIT and increased Bcl-2 expression. Novel CAR-T cells show enhanced proliferation and differentiation towards the stem cell memory T cell phenotype. C5/IL7-CAR-T cells outperformed conventional CAR-T in eradicating osteosarcoma in mouse models and displayed better survival. Additionally, CXCR5 and IL-7 co-expression enhanced CAR-T cell numbers, cytokine release, and survival in implanted tumor tissues compared to conventional CAR-T cells. Mechanistically, C5/IL7-CAR-T cells displayed enhanced STAT5 signaling.

Conclusion: These findings highlight the potential of CXCR5 and IL-7 co-expression to improve CAR-T cell therapy efficacy against osteosarcoma.

KEYWORDS

CAR-T therapy, tumor microenvironment, T cell migration, osteosarcoma, CXCR5, IL-7

1 Introduction

Osteosarcoma (OS), while relatively uncommon in the general population, presents a notable surge in incidence during the pubertal growth spurt of young adults. It is, therefore, considered an orphan disease due to the inadequate population size affected by this disease compared to other forms of cancer (1, 2). Hypoxia and acidic microenvironment promote the release of pro-angiogenic factors (HIF and VEGF) by OS tumor cells to form highly vascularized tumors, which is thought to be the main reason for the high rate of metastasis and spread of OS. In addition, the extracellular matrix (ECM) composition of OS is significantly altered, and secretion is significantly increased, resulting in a harder matrix that makes it more difficult to infiltrate for immune cells (2). There is currently a marked stagnation in its treatment progress, while adjuvant chemotherapy has remained the primary therapeutic approach for the past four decades (1). Given the recent limitations of these treatments, innovating and implementing novel treatment options for OS is unequivocally important.

A diverse array of immunotherapies, including chimeric antigen receptor (CAR)-T cell therapy, are actively being employed to identify new treatment options for OS. The efficacy of CAR-T cell therapy in solid tumors still remains a challenge despite excellent remission rates in patients with hematological malignancies (3). For OS treatment, different targets for CAR-T cells are being explored to precisely mark and eradicate target-positive malignant cells (4, 5). One promising avenue is the development of CAR-T cells targeting the natural killer group 2D (NKG2D), which has exhibited significant efficacy in eradicating OS cells both *in vitro* and in murine models (6, 7). Some studies have shown that NKG2D-based CAR-T cells are quite safe for ligand-negative cells, including normal body tissues (6, 8, 9).

Solid tumors often create an immunosuppressive microenvironment that can impede the infiltration of immune cells, including CAR-T cells. The CXC motif chemokine receptor 5 (CXCR5) receptor, which guides cells to lymphoid tissues, might also assist CAR-T cells in navigating the complex stromal architecture of solid tumors, potentially leading to improved tumor invasion. This is why CAR-T cells co-expressing CXCR5 were superior to conventional CAR-T cells in eradicating ligand-positive tumor cells (10, 11). CXC-motif chemokine ligand 13 (CXCL13), the exclusive ligand for the CXCR5 receptor, is expressed in OS cell lines and is positively correlated with $CD8^+$ T cell recruitment at tumor sites (12). However, reaching tumor sites is only part of the challenge; ensuring survival and long-term persistence at these locations is equally crucial for effective malignant cell eradication. Building on the previous success in utilizing interleukin-7 (IL-7) co-expression to enhance CAR-T cell therapy efficacy in a prostate cancer model (8), the present study presents a significant step forward. With our novel approach, we constructed a unique NKG2D-based CAR with the aim of augmenting CAR-T cell trafficking and persistence against OS. This construct co-expressed CXCR5 and IL-7 (C5/IL7) within the conventional NKG2D-CAR backbone, addressing both challenges, i.e., effective tumor penetration and sustained presence.

2 Materials and methods

2.1 Cell lines

HEK293T, U-2 OS, 143B, and Jurkat cell lines were used in this study. U-2 OS, 143B, and Mg63 are the three common osteosarcoma cell lines, they all express the ligand MICA/B of NKG2D, as well as the ligand CXCL13 of CXCR5, which are suitable for our study. All cells were obtained from the American Tissue Culture Collection (ATCC, USA) and were maintained in our laboratory. HEK293T and 143B cells were maintained in Dulbecco's modified Eagle's medium (DMEM; Gibco Laboratories, Grand Island, NY, USA), U-2 OS cells were maintained in McCoy's 5A medium (Procell, Wuhan, China), and Jurkat cells were maintained in RPMI 1640 medium (Gibco Laboratories). The culture media were supplemented with 10% fetal bovine serum (FBS; ABW, Uruguay) and 1% penicillin-streptomycin, creating an optimal growth environment referred to as the complete medium. Additionally, 143B cells were genetically modified to express luciferase through firefly-luciferase lentiviral transduction. The passage number of all cell lines was within 15.

2.2 CAR construction and lentivirus production

The second-generation CAR vector utilizing the pLL3.7 plasmid was constructed as described previously (8, 9, 13). The plasmid contained an EF-1α promoter, the human CD8α signal peptide, the NKG2D extracellular domain, the CD8α hinge, and transmembrane domains, and the cytoplasmic domain of 4-1BB fused with the CD3ζ cytoplasmic tail. Additional modifications were introduced to construct novel C5/IL7-CAR plasmid expressing human CXCR5 (aa 1-372) and IL-7 (aa 1-177) with the N-terminal secretion signals P2A or T2A cleavage peptides. For lentivirus packaging, HEK293T cells were seeded and cultured for 24 hours, followed by transfection on day 1 with the lentiviral vector and two helper vectors (psPAX2, pMD2.G) using a polyethyleneimine (PEI) system (Polysciences, Warrington, PA, USA). After a 48-hour incubation period, the supernatant was collected, filtered (0.45μm), and concentrated via ultracentrifugation (27000g, 4°C, 2 hours). The supernatant was removed, and an additional culture medium was added to the concentrated virus mixture. Aliquots were preserved at -80°C.

2.3 T-cell isolation and CAR-T cell preparation

Peripheral blood mononuclear cells (PBMCs) were isolated from the blood of healthy donors (Shanghai Blood Center, China) by the Ficoll-Paque PLUS gradient centrifugation method (HyClone, Logan, UT, USA). Primary T cells were positively selected with CD4 and CD8 microbeads, stimulated with Enceed™ (Genscript, Nanjing, China) for 48 hours, and subsequently cultured in X-VIVO 15

mediums (Lonza) supplemented with 5% FBS, 1% penicillin/streptomycin, and 200IU/mL human recombinant interleukin-2 (hIL-2, Seaform Biotech., Beijing, China). To prepare CAR-T cells, 1×10^6 T cells were transduced with the respective lentiviruses at a multiplicity of infection (MOI) 10. These transduced cells were then expanded for 2 weeks at a density of 1×10^6/mL.

2.4 Flow cytometry analysis

Flow cytometry analysis was performed according to the experimental needs. Surface staining involved a 30-minute incubation of cells with FACS antibodies, whereas, for intracellular staining, CAR-T cells were fixed and permeabilized using the BD Cytofix/Cytoperm Kit (BD Biosciences, Bergen County, NJ, USA) before staining. The gating strategies were based on forward vs scatter characteristics, followed by single-cell gating of live cells. Antibodies were purchased from Biolegend, BD Biosciences, and eBiosciences™ USA, as detailed in Supplementary Table S1. The data were acquired using a BD LSRfortessa or CantoII flow cytometer, and the acquired samples were analyzed with FlowJo software (version 10.8.1).

2.5 RT-PCR

Total RNA was extracted from CAR-T cells or cancer cells and subjected to reverse transcription for cDNA synthesis as described previously.14 The specific primers used for IL-7, CXCL13 and β-actin were as follows: IL-7 (forward 5'- TACAGTACGCATGT GAAAGTCA-3', reverse 5'-AGGAAACACAAGTCATTCAGTTT T-3'), CXCR5 (forward 5'-CCTTGCCTTGCCAGAGATTC-3', reverse 5'-TGTAGAGCATGGGGTTGAGG-3'), CXCL13 (forward 5'-TGGGGCAAACTCAAGCTTCT-3', reverse 5'-GTCTGGGG ATCTTCGAATGCTA-3'), and β-actin (forward 5'- GTAC GCCAACACAGTGCTG-3', and reverse 5'-CGTCATACTCCT GCTTGCTG-3'). The RT-PCR reaction cycles comprised pre-denaturation at 95°C for 5 minutes, followed by 30 cycles of denaturation at 95°C for 30 seconds, annealing at 60°C for 30 seconds, and extension at 72°C for 30 seconds. The PCR product was loaded on 2% agarose gel, and electrophoresis was performed.

2.6 Transwell assay

CAR-T cells (3×10^5) were seeded in the upper chamber of a 24-well transwell plate (3μm pore size, Corning), and the lower chamber was filled with DMEM (500μl) or tumor-cell supernatant. After a 4-hour incubation period, cells were collected from the lower chamber and quantified using a hemocytometer.

2.7 Cytotoxicity assay

3×104 luciferase-transduced target cells (U-2 OS, 143B, and Mg63) were seeded in a low-attachment 96-well plate. Effector cells, including Mock-T, CAR-T, and C5/IL7-CAR-T cells, were cultured at various effectors to target (E: T) ratios (1.25:1, 2.5:1, 5:1). After16-hours of coincubation, the cells were collected, and killing efficiency was quantified using a firefly Luciferase Reporter Gene Assay Kit (Beyotime Biotech, Shanghai, China).

2.8 Cell proliferation assay

A total of 1×10^6 T cells from each group were labeled with carboxyfluorescein succinimidyl ester (CFSE; 65-0850-84, eBioscience™, Waltham, MA, USA) at a concentration of 10μM. The cells were incubated in the dark at 37°C for 15 minutes, after which the unbound CFSE was removed through FBS quenching by incubating the mixture at 4°C for 10 minutes. After washing, cells were resuspended, and baseline CFSE fluorescence was analyzed on day 0 using flow cytometry. Subsequently, the labeled cells were cultured for 5 days, and post-culture CFSE dilution was assessed via flow cytometry.

2.9 Enzyme-linked immunosorbent assay

In a controlled *in vitro* setting, CAR-T cells (1.5×10^5) were cultured either alone or cocultured with 5×10^4 tumor cells in a complete X-VIVO medium. After 24 hours, the cell-free supernatant was collected, and IL-7 protein secretion was quantified using an ELISA kit following the manufacturer's instructions (1110702, Dakewe Biotech, Beijing, China). For *in vivo* assessment, blood samples were aseptically collected from mouse orbits into EDTA-coated EP tubes. After centrifugation at 3000rpm for 10 minutes, the supernatant was collected. Ferritin levels in the supernatant were assessed with a ferritin-ELISA kit according to the manufacturer's instructions (U96-3528E, YoBiBiotech, Shanghai, China), and the measurements were performed using a microplate spectrophotometer (450nm).

2.10 *In vivo* study

All animal experiments were performed with the approval of the Animal Ethics Committee of East China Normal University. Eight-week-old female NOD/SCID/γ-chain-/- (NSG) mice were used to establish osteosarcoma xenografts. Mice were anesthesia using isoflurane at 0.41ml/min fresh gas flow (2% concentration). Initially, 2×10^6 143B luciferase-positive cancer cells were subcutaneously injected into the right flank of mice. After 2 weeks, when the tumor size reached 100-150mm3, the mice were randomly divided into 6 groups (n=6), and IVIS imaging was performed. Prior to each session, the mice were injected with D-luciferin (3mg/mouse) and subsequently sedated. The photons emitted from luciferase-expressing cells were quantified using Living Image software (version 4.4). The photon intensity is represented by red (high) to blue (low), providing insight into tumor progression. Furthermore, each group either received PBS, Mock-T (5×10^6), CAR-T (5×10^6), or 3 different dosages of C5/IL7-

CAR-T (2×10^6, 5×10^6 and 1×10^7) cells intravenously, followed by IVIS imaging every week. Tumor volume was regularly assessed using calipers with the formula V=1/2(length × width^2). Peripheral blood was collected from mouse orbits on days 3, 12, and 23 after CAR-T cell therapy in EDTA tubes. Serum isolation was followed by cytokine (IL-8, IFN-γ) detection using a Cytometric Bead Array (CBA) kit (Dakewe Biotech., Beijing, China), and ferritin was detected through an ELISA kit (U96-3528E, YoBiBiotech, Shanghai, China). On day 27, the mice were sacrificed, and tumor and spleen tissues were collected for single-cell suspension preparation. Various markers were analyzed via flow cytometry, employing the antibodies specified in Supplementary Table 1.

2.11 Statistical analysis

GraphPad Prism (version 9.0) was used to generate the graphs and conduct the statistical analysis. The data are presented as the mean and standard deviation (± SD). The choice of statistical tests, including one-way ANOVA, two-way ANOVA, and two-tailed unpaired T-tests, was determined by the context of the analysis. Statistically significant differences are denoted as *P < 0.05, **P < 0.01, ***P < 0.001, ****P < 0.0001 and ns is non-significant.

3 Results

3.1 Construction and characterization of novel CAR

The second-generation chimeric antigen receptor was used in this study as described in previously published data (8, 9, 13). Briefly, our CAR consisted of an NKG2D-based extracellular domain along with 4-1BB and CD3ζ intracellular domains. The interaction between the extracellular and intracellular domains was facilitated by the presence of the CD8α hinge and transmembrane domains. Additionally, a novel CAR was constructed by incorporating the coding sequences (CDSs) of the CXCR5 and IL-7 genes into the basic CAR framework; this construct was termed C5/IL7-CAR. A schematic representation is shown in Figure 1A. The puromycin lentiviral vector was used as a control and was termed Mock.

HEK293T cells were co-transfected with either CAR or C5IL7-CAR in the presence of three plasmid packaging systems, as described previously (14, 15). The lentivirus was collected 48 and 72 h post-transfection, and titer was calculated. The lentivirus for both CAR-plasmids gave a high infection rate in HEK293T cells, giving excellent titer (Figure 1B). Activated T cells were transduced with Mock, CAR, or C5/IL7-CAR lentivirus to generate Mock-T, CAR-T, or C5/IL7-CAR-T cells, respectively. Subsequently, cells were stained with an anti-human NKG2D antibody 48 hours post-transduction. Since NKG2D is part of the CAR design, its expression directly reflects the incorporation of the CAR into the T cell population. Monitoring NKG2D expression provides insight into the extent to which engineered cells express the intended chimeric receptor. Both CAR T cells displayed notable transduction efficiency compared to that of Mock-T (Figure 1C).

To validate the efficiency of our novel C5/IL7-CAR construct, the expression levels of CXCR5 and IL-7 were determined in successive experiments. The RT-PCR data indicated that C5/IL7-CAR-T cells demonstrated higher gene expression for CXCR5 and IL-7 genes as compared with the wild-type CAR-T cells (Figure 1D). The insertion of CXCR5 and IL-7 into CAR plasmid was further confirmed by transwell assay and ELISA, respectively. The increase in the chemotaxis index in C5/IL7-CAR-T cells observed by the transwell assay confirmed the successful insertion of the CXCR5 CDS (Figure 1E). Our ELISA data indicated that IL-7 expression was elevated significantly in C5/IL7-CAR-T cells in the absence of target cells. In the presence of U-2 OS cells, IL-7 expression was further amplified (Figure 1F). These data confirmed the successful generation and functioning of the novel C5/IL7-CAR vector.

3.2 C5/IL7 amplified CAR-T cell cytotoxicity *in vitro*

To determine the suitability of osteosarcoma as a potential target for NKG2D-based CAR-T cell therapy, MICA/B expression in human OS cell lines was determined by flow cytometry. We found that OS cell lines U-2 OS, 143B, and Mg63 had increased expression of NKG2D ligands on their surface, suggesting that these cells could be suitable targets for our novel NKG2D-based CAR construct (Figure 2A). Previous data suggest increased expression of CXCL13, the ligand for CXCR5, in OS (16, 17), which was further confirmed in the present study (Supplementary Figure 1). Given the high expression of MICA/B and CXCL13, human osteosarcoma cell lines constitute the perfect avenue for studying our CAR system expressing NKG2D, CXCR5, and IL-7. To evaluate the cytotoxicity of experimental groups, we performed cytotoxicity assays targeting U-2 OS, 143B, and Mg63 transgenic cell lines as targets (Figure 2B). C5/IL7-CAR-T cells exhibited enhanced killing capacity against OS cell lines compared to that of wild-type CAR-T cells. We conducted a series of flow cytometry experiments to further investigate the effects of C5/IL7 co-expression on CAR-T cell activation, degranulation, and cytokine release. Mock-T, CAR-T, and C5/IL7-CAR-T cells were cocultured with U-2 OS for 16 hours. Subsequently, the cells were stained with C-type lectin domain (CD69) and lysosomal-associated membrane protein 1 (CD107a) flow cytometry antibodies to assess T cell activation and degranulation, respectively. C5/IL7 incorporation improved CAR-T cells' activation and degranulation capacity (Figures 2C, D). Increased CD69 expression suggested that transduced T cells are more responsive to the presence of cancer cells. Improved degranulation and activation advocate that CAR-T cells are more effective in enhancing the antitumor response (18). Furthermore, cells that exhibit increased CD107a expression are more effective at releasing cytotoxic granular contents (9). Therefore, we further analyzed the levels of intracellular granzyme B (GzmB) and interferon-gamma (IFN-γ) in the experimental cohorts by flow cytometry. As expected, C5/IL7-CAR-T cells

10.3389/fimmu.2024.1462076

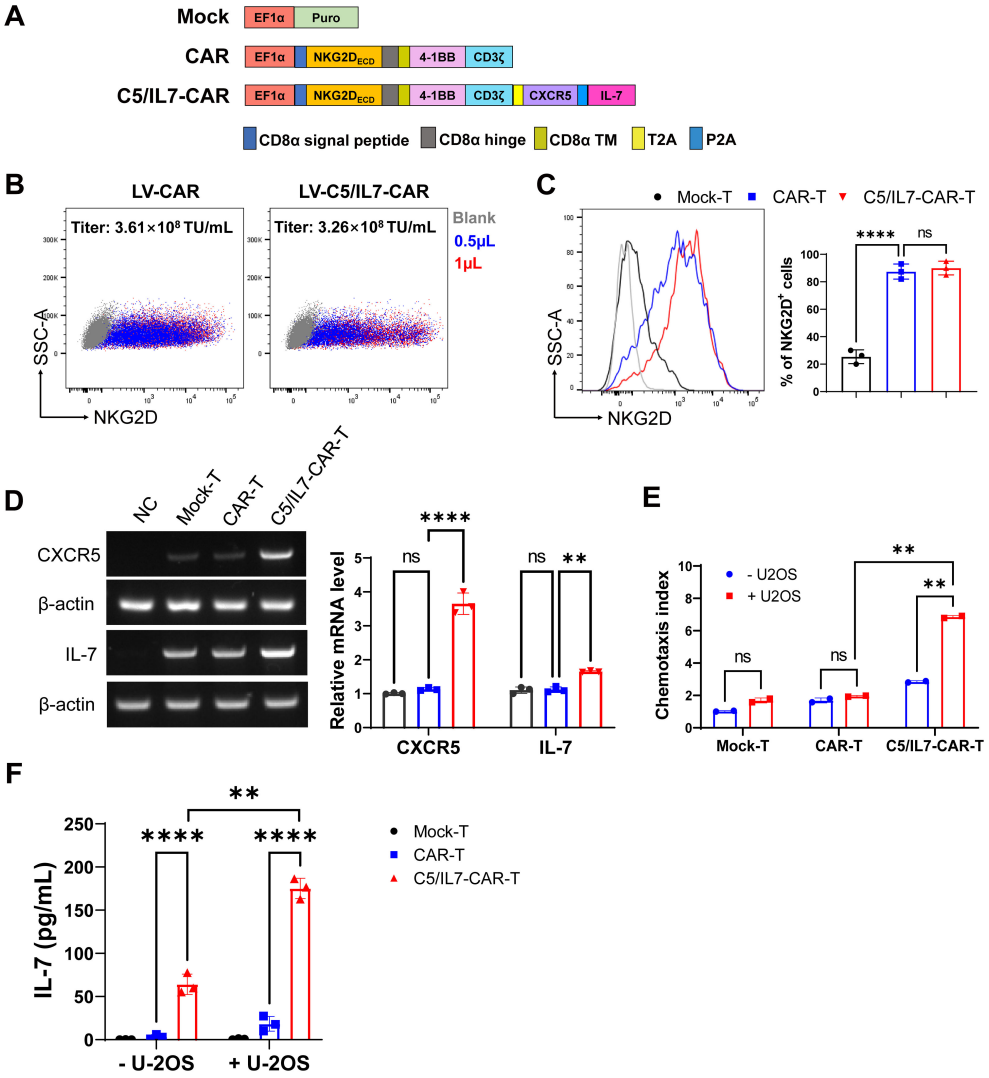

FIGURE 1
C5/IL7-CAR vector construction and validation. **(A)** Schematic representation of Mock, CAR, and C5/IL7-CAR constructs. **(B)** 2×10^5 HEK293T cells were transduced with different volumes of CAR and C5/IL7-CAR lentiviruses separately. After 48 hours, NKG2D expressions were analyzed by flow cytometry. The percentages of positive cells indicated in the dot plot and the titer (TU/mL) were calculated with the formula: (2×10^5×percentages of positive cells×1000)/Volume of lentiviruses. **(C)** 1×10^6 primary T cells were transduced with Mock, CAR, and C5/IL7-CAR lentiviruses, MOI=10. After 48 hours, cells were analyzed by flow cytometry for NKG2D expression. The percentages of positive cells are indicated in the histogram (left panel) and bar chart (right panel). **(D)** Mock-T, CAR-T, and C5/IL7-CAR-T were collected 48 hours post-transduction and were subjected to RT-PCR for CXCR5 and IL-7 gene expression analysis. HEK293T cells were used as a negative control. β-actin was used as a reference housekeeping gene. **(E)** The Chemotaxis index of CAR-T cells was determined using a transwell assay. In each experimental group, 3×10^5 cells were placed in the upper chamber of a 24-well transwell plate. After a 4-hour co-culture period, their migratory response towards the lower chamber containing either DMEM or supernatant from U-2 OS cells was evaluated. The number of migrated T cells was quantified using a hemocytometer. Data are presented based on three technical repeats with T cells cultured without cancer cell supernatant indicated in blue and those exposed to cancer cell supernatant in red. **(F)** Mock-T, CAR-T, and C5/IL7-CAR-T cohorts were cultured with or without U-2 OS cells for 24 hours, and the medium was collected and subjected to ELISA for IL-7 protein expression. Experiments were performed independently at least 3 times. For **(C)**, One-way ANOVA was used in Tukey's multiple comparison test, and for **(D–F)**, Two-way ANOVA was used in Šídák's multiple comparison test. Data represent Mean ± SD. **P < 0.01, ****P < 0.0001, ns, not significant.

expressed more GzmB and IFN-γ than did the wild-type CAR-T cells (Figures 2E, F). The data above was further confirmed in the presence of 143B target cells (Supplementary Figure 2). The results signify that incorporating C5/IL7 enhances the cytotoxic potential of CAR-T cells against osteosarcoma cell lines. This augmentation is likely achieved by increased activation, degranulation, and cytotoxic molecules and cytokines release.

3.3 C5/IL7 enhanced CAR-T cell survival

To explore the potential of co-expressing CXCR5 and IL-7 to reduce the exhaustion and apoptosis of CAR-T cells, we performed flow cytometry-based assays by staining cocultured cells with antibodies related to the respective phenomenon. The experimental groups were cocultured with target cells for 3 days. Subsequently, the

10.3389/fimmu.2024.1462076

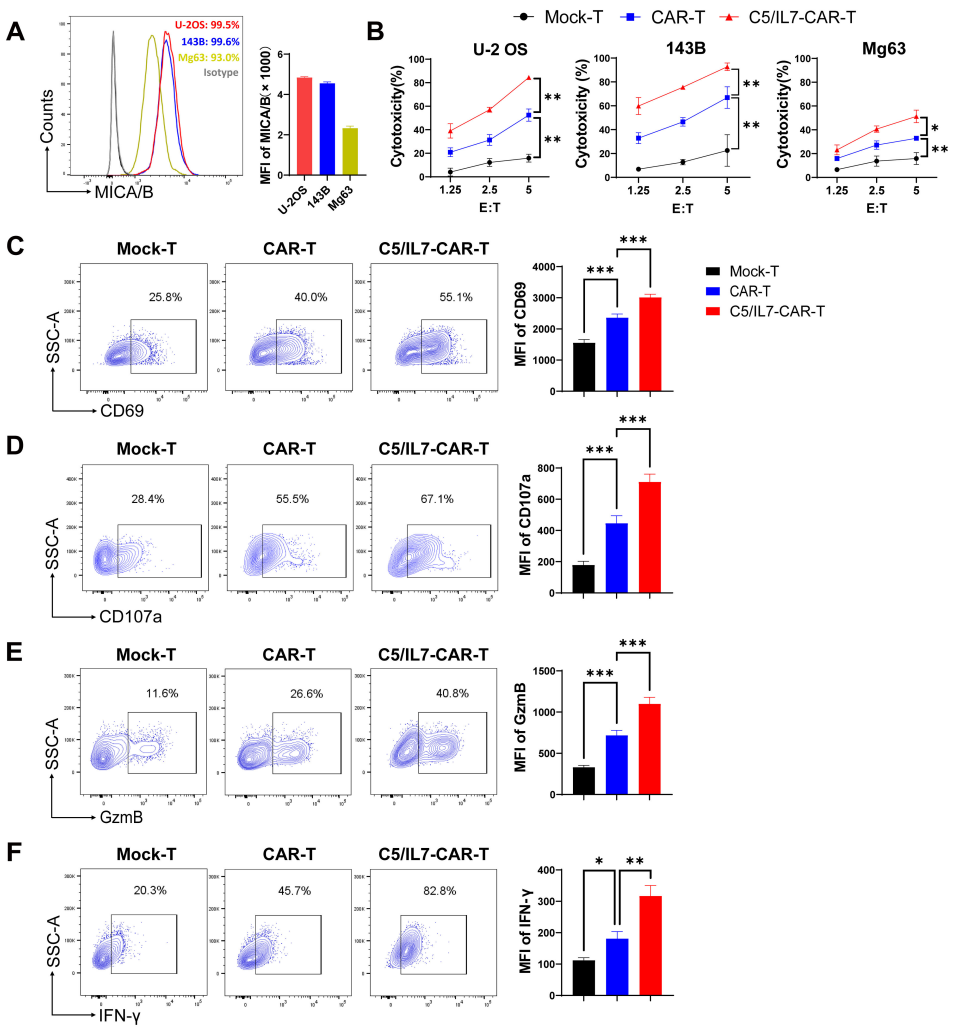

FIGURE 2
In vitro effector function of C5/IL7-CAR-T cells. **(A)** U-2 OS, 143B, and Mg63 cells were analyzed by flow cytometry for NKG2D Ligands (MICA/B) expression. U-2 OS is shown in red, 143B in blue and Mg63 in the yellow color histogram. Data are presented as Mean Fluorescence Intensity (MFI) normalized to unstained cells. **(B)** Cytotoxic analysis against U-2 OS, 143B, and Mg63 target cells. Experimental cohorts were cocultured with luciferase-transduced U-2 OS, 143B, and Mg63 target cells at varying effector-to-target (E: T) ratios for 16 hours. Percentage lysis was quantified using a luciferase-based cytotoxicity assay. **(C–F)** Flow cytometry analysis of CD69, CD107a, GzmB, and IFN-γ expression in Mock-T, CAR-T, and C5/IL7-CAR-T cohorts following a 16-hour co-culture with target cells at an E: T ratio of 3:1. Data is presented in a contour plot (left panel), and MFI is indicated by bar graphs (right panel). Experiments were performed independently at least 3 times. One-way ANOVA was used in Tukey's multiple comparison test, and Data represent Mean ± SD. *P < 0.05, **P < 0.01, ***P < 0.001.

cells were washed with PBS to remove traces of culture medium and stained with anti-human programmed cell death protein 1 (PD-1) and anti-human T cell immunoglobulin and mucin domain 3 (TIM-3) flow cytometry antibodies. FACS analysis revealed that C5/IL7-CAR-T cells had significantly lower levels of PD-1 and TIM-3 compared to the CAR-T group (Figures 3A, B). Moreover, the percentage of PD-1/TIM-3 double-positive cells was reduced in the novel-CAR transduced T cells (Supplementary Figure 3A). Similarly, T cell immunoglobulin and ITIM domain (TIGIT) expression was also decreased in CXCR5 and IL-7 expressing CAR-T experimental group (Figure 3C). In the absence of target cells, CXCR5 and IL-7 co-expression prevented CAR-T cells from undergoing IL-2-mediated exhaustion in long-term culture conditions (Supplementary Figures 3B-E). Decreased expression of exhaustion markers in CAR-T cells is beneficial because exhaustion can reduce immune responses against target cells (19). Although exhaustion and apoptosis are distinct processes, they can also be interrelated. Continued exhaustion of T cells may ultimately lead to their apoptosis as they become functionally impaired and unskilled to elicit effective immune responses. The expression of inhibitory receptors can also modulate apoptotic signaling pathways, possibly enhancing the susceptibility of exhausted T cells to cell death (20, 21). In the present study, reduced exhaustion of C5/IL7-CAR-T cells may have contributed to decreased apoptosis (Figure 3D). Flow cytometry data indicated that C5/IL7-CAR-T cells exhibited decreased Annexin V and increased B-cell lymphoma 2 (Bcl-2) expression. Bcl-2 was significantly elevated in $CD4^+$ T cells and $CD8^+$ T cells within the CD3 gate in the C5/IL7-CAR-T cohort (Figures 3D, E). These results collectively demonstrated that novel CAR-T cells are more resistant to exhaustion and apoptosis than their wild-type counterparts are.

10.3389/fimmu.2024.1462076

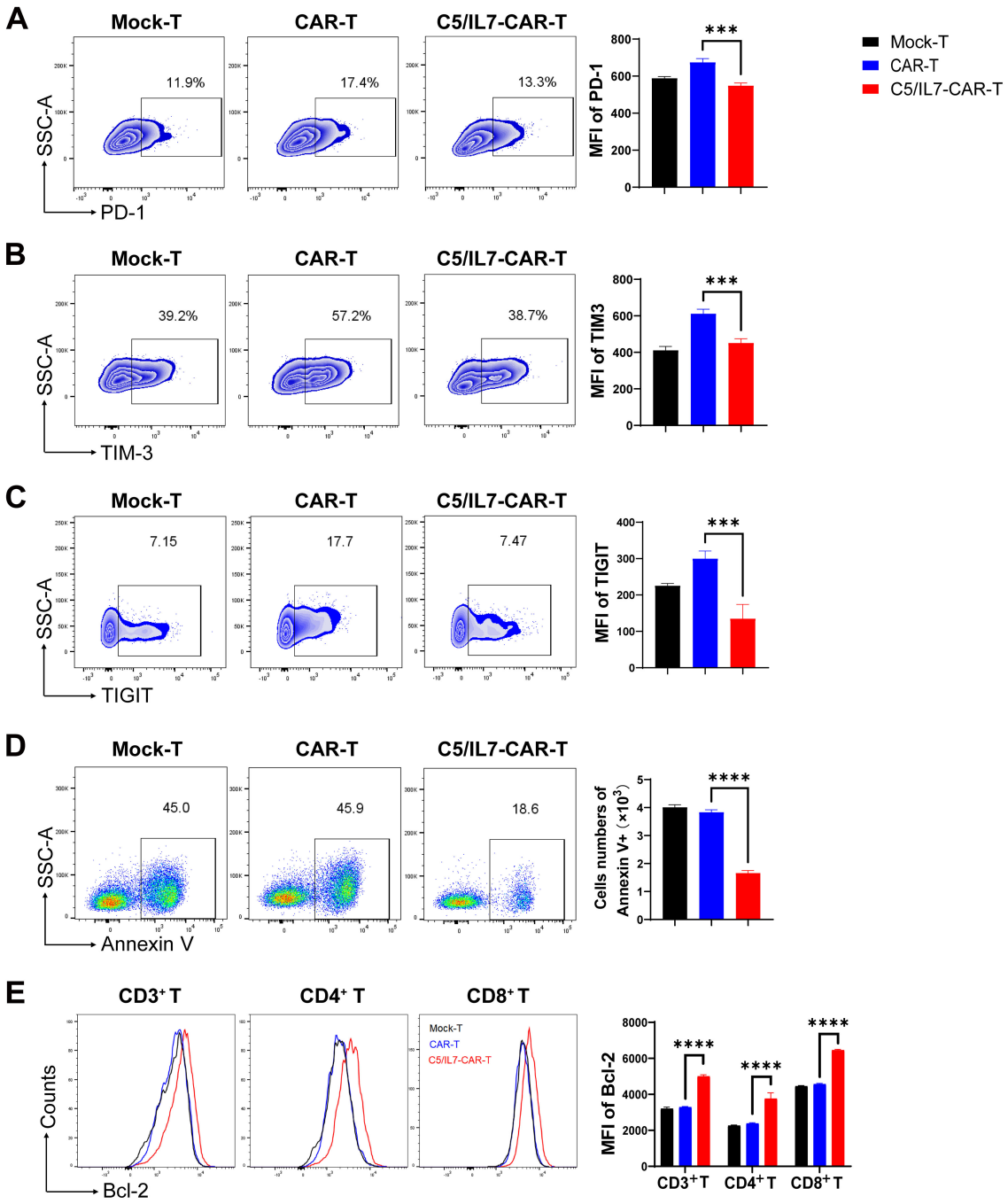

FIGURE 3
C5/IL7-CAR-T cells displayed reduced exhaustion and apoptosis *in vitro*. **(A–C)** Flow cytometry analysis of exhaustion markers PD-1, TIM-3, and TIGIT was performed after co-culturing Mock-T, CAR-T, and C5/IL7-CAR-T cells with U-2 OS for 3 days at an E: T ratio of 3:1. Representative FACS files are shown on the left, and MFI bar graph is presented on the right side. **(D)** Flow cytometry-based quantification of apoptotic cells in Mock-T, CAR-T, and C5/IL7-CAR-T cohorts. The cells were cultured for 5 days, harvested, and subsequently stained with Annexin V for 15 minutes in the dark at room temperature (RT). Flow cytometry analysis was conducted. The left and right panels displayed representative FACS files and absolute Annexin V^+ cell counts, respectively. **(E)** Following a 5-day culture of Mock-T, CAR-T, and C5/IL7-CAR-T cells were collected, and Bcl-2 expression within $CD3^+$, $CD4^+$, and $CD8^+$ T-cell populations was evaluated using flow cytometry. Representative histogram (left panel) and MFI (right panel) are shown. Experiments were performed independently at least 3 times. For **(A–D)**, One-way ANOVA was used in Tukey's multiple comparison test; for **(E)**, Two-way ANOVA was used in Tukey's multiple comparison test. Data represent Mean ± SD. ***P < 0.001, ****P < 0.0001.

10.3389/fimmu.2024.1462076

3.4 C5/IL7 augments CAR-T proliferation and persistence

Improved CAR-T cell proliferation can lead to a larger population of active cytotoxic T cells, resulting in a more effective response against cancer cells (22). Flow cytometry assays were conducted to evaluate the impact of C5/IL7 on CAR-T cell proliferation. Novel CAR-T cells demonstrated enhanced Ki67 expression than did the wild type CAR-T cells in the absence of target cells (Figure 4A). The proliferation phenomenon was further analyzed in the presence of target cells. The cells in the experimental cohorts were stained with CFSE and cultured with U-2 OS for 5 days. Flow cytometry analysis of CFSE dilution was conducted on days 0 and 5. Notably, compared with Mock-T and CAR-T cells, C5/IL7-CAR-T cells exhibited significantly greater proliferation rates (Figure 4B). Next, we investigated the differentiation of C5/IL7-CAR-T cells based on CD8 and CD4 expression. Mock-T, CAR-T, and C5/IL7-CAR-T cells were cultured in the presence or absence of target cells for 5 days and stained with CD8 and CD4 FACS antibodies. The $CD8^+/CD4^+$ T cell ratio is traditionally used

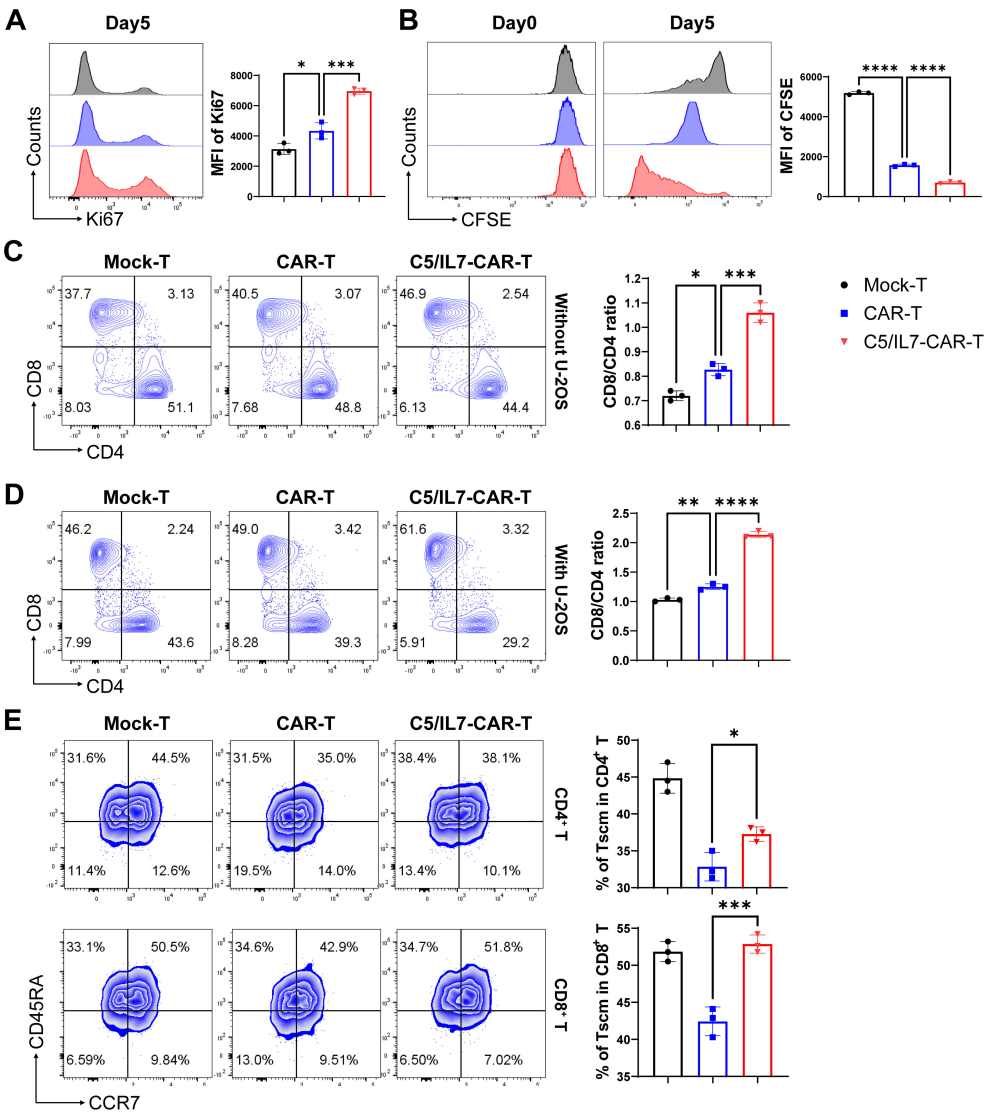

FIGURE 4
C5/IL7-CAR-T cells exhibit enhanced proliferation and differentiation. **(A)** To assess proliferation in the absence of target cells, Mock-T, CAR-T, and C5/IL7-CAR-T cells were cultured for 5 days, and analysis of Ki67 expression was detected by flow cytometry. A representative histogram is shown on the left, and MFI is presented on the right side. **(B)** To further assess proliferation in the presence of target cells, $1x10^6$ cells from Mock-T, CAR-T, and C5/IL7-CAR-T groups were initially labeled with 1μl of CFSE, and $2x10^5$ cells underwent flow cytometry analysis for CFSE dilution designated as day 0 in FITC channel. The remaining cells were co-cultured with U-2 OS for 5 days. Subsequently, on the 5th day, the CFSE dilution rate was once again measured using the same template in flow cytometry. **(C, D)** Mock-T, CAR-T, and C5/IL7-CAR-T cells were cultured with or without U-2 OS for 5 days. Flow cytometry analysis determined T cell subsets, presented in the left panel, while the calculated CD8/CD4 ratio is shown in the right panel. **(E)** For T cell differentiation, cells from each experimental group, after 5 days of co-cultured with U-2OS, were analyzed by flow cytometry. Tscm: Stem cell memory T cell ($CCR7^+CD45RA^+$), Tcm: Central memory T cell ($CCR7^+CD45RA^-$), Tem: Effector memory T cell ($CCR7^-CD45RA^-$), Teff: Effector T cell ($CCR7^-CD45RA^+$). Experiments were performed independently at least 3 times. One-way ANOVA was used in Tukey's multiple comparison test, and data represent Mean ± SD. *P < 0.05, **P < 0.01, ***P < 0.001, ****P < 0.0001.

10.3389/fimmu.2024.1462076

to measure immune cell activity, and CD8+ T cells represent the mainstay of CAR-T cell therapy (23). CAR-T cells co-expressing C5/IL7 increased the CD8/CD4 ratio, as demonstrated by flow cytometry (Figures 4C, D). An increased CD8/CD4 ratio indicated that the percentage of cytotoxic T lymphocytes was improved compared to that of helper T lymphocytes. To determine whether C5/IL7 influences the maintenance of stemness and memory properties, Mock-T, CAR-T, and C5/IL7-CAR-T cells were analyzed on the basis of CD45RA and CCR7 expression within $CD4^+$ and $CD8^+$ T cell gates in the presence of U-2 OS target cells. Remarkably, compared with wild-type CAR-T cells, C5/IL7-CAR-T cells preserved a greater percentage of Stem cell memory T cells (Tscm) (Figure 4E). The results were confirmed in the 143B OS cell line (Supplementary Figure 4). We also analyzed on the basis of CD45RO and CD62L expression within $CD4^+$ and $CD8^+$ T cell gates in the absence of target cells (Supplementary Figure 5). The increased proportions of Tscm cells in the C5/IL7-CAR-T cell cohort suggest that these cells may have a longer lifespan and will remain active over an extended period of time. This potential longevity could provide sustained tumor control and reduce the risk of relapse. Overall, the results demonstrated that incorporating C5/IL7 into CAR can enhance transduced T cells' proliferative potential and lead to the development of phenotypes well-suited for successful cancer immunotherapy.

3.5 C5/IL7 improves CAR-T therapy efficacy *in vivo*

The outcomes of our *in vitro* experiments clearly demonstrated the superior performance of the C5/IL7-CAR-T cells compared to conventional CAR-T cells. CAR-T cells that co-expressed C5/IL7 exhibited heightened activation, degranulation, cytokine release, and, ultimately, enhanced cytotoxicity against OS cell lines. Next, to determine the ability of the experimental cohorts to eradicate tumors *in vivo*, we inoculated 143B cells into NSG mice. After 14 days, the mice were randomly divided into 6 groups. The PBS, Mock, or CAR transduced T cells were injected intravenously (i.v.) through a tail vein into the respective groups of mice. The imaging of the implanted tumors was carried out with an IVIS every few days (Figure 5A). The CAR-T cell-treated mice receiving five million cells/mouse were able to control tumor growth as

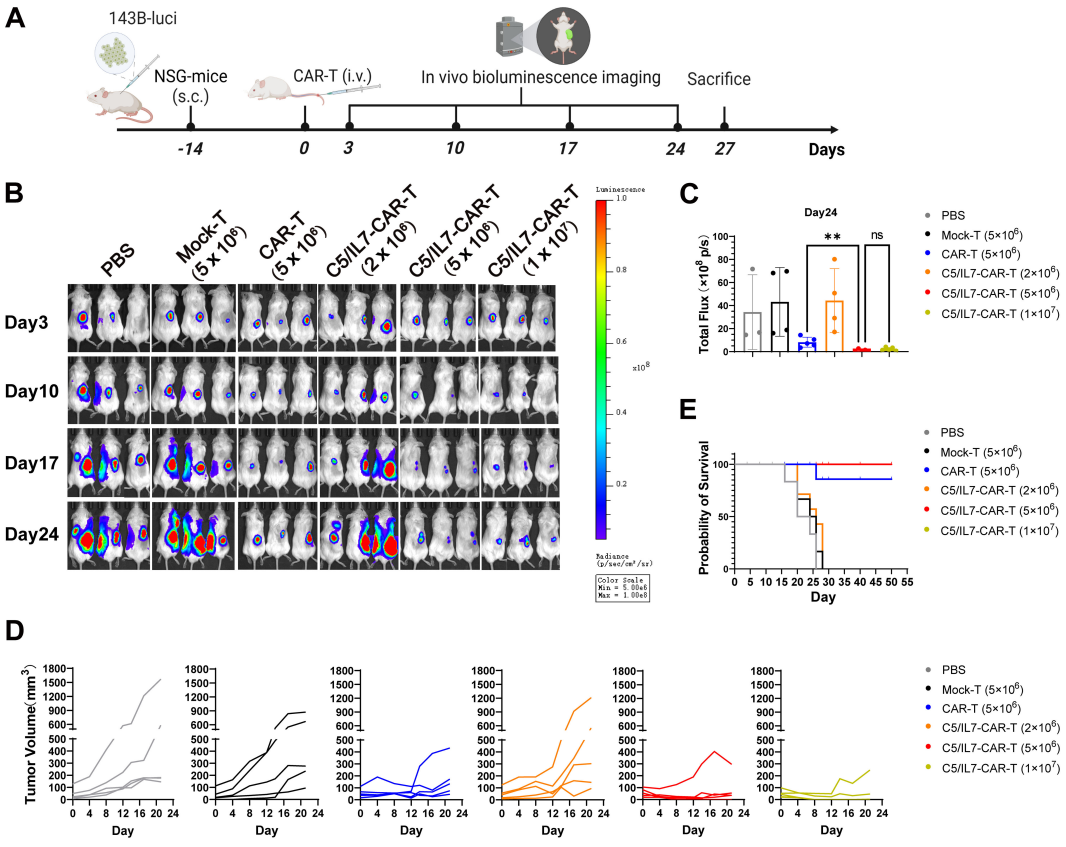

FIGURE 5
C5/IL7-CAR-T cells express advanced and enhanced antitumor activity *in vivo*. **(A)** Schematic representation of *in vivo* experimental design. NSG mice were subcutaneously (s.c.) inoculated with $2x10^6$ 143B-luciferase cells/mouse; Mice were randomly divided into 6 experimental groups (n=6), receiving treatments of PBS, Mock-T ($5x10^6$), CAR-T ($5x10^6$), and C5/IL7-CAR-T with varying cell numbers ($2x10^6$, $5x10^6$, $1x10^7$) cells/mice. **(B)** *In vivo*, bioluminescence imaging was employed to assess the progression of 143B-Luciferase+ tumors in each experimental group on days 3, 10, 17, and 24 (n=5). **(C)** On day 24, the total bioluminescence flux (photons per second) emitted by tumors was quantified through bioluminescence imaging. **(D)** Tumor volume was assessed at 3-day intervals using calipers. Each line on the graph represents the dynamic representation of tumor volume for an individual mouse (n=5). **(E)** Kaplan-Meier survival curve visually depicted the overall survival data for mice in each experimental group (n=6). Statistical significance was assessed using one-way ANOVA Tukey's test. **$p < 0.01$ and ns is non-significant.

compared to the Mock-T cell and PBS. The C5/IL7-CAR-T did not provide significant tumor control at a dose of 2 million cells per mouse. C5/IL7-CAR-T cells had better antitumor efficacy than conventional CAR-T cells at the same dose. Furthermore, doubling this dose did not improve tumor control (Figures 5B-D; Supplementary Figures 6, 7), yet the mice survived until the last observation day (Day 50) (Figure 5E). Previously, several safety concerns were raised in NKG2D-based CAR-T cell systems in OS xenograft models (7, 24). The results of ferritin, IFN-γ, and IL-8 analysis in the blood of experimental mice further support the safety of NKG2D-based CAR-T cell therapy in the OS model (Supplementary Figure 8). The results here demonstrated that in human OS mouse xenografts, mice receiving novel CAR-T cells outclassed wild-type CAR-T cells. The enhanced killing capacity of novel CAR-construct *in vivo* might correspond to the enhanced migration/tumor infiltration as well as survival ability of transduced T cells.

3.6 C5/IL7 improves CAR-T cell numbers and activities *in vivo*

Next, we wanted to determine the quantity and quality of the T lymphocytes (TILs) in experimental groups. We sought to assess the impact of co-expressing C5/IL7 in CAR-T cells. After staining with anti-human CD3 FACS antibodies and subsequent flow cytometry analysis, we observed a substantial increase in CD3+ cells within the tumor of the C5/IL7-CAR-T receiving mice group, as shown in Figure 6A. Similar results were obtained for splenic CD3 + T cells (Supplementary Figure 9). The mechanism underlying this effect might be rooted in the homing properties of CXCR5, which facilitate the directed migration of T cells (11, 25, 26). Additionally, functional analysis revealed that the C5/IL7-CAR-T cells exhibited superior cytokine production, particularly IFN-γ release, compared to that of wild-type CAR-T cells (Figure 6B). Moreover, FACS analysis revealed a notable decrease in exhaustion (Figure 6C) and an increase in the proportion of Tscm populations within the CD3 gate (Figure 6D; Supplementary Figure 10). Our novel CAR construct improved the survival of transduced T cells inside the tumor microenvironment (Figure 6E). The data in this figure explicitly demonstrate the superior performance of C5/IL7-CAR-T cells in terms of numbers at the tumor site, cytokine release, and survival in a murine model. The combination of CXCR5 and IL-7 co-expression in CAR-T cells not only augments quantity but also enhances the quality of T cells, thereby contributing to an enhanced antitumor immune response in the OS microenvironment (27).

3.7 C5/IL7 regulated CAR-T cell function via pSTAT5 signaling

To better understand the underlying molecular mechanisms, we focused on the STAT5 signaling pathway, which is known for its role in T cell functions. Flow cytometry data revealed that, compared with wild-type CAR transduced cells, C5/IL7-CAR transduced cells exhibited increased expression of phosphorylated STAT5 both in primary T cells and Jurkat cells. (Figure 7A; Supplementary Figure 11). Inhibition of STAT5 signaling in the C5/IL7-CAR cohort by Stafia-1 reversed the observed increase in STAT5 expression to a level equivalent to that of CAR-T cells (Figure 7A). To determine the role of STAT5 signaling in enhancing the functionality of C5/IL7-CAR-T cells, we employed a STAT5 inhibitor and detected different functional markers in the experimental cohorts via flow cytometry. Stafia-1 treatment decreased the levels of GzmB, INF-γ, and Ki67 markers in C5/IL7-CAR-T cells (Figures 7B-D). Moreover, the enhanced cytotoxic ability of C5/IL7-CAR-T cells was also diminished in the presence of the Stafia-1, as determined by cytotoxicity analysis (Figure 7E). These results underscore the critical role of C5/IL7 incorporation in CAR-T cell functionality.

4 Discussion

CAR-T cell therapy has achieved significant success in the treatment of blood cancers, yet its effectiveness in solid tumors has been constrained. While several factors contribute to this issue, the limited infiltration and survival of both CAR-T cells and native immune cells within the tumor microenvironment play fundamental roles in suboptimal antitumor immunity (28). In the current study, we utilized pre-synthesized CD3ζ and 4-1BB-based second-generation NKG2D-CAR systems. Additionally, we constructed a C5/IL7-CAR and compared its immunotherapeutic potential with that of conventional CAR. It was reported in some studies (although negated by others) that the second-generation CAR system outperformed the third-generation CAR system by providing a more potent antitumor response under certain circumstances (29, 30). The fact that CXCR5 and IL-7 were supposed to improve CAR-T cell numbers and activities, respectively (8, 11, 31, 32), a novel CAR co-expressing C5/IL7 was constructed. The C5/IL7-CAR transduced T cells demonstrated heightened expression of both CXCR5 and IL-7.

Osteosarcoma is the most common cancer in children and teenagers. The pursuit of novel and effective targets for CAR-T therapy in OS remains ongoing. For example, during this exploration, HER2-directed CAR-T cells achieved excellent results in preclinical studies while others are undergoing clinical trials (10). Here, we report a high expression of MICA/B in human OS cell lines U-2 OS and 143B cells, which is consistent with previously reported data (33). That is why NKG2D-based CAR-T cells demonstrated enhanced killing of OS *in vitro* compared to Mock-transduced T cells. Interestingly, C5/IL7-CAR-T cells not only displayed superior migration but also outperformed previous approaches involving CXCR5 and EGFR-based CAR-T cells, where no improvement in *in vitro* cytotoxicity was observed (11). The increased cytotoxic potential of NKG2D-based CAR-T cells *in vitro* in the current study, together with enhanced activation (CD69), degranulation (CD107a and GzmB), and cytokine release (IFN-γ) induced by C5/IL7 co-expression might owe to IL-7 signaling (34). Importantly, our *in vivo* observations mirrored the *in vitro* findings, with consistent patterns of tumor control. The tumor volume in mice receiving C5/IL7-CAR-T cells was significantly smaller than that in mice treated

10.3389/fimmu.2024.1462076

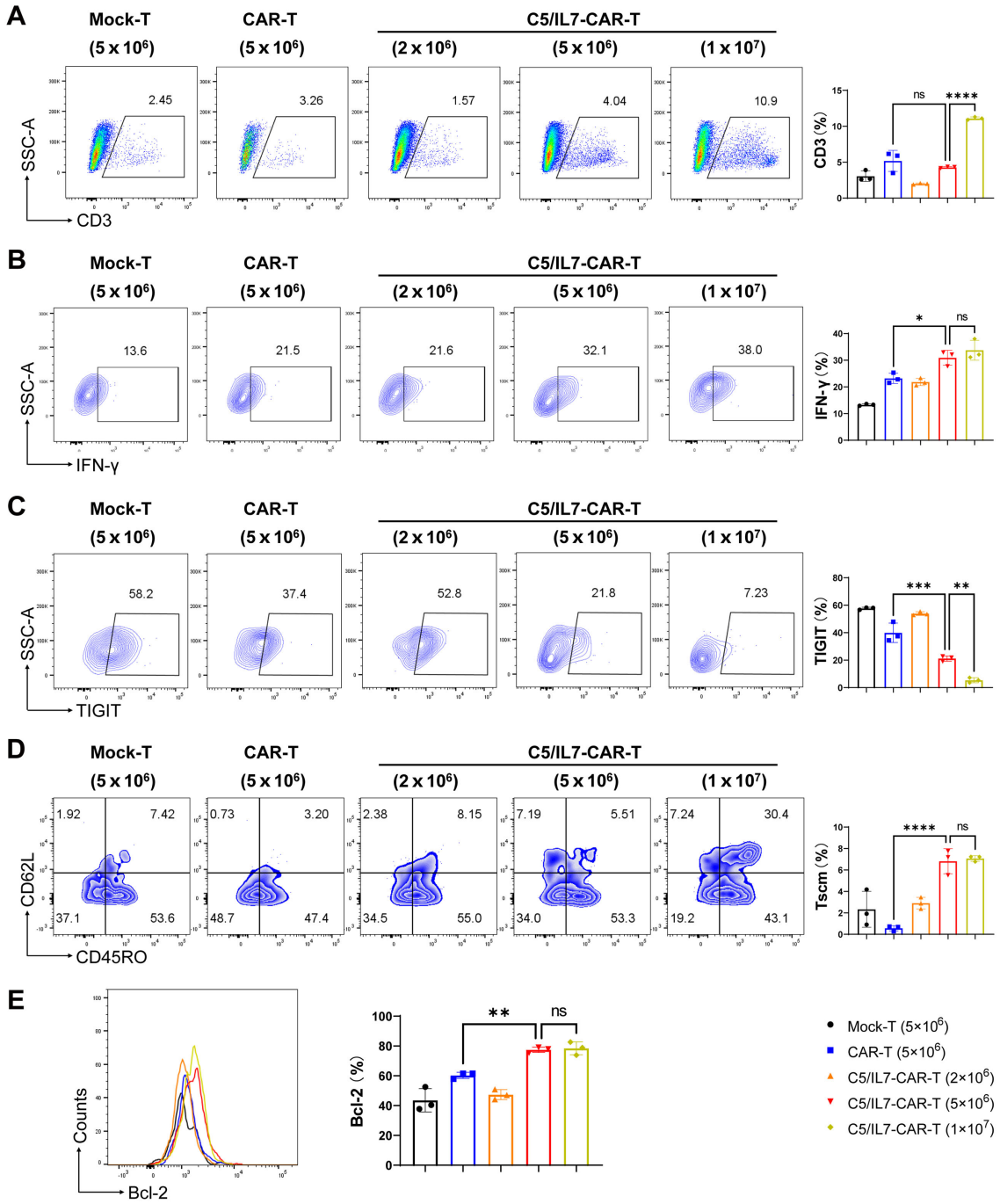

FIGURE 6
C5/IL7-CAR-T cells displayed better migration and survival *in vivo*. Mice were sacrificed on day 27 post-treatment; tumors were extracted, and single-cell suspensions were prepared for detailed immuno-profiling using flow cytometry analysis (n=3). The assessment encompassing: **(A)** $CD3^+$ T cells were quantified through staining with BV421 anti-human CD3 antibody, **(B)** IFN-γ levels were assessed by staining with APC anti-human IFN-γ antibody, **(C)** TIGIT expression was examined by BV421 anti-human TIGIT antibody, **(D)** T cell differentiation status was characterized through staining with PE anti-human CD45RO, AF700 anti-human CD62L and BV421 anti-human CD3 antibodies. **(E)** Bcl-2 expression was analyzed after intracellular staining with PE anti-human Bcl-2 antibody. Each experiment was conducted independently. FACS analysis files are presented in the left panel, while the corresponding column chats on the right. Statistical significance was measured using way one-way ANOVA. *p < 0.05, **p < 0.01, ***p < 0.001, ****p < 0.0001 and ns is non-significant.

with wild-type CAR-T cells, together with an increased number of CAR-T cells at the tumor sites.

The microenvironment of solid tumors is extremely hypoxic due to inadequate blood supply and overwhelmed oxygen demand (35). Additionally, nutrient deprivation and upregulation of coinhibitory ligands further complicate the picture. As a result, T cells in the tumor microenvironment become exhausted and are prone to apoptosis (3). The exhaustion phenomenon is characterized by the upregulation of

10.3389/fimmu.2024.1462076

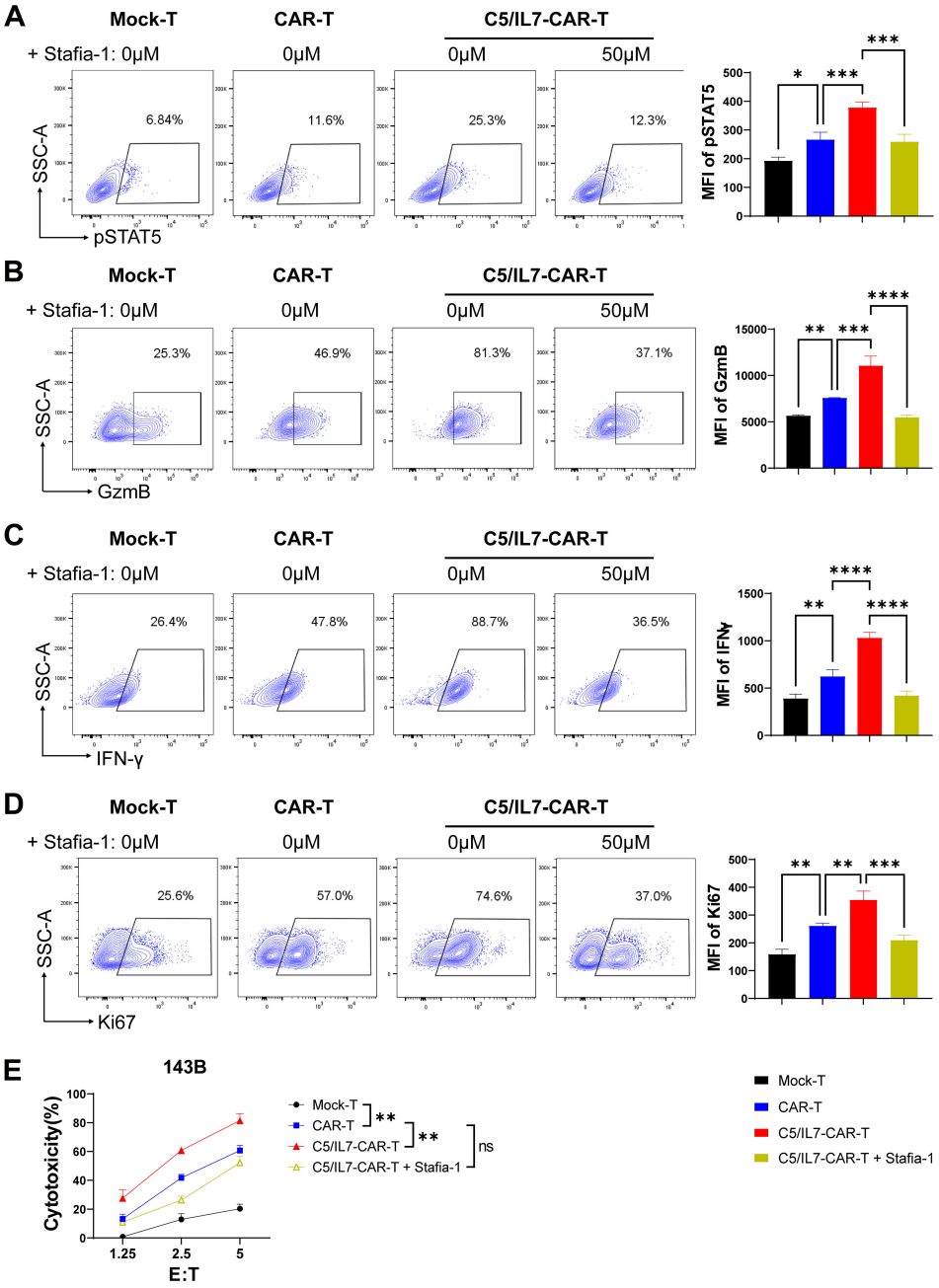

FIGURE 7
C5/IL7-CAR-T cells exhibit antitumor activity via pSTAT5 signaling. **(A–D)**, Mock-T, CAR-T, and C5/IL7-CAR-T cells, treated with either DMSO or Stafia-1 (50μM), were co-incubated with 143B cells for 24 hours at an E: T ratio of 3:1. Cells were then stained with FACS antibodies to detect pSTAT5 **(A)**, GzmB **(B)**, IFN-γ **(C)** and Ki67 **(D)** expression using flow cytometry. Representative FACS files are indicated on the left, and MFI bar graphs are shown on the right. **(E)**, Mock-T, CAR-T, C5/IL7-CAR-T and Stafia-1 treated C5/IL7-CAR-T cells were co-cultured with 143B-luciferase cells at various E: T ratios (1.25:1, 2.5:1 and 5:1) for 16-hours. Cytotoxicity was quantified using a luciferase assay. Experiments were performed independently at least 3 times. One-way ANOVA was used in Tukey's multiple comparison test, and data represent Mean ± SD. *P < 0.05, **P < 0.01, ***P < 0.001, ****P < 0.0001, ns, not significant.

checkpoint molecules, loss of ability to secrete effector cytokines, and decreased proliferative ability (36). Our data demonstrated that CAR-T cells coupled with CXCR5 and IL-7 reduced the expression of checkpoint molecules *in vitro*. Concomitantly, C5/IL7-CAR-T cells in the osteosarcoma microenvironment displayed low TIGIT expression and were able to express more IFN-γ in the NSG mouse model. Furthermore, increased expression of Bcl-2 in C5/IL7-CAR-T cells further suggested that these cells are more resilient and capable of sustaining their antitumor function than their wild-type counterparts are. C5/IL7-CAR-T cells exhibited significantly greater proliferation rates than did the other CAR-T cells, suggesting that C5/IL7-CAR-T cells more rapidly expanded in response to tumor cells. Moreover,

these cells displayed an increased CD8/CD4 ratio and Tscm phenotype, indicating a more favorable immune cell composition for CAR-T cell therapy.

STAT5 signaling is important for the survival of T lymphocytes at tumor sites. Previous studies have demonstrated that an increased STAT5 signaling can improve immunotherapeutic outcomes and hence provide better antitumor control (13, 37). In the current study, C5/IL7-CAR-T cells exhibited heightened STAT5 expression than did conventional CAR-T cells. The beneficial effects of C5/IL7 incorporation into CAR-T cells regarding proliferation, cytokine release, and cytotoxicity were diminished in the presence of Stafia-1. This fully demonstrates the importance of the STAT5 signaling pathway for CAR-T function. In the tumor microenvironment, effector T cells are typically in a state of high exhaustion, and rapid proliferation and viability maintenance of CAR-T cells can compensate for the over-exhaustion and depletion of effector T cells, resulting in better tumor clearance (38). IL-7 is a key factor in T function, and when IL-7 binds to its receptor, it can activate the JAK1 and JAK3 proteins in the cell, thereby phosphorylating the STAT3 and STAT5 proteins, forming heterodimers to enter the nucleus, activate the expression of downstream genes, and enhance the function of T cells. We also tested the STAT3 signaling pathway, which was expressed at very low levels, demonstrating that IL-7 is a STAT5 signaling pathway that promotes CAR-T cell proliferation, differentiation, and anti-apoptosis (39).

Overall, the current study suggests that C5/IL7 co-expression improves the efficacy of CAR-T cell therapy for OS. This new strategy provides a dual benefit by increasing the number and viability of transduced T cells. However, some potential limitations of the basic research include tumor immune evasion, as well as tumor heterogeneity and spread. Further improvements are necessary for the full implementation of this innovative CAR-T cell therapy in clinical translations. We will further use the osteosarcoma orthotopic model and PDX model, in combination with immune checkpoint blockade therapy, for further preclinical validation. In addition, our laboratory has also made some progress in overcoming tumor microenvironment-mediated immunosuppression for CAR-T cell therapy (13, 14). Only by combining these we can achieve the clinical translation.

5 Conclusions

In conclusion, the co-expression of CXCR5 and IL-7 in NKG2D-CAR-T cells holds promise for optimizing CAR-T cell therapy for osteosarcoma. The combined evidence from our *in vitro* and *in vivo* experiments demonstrated the multifaceted benefits of this approach, including improved cytotoxicity, resilience, and long-term persistence, which are critical for the success of immunotherapy against solid tumors. Further research and clinical investigations are warranted to fully grasp this innovative CAR-T cell therapy's potential.

Data availability statement

The original contributions presented in the study are included in the article/Supplementary Material. Further inquiries can be directed to the corresponding author.

Ethics statement

The animal study was approved by Institutional Animal Care and Use Committee of East China Normal University. The study was conducted in accordance with the local legislation and institutional requirements.

Author contributions

WJ: Conceptualization, Funding acquisition, Project administration, Supervision, Writing – review & editing. XH: Data curation, Formal analysis, Investigation, Methodology, Software, Validation, Writing – review & editing. MF: Formal analysis, Investigation, Software, Writing – original draft. YC: Data curation, Methodology, Writing – review & editing. IA: Formal analysis, Software, Writing – review & editing. YR: Writing – review & editing. MX: Formal analysis, Methodology, Writing – review & editing. YJ: Data curation, Methodology, Writing – review & editing. BD: Data curation, Methodology, Writing – review & editing. SW: Conceptualization, Investigation, Writing – review & editing.

Funding

The author(s) declare financial support was received for the research, authorship, and/or publication of this article. This work was supported by the Science and Technology Commission of Shanghai Municipality (21S11906200, 201409002900), the National Natural Science Foundation of China (81771306), the National Key Research and Development Program of China (2021YFF0702401), NMPA Key Laboratory for Quality Control of Therapeutic Monoclonal Antibodies (2023-DK-01).

Acknowledgments

We thank the East China Normal University Multifunctional Platform for Innovation (011) and the Instruments Sharing Platform of the School of Life Sciences, East China Normal University. We also express gratitude to teacher Yin Zhang for guiding us in the flow cytometry experiment.

Conflict of interest

The authors declare that the research was conducted in the absence of any commercial or financial relationships that could be construed as a potential conflict of interest.

Publisher's note

All claims expressed in this article are solely those of the authors and do not necessarily represent those of their affiliated organizations, or those of the publisher, the editors and the reviewers. Any product that may be evaluated in this article, or claim that may be made by its manufacturer, is not guaranteed or endorsed by the publisher.

Supplementary material

The Supplementary Material for this article can be found online at: https://www.frontiersin.org/articles/10.3389/fimmu.2024.1462076/full#supplementary-material

References

1. Köksal H, Müller E, Inderberg EM, Bruland Ø, Wälchli S. Treating osteosarcoma with CAR T cells. *Scand J Immunol.* (2019) 89:e12741. doi: 10.1111/sji.12741

2. Gill J, Gorlick R. Advancing therapy for osteosarcoma. *Nat Rev Clin Oncol.* (2021) 18:609–24. doi: 10.1038/s41571-021-00519-8

3. Liu G, Rui W, Zhao X, Lin X. Enhancing CAR-T cell efficacy in solid tumors by targeting the tumor microenvironment. *Cell Mol Immunol.* (2021) 18:1085–95. doi: 10.1038/s41423-021-00655-2

4. Zhang Q, Zhang Z, Liu G, Li D, Gu Z, Zhang L, et al. B7-H3 targeted CAR-T cells show highly efficient anti-tumor function against osteosarcoma both. *Vitro vivo. BMC cancer.* (2022) 22:1124. doi: 10.1186/s12885-022-10229-8

5. Wang Y, Yu W, Zhu J, Wang J, Xia K, Liang C, et al. Anti-CD166/4-1BB chimeric antigen receptor T cell therapy for the treatment of osteosarcoma. *J Exp Clin Cancer Res.* (2019) 38:1–11. doi: 10.1186/s13046-019-1147-6

6. Fernández L, Metais JY, Escudero A, Vela M, Valentín J, Vallcorba I, et al. Memory T cells expressing an NKG2D-CAR efficiently target osteosarcoma cells. *Clin Cancer Res.* (2017) 23:5824–35. doi: 10.1158/1078-0432.CCR-17-0075

7. VanSeggelen H, Hammill JA, Dvorkin-Gheva A, Tantalo DG, Kwiecien JM, Denisova GF, et al. T cells engineered with chimeric antigen receptors targeting NKG2D ligands display lethal toxicity in mice. *Mol Ther.* (2015) 23:1600–10. doi: 10.1038/mt.2015.119

8. He C, Zhou Y, Li Z, Farooq MA, Ajmal I, Zhang H, et al. Co-expression of IL-7 improves NKG2D-based CAR T cell therapy on prostate cancer by enhancing the expansion and inhibiting the apoptosis and exhaustion. *Cancers.* (2020) 12:1969. doi: 10.3390/cancers12071969

9. Gao Y, Lin H, Guo D, Cheng S, Zhou Y, Zhang L, et al. Suppression of 4.1 R enhances the potency of NKG2D-CAR T cells against pancreatic carcinoma via activating ERK signaling pathway. *Oncogenesis.* (2021) 10:62. doi: 10.1038/s41389-021-00353-8

10. Zhu J, Simayi N, Wan R, Huang W. and microenvironmental barriers of osteosarcoma. *Cytotherapy.* (2022) 24:567–76. doi: 10.1016/j.jcyt.2021.12.010

11. Li G, Guo J, Zheng Y, Ding W, Han Z, Qin L, et al. CXCR5 guides migration and tumor eradication of anti-EGFR chimeric antigen receptor T cells. *Mol Ther Oncolytics.* (2021) 22:507–17. doi: 10.1016/j.omto.2021.07.003

12. Yang H, Zhao L, Zhang Y, Li FF. A comprehensive analysis of immune infiltration in the tumor microenvironment of osteosarcoma. *Cancer Med.* (2021) 10:5696–711. doi: 10.1002/cam4.4117

13. Zhou Y, Farooq MA, Ajmal I, He C, Gao Y, Guo D, et al. Co-expression of IL-4/IL-15-based inverted cytokine receptor in CAR-T cells overcomes IL-4 signaling in immunosuppressive pancreatic tumor microenvironment. *BioMed Pharmacother.* (2023) 168:115740. doi: 10.1016/j.biopha.2023.115740

14. Ajmal I, Farooq MA, Duan Y, Yao J, Gao Y, Hui X, et al. Intrinsic ADRB2 inhibition improves CAR-T cell therapy efficacy against prostate cancer. *Mol Ther.* (2024) 32:3539–57. doi: 10.1016/j.ymthe.2024.08.028

15. Gao Y, Zhan W, Guo D, Lin H, Farooq MA, Jin C, et al. GPR97 depletion aggravates imiquimod-induced psoriasis pathogenesis via amplifying IL-23/IL-17 axis signal pathway. *BioMed Pharmacother.* (2024) 179:117431. doi: 10.1016/j.biopha.2024.117431

16. Bruserud Ø, Tronstad KJ, Berge R. *In vitro* culture of human osteosarcoma cell lines: a comparison of functional characteristics for cell lines cultured in medium without and with fetal calf serum. *J Cancer Res Clin Oncol.* (2005) 131:377–84. doi: 10.1007/s00432-004-0650-z

17. Liu JF, Lee CW, Lin CY, Chao CC, Chang TM, Han CK, et al. CXCL13/CXCR5 interaction facilitates VCAM-1-dependent migration in human osteosarcoma. *Int J Mol Sci.* (2020) 21:6095. doi: 10.3390/ijms21176095

18. Suni MA, Maino VC, Maecker HT. Ex vivo analysis of T-cell function. *Curr Opin Immunol.* (2005) 17:434–40. doi: 10.1016/j.coi.2005.05.002

19. Baldanzi G. Immune checkpoint receptors signaling in T cells. *Int J Mol Sci.* (2022) 23:3529. doi: 10.3390/ijms23073529

20. He X, Xu C. PD-1: a driver or passenger of T cell exhaustion? *Mol Cell.* (2020) 77:930–1. doi: 10.1016/j.molcel.2020.02.013

21. Zhang Q, Bi J, Zheng X, Chen Y, Wang H, Wu W, et al. Blockade of the checkpoint receptor TIGIT prevents NK cell exhaustion and elicits potent anti-tumor immunity. *Nat Immunol.* (2018) 19:723–32. doi: 10.1038/s41590-018-0132-0

22. Fultang L, Booth S, Yogev O, Martins da Costa B, Tubb V, Panetti S, et al. Metabolic engineering against the arginine microenvironment enhances CAR-T cell proliferation and therapeutic activity. *Blood.* (2020) 136:1155–60. doi: 10.1182/blood.2019004500

23. McBride JA, Striker R. Imbalance in the game of T cells: What can the CD4/CD8 T-cell ratio tell us about HIV and health? *PloS pathogens.* (2017) 13:e1006624. doi: 10.1371/journal.ppat.1006624

24. Lin Z, Wu Z, Luo W. Chimeric antigen receptor T-cell therapy: the light of day for osteosarcoma. *Cancer.* (2021) 13:4469. doi: 10.3390/cancers13174469

25. Bunse M, Pfeilschifter J, Bluhm J, Zschummel M, Joedicke JJ, Wirges A, et al. CXCR5 CAR-T cells simultaneously target B cell non-Hodgkin's lymphoma and tumor-supportive follicular T helper cells. *Nat Commun.* (2021) 12:240. doi: 10.1038/s41467-020-20488-3

26. Wang J, Jiang Y, Luo M, Lu W, He J, Zhang M, et al. Phase I clinical trial of CD19 CAR-T cells expressing CXCR5 protein for the treatment of relapsed or refractory B-cell lymphoma. *Curr Cancer Drug Targets* (2024). doi: 10.2174/0115680096304530240816111936

27. Klebanoff CA, Gattinoni L, Torabi-Parizi P, Kerstann K, Cardones AR, Finkelstein SE, et al. Central memory self/tumor-reactive CD8+ T cells confer superior antitumor immunity compared with effector memory T cells. *Proc Natl Acad Sci U S A.* (2005) 102:9571–6. doi: 10.1073/pnas.0503726102

28. Martinez M, Moon EK. CAR T cells for solid tumors: new strategies for finding, infiltrating, and surviving in the tumor microenvironment. *Front Immunol.* (2019) 10:128. doi: 10.3389/fimmu.2019.00128

29. Zhong XS, Matsushita M, Plotkin J, Riviere I, Sadelain M. Chimeric antigen receptors combining 4-1BB and CD28 signaling domains augment PI3kinase/AKT/Bcl-XL activation and CD8+ T cell–mediated tumor eradication. *Mol Ther.* (2010) 18:413–20. doi: 10.1038/mt.2009.210

30. Till BG, Jensen MC, Wang J, Qian X, Gopal AK, Maloney DG, et al. CD20-specific adoptive immunotherapy for lymphoma using a chimeric antigen receptor with both CD28 and 4-1BB domains: pilot clinical trial results. *Blood.* (2012) 119:3940–50. doi: 10.1182/blood-2011-10-387969

31. Takada I, Hidano S, Takahashi S, Yanaka K, Ogawa H, Tsuchiya M, et al. Transcriptional coregulator Ess2 controls survival of post-thymic CD4+ T cells through the Myc and IL-7 signaling pathways. *J Biol Chem.* (2022) 298:102342. doi: 10.1016/j.jbc.2022.102342

32. Li L, Li Q, Yan ZX, Sheng LS, Fu D, Xu P, et al. Transgenic expression of IL-7 regulates CAR-T cell metabolism and enhances in *vivo* persistence against tumor cells. *Sci Rep.* (2022) 12:12506. doi: 10.1038/s41598-022-16616-2

33. Lu SM, Xiao P, Xue L, Che LH, Yang P, Li Y, et al. Prevalent expression of MHC class I chain-related molecule A in human osteosarcoma. *Neoplasma.* (2008) 55:266–72.

34. Zhou J, Jin L, Wang F, Zhang Y, Liu B, Zhao T. Chimeric antigen receptor T (CAR-T) cells expanded with IL-7/IL-15 mediate superior antitumor effects. *Protein Cell.* (2019) 10:764–9. doi: 10.1007/s13238-019-0643-y

35. Schurich A, Magalhaes I, Mattsson J. Metabolic regulation of CAR T cell function by the hypoxic microenvironment in solid tumors. *Immunotherapy.* (2019) 11:335–45. doi: 10.2217/imt-2018-0141

36. Gumber D, Wang LD. Improving CAR-T immunotherapy: Overcoming the challenges of T cell exhaustion. *EbioMedicine*. (2022) 77:103941. doi. doi: 10.1016/j.ebiom.2022.103941

37. Bell M, Gottschalk S. Engineered cytokine signaling to improve CAR T cell effector function. *Front Immunol*. (2021) 12:684642. doi: 10.3389/fimmu.2021.684642

38. Adachi K, Kano Y, Nagai T, Okuyama N, Sakoda Y, Tamada K. IL-7 and CCL19 expression in CAR-T cells improves immune cell infiltration and CAR-T cell survival in the tumor. *Nat Biotechnol*. (2018) 36:346–51. doi: 10.1038/nbt.4086

39. Mackall CL, Fry TJ, Gress RE. Harnessing the biology of IL-7 for therapeutic application. *Nat Rev Immunol*. (2011) 11:330–42. doi: 10.1038/nri2970

frontiers | Frontiers in Oncology

TYPE Original Research
PUBLISHED 18 October 2024
DOI 10.3389/fonc.2024.1417459

OPEN ACCESS

EDITED BY
Yang Wang,
Sichuan Academy of Medical Sciences and Sichuan Provincial People's Hospital, China

REVIEWED BY
Zhiyu Chen,
Chongqing Medical University, China
Jie Wen,
The First Affiliated Hospital of Hunan Normal University, China
Lukas Krasny,
Lonza (United Kingdom), United Kingdom
Malik Ihsan,
University of Lahore, Pakistan
Guo-sheng Zhao,
Chongqing Medical University, China

*CORRESPONDENCE
Brock A. Lindsey
blinds10@jh.edu

RECEIVED 15 April 2024
ACCEPTED 17 September 2024
PUBLISHED 18 October 2024

CITATION
Lacinski RA, Dziadowicz SA, Roth CA, Ma L, Melemai VK, Fitzpatrick B, Chaharbakhshi E, Heim T, Lohse I, Schoedel KE, Hu G, Llosa NJ, Weiss KR and Lindsey BA (2024) Proteomic and transcriptomic analyses identify apo-transcobalamin-II as a biomarker of overall survival in osteosarcoma.
Front. Oncol. 14:1417459.
doi: 10.3389/fonc.2024.1417459

Proteomic and transcriptomic analyses identify apo-transcobalamin-II as a biomarker of overall survival in osteosarcoma

Ryan A. Lacinski[1,2], Sebastian A. Dziadowicz[3,4], Clark A. Roth[5], Li Ma[3,4], Vincent K. Melemai[1], Brody Fitzpatrick[1], Edwin Chaharbakhshi[1], Tanya Heim[5], Ines Lohse[5], Karen E. Schoedel[6], Gangqing Hu[3,4], Nicolas J. Llosa[7], Kurt R. Weiss[5] and Brock A. Lindsey[7]*

[1]Department of Orthopaedics, West Virginia University School of Medicine, Morgantown, WV, United States, [2]West Virginia University Cancer Institute, West Virginia University School of Medicine, Morgantown, WV, United States, [3]Department of Microbiology, Immunology, and Cell Biology, West Virginia University School of Medicine, Morgantown, WV, United States, [4]Bioinformatics Core, West Virginia University School of Medicine, Morgantown, WV, United States, [5]Department of Orthopaedic Surgery, University of Pittsburgh, Pittsburgh, PA, United States, [6]Department of Pathology, University of Pittsburgh Medical Center, Pittsburgh, PA, United States, [7]Department of Orthopaedic Surgery, Johns Hopkins University School of Medicine, Baltimore, MD, United States

Background: The large-scale proteomic platform known as the SomaScan® assay is capable of simultaneously measuring thousands of proteins in patient specimens through next-generation aptamer-based multiplexed technology. While previous studies have utilized patient peripheral blood to suggest serum biomarkers of prognostic or diagnostic value in osteosarcoma (OSA), the most common primary pediatric bone cancer, they have ultimately been limited in the robustness of their analyses. We propose utilizing this aptamer-based technology to describe the systemic proteomic milieu in patients diagnosed with this disease.

Methods: To determine novel biomarkers associated with overall survival in OSA, we deployed the SomaLogic SomaScan® 7k assay to investigate the plasma proteomic profile of naive primary, recurrent, and metastatic OSA patients. Following identification of differentially expressed proteins (DEPs) between 2-year deceased and survivor cohorts, publicly available databases including Survival Genie, TIGER, and KM Plotter Immunotherapy, among others, were utilized to investigate the significance of our proteomic findings.

Results: Apo-transcobalamin-II (APO-TCN2) was identified as the most DEP between 2-year deceased and survivor cohorts (Log2 fold change = 6.8, P-value = 0.0017). Survival analysis using the Survival Genie web-based platform indicated that increased intratumoral *TCN2* expression was associated with better overall survival in both OSA (TARGET-OS) and sarcoma (TCGA-SARC) datasets. Cell-cell communication analysis using the TIGER database suggested that *TCN2*+ Myeloid cells likely interact with marginal zone and immunoglobin-producing B lymphocytes expressing the TCN2 receptor (CD320) to promote

their proliferation and survival in both non-small cell lung cancer and melanoma tumors. Analysis of publicly available OSA scRNA-sequencing datasets identified similar populations in naive primary tumors. Furthermore, circulating APO-TCN2 levels in OSA were then associated with a plasma proteomic profile likely necessary for robust B lymphocyte proliferation, infiltration, and formation of intratumoral tertiary lymphoid structures for improved anti-tumor immunity.

Conclusions: Overall, APO-TCN2, a circulatory protein previously described in various lymphoproliferative disorders, was associated with 2-year survival status in patients diagnosed with OSA. The relevance of this protein and apparent immunological function (anti-tumor B lymphocyte responses) was suggested using publicly available solid tumor RNA-sequencing datasets. Further studies characterizing the biological function of APO-TCN2 and its relevance in these diseases is warranted.

KEYWORDS

osteosarcoma, plasma, proteomics, transcobalamin-II, immunotherapy

1 Introduction

The current mainstay for clinical management of solid tumors, including the determination of cancer type and staging, is predicated on the analysis of tumor specimens collected through invasive biopsy and/or surgical resection (1). Recent characterization of these specimens through next-generation genomic sequencing technologies has not only helped guide the selection of targeted therapeutics in the age of personalized medicine and precision oncology (2–4), but has also been a major driver of cancer biomarker discovery (5, 6). The collection of tumor specimens for these analyses, however, can often pose critical challenges including obtaining sufficient sample quantity (biopsy), adequately characterizing tumors which have metastasized to multiple, often unresectable locations, and repeatedly monitoring therapeutic response over time (1).

Conversely, liquid biopsies, including the collection of patient blood, saliva, or urine, are diagnostic modalities offering inherent advantages over surgically collected tumor specimens. These advantages include their minimal invasiveness in addition to the possibility of serial sampling longitudinally throughout the course of disease (1, 7). The most comprehensively evaluated liquid biopsy to date is patient peripheral blood and its liquid (plasma, serum) and cellular components. Numerous biomarkers isolated from blood specimens including circulating tumor cells (CTCs) (8, 9), tumor exosomes (10, 11), and circulating tumor DNA (ctDNA) (12, 13) have offered invaluable insight into disease processes, prognosis, and therapeutic response for a variety of solid tumors (14, 15), including pediatric malignancies such as sarcoma (16–18).

Large-scale proteomic technologies (19), capable of simultaneously characterizing hundreds to thousands of proteins in these specimens, have also gained significant traction in the field of cancer biomarker research (20). While numerous techniques have been established (21, 22), next-generation aptamer-based multiplexed proteomic technology, first published by Gold et al. in 2010, has shown extraordinary promise. These aptamer-based platforms alleviate some of the inherent limitations of previous proteomic techniques such as mass spectrometry (MS) by offering increased sample throughput, larger dynamic ranges of detection, and lower average coefficients of variation, all while necessitating minimal sample volumes (23). The basis of this technology lies in the development of chemically modified aptamers, which form complex three-dimensional matrices with robust specificity to their target proteins. This new class of aptamers, known as Slow Off-rate Modified Aptamers (SOMAmers), are an evolution of the previously described short single-stranded oligonucleotides identified by Systemic Evolution of Ligands by Exponential (SELEX) enrichment in the early 1990s (23–25).

SOMAmers and the SomaScan® platform (26, 27), developed commercially by SomaLogic, Inc. (Boulder, CO, USA), have now been used to characterize a variety of cancers, including but not limited to hepatocellular carcinoma (28), colorectal cancer (29), pancreatic cancer (30), glioma (31), lung cancer (32), oral squamous cell carcinoma (33), and ovarian cancer (34). The platform has expanded its characterization from approximately 800 proteins in 2010 to well over 7000 proteins today, offering extensive insight into nearly all biological pathways relevant to human disease (35). Due to the SomaScan's wide ranging assessment of proteins involved in the immune system including cytokine signaling, signaling by interleukins, and immunoregulatory pathways, among others, the platform has even been used to identify circulating proteins associated with immunotherapy response in diseases such as melanoma (36). As immunotherapies begin to dominate the world of oncology, systemic assessments of the immune system,

in real time, are likely critical to monitor immunotherapeutic response and better predict clinical success. To our knowledge, no study has yet utilized the SomaScan® platform for proteomic biodiscovery in osteosarcoma (OSA).

OSA is the most common primary pediatric bone malignancy (37, 38). Patients with localized disease, treated with surgical resection and neoadjuvant/adjuvant multi-drug chemotherapy (39), display five-year survival rates greater than 75% (40, 41). Unfortunately, this rate decreases to approximately 25% in those with advanced disease, most commonly in the form of metastases to the lung (42). Numerous studies have been conducted to determine biomarkers of prognostic or diagnostic value in OSA using liquid biopsies (43–47). Of utmost relevance, serum biomarkers (48) including tumor necrosis factor (TNF) (49) and other interleukins (50), vascular endothelial growth factor (VEGF) (51–53) and angiogenin (ANG) (54), macrophage migration inhibitory factor (MIF) and T-Cell Immunoglobulin and Mucin Domain-Containing Protein 3 (TIM-3) (55), as well as various chemokines including C-X-C motif chemokine ligand (CXCL)4, CXCL6, and CXCL12 (56) have shown preliminary promise as diagnostic and/or prognostic biomarkers in this disease. Additionally, analysis of plasma proteomic profiles using surface-enhanced laser desorption/ionization-time of flight (SELDI-TOF) MS identified two proteins (amyloid protein A and transthyretin) involved in the innate immune system associated with positive response to chemotherapy (57). While limited in the robustness of their analyses, these studies ultimately support that characterization of the OSA systemic proteome can offer unique insight into disease progression, therapeutic response, and prognosis in this disease.

To determine novel biomarkers associated with overall survival in OSA, we utilized the SomaScan® 7k assay to investigate the plasma proteomic profile of primary, recurrent, and metastatic OSA patients. Plasma samples, isolated from patients with confirmatory diagnosis of OSA and treated at the University of Pittsburgh, Department of Orthopaedic Surgery, were processed and analyzed for the simultaneous quantification of over 7000 circulatory proteins (Figure 1A). Following the identification of differentially expressed proteins (DEPs) between 2-year deceased and survivor patient cohorts, various analyses were then conducted to suggest their biological relevance in OSA including investigation of publicly available bulk and single cell (sc)RNA-seq datasets, further associations with overall and progression free survival in solid tumors, as well as correlations with previously published biomarkers and gene signatures (Figure 1B).

2 Materials and methods

2.1 Patients, sample collection, and processing

The human subject research protocol and subject informed consent were reviewed and approved by the University of Pittsburgh Medical Center Institutional Review Board (IRB STUDY 19060152). According to IRB guidelines, informed consent was obtained from all participants (Table 1) before study entry. Peripheral blood specimens were collected from primary, recurrent, and metastatic OSA patients diagnosed from 2014-2021 via venipuncture into Cell-Free DNA BCT tubes (Cat. #218996, Streck, La Vista, NE, USA). Blood components (buffy coat, plasma) were then separated for storage following centrifugation, with time from sample collection to processing averaging 17.4 ± 3.6 hours (ranging 0.04 to 44.06 hours).

2.2 SomaLogic SomaScan® 7k assay

Profiling of the OSA proteome was performed using the SomaScan® 7k assay, a highly multiplexed aptamer-based proteomic technology capable of determining over 7,000 protein measurements, at SomaLogic headquarters according to a previous publication (58). Briefly, frozen OSA Streck plasma samples were thawed and then buffer exchanged twice into SomaLogic Assay Buffer using Zeba 7kDa MWCO spin desalting columns (Cat. #89882, Thermo Scientific, Waltham, MA, USA) according to manufacturer's instructions. These buffer-exchanged plasma samples (diluted to 20%, 0.5%, and 0.005%) were then placed in a 96-well plate with a mix of thousands of chemically modified aptamers called SOMAmer® Reagents. These SOMAmers®, consisting of a 5' fluorophore, photocleavable linker, and biotin on streptavidin-coated beads, form complex three-dimensional shapes which bind to epitopes on their target protein with high affinity and specificity. Following the formation of SOMAmer-protein complexes, unbound proteins are washed away, captured proteins are labeled with biotin, and the SOMAmer-protein complexes are released by photocleavage with ultraviolet light in a buffer containing an unlabeled polyanionic competitor. The biotin-labeled SOMAmer-protein complexes are captured on a second set of streptavidin-coated beads before releasing SOMAmer reagents in a denaturing buffer. The amount of available protein epitope is read by hybridizing the SOMAmer reagents in the SomaScan Assay eluate to complementary sequences on a DNA microarray. Here, fluorescence is measured as relative fluorescence units (RFUs) and reflects overall epitope abundance (Figure 1A). The RFU readout is normalized by three non-consecutive steps including hybridization control normalization, intraplate median signal normalization, and median signal normalization to a reference and then delivered in a tab-delimited text file (.adat extension) for analysis using SomaLogic's web-based tool known as DataDelve Statistics alongside the DataDelve Stats v1.0 User Guide. A T-test was used to compare the means of two groups (such as 2-year deceased and survivor cohorts). Considering the exploratory nature of our study and limited OSA patient samples analyzed, differentially expressed proteins (DEPs) between comparative groups were identified as having a Log2FC > 0.585 or < -0.585 and P-value < 0.05. Median normal patient plasma RFU measurements (provided by SomaLogic) for both APO- and HOLO-transcobalamin-II (TCN2) are graphed on the associated box plot and are representative of a healthy, control patient population derived from previous publication (58). Considering these median values were determined using normal patient ethylenediaminetetraacetic acid (EDTA)-plasma samples that had been centrifuged and stored

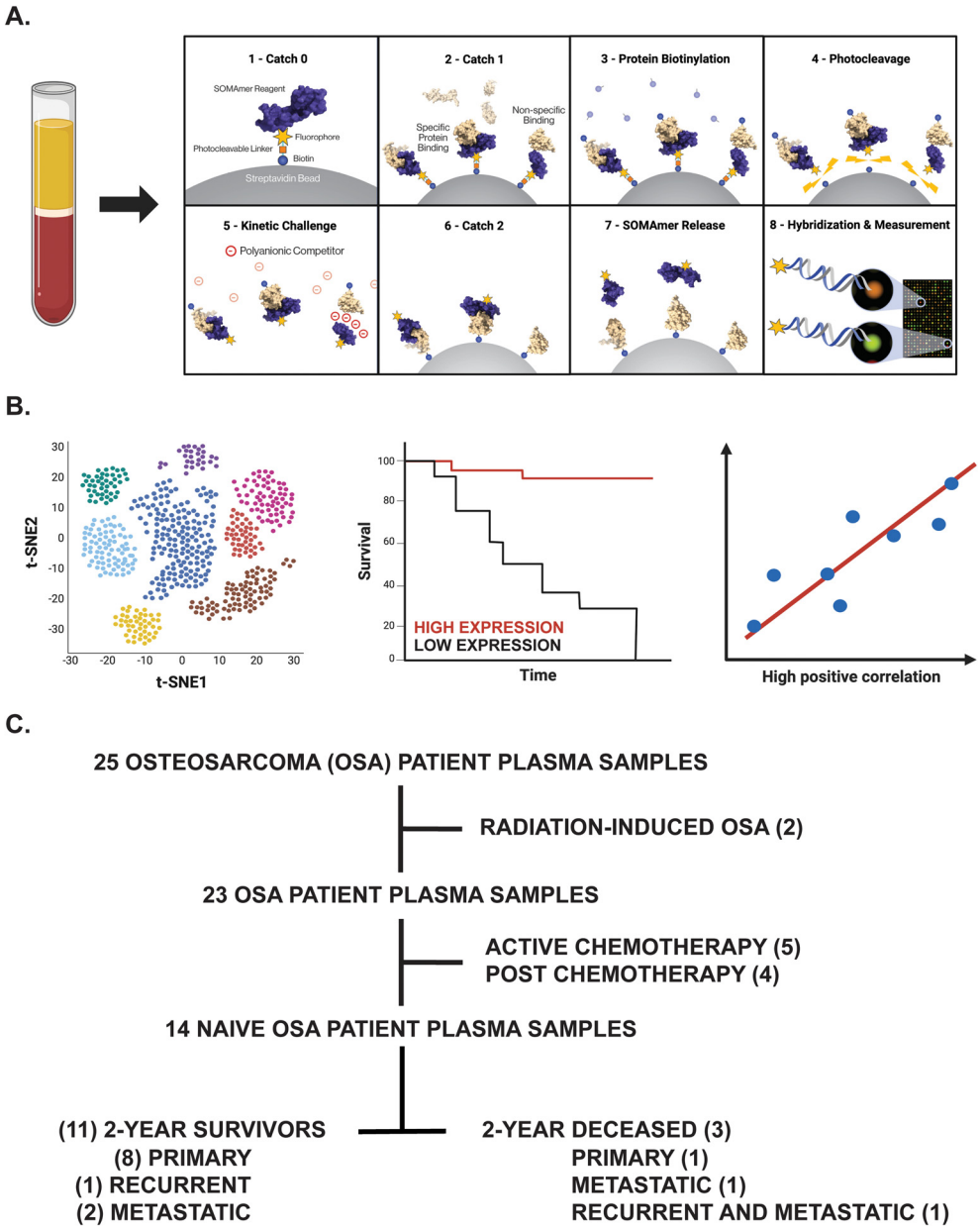

FIGURE 1
Overview of experimental design. **(A)** Proteomic investigation of OSA patient plasma samples using the SomaLogic SomaScan® 7k assay. Step-by-step process by which the SomaScan platform measures circulatory proteins (provided by SomaLogic Inc.). **(B)** Downstream analyses including cell identification using scRNA-seq analysis, overall survival analysis in publicly available datasets, and correlation analyses to support identified protein's role or association in solid tumors. Figure generated using BioRender.com. **(C)** Tree diagram depicting those OSA patient plasma samples selected for downstream analyses in this study.

2-10 hours post-blood collection (as opposed to the Streck-collected specimens analyzed here), they should only serve as a general guideline to the major findings from our analyses. A Volcano plot depicting those DEPs between comparative groups was generated using GraphPad Prism 10 (GraphPad Software, Boston, MA, USA).

2.3 Reactome pathway analysis

A pathway analysis of those DEPs between 2-year deceased and survivor cohorts (all OSA and advanced OSA cohorts) was conducted using the Reactome Pathway Analysis Tool (https://reactome.org/PathwayBrowser/, version 87) according to the Reactome User Guide (Docs – Analysis Tools) and previous publications (59–61). Briefly, all proteins with Log2FC > 0.585 or < -0.585 and P-value < 0.05 were inputted into the identifier list alongside their associated Log2FC. For consistency, proteins identified by the same SOMAmer, each with a unique sequencing ID, however, sometimes detecting multiple proteins [example seq.3714-49 quantifying both Creatine kinase M-type and Creatine kinase B-type heterodimer (P12277|P06732 or CKB|CKM)], were inputted in the identifier list multiple times with the

TABLE 1 Patient information for the 14 naive OSA patients analyzed within our proteomic biodiscovery analysis.

Patient	Sex	Vital Status	Age at sample collection	Treatment Status	Disease Status (complex)	Disease Status (simple)	2-year survival	Spin down time (hrs)
1	F	AWD	13.00	Naive	Primary	Primary	Yes	26.59
2	F	DWD	14.00	Naive	Metastatic	Advanced	No	27.16
3	M	AWD	14.00	Naive	Metastatic	Advanced	Yes	27.04
4	M	AWD	15.00	Naive	Primary	Primary	Yes	22.85
5	F	AWD	16.00	Naive	Primary	Primary	Yes	6.16
6	M	DWD	19.00	Naive	Recurrent	Advanced	Yes	0.04
7	F	DWD	19.00	Naive	Recurrent, metastatic	Advanced	No	3.93
8	M	AWD	20.00	Naive	Primary	Primary	Yes	30.52
9	F	AWD	21.00	Naive	Primary	Primary	Yes	4.87
10	M	AWD	22.00	Naive	Primary	Primary	Yes	8.27
11	M	AWD	32.00	Naive	Primary	Primary	Yes	28.85
12	F	AWD	33.00	Naive	Primary	Primary	Yes	6.78
13	M	DWD	47.00	Naive	Primary	Primary	No	44.06
14	M	DWD	69.00	Naive	Metastatic	Advanced	Yes	6.28

F - female, M - male, AWD - alive with disease, DWD - deceased with disease.

same corresponding Log2FC. Following data input and use of default analysis settings (projection to human without interactors), the pathway analysis results (.csv) and analysis report (pdf) were exported. A genome-wide overview plot is used to highlight the Reactome pathways over- (blue) or underrepresented (yellow) in the input dataset, with light grey signifying non-significant pathways. Significant Reactome pathways for the given data input were identified as having an FDR < 0.05.

2.4 Survival Genie overall survival and CIBERSORTx TIL correlation analysis

The Survival Genie web-interface (https://bhasinlab.bmi.emory.edu/SurvivalGenie/) was used for both overall survival and CIBERSORTx tumor-infiltrating lymphocyte (TIL) analyses according to the user guide and a previous publication (62). Briefly, single gene analyses [transcobalamin-II (*TCN2*), alpha 2-HS glycoprotein (*AHSG*)] were conducted using the National Cancer Institute (NCI) Therapeutically Applicable Research to Generate Effective Treatments-Osteosarcoma (TARGET-OS) and The Cancer Genome Atlas (TCGA)-Sarcoma (SARC) databases. Here, single gene normalized expression [fragments per kilobase of transcript per million mapped reads (FPKM)] from primary tumors is associated with overall survival through Cutp estimated martingale residuals (63) and patient stratification into low and high expressing groups using the survMisc package (64). Resulting Kaplan-Meier (KM) survival curves with high (red) and low (blue) group stratification are compared using the log-rank test, with log-rank P-value < 0.05 considered statistically significant (64). The provided Forest plot details the association between the high and low groups [stratified by cut point (CP)] based on the Cox Proportional Hazards regression model (survMisc package). Hazard ratio (HR) with 95% confidence interval as well as the associated Wald-test (HR) and log-rank (LR) P-values are reported (64). The relative fraction of TILs was estimated using the tumor-infiltrating immune cell type matrix LM22 gene signature from bulk tumor FPKM gene expression data and the CIBERSORTx deconvolution method (65). A Pearson correlation matrix of deconvoluted immune cell RNA-seq gene expression data and our genes of interest are reported. Shape (square or circle) denotes significance while color denotes positive (red) or negative (blue) correlation with the genes of interest (*TCN2*, *AHSG*).

2.5 TIGER scRNA-seq analysis

The Tumor Immunotherapy Gene Expression Resource (TIGER) portal (http://tiger.canceromics.org/#/) was used to investigate the target genes of interest [*TCN2*, transcobalamin receptor (*CD320*)] according to the user guide and a previous publication (66). Briefly, after inputting the genes of interest, the "Single-cell Immunity" tab was used to investigate gene expression across various scRNA-seq datasets of the TIGER database. Here, the Cell Type Marker (Log2FC) diagram represents differential expression of various clusters and subclusters in each scRNA-seq dataset of the TIGER database. These cells, organized by cancer type, dataset ID, main lineage, cell type, and Log2FC, were then sorted for highest Log2FC expression of the target genes. The top 20

clusters with increased gene expression were reported. After identifying the various cell types (myeloid, plasma, and B cells) and cancers [non-small cell lung cancer (NSCLC) – dataset NSCLC (67), NSCLC1 (68), NSCLC5 (69), NSCLC6 (70)], skin cutaneous melanoma (SKCM) – dataset SKCM1 (71)] with increased expression of the target gene(s), a subsequent cell-cell communication analysis was performed. Briefly, cell-cell communication in the NSCLC (67) and SKCM1 (71) datasets was investigated due to expression of both genes of interest (*TCN2*, *CD320*) across different cell types. Following navigation to the "Single-cell Immunity" tab and selection of the NSCLC dataset, a cell-cell communication analysis was conducted for the Mye_C1_CCL18 cluster (with greatest expression of *TCN2*) and the B_C10_MZB1 cluster (with greatest expression of *CD320*). The resulting heatmap displays the expression of all receptor-ligand interactions between any cell type of interest and its location [example – tumor, peritumoral (if applicable)]. The top three cell-cell interactions with the greatest total effect score are reported. Upon toggling the effect score between cell types of interest (example Mye_C1_CCL18 | B_C10_MZB1), the gene expression of the corresponding receptor-ligand interactions between those cells is displayed and sorted from greatest to least expression. For the top three cell-cell interactions, the top 20 receptor-ligand gene interactions (present intratumorally) and their expression were reported. A similar analysis was conducted for both the Mye_C4_C1QA (with greatest expression of *TCN2*) and the B_C2_IGHG1 (with greatest expression of *CD320*) of the SKCM1 dataset without responder/non-responder stratification (71).

2.6 scRNA-seq analysis of OSA tumor specimens

Raw OSA scRNA-seq data of GSE162454 (naive primary tumors) and GSE152048 (chemotherapy treated primary, recurrent, and metastatic tumors) were downloaded from the Gene Expression Omnibus (GEO) under their accession number. The FASTQ files were mapped to the GRCh38/hg38 reference genome using Cell Ranger (10X Genomics, Pleasanton, CA, USA, version 6.1.2). Individual cloupe files for each patient sample were then analyzed using the Loupe Browser (10X Genomics, version 7.0.1) according to the 10X Genomics Support guidelines. Briefly, each cloupe file was reanalyzed to filter barcodes through thresholds by Unique Molecular Identifiers (UMIs), threshold by Features, and mitochondrial UMIs. Considering the sheer heterogeneity of the processed samples, this filtering was performed on a sample-to-sample basis. On average, for the GSE162454 dataset, each sample was filtered by UMIs with a min = 666.67 ± 105.41 and max = 74166.67 ± 16654.16, threshold by Features with a min = 500.00 ± 0.00 and max = 9500.00 ± 500.00, and mitochondrial UMIs (%) with a min = 0.00 ± 0.00% and max = 31.33 ± 0.88%. This filtering resulted in approximately 10.3 ± 1.1% of barcodes removed from each sample (range 7.4-14.7%), in accordance with guidelines. On average, for the GSE152048 dataset, each sample was filtered by UMIs with a min = 502.18 ± 1.00 and max = 35000.00 ± 5680.91, threshold by Features with a min = 500.00 ± 0.00 and max = 5681.82 ± 527.74, and mitochondrial UMIs (%) with a min = 0.00 ± 0.00% and max = 20.91 ± 1.63%. This filtering resulted in approximately 13.0 ± 1.5% of barcodes removed from each sample (range 4.6-20.7%), again, in accordance with guidelines. Following barcode filtering, clusters were identified in each sample of both the GSE162454 and GSE152048 datasets according to canonical marker expression of the major cell types identified by Liu et al. in a previous publication including Myeloid cells 1/2 (*LYZ*, *CD68*), NK/T cells (*CD2*, *CD3D*, *CD3E*, *CD3G*, *GNLY*, *NKG7*, *KLRD1*, *KLRB1*), CAFS (*COL1A1*, *ACTA2*, *VIM*), Plasmocytes (*IGHG1*, *MZB1*), Osteoblastic OSA cells (*ALPL*, *RUNX2*, *IBSP*), Osteoclasts (*ACP5*, *CTSK*), Endothelial cells (*EGFL7*, *PLVAP*), and B cells (*MS4A1*, *CD79A*) (72). The expression of *TCN2* and *CD320* was then assessed across all major cellular clusters via visual inspection of t-distributed Stochastic Neighbor Embedding (t-SNE) plots before further downstream analysis. The expression of *TCN2* and *CD320* on Myeloid cells and Plasmocytes/B cells clusters, respectively, was then investigated. For quantification of *TCN2*+ Myeloid cells and *CD320*+ Plasmocytes and B cells, the "Feature Min" function of the Loupe Browser (displaying the minimum expression value of the features in each cluster's associated feature set when all features are expressed) was utilized. Here, for consistency across patient samples, only those cells expressing all features within a designated feature set (example: *TCN2*+ Myeloid cells with feature set *LYZ*, *CD68*, and *TCN2*) were quantified. Representative t-SNE plots with log normalized expression of the gene or feature gene set of interest are presented. In addition to total number of cells, the percent (%) of total cells and percent (%) of *TCN2*+ Myeloid cells (relative to all Myeloid cells) were calculated by dividing the cell population of interest by total number of filtered cells (barcodes) or by total number of Myeloid cells, respectively. Bar graphs quantifying abundance of various cell types across OSA specimens analyzed were generated using GraphPad Prism 10.

2.7 SomaLogic proteomic correlation analyses

Various correlations between plasma APO-TCN2 and previously described soluble markers of plasma cell maintenance (73) and B cell activation (74) [Interleukin (IL)-6, IL-6 receptor(R)a, IL-6Rb, CXCL12, TNF, IL2RA, TNF Superfamily Member 13b (TNFSF13B) or B-cell activating factor (BAFF), TNF Receptor Superfamily Member 13B (TNFRSF13B) or Transmembrane Activator and CAML Interactor (TACI), TNF Receptor Superfamily Member 17 (TNFRSF17) or B-cell maturation antigen (BCMA)], proteins critical for TLS formation [lymphotoxin alpha 1 beta 2 (LTa1b2), Fc Receptor Like 5 (FCRL5), Selectin L (SELL), TNF Superfamily Member 14 (TNFSF14)] (75), circulating immunoglobulin (Ig) levels (IgA, IgD, IgE, IgM, J chain, and IgG), as well as proteins of the 12-chemokine (12-CK) tertiary lymphoid structure (TLS) signature (75) [exception – CCL4 (not measured)] were conducted. Briefly, using GraphPad Prism 10, scatter plots representing all naive OSA patient samples (n = 14) with APO-TCN2 (RFU) on the x-axis and values of various other circulatory proteins (RFU) on the y-axis

were constructed. A Spearman correlation analysis was conducted using GraphPad Prism 10 with the correlation coefficient (R) and associated P-value (P) presented on each scatter plot.

2.8 KM Plotter Immunotherapy survival and correlation analysis

Using the Kaplan-Meier (KM) Plotter Immunotherapy online database (https://kmplot.com/analysis/), both *TCN2* and *CD320* were evaluated for overall and progression free survival in solid tumors (esophageal, gastric, head and neck, melanoma, lung, and urothelial cancer) treated with various immunotherapies (76). Specimens from all solid tumors, collected pre-treatment, irrespective of immunotherapy target [anti-programmed death cell protein 1 (PD-1), anti-programmed death ligand 1 (PD-L1), and anti-cytotoxic t-lymphocyte associated protein 4 (CTLA-4)], were included in both overall and progression free survival analysis using default KM Plotter settings (auto selection of best cutoff based on the calculation of all upper and lower quartiles with selection of the best performing threshold). For each gene of interest, a resulting KM plot was constructed with a reported HR, log-rank P-value, and FDR, with the y-axis representing probability of survival and the x-axis representing time (months). The total number of patients at risk for each time point is also reported. Similarly, an overall survival analysis was conducted for all chemokines of the 12-CK signature (75) using the same analysis parameters. Additionally, Spearman correlations between both *TCN2* and *CD320* with all chemokines of the 12-CK TLS signature including C-C Motif Chemokine Ligand (*CCL*)*2*, *CCL3*, *CCL4*, *CCL5*, *CCL8*, *CCL18*, *CCL19*, *CCL21*, *CXCL9*, *CXCL10*, *CXCL11*, *CXCL13* were also conducted. Due to an inherent limitation of the KM Plotter Immunotherapy database, a maximum of three genes of the 12-CK signature (in addition to either *TCN2* or *CD320*) were included within the same correlation analysis. Spearman correlation coefficients and P-values (* = $P < 0.05$, ** = $P < 0.01$, *** = $P < 0.001$, **** = $P < 0.0001$) were reported for all four-gene correlation matrices.

2.9 TCGA 12-CK signature correlation analysis

Using the Gene Expression Profiling Interactive Analysis 2 (GEPIA2) web server (http://gepia2.cancer-pku.cn/#index) (77), a multi-gene Spearman correlation analysis between either *TCN2* or *CD320* and the 12-CK TLS signature (75) was also performed. Two separate analyses using only the TCGA-SARC gene expression dataset or all tumor types of the TCGA were conducted. For each correlation analysis, the log2 of the transcript count per million [log2(TPM)] of the gene of interest (*TCN2* or *CD320*) was plotted on the x-axis while the log2(TPM) of the 12-CK gene signature is plotted on the y-axis. Importantly, while a log scale is used for graphical representation, the Spearman correlation is calculated on a non-log scale. The resulting Spearman correlation coefficients (R) and P-values are reported.

3 Results

3.1 Study design and patient stratification

Using the SomaLogic SomaScan® 7k assay, the plasma proteomic profile of primary, recurrent, and metastatic OSA patients was investigated. In total, 25 OSA patient plasma samples at various stages of disease and treatment status were processed in this analysis. Considering our group's inherent interest in tumor immunology, two radiation-induced OSA patient samples, five active chemotherapy patient samples, and four post-chemotherapy patient samples were excluded from downstream analysis to mitigate confounding influences to the OSA proteome. The remaining samples, representing 14 naive OSA patients collected at diagnosis (before standard of care chemotherapeutic and/or surgery regimens), were then stratified into 2-year deceased and survivor all comers cohorts (Figure 1C). Patient information including sex, vital status, treatment, disease, and 2-year survival status, in addition to Streck-plasma spin down time (hours) from blood collection to plasma isolation and frozen storage, are reported (Table 1).

3.2 Proteomic assessment of naive OSA patients reveals DEPs associated with 2-year survival status

All experimental patient plasma samples processed at SomaLogic's Boulder, CO facility passed standardized quality assessment and control (Supplementary File 1 – Supplementary Figure 1). The plasma proteomic profiles of the 2-year deceased (n = 3) and survivor (n = 11) patients from an all comers OSA cohort (n = 14) were then compared (Supplementary File 2). Importantly, a total of 24 human DEPs were identified from this analysis, including 10 significantly upregulated and 14 significantly downregulated in the 2-year survivor cohort (Figure 2A and Table 2). These 24 DEPs were then inputted into the Reactome Pathway Analysis tool. The Reactome genome-wide overview map highlighted overrepresentation of these 24 DEPs in various pathways involved in the Immune System, Signal Transduction, and Metabolism (Supplementary File 1 – Supplementary Figure 2). The most significant pathways (FDR < 0.05) and their enriched entities included those associated with FOXO-mediated transcription [catalase (CAT), resistin (RETN)], MAPK activation (IL-6R), Interleukin-6 signaling (IL-6R), and creatine metabolism [creatine kinase (CK)M, CKB] (Figure 2B).

Of the 24 individual DEPs, APO-TCN2 was the most significantly (P = 0.0017) upregulated protein associated with 2-year survival, reporting a Log2FC = 6.8. For n = 5 of total 11 patients in the 2-year survivor cohort, APO-TCN2 levels vastly exceeded median normal patient plasma RFU measurements (provided by SomaLogic) (58), with an additional two patients reporting well above minimal detectable levels. This finding contrasts with all three deceased patients, which measured near minimal detectable levels (Figure 2C). Interestingly, while the vitamin-B12 unbound

10.3389/fonc.2024.1417459

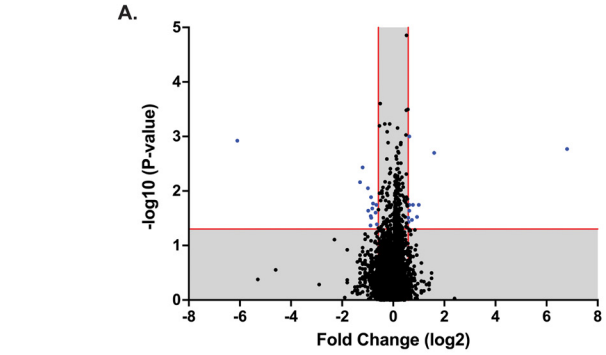

B.

Pathway identifier	Pathway name	#Entities found	#Entities total	P-Value	FDR
R-HSA-9615017	FOXO-mediated transcription of oxidative stress, metabolic and neuronal genes	4	49	3.83E-06	5.48E-04
R-HSA-9614085	FOXO-mediated transcription	4	110	8.88E-05	0.006307322
R-HSA-112411	MAPK1 (ERK2) activation	2	12	3.13E-04	0.012835285
R-HSA-110056	MAPK3 (ERK1) activation	2	13	3.67E-04	0.012835285
R-HSA-1059683	Interleukin-6 signaling	2	17	6.24E-04	0.017465828
R-HSA-71288	Creatine metabolism	2	25	0.001334694	0.030697961
R-HSA-112409	RAF-independent MAPK1/3 activation	2	28	0.001667562	0.03245642
R-HSA-6783589	Interleukin-6 family signaling	2	30	0.001909201	0.03245642

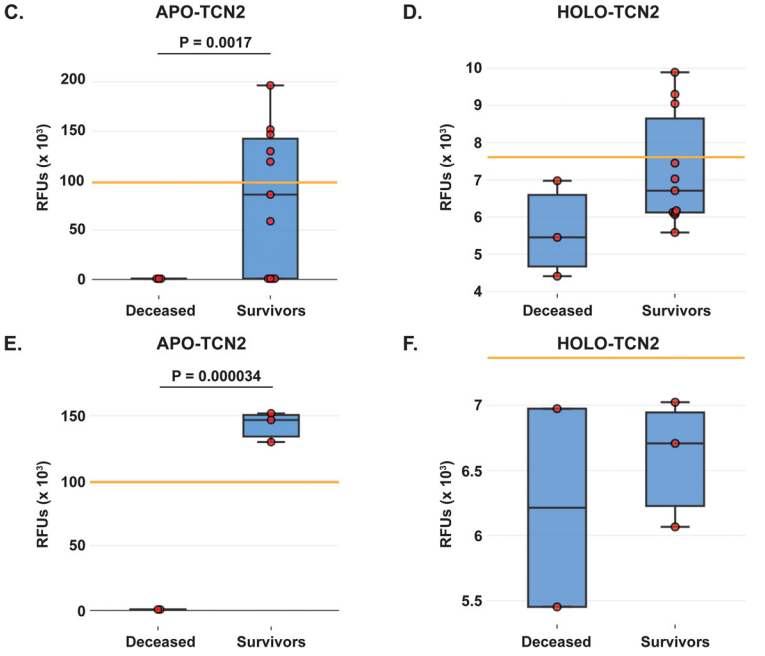

FIGURE 2
Proteomic analysis of naive OSA patients, stratified by 2-year survival status. **(A)** Volcano plot depicting those differentially expressed proteins (DEPs – blue) with a Log2FC > 0.585 or < -0.585 and P-value < 0.05. **(B)** Reactome analysis identifies those pathways associated with 2-year survival in OSA. Significant pathways include those with multiple entities and FDR < 0.05. Box plot depicting APO-TCN2 [seq.15560.52] **(C)** and HOLO-TCN2 [seq.5584.21] **(D)** levels in all naive OSA patients (n = 14) stratified by 2-year survival status, with n = 3 deceased and n = 11 survivors. Box plot depicting APO-TCN2 [seq.15560.52] **(E)** and HOLO-TCN2 [seq.5584.21] **(F)** levels in naive OSA patients with advanced disease (n = 5) stratified by 2-year survival status, with n = 2 deceased and n = 3 survivors. Each dot of the box plot is representative of an individual OSA patient. Y-axis represents the relative fluorescence units (RFUs) in thousands. Significant P-values (t-test) are presented for each comparison. Median values from assessment of plasma samples in a normal, healthy patient population (provided by SomaLogic, Inc.) are indicated by orange bar.

form of Transcobalmin-2 (APO-TCN2) differed vastly between 2-year deceased and survivor cohorts, no difference in the vitamin-B12 bound form (HOLO-TCN2) was measured (Figure 2D). Importantly, the lack of measurable differences in HOLO-TCN2 levels suggests that these OSA patients, likely, do not have a genetic *TCN2* alteration or abnormality, as previously reported in various case reports (78–81). Of note, a significant (P = 0.0012) decrease in Alpha-2-HS-glycoprotein (AHSG) was also associated with 2-year survival status, reporting a log2FC = -6.1 (Table 2). Furthermore, a secondary analysis comparing the proteome of 2-year deceased (n = 2) and survivors (n = 3) of the Advanced Disease sub-cohort (n = 5) further supported these findings. A significant (P = 0.000034) increase in plasma APO-TCN2 (Figure 2E), the most differentially upregulated protein in 2-year survivors, and no difference in HOLO-TCN2 levels (Figure 2F), was again associated with 2-year survival status. Similarly, AHSG levels were

TABLE 2 Differentially expressed proteins (DEPs) for the naive all OS 2-year survival comparison.

Sequence ID	Protein Name	UniProt ID	Gene Symbol	Log2FC	P-value
15560-52	Apo-Transcobalamin-2	P20062	TCN2	6.8	0.0017
19141-22	Death-associated protein 1	P51397	DAP	1.6	0.002
3714-49	Creatine kinase M-type:Creatine kinase B-type heterodimer	P12277|P06732	CKB|CKM	1	0.018
3488-64	Catalase	P04040	CAT	0.93	0.03
13534-20	Myomesin-2	P54296	MYOM2	0.73	0.034
11481-25	Hepatitis A virus cellular receptor 2	Q8TDQ0	HAVCR2	0.63	0.023
13691-10	Sodium-coupled monocarboxylate transporter 1	Q8N695	SLC5A8	0.63	0.018
4139-71	Interleukin-6 receptor subunit alpha	P08887	IL6R	0.63	0.001
15427-35	Lysyl oxidase homolog 3	P58215	LOXL3	0.6	0.037
15466-30	Collagen alpha-1(IX) chain	P20849	COL9A1	0.59	0.031
3216-2	Polymeric immunoglobulin receptor	P01833	PIGR	-0.64	0.041
13125-45	Vitronectin	P04004	VTN	-0.66	0.018
19323-1	Receptor-binding cancer antigen expressed on SiSo cells	O00559	EBAG9	-0.69	0.025
3199-54	Kallikrein-12	Q9UKR0	KLK12	-0.79	0.017
23569-53	START domain-containing protein 10	Q9Y365	STARD10	-0.82	0.021
12663-1	Thiosulfate sulfurtransferase	Q16762	TST	-0.86	0.031
3046-31	Resistin	Q9HD89	RETN	-0.87	0.013
17742-2	Ras-related protein R-Ras	P10301	RRAS	-0.88	0.029
13495-48	Hydroxycarboxylic acid receptor 2	Q8TDS4	HCAR2	-0.89	0.043
23259-23	EEF1A lysine methyltransferase 1	Q8WVE0	EEF1AKMT1	-0.98	0.023
4964-67	Endoplasmic reticulum aminopeptidase 1	Q9NZ08	ERAP1	-0.99	0.0089
15388-24	Low affinity immunoglobulin gamma Fc region receptor III-A	P08637	FCGR3A	-1.2	0.0037
12581-39	Inositol monophosphatase 2	O14732	IMPA2	-1.3	0.0069
10966-1	Alpha-2-HS-glycoprotein	P02765	AHSG	-6.1	0.0012

significantly (P = 0.026) reduced in the 2-year survival cohort (Supplementary File 3). Overall, a comparative proteomic analysis of OSA patient peripheral plasma identified 24 DEPs associated with 2-year survival status. Of those proteins, both APO-TCN2 and AHSG measured vastly increased or decreased levels in the survivor cohort, respectively. To further elucidate both proteins' relevance in OSA and other solid tumors, publicly available bulk and scRNA-seq tumor datasets were then examined.

3.3 Survival Genie analysis reveals association of elevated *TCN2* with overall survival in sarcoma

The Survival Genie web-based platform was then used to associate expression of *TCN2* and *AHSG* with overall survival in publicly available OSA (TARGET-OS) and sarcoma (TCGA-SARC) bulk tumor RNA-sequencing datasets (62). To begin, evaluation of *TCN2* expression in the TARGET-OS database identified 47 patients with low and 39 patients with high *TCN2* expression in OSA primary tumors. Using CIBERSORTx (65), a significant ($P \leq 0.05$) positive correlation between *TCN2* expression and T.cells.CD8, T.cells.follicular.helper, Macrophages.M1, T.cells.gamma.delta, T.cells.regulatory.Tregs, and Macrophages.M2 gene signatures was revealed. Additionally, a significant ($P \leq 0.05$) negative correlation between *TCN2* expression and Macrophages.M0, T.cells.CD4.naive, and NK.cells.resting gene signatures was also apparent. Importantly, Kaplan-Meier survival curve analysis associated an increase in intratumoral *TCN2* expression with better overall survival (log-rank P= 0.00033), with a reported HR = 0.22 (0.089 – 0.54) (Figure 3A). Considering a shared sarcomatous background, our group expanded the analysis to assess *TCN2* gene expression in the larger TCGA-SARC dataset to provide

rigor and support to the experimental findings uncovered in TARGET-OS. Analysis of the TCGA-SARC dataset identified 177 patients with low and 82 patients with high expression of *TCN2* in sarcoma primary tumors. Using CIBERSORTx (65), a significant ($P \leq 0.05$) positive correlation between *TCN2* expression and Macrophages.M2, T.cells.CD8, T.cells.CD4.memory.activated, and Macrophages.M1 was identified. Additionally, a significant ($P \leq 0.05$) negative correlation between *TCN2* expression and Macrophages.M0, T.cells.CD4.memory.resting, Eosinophils, and NK.cells.activated gene signatures was also apparent. Importantly, Kaplan-Meier curve survival analysis again associated an increase in *TCN2* expression with better overall survival (log-rank P = 0.0047), with a reported HR = 0.5 (0.31 – 0.82) (Figure 3B). These results suggest that increased intratumoral *TCN2* is associated with an activated immune signature and better overall survival. While a similar analysis revealed that low *AHSG* expression was associated with better overall survival in the TARGET-OS dataset (corroborating our proteomic findings), this trend was not apparent in the TCGA-SARC analysis, and neither finding was statistically significant. Therefore, AHSG was excluded from further downstream analysis (Supplementary File 1 – Supplementary Figure 3). Overall, Kaplan-Meier survival curve analysis associated elevated *TCN2* expression with significantly improved outcomes in both the TARGET-OS and TCGA-SARC datasets. Importantly, the association of increased intratumoral *TCN2* expression with better

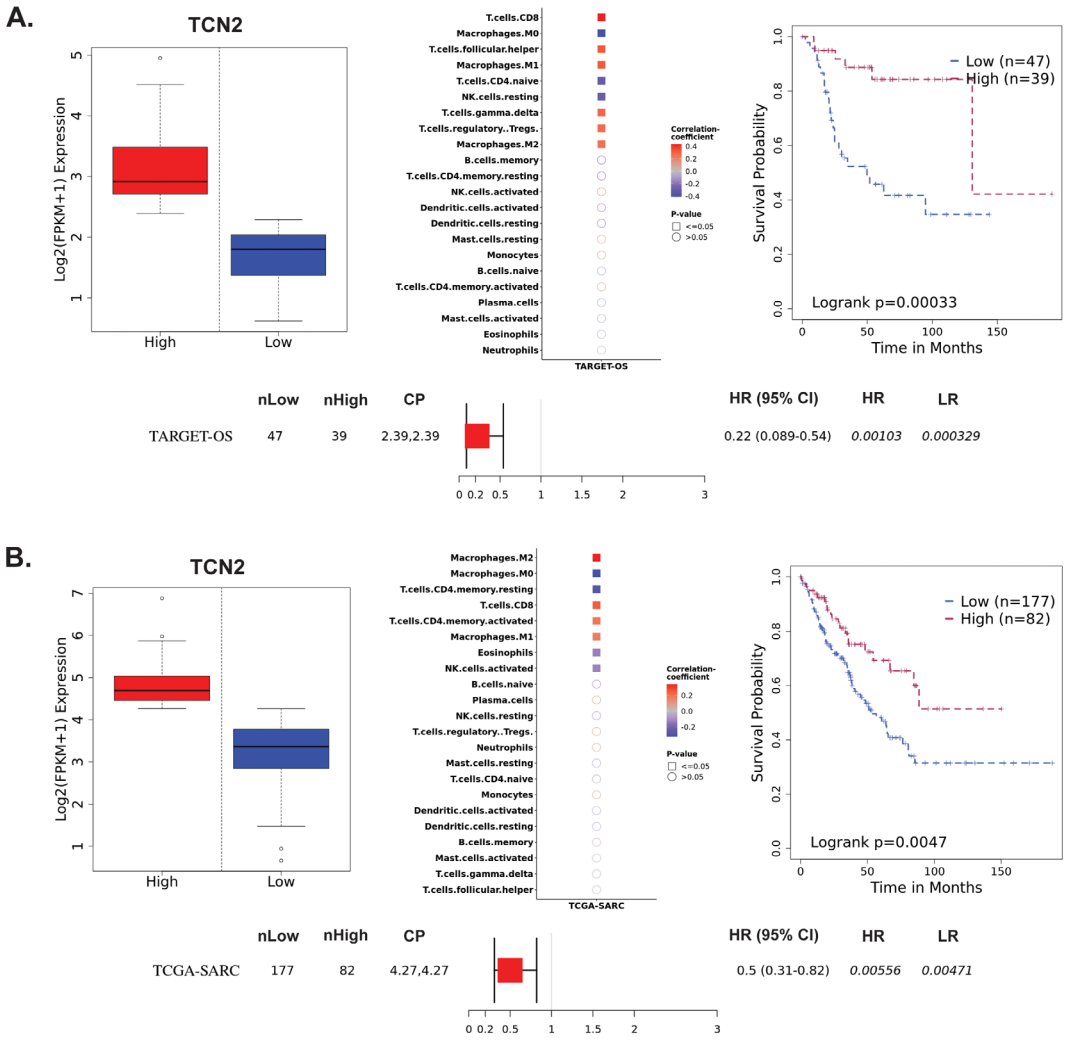

FIGURE 3
TARGET-OS and TCGA-SARC survival analysis supports TCN2 as a marker of better overall survival. Analysis of *TCN2* in TARGET-OS **(A)** and TCGA-SARC **(B)** databases using Survival Genie web-based platform. Box plots representing *TCN2* FPKM normalized expression in primary tumors with stratification into low and high expressing groups. The relative fraction of TILs was estimated using the tumor-infiltrating immune cell type matrix LM22 gene signature and CIBERSORTx deconvolution. Pearson correlation matrix of deconvoluted immune cell RNA-seq gene expression data and *TCN2*, with shape (square or circle) denoting significance and color denoting positive (red) or negative (blue) correlation with *TCN2*. Kaplan-Meier (KM) survival curves with high (red) and low (blue) group stratification are compared using the log-rank test, with log-rank P-value < 0.05 considered statistically significant. Forest plot details the association between the high and low groups [stratified by cut point (CP)] based on the Cox Proportional Hazards regression model. nLow and nHigh represent the number of patients in low and high expressing groups, respectively. Hazard ratio (HR) with 95% confidence interval as well as the associated Wald-test (HR) and log-rank (LR) P-values are reported.

overall survival correlated with our previous plasma proteomics findings (Figures 2B, D). These results ultimately support both peripheral blood plasma APO-TCN2 and intratumoral *TCN2* gene expression as possible biomarkers of overall survival in this disease.

3.4 TIGER reveals expression patterns of *TCN2* in solid tumors

The TIGER portal was then used to investigate the expression of *TCN2* across identified cellular clusters of various solid tumor scRNA-seq datasets (66). While previous analyses of bulk transcriptomic data through CIBERSORTx deconvolution had suggested the likely cellular source for *TCN2* gene expression in sarcomatous tumors, our group sought to determine which cells differentially expressed *TCN2* (for a variety of tumor types) using a method that provides single cell resolution to the complex and heterogenous tumor microenvironment (TME). Numerous cellular clusters across many solid tumors revealed differential expression of *TCN2* including non-small cell lung cancer (NSCLC), intrahepatic cholangiocarcinoma (ICC), breast cancer (BC), nasopharyngeal carcinoma (NPC), and skin cutaneous melanoma (SKCM), among others (Figure 4A). The top 20 cellular clusters with the greatest increase in *TCN2* expression were reported, highlighting apparent increases for B cell, Endothelial, and Myeloid cellular clusters, particularly in both NSCLC and SKCM datasets (Table 3). To visualize these expression changes, subsequent analysis of Uniform Manifold Approximation and Projections (UMAPs) and gene expression boxplots for the NSCLC dataset (67) confirmed isolated increases in *TCN2* expression on both Myeloid and Endothelial cellular clusters (Figures 4B, C). Subcluster analysis of the Myeloid cells revealed near ubiquitous expression of *TCN2* across myeloid populations, with the greatest increases apparent for the Mye_C1_CCL18 and Mye_C6_CCL18 subclusters (Figures 4D, E). Further visualization of the NSCLC6 (70) dataset supported increased *TCN2* expression on Endothelial, Plasma, AT2 Epithelial, and Myeloid cell populations (Figures 4F, G). Additional subcluster analysis of B cells revealed increased expression across B_C3_JCHAIN, B_C1_MZB1, and B_C7_MZB1 cellular clusters (Figures 4H, I), in accordance with the findings highlighted in Table 3. Similar results were also apparent for the SKCM1 dataset (71), which revealed increased *TCN2* expression on all Myeloid cells, various Myeloid cell subclusters including Mye_C4_C1QA, as well as the B_C2_IGHG1 B cell subcluster (Supplementary File 1 – Supplementary Figure 4). Overall, these data corroborated our Survival Genie CIBERSORTx data and previous literature (82) which suggested that *TCN2* is mainly expressed (in immune cells) on Myeloid populations.

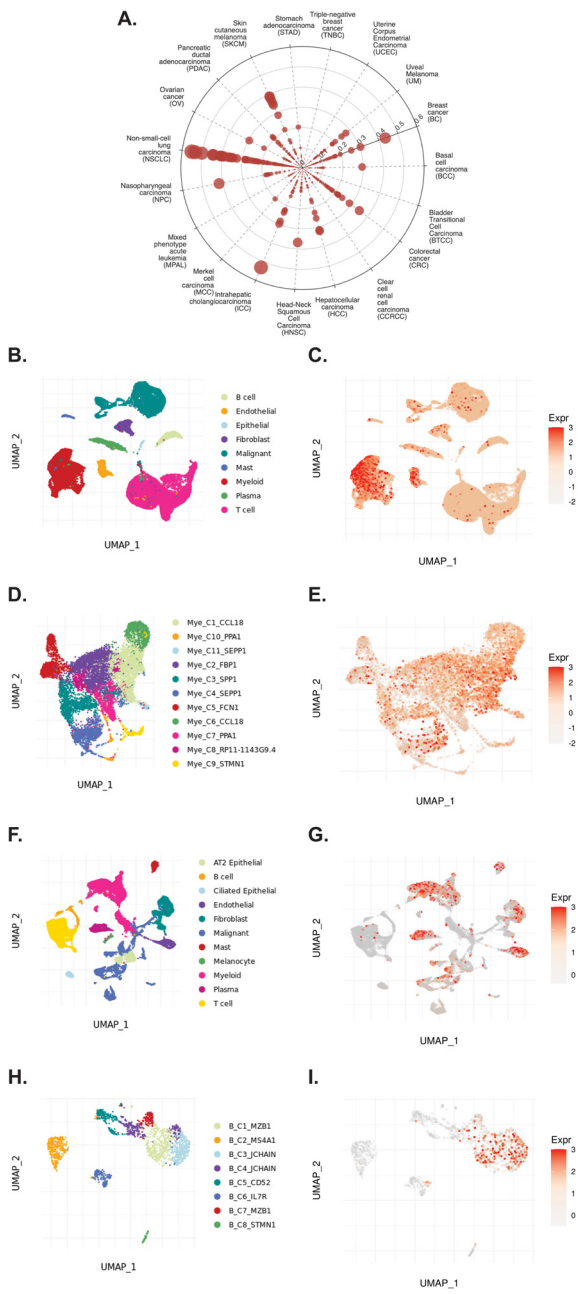

FIGURE 4
TIGER database confirms *TCN2* expression on various myeloid and B cellular clusters of NSCLC datasets. **(A)** Cell Type Marker (Log2FC) diagram represents differential expression of *TCN2* on various clusters and subclusters in each scRNA-seq tumor dataset of the TIGER database, with differential expression represented by circle size and distance from center. **(B, C)** UMAPs of all cellular clusters of the NSCLC dataset highlight expression of *TCN2* on myeloid and endothelial cells. **(D, E)** UMAPs of the Myeloid subclusters of the NSCLC dataset highlighting expression of *TCN2*. **(F, G)** UMAPs of all cellular clusters of the NSCLC6 dataset highlights expression of *TCN2* on endothelial and plasma cells. **(H, I)** UMAPs of the B cell sub-clusters of the NSCLC6 dataset highlighting expression of *TCN2*. UMAPs generated using the TIGER portal.

3.5 TIGER reveals expression patterns of *CD320* in solid tumors

The TIGER portal was also used to investigate the expression of *CD320* (83), the TCN2 receptor, across identified cellular clusters of solid tumor scRNA-seq datasets (66). Numerous cellular clusters across many solid tumors revealed differential expression of *CD320* including stomach adenocarcinoma (STAD), colorectal cancer (CRC), Merkel cell carcinoma (MCC), NSCLC, ICC, and SKCM, among others (Figure 5A). The top 20 cellular clusters with the

TABLE 3 Top 20 clusters with increased expression of *TCN2* within the TIGER database.

Cancer Type	Dataset ID	Cell Lineage	Cell Type	Log2FC
Non-small-cell lung carcinoma (NSCLC)	NSCLC6	B cell	B_C3_JCHAIN	0.5526
Non-small-cell lung carcinoma (NSCLC)	NSCLC6	All	Endothelial	0.5362
Intrahepatic cholangiocarcinoma (ICC)	ICC	All	Endothelial	0.5315
Non-small-cell lung carcinoma (NSCLC)	NSCLC	Myeloid	Mye_C1_CCL18	0.5022
Non-small-cell lung carcinoma (NSCLC)	NSCLC6	B cell	B_C1_MZB1	0.4472
Breast cancer (BC)	BC	Myeloid	Mye_C3_C1QC	0.4345
Nasopharyngeal carcinoma (NPC)	NPC	Myeloid	Mye_C2_CTSD	0.4186
Non-small-cell lung carcinoma (NSCLC)	NSCLC6	All	Plasma	0.4098
Non-small-cell lung carcinoma (NSCLC)	NSCLC5	Myeloid	Mye_C7_APOE	0.4009
Non-small-cell lung carcinoma (NSCLC)	NSCLC	All	Myeloid	0.3911
Skin cutaneous melanoma (SKCM)	SKCM1	B cell	B_C2_IGHG1	0.3895
Skin cutaneous melanoma (SKCM)	SKCM1	Myeloid	Mye_C4_C1QA	0.3865
Head-Neck Squamous Cell Carcinoma (HNSC)	HNSC	Myeloid	Mye_C7_APOE	0.3681
Non-small-cell lung carcinoma (NSCLC)	NSCLC3	Myeloid	Mye_C3_CTSB	0.357
Skin cutaneous melanoma (SKCM)	SKCM1	All	Myeloid	0.3546
Non-small-cell lung carcinoma (NSCLC)	NSCLC1	Myeloid	Mye_C6_CTSB	0.3541
Colorectal cancer (CRC)	CRC1	Myeloid	Mye_C3_APOE	0.3505
Non-small-cell lung carcinoma (NSCLC)	NSCLC6	Myeloid	Mye_C2_APOE	0.3453
Skin cutaneous melanoma (SKCM)	SKCM1	All	Plasma	0.3427
Hepatocellular carcinoma (HCC)	HCC	All	Endothelial	0.3222

greatest increase in *CD320* expression were reported, highlighting apparent increases for Endothelial, Malignant, B cell, CD4, and Myeloid cellular clusters across a variety of solid tumors (Table 4). To visualize these expression changes on immune cells of interest (B and Myeloid cells), subsequent analysis of UMAPs and gene expression boxplots for the NSCLC5 dataset confirmed increases in *CD320* expression on Endothelial, Malignant, and Fibroblast cellular clusters (Figures 5B, C). Additional subcluster analysis of B cells supported an increase in *CD320* expression on both B_C11_MZB1 and B_C4_IGHG1 (Figure 5D, E). Further visualization of UMAPs and gene expression boxplots for B cell subclusters of both the NSCLC (Figures 5F, G) and NSCLC1 (Figures 5H, I) datasets supported increased *CD320* gene expression on various Marginal Zone B and B1 Cell Specific Protein (*MZB1)*+ and *IGJ*+ B cell subclusters, in accordance with findings from Table 4. Similar results were also apparent for the SKCM1 dataset, which revealed increased *CD320* expression on all Plasma cells, Myeloid cell subclusters including Mye_C1_GZMB, as well as the B_C2_IGHG1 B cell subcluster (Supplementary File 1 – Supplementary Figure 5). Overall, these data corroborated previous publications which suggested that while *CD320* is expressed ubiquitously across many cell types (84), its expression is increased on proliferating cells (85), such as malignant cells or B lymphocytes (86), in a variety of solid tumors (87).

3.6 TIGER cell-cell communication analysis reveals interaction between *TCN2*+ myeloid cells and *CD320*+ B cells in solid tumors

To investigate a possible interaction between *TCN2*+ Myeloid and *CD320*+ B cells in these solid tumors, the TIGER portal was then used to perform a cell-cell communication analysis (66). Further investigation of both the NSCLC (67) and SKCM1 (71) datasets was warranted considering the increased expression of both *TCN2* (ligand) and *CD320* (receptor) on various immune cell populations of these tumors. To begin, a cell-cell communication analysis for the Mye_C1_CCL18 subcluster, with the greatest increase in *TCN2* expression of all myeloid cells of the NSCLC dataset (67), was performed. Analysis revealed that Mye_C1_CCL18 had greatest interaction with various other myeloid subclusters including Mye_C2_FBP1 (effect score = 97.684), Mye_C7_PPA1 (effect score = 97.64), and Mye_C6_CCL18 (effect score = 96.877). The top 20 receptor-ligand interactions driving these effect scores were reported (Table 5). Of note, this analysis consistently highlighted likely receptor-ligand interactions between CD74_MIF, CD74_COPA, CD74_APP, and HLA-DPB1_TNFSF13B as well as additional communication through HLA-DRB1_TNFSF9, CCR1_CCL18, and TNFRSF1A_GRN (Table 5). Similar cell-cell communication patterns were evident for the

10.3389/fonc.2024.1417459

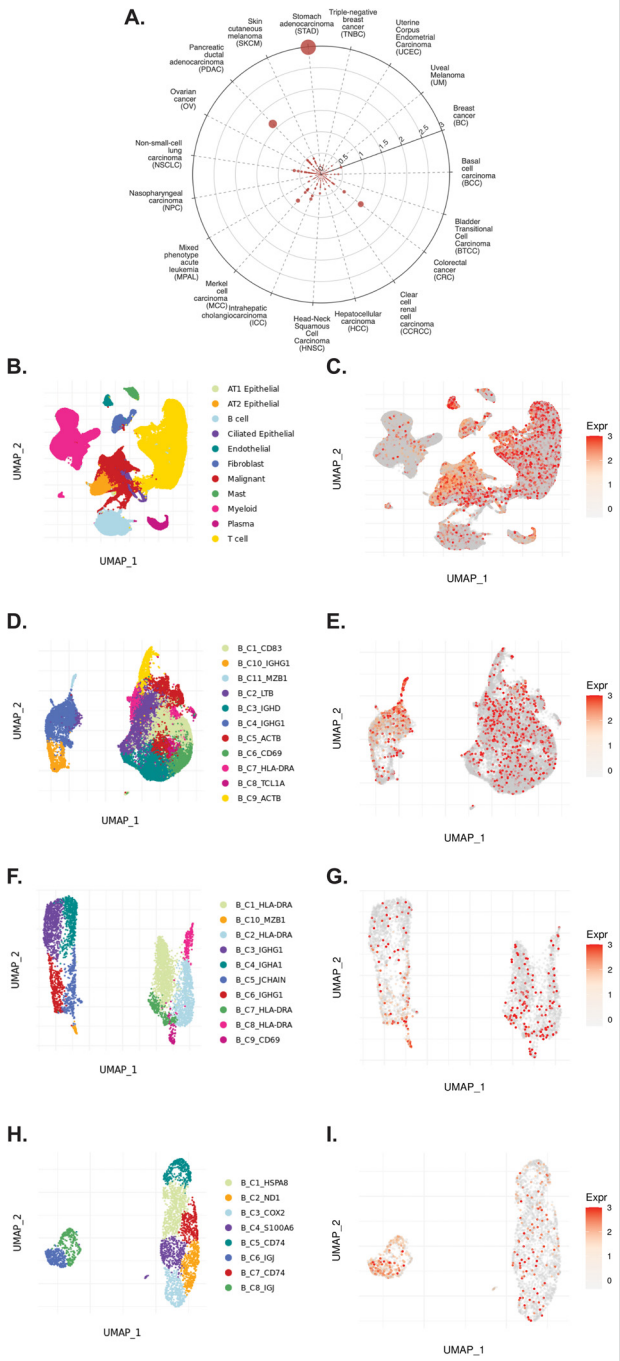

FIGURE 5
TIGER database confirms *CD320* expression on various myeloid and B cellular clusters of NSCLC datasets. **(A)** Cell Type Marker (Log2FC) diagram represents differential expression of *CD320* on various clusters and subclusters in each scRNA-seq tumor dataset of the TIGER database, with differential expression represented by circle size and distance from center. **(B, C)** UMAPs of all cellular clusters of the NSCLC5 dataset highlights expression of *CD320* on endothelial, malignant, and fibroblast cellular clusters. **(D, E)** UMAPs of the B cell subclusters of the NSCLC5 dataset highlighting expression of *CD320*. **(F, G)** UMAPs of B cell subclusters of the NSCLC dataset highlighting expression of *CD320*. **(H, I)** UMAPs of B cell subclusters of the NSCLC1 dataset highlighting expression of *CD320*. UMAPs generated using the TIGER portal.

Mye_C4_C1QA subcluster of the SKCM1 dataset (71), which displayed the greatest increase in *TCN2* expression of all SKCM1 myeloid subclusters. Here, Mye_C4_C1QA also reported the greatest cell-cell communication effects scores with other myeloid subclusters (Supplementary File 1 – Supplementary Table 1).

Additionally, a cell-cell communication analysis for the B_C10_MZB1 subcluster, with the greatest increase in *CD320* expression of all B cells of the NSCLC dataset (67), was performed. Analysis revealed that B_C10_MZB1 had the greatest interaction with various myeloid subclusters including Mye_C1_CCL18 (effect score = 48.993), Mye_C2_FBP1 (effect score = 47.944), and Mye_C7_PPA1 (effect score = 46.079). The top 20 receptor-ligand interactions driving these elevated effect scores were reported. Of note, this analysis consistently highlighted likely receptor-ligand interactions between CD74_MIF, CD74_COPA, CD74_APP, and HLA-C_FAM3C as well as additional communication through C5AR1_RPS19, HLA-DPB1_TNFSF13B, CD94:NKG2A_HLA-E, SPP1_CD44, and various chemokine axes (Table 6). Similar cell-cell communication patterns were also evident for the B_C2_IGHG1 subcluster of the SKCM1 dataset (71), which displayed the greatest increase in *CD320* expression of all SKCM1 B cell subclusters. Importantly, the B_C2_IGHG1 subcluster displayed the greatest cell-cell communication effect score with various myeloid subclusters including Mye_C4_C1QA (Supplementary File 1 – Supplementary Table 2). Overall, cell-cell communication analysis revealed that those B cell subclusters with greatest expression of *CD320* [B_C10_MZB1 (NSCLC), B_C2_IGHG1 (SKCM1)] reported the greatest cell-cell communication effect scores with those Myeloid cell subclusters with greatest expression of *TCN2* [Mye_C1_CCL18 (NSCLC), Mye_C4_C1QA (SKCM1)]. These results suggest a possible Myeloid (*TCN2*) to B/Plasma cell (*CD320*) communication network in the tumor microenvironment of immunogenic solid tumors. Considering TCN2's previously described biological functions (88–90), it was hypothesized that this interaction in solid tumors would allow for enhanced B lymphocyte infiltration, proliferation, and germinal center/TLS formation (91).

3.7 scRNA-seq of OSA tumors supports presence of *TCN2*+ myeloid and *CD320*+ plasmacytes/B cells

To investigate whether *TCN2*+ Myeloid and *CD320*+ B Lymphocyte clusters existed in OSA tumors, and whether an increase in *TCN2*+ Myeloid cells supports B lymphocyte infiltration and proliferation, scRNA-seq data from naive primary (GSE162454) and chemotherapy treated primary, recurrent, and metastatic (GSE152048) OSA tumors were analyzed. First, scRNA-seq analysis of six naive OSA primary tumors (GSE162454) was conducted. Each major cellular cluster was identified according to expression of canonical markers previously detailed by Liu et al. (72) (Figure 6A). Visualization of t-SNE plots revealed ubiquitous expression of *CD320* in OSA primary tumors, with greatest

TABLE 4 Top 20 clusters with increased expression of *CD320* within the TIGER database.

Cancer Type	Dataset ID	Cell Lineage	Cell Type	Log2FC
Stomach adenocarcinoma (STAD)	STAD	All	Endothelial	2.989
Pancreatic ductal adenocarcinoma (PDAC)	PDAC	All	Endothelial	1.6355
Colorectal cancer (CRC)	CRC1	All	Endothelial	1.1556
Merkel cell carcinoma (MCC)	MCC	All	Malignant	0.8158
Colorectal cancer (CRC)	CRC2	All	Endothelial	0.6713
Non-small-cell lung carcinoma (NSCLC)	NSCLC5	B cell	B_C11_MZB1	0.6342
Intrahepatic cholangiocarcinoma (ICC)	ICC	B cell	B_C5_HIST1H4C	0.6209
Non-small-cell lung carcinoma (NSCLC)	NSCLC	B cell	B_C10_MZB1	0.5401
Intrahepatic cholangiocarcinoma (ICC)	ICC	All	Endothelial	0.5392
Breast cancer (BC)	BC	All	Endothelial	0.4935
Pancreatic ductal adenocarcinoma (PDAC)	PDAC2	CD4	CD4_C10_GNLY	0.4653
Non-small-cell lung carcinoma (NSCLC)	NSCLC6	All	Endothelial	0.4624
Pancreatic ductal adenocarcinoma (PDAC)	PDAC2	All	Endothelial	0.4548
Head-Neck Squamous Cell Carcinoma (HNSC)	HNSC	All	Erythrocyte	0.4403
Skin cutaneous melanoma (SKCM)	SKCM1	Myeloid	Mye_C1_GZMB	0.4134
Skin cutaneous melanoma (SKCM)	SKCM1	B cell	B_C2_IGHG1	0.4074
Basal cell carcinoma (BCC)	BCC	Myeloid	Mye_C1_GZMB	0.4006
Non-small-cell lung carcinoma (NSCLC)	NSCLC1	B cell	B_C6_IGJ	0.3837
Non-small-cell lung carcinoma (NSCLC)	NSCLC5	All	Endothelial	0.3828
Colorectal cancer (CRC)	CRC2	Myeloid	Mye_C13_GZMB	0.3781

expression on Osteoblastic OSA cells, Endothelial cells, NK/T cells, and Plasmocytes (Figure 6B). For *TCN2*, t-SNE plots conveyed concentrated gene expression on Myeloid cells, with additional positivity on both Endothelial cells and Plasmocytes (Figure 6C). The number of Plasmocytes (Figure 6D), B cells (Figure 6E), and Myeloid cells (Figure 6F) expressing *CD320* (Plasmocytes/B cells, Figures 6G, H) or *TCN2* (Myeloid cells, Figure 6I) was then quantified. Unfortunately, only the OS-6 patient sample contained elevated levels of Plasmocyte or B cell populations (Supplementary File 1 – Supplementary Figure 6). This finding was unsurprising considering Li et al. noted that only one patient sample had identifiable TLSs during sample processing (72). Nevertheless, total *CD320*+ Plasmocytes, *CD320*+ B cells, and *TCN2*+ Myeloid cells, as well as the percent (%) of total cells, were quantified for each patient sample (Figures 6J, K). Importantly, while only OS-6 contained a substantial number of *CD320*+ Plasmocytes and B cells, this primary tumor also measured the greatest percentage (%) of *TCN2*+ Myeloid cells (relative to all Myeloid cells) at 38.68% (Figure 6L and Supplementary File 4).

A subsequent scRNA-seq analysis of eleven chemotherapy treated primary, recurrent, and metastatic OSA tumor specimens (GSE152048) was conducted using the same canonical markers and cellular clusters. Again, while *CD320* was ubiquitously expressed across numerous cellular populations, *TCN2* expression was concentrated on Myeloid cells. Unfortunately, subsequent quantification of Plasmocyte and B cell clusters revealed minimal B lymphocyte infiltration in the chemotherapy treated OSA tumors examined. Interestingly, these OSA samples also had substantially lower overall *TCN2*+ Myeloid cell populations in comparison to the previously analyzed naive primary tumors (GSE162454). Additionally, the percentage (%) of *TCN2*+ Myeloid cells (relative to all Myeloid cells) was no greater than 21.26% across all tumors examined (Supplementary File 1 – Supplementary Figure 7, Supplementary File 4). Overall, these analyses supported that *TCN2*+ Myeloid and *CD320*+ Plasmocyte and B cell clusters were ultimately present in OSA tumors. Considering the previous publication's note regarding isolation of these B lymphocytes from confirmed TLSs in one naive primary tumor (72), we also associated the highest % of TCN2+ Myeloid cells (relative to all Myeloid cells) with intratumoral TLS formation. Ultimately, investigation of additional OSA tumor specimens (positive for B lymphocyte and/or Plasmocyte populations) and further cell-cell communication analysis is required to support the hypothesis that *TCN2*+ Myeloid cells drive infiltration and proliferation of B lymphocyte populations through increased TCN2 (ligand) and CD320 (receptor) interactions.

TABLE 5 Top 3 interactions defined by cell-cell communication analysis for Mye_C1_CCL18 of the NSCLC dataset (TIGER), with effect score presented in parenthesis.

Gene | Gene	Mye_C2_FBP1 | Mye_C1_CCL18 (97.684)	Gene | Gene	Mye_C7_PPA1 | Mye_C1_CCL18 (97.64)	Gene | Gene	Mye_C6_CCL18 | Mye_C1_CCL18 (96.877)
CD74_MIF	2.69	CD74_MIF	3.075	CD74_MIF	2.819
CD74_COPA	2.41	CD74_COPA	2.795	HLA-DPB1_TNFSF13B	2.607
CD74_APP	2.379	CD74_APP	2.765	CD74_COPA	2.539
HLA-DPB1_TNFSF13B	2.186	HLA-DPB1_TNFSF13B	2.495	CD74_APP	2.509
HLA-DRB1_OGN	1.861	HLA-DRB1_OGN	2.111	HLA-DPA1_TNFSF9	2.016
C5AR1_RPS19	1.809	HLA-DPA1_TNFSF9	2.015	HLA-DRB1_OGN	1.864
CCR1_CCL18	1.775	C5AR1_RPS19	1.695	C5AR1_RPS19	1.798
HLA-DPA1_TNFSF9	1.605	CCR1_CCL18	1.689	HLA-C_FAM3C	1.725
SPP1_CD44	1.529	HLA-C_FAM3C	1.594	CCR1_CCL18	1.617
HLA-C_FAM3C	1.528	TNFRSF1A_GRN	1.489	TNFRSF1A_GRN	1.43
TNFRSF1A_GRN	1.46	TNFRSF1B_GRN	1.417	ANXA1_FPR3	1.324
TNFRSF1B_GRN	1.361	SPP1_CD44	1.278	ANXA1_FPR1	1.275
GRN_SORT1	1.089	EGFR_GRN	1.222	GRN_SORT1	1.27
LGALS9_CD44	1.059	GRN_SORT1	1.22	TNFRSF1B_GRN	1.255
ANXA1_FPR3	1.043	LGALS9_CD44	1.086	LGALS9_CD44	1.172
CD52_SIGLEC10	1.022	HLA-E_KLRC1	1.018	ANXA1_FPR2	1.102
SPP1_PTGER4	1.01	PTPRC_MRC1	0.978	CD52_SIGLEC10	1.097
ANXA1_FPR1	0.993	ANXA1_FPR3	0.961	ALOX5_ALOX5AP	1.089
SPP1_a4b1 complex	0.979	CD94:NKG2A_HLA-E	0.96	LGALS9_CD47	1.006
HLA-E_KLRC1	0.963	NRG1_MS4A4A	0.931	CD99_PILRA	0.991

Top 20 receptor-ligand interactions (gene | gene) driving the overall effect score between interacting cellular clusters.

3.8 Proteomic correlation analysis of APO-TCN2 reveals detectable signatures associated with plasma cell maintenance, B cell activation, TLS formation, and circulating immunoglobulins

B lymphocyte infiltration, proliferation, and formation of TLSs is well regarded as a clinical biomarker of long term survival and response to immunotherapy in many solid tumors (92–115), including soft-tissue sarcoma (116, 117). Previous literature has suggested the necessity of the CD320 receptor for germinal center B cell growth and proliferation (83). Considering the apparent association between myeloid-derived TCN2 and CD320+ B lymphocytes in various solid tumors, a subsequent correlation analysis between plasma APO-TCN2 and previously described soluble markers of plasma cell maintenance (73), B cell activation (74), proteins critical for TLS formation (75), chemokines of the 12-CK signature (75) [exception – CCL4 (not measured)], and circulating immunoglobulin levels was then conducted. To begin, for those markers of plasma cell maintenance (73) (Figures 7A–K), positive correlations between plasma APO-TCN2 and IL-6 (Figures 7A, B), IL-6Ra (Figures 7C–E), IL-6Rb (Figure 7F), and TNF (Figures 7J, K) were observed, with statistical significance apparent for IL-6Ra. Additionally, a negative correlation between APO-TCN2 and CXCL12 (Figures 7G–I) was evident. Furthermore, for the soluble markers of B cell activation (74) (Figures 7L–O), IL-2RA (Figure 7L), TNFSF13B (BAFF) (Figure 7M), and TNFRSF13B (TACI) (Figure 7N) all displayed positive yet nonsignificant correlations with plasma APO-TCN2, while a negative, nonsignificant correlation was reported for TNFRSF17 (BCMA) (Figure 7O). Overall, these data suggest that increases in plasma APO-TCN2 were associated with increases in previously described soluble markers of B lymphocyte activity, albeit nonsignificant for most associations.

Furthermore, analysis of various proteins critical for TLS formation (75) (Figures 7P–T) revealed similar trends. Positive yet nonsignificant correlations between APO-TCN2 and LTa1b2 (Figure 7P), FCRL5 (Figure 7Q), SELL (Figure 7R), and TNFSF14 (Figures 7S, T) were observed, suggesting a possible association of APO-TCN2 levels with those proteins necessary for TLS formation.

TABLE 6 Top 3 interactions defined by cell-cell communication analysis for B_C10_MZB1 of the NSCLC dataset (TIGER), with effect score presented in parenthesis.

Gene | Gene	Mye_C1_CCL18 | B_C10_MZB1 (48.993)	Gene | Gene	Mye_C2_FBP1 | B_C10_MZB1 (47.944)	Gene | Gene	Mye_C7_PPA1 | B_C10_MZB1 (46.079)
CD74_MIF	2.983	CD74_MIF	2.906	CD74_MIF	3.291
CD74_COPA	2.491	CD74_COPA	2.414	CD74_COPA	2.799
CD74_APP	2.419	CD74_APP	2.342	CD74_APP	2.727
C5AR1_RPS19	2.121	C5AR1_RPS19	2.105	HLA-DPB1_TNFSF13B	2.044
HLA-DPB1_TNFSF13B	1.873	HLA-C_FAM3C	1.758	HLA-DPA1_TNFSF9	2.018
HLA-C_FAM3C	1.777	HLA-DPB1_TNFSF13B	1.735	C5AR1_RPS19	1.991
HLA-DPA1_TNFSF9	1.732	HLA-DPA1_TNFSF9	1.607	HLA-C_FAM3C	1.824
CD94:NKG2A_HLA-E	0.892	SPP1_CD44	1.104	CD94:NKG2A_HLA-E	0.893
SPP1_CD44	0.757	SPP1_a4b1 complex	1.004	SPP1_CD44	0.853
ANXA1_FPR3	0.689	SPP1_PTGER4	0.952	LGALS9_CD47	0.77
PLD2_ARF1	0.679	CD94:NKG2C_HLA-E	0.889	SPP1_a4b1 complex	0.754
LGALS9_CD47	0.664	PLAUR_a4b1 complex	0.813	MIF_TNFRSF14	0.717
SPP1_a4b1 complex	0.658	MIF_TNFRSF14	0.796	SPP1_PTGER4	0.701
LAMP1_FAM3C	0.628	ANXA1_FPR3	0.766	ANXA1_FPR3	0.684
PECAM1_CD38	0.622	LGALS9_CD47	0.744	PLD2_ARF1	0.677
CD44_HBEGF	0.621	CXCL10_CXCR3	0.74	LGALS9_CD44	0.66
EGFR_MIF	0.609	CD44_HBEGF	0.687	LGALS9_SLC1A5	0.647
CXCL12_CXCR4	0.606	PLD2_ARF1	0.67	PTPRC_CD22	0.61
SPP1_PTGER4	0.606	LGALS9_CD44	0.634	EGFR_MIF	0.604
PLAUR_a4b1 complex	0.588	CCL2_CCR10	0.624	CXCL12_CXCR4	0.587

Top 20 receptor-ligand interactions (gene | gene) driving the overall effect score between interacting cellular clusters.

Furthermore, negative, nonsignificant correlations between APO-TCN2 and most chemokines of the 12-CK signature (75) were evident (Figure 8). Overall, these data [much like the findings for CXCL12 (Figures 7G–I)] may suggest that increased plasma APO-TCN2 is associated with the development of exacerbated chemokine axes (lower blood plasma and higher tissue levels) for potent lymphocytic infiltration into patient solid tumor and/or other tissues. Additional tissue/tumor-level analyses are necessary to further support this finding. Of note, additional correlation analyses of circulating immunoglobulin levels suggested negative correlations between plasma APO-TCN2 and IgA, IgD, IgE, IgM, and IgG, with a positive correlation to J chain (Supplementary File 1 – Supplementary Figure 8). Limited research has correlated peripheral blood immunoglobulin levels with intratumoral TLSs, therefore, the significance of these findings is unknown. However, these data may indicate the presence of improved intratumoral humoral immune responses (increased J chain) in those patients with elevated APO-TCN2. Overall, these data suggested that elevated APO-TCN2 levels may be associated with a peripheral blood plasma signature necessary for robust B lymphocyte proliferation and infiltration in OSA tumors.

3.9 KM Plotter Immunotherapy suggests association of *TCN2/CD320* with response to immunotherapy and formation of intratumoral TLSs

Our group then hypothesized that if increases in plasma APO-TCN2 (and as a result, intratumor *TCN2*) is associated with lymphocytic infiltration and possible formation of TLSs, then increased *TCN2/CD320* expression in solid tumors, treated with immunotherapy, should correlate with better overall survival. To investigate this hypothesis, both *TCN2* and *CD320* were evaluated for overall and progression free survival in solid tumors treated with various immunotherapies (anti-PD-1, anti-PD-L1, anti-CTLA-4) using the KM Plotter Immunotherapy online database (76). Increased intratumoral expression of *TCN2* was indeed associated with better overall (log-rank P = 8.6e-05, FDR = 0.03) (Figure 9A) and progression free (log-rank P = 1.6e-11, FDR = 0.01) (Figure 9B) survival. Similar findings were also evident for the TCN2 receptor, as increased *CD320* expression was associated with better overall (log-rank P = 9.4e-08, FDR = 0.01) (Figure 9C) and progression free (log-rank P = 1.3e-08, FDR = 0.01) (Figure 9D) survival in the same

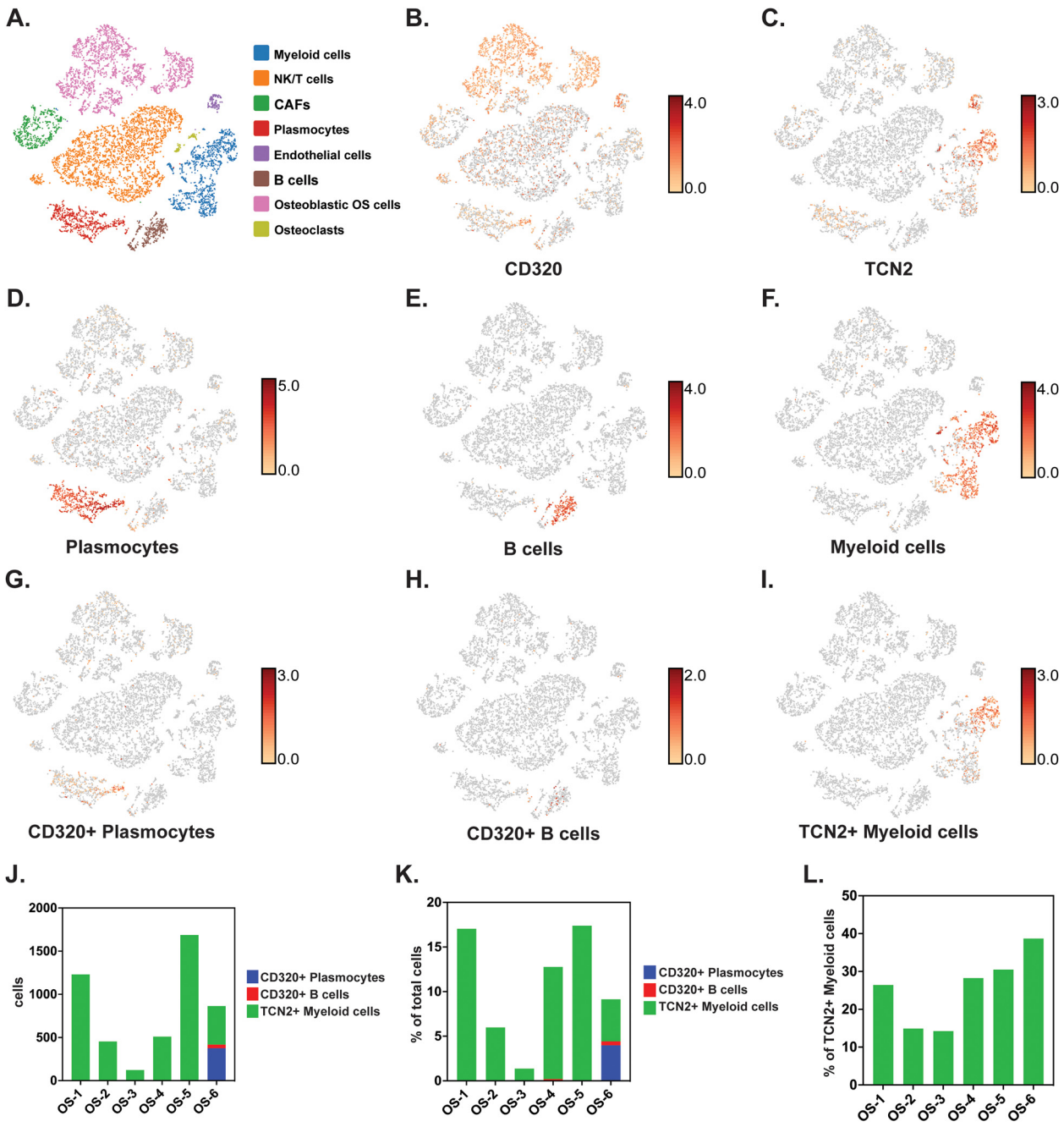

FIGURE 6
scRNA-seq analysis of naive primary OSA samples reveals *CD320* and *TCN2* expression. All clustering representative of patient OS-6 **(A)** All cellular clusters identified by canonical marker expression. **(B)** Representative log-normalized *CD320* expression across various cellular clusters. **(C)** Representative log-normalized *TCN2* expression across various cellular cluster of patient OS-6. **(D)** Representative clustering of Plasmocytes with log-normalized expression of *IGHG1* and *MZB1* using the "Feature Min" function. **(E)** Representative clustering of B cells with log-normalized expression of *MS4A1* and *CD79A* using the "Feature Min" function. **(F)** Representative clustering of Myeloid cells with log-normalized expression of *LYZ* and *CD68* using the "Feature Min" function. **(G)** Representative clustering of *CD320+* Plasmocytes with log-normalized expression of *CD320, IGHG1*, and *MZB1* using the "Feature Min" function. **(H)** Representative clustering of *CD320+* B cells with log-normalized expression of CD320, *MS4A1*, and *CD79A* using the "Feature Min" function. **(I)** Representative clustering of *TCN2+* Myeloid cells with log-normalized expression of *TCN2, LYZ*, and *CD68* using the "Feature Min" function. **(J)** Quantification of total cells for the *CD320+* Plasmocytes, *CD320+* B cells, and *TCN2+* Myeloid cells populations in all naive OSA patient tumors (n = 6). **(K)** Quantification of the percent (%) of total cells for *CD320+* Plasmocytes, *CD320+* B cells, and *TCN2+* Myeloid cells population in all naive OSA patient tumors (n = 6). **(L)** Quantification of the percent (%) of *TCN2+* Myeloid cells, relative to all Myeloid cells in all naive OSA patient tumors (n = 6).

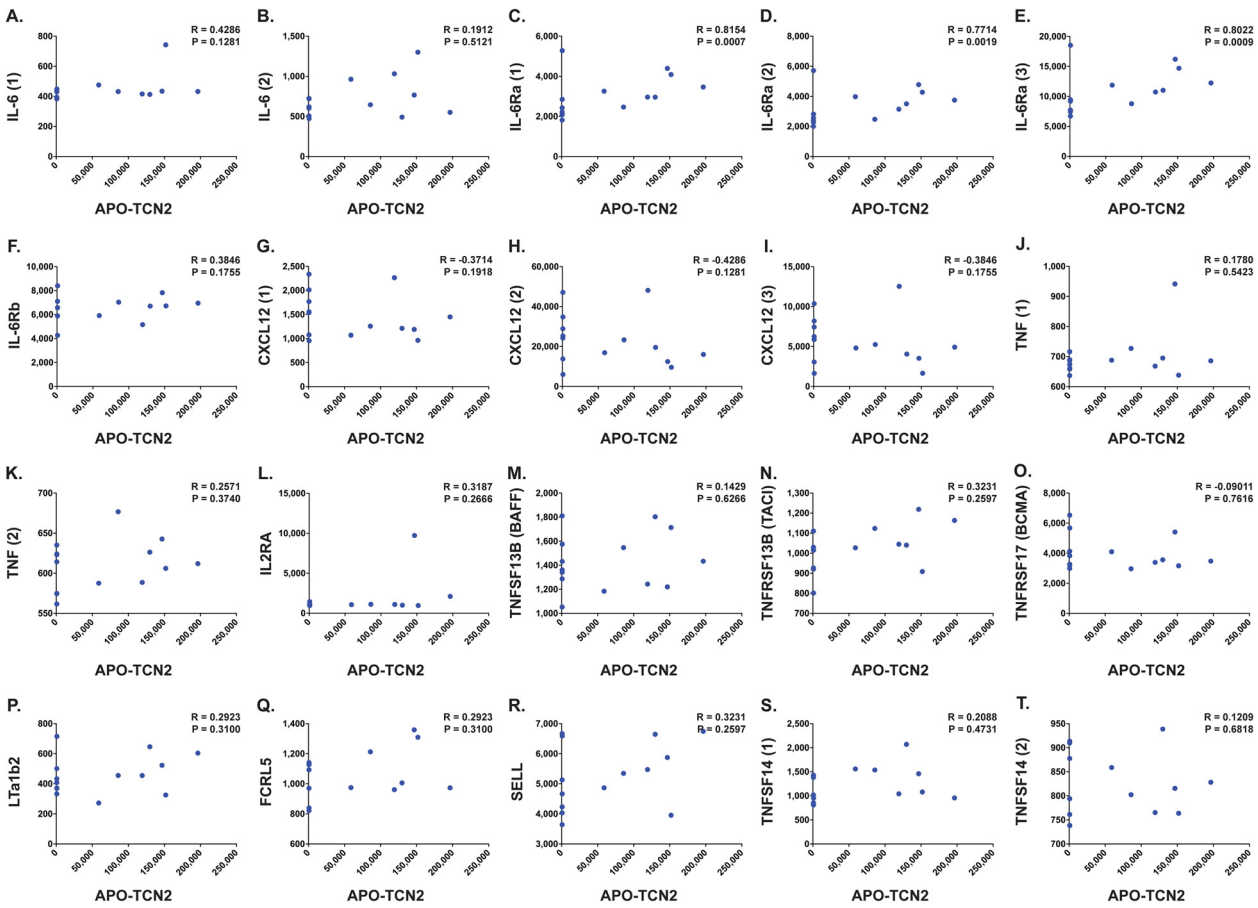

FIGURE 7
Correlation between APO-TCN2 and markers of plasma cell maintenance, B cell activation, and TLS formation. Spearman correlation analysis between measured APO-TCN2 (x-axis, RFUs) and markers of plasma cell maintenance including IL-6 [seq.2573.20, seq.4673.13] **(A, B)**, IL-6Ra [seq.15602.43, seq.4139.71, seq.8092.29] **(C–E)**, IL-6Rb [seq.2620.4] **(F)**, CXCL12 [seq.2330.2, seq.3516.60, seq.9278.9] **(G–I)**, and TNF [seq.5692.79, seq.5936.53] **(J, K)**, markers of B cell activation including IL2RA [seq.3151.6] **(L)**, TNFSF13B [seq.3059.50] **(M)**, TNFRSF13B [seq.2704.74] **(N)**, and TNFRSF17 [seq.2665.26] **(O)**, as well as markers of TLS formation including LTa1b2 [seq.3505.6] **(P)**, FCRL5 [seq.6103.70] **(Q)**, SELL [seq.4831.4] **(R)**, and TNFSF14 [seq.5355.69, seq.5988.49] **(S, T)** (y-axis, RFUs). Spearman correlation coefficient (R) and P-value (P) presented on each scatter plot. Each chemokine identified by multiple SOMAmers [example: TNFSF14 (1) and (2), representing seq.5355.69 and seq.5988.49, respectively] is presented with multiple correlation plots.

dataset. These data suggest that increased pre-treatment *TCN2* and *CD320* expression is associated with better outcomes in a variety of solid tumors treated with immunotherapy.

To further examine whether intratumoral *TCN2* and *CD320* expression is associated with TLS formation, a correlation analysis to the 12-CK TLS signature (75) was performed using the KM Plotter Immunotherapy database (76). Unsurprisingly, increased expression of all 12-CK signature chemokines was significantly (FDR < 0.05) associated with better overall survival in the solid tumors examined (exception – CCL18, HR = 0.71, log-rank P = 0.00055, FDR = 0.20) (Supplementary File 1 – Supplementary Figure 9). A Spearman correlation analysis supported significant (P < 0.05) positive correlations between *TCN2* and *CD320* expression with each chemokine of the 12-CK TLS signature (exception – *CD320* and *CCL4*) (Supplementary File 1 – Supplementary Table 3). A subsequent multi-gene Spearman correlation analysis between *TCN2* and *CD320* with the 12-CK TLS signature (75) using the GEPIA2 web server and solid tumors of the TCGA database (77) was also performed. Importantly, *TCN2* expression displayed a significant positive correlation to the 12-CK gene signature for TCGA-SARC (P-value = 5.1e-13, R = 0.43). Similar results were evident for a combinatory analysis of all TCGA tumors (P-value = 3.4e-123, R = 0.24). In contrast, *CD320* expression displayed an opposite trend, with a weak negative correlation in both datasets (Supplementary File 1 – Supplementary Figure 10). Overall, these data highlight a positive correlation between *TCN2* and the 12-CK TLS signature in a variety of solid tumors. While preliminary, these data may suggest an association between elevated peripheral plasma APO-TCN2 (alongside probable increases in intratumoral *TCN2* expression) with formation of TLSs. Further investigation of sarcoma tumor specimens is ultimately necessary to associate increased plasma APO-TCN2 with intratumoral B lymphocyte aggregation and/or TLS formation.

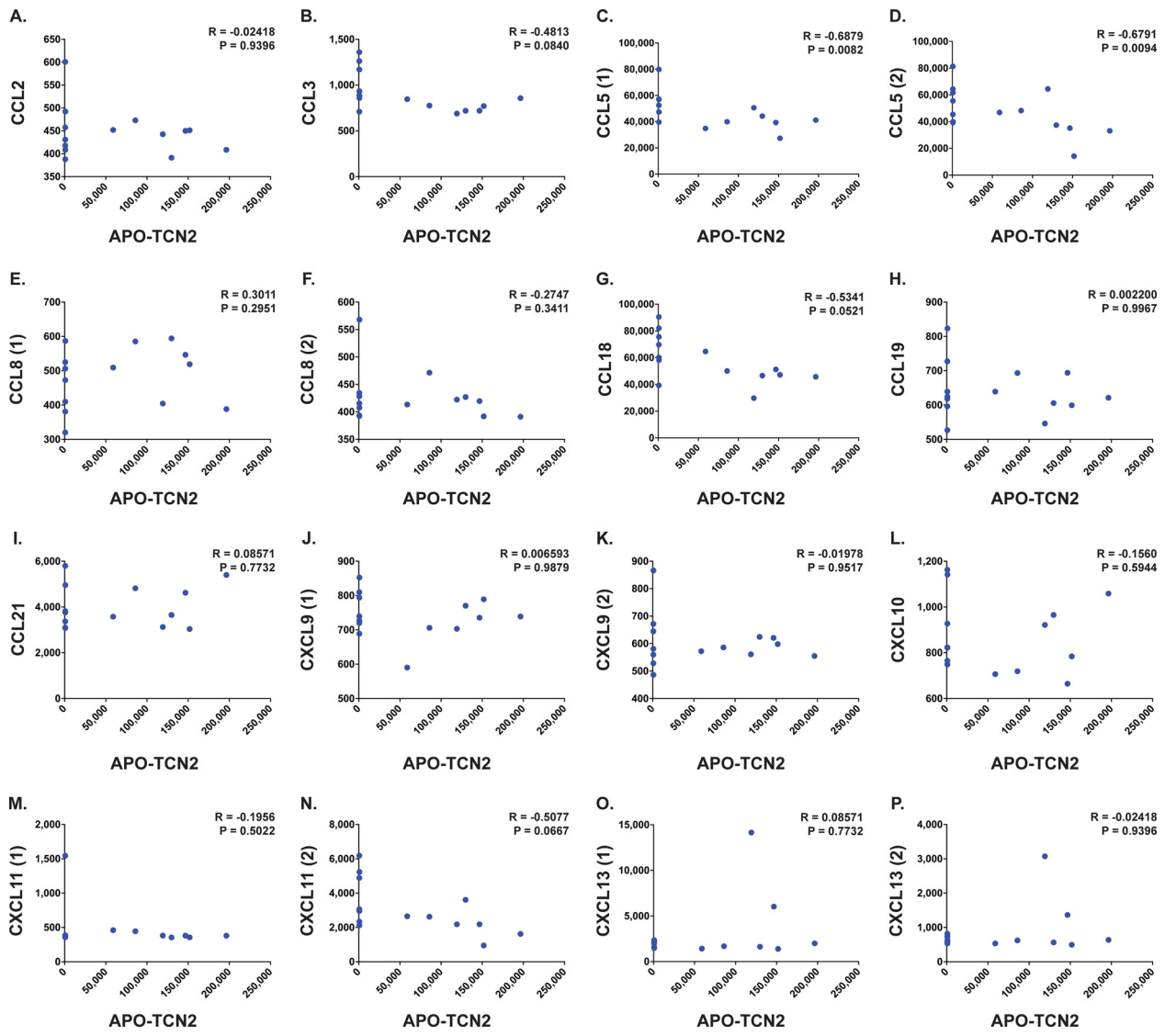

FIGURE 8
Correlation analysis between APO-TCN2 and measured chemokines of the 12-CK signature. Spearman correlation analysis between measured APO-TCN2 (x-axis, RFUs) and CCL2 [seq.2578.67] **(A)**, CCL3 [seq.3040.59] **(B)**, CCL5 [seq.2523.31, seq.5480.49] **(C, D)**, CCL8 [seq.13748.4, seq.2785.15] **(E, F)**, CCL18 [seq.3044.3] **(G)**, CCL19 [seq.4922.13] **(H)**, CCL21 [seq.2516.57] **(I)**, CXCL9 [seq.11593.21, seq.9188.119] **(J, K)**, CXCL10 [seq.4141.79] **(L)**, CXCL11 [seq.18171.25, seq.3038.9] **(M, N)**, CXCL13 [seq.13701.2, seq.3487.32] **(O, P)** (y-axis, RFUs) in naive OSA patient plasma samples (n = 14). Spearman correlation coefficient (R) and P-value (P) presented on each scatter plot. Each chemokine identified by multiple SOMAmers [example: CCL5 (1) and (2), representing seq.2523.31 and seq.5480.49, respectively] is presented with multiple correlation plots.

4 Discussion

This proteomic biodiscovery analysis of OSA patient plasma identified apo-transcobalamin-II (APO-TCN2) as a novel circulatory biomarker of survival in this disease. To our knowledge, the only known publication which previously characterized TCN2 in OSA was published by Rothzerg et al. in 2021. Here, *TCN2* was identified as one of four upregulated genes associated with better overall survival in OSA tumors of the TARGET-OS dataset (118). To our knowledge, no further characterization of TCN2 in OSA has since been conducted. Ultimately, the work presented here provides the utmost support for its relevance in this disease, as an over 6-fold increase in circulating APO-TCN2 levels was associated with better overall survival in our patient cohort. The dual association of both increased *TCN2* expression (in OSA tumors) and increased circulatory APO-TCN2 levels (in OSA peripheral blood plasma) with improved patient outcome provides credence to our findings and this biomarker's future clinical utility in this disease. While additional studies to correlate intratumoral *TCN2* expression with plasma APO-TCN2 levels are necessary, these data suggest that circulating protein measurements (through liquid biopsy) could act as a surrogate for tumoral assessments in both local and advanced OSA. Future studies to assess changes in peripheral APO-TCN2 throughout the course of disease through serial blood sampling could also further associate plasma protein levels with disease progression, therapeutic response, and/or clinical remission.

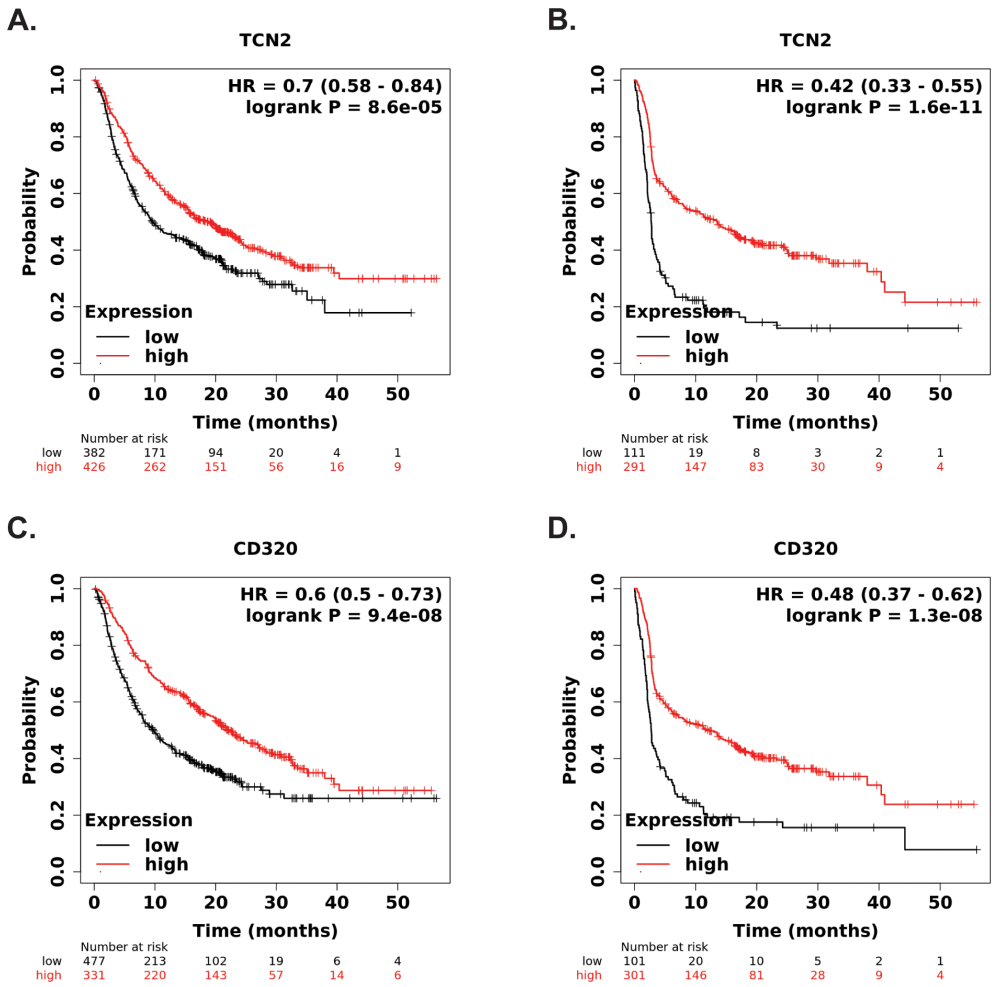

FIGURE 9
KM Plotter Immunotherapy survival analysis supports *TCN2* and *CD320* as a markers of immunotherapy response. Overall **(A)** and progression free **(B)** survival analysis of *TCN2*. Overall **(C)** and progression free **(D)** survival analysis of *CD320*. Each analysis included specimens from all solid tumors, collected pre-treatment, irrespective of immunotherapy target (anti-PD-1, anti-PD-L1, and anti-CTLA-4). Default KM Plotter settings were utilized with auto selection of best cutoff into high (red) and low (black) gene expression groups based on the calculation of all upper and lower quartiles with selection of the best performing threshold. KM survival curves with reported HR and log-rank P-value were constructed, with y-axis representing probability of survival and the x-axis representing time (months). The total number of patients at risk for each time point is reported. Survival curves generated using KM Plotter Immunotherapy.

TCN2's biological function of supporting cellular metabolic processes by transporting vitamin B12 (cobalamin, co-factor for various enzymes) through the blood stream, binding to the ubiquitously expressed CD320 surface receptor, and internalization of the receptor-ligand complex for B12's intracellular release is well known (119–121). Interestingly, numerous reports of TCN2 deficiency due to loss-of-function mutations have been described. In addition to the common presentation of failure to thrive and megaloblastic anemia (due to elevation of homocysteine and methylmalonic acid), a number of these cases reported immunological deficiencies and abnormal immunity including measured pancytopenia, neutropenia, and hypogammaglobulinemia (78–81, 122–138). TCN2 deficiency was also previously associated with abnormal granulocyte function and limited antimicrobial response to *Staphylococcus aureus* infection (139). Of note, no difference in HOLO-TCN2 levels were measured between our 2-year deceased and survivor cohorts, ruling out the possibility of a genetic abnormality in those deceased patients. These reports, however, highlight TCN2's integral role in proliferation and maintenance of cells of the immune system.

In this regard, increased TCN2 levels were previously reported in patients with a variety of inflammatory and lymphoproliferative disorders, including those diagnosed with multiple myeloma and Waldenstrom macroglobulinemia experiencing overproduction of immunoglobulins (hyperglobulinemia) (140). McLean et al. later determined that TCN2 could not only drive proliferation of human erythroleukemic and murine lymphoma cell lines *in vitro*, but antibody blockade of its receptor could also effectively inhibit cellular growth (89, 90). Furthermore, TCN2 levels in peripheral blood monocytes of patients with various inflammatory bowel diseases including shigellosis, ulcerative colitis, and Crohn's were 3-4 times higher than those measured in healthy normal patients, with levels decreasing in the setting of clinical improvement (141). TCN2 was also elevated in the setting of various infectious diseases

including malaria and typhus (142–144), supporting its role as a possible acute phase reactant (145).

Of utmost importance, increases in unsaturated TCN2 (APO-TCN2) have been reported in patients with active autoimmune diseases including systemic lupus erythematous (SLE), autoimmune hemolytic anemia, and dermatomyositis, with levels often correlating with disease activity (146–148). Haynes et al. in 2020 also identified a 93-gene signature for diagnosis of SLE through transcriptomic profiling of patient peripheral blood, of which *TCN2* was included (149). Additionally, while total serum cobalamin was no different between patients with active rheumatoid arthritis (RA) and clinical remission, APO-TCN2 was significantly elevated in those with active disease (150). These data suggest that APO-TCN2 is elevated in the setting of pathogenic immune responses in various immune-mediated disorders, often correlating with disease activity. Considering these clinical observations, Liu et al. recently investigated TCN2's pathogenic role in a murine model of lupus. Increased expression of *TCN2* in both B and T lymphocytes of SLE patients and lupus-like mice were observed. Importantly, global genetic knockout of *TCN2* in this murine model of lupus resulted in complete amelioration of lupus symptoms, as measured by lower dsDNA levels, reduced IgG deposition in the glomerulus, and decreased infiltration of both B and T follicular helper cells in the kidneys and spleen of these mice. The group suggested that TCN2 activity is associated with the abnormal germinal center responses in the setting of SLE and could act as a novel therapeutic target in this disease (91). Considering these findings, it appears that the elevated APO-TCN2 in our 2-year survival cohort, with no difference in HOLO-TCN2 levels, mirrors the heightened systemic immune activity seen in common autoimmune disorders. These *in vivo* results suggest the importance of TCN2 for germinal center-mediated immune activity, as seen in the kidneys of patients with lupus nephritis (151). While the majority of previous literature indicated that TCN2 was merely correlative in nature (152), these data ultimately suggest a causative role for this circulating protein in the development and progression of lymphoproliferative autoimmune disease.

To suggest a possible mechanism by which APO-TCN2 improves overall survival in solid tumors, various analyses were then conducted using publicly available scRNA-seq datasets. Analysis of the TIGER database supported previous literature which characterized *TCN2* expression and active production from, among others, myeloid lineage (82, 153, 154) and endothelial (155, 156) cells. This analysis also confirmed the expression of *CD320* ubiquitously across many cell types (84) including B lymphocytes (86). The cell-cell communication analyses highlighted the interaction between B lymphocytes (positive for *CD320)* with Myeloid cells (positive for *TCN2*) in both NSCLC and SKCM. These results suggest the presence of a coordinated communication network between these cellular populations which likely supports intratumoral B lymphocyte proliferation for enhanced anti-tumor immune responses. Considering the significant correlation between *TCN2* and *CD320* with the 12-CK Score (75) and previous literature's characterization of the CD320 receptor as necessary for germinal center B cell growth (83), these interactions may help coordinate the formation of intratumoral TLSs in these patients. With macrophages having been previously described as potent lymphoid tissue inducer cells necessary for T and B cell recruitment in these structures (157), and knockout of *TCN2* by Liu et al. inhibiting infiltration of B/T lymphocytes in kidneys and spleen in a murine model of lupus (91), further investigation of this intratumoral signaling network is therefore warranted.

Importantly, those B lymphocytes of the TIGER database with the greatest increased expression of *CD320* included *MZB1+* and immunoglobulin producing B cell clusters, commonly found in the marginal zone of germinal centers and tumor TLSs (158–160). Of the receptor-ligand interactions driving the cell-cell communication effect scores between these *TCN2+* Myeloid and *CD320+* B cell clusters, many are associated with promoting B cell activity. Of note, interactions between CD74 and MIF have been previously associated with both peripheral B cell survival (161) and chemotaxis (162, 163). Additionally, while interactions between CD74 and COPA (COPI coat complex subunit alpha) of malignant plasma and immune cells have been described in Waldenstrom macroglobulinemia (164), these interactions have also been shown to play a role in the maturation of B cells in the setting of antibody-mediated renal transplant rejection (165). Furthermore, scRNA-seq analysis of peripheral immune cells in patients with primary Sjogren's syndrome highlighted not only enhanced CD74-COPA interactions between monocytes and naive B cells, but also CD74-amyloid beta precursor protein (APP) interactions between monocytes and memory B cells. Considering their enrichment in those with active disease, these receptor-ligand interactions were thought to be important drivers of autoimmunity (166). Further receptor-ligand interactions between HLA class II histocompatibility antigen, DP beta chain (HLA-DPB1) and TNFSF13B (BAFF) in addition to Major Histocompatibility Complex, Class II, DP Alpha 1 (HLA-DPA1) and TNF Superfamily Member 9 (TNFSF9) suggest myeloid-mediated B lymphocyte survival and maturation (167) in germinal centers of these solid tumors, as previously proposed (168). The association of high *TCN2* and *CD320* expression with better overall survival in patients treated with immunotherapy could likely reflect the increased propensity for B lymphocyte survival, proliferation, and maturation for TLS formation within the responding patient tumors (107).

While only preliminary, both *TCN2+* Myeloid and *CD320+* Plasmocytes and B cells were identified by scRNA-seq analyses of OSA tumor specimens. Most B lymphocytes characterized in the original analysis were confirmed to have been isolated from a single primary tumor containing TLSs (72). The identification of intratumoral B cells associated with TLSs in one of six naive tumors reflects the rates previously described in the amended PEMBROSARC trial of STS (approx. 20% of patients on initial screening) (169). These preliminary results, however, suggest the necessity for elevated *TCN2+* Myeloid cells for B lymphocyte proliferation in the OSA tumor microenvironment. Additional analyses of known TLS-positive and -negative OSA or sarcoma tumor specimens are necessary to further support this interactive mechanism in sarcomas disease. Importantly, various correlation analyses presented here may indicate that elevated APO-TCN2 was associated with a favorable B lymphocyte (73, 74) proteomic profile likely necessary for potent immune cell recruitment and TLS-

formation (75) to drive antibody-mediated anti-tumor immune responses in the OSA patients examined. Ultimately, while the mechanism by which *TCN2* is associated with better overall survival in OSA was extensively postulated in these analyses, further confirmatory studies are indeed necessary.

Of note, a distinct biological function of APO-TCN2 has, to our knowledge, not yet been described. The specific elevation of APO-TCN2 (as opposed to HOLO-TCN2) was previously associated with various lymphoproliferative autoimmune disorders but not further investigated. Our group, however, can postulate several mechanisms by which the increased circulatory APO-TCN2, measured here in OSA, is associated with better overall survival. First and foremost, our group hypothesizes that increased circulatory APO-TCN2 likely reflects the development of systemic and local proliferative immune responses, driven by activated myeloid lineage cells (82), as a result of immune system detection of cancer. Previous literature suggests that not only do activated lymphocytes have a preference for TCN2 over other carriers of cobalamin (170), but TCN2 is also preferentially absorbed by normal tissues and organs, even in the setting of proliferative tumorigenesis (171). More than likely, increased APO-TCN2 improves the probability of delivering vitamin B12 (through HOLO-TCN2) to lymphoid organs to drive robust immune proliferation and activated immune responses. The elevated APO-TCN2 levels within the survivor patient cohort would then reflect an increased demand for cobalamin in the setting of enhanced lymphocytic proliferation. We provided evidence that this proliferation is occurring within B lymphocytes and associated with intratumoral germinal center formation for enhanced anti-tumor immune responses.

Secondarily, previous literature suggests that APO-TCN2 can likely act as a competitive inhibitor of the CD320 receptor. In this scenario, APO-TCN2 could block the binding and delivery of vitamin B12 (HOLO-TCN2) on CD320+ cells (172), such as malignant tumor cells, thereby limiting their proliferation. While possible, our group believes APO-TCN2's anti-tumor effect is more than likely through direct lymphocyte activation and proliferation as opposed to activity on tumor cells as a competitive inhibitor. Additionally, APO-TCN2 could possibly drive an undescribed signaling mechanism in these cells, associated with immune activation or pro-inflammatory signal transduction, through binding the CD320 receptor, binding the previously described megalin [thought to be essential in the accumulation of TCN2 in the kidney cortex and other absorptive epithelia (173)], binding an undefined receptor, or forming an additional receptor-ligand complex. Efforts to characterize the activity (if any) of APO-TCN2 are necessary for better understanding its role in both OSA and autoimmune disease. Nevertheless, these results suggest that surviving OSA patients are mounting a robust, systemic immune response as reflected through elevated levels of a biomarker (APO-TCN2) previously associated with active lymphoproliferative autoimmune disease.

While robust in our analyses, this study has inherent limitations. To begin, our plasma proteomic investigation analyzed only 14 naive OSA patients, with n = 3 in the 2-year deceased and n = 11 in the 2-year survival cohort. Considering the limited number of patient samples and the exploratory nature of the study, DEPs between comparative groups were determined based on having a Log2FC > 0.585 or < -0.585 and P-value < 0.05, leading to the possible discovery of false positive DEPs. Future investigations with larger sample sizes will utilize more stringent statistical measures [false discovery rate (FDR), corrected P-values (Bonferroni)] to determine DEPs. Importantly, however, the major finding from this study was supported by gene expression analysis of the largest known OSA RNA-seq dataset (TARGET-OS) in addition to other solid tumors (i.e. TCGA-SARC). Furthermore, several of the analyses presented here, including APO-TCN2's relationship to other plasma proteins and scRNA-seq cell-cell communication analysis, are mostly correlative and associative in nature. These findings ultimately require further validation in confirmatory studies. Additionally, as to be expected with clinical specimens, the Streck-collected plasma samples analyzed here were processed and stored over varying periods of time. It is well understood that delays in sample processing can affect the measured proteome of patient samples. Fortunately, a previous analysis by Savage et al. using the O-link proteomic platform reported no change in TCN2 levels (in comparison to fresh samples) even after 18 hours of room temperature storage prior to blood specimen processing (log2FC = -0.0087, P-value = 0.860127) (174). These results suggest that the measured APO-TCN2 levels reported here were likely minimally influenced by differential processing times. Ultimately, future studies which plan to expand our OSA patient cohort will be more cognizant of sample collection and processing time to limit confounding influences during comparative analyses.

In conclusion, this study identified apo-transcobalamin-II (APO-TCN2) as a novel plasma proteomic biomarker of survival in OSA. We provide evidence that increases in APO-TCN2 likely reflect a systemic and local inflammatory myeloid response which drives proliferation and intratumoral infiltration of B lymphocytes for improved anti-tumor immunity in these patients. This finding correlated with the only known documented investigation of TCN2 in this disease, which previously suggested *TCN2* as one of four upregulated survival genes in OSA tumors of the TARGET-OS dataset (118). Further expansion of our patient cohort for validation of APO-TCN2's clinical utility as a biomarker of improved overall survival is warranted. Future studies to investigate the distinct biological function of APO-TCN2 in both OSA and lymphoproliferative autoimmune disorders are necessary. Considering the availability of recombinant forms of this globulin protein, studies which investigate therapeutic injection of APO-TCN2 in murine models of metastatic OSA could ultimately suggest a future therapeutic role for this protein. Exogenous TCN2 may be critical to drive the robust expansion and lymphocytic proliferation necessary for enhanced anti-tumor immune responses in these patients.

Data availability statement

The datasets used and/or analyzed during this study are available in the Supplementary Files, the GEO repository (https://

www.ncbi.nlm.nih.gov/geo/query/acc.cgi?acc=GSE162454, https://www.ncbi.nlm.nih.gov/geo/query/acc.cgi?acc=GSE152048), the corresponding web-based platforms (https://bhasinlab.bmi.emory.edu/Survival Genie/, http://tiger.canceromics.org/#/, https://kmplot.com/analysis/, http://gepia2.cancer-pku.cn/#index), or from the corresponding author on reasonable request.

Ethics statement

The studies involving humans were approved by the University of Pittsburgh Medical Center Institutional Review Board (IRB STUDY 19060152). The studies were conducted in accordance with the local legislation and institutional requirements. Written informed consent for participation in this study was provided by the participants' legal guardians/next of kin.

Author contributions

RL: Writing – original draft, Writing – review & editing, Conceptualization, Data curation, Formal analysis, Investigation, Visualization. SD: Data curation, Formal analysis, Investigation, Visualization, Writing – original draft, Writing – review & editing. CR: Data curation, Writing – review & editing. LM: Investigation, Writing – original draft, Writing – review & editing. VM: Formal analysis, Writing – review & editing. BF: Formal analysis, Writing – original draft, Writing – review & editing. EC: Formal analysis, Writing – original draft, Writing – review & editing. TH: Formal analysis, Project administration, Writing – review & editing. IL: Formal analysis, Project administration, Writing – review & editing. KS: Formal analysis, Project administration, Writing – review & editing. GH: Funding acquisition, Project administration, Resources, Writing – review & editing. NL: Formal analysis, Project administration, Supervision, Writing – review & editing. KW: Formal analysis, Project administration, Resources, Supervision, Writing – review & editing. BL: Conceptualization, Formal analysis, Funding acquisition, Investigation, Project administration, Resources, Supervision, Writing – review & editing.

Funding

The author(s) declare financial support was received for the research, authorship, and/or publication of this article. This work was supported through grant funding by the Pittsburgh Cure Sarcoma Foundation and internal funding by the West Virginia University School of Medicine, Department of Orthopaedics. This project used the Musculoskeletal Oncology Tumor Registry and Tissue Bank at the University of Pittsburgh Medical Center. This project also utilized the Bioinformatics Core at the West Virginia University School of Medicine with funding through both WV-INBRE grant P20 GM103434 and NIGMS grant U54 GM-104942.

Acknowledgments

We acknowledge SomaLogic Inc. including Jennifer Yoon, Alan Horgan, Will Schwarzmann, and Christopher Dimapasok, among others, for their support of this work.

Conflict of interest

The authors declare that the research was conducted in the absence of any commercial or financial relationships that could be construed as a potential conflict of interest.

Publisher's note

Supplementary material

The Supplementary Material for this article can be found online at: https://www.frontiersin.org/articles/10.3389/fonc.2024.1417459/full#supplementary-material

SUPPLEMENTARY FILE 1
Supplementary Figures and Tables: Supplementary Figures 1-11 and Supplementary Tables 1-3 including titles and legends.

SUPPLEMENTARY FILE 2
All Naive OSA, 2-year Survival Analysis: Raw proteomics data (RFUs), comparison between naive, all OSA, 2-year survival analysis, and Reactome pathway analysis.

SUPPLEMENTARY FILE 3
Naive, Advanced Disease OSA, 2-year Survival Analysis: Raw data for comparison between naive, advanced disease OSA, 2-year survival analysis with additional data from Reactome pathway analysis.

SUPPLEMENTARY FILE 4
scRNA-seq of Naive and Chemotherapy Treated OSA tumor: Raw data derived from Loupe Browser used in analysis of various cellular populations of interest and reported in manuscript.

References

1. Diaz PM, Leehans A, Ravishankar P, Daily A. Multiomic approaches for cancer biomarker discovery in liquid biopsies: advances and challenges. *biomark Insights*. (2023) 18:11772719231204508. doi: 10.1177/11772719231204508

2. Pruis MA, Groenendijk FH, Badloe KS, van Puffelen A, Robbrecht D, Dinjens WNM, et al. Personalised selection of experimental treatment in patients with advanced solid cancer is feasible using whole-genome sequencing. *Br J Cancer*. (2022) 127:776–83. doi: 10.1038/s41416-022-01841-3

3. Jiménez-Santos MJ, García-Martín S, Fustero-Torre C, Di Domenico T, Gómez-López G, Al-Shahrour F. Bioinformatics roadmap for therapy selection in cancer genomics. *Mol Oncol*. (2022) 16:3881–908. doi: 10.1002/1878-0261.13286

4. Avila M, Meric-Bernstam F. Next-generation sequencing for the general cancer patient. *Clin Adv Hematol Oncol*. (2019) 17:447–54.

5. Yang X, Kui L, Tang M, Li D, Wei K, Chen W, et al. High-throughput transcriptome profiling in drug and biomarker discovery. *Front Genet*. (2020) 11:19. doi: 10.3389/fgene.2020.00019

6. Hristova VA, Chan DW. Cancer biomarker discovery and translation: proteomics and beyond. *Expert Rev Proteomics*. (2019) 16:93–103. doi: 10.1080/14789450.2019.1559062

7. Sisodiya S, Kasherwal V, Khan A, Roy B, Goel A, Kumar S, et al. Liquid Biopsies: Emerging role and clinical applications in solid tumours. *Transl Oncol*. (2023) 35:101716. doi: 10.1016/j.tranon.2023.101716

8. Lin D, Shen L, Luo M, Zhang K, Li J, Yang Q, et al. Circulating tumor cells: biology and clinical significance. *Signal Transduct Target Ther*. (2021) 6:404. doi: 10.1038/s41392-021-00817-8

9. Cortés-Hernández LE, Eslami-S Z, Pantel K, Alix-Panabières C. Circulating tumor cells: from basic to translational research. *Clin Chem*. (2024) 70:81–9. doi: 10.1093/clinchem/hvad142

10. Zhou B, Xu K, Zheng X, Chen T, Wang J, Song Y, et al. Application of exosomes as liquid biopsy in clinical diagnosis. *Signal Transduct Target Ther*. (2020) 5:144. doi: 10.1038/s41392-020-00258-9

11. Yu D, Li Y, Wang M, Gu J, Xu W, Cai H, et al. Exosomes as a new frontier of cancer liquid biopsy. *Mol Cancer*. (2022) 21:56. doi: 10.1186/s12943-022-01509-9

12. Cescon DW, Bratman SV, Chan SM, Siu LL. Circulating tumor DNA and liquid biopsy in oncology. *Nat Cancer*. (2020) 1:276–90. doi: 10.1038/s43018-020-0043-5

13. Ma M, Zhu H, Zhang C, Sun X, Gao X, Chen G. "Liquid biopsy"-ctDNA detection with great potential and challenges. *Ann Transl Med*. (2015) 3:235. doi: 10.3978/j.issn.2305-5839.2015.09.29

14. Mathai RA, Vidya RVS, Reddy BS, Thomas L, Udupa K, Kolesar J, et al. Potential utility of liquid biopsy as a diagnostic and prognostic tool for the assessment of solid tumors: implications in the precision oncology. *J Clin Med*. (2019) 8. doi: 10.3390/jcm8030373

15. Pinzani P, D'Argenio V, Del Re M, Pellegrini C, Cucchiara F, Salvianti F, et al. Updates on liquid biopsy: current trends and future perspectives for clinical application in solid tumors. *Clin Chem Lab Med*. (2021) 59:1181–200. doi: 10.1515/cclm-2020-1685

16. Weiser DA, West-Szymanski DC, Fraint E, Weiner S, Rivas MA, Zhao CWT, et al. Progress toward liquid biopsies in pediatric solid tumors. *Cancer Metastasis Rev*. (2019) 38:553–71. doi: 10.1007/s10555-019-09825-1

17. van der Laan P, van Houdt WJ, van den Broek D, Steeghs N, van der Graaf WTA. Liquid biopsies in sarcoma clinical practice: where do we stand? *Biomedicines*. (2021) 9. doi: 10.3390/biomedicines9101315

18. Li X, Seebacher NA, Hornicek FJ, Xiao T, Duan Z. Application of liquid biopsy in bone and soft tissue sarcomas: Present and future. *Cancer Lett*. (2018) 439:66–77. doi: 10.1016/j.canlet.2018.09.012

19. Ding Z, Wang N, Ji N, Chen ZS. Proteomics technologies for cancer liquid biopsies. *Mol Cancer*. (2022) 21:53. doi: 10.1186/s12943-022-01526-8

20. Sallam RM. Proteomics in cancer biomarkers discovery: challenges and applications. *Dis Markers*. (2015) 2015:321370. doi: 10.1155/2015/321370

21. Mesri M. Advances in proteomic technologies and its contribution to the field of cancer. *Adv Med*. (2014) 2014:238045. doi: 10.1155/2014/238045

22. Khalilpour A, Kilic T, Khalilpour S, Álvarez MM, Yazdi IK. Proteomic-based biomarker discovery for development of next generation diagnostics. *Appl Microbiol Biotechnol*. (2017) 101:475–91. doi: 10.1007/s00253-016-8029-z

23. Gold L, Ayers D, Bertino J, Bock C, Bock A, Brody EN, et al. Aptamer-based multiplexed proteomic technology for biomarker discovery. *PLoS One*. (2010) 5: e15004. doi: 10.1371/journal.pone.0015004

24. Tuerk C, Gold L. Systematic evolution of ligands by exponential enrichment: RNA ligands to bacteriophage T4 DNA polymerase. *Science*. (1990) 249:505–10. doi: 10.1126/science.2200121

25. Ellington AD, Szostak JW. *In vitro* selection of RNA molecules that bind specific ligands. *Nature*. (1990) 346:818–22. doi: 10.1038/346818a0

26. Kraemer S, Vaught JD, Bock C, Gold L, Katilius E, Keeney TR, et al. From SOMAmer-based biomarker discovery to diagnostic and clinical applications: a SOMAmer-based, streamlined multiplex proteomic assay. *PLoS One*. (2011) 6: e26332. doi: 10.1371/journal.pone.0026332

27. Gold L, Walker JJ, Wilcox SK, Williams S. Advances in human proteomics at high scale with the SOMAscan proteomics platform. *N Biotechnol*. (2012) 29:543–9. doi: 10.1016/j.nbt.2011.11.016

28. Qiao Z, Pan X, Parlayan C, Ojima H, Kondo T. Proteomic study of hepatocellular carcinoma using a novel modified aptamer-based array (SOMAscan™) platform. *Biochim Biophys Acta Proteins Proteom*. (2017) 1865:434–43. doi: 10.1016/j.bbapap.2016.09.011

29. Li H, Vanarsa K, Zhang T, Soomro S, Cicalese PA, Duran V, et al. Comprehensive aptamer-based screen of 1317 proteins uncovers improved stool protein markers of colorectal cancer. *J Gastroenterol*. (2021) 56:659–72. doi: 10.1007/s00535-021-01795-y

30. Narasimhan A, Shahda S, Kays JK, Perkins SM, Cheng L, Schloss KNH, et al. Identification of potential serum protein biomarkers and pathways for pancreatic cancer cachexia using an aptamer-based discovery platform. *Cancers (Basel)*. (2020) 12. doi: 10.3390/cancers12123787

31. Thanasupawat T, Glogowska A, Pascoe C, Krishnan SN, Munir M, Begum F, et al. Slow off-rate modified aptamer (SOMAmer) proteomic analysis of patient-derived Malignant glioma identifies distinct cellular proteomes. *Int J Mol Sci*. (2021) 22. doi: 10.3390/ijms22179566

32. Ostroff RM, Bigbee WL, Franklin W, Gold L, Mehan M, Miller YE, et al. Unlocking biomarker discovery: large scale application of aptamer proteomic technology for early detection of lung cancer. *PLoS One*. (2010) 5:e15003. doi: 10.1371/journal.pone.0015003

33. Blatt S, Kämmerer PW, Krüger M, Surabattula R, Thiem DGE, Dillon ST, et al. High-multiplex aptamer-based serum proteomics to identify candidate serum biomarkers of oral squamous cell carcinoma. *Cancers (Basel)*. (2023) 15. doi: 10.3390/cancers15072071

34. Finkernagel F, Reinartz S, Schuldner M, Malz A, Jansen JM, Wagner U, et al. Dual-platform affinity proteomics identifies links between the recurrence of ovarian carcinoma and proteins released into the tumor microenvironment. *Theranostics*. (2019) 9:6601–17. doi: 10.7150/thno.37549

35. Candia J, Daya GN, Tanaka T, Ferrucci L, Walker KA. Assessment of variability in the plasma 7k SomaScan proteomics assay. *Sci Rep*. (2022) 12:17147. doi: 10.1038/s41598-022-22116-0

36. Lim SY, Lee JH, Welsh SJ, Ahn SB, Breen E, Khan A, et al. Evaluation of two high-throughput proteomic technologies for plasma biomarker discovery in immunotherapy-treated melanoma patients. *biomark Res*. (2017) 5:32. doi: 10.1186/s40364-017-0112-9

37. Gill J, Gorlick R. Advancing therapy for osteosarcoma. *Nat Rev Clin Oncol*. (2021) 18:609–24. doi: 10.1038/s41571-021-00519-8

38. Yang C, Tian Y, Zhao F, Chen Z, Su P, Li Y, et al. Bone microenvironment and osteosarcoma metastasis. *Int J Mol Sci*. (2020) 21:6985. doi: 10.3390/ijms21196985

39. Smrke A, Anderson PM, Gulia A, Gennatas S, Huang PH, Jones RL. Future directions in the treatment of osteosarcoma. *Cells*. (2021) 10. doi: 10.3390/cells10010172

40. Corre I, Verrecchia F, Crenn V, Redini F, Trichet V. The osteosarcoma microenvironment: A complex but targetable ecosystem. *Cells*. (2020) 9. doi: 10.3390/cells9040976

41. Gaspar N, Marques Da Costa ME, Fromigue O, Droit R, Berlanga P, Marchais A. Recent advances in understanding osteosarcoma and emerging therapies. *Faculty Rev*. (2020) 9. doi: 10.12703/r/9-18

42. Cascini C, Chiodoni C. The immune landscape of osteosarcoma: implications for prognosis and treatment response. *Cells*. (2021) 10. doi: 10.3390/cells10071668

43. Aran V, Devalle S, Meohas W, Heringer M, Cunha Caruso A, Pinheiro Aguiar D, et al. Osteosarcoma, chondrosarcoma and Ewing sarcoma: Clinical aspects, biomarker discovery and liquid biopsy. *Crit Rev Oncol Hematol*. (2021) 162:103340. doi: 10.1016/j.critrevonc.2021.103340

44. Ucci A, Rucci N, Ponzetti M. Liquid biopsies in primary and secondary bone cancers. *Cancer Drug Resist*. (2022) 5:541–59. doi: 10.20517/cdr.2022.17

45. Raimondi L, De Luca A, Costa V, Amodio N, Carina V, Bellavia D, et al. Circulating biomarkers in osteosarcoma: new translational tools for diagnosis and treatment. *Oncotarget*. (2017) 8:100831–51. doi: 10.18632/oncotarget.19852

46. Evola FR, Costarella L, Pavone V, Caff G, Cannavò L, Sessa A, et al. Biomarkers of osteosarcoma, chondrosarcoma, and ewing sarcoma. *Front Pharmacol*. (2017) 8:150. doi: 10.3389/fphar.2017.00150

47. Wan-Ibrahim WI, Singh VA, Hashim OH, Abdul-Rahman PS. Biomarkers for bone tumors: discovery from genomics and proteomics studies and their challenges. *Mol Med*. (2016) 21:861–72. doi: 10.2119/molmed.2015.00183

48. Savitskaya YA, Rico-Martínez G, Linares-González LM, Delgado-Cedillo EA, Téllez-Gastelum R, Alfaro-Rodríguez AB, et al. Serum tumor markers in pediatric osteosarcoma: a summary review. *Clin Sarcoma Res*. (2012) 2:9. doi: 10.1186/2045-3329-2-9

49. Holzer G, Pfandlsteiner T, Blahovec H, Trieb K, Kotz R. Serum levels of TNF-beta and sTNF-R in patients with Malignant bone tumours. *Anticancer Res*. (2003) 23:3057–9.

50. Markiewicz K, Zeman K, Kozar A, Gołebiowska-Wawrzyniak M. Evaluation of selected cytokines in children and adolescents with osteosarcoma at diagnosis - preliminary report. *Med Wieku Rozwoj*. (2011) 15:25–31.

51. Zhang C, Wang L, Xiong C, Zhao R, Liang H, Luo X. The role of vascular endothelial growth factor as a prognostic and clinicopathological marker in osteosarcoma: a systematic review and meta-analysis. *J Orthop Surg Res*. (2021) 16:738. doi: 10.1186/s13018-021-02888-3

52. Chen D, Zhang YJ, Zhu KW, Wang WC. A systematic review of vascular endothelial growth factor expression as a biomarker of prognosis in patients with osteosarcoma. *Tumour Biol*. (2013) 34:1895–9. doi: 10.1007/s13277-013-0733-z

53. Qu JT, Wang M, He HL, Tang Y, Ye XJ. The prognostic value of elevated vascular endothelial growth factor in patients with osteosarcoma: a meta-analysis and systemic review. *J Cancer Res Clin Oncol*. (2012) 138:819–25. doi: 10.1007/s00432-012-1149-7

54. Kushlinskii NE, Babkina IV, Solov'ev YN, Trapeznikov NN. Vascular endothelium growth factor and angiogenin in the serum of patients with osteosarcoma and Ewing's tumor. *Bull Exp Biol Med*. (2000) 130:691–3. doi: 10.1007/BF02682107

55. Liu G, Liu B, Tang L, Liu Z, Dai H. Cytokines as prognostic biomarkers in osteosarcoma patients: A systematic review and meta-analysis. *J Interferon Cytokine Res*. (2023) 43:335–43. doi: 10.1089/jir.2023.0083

56. Li Y, Flores R, Yu A, Okcu MF, Murray J, Chintagumpala M, et al. Elevated expression of CXC chemokines in pediatric osteosarcoma patients. *Cancer*. (2011) 117:207–17. doi: 10.1002/cncr.v117.1

57. Li Y, Dang TA, Shen J, Hicks J, Chintagumpala M, Lau CC, et al. Plasma proteome predicts chemotherapy response in osteosarcoma patients. *Oncol Rep*. (2011) 25:303–14. doi: 10.3892/or.2010.1111

58. Williams SA, Kivimaki M, Langenberg C, Hingorani AD, Casas JP, Bouchard C, et al. Plasma protein patterns as comprehensive indicators of health. *Nat Med*. (2019) 25:1851–7. doi: 10.1038/s41591-019-0665-2

59. Fabregat A, Sidiropoulos K, Garapati P, Gillespie M, Hausmann K, Haw R, et al. The reactome pathway knowledgebase. *Nucleic Acids Res*. (2016) 44:D481–7. doi: 10.1093/nar/gkv1351

60. Fabregat A, Jupe S, Matthews L, Sidiropoulos K, Gillespie M, Garapati P, et al. The reactome pathway knowledgebase. *Nucleic Acids Res*. (2018) 46:D649–D55. doi: 10.1093/nar/gkx1132

61. Fabregat A, Sidiropoulos K, Viteri G, Forner O, Marin-Garcia P, Arnau V, et al. Reactome pathway analysis: a high-performance in-memory approach. *BMC Bioinf*. (2017) 18:142. doi: 10.1186/s12859-017-1559-2

62. Dwivedi B, Mumme H, Satpathy S, Bhasin SS, Bhasin M. Survival Genie, a web platform for survival analysis across pediatric and adult cancers. *Sci Rep*. (2022) 12:3069. doi: 10.1038/s41598-022-06841-0

63. Contal C, O'Quigley J. An application of changepoint methods in studying the effect of age on survival in breast cancer. *Comput Stat Data Anal* (1999) 30:253–70. doi: 10.1016/S0167-9473(98)00096-6

64. Dardis C. survMisc: miscellaneous functions for survival data. *R-project*. (2022) 0.5:6.

65. Chen B, Khodadoust MS, Liu CL, Newman AM, Alizadeh AA. Profiling tumor infiltrating immune cells with CIBERSORT. *Methods Mol Biol*. (2018) 1711:243–59. doi: 10.1007/978-1-4939-7493-1_12

66. Chen Z, Luo Z, Zhang D, Li H, Liu X, Zhu K, et al. TIGER: A web portal of tumor immunotherapy gene expression resource. *Genomics Proteomics Bioinf*. (2023) 21:337–48. doi: 10.1016/j.gpb.2022.08.004

67. Lambrechts D, Wauters E, Boeckx B, Aibar S, Nittner D, Burton O, et al. Phenotype molding of stromal cells in the lung tumor microenvironment. *Nat Med*. (2018) 24:1277–89. doi: 10.1038/s41591-018-0096-5

68. Wu TD, Madireddi S, de Almeida PE, Banchereau R, Chen YJ, Chitre AS, et al. Peripheral T cell expansion predicts tumour infiltration and clinical response. *Nature*. (2020) 579:274–8. doi: 10.1038/s41586-020-2056-8

69. Kim N, Kim HK, Lee K, Hong Y, Cho JH, Choi JW, et al. Single-cell RNA sequencing demonstrates the molecular and cellular reprogramming of metastatic lung adenocarcinoma. *Nat Commun*. (2020) 11:2285. doi: 10.1038/s41467-020-16164-1

70. Maynard A, McCoach CE, Rotow JK, Harris L, Haderk F, Kerr DL, et al. Therapy-induced evolution of human lung cancer revealed by single-cell RNA sequencing. *Cell*. (2020) 182:1232–51.e22. doi: 10.1016/j.cell.2020.07.017

71. Sade-Feldman M, Yizhak K, Bjorgaard SL, Ray JP, de Boer CG, Jenkins RW, et al. Defining T cell states associated with response to checkpoint immunotherapy in melanoma. *Cell*. (2019) 176:404. doi: 10.1016/j.cell.2018.12.034

72. Liu Y, Feng W, Dai Y, Bao M, Yuan Z, He M, et al. Single-cell transcriptomics reveals the complexity of the tumor microenvironment of treatment-naive osteosarcoma. *Front Oncol*. (2021) 11:709210. doi: 10.3389/fonc.2021.709210

73. Khodadadi L, Cheng Q, Radbruch A, Hiepe F. The maintenance of memory plasma cells. *Front Immunol*. (2019) 10:721. doi: 10.3389/fimmu.2019.00721

74. Sanges S, Guerrier T, Duhamel A, Guilbert L, Hauspie C, Largy A, et al. Soluble markers of B cell activation suggest a role of B cells in the pathogenesis of systemic sclerosis-associated pulmonary arterial hypertension. *Front Immunol*. (2022) 13:954007. doi: 10.3389/fimmu.2022.954007

75. Li R, Berglund A, Zemp L, Dhillon J, Putney R, Kim Y, et al. The 12-CK score: global measurement of tertiary lymphoid structures. *Front Immunol*. (2021) 12:694079. doi: 10.3389/fimmu.2021.694079

76. Kovács SA, Fekete JT, Győrffy B. Predictive biomarkers of immunotherapy response with pharmacological applications in solid tumors. *Acta Pharmacol Sin*. (2023) 44:1879–89. doi: 10.1038/s41401-023-01079-6

77. Tang Z, Kang B, Li C, Chen T, Zhang Z. GEPIA2: an enhanced web server for large-scale expression profiling and interactive analysis. *Nucleic Acids Res*. (2019) 47:W556–W60. doi: 10.1093/nar/gkz430

78. Kose E, Besci O, Gudeloglu E, Suncak S, Oymak Y, Ozen S, et al. Transcobalamin II deficiency in twins with a novel variant in the TCN2 gene: case report and review of literature. *J Pediatr Endocrinol Metab*. (2020) 33:1487–99. doi: 10.1515/jpem-2020-0096

79. Ratschmann R, Minkov M, Kis A, Hung C, Rupar T, Mühl A, et al. Transcobalamin II deficiency at birth. *Mol Genet Metab*. (2009) 98:285–8. doi: 10.1016/j.ymgme.2009.06.003

80. Unal S, Tezol O, Oztas Y. A novel mutation of the transcobalamin II gene in an infant presenting with hemophagocytic lymphohistiocytosis. *Int J Hematol*. (2014) 99:659–62. doi: 10.1007/s12185-014-1545-7

81. Zhan S, Cheng F, He H, Hu S, Feng X. Identification of transcobalamin deficiency with two novel mutations in the TCN2 gene in a Chinese girl with abnormal immunity: a case report. *BMC Pediatr*. (2020) 20:460. doi: 10.1186/s12887-020-02357-6

82. Fehr J, De Vecchi P. Transcobalamin II: a marker for macrophage/histiocyte proliferation. *Am J Clin Pathol*. (1985) 84:291–6. doi: 10.1093/ajcp/84.3.291

83. Li L, Zhang X, Kovacic S, Long AJ, Bourque K, Wood CR, et al. Identification of a human follicular dendritic cell molecule that stimulates germinal center B cell growth. *J Exp Med*. (2000) 191:1077–84. doi: 10.1084/jem.191.6.1077

84. Quadros EV, Sequeira JM. Cellular uptake of cobalamin: transcobalamin and the TCblR/CD320 receptor. *Biochimie*. (2013) 95:1008–18. doi: 10.1016/j.biochi.2013.02.004

85. Lai SC, Nakayama Y, Sequeira JM, Quadros EV. Down-regulation of transcobalamin receptor TCblR/CD320 by siRNA inhibits cobalamin uptake and proliferation of cells in culture. *Exp Cell Res*. (2011) 317:1603–7. doi: 10.1016/j.yexcr.2011.02.016

86. Cho W, Choi J, Park CH, Yoon SO, Jeoung DI, Kim YM, et al. Expression of CD320 in human B cells in addition to follicular dendritic cells. *BMB Rep*. (2008) 41:863–7. doi: 10.5483/BMBRep.2008.41.12.863

87. Sysel AM, Valli VE, Nagle RB, Bauer JA. Immunohistochemical quantification of the vitamin B12 transport protein (TCII), cell surface receptor (TCII-R) and Ki-67 in human tumor xenografts. *Anticancer Res*. (2013) 33:4203–12.

88. Oreshkin AE, Gudkova MV, Miasishcheva NV. The expression of plasmalemma transcobalamin-II receptors on human blood lymphocytes stimulated by mitogens. *Biull Eksp Biol Med*. (1992) 114:185–7. doi: 10.1007/BF00800082

89. McLean GR, Quadros EV, Rothenberg SP, Morgan AC, Schrader JW, Ziltener HJ. Antibodies to transcobalamin II block in *vitro* proliferation of leukemic cells. *Blood*. (1997) 89:235–42. doi: 10.1182/blood.V89.1.235

90. McLean GR, Williams MJ, Woodhouse CS, Ziltener HJ. Transcobalamin II and in vitro proliferation of leukemic cells. *Leuk Lymphoma*. (1998) 30:101–9. doi: 10.3109/10428199809050933

91. Liu B, Xu K, Li A, Xu J, Cui Y. Inhibition of transcolbalamin2 overexpression ameliorated renal injury in systemic lupus erythema via reducing pathogenic Tfh and B cell infiltration. *Lupus Sci Med*. (2023) 10. doi: 10.1136/lupus-2023-KCR.37

92. Calderaro J, Petitprez F, Becht E, Laurent A, Hirsch TZ, Rousseau B, et al. Intra-tumoral tertiary lymphoid structures are associated with a low risk of early recurrence of hepatocellular carcinoma. *J Hepatol*. (2019) 70:58–65. doi: 10.1016/j.jhep.2018.09.003

93. Ding GY, Ma JQ, Yun JP, Chen X, Ling Y, Zhang S, et al. Distribution and density of tertiary lymphoid structures predict clinical outcome in intrahepatic cholangiocarcinoma. *J Hepatol*. (2022) 76:608–18. doi: 10.1016/j.jhep.2021.10.030

94. Domblides C, Rochefort J, Riffard C, Panouillot M, Lescaille G, Teillaud JL, et al. Tumor-associated tertiary lymphoid structures: from basic and clinical knowledge to therapeutic manipulation. *Front Immunol*. (2021) 12:698604. doi: 10.3389/fimmu.2021.698604

95. Germain C, Gnjatic S, Tamzalit F, Knockaert S, Remark R, Goc J, et al. Presence of B cells in tertiary lymphoid structures is associated with a protective immunity in patients with lung cancer. *Am J Respir Crit Care Med*. (2014) 189:832–44. doi: 10.1164/rccm.201309-1611OC

96. He W, Zhang D, Liu H, Chen T, Xie J, Peng L, et al. The high level of tertiary lymphoid structure is correlated with superior survival in patients with advanced gastric cancer. *Front Oncol*. (2020) 10:980. doi: 10.3389/fonc.2020.00980

97. Jiang Q, Tian C, Wu H, Min L, Chen H, Chen L, et al. Tertiary lymphoid structure patterns predicted anti-PD1 therapeutic responses in gastric cancer. *Chin J Cancer Res*. (2022) 34:365–82. doi: 10.21147/j.issn.1000-9604.2022.04.05

98. Kemi N, Ylitalo O, Väyrynen JP, Helminen O, Junttila A, Mrena J, et al. Tertiary lymphoid structures and gastric cancer prognosis. *APMIS*. (2023) 131:19–25. doi: 10.1111/apm.v131.1

99. Kroeger DR, Milne K, Nelson BH. Tumor-infiltrating plasma cells are associated with tertiary lymphoid structures, cytolytic T-cell responses, and superior prognosis in ovarian cancer. *Clin Cancer Res*. (2016) 22:3005–15. doi: 10.1158/1078-0432.CCR-15-2762

100. Li Q, Liu X, Wang D, Wang Y, Lu H, Wen S, et al. Prognostic value of tertiary lymphoid structure and tumour infiltrating lymphocytes in oral squamous cell carcinoma. *Int J Oral Sci*. (2020) 12:24. doi: 10.1038/s41368-020-00092-3

101. Liu Z, Meng X, Tang X, Zou W, He Y. Intratumoral tertiary lymphoid structures promote patient survival and immunotherapy response in head neck squamous cell carcinoma. *Cancer Immunol Immunother*. (2022) 72(6):1505–21. doi: 10.21203/rs.3.rs-1987850/v1

102. Mori T, Tanaka H, Deguchi S, Yamakoshi Y, Miki Y, Yoshii M, et al. Clinical efficacy of nivolumab is associated with tertiary lymphoid structures in surgically resected primary tumors of recurrent gastric cancer. *PloS One*. (2022) 17:e0262455. doi: 10.1371/journal.pone.0262455

103. J N, T J, N Sl, B Gt. Tertiary lymphoid structures and B lymphocytes in cancer prognosis and response to immunotherapies. *Oncoimmunology*. (2021) 10:1900508. doi: 10.1080/2162402X.2021.1900508

104. Sautès-Fridman C, Lawand M, Giraldo NA, Kaplon H, Germain C, Fridman WH, et al. Tertiary lymphoid structures in cancers: prognostic value, regulation, and manipulation for therapeutic intervention. *Front Immunol*. (2016) 7:407. doi: 10.3389/fimmu.2016.00407

105. Schumacher TN, Thommen DS. Tertiary lymphoid structures in cancer. *Science*. (2022) 375:eabf9419. doi: 10.1126/science.abf9419

106. Trüb M, Zippelius A. Tertiary lymphoid structures as a predictive biomarker of response to cancer immunotherapies. *Front Immunol*. (2021) 12:674565. doi: 10.3389/fimmu.2021.674565

107. Vaghjiani RG, Skitzki JJ. Tertiary lymphoid structures as mediators of immunotherapy response. *Cancers (Basel)*. (2022) 14. doi: 10.3390/cancers14153748

108. Vanhersecke L, Brunet M, Guégan JP, Rey C, Bougouin A, Cousin S, et al. Mature tertiary lymphoid structures predict immune checkpoint inhibitor efficacy in solid tumors independently of PD-L1 expression. *Nat Cancer*. (2021) 2:794–802. doi: 10.1038/s43018-021-00232-6

109. Wakasu S, Tagawa T, Haratake N, Kinoshita F, Oku Y, Ono Y, et al. Preventive effect of tertiary lymphoid structures on lymph node metastasis of lung adenocarcinoma. *Cancer Immunol Immunother*. (2023) 72(6):1823–34. doi: 10.21203/rs.3.rs-2055351/v1

110. Wang B, Liu J, Han Y, Deng Y, Li J, Jiang Y. The presence of tertiary lymphoid structures provides new insight into the clinicopathological features and prognosis of patients with breast cancer. *Front Immunol*. (2022) 13:868155. doi: 10.3389/fimmu.2022.868155

111. Yu JS, Huang WB, Zhang YH, Chen J, Li J, Fu HF, et al. The association of immune cell infiltration and prognostic value of tertiary lymphoid structures in gastric cancer. *Neoplasma*. (2022) 69:886–98. doi: 10.4149/neo_2022_220128N123

112. Zhang Q, Wu S. Tertiary lymphoid structures are critical for cancer prognosis and therapeutic response. *Front Immunol*. (2022) 13:1063711. doi: 10.3389/fimmu.2022.1063711

113. Zhang K, Xie X, Zou LH, Guo SQ. Tertiary lymphoid structures are associated with a favorable prognosis in high-grade serous ovarian cancer patients. *Reprod Sci*. (2023) 30(8):2468–80. doi: 10.1007/s43032-023-01188-x

114. Zhou L, Xu B, Liu Y, Wang Z. Tertiary lymphoid structure signatures are associated with survival and immunotherapy response in muscle-invasive bladder cancer. *Oncoimmunology*. (2021) 10:1915574. doi: 10.1080/2162402X.2021.1915574

115. Zou J, Zhang Y, Zeng Y, Peng Y, Liu J, Xiao C, et al. Tertiary lymphoid structures: A potential biomarker for anti-cancer therapy. *Cancers (Basel)*. (2022) 14. doi: 10.3390/cancers14235968

116. Italiano A, Bessede A, Pulido M, Bompas E, Piperno-Neumann S, Chevreau C, et al. Pembrolizumab in soft-tissue sarcomas with tertiary lymphoid structures: a phase 2 PEMBROSARC trial cohort. *Nat Med*. (2022) 28:1199–206. doi: 10.1038/s41591-022-01821-3

117. Petitprez F, de Reyniès A, Keung EZ, Chen TW, Sun CM, Calderaro J, et al. B cells are associated with survival and immunotherapy response in sarcoma. *Nature*. (2020) 577:556–60. doi: 10.1038/s41586-019-1906-8

118. Rothzerg E, Xu J, Wood D, Kõks S. 12 Survival-related differentially expressed genes based on the TARGET-osteosarcoma database. *Exp Biol Med (Maywood)*. (2021) 246:2072–81. doi: 10.1177/15353702211007410

119. Seetharam B, Bose S, Li N. Cellular import of cobalamin (Vitamin B-12). *J Nutr*. (1999) 129:1761–4. doi: 10.1093/jn/129.10.1761

120. Seetharam B. Receptor-mediated endocytosis of cobalamin (vitamin B12). *Annu Rev Nutr*. (1999) 19:173–95. doi: 10.1146/annurev.nutr.19.1.173

121. Seetharam B, Li N. Transcobalamin II and its cell surface receptor. *Vitam Horm*. (2000) 59:337–66. doi: 10.1016/S0083-6729(00)59012-8

122. Barshop BA, Wolff J, Nyhan WL, Yu A, Prodanos C, Jones G, et al. Transcobalamin II deficiency presenting with methylmalonic aciduria and homocystinuria and abnormal absorption of cobalamin. *Am J Med Genet*. (1990) 35:222–8. doi: 10.1002/ajmg.1320350216

123. Bibi H, Gelman-Kohan Z, Baumgartner ER, Rosenblatt DS. Transcobalamin II deficiency with methylmalonic aciduria in three sisters. *J Inherit Metab Dis*. (1999) 22:765–72. doi: 10.1023/A:1005507204491

124. Chao MM, Illsinger S, Yoshimi A, Das AM, Kratz CP. Congenital transcobalamin II deficiency: A rare entity with a broad differential. *Klin Padiatr*. (2017) 229:355–7. doi: 10.1055/s-0043-120266

125. Hitzig WH, Dohmann U, Pluss HJ, Vischer D. Hereditary transcobalamin II deficiency: clinical findings in a new family. *J Pediatr*. (1974) 85:622–8. doi: 10.1016/S0022-3476(74)80503-2

126. Hitzig WH, Fràter-Schröder M, Seger R. Immunodeficiency due to transcobalamin II deficiency. *Ciba Found Symp*. (1978) 68:77–91. doi: 10.1002/9780470720516

127. Kaikov Y, Wadsworth LD, Hall CA, Rogers PC. Transcobalamin II deficiency: case report and review of the literature. *Eur J Pediatr*. (1991) 150:841–3. doi: 10.1007/BF01955004

128. Meyers PA, Carmel R. Hereditary transcobalamin II deficiency with subnormal serum cobalamin levels. *Pediatrics*. (1984) 74:866–71. doi: 10.1542/peds.74.5.866

129. Niebrugge DJ, Benjamin DR, Christie D, Scott CR. Hereditary transcobalamin II deficiency presenting as red cell hypoplasia. *J Pediatr*. (1982) 101:732–5. doi: 10.1016/S0022-3476(82)80304-1

130. Prasad C, Rosenblatt DS, Corley K, Cairney AE, Rupar CA. Transcobalamin (TC) deficiency–potential cause of bone marrow failure in childhood. *J Inherit Metab Dis*. (2008) 31 Suppl 2:S287–92. doi: 10.1007/s10545-008-0864-3

131. Rana SR, Colman N, Goh KO, Herbert V, Klemperer MR. Transcobalamin II deficiency associated with unusual bone marrow findings and chromosomal abnormalities. *Am J Hematol*. (1983) 14:89–96. doi: 10.1002/ajh.2830140111

132. Sakiyama Y. Hereditary transcobalamin II deficiency. *Ryoikibetsu Shokogun Shirizu*. (2000) 32:346–8.

133. Scott CR, Hakami N, Teng CC, Sagerson RN. Hereditary transcobalamin II deficiency: the role of transcobalamin II in vitamin B 12 -mediated reactions. *J Pediatr*. (1972) 81:1106–11. doi: 10.1016/S0022-3476(72)80239-7

134. Sourial NA. Transcobalamin II deficiency in infancy and the diagnostic value of serum B12 binders. *Scand J Haematol*. (1984) 33:327–8. doi: 10.1111/j.1600-0609.1984.tb02237.x

135. Thomas PK, Hoffbrand AV. Hereditary transcobalamin II deficiency: a 22 year follow up. *J Neurol Neurosurg Psychiatry*. (1997) 62:197. doi: 10.1136/jnnp.62.2.197

136. Toret E, Özdemir ZC, Bor Ö. Transcobalamin II deficiency in an infant with a novel mutation. *Turk Arch Pediatr*. (2022) 57:670–2. doi: 10.5152/TurkArchPediatr.2022.22100

137. Ünal Ş, Rupar T, Yetgin S, Yaralı N, Dursun A, Gürsel T, et al. Transcobalamin II deficiency in four cases with novel mutations. *Turk J Haematol*. (2015) 32:317–22. doi: 10.4274/Tjh.2014.0154

138. Ünal S, Karahan F, Arıkoğlu T, Akar A, Kuyucu S. Different presentations of patients with transcobalamin II deficiency: A single-center experience from Turkey. *Turk J Haematol*. (2019) 36:37–42. doi: 10.4274/tjh.galenos.2018.2018.0230

139. Seger R, Fràter-Schröder M, Hitzig WH, Wildfeuer A, Linnell JC. Granulocyte dysfunction in transcobalamin II deficiency responding to leucovorin or hydroxocobalamin-plasma transfusion. *J Inherit Metab Dis*. (1980) 3:3–9. doi: 10.1007/BF02312515

140. Carmel R, Hollander D. Extreme elevation of transcobalamin II levels in multiple myeloma and other disorders. *Blood*. (1978) 51:1057–63. doi: 10.1182/blood.V51.6.1057.1057

141. Rachmilewitz D, Ligumsky M, Rachmilewitz B, Rachmilewitz M, Tarcic N, Schlesinger M. Transcobalamin II level in peripheral blood monocytes–a biochemical marker in inflammatory diseases of the bowel. *Gastroenterology*. (1980) 78:43–6. doi: 10.1016/0016-5085(80)90190-0

142. Areekul S, Churdchu K, Cheeramakara C, Wilairatana P, Charoenlarp P. Persistently elevated serum transcobalamin II in a patient with cerebral malaria and typhus infections. *J Med Assoc Thai*. (1995) 78:48–52.

143. Cheeramakara C, Thanomsak W, Songmeang K, Nontprasert A, Sanghirun C, Suthisai N, et al. Elevation of serum transcobalamin II in patients with scrub typhus. *Southeast Asian J Trop Med Public Health*. (2005) 36:113–7.

144. Cheeramakara C, Songmeang K, Nakosiri W, Suthisai N, Nontprasert A, Areekul S. Study on serum transcobalamin II in patients with murine typhus. *Southeast Asian J Trop Med Public Health*. (2006) 37 Suppl 3:145–8.

145. Bauer A, Pachl E, Hellmuth JC, Kneidinger N, Heydarian M, Frankenberger M, et al. Proteomics reveals antiviral host response and NETosis during acute COVID-19 in high-risk patients. *Biochim Biophys Acta Mol Basis Dis*. (2023) 1869:166592. doi: 10.1016/j.bbadis.2022.166592

146. Fráter-Schröder M, Hitzig WH, Grob PJ, Kenny AB. Increase of unsaturated transcobalamine II in autoimmune diseases; effect of immunosuppressive therapy (proceedings). *Schweiz Med Wochenschr*. (1978) 108:1604.

147. Fràter-Schröder M, Hitzig WH, Grob PJ, Kenny AB. Increased unsaturated transcobalamin II in active autoimmune disease. *Lancet*. (1978) 2:238–9. doi: 10.1016/S0140-6736(78)91747-6

148. Lässer U, Kierat L, Grob PJ, Hitzig WH, Fráter-Schröder M. Transcobalamin II, a serum protein reflecting autoimmune disease activity, its plasma dynamics, and the relationship to established serum parameters in systemic lupus erythematosus. *Clin Immunol Immunopathol*. (1985) 36:345–57. doi: 10.1016/0090-1229(85)90055-8

149. Haynes WA, Haddon DJ, Diep VK, Khatri A, Bongen E, Yiu G, et al. Integrated, multicohort analysis reveals unified signature of systemic lupus erythematosus. *JCI Insight*. (2020) 5. doi: 10.1172/jci.insight.122312

150. Arnalich F, Zamorano AF, Benito-Urbina S, Gijón-Baños J, De Miguel E, Peña JM, et al. Increased apotranscobalamin II levels in rheumatoid arthritis. *Br J Rheumatol*. (1990) 29:171–3. doi: 10.1093/rheumatology/29.3.171

151. Dorraji SE, Kanapathippillai P, Hovd AK, Stenersrød MR, Horvei KD, Ursvik A, et al. Kidney tertiary lymphoid structures in lupus nephritis develop into large interconnected networks and resemble lymph nodes in gene signature. *Am J Pathol*. (2020) 190:2203–25. doi: 10.1016/j.ajpath.2020.07.015

152. Vreugdenhil G, Lindemans J, van Eijk HG, Swaak AJ. Elevated serum transcobalamin levels in anaemia of rheumatoid arthritis: correlation with disease activity but not with serum tumour necrosis factor alpha and interleukin 6. *J Intern Med*. (1992) 231:547–50. doi: 10.1111/j.1365-2796.1992.tb00972.x

153. Rachmilewitz B, Rachmilewitz M, Chaouat M, Schlesinger M. The synthesis of transcobalamin II, a vitamin B12 transport protein, by stimulated mouse peritoneal macrophages. *Biomedicine*. (1977) 27:213–4.

154. Rabinowitz R, Rachmilewitz B, Rachmilewitz M, Schlesinger M. Production of transcobalamin II by various murine and human cells in culture. *Isr J Med Sci*. (1982) 18:740–5.

155. Carmel R, Neely SM, Francis RB. Human umbilical vein endothelial cells secrete transcobalamin II. *Blood*. (1990) 75:251–4. doi: 10.1182/blood.V75.1.251.251

156. Quadros EV, Rothenberg SP, Jaffe EA. Endothelial cells from human umbilical vein secrete functional transcobalamin II. *Am J Physiol*. (1989) 256:C296–303. doi: 10.1152/ajpcell.1989.256.2.C296

157. Johansson-Percival A, Ganss R. Therapeutic induction of tertiary lymphoid structures in cancer through stromal remodeling. *Front Immunol*. (2021) 12:674375. doi: 10.3389/fimmu.2021.674375

158. Miyagawa-Hayashino A, Yoshifuji H, Kitagori K, Ito S, Oku T, Hirayama Y, et al. Increase of MZB1 in B cells in systemic lupus erythematosus: proteomic analysis of biopsied lymph nodes. *Arthritis Res Ther*. (2018) 20:13. doi: 10.1186/s13075-018-1511-5

159. Siu JHY, Pitcher MJ, Tull TJ, Velounias RL, Guesdon W, Montorsi L, et al. Two subsets of human marginal zone B cells resolved by global analysis of lymphoid tissues and blood. *Sci Immunol*. (2022) 7:eabm9060. doi: 10.1126/sciimmunol.abm9060

160. Meylan M, Petitprez F, Becht E, Bougoüin A, Pupier G, Calvez A, et al. Tertiary lymphoid structures generate and propagate anti-tumor antibody-producing plasma cells in renal cell cancer. *Immunity*. (2022) 55:527–41.e5. doi: 10.1016/j.immuni.2022.02.001

161. Shachar I, Haran M. The secret second life of an innocent chaperone: the story of CD74 and B cell/chronic lymphocytic leukemia cell survival. *Leuk Lymphoma*. (2011) 52:1446–54. doi: 10.3109/10428194.2011.565437

162. Ives A, Le Roy D, Théroude C, Bernhagen J, Roger T, Calandra T. Macrophage migration inhibitory factor promotes the migration of dendritic cells through CD74 and the activation of the Src/PI3K/myosin II pathway. *FASEB J*. (2021) 35:e21418. doi: 10.1096/fj.202001605R

163. Klasen C, Ohl K, Sternkopf M, Shachar I, Schmitz C, Heussen N, et al. MIF promotes B cell chemotaxis through the receptors CXCR4 and CD74 and ZAP-70 signaling. *J Immunol*. (2014) 192:5273–84. doi: 10.4049/jimmunol.1302209

164. Sun H, Fang T, Wang T, Yu Z, Gong L, Wei X, et al. Single-cell profiles reveal tumor cell heterogeneity and immunosuppressive microenvironment in Waldenström macroglobulinemia. *J Transl Med*. (2022) 20:576. doi: 10.1186/s12967-022-03798-6

165. Kong F, Ye S, Zhong Z, Zhou X, Zhou W, Liu Z, et al. Single-cell transcriptome analysis of chronic antibody-mediated rejection after renal transplantation. *Front Immunol*. (2021) 12:767618. doi: 10.3389/fimmu.2021.767618

166. Liu J, Gao H, Li C, Zhu F, Wang M, Xu Y, et al. Expression and regulatory characteristics of peripheral blood immune cells in primary Sjögren's syndrome patients using single-cell transcriptomic. *iScience*. (2022) 25:105509. doi: 10.1016/j.isci.2022.105509

167. Mackay F, Browning JL. BAFF: a fundamental survival factor for B cells. *Nat Rev Immunol*. (2002) 2:465–75. doi: 10.1038/nri844

168. Zhao S, Zhang H, Xing Y, Natkunam Y. CD137 ligand is expressed in primary and secondary lymphoid follicles and in B-cell lymphomas: diagnostic and therapeutic implications. *Am J Surg Pathol*. (2013) 37:250–8. doi: 10.1097/PAS.0b013e318268c6ea

169. Kendal JK, Shehata MS, Lofftus SY, Crompton JG. Cancer-associated B cells in sarcoma. *Cancers (Basel)*. (2023) 15. doi: 10.3390/cancers15030622

170. Meyer LM, Miller IF, Gizis E, Tripp E, Hoffbrand AV. Delivery of vitamin B12 to human lymphocytes by transcobalamins I, II and 3. *Proc Soc Exp Biol Med*. (1974) 146:747–50. doi: 10.3181/00379727-146-38185

171. Waibel R, Treichler H, Schaefer NG, van Staveren DR, Mundwiler S, Kunze S, et al. New derivatives of vitamin B12 show preferential targeting of tumors. *Cancer Res*. (2008) 68:2904–11. doi: 10.1158/0008-5472.CAN-07-6771

172. Hall CA, Green PD. Competition between apo and holo transcobalamin II (TC-II) for the TC-II mediated uptake process. *Proc Soc Exp Biol Med*. (1978) 158:206–9. doi: 10.3181/00379727-158-40172

173. Birn H, Willnow TE, Nielsen R, Norden AG, Bönsch C, Moestrup SK, et al. Megalin is essential for renal proximal tubule reabsorption and accumulation of transcobalamin-B(12). *Am J Physiol Renal Physiol*. (2002) 282:F408–16. doi: 10.1152/ajprenal.00206.2000

174. Savage AK, Gutschow MV, Chiang T, Henderson K, Green R, Chaudhari M, et al. Multimodal analysis for human. *iScience*. (2021) 24:102404. doi: 10.1016/j.isci.2021.102404

Glossary

12-CK	12-chemokine
ACP5	Acid Phosphatase 5, Tartrate Resistant
ACTA2	Actin Alpha 2, Smooth Muscle
AHSG	Alpha 2-HS Glycoprotein
ALPL	Alkaline Phosphatase, Biomineralization Associated
ANG	Angiogenin
APO-TCN2	Apo-Transcobalamin-II
APP	Amyloid Beta Precursor Protein
AT2	Alveolar epithelial type II
BC	Breast Cancer
C1QA	Complement C1q A Chain
C5AR1	Complement C5a Receptor 1
CAT	Catalase
CCL18	C-C Motif Chemokine Ligand 18
CCL19	C-C Motif Chemokine Ligand 19
CCL2	C-C Motif Chemokine Ligand 2
CCL21	C-C Motif Chemokine Ligand 21
CCL3	C-C Motif Chemokine Ligand 3
CCL4	C-C Motif Chemokine Ligand 4
CCL5	C-C Motif Chemokine Ligand 5
CCL8	C-C Motif Chemokine Ligand 8
CCR1	C-C Motif Chemokine Receptor 1
CD2	T-Cell Surface Antigen CD2
CD320	Transcobalamin Receptor
CD3D	CD3 Delta Subunit Of T-Cell Receptor Complex
CD3E	CD3 Epsilon Subunit Of T-Cell Receptor Complex
CD3G	CD3 Gamma Subunit Of T-Cell Receptor Complex
CD44	Cluster of differentiation 44
CD68	Cluster of differentiation 68
CD74	Cluster of differentiation 74
CD79A	Cluster of differentiation 79A
CD94	Cluster of differentiation 94
CKB	Creatine Kinase B
CKM	Creatine Kinase, M-Type
COL1A1	Collagen Type I Alpha 1 Chain
COPA	COPI Coat Complex Subunit Alpha
CP	Cutpoint
CRC	Colorectal cancer
CTC	Circulating tumor cells
ctDNA	Circulating tumor DNA
CTLA-4	Cytotoxic T-Lymphocyte Associated Protein 4
CTSK	Cathepsin K
CXCL10	C-X-C Motif Chemokine Ligand 10
CXCL11	C-X-C Motif Chemokine Ligand 11
CXCL12	C-X-C Motif Chemokine Ligand 12
CXCL13	C-X-C Motif Chemokine Ligand 13
CXCL4	C-X-C Motif Chemokine Ligand 4
CXCL6	C-X-C Motif Chemokine Ligand 6
CXCL9	C-X-C Motif Chemokine Ligand 9
DEP	Differential expressed protein
EDTA	Ethylenediaminetetraacetic acid
EGFL7	EGF Like Domain Multiple 7
FAM3C	FAM3 Metabolism Regulating Signaling Molecule C
FBP1	Fructose-Bisphosphatase 1
FCRL5	Fc Receptor Like 5
FDR	False discovery rate
FOXO	Forkhead Box-O
FPKM	Fragments Per Kilobase of transcript per Million mapped reads
GEPIA2	Gene Expression Profiling Interactive Analysis 2
GNLY	Granulysin
GRN	Granulin Precursor
GZMB	Granzyme B
HLA-DPA1	Major Histocompatibility Complex, Class II, DP Alpha 1
HLA-DPB1	Major Histocompatibility Complex, Class II, DP Beta 1
HLA-DRB1	HLA class II histocompatibility antigen, DRB1 beta chain
HLA-E	Major histocompatibility complex, class I, E
HOLO-TCN2	Holo-Transcobalamin-II
HR	Hazard Ratio
IBSP	Integrin Binding Sialoprotein
ICC	Intrahepatic Cholangiocarcinoma
IgA	Immunoglobulin A
IgD	Immunoglobulin D
IgE	Immunoglobulin E
IgG	Immunoglobulin G
IGHG1	Immunoglobulin Heavy Constant Gamma 1
IGJ	Joining Chain of Multimeric IgA and IgM
IgM	Immunoglobulin M
IL-6	Interleukin-6
IL-6Ra	Interleukin-6 receptor, alpha
IL-6Rb	Interleukin-6 receptor, beta
IL2RA	Interleukin-2 receptor subunit alpha
IRB	Institutional Review Board
KLRB1	Killer Cell Lectin Like Receptor B1
KLRD1	Killer Cell Lectin Like Receptor D1
KM	Kaplan Meier
LR	Log-rank
LTa1b2	Lymphotoxin alpha1:beta2
LYZ	Lysozyme
MAPK	Mitogen-activated protein kinases
MCC	Merkel cell carcinoma
MIF	Macrophage Migration Inhibitory Factor
MS	Mass Spectrometry
MS4A1	Membrane Spanning 4-Domains A1

MZB1	Marginal Zone B and B1 Cell Specific Protein
NCI	National Cancer Institute
TARGET-OS	Therapeutically Applicable Research to Generate Effective Treatments-Osteosarcoma
NKG2A	Killer Cell Lectin Like Receptor C1
NKG7	Natural Killer Cell Granule Protein 7
NPC	Nasopharyngeal carcinoma
NSCLC	Non-small cell lung carcinoma
OSA	Osteosarcoma
PD-1	Programmed cell death protein 1
PD-L1	Programmed death-ligand 1
PPA1	Inorganic Pyrophosphatase 1
RA	Rheumatoid Arthritis
RETN	Resistin
RFU	Relative fluorescent unit
RPS19	Ribosomal Protein S19
RUNX2	RUNX Family Transcription Factor 2
scRNA-seq	single cell RNA-sequencing
SELDI-TOF	Surface-enhanced laser desorption/ionization with time of flight
SELEX	Systemic Evolution of Ligands by Exponential
SELL	Selectin L
SKCM	Skin cutaneous melanoma
SLE	Systemic Lupus Erythematous
SPP1	Secreted Phosphoprotein 1
STAD	Stomach adenocarcinoma
t-SNE	t-distributed Stochastic Neighbor Embedding
TCGA	The Cancer Genome Atlas
SARC	Sarcoma
TCN2	Transcobalamin-II
TIGER	Tumor Immunotherapy Gene Expression Resource
TIL	Tumor-infiltrating lymphocyte
TIM-3 (HAVCR2)	T-Cell Immunoglobulin and Mucin Domain-Containing Protein 3 (Hepatitis A Virus Cellular Receptor 2)
TLS	Tertiary lymphoid structure
TNF	Tumor necrosis factor
TNFRSF13B (TACI)	TNF Receptor Superfamily Member 13B (Transmembrane Activator and CAML Interactor)
TNFRSF17 (BCMA)	TNF Receptor Superfamily Member 17 (B-cell maturation antigen)
TNFRSF1A	TNF Receptor Superfamily Member 1A
TNFSF13B (BAFF)	TNF Superfamily Member 13b (B-cell activating factor)
TNFSF14	TNF Superfamily Member 14
TNFSF9	TNF Superfamily Member 9
UMAP	Uniform Manifold Approximation and Projection
UMI	Unique Molecular Identifier
VEGF	Vascular endothelial growth factor
VIM	Vimentin

frontiers | Frontiers in Immunology

TYPE Review
PUBLISHED 08 November 2024
DOI 10.3389/fimmu.2024.1490712

OPEN ACCESS

EDITED BY
Gaia Codolo,
University of Padua, Italy

REVIEWED BY
Bikesh Kumar Nirala,
Emory University, United States
Yang Wang,
Sichuan Academy of Medical Sciences and Sichuan Provincial People's Hospital, China

*CORRESPONDENCE
Dongsong Li
lidongsong@jlu.edu.cn

RECEIVED 04 September 2024
ACCEPTED 21 October 2024
PUBLISHED 08 November 2024

CITATION
Xia M, Han Y, Sun L, Li D, Zhu C and Li D (2024) The role of neutrophils in osteosarcoma: insights from laboratory to clinic.
Front. Immunol. 15:1490712.
doi: 10.3389/fimmu.2024.1490712

The role of neutrophils in osteosarcoma: insights from laboratory to clinic

Ming Xia, Yu Han, Lihui Sun, Dongbo Li, Chunquan Zhu and Dongsong Li*

Department of Orthopedics, The First Hospital of Jilin University, Changchun, Jilin, China

Osteosarcoma, a highly aggressive malignant bone tumor, is significantly influenced by the intricate interactions within its tumor microenvironment (TME), particularly involving neutrophils. This review delineates the multifaceted roles of neutrophils, including tumor-associated neutrophils (TANs) and neutrophil extracellular traps (NETs), in osteosarcoma's pathogenesis. TANs exhibit both pro- and anti-tumor phenotypes, modulating tumor growth and immune evasion, while NETs facilitate tumor cell adhesion, migration, and immunosuppression. Clinically, neutrophil-related markers such as the neutrophil-to-lymphocyte ratio (NLR) predict patient outcomes, highlighting the potential for neutrophil-targeted therapies. Unraveling these complex interactions is crucial for developing novel treatment strategies that harness the TME to improve osteosarcoma management.

KEYWORDS

osteosarcoma, neutrophils, tumor microenvironment, neutrophil extracelluar traps, TANs

Introduction

Osteosarcoma is a primary malignant bone tumor characterized by the uncontrolled proliferation of osteoblastic cells, predominantly affecting children and adolescents (1). This aggressive cancer is associated with significant morbidity and mortality, necessitating a deeper understanding of its pathogenesis and progression (2).

The tumor microenvironment (TME) plays a pivotal role in the development and progression of cancer. TME encompassing a complex milieu of cellular and molecular components that interact with tumor cells and influence their behavior (3). In TME, various cell types, including immune cells, fibroblasts, endothelial cells, and extracellular matrix components, dynamically interact with tumor cells to create a supportive niche for tumor growth and dissemination (4). In osteosarcoma, the tumor microenvironment is characterized by an immunosuppressive milieu, driven by the secretion of cytokines, chemokines, growth factors, and extracellular matrix remodeling enzymes (5). These factors not only promote tumor cell proliferation, survival, and invasion but also

modulate the immune response, angiogenesis, and metastatic potential of osteosarcoma (6).

Neutrophils are white blood cells that play a key role in the innate immune response to infection and inflammation (7). In recent years, evidence has highlighted the multifaceted roles of neutrophils in the TME of various cancers, including osteosarcoma (8). Neutrophils can be recruited to the TME in response to tumor-derived signals and inflammatory mediators, where they interact with tumor cells and other stromal components (9).

Neutrophils have long been recognized for their role in osteosarcoma. Initially, the prognostic significance of the neutrophil-to-lymphocyte ratio in osteosarcoma was identified (10). Subsequent research has further elucidated the involvement of neutrophils, particularly neutrophil extracellular traps (NETs) and tumor-associated neutrophils (TANs), in the immune microenvironment and progression of osteosarcoma (8).

While neutrophils can promote tumor progression in various cancers, the specific mechanisms and the extent of their influence may vary. In osteosarcoma, neutrophils may contribute more significantly to the immunosuppressive tumor microenvironment and the promotion of metastasis due to the unique interactions between neutrophils and the bone matrix, as well as the high propensity of osteosarcoma cells to metastasize to the lung and the roles of neutrophils in the body after surgery (5). Previous findings underscore the intricate involvement of neutrophils in the complex interplay within TME of osteosarcoma, highlighting their potential as key modulators and therapeutic targets for improving clinical outcomes in this aggressive bone cancer (11). In the context of osteosarcoma, neutrophils have been shown to interact uniquely with the tumor microenvironment (12). The osteosarcoma microenvironment is a complex ecosystem that includes not only the tumor cells but also a variety of immune cells, bone cells, extracellular matrix components, and signaling molecules (1). Neutrophils in this context can be affected by the tumor to promote tumor growth, survival, and metastasis (13).

Understanding the interactions between TANs, NETs, and TME in osteosarcoma is essential for elucidating the mechanisms underlying tumor progression and identifying potential therapeutic targets. Targeting the immune cell components and inflammatory pathways within the tumor microenvironment may offer novel strategies for the treatment of osteosarcoma and improve patient outcomes. This review aims to provide insights into the multifaceted roles of neutrophils in osteosarcoma, spanning from fundamental laboratory research to potential clinical implications. By elucidating the intricate interactions between neutrophils and osteosarcoma, this review seeks to enhance our understanding of the complex tumor microenvironment and identify novel therapeutic strategies for the management of this aggressive bone cancer (Figure 1).

TANs in the tumor

Neutrophils are the most abundant immune cells in the human body and constitute 50%-70% of all white blood cells (14). Due to the limited proliferation capacity and lifespan of neutrophils, the

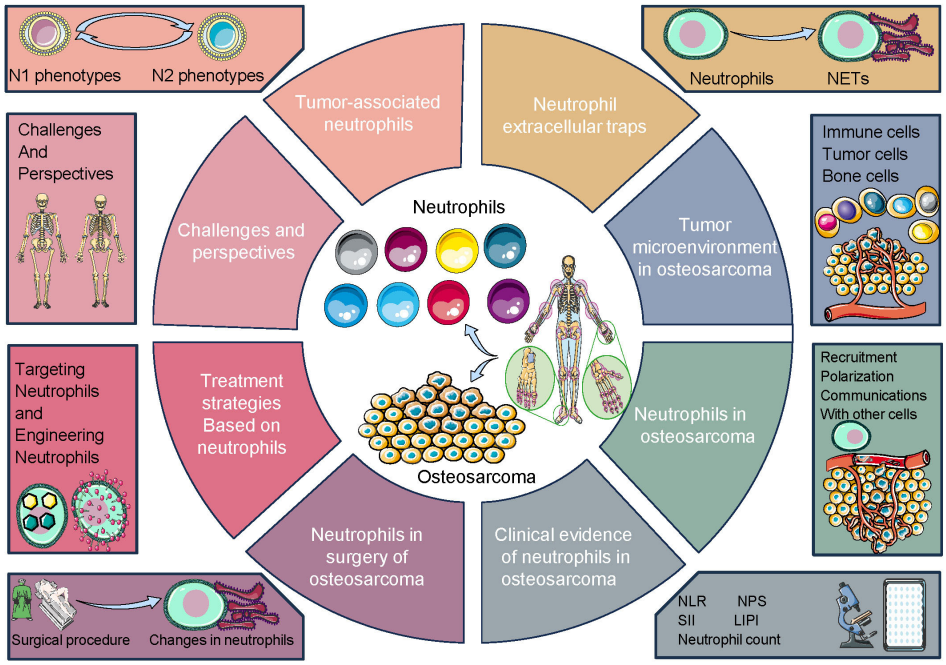

FIGURE 1
Overall design of our study. The nuanced interactions between neutrophils, specifically tumor-associated neutrophils (TANs) and neutrophil extracellular traps (NETs), with key osteosarcoma microenvironment (TME) constituents. It emphasizes the reciprocal modulation between TANs and TME cellular components, such as cancer-associated fibroblasts (CAFs) and regulatory T cells (Tregs), and molecular mediators including cytokines and chemokines, which orchestrate a pro-tumorigenic or tumor-suppressive milieu.

understanding of the roles of neutrophils in heterogeneous tumors has been lacking in recent decades (15). In recent years, owing to novel biotechnology, such as single-cell sequencing, there has been increasing attention on neutrophils in tumor-related research (16). Nowadays, the heterogeneity of TANs far exceeds the simple classification of several groups (17). According to their roles and functions in TME, TANs are classified into anti-tumor (N1) and pro-tumor (N2) phenotypes (Figure 2), and these two TANs phenotypes with opposing effects may regulate the initiation, proliferation, metastasis, and immune suppression (18).

Usually, neutrophils are continuously produced in the hematopoietic cords of the bone marrow and are regulated by transcription factors and proteins such as CCAAT-enhancer binding protein (CEBP/α) and colony-stimulating factors (19). In the tumor tissues, the function and polarization of neutrophils were mainly regulated by the factors in inflammatory TME. Different transcription factors and proteins may contribute to different neutrophil phenotypes (20). For example, interferon type 1 (IFN-1) may enhance the ability of adhesion and phagocytosis of neutrophils and force neutrophils to polarized towards N1 phenotype, and reversely, transforming growth factor-β (TGF-β) is a driver for N2 phenotype (21, 22). Furthermore, many other factors were also identified as the drivers of the polarization of neutrophils, including adenosine triphosphate, S100A9, adenosine, and so on (23, 24).

In recent years, some downstream pathways related to TANs were identified. N1 cell phenotypes usually perform their anti-tumor effects via reactive oxygen species (ROS) related pathways (25). ROS may up-regulate the superoxide-dependent Ca2+ channel of the tumor cells, contribute to the disorder of the Ca2+ levels, and lastly inhibit the development of the cancer (26). Reversely, tumor development may be upregulated by the factors produced by N2 phenotypes, including neutrophil elastase (NE) and matrix metalloproteinases (15).

In addition to immune regulations, TANs were also regulated by metabolic factors: the factors produced in the glucose metabolism, lipid metabolism, tricarboxylic acid cycle, and amino acid metabolism were able to reprogram the metabolism of TANs (7, 27). The oxygen deprivation TME may contribute to the glycolytic effects of TANs (28), and the factors produced in the glycolysis may inhibit the proliferation of movement of T cells and play their immunosuppressive functions (29). The TANs after metabolism reprogramming may contribute to a higher level of hypoxia-inducible factor 1 alpha (HIF-1α) expression (30). HIF-1α is a key transcription factor that plays a critical role in cellular responses to low oxygen levels, or hypoxia. In the context of tumors, HIF-1α is known to be a master regulator of the adaptive mechanisms that cancer cells employ to survive and proliferate under hypoxic conditions (31). Activation of HIF-1α in tumor cells leads to the upregulation of genes involved in angiogenesis, glycolysis, and cell survival, promoting tumor growth and metastasis (31, 32).

NETs in tumor

In addition to neutrophils, neutrophil-related components have also attracted increasing attention. Neutrophil extracellular traps (NETs) are web-like structures composed of chromatin, histones, and antimicrobial proteins released by activated neutrophils in response to various stimuli, including infection, inflammation, and cancer (33). In the context of tumors, emerging evidence

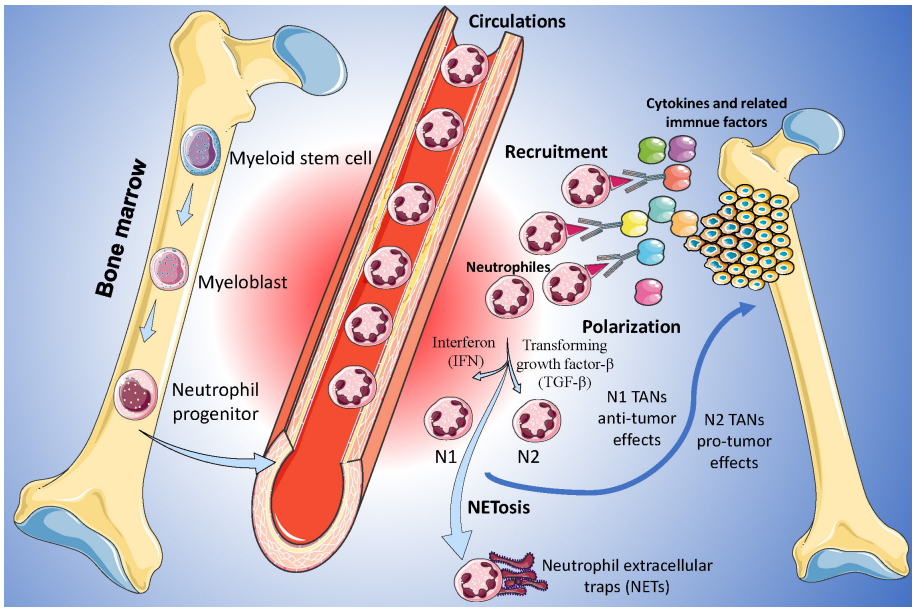

FIGURE 2
Function and roles of Tumor-Associated Neutrophils (TANs) in Osteosarcoma. N1 TANs, characterized by their anti-tumoral functions, are depicted engaging in ROS-mediated cytotoxicity and antigen presentation, while N2 TANs are portrayed as pro-tumorigenic, secreting factors such as MMP-9 and VEGF that facilitate angiogenesis and immunosuppression.

suggests that NETs play an important role in the tumor microenvironment (34). NETs have been implicated in promoting tumor progression by facilitating tumor cell adhesion, migration, and invasion, as well as inducing immunosuppression and angiogenesis (35).

The formation of NETs is not spontaneous but rather occurs abundantly in activated neutrophils (33). The formation of NETs is related to a distinct form of cell death, mediated by ROS and termed neutrophilic inflammatory cell death (NETosis), distinguishing it from traditional apoptosis and necrosis (36). Upon stimulation by extracellular physicochemical factors, the chromatin within the nucleus undergoes abnormal changes, and enzymes within cytoplasmic vesicles are activated, ultimately leading to the rupture of the cell membrane and release of the contents (37). In certain instances, neutrophils do not need to sacrifice themselves to release NETs, as non-lytic NETosis can occur during Staphylococcus aureus infection. In this scenario, neutrophils rapidly release chromatin extracellularly and undergo degranulation to release various enzymes, thereby forming extracellular NETs (33).

Initially, the roles of NETs in cancer metastasis, especially in the premetastatic niche, were recognized. NETs may facilitate tumor cell migration and invasion by releasing pro-inflammatory cytokines and chemokines that attract tumor cells to the site of NETs deposition, including IL-1, IL-6, IL-8, and so on, promoting their movement toward distant sites (38). Additionally, NETs induce an epithelial-mesenchymal transition (EMT) in cancer cells, leading to the acquisition of a mesenchymal phenotype that enhances their migratory and invasive abilities (39). Furthermore, NETs interact with endothelial cells, causing a loss of cell-to-cell junctions and altering the morphology of the endothelium, facilitating tumor cell intravasation and extravasation (40). By capturing circulating tumor cells and creating a permissive environment in pre-metastatic and metastatic niches, NETs promote the establishment and growth of metastatic lesions (41).

Nowadays, studies have proven that NETs also contribute significantly to cancer progression. NETs may induce tumor cell proliferation by releasing factors that enhance the proliferative ability of cancer cells (42). They also contribute to the immunosuppressive tumor microenvironment by hindering the migration of cytotoxic immune cells and shielding tumor cells from immune-mediated killing (43). Furthermore, NETs play a role in awakening dormant cancer cells, promoting their proliferation and metastatic growth (44). By facilitating cell migration and metastatic microenvironment, NETs contribute to the overall progression of cancer (45).

The formation of NETs requires the presence of two essential proteins: integrin αvβ1 and matrix metalloproteinase 9 (MMP-9), which can capture and activate TGF-β (46). The activation of TGF-β triggers EMT in cancer cells and is associated with the progression of tumor cells (46, 47). The DNA component of NETs also plays a crucial role in tumors by interacting with receptors on tumor cells, influencing their behavior and contributing to the complex interplay between the immune system and cancer cells in the tumor microenvironment (48). Additionally, the chemical composition of NETs may also be a key factor, for example, IL-17 found in NETs can interact with cytotoxic CD8 T cells and exclude them from the tumor tissue (49).

Tumor microenvironment in osteosarcoma

The basis of understanding the roles of neutrophils in osteosarcoma is to decode the TME of osteosarcoma (Figure 3). The TME of osteosarcoma comprises a heterogeneous milieu of cellular components, including bone cells, stromal cells, vascular cells, immune cells, and the extracellular matrix (ECM) (5). Within the TME of osteosarcoma, interactions between tumor cells and stromal cells contribute to tumor growth, invasion, and metastasis (50). In this complex microenvironment, the immune system plays a paradoxical role: it may promote or suppress the progression of osteosarcoma, according to different TME and cellular phenotypes (51). Moreover, the ECM components in the TME of osteosarcoma provide structural support and signaling cues that influence tumor cell behavior, including migration, invasion, and drug resistance (52). Recent evidence also suggested that EVs, small membrane-bound vesicles released by cells into the ECM, may serve as a bridge of intercellular communication and metastasis (53).

In osteosarcoma, bone cells, including osteoblasts, osteoclasts, and osteocytes, play a crucial role in the TME (5). Osteoblast, a type of bone-forming cell, is originating from pluripotent mesenchymal stem cells. In the TME of osteosarcoma, osteoblasts may regulate the osteoclasts' metabolism and communicate with osteosarcoma cells via multiple pathways, such as OPG/RANK/RANKL and Fas/FasL (54). Moreover, a recent study also reported that osteoblast may also regulate the TME by extracellular vesicles (55). Compared to osteoblasts, osteoclasts, cells derived from myeloid precursor cells and playing bone resorption effect, may play a more active area in osteosarcoma (50). From views of the population level, individuals with higher levels of osteoclast activity may have a lower risk of osteosarcoma and more satisfactory chemotherapy efficacy (56). Osteoclasts may activate $CD4^+$ and $CD8^+$ T cells and play an antigen-presenting cells-like role (57). However, in the different stages of osteosarcoma, osteoclasts may have different effects: in the early stage, osteoclasts may establish a niche containing osteosarcoma and suppress the metastasis, while in the later stage, accumulated tumor cells may have a stronger metastatic (58). Osteoclasts may also regulate the TME of osteosarcoma by interacting with CD4+ Tregs (59). Lastly, osteocytes as mature bone cells were also reported to have contributions to TME of osteosarcoma: osteocytes may have communications with osteosarcoma via the CXCL12-CXCR4 axis and by secreting TGF-β and VEGFA (60).

Another crucial cell in the TME of osteosarcoma is the mesenchymal stem cell (MSC), due to their potential roles as the precursors of osteosarcoma cells (61). The communications between MSCs and osteosarcoma cells have been reported in previous studies, and many factors, including CXCL12, IL-6, and VEGF, have been proven to be included (61). Moreover, extracellular vesicles may also mediate the interaction between MSCs and osteosarcoma cells by regulating the MALAT1/Wnt/β-

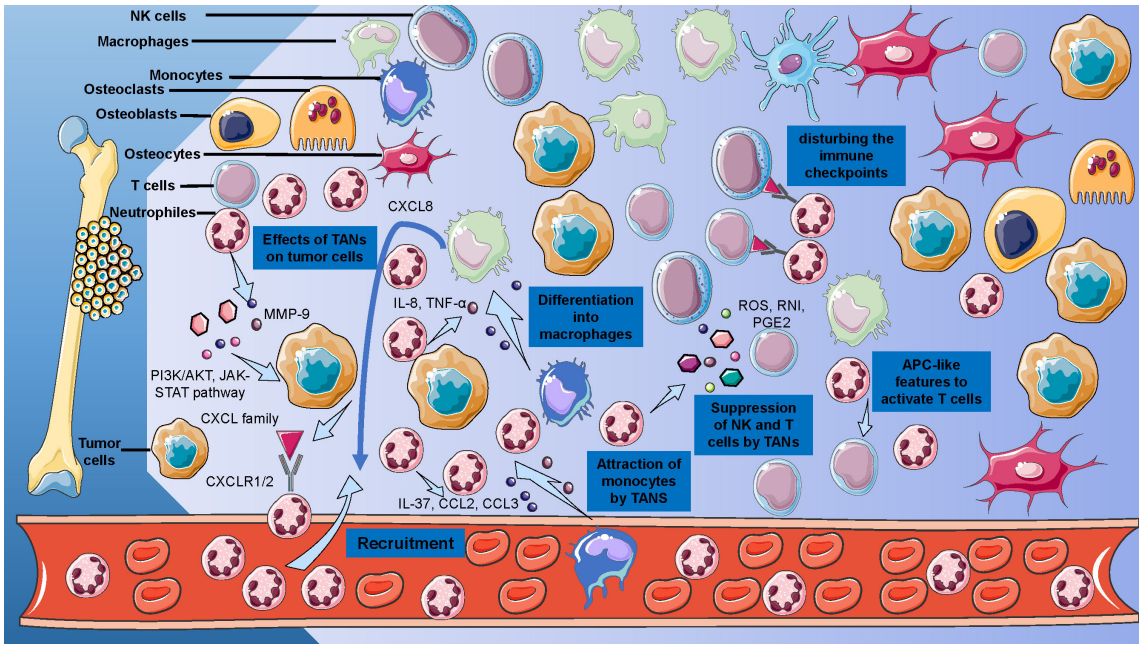

FIGURE 3
Cellular and Acellular Elements of the Osteosarcoma Tumor Microenvironment. Detailed representation of the osteosarcoma TME, delineates the interplay between osteoblasts, osteoclasts, MSCs, and immune cells, including T cells and macrophages.

catenin pathway and autophagy (62). Due to the characteristics and the roles of the extracellular vesicles from MSCs in the development of osteosarcoma, engineered extracellular vesicles may become a potential treatment for osteosarcoma by encapsulating drugs (63).

Recently, with the development of single-cell transcription, more understandings of immune TME of osteosarcoma are emerging. T cells play different roles in the TME of osteosarcoma due to the heterogeneity. Usually, $CD8^+$T cells may directly attack tumor cells, and CD4 T cells may orchestrate the immunity, while Tregs act as an immune suppressor role (64). In the single-cell dynasty, the landscapes of T cells in osteosarcoma are more complex and diverse (13). T cells may also be regulated by TME. In TME, many chemokines, such as CXCL12, and many cell phenotypes, such as Tregs and myeloid-derived suppressor cells (MDSCs), may regulate the migration of T cells and contribute to the progression of osteosarcoma (13). Compared to T cells, B cells may mainly play tumor-promotion roles in osteosarcoma by secreting immune suppressive cytokines and activating Tregs (65). Recent studies have reported the potential checkpoint molecules on B cells, and targeting these checkpoints may become a potential strategy for osteosarcoma treatment (66). Another lymphoid cell in TME of osteosarcoma is the NK cell, a type of cell featured by its strong cytotoxic activity on malignant cells (67). NK cells may directly regulate the TME and establish the antitumor microenvironment by releasing IFN-γ (68). However, recent understandings from single-cell levels indicated that TME may also have an effect on NK cells and cause high levels of heterogeneity by regulating NK cell receptor signals and Tregs (13). Many studies have tried to develop potential methods based on NK cells to treat osteosarcoma, and these methods may enhance the anti-tumor effect of NK cells by targeting IL-12, IL-15, and so on (69).

Another immune cell lineage in osteosarcoma TME is monocyte lineage, including monocytes, macrophages, and dendritic cells (DCs). Monocytes play roles of antigen-presenting cells and could further differentiate into macrophages or DCs (70). Monocytes may release chemokine monocyte chemoattractant protein-1 (MCP-1), and MCP-1 may regulate the growth, metastasis, and progression of osteosarcoma cells (71). The recruitment of monocytes in TME is mainly regulated by CCL2, and by inhibiting the CCL2 receptor, the monocyte recruitment in TME may significantly decrease (72).

Monocytes may further differentiate into macrophages, which are the most abundant immune cells in the TME of osteosarcoma (73). Polarizing into M1 or M2 phenotype, macrophages may have contrast effects on tumor progression (74). M1 macrophages release proinflammatory cytokines, including nitric oxide synthase (iNOS), and tumor necrosis factor-alpha (TNF-α), and factors may lead to anti-tumor activity and induce the Th1 cells (75). Compared to M1 macrophages, M2 phenotype cells have contrasting activity: M2 macrophages exert their pro-tumor activities through various mechanisms in TME, including immune suppression, tissue remodeling, tumor progression, and angiogenesis (12). M2 macrophages promote osteosarcoma metastasis by secreting factors such as CCL18, MMP-12, COX-2, and IL-1β, and these factors may contribute to metastasis through the NF-κB/miR-181α-5p/RASSF1A/Wnt pathway (76, 77). M2 macrophages may also contribute to tumor angiogenesis by releasing vascular endothelial growth factor (VEGF) and fibroblast growth factor (FGF) (78). Recent studies also reported that M2 macrophages may inhibit the

activity of T cells due to their expression of PD-1 (79). Repolarization of M2-like macrophages to M1-like macrophages is emerging as an innovative anticancer approach.

Another phenotype differentiated from monocytes is DCs, kinds of professional antigen-presenting cells (APCs) (68). By producing IFN-1α and IFN-1β, DCs may regulate anti-tumor effects (80). High levels of DCs may relate to high levels of heat shock promoter 70 (HSP70) and high activity of T cells (81). In view of results from single-cell RNAseq, DCs may have different phenotypes, and some of them may play immunosuppressive roles (82).

Roles of neutrophils in osteosarcoma

The recruitment of neutrophils from the circulatory system to TME may undergo several stages, including attachment, adhesion, crawling, and transmigration (83). Chemokine of the CXC family is the major system that regulates the attraction of neutrophils, including seven chemokines and two receptors. Usually, the CXC family chemokines secreted by tumor tissues may attract the neutrophils by interacting with CXC receptors CXCR1 and CXCR2 expressed on neutrophils (84). After the receptor binding, the G-protein and β-arrestin signaling pathways were activated, which may further regulate the activation of calcium channels, phospholipase C, MAP, and tyrosine kinase pathways (85). The activation of these pathways may promote neutrophil migration by remodeling dynamic actin (86). Previous studies have reported that many neutrophil-regulating factors, such as CSF and IL-17, may regulate neutrophil attraction by regulating the levels of CXC chemokines and the receptions (87, 88). Many factors that play significant roles in neutrophil migration have been explored in osteosarcoma, including CXCL1, IL-6, CCL2, and so on (89). CXCL1 has higher expression in the tumor tissues compared to normal tissues, and the levels of CXCL1 expression may increase with the tumor progression, many factors were found to relate to this phenomenon, including the extracellular vesicles secreted by osteosarcoma cells, pH levels, and other cytokines released by tumor-relating cells (90, 91).

The recruitment of neutrophils to other organs is also significantly related to the formation of a pre-metastatic niche (92). Previous studies have proven that CXCL1 releasing by human pulmonary artery endothelial cells may significantly increase osteosarcoma cell mobility, and this phenomenon was mediated by VCAM-1 (93). Moreover, it was also reported that ANGPTL2 may contribute to the recruitment of neutrophils to the lung and promote the formation of lung pre-metastatic (92). Moreover, evidence from transcriptomic and histological analysis of premetastatic lungs has identified the characteristics of pro-metastatic events including inflammatory-induced stromal fibroblast activation, neutrophil infiltration, and ECM remodeling (94).

Though the research on TANs in osteosarcoma is still limited, the neutrophils and their related phenotypes have also been proven to have effects on the development and progression of osteosarcoma (95). In osteosarcoma, the N1 subtype of TANs may be more prevalent in the early stages of the disease, correlating with a favorable response to treatment and a better prognosis, while the N2 subtype could foster an immunosuppressive microenvironment that hinders effective immunotherapy (96). The unique behavior of neutrophils in osteosarcoma may be attributed to the bone matrix components and the specific cytokine milieu present in the OS microenvironment, which can influence neutrophil polarization and function (97).

Furthermore, recent multi-omics analyses identified distinct molecular subtypes of osteosarcoma, each with varying prognoses and responses to treatment (98). These subtypes exhibit different patterns of neutrophil infiltration and activation, suggesting that the regulatory mechanisms controlling neutrophil behavior may vary between osteosarcoma subtypes (98). TANs may regulate the development of osteosarcoma via matrix metalloproteinases -9 (MMP-9): the high levels of MMP-9 mediated by TANs are correlated with poorer prognosis (99). MMP-9 secreted from TANs may interact with insulin receptor substrate 1 (IRS-1), and further regulate the PI3K/AKT signaling pathway to contribute to the proliferation of tumor cells (100). From the insights of single-cell sequencing, the expressions of PPP2R5C, PPP2R5E, YWHAG, and CREBBP on TANs were significantly related to the metastatic of osteosarcoma, and these genes may play their roles via HIF-1, PI3K-AKT, and JAK-STAT signaling pathways (101). Similar to MMP-9, the PPP2R5C, a subunit of protein phosphatase 2A, was expressed on TANs, and may also regulate the proliferation of osteosarcoma via PI3K/AKT pathway (101). By comprehensively analyzing the significant genes from osteosarcoma and neutrophils at the single-cell level, hundreds of genes were identified, and C3AR1 and FCER1G as two neutrophil-related genes were validated to play critical roles in the communication between neutrophils and osteosarcoma cells (102). C3AR1 and FCER1G were highly regulated in the osteosarcoma mice induced by K7M2, and these two genes were proven to have significant prognostic value in osteosarcoma (102).

TANs may also act by communicating with other immune cells (103). The most significant cell phenotypes that relate to TANs are myeloid-derived suppressor cells (MDSCs), due to their shared origin (15). MDSCs, the immature myeloid cells, play significant roles in TME. In humans and mice, there are two major classes of myeloid-derived suppressor cells (MDSCs), classified based on their origins from the granulocytic lineage and monocytic lineage, namely polymorphonuclear-MDSCs (PMN-MDSCs) and monocytic-MDSCs (M-MDSCs) (104). The common feature of MDSCs is their appearance in immunologically activated pathological states, due to sustained stimulation of myeloid cells in environments such as cancer, chronic infections or inflammation, and autoimmune diseases, as a result of prolonged presence of myeloid growth factors and inflammatory signals. The main characteristic of MDSCs is their ability to suppress immune responses, including those mediated by T cells, B cells, and natural killer (NK) cells (105). M-MDSCs and PMN-MDSCs possess key biochemical features that contribute to immune response suppression, including upregulation of signal transducer and

activator of transcription 3 (STAT3), induction of endoplasmic reticulum stress, expression of arginase 1, and expression of S100A8/A9 (106).

MDSCs may inhibit the migration of T cells and reduce T cell activity to protect osteosarcoma cells (107, 108). This function of MDSCs may be achieved by several pathways and factors, such as the production of nitric oxide (NO) and ROS, and the consumption of L-arginine (109). MDSCs may also contribute to the metastasis of osteosarcoma by forcing T-cell tolerance and releasing TGF-β and hepatocyte growth factor (HGF) (110). Moreover, MDSCs may also regulate tumor angiogenesis by releasing VEGF and MMP-9 (111).

Another remarkable cell interaction with neutrophils is tumor-associated macrophages (15). The neutrophils may attract monocytes by secreting IL-37, CCL2, and CCL3, and these monocytes may differentiate into macrophages via IL-8 and TNF-α (112). It was also reported that in the development of sarcoma, TANs may regulate the IL-12 releasing of macrophages, and IL-12 may contribute to the activation of unconventional T cells due to their high levels of IL-12R expression, which further regulate the secreting of IFN-γ and tumor suppression (113). During the nascent stages of oncogenesis, macrophages exhibit tumoricidal properties due to their activated state, generating reactive oxygen and nitrogen species that can induce DNA damage and genetic instability (114). The cytokines from neutrophils in the tumor microenvironment may significantly impact macrophage functions and phenotypes (115). Furthermore, macrophages may contribute to malignant transformation through the secretion of angiogenic factors, proteases, and growth factors (116). These factors stimulate cancer cell proliferation and support the epithelial-mesenchymal transition in tumor cells, thereby facilitating tumor growth and metastasis (117). Recent studies also reported that these recruited monocytes and macrophages may release CXCL8 to further attract neutrophils, which may become a feedback loop (118).

TANs may also interact with lymphoid cells and have paradoxical effects on the functions of lymphoid cells (119). TANs may release ROS, reactive nitrogen intermediates (RNI), and prostaglandin E2 (PGE2), and these factors may directly inhibit the functions of T cells and NK cells (120, 121). The release function of TANs may relate to their metabolism status. Facing limited glucose supply, neutrophils may have high levels of mitochondrial fatty acid oxidation and high ROS production (120). Moreover, TANs with endoplasmic reticulum stress and altered lipid metabolism may also have higher levels of ROS production (122). In addition to the release of mediate factors, TANs may also interact with lymphocytes by disturbing the immune checkpoints, due to the expression of PD-L1 and VISTA on neutrophils, which may result in the dysfunction of T cells and NK cells by interacting with their ligands (123). It was also reported that some types of neutrophils may directly contact CD4+ T cells physically to inhibit the functions of the cells (124). TANs may regulate the activity of T cells by attracting Tregs and formatting the TME. Interestingly, TANs may also have positive effects on lymphoid cell activation. TANs may activate T cells by showing their APC-like features, and these APC-like features in TANs are activated by TME-derived CSF and IFN-γ (125). Furthermore, the activation of T cells may contribute to the expression of CD54 and CD86 on TANs, which may further strengthen the APC-like features of TNAs and construct a positive feedback loop (126). By secreting IL-1β and IL-18, neutrophils also directly attract and activate NK cells (127).

Within the context of the tumor microenvironment, the intricate interplay between neutrophils and B cells holds substantial implications for cancer progression and therapeutic strategies (124). Neutrophils have been shown to facilitate the migration of B cells through the release of TNF-α, with this effect being notably enhanced by the presence of specific chemokines, including CXCL13 and CXCL12 (128). While the precise nature of the interaction between neutrophils and follicular B cells remains to be fully elucidated, it is observed that neutrophils tend to concentrate in areas rich in B cells and secrete B-cell-activating factor (BAFF) under the influence of G-CSF, which in turn, bolsters the rapid production of plasma cells (129). Furthermore, neutrophils are known to regulate immunoglobulin production by interacting with the BAFF receptor on B cells, a pivotal mechanism in the modulation of the humoral immune response (130). This capability of neutrophils to influence B cell activity is particularly significant when considering the diverse functions of B cells in countering tumorigenesis and their ability to stimulate other immune cells, including T and NK cells (131).

The roles of NETs in osteosarcoma were also reported in previous studies. In the osteosarcoma gene profiles, more than 90 NETs genes were identified, and these genes were related to immune cell infiltration, including NK cells and CD8+ T cells (8). Previous studies tried to establish a prognostic signature based on NETs-related genes to predict the overall prognosis of osteosarcoma and proved the strong performance of this signature (11). Similarly, the TME between groups with different levels of NETs-related signatures may have different types of immune cell infiltration.

Though few functional and experimental studies tried to explore the specific mechanism of NETs in osteosarcoma, the normal function and features of NETs in general tumors may provide us with a potential hypothesis. In the context of tumor development, NETs may serve to limit tumor spread in the early stages by directly entrapping and killing cancer cells (132). Moreover, NETs can enhance the local immune response by promoting the recruitment and activation of immune cells such as T cells and natural killer (NK) cells. This can lead to the secretion of cytokines and chemokines that reinforce the inflammatory response and potentially contribute to the elimination of cancer cells (133). Generally, some NETs-related factors, such as IL-8, G-CSF, and CXC chemokine receptor family, have been also proven to relate to the progression of osteosarcoma (134). Similarly, MMP-9, mentioned many times in this review, as a critical protein of NETs, is also proven as a key factor in osteosarcoma (135). In addition, the roles of NETs in blocking immune cells and protecting cancer cells physically may also exist in the TME of osteosarcoma. The overall roles of neutrophils in osteosarcoma are summarized in Figure 3.

Clinical evidence of neutrophils in osteosarcoma

Previous studies reported the neutrophil count was an independent risk factor for the metastasis of osteosarcoma (136).

However, the most widely used predictive parameter related to neutrophils in osteosarcoma is the neutrophil-to-lymphocyte ratio (NLR), which may predict many kinds of prognoses, including overall survival, progression-free survival (PFS), disease-free survival (DFS), metastasis, and so on (137–139). In a cohort enrolling 359 individuals after surgeries for osteosarcoma, pre-treatment NLR may independently predict the overall survival and PFS: the individuals with higher NLR may have lower 5-year overall survival (HR = 1.80, 95% CI = 1.35-2.41, P < 0.001) and PFS (HR = 1.65, 95% CI = 1.26-2.15, P < 0.001) compared with those with low levels of NLR (137). Similar results were also reported in a study that included 100 children with osteosarcoma, rhabdomyosarcoma, and Ewing sarcoma: the NLR > 2 may independently predict the overall survival (HR = 2.27, 95% CI = 1.07-5.30, P = 0.046) for children with osteosarcoma (10). Compared to other hemogram parameters, such as platelet-to-lymphocyte ratio (PLR) (AUC = 0.668 and AUC = 0.600) and lymphocyte-to-monocyte ratio (LMR) (AUC = 0.609 and AUC = 0.407), NLR (AUC = 0.749 and AUC = 0.663) has the highest predictive value for overall survival (140, 141). Pre-treatment NLR may also predict the efficacy of neoadjuvant chemotherapy in osteosarcoma, and the results from multicenter cohorts showed that the patients with lower NLR may be more likely to achieve pathological complete response (OR = 2.82, 95% CI = 1.36-5.17, P = 0.020) compared with patients with high NLR (142). Similarly, a cohort from Iran with 186 individuals also reported that the pre-treatment NLR may effectively predict the response after neoadjuvant chemotherapy and overall survival: the patients with high NLR have significantly low overall survival (20.7 months vs. 34.6 months, P = 0.003) and DFS (20.4 months vs. 32.7 months, P = 0.020) compared with individuals with normal NLR (143). The prognostic abilities of increased NLR for overall survival (HR = 1.30, 95% CI = 1.10-1.50, P = 0.002) were also reported in individuals with osteosarcoma and treated with high-dose methotrexate and etoposide/ifosfamide chemotherapy (144). Beyond the pre-treatment NLR, a recent study also reported the prognostic value of dynamic changes of NLR during the treatment: by combining the baseline NLR and Delta NLR, the NLR staging system (HR = 2.46, 95% CI = 1.63-3.71, P < 0.001) may have better predictive values (145).

In addition to the simple immune inflammation index such as NLR, many immune indices related to neutrophils were also reported to be used to predict the outcome of osteosarcoma. For example, the systemic immune inflammation index (SII), defined as platelet × neutrophil/lymphocyte counts, was reported to relate to tumor size, histological type, Enneking stage, and neoadjuvant chemotherapy, and high SII (HR = 1.22, 95% CI = 1.10-1.45, P = 0.029 and HR = 1.01, 95% CI = 1.00-1.02, P = 0.015) may independently predict the overall survival (146, 147). A multicenter study also reported the prognostic values of pre-operative SII in the overall survival of both young (≤20 years) individuals (HR = 2.38, 95% CI = 1.02-5.56, P = 0.045) and older (60-80 years) individuals (HR = 2.42, 95% CI = 1.03-5.68, P = 0.043) with osteosarcoma (148). In addition to SII, the lung immune prognostic index (LIPI), calculated by serum lactate dehydrogenase (LDH) and neutrophil to lymphocyte ratio (NLR), was also proven to predict the metastasis (HR = 1.864, 95% CI = 1.11-3.13, P = 0.018) of osteosarcoma (149). Moreover, studies included 133 individuals with osteosarcoma reported that the pre-treatment Naples prognostic score (NPS), composed of serum albumin level, serum total cholesterol (TC), lymphocyte-to-monocyte ratio (LMR), and neutrophil-to-lymphocyte ratio (NLR), was able to predict the overall survival (HR = 5.87, 95% CI = 1.03-6.43, P < 0.001; HR = 6.55, 95% CI = 1.15-13.62, P < 0.001) and PFS (HR = 5.27, 95% CI = 1.02-11.49, P < 0.001; HR = 6.78, 95% CI = 1.23-10.58, P < 0.001), and was significantly related to tumor location (P = 0.009), Enneking stage (P < 0.001), pathological fracture (P = 0.005), local recurrence (P < 0.001), and metastasis (P = 0.003) (150). The studies related to the clinical roles of neutrophils are summarized in Table 1.

Neutrophils in the surgery of osteosarcoma

In the treatment of osteosarcoma, surgical resection is the most critical treatment strategy. However, even after the surgical procedure, patients with osteosarcoma may also face a high risk of postoperative metastasis (151). Recent studies reported that the postoperative metastasis was partly driven by the immune response caused by infection, tissue damage, and cell injury, and the surgical procedure of osteosarcoma is the major cause, due to the extensive tissue resection and reconstruction (152). Even after surgery, the tissue healing process also activates systemic inflammatory reaction, which establishes a favorable microenvironment for tumor growth and metastasis (153). Neutrophils may play critical roles in this kind of acute inflammatory response (Figure 4).

After the surgical procedures of osteosarcoma, the extensive trauma caused by surgery may result in high levels of release of intracellular factors and cytokines, which may initiate the immune response and naturally increase the circulation neutrophil counts (154). The damaged cells after surgery expressed increased levels of damage-associated molecular patterns (DAMPs), groups of cellular components including ATP, DNA, cytokines, and so on (155). DAMPs in the local tissues may attract the circulation of neutrophils and contribute to the activation of neutrophils (116). A recent study reported that with the cell destruction, mitochondrial DNA (mtDNA) was released into circulation, and attracted neutrophils to format the pre-metastatic niche, which indicated the roles of neutrophils in the surgery-induced osteosarcoma metastasis (156).

Facing the extensive simulation, the NETosis of neutrophils would be activated. Previous studies have proven that after major surgeries, especially the large removal and reconstruction in tumor surgeries, the NETs markers in circulation may significantly increase (157, 158). Additionally, the intraoperative surgical vascular occlusion and hypoxia in the surgery procedures may also contribute to NETosis (159). The extensive release of NETs may finally promote the metastasis of tumors and result in the failure of radical surgery.

TABLE 1 Studies focusing on the clinical roles of neutrophils in osteosarcoma.

Index	Sample size	Location	Population Characteristics	Study type	Outcome	Conclusion	Ref
Pretreatment Neutrophil count	65	Japan	First visit osteosarcoma patients without metastasis	Single-center retrospective study	Metastasis	Low neutrophil count as a risk factor for metastasis of osteosarcoma	(122)
Pretreatment NLR	359	China	Patients who underwent curative surgery for osteosarcoma	Single-center retrospective study	5-years OS/PFS	High levels of NLR as risk factors for survival of osteosarcoma	(123)
NLR	2087	–	Patients with osteosarcoma	Meta-analysis	OS/DFS	High levels of NLR as risk factors for survival of osteosarcoma	(124)
NLR	2162	–	Patients with osteosarcoma	Meta-analysis	OS/DPS	High levels of NLR as risk factors for survival of osteosarcoma	(125)
Pretreatment NLR	172	Turkey	Pretreatment patients with osteosarcoma	Single-center retrospective study	OS	High levels of NLR as risk factors for survival of osteosarcoma	(126)
Pretreatment NLR	162	China	Pretreatment patients with osteosarcoma	Single-center retrospective study	OS	High levels of NLR as risk factors for survival of osteosarcoma	(127)
NLR at the first cycle of chemotherapy	96	China	Patients who underwent NACT for osteosarcoma	Multi-center retrospective study	pCR	High levels of NLR as risk factors for the effect of NACT	(128)
NLR at the first cycle of chemotherapy	186	Iran	Patients who underwent NACT for osteosarcoma	Multi-center prospective study	OS/DFS	High levels of NLR as risk factors for survival of osteosarcoma	(129)
NLR during chemotherapy	164	France	Patients with osteosarcoma and treated with M-EI chemotherapy	Multi-center prospective study	OS/EFS	High levels of NLR at 4 weeks as risk factors for survival of osteosarcoma	(130)
NLR (baseline, during treatment, delta)	251	China	Pretreatment patients with osteosarcoma	Single-center retrospective study	OS	High levels of baseline NLR and delta NLR as risk factors for survival of osteosarcoma	(131)
Pretreatment SII	126	China	Pretreatment patients with osteosarcoma	Single-center retrospective study	OS	High levels of SII as risk factors for survival of osteosarcoma	(132)
Pretreatment SII	86	China	Pretreatment patients with osteosarcoma	Single-center retrospective study	EFS/CSS	High levels of SII as risk factors for survival of osteosarcoma	(133)
Pretreatment SII	125	China	Pretreatment patients with osteosarcoma	Single-center retrospective study	OS	High levels of SII as risk factors for survival of osteosarcoma	(134)
Pretreatment LIPI	184	China	Pretreatment patients with osteosarcoma	Single-center retrospective study	Metastasis	Low levels of LIPI as risk factors for metastasis of osteosarcoma	(135)
Pretreatment NPS	133	China	Pretreatment patients with osteosarcoma	Single-center retrospective study	OS/PFS	High levels of NPS as risk factors for survival of osteosarcoma	(136)

Potential treatments based on neutrophils

How to benefit the patients more by targeting neutrophils? Many researchers have begun their explorations in the engineering and targeting of neutrophil strategies. Due to the limited recognition of the neutrophils in the cancer, especially in osteosarcoma, few studies about the neutrophil treatment in osteosarcoma have been reported. Here, we reviewed the progress and explorations in targeting and engineering neutrophils for cancer treatment to provide potential ways to treat osteosarcoma (Figure 5).

The recruitment of neutrophils in local tissues plays a significant role in tumor development and metastasis, so many studies tried to inhibit this process to achieve the goals of cancer therapy. Targeting CXCL/CXCR2 signaling has been reported as a potential treatment in cancer: by regulating neutrophil infiltration, CXCR2 inhibition, and interference may significantly suppress the tumor growth and prolong the survival of mice with tumor, as well

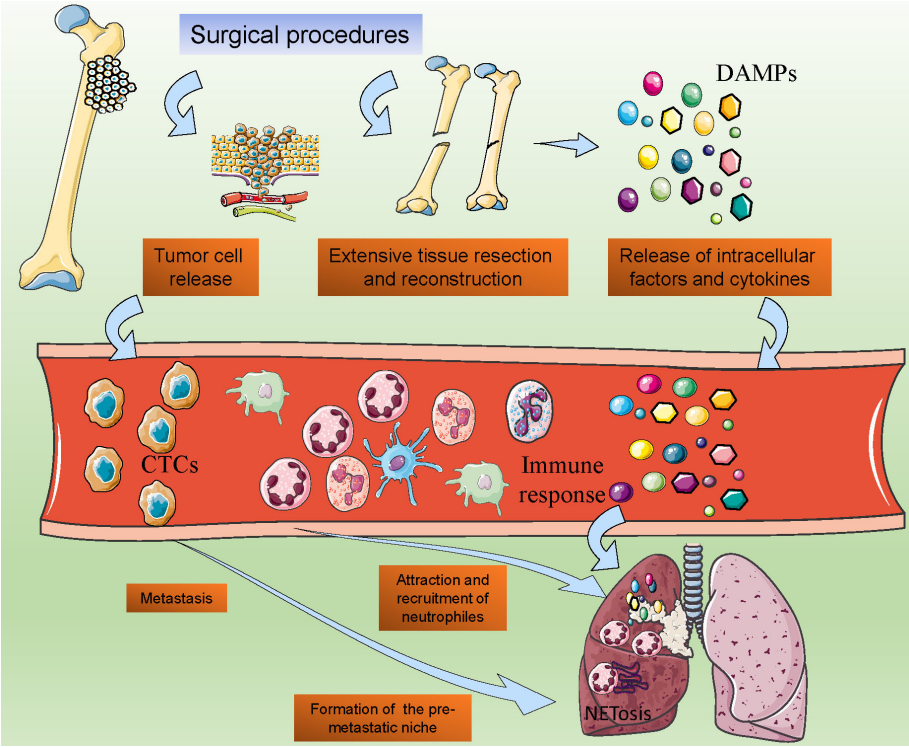

FIGURE 4
Post-surgical Neutrophil Activation and Its Implications in Osteosarcoma Metastasis. The post-operative surge in neutrophil activity following osteosarcoma surgery, showcasing the release of damage-associated molecular patterns (DAMPs) and subsequent neutrophil chemotaxis. It suggests a model where surgical stress-induced NETosis and the formation of pre-metastatic niches in distal organs are potential drivers of tumor cell dissemination.

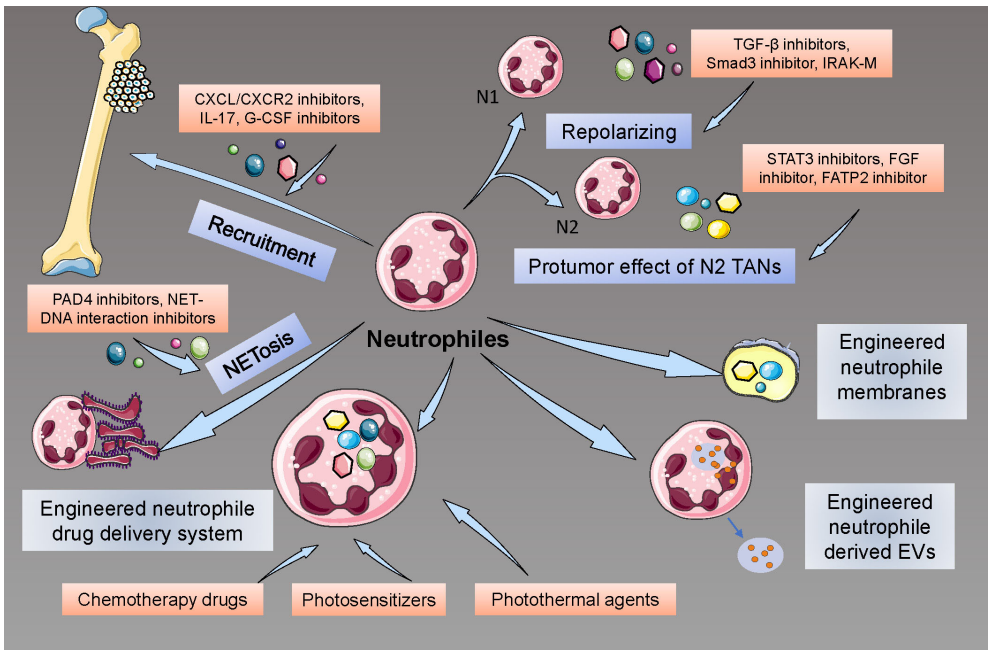

FIGURE 5
Therapeutic Interventions Targeting Neutrophils in Osteosarcoma. These include neutralizing chemokine gradients that recruit neutrophils to the TME, pharmacological repolarization of TAN phenotypes using TGF-β inhibitors, and the innovative use of engineered neutrophils for precision drug delivery, highlighting the potential of these approaches to disrupt osteosarcoma progression and enhance therapeutic responses.

as improve the quality of chemotherapy (160, 161). In addition to the direct effects on tumor development, anti-CXCR2 may also improve the effectiveness of PD-1 strategies, suppress the inflammatory microenvironment caused by neutrophils, and inhibit the formation of NETs (162). Similarly to CXCR2-related strategies, targeting CXCR4 may also have effects on tumor development by disturbing the recruitment of neutrophils (163). Additionally, many cytokines, proteins, and novel nanomaterial drugs, such as CEMIP (cell migration-inducing protein), IL-17, G-CSF-inhibiting antibodies, and colchicine, were reported to have a potential suppressive effect on neutrophil recruitment and have potential to become a treatment of cancers (164–166).

Due to the different phenotypes of TANs, researchers also tried to develop methods to repolarize pro-tumor TANs to anti-tumor TANs. As the TGF-β/Smad pathway is critical to the polarization of N2 TANs, some studies explored the potential strategies that may inhibit this signal, and usage of TGF-β receptor inhibitor and Smad3 inhibitor, as well as knockdown of Smad3, can effectively contribute to the repolarization to N1 phenotypes and enhance the anti-tumor effect of neutrophils (167). Similarly, enhancing the pathways that contribute to the polarization of TANs to anti-tumor phenotypes may also provide a potential effect on tumor suppression, such as interferon therapy (22). Recently, many new factors that may affect the repolarization of TANs were also reported, including Interleukin-1 receptor-associated kinase M (IRAK-M), nicotinamide phosphoribosyltransferase (NAMPT), novel TGF-β inhibitor, and proteins for inflammation resolution (168–170).

Trying to eliminate the effects caused by pro-tumor TANs may also be a potential intervention in targeting neutrophils for cancer treatments. Studies reported that by using STAT3 inhibitors, the activation of neutrophils was suppressed and turned into an anti-tumor phenotype (171). Targeting the angiogenesis effect of neutrophils may also inhibit the development and metastasis of tumors (172). A recent study also proved that inhibiting the FGF pathway could eliminate the neutrophil-activated effect on tumor cells (173). Moreover, many factors and proteins were found to have a regulatory impact on neutrophil activity by inhibiting specific pathways, such as fatty acid transport protein 2 (FATP2) inhibitor, HDAC inhibitor, leukotriene-generating enzyme arachidonate 5-lipoxygenase (Alox5) inhibitor, and so on (174, 175).

Targeting NETs is also a potential strategy. Targeting the protein structures of NETs, previous studies tried to use DNase I and (protein-arginine deaminase 4) PAD4 inhibitors, as well as laminin antibodies, to inhibit the protective roles of NETs in tumor progress (176). Due to the unstable nature of these inhibitor proteins, some nanomaterials were designed to precisely release the protein inhibitors at the accurate tumor location, which has achieved satisfactory effects (177). Similarly, studies also reported the exploration of targeting NETs-DNA. By designing cationic materials that may inhibit the interaction between NETs-DNA and CCDC25, researchers significantly reduced the infiltration of NETs-DNA and suppressed the metastasis of tumors (178).

Based on the characteristics of neutrophils that neutrophils may release cargo in certain microenvironments, engineering neutrophils were also considered as a potential treatment for tumors. Recent studies have reported that neutrophils may be engineered as cell drug delivery systems to transport chemotherapy drugs, photosensitizers, photothermal agents, and so on to tumor tissues efficiently and safely (179, 180). Neutrophil membranes have also been engineered for novel therapy strategies for tumors. The cell membranes derived from different cells have similar structures and functions to their derived cells, which were considered to have the potential to interact with tumor cells and to deliver drugs accurately (181). Recent studies designed the neutrophil membranes loaded celastrol (CLT), paclitaxel (PTX), and so on to treat cancer and achieved significant anti-tumor efficacy (182, 183). It was also proven that irreversible electroporation may induce the attraction of neutrophils and then improve the drug delivery effectiveness mediated by neutrophils (184). Additionally, neutrophil-derived extracellular vesicles (EVs) were also considered as potential platforms for drug delivery. Due to the inflammatory chemotaxis of neutrophil-derived EVs, EVs may automatically migrate to the inflammatory site, as well as tumor location (185). Engineered neutrophil-derived EVs may directly kill tumor cells and regulate TME by carrying drugs, miRNAs, and cytotoxic factors such as doxorubicin, granzyme, perforin, and so on (186, 187).

In addition to normal engineered neutrophil systems, many other engineered strategies based on neutrophils have also been developed. A recent study developed a two-pronged delivery system to inhibit the effect of neutrophils in TME by both eliminating NETs and reducing mitochondrial biogenesis (188). The design of this strategy was based on the positive feedback loop that hypoxia caused by exceeding mitochondrial activity may promote the formation of NETs and NETs may positively contribute to the mitochondrial metabolism. It was also reported that a drug delivery system based on a platelet-neutrophil hybrid Membrane may achieve efficient drug delivery guided by neutrophil-related inflammatory microenvironment and enhance the anti-tumor effect of macrophage (189).

However, the challenges and potential side effects associated with neutrophil-related therapies should also be noticed. Usually, chemokine inhibitors and chemokine receptor inhibitors were usually employed to achieve the strategies targeting on the recruitment, repolarization, pro-tumor effect, and NETosis (162). The human chemokine system is characterized by its intricate and diverse nature. The inhibition of a pivotal chemokine receptor could potentially result in significant adverse effects (72). Moreover, the redundancy inherent in chemokines and their receptors necessitates the use of appropriate initiating doses and metabolic stabilizers for the antagonists to be effective. This requirement significantly constrains the development of chemokine receptor antagonists and their clinical efficacy (190). Consequently, there is a pressing need to optimize chemokine receptor antagonists in future research and development endeavors. Moreover, we have to further explore the effects of neutrophil subtypes. As neutrophils play a critical role in innate immunity, broad targeting of these cells can increase the risk of infections and other diseases (98). Therefore, therapies must be tailored to minimize off-target effects on normal neutrophil functions. Engineered neutrophil systems may achieve more satisfactory effect due to their ability in precision targeting, immunomodulation, and rapid response (187). They can be designed to deliver drugs directly to the tumor site, increasing the

efficacy of chemotherapy and reducing systemic side effects (173). Despite these advantages, their stability within the complex *in vivo* environment can be a concern, potentially affecting their therapeutic efficacy. Ensuring biocompatibility to avoid adverse immune responses is also a significant hurdle (173).

In summary, while neutrophil-based therapeutic strategies show promise in the fight against cancer, they also present significant scientific and technical challenges. Future research must focus on overcoming these hurdles, refining these therapies to maximize their efficacy and minimize adverse effects, and identifying biomarkers that can predict treatment response. This will be crucial in translating these innovative approaches into clinical practice, offering new hope for cancer patients.

Challenges and perspectives

With the development of single-cell sequencing, the roles of neutrophils in tumor development and metastasis are gradually recognized and understood. However, their involvement in bone cancer, specifically osteosarcoma, remains relatively understudied compared to other types of tumors. Recent research has partly demonstrated the roles of neutrophils in osteosarcoma, but the specific roles of neutrophils in osteosarcoma, including the interaction with bone cells (osteoclasts and osteoblasts), the communication with immune cells, and the effects of NETs, were still not fully understood. Moreover, further engineering and targeting therapies based on neutrophils were still limited.

In the future, further research is needed to elucidate the complex interplay between neutrophils and tumor cells in osteosarcoma, as well as to identify novel therapeutic targets to modulate neutrophil function and improve patient outcomes. Single-cell transcriptomics allows for a detailed analysis of the transcriptomic profiles of neutrophils in different osteosarcoma subtypes (191). By comparing the gene expression profiles of N1 and N2 neutrophils in various osteosarcoma subtypes, we can gain insights into the molecular mechanisms underlying their polarization and function. This can be optimized by using advanced computational methods to analyze the single-cell data and by integrating the data with proteomic and metabolomic profiles. Moreover, given the role of exosomes and other extracellular vesicles in cell-cell communication, future research should focus on their role in neutrophil-bone cell interactions (187). Isolation and characterization of these vesicles from osteosarcoma subtypes can reveal novel biomarkers and therapeutic targets. Additionally, the development of preclinical models that accurately recapitulate the bone tumor microenvironment will be essential for advancing our understanding of neutrophil biology in osteosarcoma and translating these findings into clinical practice. Many models in bone metabolism research may achieve the regulation of different bone cells, such as B-hRANKL mice, B-hSOST mice, B-hRSPO1 mice, and so on (192). Integrating the bone-related diseases models, orthotopic osteosarcoma models and neutrophil models, we may further explore the potential mechanism of the neutrophils in osteosarcoma.

Conclusion

In this review, we tried to summarize the roles of neutrophils in osteosarcoma from various dimensions, including the NETs, TANs in immune TME, interaction between neutrophils and immune cells, clinical evidence of neutrophils in osteosarcoma, the roles of neutrophils in surgery, and the potential therapy based on neutrophils. Though the studies on neutrophils in osteosarcoma were still limited, taking inspiration from studies on neutrophils in other types of cancer can also provide valuable insights for future research on their role in osteosarcoma development.

Author contributions

MX: Conceptualization, Data curation, Formal Analysis, Funding acquisition, Investigation, Methodology, Project administration, Resources, Software, Supervision, Validation, Visualization, Writing – original draft, Writing – review & editing. YH: Conceptualization, Data curation, Formal Analysis, Funding acquisition, Investigation, Methodology, Project administration, Resources, Software, Supervision, Validation, Visualization, Writing – original draft, Writing – review & editing. LS: Conceptualization, Data curation, Formal Analysis, Funding acquisition, Investigation, Methodology, Project administration, Resources, Software, Supervision, Validation, Visualization, Writing – original draft, Writing – review & editing. DBL: Conceptualization, Data curation, Formal Analysis, Funding acquisition, Investigation, Methodology, Project administration, Resources, Software, Supervision, Validation, Visualization, Writing – original draft, Writing – review & editing. CZ: Conceptualization, Data curation, Formal Analysis, Funding acquisition, Investigation, Methodology, Project administration, Resources, Software, Supervision, Validation, Visualization, Writing – original draft, Writing – review & editing. DSL: Conceptualization, Data curation, Formal Analysis, Funding acquisition, Investigation, Methodology, Project administration, Resources, Software, Supervision, Validation, Visualization, Writing – original draft, Writing – review & editing.

Funding

The author(s) declare that financial support was received for the research, authorship, and/or publication of this article. Jilin Provincial Scientific and Technological Development Program (20230204077YY).

Conflict of interest

The authors declare that the research was conducted in the absence of any commercial or financial relationships that could be construed as a potential conflict of interest.

Publisher's note

References

1. Bian J, Liu Y, Zhao X, Meng C, Zhang Y, Duan Y, et al. Research progress in the mechanism and treatment of osteosarcoma. *Chin Med J (Engl)*. (2023) 136:2412–20. doi: 10.1097/CM9.0000000000002800

2. Nirala BK, Yamamichi T, Yustein JT. Deciphering the signaling mechanisms of osteosarcoma tumorigenesis. *Int J Mol Sci*. (2023) 24:11367. doi: 10.3390/ijms241411367

3. Acharya SS, Kundu CN. Havoc in harmony: Unravelling the intricacies of angiogenesis orchestrated by the tumor microenvironment. *Cancer Treat Rev*. (2024) 127:102749. doi: 10.1016/j.ctrv.2024.102749

4. Lv D, Fei Y, Chen H, Wang J, Han W, Cui B, et al. Crosstalk between T lymphocyte and extracellular matrix in tumor microenvironment. *Front Immunol*. (2024) 15:1340702. doi: 10.3389/fimmu.2024.1340702

5. Nirala BK, Yamamichi T, Petrescu DI, Shafin TN, Yustein JT. Decoding the impact of tumor microenvironment in osteosarcoma progression and metastasis. *Cancers (Basel)*. (2023) 15:5108. doi: 10.3390/cancers15205108

6. Cheng S, Wang H, Kang X, Zhang H. Immunotherapy innovations in the fight against osteosarcoma: emerging strategies and promising progress. *Pharmaceutics*. (2024) 16:251. doi: 10.3390/pharmaceutics16020251

7. Thind MK, Uhlig HH, Glogauer M, Palaniyar N, Bourdon C, Gwela A, et al. A metabolic perspective of the neutrophil life cycle: new avenues in immunometabolism. *Front Immunol*. (2023) 14:1334205. doi: 10.3389/fimmu.2023.1334205

8. Tang H, Xie J, Du YX, Tan ZJ, Liang ZT. Osteosarcoma neutrophil extracellular trap network-associated gene recurrence and metastasis model. *J Cancer Res Clin Oncol*. (2024) 150:48. doi: 10.1007/s00432-023-05577-2

9. Li X, Hu L, Naeem A, Xiao S, Yang M, Shang H, et al. Neutrophil extracellular traps in tumors and potential use of traditional herbal medicine formulations for its regulation. *Int J Nanomed*. (2024) 19:2851–77. doi: 10.2147/IJN.S449181

10. Vasquez L, Leon E, Beltran B, Maza I, Oscanoa M, Geronimo J. Pretreatment neutrophil-to-lymphocyte ratio and lymphocyte recovery: independent prognostic factors for survival in pediatric sarcomas. *J Pediatr Hematol Oncol*. (2017) 39:538–46. doi: 10.1097/MPH.0000000000000911

11. Lin Y, Tang H, Teng H, Feng W, Li F, Liu S, et al. Development and validation of neutrophil extracellular traps-derived signature to predict the prognosis for osteosarcoma patients. *Int Immunopharmacol*. (2024) 127:111364. doi: 10.1016/j.intimp.2023.111364

12. Cersosimo F, Lonardi S, Bernardini G, Telfer B, Mandelli GE, Santucci A, et al. Tumor-associated macrophages in osteosarcoma: from mechanisms to therapy. *Int J Mol Sci*. (2020) 21:5207. doi: 10.3390/ijms21155207

13. Wu CC, Beird HC, Andrew Livingston J, Advani S, Mitra A, Cao S, et al. Immuno-genomic landscape of osteosarcoma. *Nat Commun*. (2020) 11:1008. doi: 10.1038/s41467-020-14646-w

14. Coffelt SB, Wellenstein MD, de Visser KE. Neutrophils in cancer: neutral no more. *Nat Rev Cancer*. (2016) 16:431–46. doi: 10.1038/nrc.2016.52

15. Yang S, Jia J, Wang F, Wang Y, Fang Y, Yang Y, et al. Targeting neutrophils: Mechanism and advances in cancer therapy. *Clin Transl Med*. (2024) 14:e1599. doi: 10.1002/ctm2.v14.3

16. Hedrick CC, Malanchi I. Neutrophils in cancer: heterogeneous and multifaceted. *Nat Rev Immunol*. (2022) 22:173–87. doi: 10.1038/s41577-021-00571-6

17. Xie X, Shi Q, Wu P, Zhang X, Kambara H, Su J, et al. Single-cell transcriptome profiling reveals neutrophil heterogeneity in homeostasis and infection. *Nat Immunol*. (2020) 21:1119–33. doi: 10.1038/s41590-020-0736-z

18. Mollinedo F. Neutrophil degranulation, plasticity, and cancer metastasis. *Trends Immunol*. (2019) 40:228–42. doi: 10.1016/j.it.2019.01.006

19. Mistry P, Nakabo S, O'Neil L, Goel RR, Jiang K, Carmona-Rivera C, et al. Transcriptomic, epigenetic, and functional analyses implicate neutrophil diversity in the pathogenesis of systemic lupus erythematosus. *Proc Natl Acad Sci U S A*. (2019) 116:25222–8. doi: 10.1073/pnas.1908576116

20. Rosmarin AG, Yang Z, Resendes KK. Transcriptional regulation in myelopoiesis: Hematopoietic fate choice, myeloid differentiation, and leukemogenesis. *Exp Hematol*. (2005) 33:131–43. doi: 10.1016/j.exphem.2004.08.015

21. Fridlender ZG, Sun J, Kim S, Kapoor V, Cheng G, Ling L, et al. Polarization of tumor-associated neutrophil phenotype by TGF-beta: "N1" versus "N2" TAN. *Cancer Cell*. (2009) 16:183–94. doi: 10.1016/j.ccr.2009.06.017

22. Andzinski L, Kasnitz N, Stahnke S, Wu CF, Gereke M, von Kockritz-Blickwede M, et al. Type I IFNs induce anti-tumor polarization of tumor associated neutrophils in mice and human. *Int J Cancer*. (2016) 138:1982–93. doi: 10.1002/ijc.v138.8

23. Mihaila AC, Ciortan L, Macarie RD, Vadana M, Cecoltan S, Preda MB, et al. Transcriptional profiling and functional analysis of N1/N2 neutrophils reveal an immunomodulatory effect of S100A9-blockade on the pro-inflammatory N1 subpopulation. *Front Immunol*. (2021) 12:708770. doi: 10.3389/fimmu.2021.708770

24. Lovaszi M, Nemeth ZH, Pacher P, Gause WC, Wagener G, Hasko G. A(2A) adenosine receptor activation prevents neutrophil aging and promotes polarization from N1 towards N2 phenotype. *Purinergic Signal*. (2022) 18:345–58. doi: 10.1007/s11302-022-09884-0

25. Granot Z, Henke E, Comen EA, King TA, Norton L, Benezra R. Tumor entrained neutrophils inhibit seeding in the premetastatic lung. *Cancer Cell*. (2011) 20:300–14. doi: 10.1016/j.ccr.2011.08.012

26. Gershkovitz M, Caspi Y, Fainsod-Levi T, Katz B, Michaeli J, Khawaled S, et al. TRPM2 mediates neutrophil killing of disseminated tumor cells. *Cancer Res*. (2018) 78:2680–90. doi: 10.1158/0008-5472.CAN-17-3614

27. Ralph SJ, Reynolds MJ. Intratumoral pro-oxidants promote cancer immunotherapy by recruiting and reprogramming neutrophils to eliminate tumors. *Cancer Immunol Immunother*. (2023) 72:527–42. doi: 10.1007/s00262-022-03248-8

28. Pelletier M, Billingham LK, Ramaswamy M, Siegel RM. Extracellular flux analysis to monitor glycolytic rates and mitochondrial oxygen consumption. *Methods Enzymol*. (2014) 542:125–49. doi: 10.1016/B978-0-12-416618-9.00007-8

29. Leone RD, Powell JD. Fueling the revolution: targeting metabolism to enhance immunotherapy. *Cancer Immunol Res*. (2021) 9:255–60. doi: 10.1158/2326-6066.CIR-20-0791

30. Korbecki J, Siminska D, Gassowska-Dobrowolska M, Listos J, Gutowska I, Chlubek D, et al. Chronic and cycling hypoxia: drivers of cancer chronic inflammation through HIF-1 and NF-kappaB activation: A review of the molecular mechanisms. *Int J Mol Sci*. (2021) 22:10701. doi: 10.3390/ijms221910701

31. Magar AG, Morya VK, Kwak MK, Oh JU, Noh KC. A molecular perspective on HIF-1alpha and angiogenic stimulator networks and their role in solid tumors: an update. *Int J Mol Sci*. (2024) 25:3313. doi: 10.3390/ijms25063313

32. Bae T, Hallis SP, Kwak MK. Hypoxia, oxidative stress, and the interplay of HIFs and NRF2 signaling in cancer. *Exp Mol Med*. (2024) 56:501–14. doi: 10.1038/s12276-024-01180-8

33. Papayannopoulos V. Neutrophil extracellular traps in immunity and disease. *Nat Rev Immunol*. (2018) 18:134–47. doi: 10.1038/nri.2017.105

34. Yan M, Gu Y, Sun H, Ge Q. Neutrophil extracellular traps in tumor progression and immunotherapy. *Front Immunol*. (2023) 14:1135086. doi: 10.3389/fimmu.2023.1135086

35. Shang B, Cui H, Xie R, Wu J, Shi H, Bi X, et al. Neutrophil extracellular traps primed intercellular communication in cancer progression as a promising therapeutic target. *biomark Res*. (2023) 11:24. doi: 10.1186/s40364-023-00463-y

36. Fuchs TA, Abed U, Goosmann C, Hurwitz R, Schulze I, Wahn V, et al. Novel cell death program leads to neutrophil extracellular traps. *J Cell Biol*. (2007) 176:231–41. doi: 10.1083/jcb.200606027

37. Chen T, Li Y, Sun R, Hu H, Liu Y, Herrmann M, et al. Receptor-mediated NETosis on neutrophils. *Front Immunol*. (2021) 12:775267. doi: 10.3389/fimmu.2021.775267

38. De Meo ML, Spicer JD. The role of neutrophil extracellular traps in cancer progression and metastasis. *Semin Immunol*. (2021) 57:101595. doi: 10.1016/j.smim.2022.101595

39. Kaltenmeier C, Simmons RL, Tohme S, Yazdani HO. Neutrophil extracellular traps (NETs) in cancer metastasis. *Cancers (Basel)*. (2021) 13:6131. doi: 10.3390/cancers13236131

40. McDowell SAC, Luo RBE, Arabzadeh A, Dore S, Bennett NC, Breton V, et al. Neutrophil oxidative stress mediates obesity-associated vascular dysfunction and metastatic transmigration. *Nat Cancer*. (2021) 2:545–62. doi: 10.1038/s43018-021-00194-9

41. Cools-Lartigue J, Spicer J, McDonald B, Gowing S, Chow S, Giannias B, et al. Neutrophil extracellular traps sequester circulating tumor cells and promote metastasis. *J Clin Invest*. (2013) 123:3446–58. doi: 10.1172/JCI67484

42. Schedel F, Mayer-Hain S, Pappelbaum KI, Metze D, Stock M, Goerge T, et al. Evidence and impact of neutrophil extracellular traps in Malignant melanoma. *Pigment Cell Melanoma Res.* (2020) 33:63–73. doi: 10.1111/pcmr.12818

43. Kaltenmeier C, Yazdani HO, Morder K, Geller DA, Simmons RL, Tohme S. Neutrophil extracellular traps promote T cell exhaustion in the tumor microenvironment. *Front Immunol.* (2021) 12:785222. doi: 10.3389/fimmu.2021.785222

44. Albrengues J, Shields MA, Ng D, Park CG, Ambrico A, Poindexter ME, et al. Neutrophil extracellular traps produced during inflammation awaken dormant cancer cells in mice. *Science.* (2018) 361:eaao4227. doi: 10.1126/science.aao4227

45. He XY, Gao Y, Ng D, Michalopoulou E, George S, Adrover JM, et al. Chronic stress increases metastasis via neutrophil-mediated changes to the microenvironment. *Cancer Cell.* (2024) 42:474–86 e12. doi: 10.1016/j.ccell.2024.01.013

46. Zhang F, Yan Y, Cao X, Guo C, Wang K, Lv S. TGF-beta-driven LIF expression influences neutrophil extracellular traps (NETs) and contributes to peritoneal metastasis in gastric cancer. *Cell Death Dis.* (2024) 15:218. doi: 10.1038/s41419-024-06594-w

47. Mousset A, Lecorgne E, Bourget I, Lopez P, Jenovai K, Cherfils-Vicini J, et al. Neutrophil extracellular traps formed during chemotherapy confer treatment resistance via TGF-beta activation. *Cancer Cell.* (2023) 41:757–75 e10. doi: 10.1016/j.ccell.2023.03.008

48. Yang L, Liu Q, Zhang X, Liu X, Zhou B, Chen J, et al. DNA of neutrophil extracellular traps promotes cancer metastasis via CCDC25. *Nature.* (2020) 583:133–8. doi: 10.1038/s41586-020-2394-6

49. Zhang Y, Chandra V, Riquelme Sanchez E, Dutta P, Quesada PR, Rakoski A, et al. Interleukin-17-induced neutrophil extracellular traps mediate resistance to checkpoint blockade in pancreatic cancer. *J Exp Med.* (2020) 217:e20190354. doi: 10.1084/jem.20190354

50. Chen F, Liu J, Yang T, Sun J, He X, Fu X, et al. Analysis of intercellular communication in the osteosarcoma microenvironment based on single cell sequencing data. *J Bone Oncol.* (2023) 41:100493. doi: 10.1016/j.jbo.2023.100493

51. Zhu T, Han J, Yang L, Cai Z, Sun W, Hua Y, et al. Immune microenvironment in osteosarcoma: components, therapeutic strategies and clinical applications. *Front Immunol.* (2022) 13:907550. doi: 10.3389/fimmu.2022.907550

52. Cortini M, Macchi F, Reggiani F, Vitale E, Lipreri MV, Perut F, et al. Endogenous extracellular matrix regulates the response of osteosarcoma 3D spheroids to doxorubicin. *Cancers (Basel).* (2023) 15:1221. doi: 10.3390/cancers15041221

53. Deng C, Xu Y, Chen H, Zhu X, Huang L, Chen Z, et al. Extracellular-vesicle-packaged S100A11 from osteosarcoma cells mediates lung premetastatic niche formation by recruiting gMDSCs. *Cell Rep.* (2024) 43:113751. doi: 10.1016/j.celrep.2024.113751

54. Chen X, Wang Z, Duan N, Zhu G, Schwarz EM, Xie C. Osteoblast-osteoclast interactions. *Connect Tissue Res.* (2018) 59:99–107. doi: 10.1080/03008207.2017.1290085

55. Ponzetti M, Ucci A, Puri C, Giacchi L, Flati I, Capece D, et al. Effects of osteoblast-derived extracellular vesicles on aggressiveness, redox status and mitochondrial bioenergetics of MNNG/HOS osteosarcoma cells. *Front Oncol.* (2022) 12:983254. doi: 10.3389/fonc.2022.983254

56. Araki Y, Yamamoto N, Hayashi K, Takeuchi A, Miwa S, Igarashi K, et al. The number of osteoclasts in a biopsy specimen can predict the efficacy of neoadjuvant chemotherapy for primary osteosarcoma. *Sci Rep.* (2021) 11:1989. doi: 10.1038/s41598-020-80504-w

57. Li H, Hong S, Qian J, Zheng Y, Yang J, Yi Q. Cross talk between the bone and immune systems: osteoclasts function as antigen-presenting cells and activate CD4+ and CD8+ T cells. *Blood.* (2010) 116:210–7. doi: 10.1182/blood-2009-11-255026

58. Endo-Munoz L, Evdokiou A, Saunders NA. The role of osteoclasts and tumour-associated macrophages in osteosarcoma metastasis. *Biochim Biophys Acta.* (2012) 1826:434–42. doi: 10.1016/j.bbcan.2012.07.003

59. Li F, Tang H, Luo X, Li X, Luo K, Liu S, et al. Interaction gene set between osteoclasts and regulatory CD4(+) T cells can accurately predict the prognosis of patients with osteosarcoma. *Cancer Sci.* (2023) 114:3014–26. doi: 10.1111/cas.v114.7

60. Anloague A, Delgado-Calle J. Osteocytes: new kids on the block for cancer in bone therapy. *Cancers (Basel).* (2023) 15:2645. doi: 10.3390/cancers15092645

61. Zheng Y, Wang G, Chen R, Hua Y, Cai Z. Mesenchymal stem cells in the osteosarcoma microenvironment: their biological properties, influence on tumor growth, and therapeutic implications. *Stem Cell Res Ther.* (2018) 9:22. doi: 10.1186/s13287-018-0780-x

62. Li F, Chen X, Shang C, Ying Q, Zhou X, Zhu R, et al. Bone Marrow Mesenchymal Stem Cells-Derived Extracellular Vesicles Promote Proliferation, Invasion and Migration of Osteosarcoma Cells via the lncRNA MALAT1/miR-143/NRSN2/Wnt/beta-Catenin Axis. *Onco Targets Ther.* (2021) 14:737–49. doi: 10.2147/OTT.S283459

63. Wei H, Chen J, Wang S, Fu F, Zhu X, Wu C, et al. A nanodrug consisting of doxorubicin and exosome derived from mesenchymal stem cells for osteosarcoma treatment *in vitro*. *Int J Nanomed.* (2019) 14:8603–10. doi: 10.2147/IJN.S218988

64. Mani N, Andrews D, Obeng RC. Modulation of T cell function and survival by the tumor microenvironment. *Front Cell Dev Biol.* (2023) 11:1191774. doi: 10.3389/fcell.2023.1191774

65. Kendal JK, Shehata MS, Lofftus SY, Crompton JG. Cancer-associated B cells in sarcoma. *Cancers (Basel).* (2023) 15:622. doi: 10.3390/cancers15030622

66. Bod L, Kye YC, Shi J, Torlai Triglia E, Schnell A, Fessler J, et al. B-cell-specific checkpoint molecules that regulate anti-tumour immunity. *Nature.* (2023) 619:348–56. doi: 10.1038/s41586-023-06231-0

67. Quamine AE, Olsen MR, Cho MM, Capitini CM. Approaches to enhance natural killer cell-based immunotherapy for pediatric solid tumors. *Cancers (Basel).* (2021) 13:2796. doi: 10.3390/cancers13112796

68. Marchais A, Marques da Costa ME, Job B, Abbas R, Drubay D, Piperno-Neumann S, et al. Immune Infiltrate and Tumor Microenvironment Transcriptional Programs Stratify Pediatric Osteosarcoma into Prognostic Groups at Diagnosis. *Cancer Res.* (2022) 82:974–85. doi: 10.1158/0008-5472.CAN-20-4189

69. Omer N, Nicholls W, Ruegg B, Souza-Fonseca-Guimaraes F, Rossi GR. Enhancing natural killer cell targeting of pediatric sarcoma. *Front Immunol.* (2021) 12:791206. doi: 10.3389/fimmu.2021.791206

70. Pratt HG, Justin EM, Lindsey BA. Applying osteosarcoma immunology to understand disease progression and assess immunotherapeutic response. *Adv Exp Med Biol.* (2020) 1258:91–109. doi: 10.1007/978-3-030-43085-6_6

71. Liu JF, Chen PC, Chang TM, Hou CH. Monocyte Chemoattractant Protein-1 promotes cancer cell migration via c-Raf/MAPK/AP-1 pathway and MMP-9 production in osteosarcoma. *J Exp Clin Cancer Res.* (2020) 39:254. doi: 10.1186/s13046-020-01756-y

72. Regan DP, Coy JW, Chahal KK, Chow L, Kurihara JN, Guth AM, et al. The angiotensin receptor blocker losartan suppresses growth of pulmonary metastases via AT1R-independent inhibition of CCR2 signaling and monocyte recruitment. *J Immunol.* (2019) 202:3087–102. doi: 10.4049/jimmunol.1800619

73. He J, Shan S, Jiang T, Zhou S, Qin J, Li Q, et al. Mechanical stretch preconditioned adipose-derived stem cells elicit polarization of anti-inflammatory M2-like macrophages and improve chronic wound healing. *FASEB J.* (2024) 38:e23626. doi: 10.1096/fj.202300586R

74. Luo ZW, Liu PP, Wang ZX, Chen CY, Xie H. Macrophages in osteosarcoma immune microenvironment: implications for immunotherapy. *Front Oncol.* (2020) 10:586580. doi: 10.3389/fonc.2020.586580

75. Mao X, Song F, Jin J, Zou B, Dai P, Sun M, et al. Prognostic and immunological significance of an M1 macrophage-related gene signature in osteosarcoma. *Front Immunol.* (2023) 14:1202725. doi: 10.3389/fimmu.2023.1202725

76. Zhou Q, Xian M, Xiang S, Xiang D, Shao X, Wang J, et al. All-trans retinoic acid prevents osteosarcoma metastasis by inhibiting M2 polarization of tumor-associated macrophages. *Cancer Immunol Res.* (2017) 5:547–59. doi: 10.1158/2326-6066.CIR-16-0259

77. Han Y, Guo W, Ren T, Huang Y, Wang S, Liu K, et al. Tumor-associated macrophages promote lung metastasis and induce epithelial-mesenchymal transition in osteosarcoma by activating the COX-2/STAT3 axis. *Cancer Lett.* (2019) 440-441:116–25. doi: 10.1016/j.canlet.2018.10.011

78. Huang R, Kang T, Chen S. The role of tumor-associated macrophages in tumor immune evasion. *J Cancer Res Clin Oncol.* (2024) 150:238. doi: 10.1007/s00432-024-05777-4

79. Cassetta L, Pollard JW. Targeting macrophages: therapeutic approaches in cancer. *Nat Rev Drug Discovery.* (2018) 17:887–904. doi: 10.1038/nrd.2018.169

80. Soto JA, Galvez NMS, Andrade CA, Pacheco GA, Bohmwald K, Berrios RV, et al. The role of dendritic cells during infections caused by highly prevalent viruses. *Front Immunol.* (2020) 11:1513. doi: 10.3389/fimmu.2020.01513

81. Zhang F, Zhu Y, Fan G, Hu S. Photodynamic therapy reduces the inhibitory effect of osteosarcoma cells on dendritic cells by upregulating HSP70. *Oncol Lett.* (2018) 16:5034–40. doi: 10.3892/ol.2018.9322

82. Pan R, Pan F, Zeng Z, Lei S, Yang Y, Yang Y, et al. A novel immune cell signature for predicting osteosarcoma prognosis and guiding therapy. *Front Immunol.* (2022) 13:1017120. doi: 10.3389/fimmu.2022.1017120

83. Shafqat A, Khan JA, Alkachem AY, Sabur H, Alkattan K, Yaqinuddin A, et al. How neutrophils shape the immune response: reassessing their multifaceted role in health and disease. *Int J Mol Sci.* (2023) 24:17583. doi: 10.3390/ijms242417583

84. Cambier S, Gouwy M, Proost P. The chemokines CXCL8 and CXCL12: molecular and functional properties, role in disease and efforts towards pharmacological intervention. *Cell Mol Immunol.* (2023) 20:217–51. doi: 10.1038/s41423-023-00974-6

85. Bhattacharya M, Anborgh PH, Babwah AV, Dale LB, Dobransky T, Benovic JL, et al. Beta-arrestins regulate a Ral-GDS Ral effector pathway that mediates cytoskeletal reorganization. *Nat Cell Biol.* (2002) 4:547–55. doi: 10.1038/ncb821

86. Alon R, Shulman Z. Chemokine triggered integrin activation and actin remodeling events guiding lymphocyte migration across vascular barriers. *Exp Cell Res.* (2011) 317:632–41. doi: 10.1016/j.yexcr.2010.12.007

87. Awane M, Andres PG, Li DJ, Reinecker HC. NF-kappa B-inducing kinase is a common mediator of IL-17-, TNF-alpha-, and IL-1 beta-induced chemokine promoter activation in intestinal epithelial cells. *J Immunol.* (1999) 162:5337–44. doi: 10.4049/jimmunol.162.9.5337

88. Kim HK, de la Luz Sierra M, Williams CK, Gulino AV, Tosato G. G-CSF down-regulation of CXCR4 expression identified as a mechanism for mobilization of myeloid cells. *Blood.* (2006) 108:812–20. doi: 10.1182/blood-2005-10-4162

89. Ucci A, Cappariello A, Ponzetti M, Tennant F, Loftus AEP, Shefferd K, et al. Anti-osteoblastogenic, pro-inflammatory and pro-angiogenic effect of extracellular

vesicles isolated from the human osteosarcoma cell line MNNG/HOS. *Bone*. (2021) 153:116130. doi: 10.1016/j.bone.2021.116130

90. Avnet S, Di Pompo G, Chano T, Errani C, Ibrahim-Hashim A, Gillies RJ, et al. Cancer-associated mesenchymal stroma fosters the stemness of osteosarcoma cells in response to intratumoral acidosis via NF-kappaB activation. *Int J Cancer*. (2017) 140:1331–45. doi: 10.1002/ijc.30540

91. Tieken C, Verboom MC, Ruf W, Gelderblom H, Bovee JV, Reitsma PH, et al. Tissue factor associates with survival and regulates tumour progression in osteosarcoma. *Thromb Haemost*. (2016) 115:1025–33. doi: 10.1160/TH15-07-0541

92. Charan M, Dravid P, Cam M, Setty B, Roberts RD, Houghton PJ, et al. Tumor secreted ANGPTL2 facilitates recruitment of neutrophils to the lung to promote lung pre-metastatic niche formation and targeting ANGPTL2 signaling affects metastatic disease. *Oncotarget*. (2020) 11:510–22. doi: 10.18632/oncotarget.27433

93. Chao CC, Lee CW, Chang TM, Chen PC, Liu JF. CXCL1/CXCR2 paracrine axis contributes to lung metastasis in osteosarcoma. *Cancers (Basel)*. (2020) 12:459. doi: 10.3390/cancers12020459

94. Almeida SFF, Santos L, Sampaio-Ribeiro G, Ferreira HRS, Lima N, Caetano R, et al. Unveiling the role of osteosarcoma-derived secretome in premetastatic lung remodelling. *J Exp Clin Cancer Res*. (2023) 42:328. doi: 10.1186/s13046-023-02886-9

95. Ji Y, Lin Z, Li G, Tian X, Wu Y, Wan J, et al. Identification and validation of novel biomarkers associated with immune infiltration for the diagnosis of osteosarcoma based on machine learning. *Front Genet*. (2023) 14:1136783. doi: 10.3389/fgene.2023.1136783

96. Jaillon S, Ponzetta A, Di Mitri D, Santoni A, Bonecchi R, Mantovani A. Neutrophil diversity and plasticity in tumour progression and therapy. *Nat Rev Cancer*. (2020) 20:485–503. doi: 10.1038/s41568-020-0281-y

97. Misaghi A, Goldin A, Awad M, Kulidjian AA. Osteosarcoma: a comprehensive review. *SICOT J*. (2018) 4:12. doi: 10.1051/sicotj/2017028

98. Jiang Y, Wang J, Sun M, Zuo D, Wang H, Shen J, et al. Multi-omics analysis identifies osteosarcoma subtypes with distinct prognosis indicating stratified treatment. *Nat Commun*. (2022) 13:7207. doi: 10.1038/s41467-022-34689-5

99. Zhou J, Liu T, Wang W. Prognostic significance of matrix metalloproteinase 9 expression in osteosarcoma: A meta-analysis of 16 studies. *Med (Baltimore)*. (2018) 97: e13051. doi: 10.1097/MD.0000000000013051

100. Bonecchi R, Mantovani A, Jaillon S. Chemokines as regulators of neutrophils: focus on tumors, therapeutic targeting, and immunotherapy. *Cancers (Basel)*. (2022) 14:680. doi: 10.3390/cancers14030680

101. Tan S, Chao R. An exploration of osteosarcoma metastasis diagnostic markers based on tumor-associated neutrophils. *Discovery Med*. (2023) 35:300–11. doi: 10.24976/Discov.Med.202335176.31

102. Lu J, Rui J, Xu XY, Shen JK. Exploring the role of neutrophil-related genes in osteosarcoma via an integrative analysis of single-cell and bulk transcriptome. *Biomedicines*. (2024) 12:1513. doi: 10.3390/biomedicines12071513

103. Segal BH, Giridharan T, Suzuki S, Khan ANH, Zsiros E, Emmons TR, et al. Neutrophil interactions with T cells, platelets, endothelial cells, and of course tumor cells. *Immunol Rev*. (2023) 314:13–35. doi: 10.1111/imr.v314.1

104. Veglia F, Sanseviero E, Gabrilovich DI. Myeloid-derived suppressor cells in the era of increasing myeloid cell diversity. *Nat Rev Immunol*. (2021) 21:485–98. doi: 10.1038/s41577-020-00490-y

105. Joshi S, Sharabi A. Targeting myeloid-derived suppressor cells to enhance natural killer cell-based immunotherapy. *Pharmacol Ther*. (2022) 235:108114. doi: 10.1016/j.pharmthera.2022.108114

106. Marvel D, Gabrilovich DI. Myeloid-derived suppressor cells in the tumor microenvironment: expect the unexpected. *J Clin Invest*. (2015) 125:3356–64. doi: 10.1172/JCI80005

107. Ling Z, Yang C, Tan J, Dou C, Chen Y. Beyond immunosuppressive effects: dual roles of myeloid-derived suppressor cells in bone-related diseases. *Cell Mol Life Sci*. (2021) 78:7161–83. doi: 10.1007/s00018-021-03966-9

108. Tumino N, Fiore PF, Pelosi A, Moretta L, Vacca P. Myeloid derived suppressor cells in tumor microenvironment: Interaction with innate lymphoid cells. *Semin Immunol*. (2022) 61-64:101668. doi: 10.1016/j.smim.2022.101668

109. Siret C, Collignon A, Silvy F, Robert S, Cheyrol T, Andre P, et al. Deciphering the crosstalk between myeloid-derived suppressor cells and regulatory T cells in pancreatic ductal adenocarcinoma. *Front Immunol*. (2019) 10:3070. doi: 10.3389/fimmu.2019.03070

110. Umansky V, Blattner C, Gebhardt C, Utikal J. The role of myeloid-derived suppressor cells (MDSC) in cancer progression. *Vaccines (Basel)*. (2016) 4:36. doi: 10.3390/vaccines4040036

111. Ran S, Wilber A. Novel role of immature myeloid cells in formation of new lymphatic vessels associated with inflammation and tumors. *J Leukoc Biol*. (2017) 102:253–63. doi: 10.1189/jlb.1MR1016-434RR

112. Soehnlein O, Lindbom L, Weber C. Mechanisms underlying neutrophil-mediated monocyte recruitment. *Blood*. (2009) 114:4613–23. doi: 10.1182/blood-2009-06-221630

113. Ponzetta A, Carriero R, Carnevale S, Barbagallo M, Molgora M, Perucchini C, et al. Neutrophils driving unconventional T cells mediate resistance against murine sarcomas and selected human tumors. *Cell*. (2019) 178:346–60 e24. doi: 10.1016/j.cell.2019.05.047

114. Canli O, Nicolas AM, Gupta J, Finkelmeier F, Goncharova O, Pesic M, et al. Myeloid cell-derived reactive oxygen species induce epithelial mutagenesis. *Cancer Cell*. (2017) 32:869–83 e5. doi: 10.1016/j.ccell.2017.11.004

115. Russo M, Nastasi C. Targeting the tumor microenvironment: A close up of tumor-associated macrophages and neutrophils. *Front Oncol*. (2022) 12:871513. doi: 10.3389/fonc.2022.871513

116. Hanahan D, Coussens LM. Accessories to the crime: functions of cells recruited to the tumor microenvironment. *Cancer Cell*. (2012) 21:309–22. doi: 10.1016/j.ccr.2012.02.022

117. Pollard JW. Trophic macrophages in development and disease. *Nat Rev Immunol*. (2009) 9:259–70. doi: 10.1038/nri2528

118. Di Ceglie I, Carnevale S, Rigatelli A, Grieco G, Molisso P, Jaillon S. Immune cell networking in solid tumors: focus on macrophages and neutrophils. *Front Immunol*. (2024) 15:1341390. doi: 10.3389/fimmu.2024.1341390

119. Carnevale S, Ghasemi S, Rigatelli A, Jaillon S. The complexity of neutrophils in health and disease: Focus on cancer. *Semin Immunol*. (2020) 48:101409. doi: 10.1016/j.smim.2020.101409

120. Rice CM, Davies LC, Subleski JJ, Maio N, Gonzalez-Cotto M, Andrews C, et al. Tumour-elicited neutrophils engage mitochondrial metabolism to circumvent nutrient limitations and maintain immune suppression. *Nat Commun*. (2018) 9:5099. doi: 10.1038/s41467-018-07505-2

121. Li P, Lu M, Shi J, Hua L, Gong Z, Li Q, et al. Dual roles of neutrophils in metastatic colonization are governed by the host NK cell status. *Nat Commun*. (2020) 11:4387. doi: 10.1038/s41467-020-18125-0

122. Condamine T, Kumar V, Ramachandran IR, Youn JI, Celis E, Finnberg N, et al. ER stress regulates myeloid-derived suppressor cell fate through TRAIL-R-mediated apoptosis. *J Clin Invest*. (2014) 124:2626–39. doi: 10.1172/JCI74056

123. Cheng Y, Li H, Deng Y, Tai Y, Zeng K, Zhang Y, et al. Cancer-associated fibroblasts induce PDL1+ neutrophils through the IL6-STAT3 pathway that foster immune suppression in hepatocellular carcinoma. *Cell Death Dis*. (2018) 9:422. doi: 10.1038/s41419-018-0458-4

124. Zhang M, Qin H, Wu Y, Gao Q. Complex role of neutrophils in the tumor microenvironment: an avenue for novel immunotherapies. *Cancer Biol Med*. (2024) 21:20240192. doi: 10.20892/j.issn.2095-3941.2024.0192

125. Singhal S, Bhojnagarwala PS, O'Brien S, Moon EK, Garfall AL, Rao AS, et al. Origin and role of a subset of tumor-associated neutrophils with antigen-presenting cell features in early-stage human lung cancer. *Cancer Cell*. (2016) 30:120–35. doi: 10.1016/j.ccell.2016.06.001

126. Eruslanov EB, Bhojnagarwala PS, Quatromoni JG, Stephen TL, Ranganathan A, Deshpande C, et al. Tumor-associated neutrophils stimulate T cell responses in early-stage human lung cancer. *J Clin Invest*. (2014) 124:5466–80. doi: 10.1172/JCI77053

127. Riise RE, Bernson E, Aurelius J, Martner A, Pesce S, Della Chiesa M, et al. TLR-stimulated neutrophils instruct NK cells to trigger dendritic cell maturation and promote adaptive T cell responses. *J Immunol*. (2015) 195:1121–8. doi: 10.4049/jimmunol.1500709

128. Shaul ME, Zlotnik A, Tidhar E, Schwartz A, Arpinati L, Kaisar-Iluz N, et al. Tumor-associated neutrophils drive B-cell recruitment and their differentiation to plasma cells. *Cancer Immunol Res*. (2021) 9:811–24. doi: 10.1158/2326-6066.CIR-20-0839

129. Hampton HR, Chtanova T. The lymph node neutrophil. *Semin Immunol*. (2016) 28:129–36. doi: 10.1016/j.smim.2016.03.008

130. Tomay F, Wells K, Duong L, Tsu JW, Dye DE, Radley-Crabb HG, et al. Aged neutrophils accumulate in lymphoid tissues from healthy elderly mice and infiltrate T- and B-cell zones. *Immunol Cell Biol*. (2018) 96:831–40. doi: 10.1111/imcb.2018.96.issue-8

131. Parsa R, Lund H, Georgoudaki AM, Zhang XM, Ortlieb Guerreiro-Cacais A, Grommisch D, et al. BAFF-secreting neutrophils drive plasma cell responses during emergency granulopoiesis. *J Exp Med*. (2016) 213:1537–53. doi: 10.1084/jem.20150577

132. Guan X, Guan X, Zhao Z, Yan H. NETs: Important players in cancer progression and therapeutic resistance. *Exp Cell Res*. (2024) 441:114191. doi: 10.1016/j.yexcr.2024.114191

133. Wang H, Kim SJ, Lei Y, Wang S, Wang H, Huang H, et al. Neutrophil extracellular traps in homeostasis and disease. *Signal Transduct Target Ther*. (2024) 9:235. doi: 10.1038/s41392-024-01933-x

134. Tatsuno R, Ichikawa J, Komohara Y, Pan C, Kawasaki T, Enomoto A, et al. Pivotal role of IL-8 derived from the interaction between osteosarcoma and tumor-associated macrophages in osteosarcoma growth and metastasis via the FAK pathway. *Cell Death Dis*. (2024) 15:108. doi: 10.1038/s41419-024-06487-y

135. Tajvar Nasab N, Jalili-Nik M, Afshari AR, Rezaei Farimani A, Soukhtanloo M. Urolithin B inhibits proliferation and migration and promotes apoptosis and necrosis by inducing G2/M arrest and targeting MMP-2/-9 expression in osteosarcoma cells. *J Biochem Mol Toxicol*. (2023) 37:e23486. doi: 10.1002/jbt.23486

136. Araki Y, Yamamoto N, Hayashi K, Takeuchi A, Miwa S, Igarashi K, et al. Pretreatment neutrophil count and platelet-lymphocyte ratio as predictors of metastasis in patients with osteosarcoma. *Anticancer Res*. (2022) 42:1081–9. doi: 10.21873/anticanres.15570

137. Xia WK, Liu ZL, Shen D, Lin QF, Su J, Mao WD. Prognostic performance of pre-treatment NLR and PLR in patients suffering from osteosarcoma. *World J Surg Oncol*. (2016) 14:127. doi: 10.1186/s12957-016-0889-2

138. Peng LP, Li J, Li XF. Prognostic value of neutrophil/lymphocyte, platelet/lymphocyte, lymphocyte/monocyte ratios and Glasgow prognostic score in osteosarcoma: A meta-analysis. *World J Clin Cases*. (2022) 10:2194–205. doi: 10.12998/wjcc.v10.i7.2194

139. Song X, Zhang H, Yin F, Guo P, Yang X, Liu J, et al. Systemic inflammatory markers for predicting overall survival in patients with osteosarcoma: A systematic review and meta-analysis. *Mediators Inflamm*. (2021) 2021:3456629. doi: 10.1155/2021/3456629

140. Yapar A, Tokgoz MA, Yapar D, Atalay IB, Ulucakoy C, Gungor BS. Diagnostic and prognostic role of neutrophil/lymphocyte ratio, platelet/lymphocyte ratio, and lymphocyte/monocyte ratio in patients with osteosarcoma. *Jt Dis Relat Surg*. (2021) 32:489–96. doi: 10.52312/jdrs

141. Liu B, Huang Y, Sun Y, Zhang J, Yao Y, Shen Z, et al. Prognostic value of inflammation-based scores in patients with osteosarcoma. *Sci Rep*. (2016) 6:39862. doi: 10.1038/srep39862

142. Tang H, Liu D, Lu J, He J, Ji S, Liao S, et al. Significance of the neutrophil-to-lymphocyte ratio in predicting the response to neoadjuvant chemotherapy in extremity osteosarcoma: a multicentre retrospective study. *BMC Cancer*. (2022) 22:33. doi: 10.1186/s12885-021-09130-7

143. Arefpour AM, Garousi M, Foroughi A, Hosseini S, Shahin M, Javadinia SA. Significance of the pretreatment neutrophil-to-lymphocyte and platelet-to-lymphocyte ratios in predicting the response to neoadjuvant chemotherapy and survival rates in extremity osteosarcoma: A multicentre prospective study. *Cancer Invest*. (2023) 41:816–20. doi: 10.1080/07357907.2023.2283456

144. Bastard P, Cozic N, Brion R, Gaspar N, Piperno-Neumann S, Cordero C, et al. Prognostic value of hemogram parameters in osteosarcoma: The French OS2006 experience. *Pediatr Blood Cancer*. (2024) 71:e31029. doi: 10.1002/pbc.31029

145. Li L, Li Y, Lu M, Wang Y, Li Z, Hu X, et al. The combination of baseline neutrophil to lymphocyte ratio and dynamic changes during treatment can better predict the survival of osteosarcoma patients. *Front Oncol*. (2023) 13:1235158. doi: 10.3389/fonc.2023.1235158

146. Huang X, Hu H, Zhang W, Shao Z. Prognostic value of prognostic nutritional index and systemic immune-inflammation index in patients with osteosarcoma. *J Cell Physiol*. (2019) 234:18408–14. doi: 10.1002/jcp.v234.10

147. Ouyang H, Wang Z. Predictive value of the systemic immune-inflammation index for cancer-specific survival of osteosarcoma in children. *Front Public Health*. (2022) 10:879523. doi: 10.3389/fpubh.2022.879523

148. Ma C, Yu R, Li J, Guo J, Xu J, Wang X, et al. Preoperative prognostic nutritional index and systemic immune-inflammation index predict survival outcomes in osteosarcoma: A comparison between young and elderly patients. *J Surg Oncol*. (2022) 125:754–65. doi: 10.1002/jso.v125.4

149. He X, Wang Y, Ye Q, Wang Y, Min L, Luo Y, et al. Lung immune prognostic index could predict metastasis in patients with osteosarcoma. *Front Surg*. (2022) 9:923427. doi: 10.3389/fsurg.2022.923427

150. Yang Q, Chen T, Yao Z, Zhang X. Prognostic value of pre-treatment Naples prognostic score (NPS) in patients with osteosarcoma. *World J Surg Oncol*. (2020) 18:24. doi: 10.1186/s12957-020-1789-z

151. Smeland S, Bielack SS, Whelan J, Bernstein M, Hogendoorn P, Krailo MD, et al. Survival and prognosis with osteosarcoma: outcomes in more than 2000 patients in the EURAMOS-1 (European and American Osteosarcoma Study) cohort. *Eur J Cancer*. (2019) 109:36–50. doi: 10.1016/j.ejca.2018.11.027

152. Huber-Lang M, Lambris JD, Ward PA. Innate immune responses to trauma. *Nat Immunol*. (2018) 19:327–41. doi: 10.1038/s41590-018-0064-8

153. Krall JA, Reinhardt F, Mercury OA, Pattabiraman DR, Brooks MW, Dougan M, et al. The systemic response to surgery triggers the outgrowth of distant immune-controlled tumors in mouse models of dormancy. *Sci Transl Med*. (2018) 10:eaan3464. doi: 10.1126/scitranslmed.aan3464

154. Chen GY, Nunez G. Sterile inflammation: sensing and reacting to damage. *Nat Rev Immunol*. (2010) 10:826–37. doi: 10.1038/nri2873

155. Wheeler DS, Chase MA, Senft AP, Poynter SE, Wong HR, Page K. Extracellular Hsp72, an endogenous DAMP, is released by virally infected airway epithelial cells and activates neutrophils via Toll-like receptor (TLR)-4. *Respir Res*. (2009) 10:31. doi: 10.1186/1465-9921-10-31

156. Tang F, Tie Y, Lan TX, Yang JY, Hong WQ, Chen SY, et al. Surgical treatment of osteosarcoma induced distant pre-metastatic niche in lung to facilitate the colonization of circulating tumor cells. *Adv Sci (Weinh)*. (2023) 10:e2207518. doi: 10.1002/advs.202207518

157. von Meijenfeldt FA, Burlage LC, Bos S, Adelmeijer J, Porte RJ, Lisman T. Elevated plasma levels of cell-free DNA during liver transplantation are associated with activation of coagulation. *Liver Transpl*. (2018) 24:1716–25. doi: 10.1002/lt.25329

158. Banki F, Mason RJ, Oh D, Hagen JA, DeMeester SR, Lipham JC, et al. Plasma DNA as a molecular marker for completeness of resection and recurrent disease in patients with esophageal cancer. *Arch Surg*. (2007) 142:533–8; discussion 8-9. doi: 10.1001/archsurg.142.6.533

159. Tohme S, Yazdani HO, Al-Khafaji AB, Chidi AP, Loughran P, Mowen K, et al. Neutrophil extracellular traps promote the development and progression of liver metastases after surgical stress. *Cancer Res*. (2016) 76:1367–80. doi: 10.1158/0008-5472.CAN-15-1591

160. Raccosta L, Fontana R, Maggioni D, Lanterna C, Villablanca EJ, Paniccia A, et al. The oxysterol-CXCR2 axis plays a key role in the recruitment of tumor-promoting neutrophils. *J Exp Med*. (2013) 210:1711–28. doi: 10.1084/jem.20130440

161. Cheng Y, Mo F, Li Q, Han X, Shi H, Chen S, et al. Targeting CXCR2 inhibits the progression of lung cancer and promotes therapeutic effect of cisplatin. *Mol Cancer*. (2021) 20:62. doi: 10.1186/s12943-021-01355-1

162. Teijeira A, Garasa S, Gato M, Alfaro C, Migueliz I, Cirella A, et al. CXCR1 and CXCR2 chemokine receptor agonists produced by tumors induce neutrophil extracellular traps that interfere with immune cytotoxicity. *Immunity*. (2020) 52:856–71 e8. doi: 10.1016/j.immuni.2020.03.001

163. Tulotta C, Stefanescu C, Chen Q, Torraca V, Meijer AH, Snaar-Jagalska BE. CXCR4 signaling regulates metastatic onset by controlling neutrophil motility and response to Malignant cells. *Sci Rep*. (2019) 9:2399. doi: 10.1038/s41598-019-38643-2

164. Wang PF, Zhang YX, Su J, Yao K, Li SW, Huang GR, et al. Neutrophil depletion enhances the therapeutic effect of PD-1 antibody on glioma. *Aging (Albany NY)*. (2020) 12:15290–301. doi: 10.18632/aging.103428

165. Zhang L, Yao J, Wei Y, Zhou Z, Li P, Qu J, et al. Blocking immunosuppressive neutrophils deters pY696-EZH2-driven brain metastases. *Sci Transl Med*. (2020) 12:eaaz5387. doi: 10.1126/scitranslmed.aaz5387

166. Coffelt SB, Kersten K, Doornebal CW, Weiden J, Vrijland K, Hau CS, et al. IL-17-producing gammadelta T cells and neutrophils conspire to promote breast cancer metastasis. *Nature*. (2015) 522:345–8. doi: 10.1038/nature14282

167. Chung JY, Tang PC, Chan MK, Xue VW, Huang XR, Ng CS, et al. Smad3 is essential for polarization of tumor-associated neutrophils in non-small cell lung carcinoma. *Nat Commun*. (2023) 14:1794. doi: 10.1038/s41467-023-37515-8

168. Mattoscio D, Isopi E, Lamolinara A, Patruno S, Medda A, De Cecco F, et al. Resolvin D1 reduces cancer growth stimulating a protective neutrophil-dependent recruitment of anti-tumor monocytes. *J Exp Clin Cancer Res*. (2021) 40:129. doi: 10.1186/s13046-021-01937-3

169. Zhang Y, Diao N, Lee CK, Chu HW, Bai L, Li L. Neutrophils deficient in innate suppressor IRAK-M enhances anti-tumor immune responses. *Mol Ther*. (2020) 28:89–99. doi: 10.1016/j.ymthe.2019.09.019

170. Pylaeva E, Harati MD, Spyra I, Bordbari S, Strachan S, Thakur BK, et al. NAMPT signaling is critical for the proangiogenic activity of tumor-associated neutrophils. *Int J Cancer*. (2019) 144:136–49. doi: 10.1002/ijc.v144.1

171. Tyagi A, Wu SY, Sharma S, Wu K, Zhao D, Deshpande R, et al. Exosomal miR-4466 from nicotine-activated neutrophils promotes tumor cell stemness and metabolism in lung cancer metastasis. *Oncogene*. (2022) 41:3079–92. doi: 10.1038/s41388-022-02322-w

172. Itatani Y, Yamamoto T, Zhong C, Molinolo AA, Ruppel J, Hegde P, et al. Suppressing neutrophil-dependent angiogenesis abrogates resistance to anti-VEGF antibody in a genetic model of colorectal cancer. *Proc Natl Acad Sci U S A*. (2020) 117:21598–608. doi: 10.1073/pnas.2008112117

173. Zhang J, Ji C, Zhang H, Shi H, Mao F, Qian H, et al. Engineered neutrophil-derived exosome-like vesicles for targeted cancer therapy. *Sci Adv*. (2022) 8:eabj8207. doi: 10.1126/sciadv.abj8207

174. Perego M, Tyurin VA, Tyurina YY, Yellets J, Nacarelli T, Lin C, et al. Reactivation of dormant tumor cells by modified lipids derived from stress-activated neutrophils. *Sci Transl Med*. (2020) 12:eabb5817. doi: 10.1126/scitranslmed.abb5817

175. Veglia F, Tyurin VA, Blasi M, De Leo A, Kossenkov AV, Donthireddy L, et al. Fatty acid transport protein 2 reprograms neutrophils in cancer. *Nature*. (2019) 569:73–8. doi: 10.1038/s41586-019-1118-2

176. Park J, Wysocki RW, Amoozgar Z, Maiorino L, Fein MR, Jorns J, et al. Cancer cells induce metastasis-supporting neutrophil extracellular DNA traps. *Sci Transl Med*. (2016) 8:361ra138. doi: 10.1126/scitranslmed.aag1711

177. Chen J, Hou S, Liang Q, He W, Li R, Wang H, et al. Localized degradation of neutrophil extracellular traps by photoregulated enzyme delivery for cancer immunotherapy and metastasis suppression. *ACS Nano*. (2022) 16:2585–97. doi: 10.1021/acsnano.1c09318

178. Liang H, Du Y, Zhu C, Zhang Z, Liao G, Liu L, et al. Nanoparticulate cationic poly(amino acid)s block cancer metastases by destructing neutrophil extracellular traps. *ACS Nano*. (2023) 17:2868–80. doi: 10.1021/acsnano.2c11280

179. Mu Q, Yao K, Syeda MZ, Zhang M, Cheng Q, Zhang Y, et al. Ligustrazine nanoparticle hitchhiking on neutrophils for enhanced therapy of cerebral ischemia-reperfusion injury. *Adv Sci (Weinh)*. (2023) 10:e2301348. doi: 10.1002/advs.202301348

180. Chen K, Zhou A, Zhou X, He J, Xu Y, Ning X. Cellular Trojan Horse initiates bimetallic Fe-Cu MOF-mediated synergistic cuproptosis and ferroptosis against Malignancies. *Sci Adv*. (2024) 10:eadk3201. doi: 10.1126/sciadv.adk3201

181. Yu X, Xing G, Sheng S, Jin L, Zhang Y, Zhu D, et al. Neutrophil camouflaged stealth nanovehicle for photothermal-induced tumor immunotherapy by triggering pyroptosis. *Adv Sci (Weinh)*. (2023) 10:e2207456. doi: 10.1002/advs.202207456

182. Zhou X, Yu R, Cao X, Zhang ZR, Deng L. Bio-mimicking nanoparticles for targeted therapy of Malignant melanoma. *J BioMed Nanotechnol*. (2019) 15:993–1004. doi: 10.1166/jbn.2019.2739

183. Chen S, Chen E, Guan X, Li J, Qin A, Wang C, et al. Magnetically controlled nanorobots induced oriented and rapid clearance of the cytokine storm for acute lung injury therapy. *Colloids Surf B Biointerfaces*. (2024) 234:113731. doi: 10.1016/j.colsurfb.2023.113731

184. Huang T, Wen X, Liang Y, Liu X, Zhao J, Long X. Irreversible electroporation-induced inflammation facilitates neutrophil-mediated drug delivery to enhance pancreatic cancer therapy. *Mol Pharm*. (2024) 21:1998–2011. doi: 10.1021/acs.molpharmaceut.4c00006

185. Wang H, Zang J, Zhao Z, Zhang Q, Chen S. The advances of neutrophil-derived effective drug delivery systems: A key review of managing tumors and inflammation. *Int J Nanomed*. (2021) 16:7663–81. doi: 10.2147/IJN.S328705

186. Yu D, Zhang J, Wang M, Ji R, Qian H, Xu W, et al. Exosomal miRNAs from neutrophils act as accurate biomarkers for gastric cancer diagnosis. *Clin Chim Acta*. (2024) 554:117773. doi: 10.1016/j.cca.2024.117773

187. Zhang J, Gu J, Wang X, Ji C, Yu D, Wang M, et al. Engineering and targeting neutrophils for cancer therapy. *Adv Mater*. (2024) 36:e2310318. doi: 10.1002/adma.202310318

188. Kong J, Deng Y, Xu Y, Zhang P, Li L, Huang Y. A two-pronged delivery strategy disrupting positive feedback loop of neutrophil extracellular traps for metastasis suppression. *ACS Nano*. (2024) 18:15432–51. doi: 10.1021/acsnano.3c09165

189. Sheng S, Jin L, Zhang Y, Sun W, Mei L, Zhu D, et al. A twindrive precise delivery system of platelet-neutrophil hybrid membrane regulates macrophage combined with CD47 blocking for postoperative immunotherapy. *ACS Nano*. (2024) 18:4981–92. doi: 10.1021/acsnano.3c10862

190. Hawash M. Advances in cancer therapy: A comprehensive review of CDK and EGFR inhibitors. *Cells*. (2024) 13:1656. doi: 10.3390/cells13191656

191. Zhou W, Cao X, Xu Q, Qu J, Sun Y. The double-edged role of neutrophil heterogeneity in inflammatory diseases and cancers. *MedComm (2020)*. (2023) 4:e325. doi: 10.1002/mco2.v4.4

192. Koh NYY, Miszkiewicz JJ, Fac ML, Wee NKY, Sims NA. Preclinical rodent models for human bone disease, including a focus on cortical bone. *Endocr Rev*. (2024) 45:493–520. doi: 10.1210/endrev/bnae004

frontiers | Frontiers in Oncology

TYPE Original Research
PUBLISHED 09 January 2025
DOI 10.3389/fonc.2024.1485605

OPEN ACCESS

EDITED BY
Brian D. Adams,
Brain Institute of America, United States

REVIEWED BY
Juliano Andreoli Miyake,
Federal University of Santa Catarina, Brazil
Yang Wang,
Sichuan Academy of Medical Sciences and Sichuan Provincial People's Hospital, China

*CORRESPONDENCE
Naiqiang Zhu
zhunq2010@163.com

RECEIVED 24 August 2024
ACCEPTED 18 December 2024
PUBLISHED 09 January 2025

CITATION
Zhang Y, Lun H, Zhu N, Yang N, Ding K, Chen B, Chang C, Gu H and Liu Y (2025) Deciphering the oncogenic network: how C1QTNF1-AS1 modulates osteosarcoma through miR-34a-5p and glycolytic pathways. *Front. Oncol.* 14:1485605. doi: 10.3389/fonc.2024.1485605

Deciphering the oncogenic network: how C1QTNF1-AS1 modulates osteosarcoma through miR-34a-5p and glycolytic pathways

Yu Zhang[1], Hailong Lun[2], Naiqiang Zhu[3,4]*, Ning Yang[3], Kaikai Ding[1], Bin Chen[4], Chengbing Chang[4], Haipeng Gu[4] and Yanqi Liu[4]

[1]Graduate School of Chengde Medical University, Chengde, Hebei, China, [2]Tangshan Nanhu Hospital, Department of Orthopedic, Tangshan, Hebei, China, [3]Hebei Key Laboratory of Panvascular Diseases, Affiliated Hospital of Chengde Medical University, Chengde, Hebei, China, [4]Department of Minimally Invasive Spine Surgery, Affiliated Hospital of Chengde Medical University, Chengde, Hebei, China

Introduction: Osteosarcoma (OS), a prevalent metastatic cancer among young individuals, is associated with a grim prognosis. Long non-coding RNAs (lncRNAs), including C1QTNF1-AS1, are pivotal regulators of cancer cell proliferation and motility. As an oncogene, C1QTNF1-AS1 is implicated in various tumor types, such as colorectal, pancreatic, hepatocellular carcinomas, and OS. The aim of this study was to investigate the functions and underlying mechanisms of C1QTNF1-AS1 in the progression of osteosarcoma.

Methods: This investigation focused on elucidating the functional roles and mechanisms of C1QTNF1-AS1 in OS cells. Bioinformatics tools were utilized to identify the interaction between microRNA miR-34a-5p and C1QTNF1-AS1, as well as the targeting of LDHA and PDK3 by miR-34a-5p. Dual-luciferase reporter assays and RNA immunoprecipitation were employed to validate these interactions. Expression profiles of C1QTNF1-AS1, miR-34a-5p, LDHA, and PDK3 in osteosarcoma cells were analyzed using RT-PCR and western blot analyses, revealing their intricate relationships. The impact of these molecules on OS cell proliferation, invasion, and migration was assessed through CCK-8, Transwell, and Cell scratch assay. Moreover, the effects on aerobic glycolysis in OS cells were examined by quantifying ATP levels, lactate production, glucose uptake capacity, and the extracellular acidification rate.

Results: The findings indicated a significant decrease in C1QTNF1-AS1 expression levels in OS cells compared to normal osteoblasts. A parallel downregulation trend of miR-34a-5p was also observed in OS cells. Silencing C1QTNF1-AS1 led to a marked upregulation of LDHA and PDK3 in OS cells, which was partially attenuated by miR-34a-5p mimics. Functional evaluations demonstrated that suppression of C1QTNF1-AS1 accelerated OS cell growth, motility, invasiveness, and the Warburg effect. Conversely, the overexpression of miR-34a-5p mitigated these stimulatory effects, suggesting a regulatory role in modulating OS progression.

Discussion: Our research emphasizes the critical role of C1QTNF1-AS1 in the pathogenesis of osteosarcoma (OS). We discovered that the downregulation of C1QTNF1-AS1 indirectly upregulates the expression of LDHA and PDK3 by

suppressing miR-34a-5p, which functions as a regulator of the Warburg effect. This cascade of events promotes OS progression by enhancing glycolytic metabolism and supplying energy for cancer cell growth, migration, and invasion. These findings suggest a potential therapeutic target and highlight the importance of understanding the regulatory network involving lncRNAs in cancer metabolism and progression.

KEYWORDS

OS, C1QTNF1-AS1, miR-34a-5p, LDHA, PDK3, Warburg effect

1 Introduction

Osteosarcoma, commonly abbreviated as OS, represents a highly aggressive form of connective tissue malignancy characterized by the capability of cancerous cells to produce bone and osteoid tissues (1). It is the leading primary malignancy affecting bone tissues. Posing significant challenges for treatment due to its aggressive nature and propensity for dissemination (2). OS continues to yield poor patient outcomes despite rigorous therapeutic interventions (3). Consequently, there is an urgent need to unravel the intricate molecular mechanisms underpinning OS development, identify novel biomarkers to facilitate early diagnosis, and explore innovative therapeutic strategies to address this formidable disease.

To elucidate the Warburg effect, it implies that cancer cells, under hypoxic conditions, favor lactate fermentation over oxidative phosphorylation for energy generation (4). This metabolic shift is marked by intensified glycolysis, augmented glucose consumption, escalated lactate excretion, and decreased oxygen utilization within tumor cells (5, 6). Extensive research has confirmed the manifestation of the Warburg effect in cancer cells, emphasizing its pivotal contribution to tumor progression and expansion. This phenomenon underscores the metabolic reprogramming of tumor cells, pivotal for their survival and aggressive growth.

PDK3, or pyruvate dehydrogenase kinase isoform 3, serves as a key regulator of intracellular energy metabolism, particularly within tumor cells (7). By inhibiting pyruvate dehydrogenase activity, PDK3 exerts a pronounced influence on the metabolic profile of cancer cells (8). This enzyme plays a central role in perpetuating the Warburg effect, a phenomenon intimately tied to energy metabolism and tumor cell vitality (9). Meanwhile, lactate dehydrogenase A (LDHA), a pivotal player in intracellular lactate dynamics, is intricately linked to both glycolysis and the Warburg effect (10). As a gene and enzyme implicated in glycolysis, LDHA facilitates the generation and accumulation of lactate, thereby bolstering cell survival and proliferation (11). This metabolic pathway is fundamental to cellular energy procurement and, as previous investigations have attested, is a hallmark of OS, underscoring its critical role in the disease.

Long non-coding RNAs (lncRNAs), comprising RNA molecules longer than 200 nucleotides without protein-coding capability, pervade the human genome (12). These transcripts exert substantial influence on the initiation, progression, and development of tumors, either bolstering or retarding these processes (13, 14). For example, FEZF1-AS1, through its interaction with miR-4443, modulates the NUPR1-axis, thereby fostering the development of OS (15). In breast cancer, augmented levels of C1QTNF1-AS1 perturb growth, invasion, and dissemination of cancer cells by regulating various signaling cascades, such as Wnt/β-catenin, PI3K/Akt, and NF-κB (16–19). Likewise, in lung cancer, high expression of C1QTNF1-AS1 orchestrates critical cellular functions, including proliferation, invasion, and angiogenesis, by targeting genes like EGFR, HIF-1α, and VEGF (20–22). However, the precise function of C1QTNF1-AS1 in OS remains an enigma, necessitating further investigation.

MicroRNAs (miRNAs), consisting of approximately 22 nucleotides, are single-stranded, non-coding RNAs that have garnered substantial research attention (23). miR-323a-3p, for instance, amplifies LDHA expression, thereby augmenting lactate generation and fostering metastatic and invasive capabilities in osteosarcoma (24). Conversely, miR-199b-3p retards the expansion of OS by targeting PDK1 (25). Notably, miR-34a-5p exhibits abnormal expression patterns in OS cells, and its levels are intimately tied to cellular responsiveness, tumor stage, lung metastasis potential, and patient prognosis (26, 27).

Competitive endogenous RNA (ceRNA) are RNA molecules that modulate gene expression by interacting with microRNA (miRNA) (28). This class includes various types such as mRNA, lncRNA, pseudogenes, and circRNA (29). The ceRNA mechanism centers on the "sponge effect," where these molecules bind to miRNA, preventing it from binding to and inhibiting target mRNAs (30, 31). This interaction is based on complementary sequences between ceRNA and miRNA targeting sites (32). The biological significance of ceRNA lies in its role within a gene regulatory network, where ceRNAs compete for miRNAs, creating a complex regulatory system (33). This discovery enhances our comprehension of RNA functions and gene regulation, offering insights into disease mechanisms.

Abbreviations: miR, microRNA; lncRNA, long noncoding RNA; OS, osteosarcoma; si, knockdown; mim, overexpression; LDHA, lactate dehydrogenase A; PDK3, also known as pyruvate dehydrogenase kinase isoform 3; NC, negative control; ceRNA, competing endogenous RNA.

The study unveiled intriguing findings regarding the roles of C1QTNF1-AS1 and miR-34a-5p in OS cells. Specifically, it was observed that both C1QTNF1-AS1 and miR-34a-5p exhibited reduced expression levels in OS cells compared to normal osteoblasts. Furthermore, silencing C1QTNF1-AS1 led to a marked enhancement in OS cell proliferation and the Warburg effect, a phenomenon wherein cancer cells preferentially utilize glycolysis for energy generation even in the presence of oxygen. Bioinformatics analysis illuminated a potential interaction between C1QTNF1-AS1 and miR-34a-5p, suggesting that they partially base pair. Moreover, it was hypothesized that LDHA and PDK3, enzymes implicated in glycolysis and energy metabolism, could be target genes of miR-34a-5p. This interaction was subsequently validated using dual-luciferase reporter assays. The study delved deeper into the underlying mechanisms by exploring whether suppressing C1QTNF1-AS1 indirectly elevated LDHA and PDK3 expression levels through downregulation of miR-34a-5p. This, in turn, was postulated to influence the Warburg effect and accelerate tumor progression.

The research provides valuable insights into the complex interplay between lncRNAs, miRNAs, and their target genes in modulating cancer cell behavior. By shedding light on the regulatory mechanisms governing glycolysis and energy metabolism in OS cells, this study opens new avenues for the development of targeted therapies aimed at disrupting these pathways and ultimately retarding tumor growth and progression.

2 Methods

2.1 Cell culture and reagents

Human osteosarcoma cell lines (including MG63, Saos-2, U2OS and HOS) and normal osteoblasts (HFOB1.19) were obtained from the ATCC Cell Bank located in Manassas, Virginia, USA. These cells were cultivated in Eagle's medium supplemented with 10% fetal bovine serum sourced from Thermo Fisher Scientific (Manassas, VA, USA), along with 0.1% penicillin and 0.1% streptomycin procured from Invitrogen (Carlsbad, CA, USA). All osteosarcoma cell lines were cultured at 37°C, whereas the HFOB1.19 cells were maintained at 34°C. All cells were incubated in an environment containing 5% carbon dioxide.

2.2 Bioinformatics analysis

The dataset GSE42352 originates from the Gene Expression Omnibus (GEO) database, which is accessible at http://www.ncbi.nlm.nih.gov/geo. The downloaded data comprised 84 disease samples and three healthy controls. The SangerBox platform (http://sangerbox.com) and the limma package (version 3.46.0, Linear Models for Microarray Data, from Bioconductor) were utilized to analyze the two sample groups.

2.3 Database analysis

Data pertaining to potential target genes of miR-34a-5p were acquired utilizing the online software tools TarBase (accessible at https://dianalab.e-ce.uth.gr), miRDB (located at https://mirdb.org), and TargetScan (found at https://www.targetscan.org). Analysis conducted with RNAhybrid and miRanda indicated that C1QTNF1-AS1 targets miR-34a-5p. Furthermore, predictions from TargetScan, miRanda, and miRWalk databases suggested that LDHA and PDK3 are potential targets of miR-34a-5p.

2.4 Real-time quantitative PCR

In accordance with the manufacturer's protocol, RNA extraction from osteosarcoma cell lines including MG63, Saos-2, U2OS and HOS was accomplished using the TRIzol reagent sourced from Thermo Fisher Scientific. Subsequently, the RNA samples were reverse transcribed into cDNA using the PrimeScript RT Kit provided by Takara. Gene expression levels were then quantified via qRT-PCR on an ABI7500 Quantitative PCR instrument from ABI Corporation, employing the SYBR Prex Ex Taq II Kit also from Takara. GAPDH served as the stable reference gene for normalization during the analysis.

2.5 Western blotting

Total protein extraction was carried out using RIPA buffer (Sigma) supplemented with a protease inhibitor from Roche. The extracted proteins were then resolved on a 12% SDS-PAGE gel. After electrophoresis, the proteins were transferred to membranes which were subsequently blocked with 5% skim milk for an hour. Overnight incubation with the primary antibody at 4°C was followed by rinsing the membranes with TBST. Subsequently, the membranes were incubated with secondary antibodies and washed again with TBST. Luminescence was detected using an ECL detection kit from Share-bio. For quantification, densitometric analysis of the immunoblotted proteins was conducted utilizing ImageJ software.

2.6 Cell count kit-8 test

Following transfection, U2OS and MG63 cells were plated in 96-well plates at a concentration of 3,000 cells per well. Each well received 10μL of CCK-8 solution (Dojindo Molecular Technologies) and was incubated at 37°C with 5% CO2 for 0, 24, and 48 hours. The optical density at 450 nm was then determined using a BioTek microplate reader. The findings reflect three separate trials.

2.7 Cell transfection

Cells with C1QTNF1-AS1 knockdown (si-lnc) and those with a negative control (si-NC) were produced. GenePharma (Shanghai, China) supplied the miR-34a-5p mimic (miR-mim) along with its control (miR-NC). Lipofectamine 3000 reagent (Invitrogen) was utilized for transfection, following the guidelines provided by the manufacturer.

2.8 Measurement of glucose metabolism, lactate production, and intracellular ATP levels

The rate of glucose metabolism was assessed using the colorimetric glucose uptake test kit provided by Sigma-Aldrich. The determination of intracellular ATP concentration was carried out according to the protocol provided by Promega Corporation (Madison, Wisconsin, USA), using their ATP Assay Kit. Fluorescence measurements of bioluminescence were taken using a fluorometer produced by Perkin Elmer located in Waltham, Massachusetts, USA. ATP levels were calculated based on the standard curve method. Furthermore, the extracellular lactate levels were measured utilizing a lactate assay kit sourced from BioVision (Zurich, Switzerland), in accordance with the manufacturer's protocol. All measurements were normalized to the cellular protein levels. The experiment was independently replicated three times.

2.9 Transwell assay

A matrix-coated 24-well span chamber (8μm aperture) was prepared for cell invasion assays. U2OS and MG63 cells were incubated in a serum-free medium in the upper chamber. The lower chamber received medium with 10% FBS. Following a 48-hour incubation period, the cells that had migrated to the lower chamber were treated with methanol and stained using a 0.1% crystal violet solution. The invading cells were examined using an Olympus inverted microscope.

2.10 Cell scratch assay

Cell scratch tests were utilized to evaluate the movement of OS cell lines. Once the U2OS and MG63 cells achieved 90% confluence in 24-well plates, a sterile plastic tip was used to scrape the monolayer, followed by two washes with phosphate-buffered saline (PBS) to eliminate cell debris. The cells were then incubated in complete growth medium. Ultimately, the cells that moved to the damaged region were gathered at 0 and 24 hours following the initial scratch and examined using an inverted microscope (Olympus) for each injury. The relative distances of the cell scratches were analyzed using ImageJ software.

2.11 Dual-luciferase activity measurement

A dual-luciferase reporter assay was conducted by inserting either wild-type or mutant lncRNA-C1QTNF1-AS1/LDHA/PDK3 into the pmirGLO vector (Universal Biotech, China). MG63 cells were planted in 48-well plates at a concentration of 5×104 cells per well. For 48 hours, the luciferase reporter plasmid along with miR-34a-5p mimic or mimic-NC were introduced using Liposome 3000 (Invitrogen). The activities of firefly and Renilla luciferase were evaluated using a dual-luciferase reporter assay kit from Promega, USA. The activity of Firefly luciferase was adjusted relative to that of Renilla luciferase. Every test was conducted three times.

2.12 Measurement of glycolysis

The extracellular acidification rate (ECAR) of cultured cells was measured using an XF96 metabolic flux analyzer from Seahorse Biosciences, located in Billerica, MA, USA, in accordance with the manufacturer's instructions. Briefly, 80 μL of a suspension containing 3 × 10^4 target cells were dispensed into each well of an XF96 96-well plate provided by Seahorse Biosciences and incubated overnight at 37°C. The XF sensor box, manufactured by Seahorse Bioscience, was prepared with XF calibration solution and left to incubate overnight at 37°C, without the addition of CO2. On the subsequent day, the standard medium was replaced with XF assay-adapted DMEM (containing 1 g/mL glucose, pH 7.4; sourced from Seahorse Biosciences), and the cells were further incubated for an hour at 37°C in a CO2-free environment. Sequential additions of 10 mM glucose, 1 mM oligomycin (provided by Sigma-Aldrich), and 80 mM 2-deoxyglucose (D8375; Sigma-Aldrich) were made to assess ECAR. The obtained data were analyzed using XFe Wave software, also provided by Seahorse Biosciences.

2.13 RNA immunoprecipitation assay

This study employed the RIP Kit manufactured by Bersinbio Company (Guangzhou, China), adhering strictly to the manufacturer's operating instructions, to assess the interactions among LDHA, PDK3, miR-34a-5p, and the AGO2 protein. During the experimental procedure, cells subjected to oxidative stress were initially washed with phosphate-buffered saline (PBS). Following this, cell lysis was conducted in RIP buffer supplemented with proteasome inhibitors. The resultant lysate was then co-incubated overnight with antibodies specifically targeting the AGO2 protein or with control IgG antibodies, to facilitate the formation of RNA-protein complexes. Subsequently, these complexes were bound to protein A/G magnetic beads and subjected to proteinase K treatment to eliminate the protein components. Ultimately, the purified RNA was analyzed using qRT-PCR.

2.14 Statistical analysis

Data were analyzed and graphed using GraphPad Prism 9 (version 9.4.0). Data are presented as mean ± standard deviation, and group differences were analyzed using the t-test Or the One-way test. A p-value of less than 0.05 was considered statistically significant.

3 Results

3.1 C1QTNF1-AS1 expression was significantly downregulated in OS cells

The SangerBox platform was utilized to analyze gene expression profiles from the GSE42352 dataset on GEO, aiming to pinpoint genes with differential expression in OS cells. Differentially expressed genes between OS cells and normal osteoblasts were identified using the limma package (log FC > 1 and $p < 0.05$) and volcano and heatmap

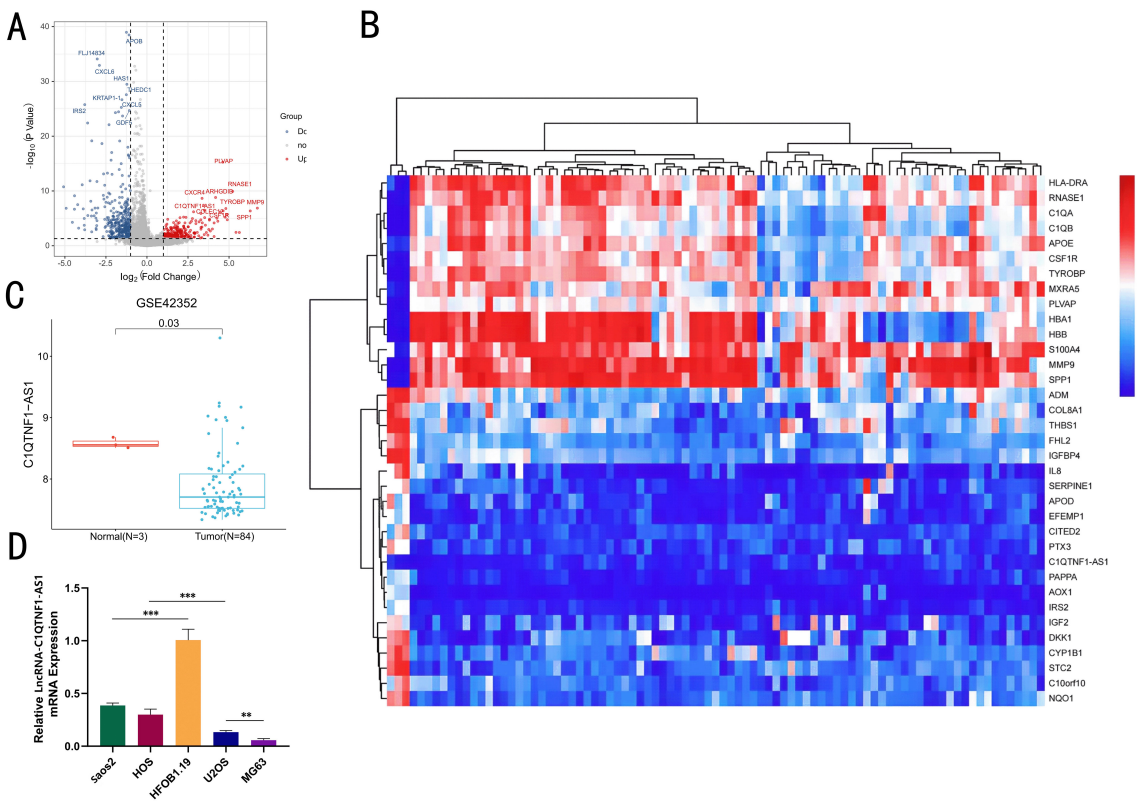

FIGURE 1
The levels of LncRNA-C1QTNF1-AS1 are reduced in OS. A volcano plot showcasing the LncRNA with differential expression in GEO datasets **(A)**. A heatmap illustrating the variably expressed LncRNA in GSE42352, sourced from the GEO database **(B)**. Expression of LncRNA C1QTNF1-AS1 in normal cells and OS cells of dataset **(C)**. Quantitative real-time PCR **(D)** was employed to measure the levels of LncRNA-C1QTNF1-AS1 in U2OS, Saos2, MG63, and HOS cells compared to hFOB1.19 cells. Results are shown as average ± standard deviation. **P<0.01, ***P<0.001.

plots were prepared in The R Project for Statistical Computing (R version 4.4.0) (Figures 1A, B). Among these differentially expressed genes, C1QTNF1-AS1 was significantly downregulated in OS cells compared to that in normal osteoblasts (Figure 1C). Initially, we assessed the expression levels of C1QTNF1-AS1 in both osteoblasts (HFOB 1.19) and various osteosarcoma cell lines (Saos2, MG63, HOS, and U2OS) through qRT-PCR analysis. The findings indicated that C1QTNF1-AS1 expression was notably reduced in osteosarcoma cell lines relative to normal human osteogenic cell lines, with a marked decrease observed in MG63 and U2OS cell lines (Figure 1D).

3.2 Silencing of C1QTNF1-AS1 significantly promoted OS cell development and the Warburg effect *in vitro*

To investigate the precise role of C1QTNF1-AS1 in osteosarcoma cells, we created a cell line with C1QTNF1-AS1 knocked down (si-lnc) and a corresponding negative control (si-NC). The results of the CCK-8 proliferation assay (Figure 2A), cell scratch tests (Figures 2B, C), along with the Transwell experiment (Figures 2D, E) demonstrated that reducing C1QTNF1-AS1 levels enhanced the growth, movement, and invasive capabilities of MG63 and U2OS cells. The Warburg effect is essential for tumor progression and aids in the proliferation of cancer cells. We investigated the potential correlation between C1QTNF1-AS1 and the Warburg effect in the development of osteosarcoma (OS) by examining glucose levels, ATP production, and lactate production in the supernatants of OS cell cultures. To ascertain whether the silencing of C1QTNF1-AS1 contributes to the regulation of aerobic glycolysis, we utilized a metabolic flux analyzer to measure extracellular acidification rates (ECAR). Our research revealed that the silencing of C1QTNF1-AS1 led to a substantial increase in ATP production (Figure 2F) and lactate production (Figure 2G) in MG63 and U2OS cells. Simultaneously, it notably decreased the glucose levels in the supernatants of these cells (Figure 2H), indicating that the cells consumed more glucose. Furthermore, we found that the knockdown of C1QTNF1-AS1 resulted in enhanced glycolysis levels in U2OS and MG63 cells (Figure 2I). Taken together, these data suggest that the silencing of C1QTNF1-AS1 promotes aerobic glycolysis in OS cells.

3.3 miR-34a-5p was identified as a direct target of C1QTNF1-AS1 and showed consistent expression trends in OS cells

In order to investigate how C1QTNF1-AS1 influences aerobic glycolysis in OS, we employed three gene prediction tools—

10.3389/fonc.2024.1485605

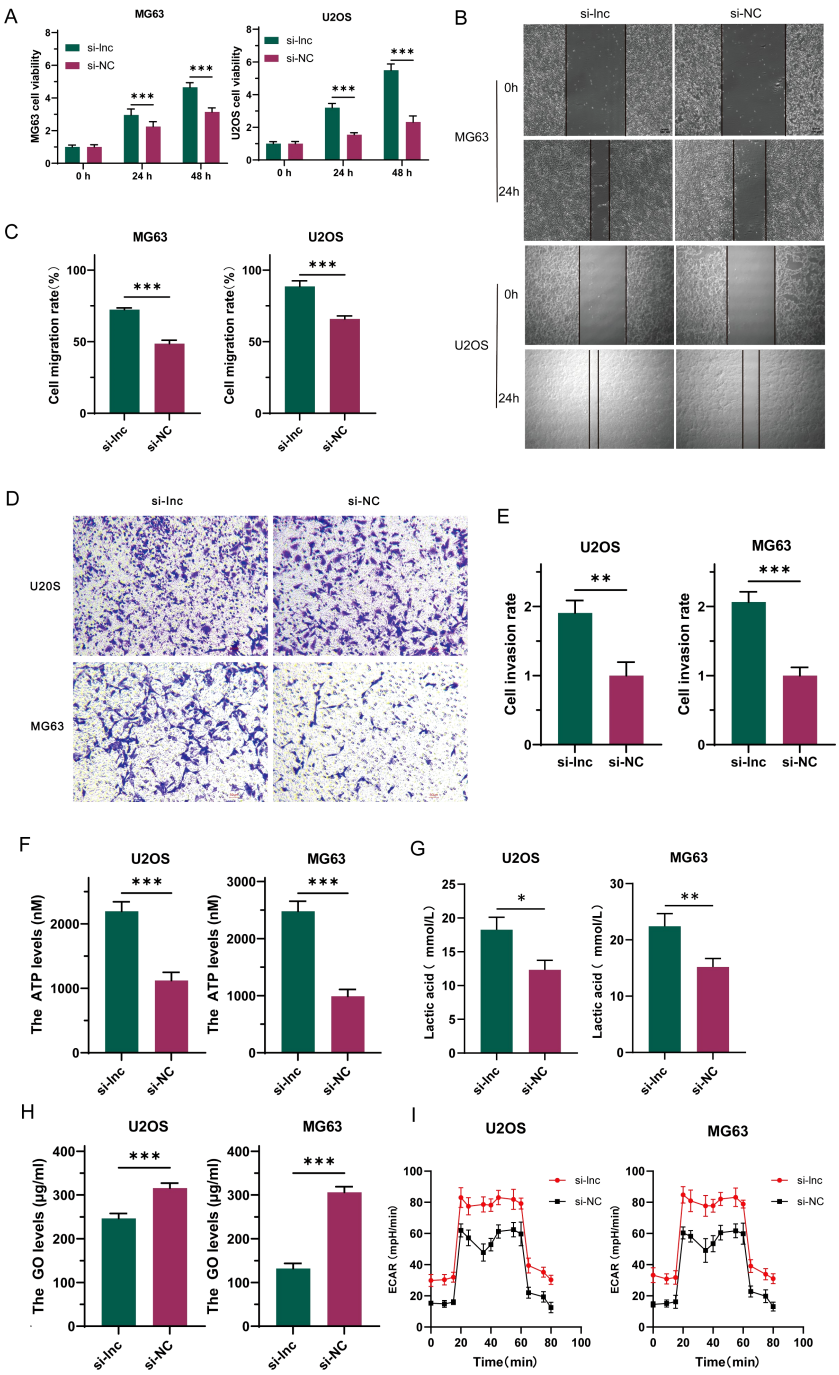

FIGURE 2
LncRNA-C1QTNF1-AS1 exhibits inhibitory effects on the progression of osteosarcoma (OS) in laboratory conditions. The CCK-8 assay was utilized to evaluate the growth rate of OS cells following the inhibition of C1QTNF1-AS1 **(A)**. The migration capability of cells after C1QTNF1-AS1 knockdown was assessed through a cell scratch assay **(B, C)**. The invasive potential post-inhibition of C1QTNF1-AS1 was further examined using a Transwell assay **(D, E)**. To gain insights into the metabolic alterations, ATP **(F)** and lactate production levels **(G)** in C1QTNF1-AS1 knockdown cells were measured using respective assays, while glucose concentrations in cell supernatants were determined via a glucose assay **(H)**. To definitively determine the impact of C1QTNF1-AS1 silencing on glycolysis rates, the extracellular acidification rate (ECAR) was assessed using a metabolic flux analyzer **(I)**. Results are shown as average ± standard deviation. *P<0.05, **P<0.01, ***P<0.001.

TarBase, miRDB, and TargetScan—to identify mRNA candidates targeted by C1QTNF1-AS1.Intersection of the three databases revealed that only miR-34a-5p was associated with aerobic glycolysis (Figure 3A). The binding site of C1QTNF1-AS1 to miR-34a-5p was predicted using the RNAhybrid and miRanda algorithms, and a mutated sequence, mut, was designed. The dual-luciferase assay results showed that the miR-34a-5p mimic could bind to C1QTNF1-AS1 wild-type to increase luciferase activity compared to the expression of the NC mimic. Nonetheless, altering the binding site resulted in the miR-34a-5p

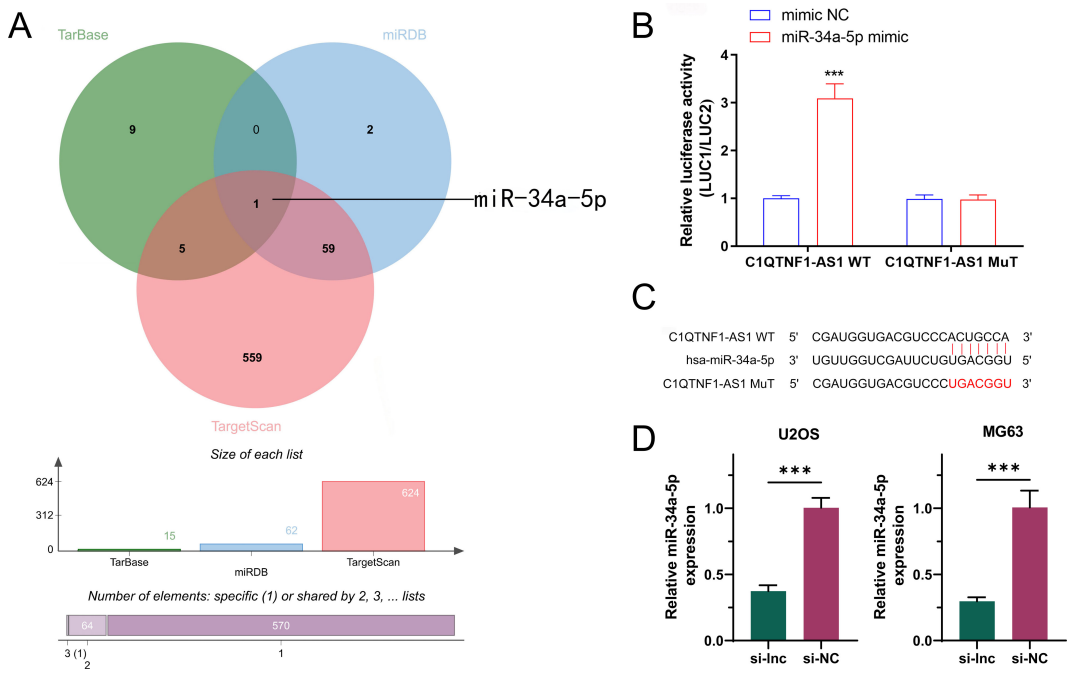

FIGURE 3
miR-34a-5p is an authentic target of LncRNA-C1QTNF1-AS1.A Venn diagram illustrating the anticipated glycolysis-associated target genes of lncRNA C1QTNF1-AS1, derived from the TarBase miRDB, and TargetScan databases **(A)**. Dual-luciferase reporter experiments were conducted on OS cells transfected with either miR-34a-5p UTR wild-type (WT) or mutant (MUT) forms, alongside lncRNA C1QTNF1-AS1 plasmid or a control plasmid **(B)**. miR-34a-5p 3′-UTR contains one predicted LncRNA C1QTNF1-AS1 binding site **(C)**. Expression levels of miR-34a-5p in OS cells after transfection with either a negative control or a C1QTNF1-AS1 knockdown plasmid **(D)**. Results are shown as the average ± standard deviation. Results are shown as average ± standard deviation. ***P<0.001.

mimic showing no notable impact on luciferase activity (Figure 3B). This suggested that miR-34a-5p attaches to C1QTNF1-AS1 at this location (Figure 3C). In order to investigate the connection between C1QTNF1-AS1 and miR-34a-5p in osteosarcoma cells, we created a stable cell line (si-lnc) and a negative control (si-NC). The qRT-PCR analysis indicated that miR-34a-5p levels in osteosarcoma cells decreased following the silencing of C1QTNF1-AS1 (Figure 3D).

3.4 miR-34a-5p suppressed the growth and progression of OS cells by modulating the Warburg effect

To explore the function of miR-34a-5p in osteosarcoma, this study constructed stable cell lines overexpressing miR (miR-mim) and negative controls (mim-NC) and performed CCK-8 proliferation assays. The results showed that increased expression levels of miR-34a-5p inhibited the growth of OS cells (Figure 4A). Transwell assay results indicated that elevated miR-34a-5p expression levels suppressed the invasion of OS cells (Figures 4B, C). Scratch assays demonstrated that overexpression of miR-34a-5p inhibited the migration of OS cells (Figures 4D, E). This study found that the overexpression of miR-34a-5p significantly reduced ATP production (Figure 4F) and lactate production (Figure 4G) in MG63 and U2OS cell lines, while significantly increasing the glucose level in the cell supernatant (Figure 4H). This indicated a reduction in glucose consumption by osteosarcoma cells. Metabolic flux analysis revealed that the overexpression of miR-34a-5p significantly decreased the extracellular acidification rate (ECAR) (Figure 4I) in both MG63 and U2OS cell lines, thereby inhibiting the Warburg effect. In summary, miR-34a-5p inhibited the proliferation, migration, and invasion of osteosarcoma cells, as well as aerobic glycolysis.

3.5 Silencing of C1QTNF1-AS1 promoted OS progression through miR-34-a-5p–mediated glycolysis

To deeply explore whether C1QTNF1-AS1 inhibits the development and progression of osteosarcoma cells by targeting miR-34a-5p, this study selected U2OS and MG63 cell lines for rescue experiments. By comparing the data from CCK-8 assays (Figure 5A), Transwell assays (Figures 5B, C), and cell scratch assays (Figures 5D, E), it was found that knockdown of C1QTNF1-AS1 significantly promoted the proliferation, migration, and invasion abilities of osteosarcoma cells, while the overexpression of miR-34a-5p partially reversed this effect. Similarly, the elevation of miR-34a-5p levels partially alleviated the impact of C1QTNF1-AS1 inhibition on the Warburg effect of osteosarcoma cells. Further confirmation of this effect was provided by measuring ATP production (Figure 5F), lactate production (Figure 5G), glucose consumption (Figure 5H), and ECAR (Figure 5I). Based on these results, this study revealed that inhibiting C1QTNF1-AS1 enhances the proliferation, migration, and invasion abilities of osteosarcoma cells by blocking the glycolysis driven by miR-34a-5p.

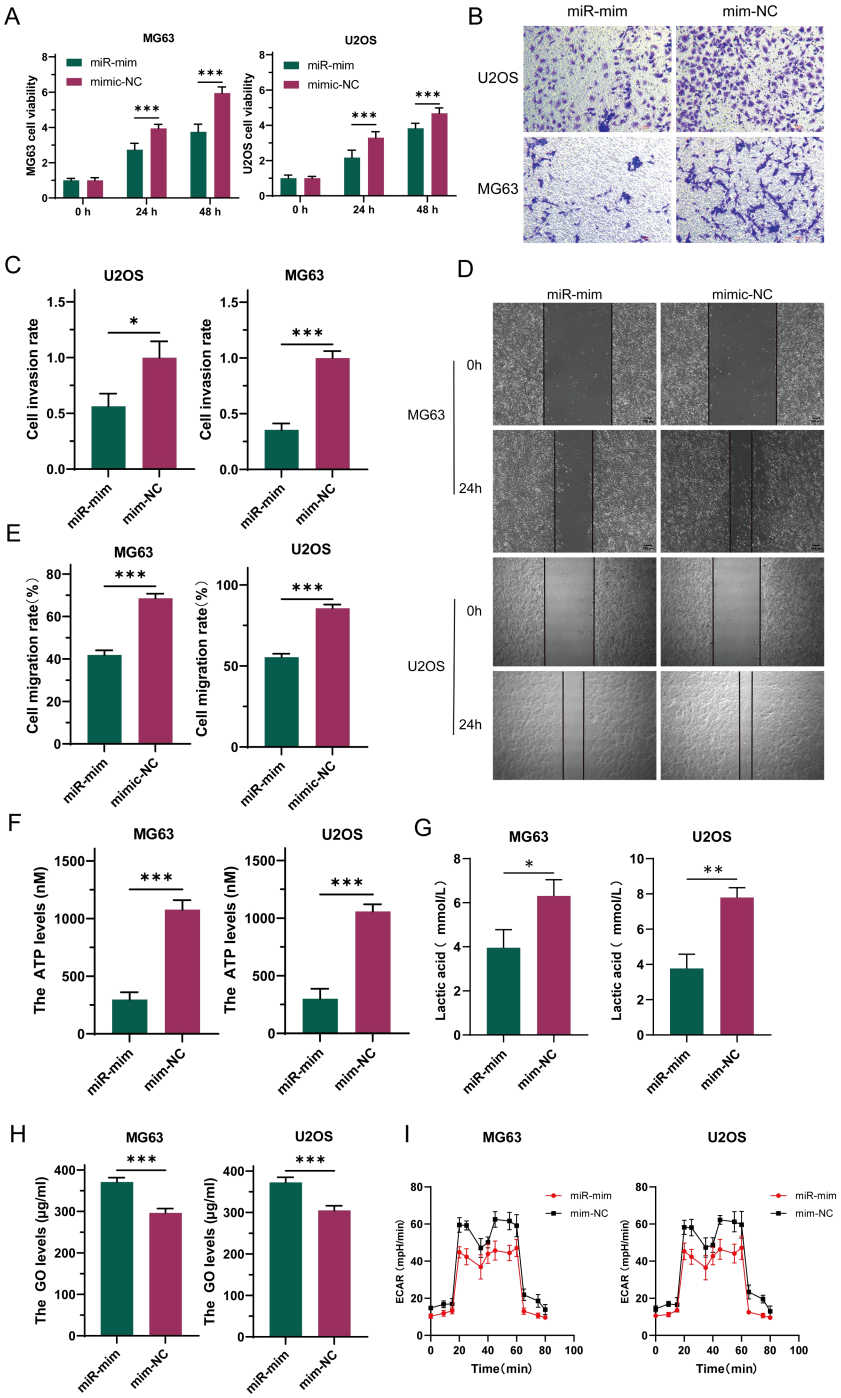

FIGURE 4
Under laboratory conditions, miR-34a-5p has been demonstrated to inhibit the progression of osteosarcoma (OS). To investigate this, the proliferation rate of OS cells was assessed following miR-34a-5p overexpression using CCK-8 assays **(A)**. Furthermore, the invasive potential of these cells with miR-34a-5p overexpression was evaluated through Transwell experiments **(B, C)**. To determine the effect of miR-34a-5p overexpression on cell migration, scratch assays were conducted on the cells **(D, E)**. Additionally, to assess the production of ATP and lactate in cells overexpressing miR-34a-5p, ATP levels **(F)**, lactate levels **(G)**, and glucose content in the cell supernatant **(H)** were measured using appropriate assays. Moreover, ECAR detection was performed to evaluate the glycolytic rate of the cells after miR-34a-5p overexpression **(I)**. Results are shown as average ± standard deviation. *P<0.05, **P<0.01, ***P<0.001.

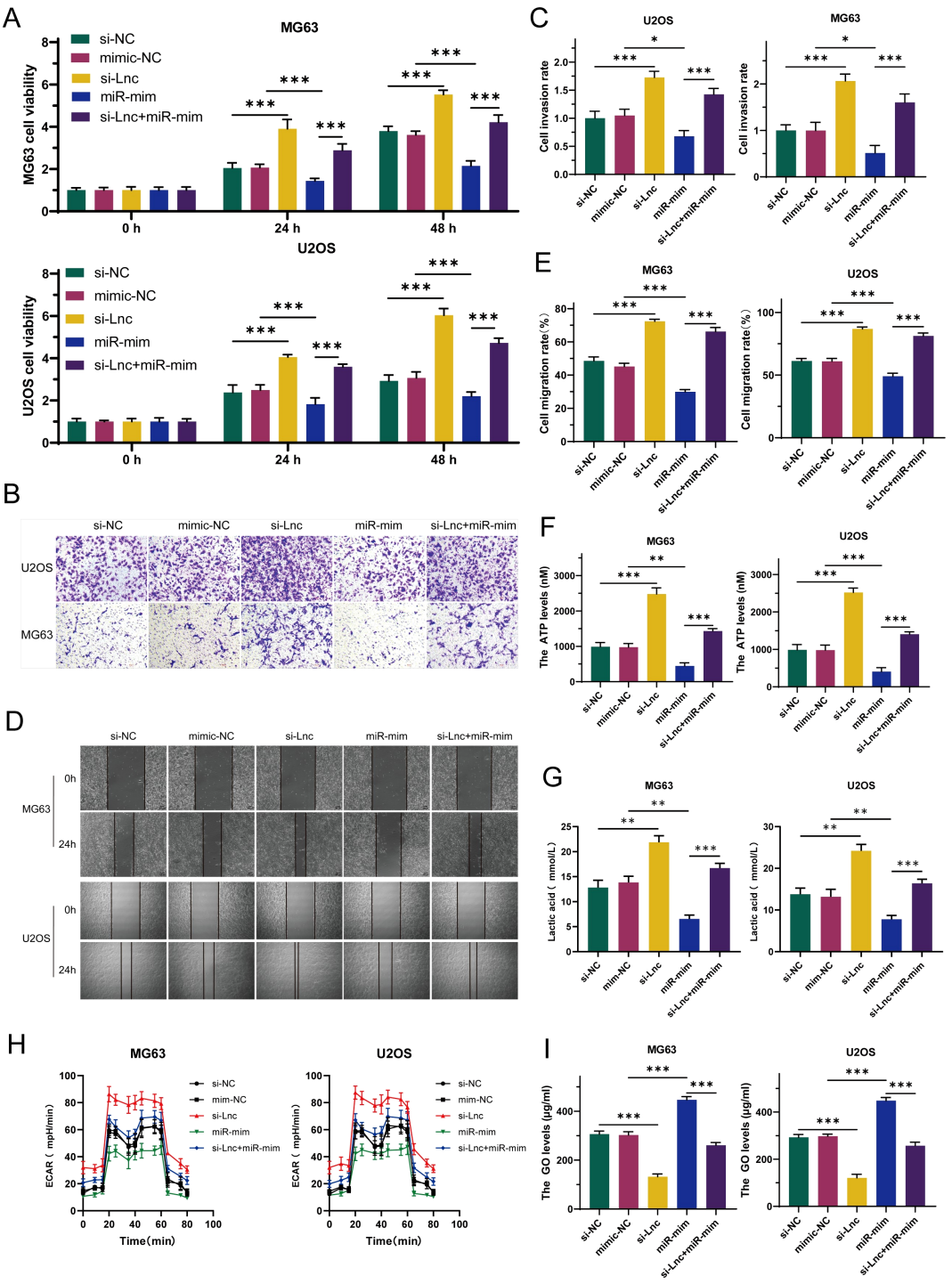

FIGURE 5
Elevated levels of miR-34a-5p partially restore the oncogenic role suppressed by the downregulation of C1QTNF1-AS1 in osteosarcoma. CCK-8 tests **(A)**, Transwell assays **(B, C)**, and cell scratch tests **(D, E)** demonstrate that the overexpression of miR-34a-5p somewhat counteracts the enhancement of OS cell proliferation, invasion, and migration induced by the knockdown of C1QTNF1-AS1. Furthermore, assessments of ATP levels **(F)**, lactate production **(G)**, glucose consumption **(H)**, and ECAR **(I)** indicate that the overexpression of miR-34a-5p also somewhat mitigates the impact of C1QTNF1-AS1 silencing on the Warburg effect in osteosarcoma cells. Results are shown as average ± standard deviation. *P<0.05, **P<0.01, ***P<0.001.

3.6 LDHA and PDK3 were identified as direct targets of miR-34a-5p and showed opposite expression trends in OS cells

The binding sites for LDHA, PDK3, and miR-34a-5p were predicted utilizing the TargetScan, miRanda, and miRWalk algorithms, and a mutated sequence (mut) was subsequently designed. The dual-luciferase assay revealed that the miR-34a-5p mimic attached to both wild-type LDHA and PDK3, resulting in a reduction in luciferase activity compared to the NC mimic expression. However, mutating the binding site rendered the miR-34a-5p mimic ineffective in altering luciferase activity (Figures 6A, B). These findings demonstrated that miR-34a-5p binds to LDHA and PDK3 at the predicted sites (Figures 6C, D). Furthermore, stable cell lines overexpressing miR-34a-5p (miR-mim) and a negative control (mim-NC) were established. The qRT-PCR analysis results indicated that the expression levels of both PDK3 and LDHA were significantly downregulated in osteosarcoma cells following the overexpression of miR-34a-5p (Figure 6E). Western blot analysis further confirmed this observation, demonstrating a significant decrease in the protein expression of PDK3 and LDHA in osteosarcoma cells due to the overexpression of miR-34a-5p (Figures 6F, G). RNA immunoprecipitation (RIP) experiments revealed that the enrichment levels of LDHA and PDK3 were significantly increased in the group overexpressing miR-34a-5p and targeting Argonaute2 (Ago2) (Figures 6H, I). These experimental data collectively demonstrated that miR-34a-5p inhibited the expression of LDHA and PDK3 by directly interacting with their 3′ untranslated regions (3′UTR).

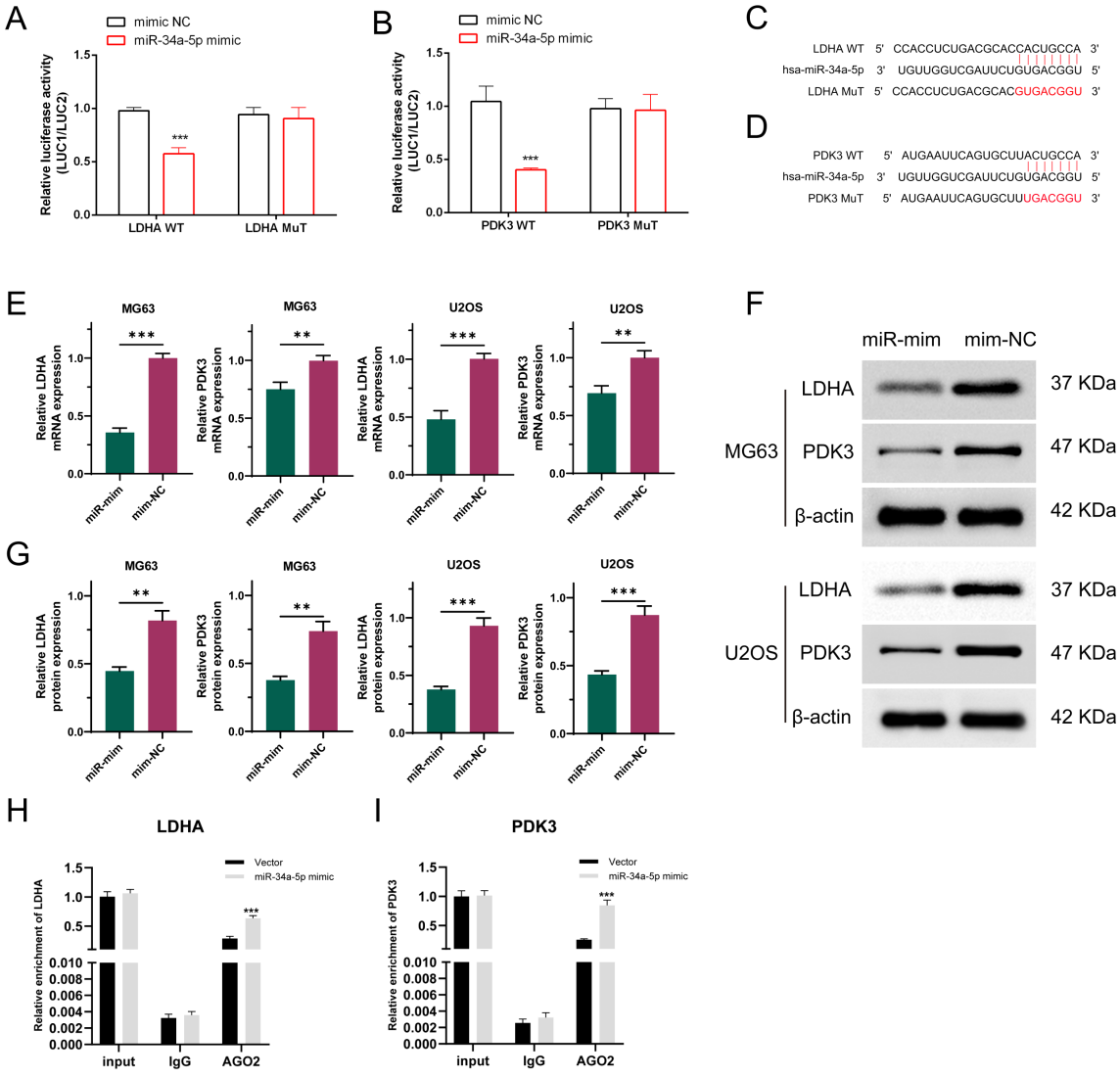

FIGURE 6
LDHA and PDK3 are authentic targets of miR-34a-5p. Dual-luciferase reporter experiments were conducted on OS cells transfected with either wild-type or mutant LDHA and PDK3 UTR, alongside miR-34a-5p plasmid or a control plasmid **(A, B)**. The 3′-UTRs of LDHA and PDK3 both have a predicted binding site for miR-34a-5p **(C, D)**. As demonstrated by qRT-PCR **(E)** and Western blot analyses **(F, G)**, the expression levels of LDHA and PDK3 were assessed in osteosarcoma cells transfected with either a negative control plasmid or a plasmid overexpressing miR-34a-5p. RIP experiments were conducted using MG63 cell lysates with AGO2 or IgG antibodies. qRT-PCR results showed the relative enrichment of LDHA and PDK3 mRNA in cells transfected with miR-34a-5p mimics compared to those transfected with NC mimics **(H, I)**. Results are shown as average ± standard deviation. **P<0.01, ***P<0.001.

3.7 Silencing of C1QTNF1-AS1 upregulates LDHA and PDK3 expression in OS cells through inhibition of miR-34a-5p

To explore the interactions between C1QTNF1-AS1, miR-34a-5p, LDHA, and PDK3 in OS cells, we constructed C1QTNF1-AS1 knockdown stable cell lines (si-lnc) and miR-34a-5p overexpression stable cell lines (miR-mim). As demonstrated by qRT-PCR (Figure 7A) and Western blot analyses (Figures 7B, C), the suppression of C1QTNF1-AS1 in OS cells led to a notable rise in LDHA and PDK3 levels. As demonstrated by qRT-PCR (Figure 7D) and Western blot analyses (Figures 7E, F), our rescue experiments revealed that elevating miR-34a-5p levels partially mitigated the enhancement induced by LDHA and PDK3 following the knockdown of C1QTNF1-AS1.

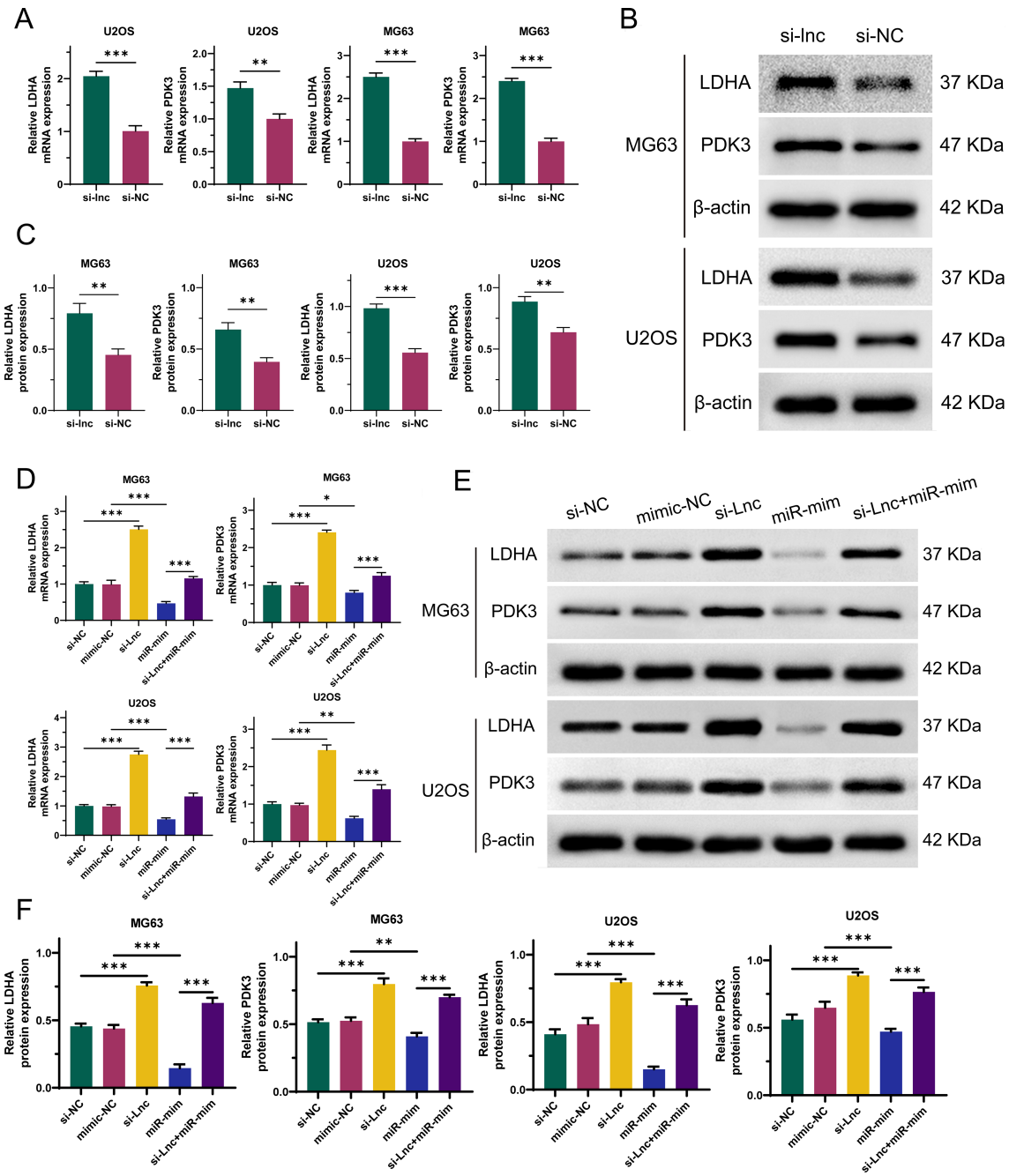

FIGURE 7
Silencing of C1QTNF1-AS1 upregulates the expression of LDHA and PDK3 in osteosarcoma (OS) cells by inhibiting miR-34a-5p. The altered expression levels of LDHA and PDK3 in OS cells subsequent to C1QTNF1-AS1 silencing are demonstrated through qRT-PCR **(A)** and Western blot analysis **(B, C)**. As illustrated by qRT-PCR **(D)** and Western blot analysis **(E, F)**, overexpression of miR-34a-5p partially reverses the enhanced expression of LDHA and PDK3 that is observed following the knockdown of C1QTNF1-AS1. Results are shown as average ± standard deviation. *P<0.05, **P<0.01, ***P<0.001.

4 Discussion

OS, a common form of primary bone malignancy encountered in clinical practice, predominantly strikes adolescents and children and boasts the highest incidence rate among its kind. Characterized by rapid progression and a high tendency for metastasis (34). OS is considered a highly aggressive cancer. In the realm of cancer development, long non-coding RNAs (lncRNAs) occupy a pivotal position (35). This particular study delves into the functional roles and underlying mechanisms of the lncRNA, C1QTNF1-AS1, in the context of osteosarcoma. The findings of this investigation reveal that the inhibition or silencing of C1QTNF1-AS1 leads to an upregulation of LDHA and PDK3 expressions, a phenomenon mediated through the sequestration of miR-34a-5p. This observation underscores the intricate interplay between various regulatory elements within the cancer cell landscape.

The provided text discusses the role of C1QTNF1-AS1 in various types of cancer, including OS. It highlights that C1QTNF1-AS1 expression is reduced in certain cancer cells and that it inhibits multiple types of cancer by affecting proliferation, invasion, epithelial-mesenchymal transition, and apoptosis induction (36, 37). Additionally, C1QTNF1-AS1 counteracts the Warburg effect in hepatocellular carcinoma (38). The study confirms the function of C1QTNF1-AS1 in OS cells, showing that silencing C1QTNF1-AS1 promotes proliferation, migration, invasion, and the Warburg effect in OS cells. Overall, the findings indicate that C1QTNF1-AS1 is essential in the advancement of OS.

miR-34a-5p inhibits Thyroid cancer progression by restricting cell growth and spread and also hampers Head and neck squamous cell carcinoma development by targeting Flotillin-2 (39). In this research, miR-34a-5p was identified as a target of C1QTNF1-AS1, confirmed through dual-luciferase reporter tests. Our analysis revealed a significant association between the levels of miR-34a-5p and C1QTNF1-AS1 in OS cells. Functional assays confirmed that miR-34a-5p overexpression suppresses cell growth, movement, invasion, and the Warburg effect in OS cells. Rescue experiments showed that silencing C1QTNF1-AS1 led to increased OS cell growth, invasion, migration, and the Warburg effect by sequestering miR-34a-5p. These data indicate that C1QTNF1-AS1 regulates OS progression by adsorbing miR-34a-5p.

The Warburg effect plays a pivotal role in fostering the growth and progression of malignant tumors (40). This effect reveals a biological phenomenon wherein, despite ample oxygen availability, osteosarcoma cells preferentially obtain energy through glycolysis rather than through the normal oxidative phosphorylation pathway (41). This metabolic pattern not only provides the necessary energy and biosynthetic precursors for rapid tumor cell proliferation but may

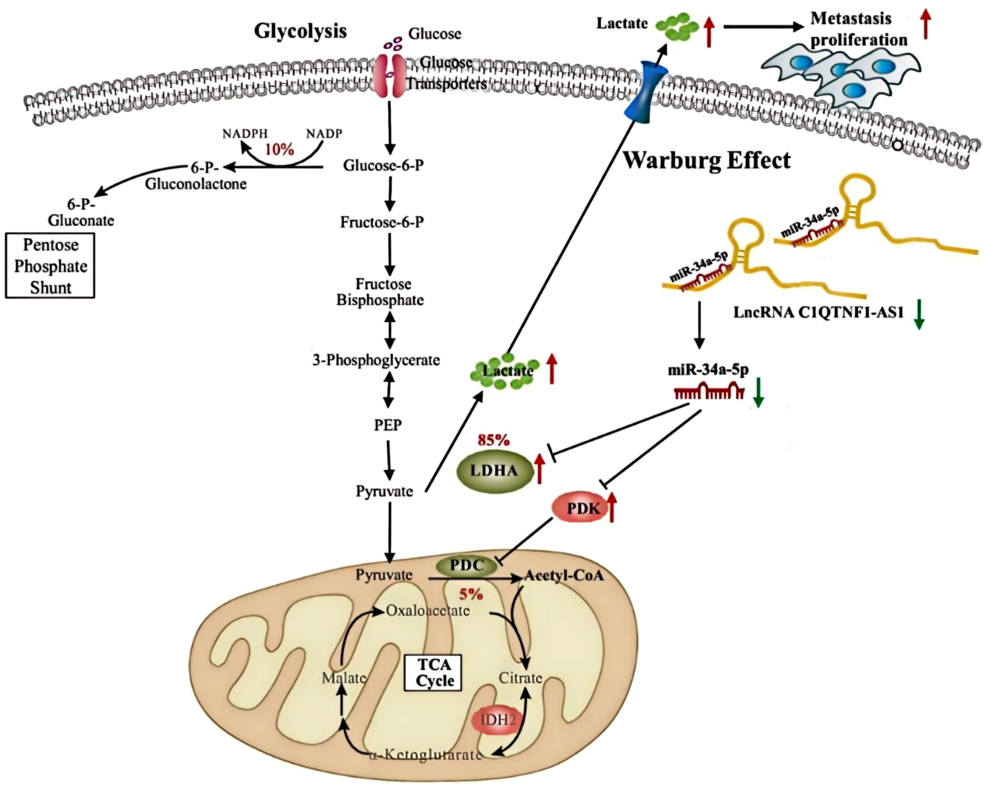

FIGURE 8
Silent lncRNA-C1QTNF1-AS1 promotes the expression of LDHA and PDK3 by adsorbing miR-34a-5p, indirectly regulating the Warburg effect and facilitating tumor development.

also promote tumor invasion and metastasis by altering the tumor microenvironment (42). The presence of the Warburg effect offers new avenues for osteosarcoma treatment. Firstly, researchers can target key enzymes in the glycolytic pathway, such as hexokinase and lactate dehydrogenase, to develop specific inhibitors. These inhibitors can effectively suppress the energy metabolism of tumor cells, thereby inhibiting their growth (43). Secondly, by exacerbating mitochondrial dysfunction and promoting mitochondria-mediated apoptosis, the survival capacity of tumor cells can be further compromised (44). Additionally, intervention in the Warburg effect may synergize with existing chemotherapeutic agents, enhancing the sensitivity of tumor cells to drugs and thus intensifying the efficacy of chemotherapy (45). The development of these therapeutic strategies not only promises to improve the survival rates of osteosarcoma patients but may also enhance their quality of life. Through in-depth investigation of the relationship between the Warburg effect and osteosarcoma, scientists are progressively unveiling the mechanisms of aberrant tumor metabolism, laying a solid foundation for future personalized and precision medicine approaches. With ongoing research, there is good reason to believe that further breakthroughs in the field of osteosarcoma treatment will be achieved, offering more hope and possibilities for patients.

Notably, lactate dehydrogenase A (LDHA), a pivotal enzyme in the final phase of this metabolic shift, is prevalent in multiple cancer cells and is intimately linked to tumor dimensions and clinical outcomes (46, 47). Pyruvate dehydrogenase kinase (PDK), with its four isoforms, contributes significantly to the emergence of the Warburg effect and balances glycolysis with oxidative phosphorylation (48, 49). Our study pinpointed LDHA and PDK3 as direct targets of microRNA-34a-5p (miR-34a-5p), validated through dual-luciferase reporter assays and RNA immunoprecipitation. Additionally, analyzing the expression patterns of C1QTNF1-AS1, miR-34a-5p, LDHA, and PDK3 in OS cells, along with rescue experiments, revealed that the silencing of C1QTNF1-AS1 upregulates LDHA and PDK3 levels in OS cells by sequestering miR-34a-5p.

In summary, this study elucidates the potential biomarker value of C1QTNF1-AS1 and miR-34a-5p in the early diagnosis of osteosarcoma. By quantitatively analyzing the expression levels of these two molecules in patients, early identification and diagnosis of osteosarcoma can be achieved, thereby facilitating timely and effective therapeutic interventions aimed at improving patient survival rates. Furthermore, the study reveals the unique metabolic characteristics of osteosarcoma cells, namely the Warburg effect. This research provides a novel perspective for the formulation of treatment strategies: 1. The restoration or enhancement of miR-34a-5p function can effectively inhibit the proliferation and invasiveness of osteosarcoma cells, and by modulating the expression of enzymes such as LDHA and PDK3, the metabolic profile of osteosarcoma cells can be altered. This lays the theoretical groundwork for the development of miR-34a-5p-targeted therapeutic approaches, potentially representing a novel method for treating osteosarcoma. 2. Suppressing the expression of LDHA and PDK3 *in vivo* can disrupt the metabolic pathways of osteosarcoma cells, thereby inhibiting their proliferation and invasiveness. This provides a basis for the development of targeted drugs against LDHA and PDK3. 3. Combining miR-34a-5p-targeted therapies with current conventional treatments for osteosarcoma may yield superior therapeutic outcomes. By restoring miR-34a-5p function or inhibiting LDHA and PDK3 activity, patient sensitivity to chemotherapy or radiotherapy can be enhanced, thus improving treatment efficacy and reducing side effects. In summary, this study offers new biomarkers for clinical diagnosis through an in-depth exploration of the mechanisms of action of C1QTNF1-AS1 and miR-34a-5p within osteosarcoma cells, reveals the metabolic characteristics of osteosarcoma, and provides new targets for treatment strategies as well as theoretical support for combination therapy. These findings offer novel insights and approaches for the clinical practice and treatment of osteosarcoma, promising better therapeutic outcomes and quality of life for patients with this condition.

The mechanism diagram of this study can be found in Figure 8.

Data availability statement

The datasets presented in this study can be found in online repositories. The names of the repository/repositories and accession number(s) can be found in the article/Supplementary Material.

Author contributions

YZ: Writing – original draft, Writing – review & editing. HL: Writing – review & editing. NZ: Validation, Writing – review & editing. NY: Data curation, Supervision, Writing – review & editing. KD: Writing – review & editing. BC: Supervision, Validation, Writing – review & editing. CC: Data curation, Writing – review & editing. HG: Formal Analysis, Writing – review & editing. YL: Methodology, Writing – review & editing.

Funding

The author(s) declare financial support was received for the research, authorship, and/or publication of this article. This study was supported by Hebei Natural Science Foundation (H2022406038).

Acknowledgments

We thank all the teachers at the Central Laboratory of the Affiliated Hospital of Chengde Medical College for their contributions to this study.

Conflict of interest

The authors declare that the research was conducted in the absence of any commercial or financial relationships that could be construed as a potential conflict of interest.

Publisher's note

All claims expressed in this article are solely those of the authors and do not necessarily represent those of their affiliated organizations, or those of the publisher, the editors and the reviewers. Any product that may be evaluated in this article, or claim that may be made by its manufacturer, is not guaranteed or endorsed by the publisher.

Supplementary material

The Supplementary Material for this article can be found online at: https://www.frontiersin.org/articles/10.3389/fonc.2024.1485605/full#supplementary-material

References

1. Yu X, Duan W, Wu F, Yang D, Wang X, Wu J, et al. LncRNA-HOTAIRM1 promotes aerobic glycolysis and proliferation in osteosarcoma via the miR-664b-3p/Rheb/mTOR pathway. *Cancer Sci*. (2023) 114:3537–52. doi: 10.1111/cas.v114.9

2. Zheng C, Li R, Zheng S, Fang H, Xu M, Zhong L, et al. The knockdown of lncRNA DLGAP1-AS2 suppresses osteosarcoma progression by inhibiting aerobic glycolysis via the miR-451a/HK2 axis. *Cancer Sci*. (2023) 114:4747–62. doi: 10.1111/cas.v114.12

3. Zhu Y, Yang L, Yu Y, Xiong Y, Xiao P, Fu X, et al. Hydroxysafflor yellow A induced ferroptosis of Osteosarcoma cancer cells by HIF-1α/HK2 and SLC7A11 pathway. *Oncol Res*. (2024) 32:899–910. doi: 10.32604/or.2023.042604

4. Halma MTJ, Tuszynski JA, Marik PE. Cancer metabolism as a therapeutic target and review of interventions. *Nutrients*. (2023) 15:4245. doi: 10.3390/nu15194245

5. Mathew M, Nguyen NT, Bhutia YD, Sivaprakasam S, Ganapathy V. Metabolic signature of warburg effect in cancer: an effective and obligatory interplay between nutrient transporters and catabolic/anabolic pathways to promote tumor growth. *Cancers (Basel)*. (2024) 16:504. doi: 10.3390/cancers16030504

6. Niepmann M. Importance of michaelis constants for cancer cell redox balance and lactate secretion—Revisiting the warburg effect. *Cancers (Basel)*. (2024) 16:2290. doi: 10.3390/cancers16132290

7. Rai S, Roy G, Hajam YA. Melatonin: a modulator in metabolic rewiring in T-cell Malignancies. *Front Oncol*. (2024) 13:1248339. doi: 10.3389/fonc.2023.1248339

8. Pucci G, Minafra L, Bravata V, Calvaruso M, Turturici G, Cammarata F, et al. Glut-3 gene knockdown as a potential strategy to overcome glioblastoma radioresistance. *Int J Mol Sci*. (2024) 25:2079. doi: 10.3390/ijms25042079

9. Anwar S, Shamsi A, Mohammad T, Islam A, Hassan Md. I. Targeting pyruvate dehydrogenase kinase signaling in the development of effective cancer therapy. *Biochim Biophys Acta (BBA) - Rev Cancer*. (2021) 1876:188568. doi: 10.1016/j.bbcan.2021.188568

10. Yang W, Wei Y, Wang T, Xu Y, Jin X, Qian H, et al. Cytoplasmic localization of SETDB1-induced Warburg effect via c-MYC-LDHA axis enhances migration and invasion in breast carcinoma. *Int J Mol Med*. (2024) 53:40. doi: 10.3892/ijmm.2024.5364

11. Lin J, Zhong W, Lyu Z, Peng J, Rong Y, Zeng K, et al. Circular RNA circTATDN3 promotes the Warburg effect and proliferation in colorectal cancer. *Cancer Lett*. (2024) 589:216825. doi: 10.1016/j.canlet.2024.216825

12. Liu C, Shen A, Song J, Cheng L, Zhang M, Wang Y, et al. LncRNA-CCAT5-mediated crosstalk between Wnt/β-Catenin and STAT3 signaling suggests novel therapeutic approaches for metastatic gastric cancer with high Wnt activity. *Cancer Commun (Lond)*. (2023) 44:76–100. doi: 10.1002/cac2.12507

13. Li L, Gao Y, Yu B, Zhang J, Ma G, Jin X. Role of LncRNA H19 in tumor progression and treatment. *Mol Cell Probes*. (2024) 75:101961. doi: 10.1016/j.mcp.2024.101961

14. Wan Q, Deng Y, Wei R, Ma K, Tang J, Deng Y. Tumor-infiltrating macrophage associated lncRNA signature in cutaneous melanoma: implications for diagnosis, prognosis, and immunotherapy. *Aging (Albany NY)*. (2024) 16:4518–40. doi: 10.18632/aging.205606

15. Zhou C, Xu J, Lin J, Lin R, Chen K, Kong J, et al. Long noncoding RNA FEZF1-AS1 promotes osteosarcoma progression by regulating the miR-4443/NUPR1 axis. *Oncol Res*. (2018) 26:1335–43. doi: 10.3727/096504018X15188367859402

16. Yang Q, Fu Y, Wang J, Yang H, Zhang X. Roles of lncRNA in the diagnosis and prognosis of triple-negative breast cancer. *J Zhejiang Univ Sci B*. (2023) 24:1123–40. doi: 10.1631/jzus.B2300067

17. Cai Z, Shi Q, Li Y, Jin L, Li S, LamWong L, et al. LncRNA EILA promotes CDK4/6 inhibitor resistance in breast cancer by stabilizing cyclin E1 protein. *Sci Adv*. (2023) 9:eadi3821. doi: 10.1126/sciadv.adi3821

18. Zhang K-J, Tan X-L, Guo L. LncRNA TYMSOS facilitates breast cancer metastasis and immune escape through downregulating ULBP3. *iScience*. (2023) 26:107556. doi: 10.1016/j.isci.2023.107556

19. Dong Y, Zhang T, Li X, Yu F, Guo Y. Comprehensive analysis of coexpressed long noncoding RNAs and genes in breast cancer. *J Obstetrics Gynaecology Res*. (2019) 45:428–37. doi: 10.1111/jog.2019.45.issue-2

20. Braga EA, Fridman M, Burdennyy A, Loginov V, Dmitriev A, Dmitriev A, et al. Various lncRNA mechanisms in gene regulation involving miRNAs or RNA-binding proteins in non-small-cell lung cancer: main signaling pathways and networks. *Int J Mol Sci*. (2023) 24. doi: 10.3390/ijms241713617

21. Yang Q, Wang M, Xu J, Yu D, Li Y, Chen Y, et al. LINC02159 promotes non-small cell lung cancer progression via ALYREF/YAP1 signaling. *Mol Cancer*. (2023) 22:122. doi: 10.1186/s12943-023-01814-x

22. Chen Y-L, Liu Y, Lin Y, Tsai M, Wu S, Chang T, et al. LncRNA SLCO4A1-AS1 suppresses lung cancer progression by sequestering the TOX4-NTSR1 signaling axis. *J Biomed Sci*. (2023) 30:80. doi: 10.1186/s12929-023-00973-9

23. Yang J, Wang X, Hao W, Wang Y, Li Z, Han Q, et al. MicroRNA-488: A miRNA with diverse roles and clinical applications in cancer and other human diseases. *Biomedicine Pharmacotherapy*. (2023) 165:115115. doi: 10.1016/j.biopha.2023.115115

24. Chen H, Gao S, Cheng C. MiR-323a-3p suppressed the glycolysis of osteosarcoma via targeting LDHA. *Hum Cell*. (2018) 31:300–9. doi: 10.1007/s13577-018-0215-0

25. Zhu D, Qi H, Zhu H. hsa-miR-199b-3p suppresses osteosarcoma progression by targeting CCDC88A, inhibiting epithelial-to-mesenchymal transition, and Wnt/beta-catenin signaling pathway. *Sci Rep*. (2023) 13:12544. doi: 10.1038/s41598-023-39537-0

26. Zhang Y, Mi Y, He C. 2-methoxyestradiol restrains non-small cell lung cancer tumorigenesis through regulating circ_0010235/miR-34a-5p/NFAT5 axis. *Thorac Cancer*. (2023) 14:2105–15. doi: 10.1111/1759-7714.14993

27. Dai L, Zhang W, Wang Y, Yu K, Le Q, Wu X. circAGTPBP1 promotes the progression of papillary thyroid cancer through the notch pathway via the miR-34a-5p/notch1 axis. *iScience*. (2023) 26:107564. doi: 10.1016/j.isci.2023.107564

28. Li R, Xu H, Gao X. The ceRNA network regulates epithelial-mesenchymal transition in colorectal cancer. *Heliyon*. (2023) 9:e14143. doi: 10.1016/j.heliyon.2023.e14143

29. Mao M, Zhang J, Xiang Y, Gong M, Deng Y, Ye D. Role of exosomal competitive endogenous RNA (ceRNA) in diagnosis and treatment of Malignant tumors. *Bioengineered*. (2022) 13:12156. doi: 10.1080/21655979.2022.2073130

30. Yang S, Wang X, Zhou X, Hou L, Wu J, Zhang W, et al. ncRNA-mediated ceRNA regulatory network: Transcriptomic insights into breast cancer progression and treatment strategies. *Biomed Pharmacother*. (2023) 162:114698. doi: 10.1016/j.biopha.2023.114698

31. Zhang C, Yu Z, Yang S, Liu Y, Song J, Mao J, et al. ZNF460-mediated circRPPH1 promotes TNBC progression through ITGA5-induced FAK/PI3K/AKT activation in a ceRNA manner. *Mol Cancer*. (2024) 23:33. doi: 10.1186/s12943-024-01944-w

32. Wu X, Sui Z, Zhang H, Wang Y, Yu Z. Integrated Analysis of lncRNA–Mediated ceRNA Network in Lung Adenocarcinoma. *Front Oncol*. (2020) 10:554759. doi: 10.3389/fonc.2020.554759

33. Jiang J, Gareev I, Ilyasova T, Shumadalova A, Du W, Yang B, et al. The role of lncRNA-mediated ceRNA regulatory networks in liver fibrosis. *Non-coding RNA Res*. (2024) 9:463. doi: 10.1016/j.ncrna.2024.01.001

34. Yang Z, Liu Z, Lu W, Guo H, Chen J, Zhang Y. LncRNA WAC-AS1 promotes osteosarcoma Metastasis and stemness by sponging miR-5047 to upregulate SOX2. *Biol Direct*. (2023) 18:74. doi: 10.1186/s13062-023-00433-2

35. Wang P, Zhu J, Long Q, Wang Y, Xu H, Tao H, et al. LncRNA SATB2-AS1 promotes tumor growth and metastasis and affects the tumor immune microenvironment in osteosarcoma by regulating SATB2. *J Bone Oncol*. (2023) 41:100491. doi: 10.1016/j.jbo.2023.100491

36. Yu H, Yan X, Chen G, Li R, Yang Z, Liang Z, et al. Dynamic network biomarker C1QTNF1 regulates tumor formation at the tipping point of hepatocellular carcinoma. *Biomolecules Biomedicine*. (2024) 24:939–51. doi: 10.17305/bb.2024.10103

37. Qiu J, Wang Z, Zhao L, Zhang P, Xu Y, Xia Q. High C1QTNF1 expression mediated by potential ncRNAs is associated with poor prognosis and tumor immunity in kidney renal clear cell carcinoma. *Front Mol Biosci*. (2023) 10:1201155. doi: 10.3389/fmolb.2023.1201155

38. Lin J. C1QTNF1-AS1 regulates the occurrence and development of hepatocellular carcinoma by regulating miR-221-3p/SOCS3. *Hepatol Int*. (2021) 15:526–6. doi: 10.1007/s12072-021-10152-3

39. Lu S, Zeng L, Mo G, Lei D, Li Y, Ou G, et al. Long non-coding RNA SNHG17 may function as a competitive endogenous RNA in diffuse large B-cell lymphoma progression by sponging miR-34a-5p. *PloS One*. (2023) 18:e0294729. doi: 10.1371/journal.pone.0294729

40. Upadhyay S, Khan S, Hassan Md. I. Exploring the diverse role of pyruvate kinase M2 in cancer: Navigating beyond glycolysis and the Warburg effect. *Biochim Biophys Acta (BBA) - Rev Cancer*. (2024) 1879:189089. doi: 10.1016/j.bbcan.2024.189089

41. Pascale RM, Calvisi DF, Simile MM, Feo CF, Feo F. The warburg effect 97 years after its discovery. *Cancers*. (2020) 12:2819. doi: 10.3390/cancers12102819

42. Zhong X, He X, Wang Y, Hu Z, Huang H, Zhao S, et al. Warburg effect in colorectal cancer: the emerging roles in tumor microenvironment and therapeutic implications. *J Hematol Oncol*. (2022) 15:160. doi: 10.1186/s13045-022-01358-5

43. Liao M, Yao D, Wu L, Luo C, Wang Z, Zhang J, et al. Targeting the Warburg effect: A revisited perspective from molecular mechanisms to traditional and innovative therapeutic strategies in cancer. *Acta Pharm Sinica B*. (2023) 14:953. doi: 10.1016/j.apsb.2023.12.003

44. Barba I, Carrillo-Bosch L, Seoane J. Targeting the warburg effect in cancer: where do we stand? *Int J Mol Sci*. (2024) 25:3142. doi: 10.3390/ijms25063142

45. Kocianova E, Piatrikova V, Golias T. Revisiting the warburg effect with focus on lactate. *Cancers*. (2022) 14:6028. doi: 10.3390/cancers14246028

46. Wu C, Zheng C, Chen S, He Z, Hua H, Sun C, et al. FOXQ1 promotes pancreatic cancer cell proliferation, tumor stemness, invasion and metastasis through regulation of LDHA-mediated aerobic glycolysis. *Cell Death Dis*. (2023) 14:699. doi: 10.1038/s41419-023-06207-y

47. Chen M, Xiao Z, Huang Z, Xue K, Xia H, Zhou J, et al. Glycine decarboxylase (GLDC) plays a crucial role in regulating energy metabolism, invasion, metastasis and immune escape for prostate cancer. *Int J Biol Sci*. (2023) 19:4726–43. doi: 10.7150/ijbs.85893

48. Gan L, Yang Y, Liang Z, Zhang M, He Y, Zhang S. Targeting the pyruvate dehydrogenase complex/pyruvate dehydrogenase kinase (PDC/PDK) axis to discover potent PDK inhibitors through structure-based virtual screening and pharmacological evaluation. *Eur J Medicinal Chem*. (2024) 264:116008. doi: 10.1016/j.ejmech.2023.116008

49. Li X-N, Yang S, Li M, Li X, Tian Q, Xiao F, et al. Formaldehyde induces ferroptosis in hippocampal neuronal cells by upregulation of the Warburg effect. *Toxicology*. (2021) 448:152650. doi: 10.1016/j.tox.2020.152650

frontiers | Frontiers in Immunology

TYPE Systematic Review
PUBLISHED 10 February 2025
DOI 10.3389/fimmu.2024.1485053

OPEN ACCESS

EDITED BY
Tong-Chuan He,
University of Chicago Medicine, United States

REVIEWED BY
Saroj Kumari,
Nation Institute of Immunology, India
Bikesh Kumar Nirala,
Emory University, United States
Malik Ihsan,
University of Lahore, Pakistan

*CORRESPONDENCE
Yunxiang Hu
hooshawnzeee@dmu.edu.cn

†These authors have contributed equally to this work and share first authorship

RECEIVED 23 August 2024
ACCEPTED 24 December 2024
PUBLISHED 10 February 2025

CITATION
Hu Y, Yang R, Ni S and Song Z (2025) Bibliometric analysis of targeted immunotherapy for osteosarcoma-current knowledge, hotspots and future perspectives. *Front. Immunol.* 15:1485053. doi: 10.3389/fimmu.2024.1485053

Bibliometric analysis of targeted immunotherapy for osteosarcoma-current knowledge, hotspots and future perspectives

Yunxiang Hu[1,2*†], Rui Yang[2†], Shuai Ni[1,2†] and Zefeng Song[3]

[1]Department of Orthopaedic Trauma, The Second Affiliated Hospital of Dalian Medical University, Dalian, Liaoning, China, [2]School of Graduates, Dalian Medical University, Dalian, Liaoning, China, [3]School of Graduates, Dalian University of Technology, Dalian, Liaoning, China

Objective: The objective of this study is to conduct a bibliometric analysis on examining the current condition, areas of interest, and rising trends of immunotherapy for osteosarcoma (ITFOS), as well as its importance in associated research domains.

Methods: An extensive collection of academic papers on the use of ITFOS was obtained from the Web of Science between January 1, 2000 and October 20, 2023. Then, using a variety of tools like HisCite, VOSviewer, CiteSpace, and the bibliometrix package, a bibliometric study was carried out. This study included the collection of information on country, institution, author, journal, and keywords.

Results: A comprehensive analysis was undertaken on a total of 616 publications obtained from 247 journals, encompassing the contributions of 3725 authors affiliated with 831 institutes spanning across 43 countries/regions. Notably, China exhibited the highest quantity of published 277 (44.99%) articles on ITFOS. The most productive institution was Zhejiang University, with 26 (4.22%) publications. The author with the highest publication output was Tsukahara, Tomohide from Japan with 15 (2.44%) publications. The article with the most citation was "DOI: 10.1200/JCO.2014.58.0225". Frontiers in Immunology demonstrated the highest level of productivity, having published a total of 31 (5.03%) articles. The most frequently used were "osteosarcoma," "immunotherapy," and "cancer,". Meanwhile, "sequencing", "prognostic signature" and "immune microenvironment" have been identified as the research frontiers for the forthcoming years.

Conclusion: This paper provides a thorough evaluation of current research trends and advancements in ITFOS. It includes relevant research findings and emphasizes collaborative efforts among authors, institutions, and countries.

KEYWORDS

osteosarcoma, immune function, immunotherapy, immune checkpoint inhibitor, targeted therapy

Introduction

Osteosarcoma is the most common primary malignant bone tumor characterized by highly aggressive and metastatic behavior, accounting for approximately 56% of primary malignant bone tumors (1). It predominantly affects children and adolescents with a median age of 16 years and occurs most frequently in the metaphysis of long bones, including the distal femur and proximal tibia (2). According to the 5th edition of the World Health Organization (WHO) classification of bone and soft tissue tumors, osteosarcoma is classified into several subtypes, including low-grade central osteosarcoma, conventional osteosarcoma, telangiectatic osteosarcoma, small cell osteosarcoma, parosteal osteosarcoma, periosteal osteosarcoma, high-grade surface osteosarcoma, and secondary osteosarcoma (3). Surgical intervention is an important treatment modality for osteosarcoma. With the introduction of neoadjuvant chemotherapy, the combination of chemotherapy and surgery has improved the 5-year survival rate to 70% for non-metastatic osteosarcoma patients. However, for advanced and recurrent osteosarcoma patients, despite the incorporation of various chemotherapy regimens, the treatment outcomes have remained poor based on decades of research, with a 5-year survival rate of only 20% (4, 5). Consequently, there is an urgent need to explore novel treatment approaches that can fundamentally improve the prognosis of osteosarcoma. In recent years, researchers have made significant progress in the study of tumor immune responses, leading to the development of targeted therapies focusing on T cells or their receptors in the tumor microenvironment. One such example is the use of immune checkpoint inhibitors, such as PD-1/PD-L1 monoclonal antibodies, which have shown promising therapeutic effects in various types of tumors, including melanoma, lung cancer, and breast cancer (6–9). These successes have reignited the enthusiasm for tumor immunotherapy research. In the case of osteosarcoma, researchers have increasingly conducted basic research and clinical trials exploring the potential of immunotherapy due to the challenges faced in achieving standardized treatment for osteosarcoma patients.

In the field of science, bibliometric analyses are frequently used to evaluate published research and predict future trends. The field of bibliometrics examines the relationships between scientific fields, countries, organizations, authors, and publications by using mathematical and statistical approaches (9, 10). In recent years, significant advancements have been made in the study of ITFOS, yet a bibliometric analysis of this research is lacking. This study aims to conduct a bibliometric analysis of ITFOS research. By utilizing knowledge maps, scientists can efficiently analyze large datasets and gain insights into the development and emerging trends in this field. This methodology enhances the ability to identify research hotspots and allows for a comprehensive examination of research patterns. Furthermore, the analysis may offer valuable insights for future research projects and decision-making processes.

Materials and methods

Search strategy

Using the Web of Science Core Collection (WoSCC), a literature search was carried out at Dalian Municipal Central Hospital on October 20th, 2023. Use the following search parameters to find results: (((TS = (Osteosarcoma OR Osteosarcomas OR Osteosarcoma Tumor OR Osteosarcoma Tumors OR Tumor, Osteosarcoma OR Tumors, Osteosarcoma OR Sarcoma, Osteogenic OR Osteogenic Sarcomas OR Sarcomas, Osteogenic OR Osteogenic Sarcoma)) AND TS=(immunotherapy)) AND DT= (Article OR Review)) AND LA=(English). Articles that mentioned ITFOS or its synonyms in their title, abstract, or keywords were found as a result of the search query. Articles and reviews published between January 1, 2000, and October 20, 2023 were the only document kinds included in the search; publications earlier than January 1, 2000, case reports, meeting abstracts, editorial materials, and other document types were not included. Documents written in the English language were the only ones that met the inclusion criterion.

Data collection

On October 20, 2023, a literature search query was performed in order to retrieve data from the WoSCC. The information retrieved covered a wide range of features of the literature, including authorship, title, source, sponsorship, citation count, accession number, abstract, address, document type, and cited references. To aid further analysis, the data was collected in both txt and BibTex formats. Web of Science was used to obtain the H-index of the top 10 authors with the most publication output. Furthermore, the 2022 impact factor and Journal Citation Report category quartile of the ten key journals relevant to ITFOS were obtained from Web of Science.

Statistical analysis

HisCite (version 12.03.17), VOSviewer (version 1.6.18), CiteSpace (version 6.1.R3), and the bibliometrix package (version 3.2.1; https://cran.r-project.org/web/packages/bibliometrix/) based on R language (version 4.1.2) were used to analyze the bibliometric data. HisCite was used to calculate the total number of publications and citations for producing countries, institutions, and authors. In addition, using HisCite, the top ten papers with the highest citation count in ITFOS were discovered. The yearly count of publications was calculated using HisCite and graphically represented in the R programming language using the ggplot2 package (version 3.3.6; https://github.com/tidyverse/ggplot2). VOSviewer was used to identify the top 10 keywords with the highest occurrence, bibliometric coupling within journals, and clustering of the top 54 keywords. CiteSpace was also used to create a dual-map overlay of

the journals connected with ITFOS. CiteSpace was used to assess the level of collaborative centrality among countries/regions, institutions, and authors. Following that, trend topic detection within the bibliomatrix program was used as an alternate methodology. This program was also used to build visual representations of publication volume and collaborative relationship networks. When analyzing different subjects, it's important to choose appropriate tools based on their specific characteristics. For example, in clustering diagrams for keywords, countries, and authorses,sti algorithmic influence is minimalcei focus on the compactness and aesthetics, making VOSviewer a suitable choice. In contrast, Citespace is better for citation bursts, co-citation networks, and timelines. The bibliometrix R package provides intuitive visualizations for trend topics, while the interactive tool biblioshiny has limited interactivity. However, bibliometrix also allows for custom visualizations, such as keyword time heatmaps. These tool differences necessitate careful selection based on research objectives. To mitigate discrepancies from using different tools, we analyze identified trends or clusters with multiple tools and compare the results. If consistent trends are found across tools for the same keyword or topic, we consider these findings robust. In our final reports, we prioritize keywords or topics identified as hotspots across various analyses to ensure the reliability and generalizability of the results.

Results

Overview

A comprehensive search was conducted in the WoSCC database, resulting in the identification of 616 publications pertaining to ITFOS. The search period spanned from January 1, 2000, to October 20, 2023 (Figure 1).

Among these publications, 469 were categorized as original articles, while 147 were classified as review articles. Notably, the frequency of ITFOS-related publications exhibited an irregular pattern, albeit showing an overall upward trend in terms of total citations (Figure 2).

It is worth mentioning that the proportion of original articles consistently surpassed that of review articles on an annual basis. The cumulative collection of published articles has garnered a total of 14355 citations, resulting in an average of 23.31 citations per article, which holds significant scholarly value.

Leading countries/regions

From January 1, 2000, to October 20, 2023, scholarly articles on ITFOS were disseminated across 43 countries/regions spanning six continents. Notable collaboration was observed among East Asia, North America, and Western Europe (Figure 3).

This study highlights the top 10 countries in terms of productivity in publishing articles on ITFOS. China emerged as the most prolific country, contributing 277 (44.99%) articles, followed by USA with 192 (31.17%) articles, Japan with 68 (11.04%) articles, Italy with 32 (5.19%) articles, and Germany with 25 (4.06%) articles. It is noteworthy that articles originating from the United States received the highest total number of citations, amounting to 6826, while articles from Germany had the highest average number of citations per article, with 57.16 (Table 1).

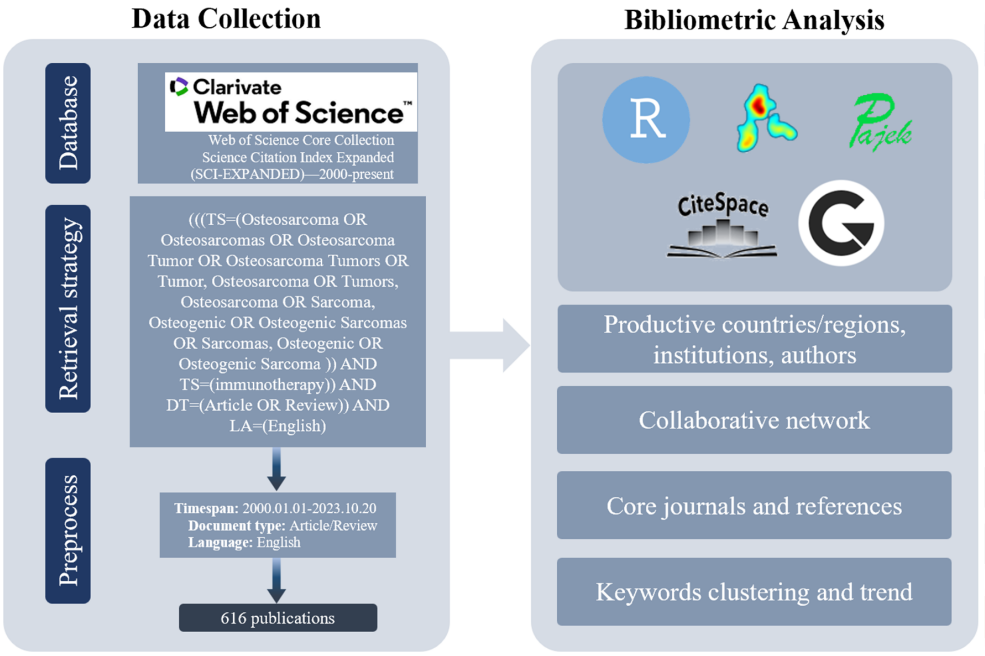

FIGURE 1
Hierarchical chart depicting the process of publication selection.

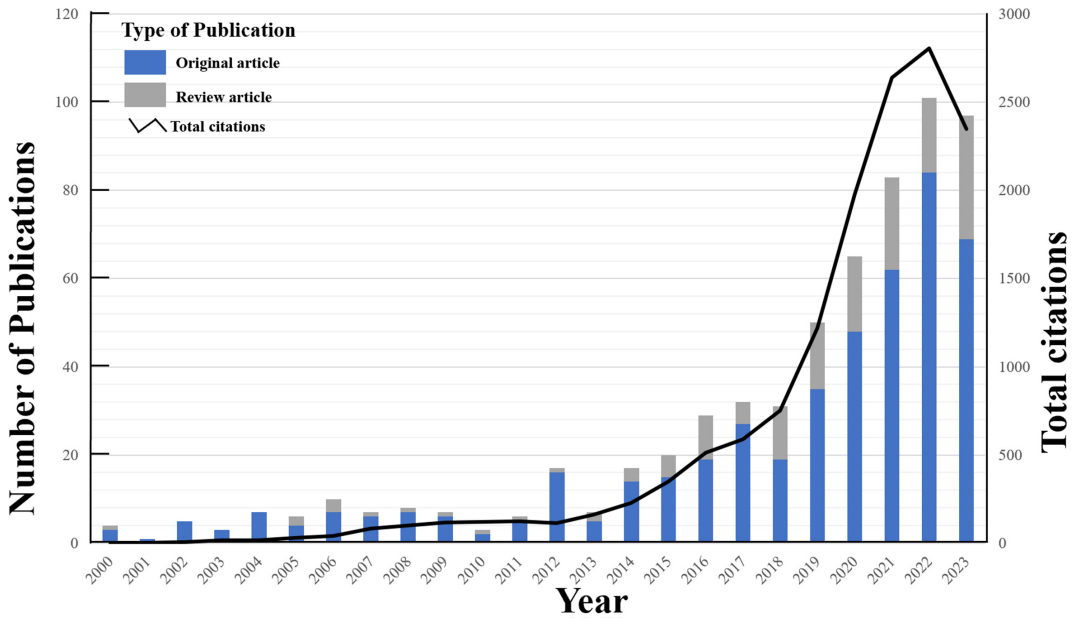

FIGURE 2
The yearly quantity and citations of publications pertaining to ITFOS.

Active institutions and authors

Through an extensive investigation, a total of 616 publications were identified, authored by 3725 individuals affiliated with 831 institutes across 43 countries/regions. Among the identified institutes, Zhejiang University in the China emerged as the most prolific, contributing 26 (4.22%) publications. This was followed by the Central South University, China with 22 (3.57%) publications, University of Texas MD Anderson Cancer Center, USA with 21 (3.41%) publications, Sapporo Medical University in Japan with 20 (3.25%) publications, and Shanghai Jiao Tong University, China with18 (2.92%) publications. Notably, among the top ten institutions, six were located in the China, three in USA, and one in Japan (Table 2).

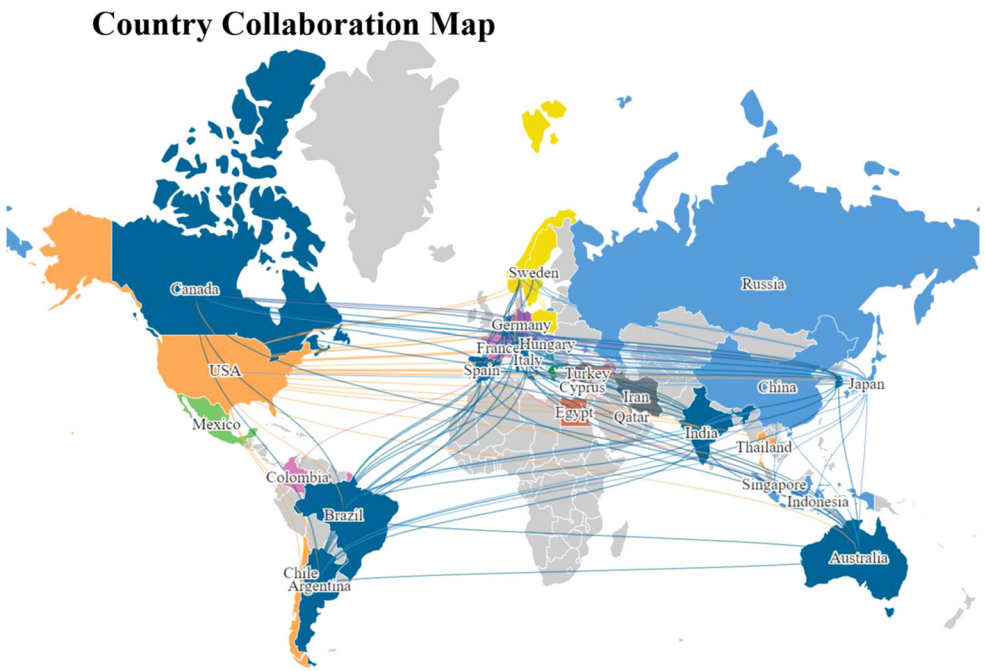

FIGURE 3
The collaborative map of the country.

TABLE 1 The top 10 countries/regions with the highest productivity.

Rank	Country	Publications n(%)	Total citations	Average citations	Collaborative centrality
1	China	277 (44.99%)	3964	14.31	0.00
2	USA	192 (31.17%)	6826	35.55	0.22
3	Japan	68 (11.04%)	1992	29.29	0.06
4	Italy	32 (5.19%)	762	23.81	0.02
5	Germany	25 (4.06%)	1429	57.16	0. 12
6	United Kingdom	24 (3.90%)	937	39.04	0.13
7	France	21 (3.41%)	722	34.38	0.02
8	Australia	13 (2.11%)	309	23.77	0. 01
9	Netherlands	12 (1.95%)	607	50.58	0.03
10	Spain	12 (1.95%)	306	25.50	0. 04

The study also revealed four distinct clusters of institutional collaboration, with Zhejiang University, University of Texas MD Anderson Cancer Center, Nationwide Children's Hospital and National Cancer Institute (NCI) exhibiting the highest level of collaboration (Figure 4A). Regarding authors, the most prolific author identified was Tsukahara, Tomohide, Japan with 15 (2.44%) publications, followed by Sato, Noriyuki, Japan with 13 (2.11%) publications, and Torigoe, Toshihiko, Japan, with 13 (2.11%) publications. Among the top ten most productive authors, four were affiliated with institutions in Japan, two with institutions in China, one with an institution in USA, one with an institution in Germany, and one with an institution in Australia. Notably, Gottschalk, Stephen from Germany had the highest H-index of 64 (Table 3).

The authors demonstrated a notable level of cooperation, as evidenced by the presence of five clusters. Torigoe, Toshihiko, Tsukahara, Tomohide, Canter, Robert J., Tao Huimin, and Lee, Dean A. displayed a significant degree of collaborative centrality (Figure 4B).

Core journals and references

A total of 43 journals have published research on ITFOS. Among these journals, Frontiers in Immunology demonstrated the highest productivity, publishing 31 (5.03%) articles related to ITFOS. This was followed by Frontiers in Oncology with 25 (4.07%) articles, Cancers with 20 (3.25%) articles, Journal for Immunotherapy of Cancer with 15 (2.44%) articles, and International Journal of Molecular Sciences with 11 (1.79%) articles. Notably, Clinical Cancer Research achieved the highest average citation rate, with an average of 74.40 citations per article (Table 4).

The dual-map overlay revealed a single citation pathway among the numerous inter-domain linkages between journals. Interestingly, publications in Molecular/Biology/Immunology were primarily referenced by publications in Molecular/Biology/Genetics (Figure 5A). Bradford's Law, a bibliometric principle, describes the distribution of scientific literature in a specific field. It suggests that a few core information sources or journals

TABLE 2 The top 10 productive institutions.

Rank	Institution	Country	Publications n(%)	Total citation	Average citation
1	Zhejiang University	China	26 (4.22%)	709	27.27
2	Central South University	China	22 (3.57%)	118	5.36
3	University of Texas MD Anderson Cancer Center	USA	21 (3.41%)	1480	70.48
4	Sapporo Medical University	Japan	20 (3.25%)	373	18.65
5	Shanghai Jiao Tong University	China	18 (2.92%)	330	18.33
6	Memorial Sloan Kettering Cancer Center	USA	17 (2.76%)	798	46.94
7	Peking University	China	14 (2.27%)	358	25.57
8	Fourth Military Medical University	China	13 (2.11%)	186	14.31
9	Sun Yat-sen University	China	13 (2.11%)	177	13.62
10	National Cancer Institute (NCI)	USA	12 (1.95%)	595	49.58

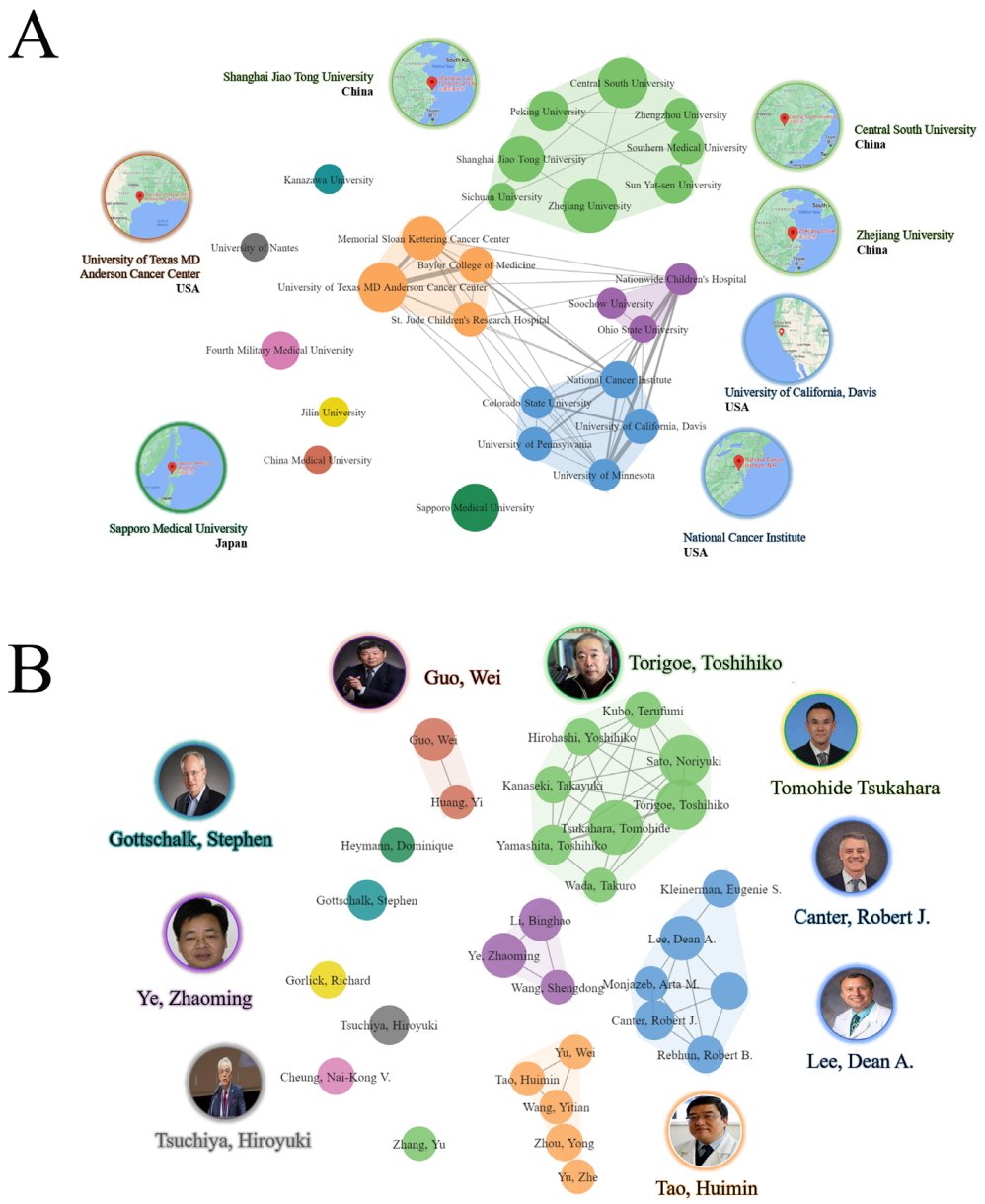

FIGURE 4
Collaborative clustering of institutions and authors. **(A)** Collaborative clustering of institutions. **(B)** Collaborative clustering of authors.

contribute significantly to the published research in that field. In the context of ITFOS research, three clusters were identified, Frontiers in Immunology, Cancers, and Oncoimmunology emerged as the top three influential journals (Figure 5B).

Clusters located on the right-hand side, characterized by a higher incidence of red nodes, indicate a greater prevalence of recent references. The clusters labeled "#0" (TME) and "#2" (tumor-infiltrating lymphocytes) were found to be the most temporally proximate (Figure 6A). A list of the top 10 papers with the most citations can be found in (Table 5). The article with the most citation was "DOI: 10.1200/JCO.2014.58.0225". Ahmed et al. conducted a study that evaluated the safety and efficacy of HER2-CAR T cells in cancer patients. They found that these cells can persist for 6 weeks without significant toxicities, paving the way for future studies that combine HER2-CAR T cells with other immunomodulatory approaches to enhance their expansion and persistence (11).

Moreover, reference burst detection was employed to identify research frontiers and emerging reference. The study examined the top 25 references with the most robust emergent properties. The reference " doi: 10.3390/cells9040976" (21) " doi: 10.1038/s41467-020-14646-w" (22) and " doi: 10.1080/14737140.2018.1413939" (23) were identified as the most emergent reference in 2023 (Figure 6B).

TABLE 3 Top 10 productive authors.

Rank	Author	Institution	Country	Publications n(%)	Total citation	Average citation	H-index
1	Tsukahara, Tomohide	Sapporo Medical University	Japan	15 (2.44%)	272	18.13	29
2	Sato, Noriyuki	Fukushima Univ Child Mental Hlth	Japan	13 (2.11%)	267	20.54	42
3	Torigoe, Toshihiko	Sapporo Medical University	Japan	13 (2.11%)	246	18.92	42
4	Lee, Dean A.	Nationwide Children's Hospital	USA	10 (1.62%)	314	31.40	47
5	Ye, Zhaoming	Zhejiang University School of Medicine	China	10 (1.62%)	320	32.00	28
6	Guo, Wei	Peking University	China	9 (1.46%)	369	41.00	19
7	Li, Binghao	University of New South Wales Sydney	Australia	9 (1.46%)	292	32.44	22
8	Canter, Robert J.	University of California Davis	USA	8 (1.30%)	258	32.25	36
9	Gottschalk, Stephen	St. Jude Children's Research Hospital	Germany	8 (1.30%)	325	40.63	64
10	Tsuchiya, Hiroyuki	Kanazawa University	Japan	8 (1.30%)	278	34.75	41

An analysis of keywords

We presented the fifteen most frequently appearing keywords in ITFOS research after consolidating synonymous terms, with " osteosarcoma " being the most commonly referenced (Table 6).

An analysis of keyword co-occurrence among the top 43 keywords revealed the presence of five distinct clusters. The cluster consisting of "osteosarcoma," "immunotherapy," "cancer," "chemotherapy," and "blockade" exhibited the highest frequency of occurrence (Figure 7A). Furthermore, an examination of the trend topics from 2000 to 2023 identified "sequencing", "prognostic signature" and "immune microenvironment " as the research frontiers for the upcoming years (Figure 7B).

Discussion

As early as 1891, the potential of immunotherapy for the treatment of osteosarcoma was recognized (24). In recent years, new immunotherapy approaches have emerged rapidly, and the scope of treatment has been expanding, bringing a hopeful outlook for breakthroughs in osteosarcoma treatment, which has been stagnant

TABLE 4 Top 10 core journals.

Rank	Journal	Publications n(%)	Total citations	Average citations	2022 JCR category quartile	2022 IF
1	Frontiers in Immunology	31 (5.03%)	340	10.97	Q1	7.3
2	Frontiers in Oncology	25 (4.07%)	432	17.28	Q2	4.7
3	Cancers	20 (3.25%)	180	9.00	Q1	5.2
4	Journal for Immunotherapy of Cancer	15 (2.44%)	573	38.20	Q1	10.9
5	International Journal of Molecular Sciences	11 (1.79%)	257	23.36	Q1	5.6
6	Clinical Cancer Research	10 (1.62%)	744	74.40	Q1	11.5
7	Journal of Bone Oncology	10 (1.62%)	172	17.20	Q2	3.4
8	Oncoimmunology	10 (1.62%)	231	23.10	Q1	7.2
9	Cancer Immunology Immunotherapy	9 (1.46%)	339	37.67	Q1	5.8
10	Oncology Letters	9 (1.46%)	106	11.78	Q3	2.9

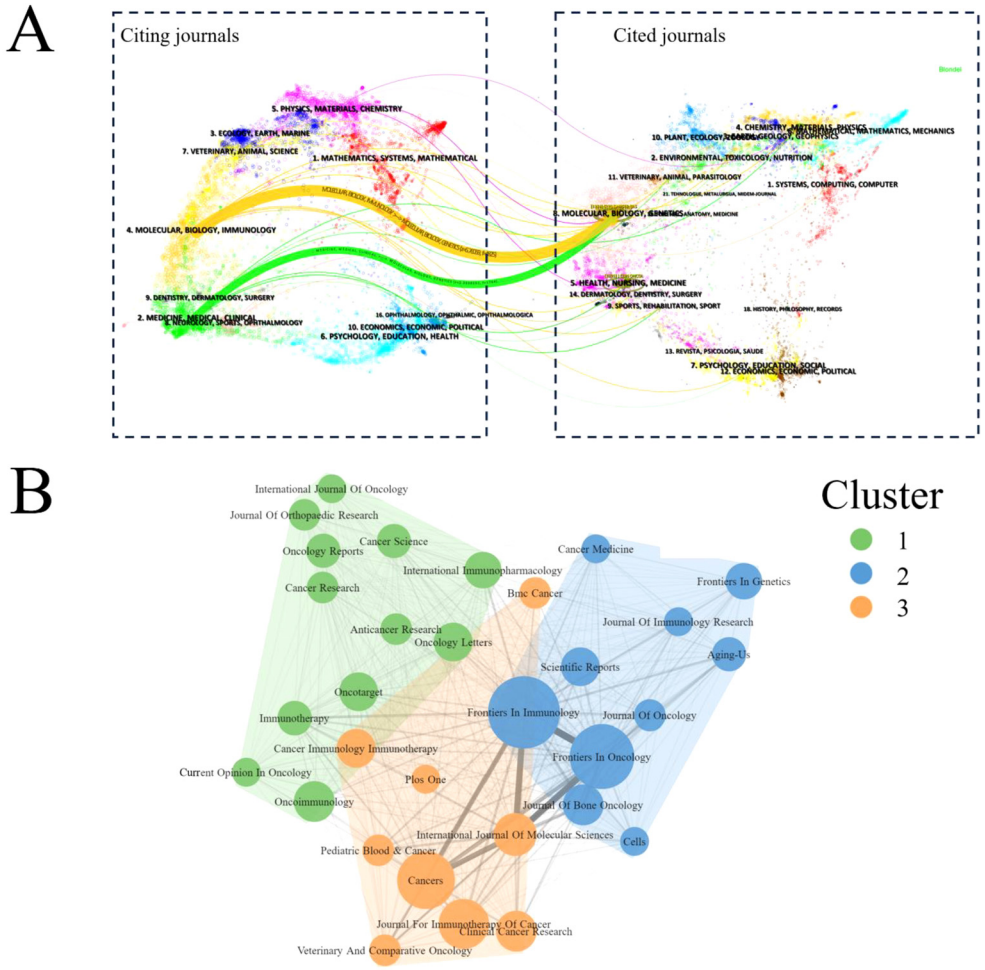

FIGURE 5
Analysis of journals. **(A)** The dual-map overlay of journals publishing studies on ITFOS. Citing journals are on the left, cited journals are on the right, and lines represent the citation relationship. **(B)** Bibliometric coupling within journals. Three clusters were identified based on journals that had published more than five articles.

for several decades (25, 26). Currently, a substantial body of preclinical experiments supports the significant potential of immunotherapy in the treatment of osteosarcoma. Furthermore, several clinical trials have been initiated, involving various aspects such as T cells and immune checkpoint inhibitors (27, 28). Therefore, we conducted a bibliometric analysis and found that China exhibited the highest quantity of published 277 (44.99%) articles on ITFOS. The most productive institution was Zhejiang University, with 26 (4.22%) publications. China and Zhejiang University lead in publication counts. Possible reasons include: Osteosarcoma is a highly heterogeneous malignant tumor with a complex pathogenesis involving multiple biological processes, prompting researchers to explore it in depth. The study of osteosarcoma involves multiple disciplines, including oncology, molecular biology, immunology, and pharmacology, which fosters interdisciplinary collaboration and innovation. Advances in technology, such as genomics, transcriptomics, and immunotherapy, provide new research tools and platforms that enhance the progress of osteosarcoma research. Furthermore, international collaboration is also significant, with many research institutions and teams engaging in joint efforts in the field, sharing resources and data to facilitate rapid scientific outcomes. Additionally, increased funding support from governments and academic institutions has led to growing attention on osteosarcoma research, enabling the implementation of related projects and boosting research output. Lastly, active academic exchanges through frequent conferences and forums offer researchers opportunities to share and showcase their findings, further promoting scientific development. The study also revealed four distinct clusters of institutional collaboration, with Zhejiang University, University of Texas MD Anderson Cancer Center, Nationwide Children's Hospital and National Cancer Institute (NCI) exhibiting the highest level of collaboration. The benefits of closer collaboration between research institutions include: Resource sharing: Collaborative institutions can share equipment, data, and funding, which enhances research efficiency and reduces costs. Improved research quality: Through collaboration, research teams can gain broader perspectives and specialized skills, thereby increasing the rigor and credibility of their research. Accelerated translation of results: Close collaboration can shorten the time required to translate research findings into practical applications, facilitating rapid technology dissemination. Enhanced

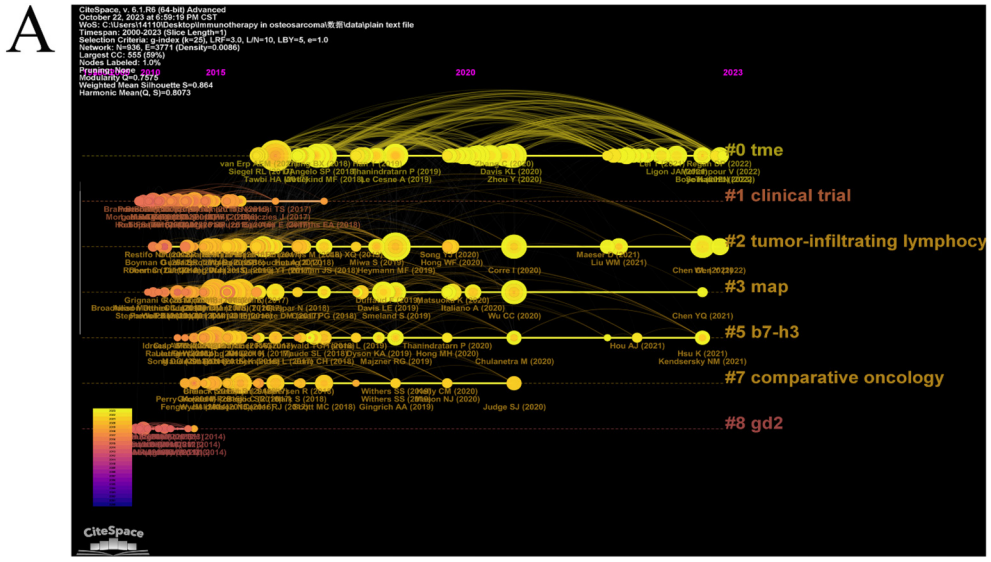

B

Top 25 References with the Strongest Citation Bursts

References	Year	Strength	Begin	End	2000 - 2023
Tsukahara T, 2004, CANCER RES, V64, P5442, DOI 10.1158/0008-5472.CAN-04-0522, DOI	2004	6.55	2005	2008	
Ahmed N, 2009, MOL THER, V17, P1779, DOI 10.1038/mt.2009.133, DOI	2009	5.75	2012	2014	
Topalian SL, 2012, NEW ENGL J MED, V366, P2443, DOI 10.1056/NEJMoa1200690, DOI	2012	8.89	2013	2016	
Hodi FS, 2010, NEW ENGL J MED, V363, P711, DOI 10.1056/NEJMoa1003466, DOI	2010	6.78	2013	2015	
Robbins PF, 2011, J CLIN ONCOL, V29, P917, DOI 10.1200/JCO.2010.32.2537, DOI	2011	6.77	2014	2016	
Huang GX, 2012, CANCER RES, V72, P271, DOI 10.1158/0008-5472.CAN-11-2778, DOI	2012	6.24	2014	2017	
Shen JK, 2014, CANCER IMMUNOL RES, V2, P690, DOI 10.1158/2326-6066.CIR-13-0224, DOI	2014	12.28	2015	2019	
Kim JR, 2013, PLOS ONE, V8, P0, DOI 10.1371/journal.pone.0082870, DOI	2013	9.5	2015	2018	
Lussier DM, 2015, J IMMUNOTHER, V38, P96, DOI 10.1097/CJI.0000000000000065, DOI	2015	13.39	2016	2020	
Ahmed N, 2015, J CLIN ONCOL, V33, P1688, DOI 10.1200/JCO.2014.58.0225, DOI	2015	13.06	2016	2020	
Lussier DM, 2015, J IMMUNOTHER CANCER, V3, P0, DOI 10.1186/s40425-015-0067-z, DOI	2015	12.37	2016	2019	
Isakoff MS, 2015, J CLIN ONCOL, V33, P3029, DOI 10.1200/JCO.2014.59.4895, DOI	2015	8.12	2016	2020	
Kansara M, 2014, NAT REV CANCER, V14, P722, DOI 10.1038/nrc3838, DOI	2014	7.78	2016	2019	
Bielack SS, 2015, J CLIN ONCOL, V33, P2279, DOI 10.1200/JCO.2014.60.0734, DOI	2015	6.16	2016	2020	
Koirala P, 2016, SCI REP-UK, V6, P0, DOI 10.1038/srep30093, DOI	2016	12.27	2017	2021	
Merchant MS, 2016, CLIN CANCER RES, V22, P1364, DOI 10.1158/1078-0432.CCR-15-0491, DOI	2016	7.14	2018	2021	
Sundara YT, 2017, CANCER IMMUNOL IMMUN, V66, P119, DOI 10.1007/s00262-016-1925-3, DOI	2017	6.54	2018	2021	
Tawbi HA, 2017, LANCET ONCOL, V18, P1493, DOI 10.1016/S1470-2045(17)30624-1, DOI	2017	12.79	2019	2021	
Mason NJ, 2016, CLIN CANCER RES, V22, P4380, DOI 10.1158/1078-0432.CCR-16-0088, DOI	2016	7.07	2019	2021	
Fritzsching B, 2015, ONCOIMMUNOLOGY, V4, P0, DOI 10.4161/2162402X.2014.990800, DOI	2015	5.82	2019	2020	
Gomez-Brouchet A, 2017, ONCOIMMUNOLOGY, V6, P0, DOI 10.1080/2162402X.2017.1331193, DOI	2017	5.7	2019	2021	
Thanindratarn P, 2019, J BONE ONCOL, V15, P0, DOI 10.1016/j.jbo.2019.100221, DOI	2019	5.98	2020	2021	
Corre I, 2020, CELLS-BASEL, V9, P0, DOI 10.3390/cells9040976, DOI	2020	7.23	2021	2023	
Wu CC, 2020, NAT COMMUN, V11, P0, DOI 10.1038/s41467-020-14646-w, DOI	2020	5.99	2021	2023	
Harrison DJ, 2018, EXPERT REV ANTICANC, V18, P39, DOI 10.1080/14737140.2018.1413939, DOI	2018	5.83	2021	2023	

FIGURE 6
Analysis of citations and references. **(A)** Timeline of co-cited references related to ITFOS. **(B)** Reference burst detection of the top 25 references with the strongest emergent strength.

impact: Collaboration enables research institutions to better expand the influence of their findings and enhance their reputation within the academic community and society at large. The author with the highest publication output was Tsukahara, Tomohide from Japan with 15 (2.44%) publications. Frontiers in Immunology demonstrated the highest level of productivity, having published a total of 31 (5.03%) articles. The most frequently used keywords were "osteosarcoma," "immunotherapy," and "cancer,". The trend in keyword frequency is identified by observing its growth or decline over time, thereby marking keywords with increasing frequency (emerging trends) or decreasing frequency (declining trends). "sequencing", "prognostic signature" and "immune microenvironment" have been identified as the research frontiers for the forthcoming years. As predicted, research on "sequencing" (29, 30), "prognostic signature" and "immune microenvironment" (16, 31–36) in osteosarcoma has gained momentum, with the number of published studies increasing annually. These topics are expected to remain prominent in the near future. Zhong et al. developed a signature (ZNF583, CGNL1, CXCL13) to predict overall survival in osteosarcoma patients, focusing on the anoikis subcluster. This signature showed strong performance in external validation, with stratification revealing significant prognostic differences. It was identified as an independent prognostic factor (29). Wu et al. found that the TMEindex is a promising biomarker for predicting prognosis in osteosarcoma patients, assessing their response to immune checkpoint inhibitor (ICI) therapy, and distinguishing molecular and immune characteristics (34). The application of immunotherapy in osteosarcoma primarily involves two aspects: enhancing the patient's own immune system response to the tumor and exogenously boosting the immune function of the patient.

TABLE 5 Top 10 core literatures.

Rank	First author	Title	Journal	Type	Year of publication	Total citations
1	Ahmed et al (11)	Human Epidermal Growth Factor Receptor 2 (HER2) -Specific Chimeric Antigen Receptor-Modified T Cells for the Immunotherapy of HER2-Positive Sarcoma	Journal of Clinical Oncology	Article	2015	719
2	Majzner et al (12)	CAR T Cells Targeting B7-H3, a Pan-Cancer Antigen, Demonstrate Potent Preclinical Activity Against Pediatric Solid Tumors and Brain Tumors	Clinical Cancer Research	Article	2019	301
3	Nakatsuka et al (13)	Immunohistochemical detection of WT1 protein in a variety of cancer cells	Modern Pathology	Article	2006	258
4	Bishop et al (14)	Future directions in the treatment of osteosarcoma	Current Opinion in Pediatrics	Review	2016	229
5	Koirala et al (15)	Immune infiltration and PD-L1 expression in the tumor microenvironment are prognostic in osteosarcoma	Scientific Reports	Article	2016	202
6	Zhou et al (16)	Single-cell RNA landscape of intratumoral heterogeneity and immunosuppressive microenvironment in advanced osteosarcoma	Nature Communications	Article	2020	187
7	Kager et al (17)	Novel insights and therapeutic interventions for pediatric osteosarcoma	Future Oncology	Review	2017	176
8	Lu et al (18)	Treatment of Patients with Metastatic Cancer Using a Major Histocompatibility Complex Class II-Restricted T-Cell Receptor Targeting the Cancer Germline Antigen MAGE-A3	Journal of Clinical Oncology	Article	2017	172
9	Chen et al (19)	Immunotherapy for osteosarcoma: Fundamental mechanism, rationale, and recent breakthroughs	Cancer Letters	Review	2021	161
10	Travis et al (20)	IASLC Multidisciplinary Recommendations for Pathologic Assessment of Lung Cancer Resection Specimens After Neoadjuvant Therapy	Journal of Thoracic Oncology	Article	2020	174

TABLE 6 Top 15 keywords by frequency.

Rank	Keyword	Occurrence	Cluster	Centrality
1	osteosarcoma	378	2	0.05
2	immunotherapy	364	1	0.12
3	cancer	158	3	0.16
4	expression	137	2	0.11
5	survival	81	2	0.03
6	t-cell	78	1	0.10
7	chemotherapy	74	5	0.10
8	cell	73	2	0.06
9	sarcoma	63	1	0.01
10	therapy	62	3	0.05
11	prognosis	54	2	0.01
12	tumor microenvironment	53	2	0.02
13	high-grade osteosarcoma	52	1	0.08
14	open-label	52	1	0.02
15	tumor	52	3	0.02

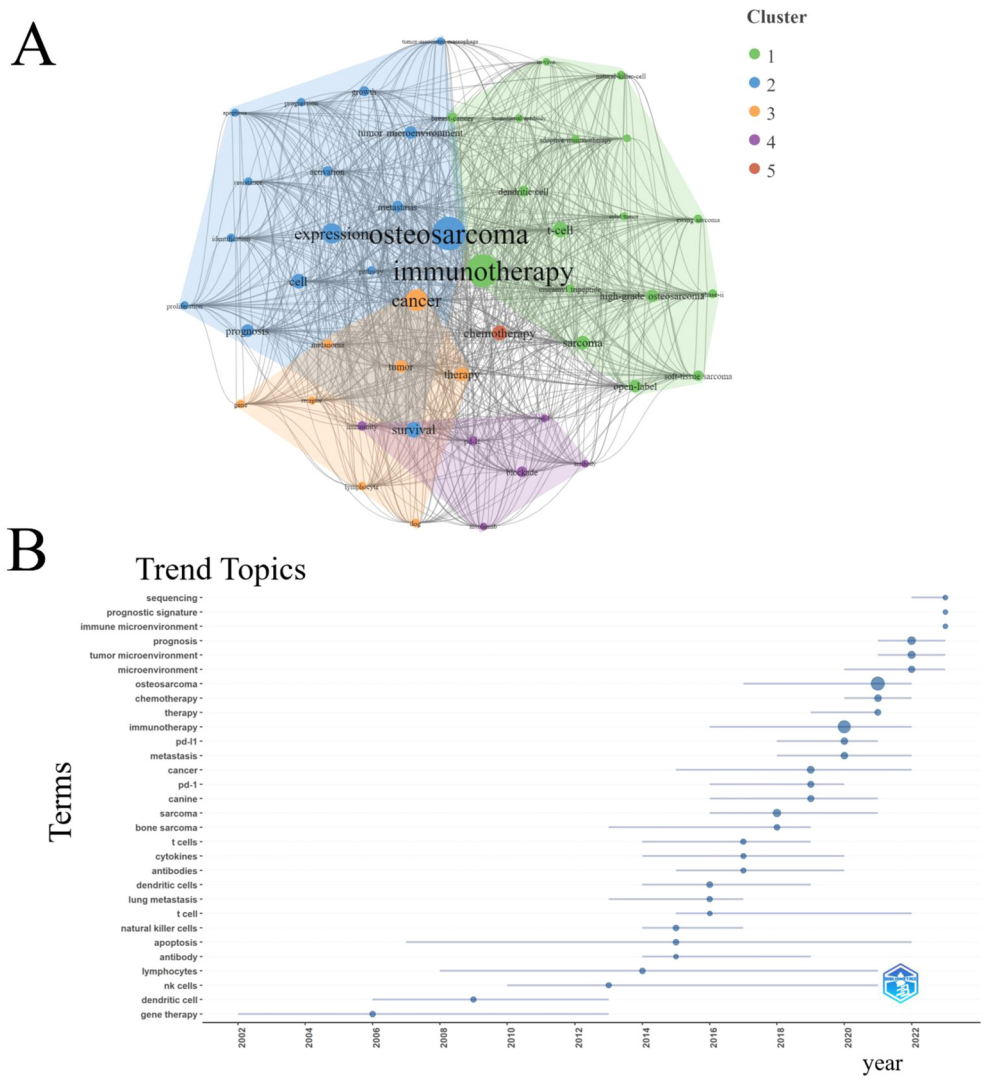

FIGURE 7
Analysis of keywords. **(A)** Clustering of the top 43 keywords with the highest number of occurrences. **(B)** Trend topics from 2000 to 2023.

Enhancing the patient's immune function

The human immune system is highly complex, with various immune cells and factors working together to defend against external threats such as infections and tumors. Tumor cells can escape immune surveillance through mechanisms such as antigen concealment, downregulation of human leukocyte antigen (HLA) expression, release of inhibitory cytokines, recruitment of Treg cells, generation of bone marrow-derived suppressor cells, and promotion of tumor-associated M2 macrophages (37, 38). Therefore, enhancing the patient's own immune function aims to eliminate tumor immune escape and reawaken the recognition of tumor cells by the body's immune system, ultimately leading to tumor cell clearance.

Tumor vaccines

Tumor vaccines aim to induce an anti-tumor immune response in the human body by exposing tumor antigens. Currently, the most mature technology for tumor vaccines is the cervical cancer vaccine. Cervical cancer is predominantly induced by human papillomavirus (HPV), so cervical cancer vaccines are divided into preventive vaccines (targeting HPV infection) and therapeutic vaccines (exposing tumor antigens) (39, 40). Dendritic cell (DC) vaccines, as the main type of tumor vaccine, have been applied in various types of tumor treatment to eliminate tumor cells in refractory tumors. DC vaccines are commonly used in osteosarcoma treatment (41, 42).

Enhancing innate immunity

Recently, the role of innate immune cells in controlling tumor progression has been established. Innate immunity inhibits tumor progression by directly recognizing and killing tumor cells and triggering a strong adaptive immune response (43, 44). The cyclic GMP-AMP synthase-stimulator of interferon genes (cGAS-STING) pathway has gained significant attention due to its ability to activate

the production of type I interferon, thereby enhancing anti-tumor immune responses (45). The application of STING (DMXAA, CDN, MSA-2, etc.) agonists in the treatment of osteosarcoma may be an effective strategy (46).

Improving the tumor microenvironment

The occurrence and development of tumors are closely related to changes in the surrounding tumor tissue environment, which occurs simultaneously. Tumor cells functionally shape the tumor microenvironment by secreting various cytokines, chemokines, and other factors. This microenvironment, in turn, influences the occurrence and development of tumors, known as the tumor microenvironment. The tumor microenvironment consists of various cells (such as macrophages, neutrophils, dendritic cells, bone marrow-derived suppressor cells, NK cells, T cells, B cells, tumor-associated fibroblasts) and abundant extracellular matrix (such as collagen, fibronectin, laminin, proteoglycans), as well as various cytokines (such as IL-1β, IL-6, IFN-γ, TGF-β) (47–49). Research on the tumor microenvironment of osteosarcoma has been ongoing, and in recent years, numerous studies have demonstrated that osteosarcoma-derived extracellular vesicle (EV) play a significant role in promoting widespread immune suppression. These EV can inhibit the activity of T cells and NK cells through various pathways, and can even induce T cell apoptosis. Furthermore, they enhance the activity of bone marrow-derived suppressor cells (MDSCs) to support immune evasion by osteosarcoma cells. These research findings highlight the importance of immune suppression mechanisms in the osteosarcoma microenvironment and provide new insights for the development of therapeutic strategies targeting this microenvironment (50).

Immune check point inhibitors

In recent years, researchers have developed targeted antibodies against cytotoxic T-lymphocyte-associated antigen 4 (CTLA-4) and programmed cell death protein 1 (PD-1) or its ligand PD-L1. These immune checkpoint inhibitors have shown promising therapeutic effects in malignant tumors such as melanoma, lung cancer (51–53). PD-1/PD-L1 as immune therapy targets have ushered in a new era of immunotherapy and accelerated research on immune treatment for osteosarcoma. Studies have shown that blocking the interaction between PD-1 and PD-L1 with antibodies significantly improves the responsiveness of osteosarcoma to cytotoxic T lymphocytes (CTLs), leading to reduced tumor burden and increased survival rates in mouse models of metastatic osteosarcoma (54). Koirala et al (15) reported a significant association between PD-L1 expression and the presence of T cells, dendritic cells, and natural killer cells in osteosarcoma. While all examined immune cell types were present in osteosarcoma samples, only infiltration of dendritic cells (28.3% vs. 83.9%, $p = 0.001$) and macrophages (45.5% vs. 84.4%, $p = 0.031$) was correlated with worse five-year event-free survival (EFS). Furthermore, PD-L1 expression was significantly associated with poorer five-year EFS (25.0% vs. 69.4%, $p = 0.014$). In addition, blockade of the PD-1/PD-L1 axis has also been shown to enhance the chemotherapeutic efficacy of cisplatin in osteosarcoma (55). However, there are differing opinions as well. Le et al. conducted a phase II clinical trial in 17 patients with advanced osteosarcoma and found a progression-free survival rate of only 13.3% at 6 months. They concluded that the efficacy of PD-1 inhibition in immunotherapy for osteosarcoma is limited (56). CTLA-4 is expressed on the surface of regulatory T cells (Tregs) and memory T cells. Overexpression of CTLA-4 can competitively inhibit the CD28 co-stimulatory signal required for optimal T cell activation, leading to a loss of anti-cancer activity. Additionally, binding of CTLA-4 to CD80/86 on dendritic cells can result in functional suppression of dendritic cells (57).Ipilimumab, a monoclonal antibody targeting CTLA-4 developed in 2011, was approved by the U.S. Food and Drug Administration (FDA) as the first-line immunotherapy for the treatment of melanoma (58). A phase I clinical trial demonstrated that 25% of osteosarcoma patients achieved disease stabilization following treatment with ipilimumab (59).

Exogenous immune effector cells targeting osteosarcoma tissue

Enhancement of patient immune function through the infusion of immune cells, also known as adoptive cell-transfer therapy (ACT), is a primary approach for augmenting immune function (60). Tumor cells may downregulate the expression of their own HLA and tumor antigens, rendering them unrecognizable by T cells. Engineered T cells with high affinity for tumor-specific antigens, known as chimeric antigen receptor T cells (CAR-T cells) can recognize tumor cells independent of HLA presentation (61, 62). CAR-T cells have undergone extensive clinical trials for the treatment of hematological malignancies, achieving significant breakthroughs. In a clinical trial, CD22 CAR-T cells demonstrated an 80% response rate (24/30 patients) in the treatment of refractory or relapsed B-cell acute lymphoblastic leukemia, providing a valuable window of time for subsequent hematopoietic stem cell transplantation (63). Majzner et al (12) discovered that B7-H3 CAR T cells exhibited significant antitumor activity *in vivo*, leading to the regression of established solid tumors in xenograft models, including osteosarcoma, medulloblastoma, and Ewing sarcoma. Their findings revealed that the effectiveness of B7-H3 CAR T cells relied heavily on the high density of the target antigen on tumor tissues. Conversely, the activity of these CAR T cells was substantially reduced against target cells expressing low levels of the antigen. This observation suggests the potential for a therapeutic window, despite the low-level expression of B7-H3 in normal tissues. In osteosarcoma, primary bone tumors typically exhibit low mutation burden and are accompanied by rare naturally occurring anti-tumor T cells. Therefore, CAR-T cell therapy may be an effective strategy (64). Other adoptive cell transfer therapy approaches include CAR-NK cells and CAR-tumor infiltrating lymphocytes (TILs). Unlike T cells, NK cells are innate immune cells with cytotoxic and immunoregulatory functions (65, 66).

Since the 1970s, although there has been some improvement in the overall treatment of osteosarcoma, the therapeutic options remain limited, particularly for recurrent and metastatic osteosarcoma. Osteosarcoma cannot be cured with a single treatment. Experts

from the SARC028 clinical trial indicate that resistance to immunotherapy may stem from PTEN inactivation, resulting in hyperactivation of the PI3K-AKT pathway. This highlights the necessity of a combination treatment strategy (67). Surgical interventions and conventional chemotherapy often yield unsatisfactory results (68, 69). In recent years, the rapid advancement of immunotherapy techniques, methods, and new drugs has brought new opportunities for the stagnant field of osteosarcoma treatment (70, 71). However, these opportunities come with challenges. Many preclinical studies suggest that immunotherapy may benefit osteosarcoma patients, but clinical trials of single-agent therapies often yield disappointing results, hindering effective treatment. Several promising drugs have faced setbacks, primarily because trials included advanced cases of osteosarcoma that had relapsed or metastasized after conventional chemotherapy. In such cases, patients often have severely compromised immune systems, limiting immunotherapy's effectiveness. Additionally, the immune microenvironment in tumor patients is complex and dynamic, with tumor cells employing various mechanisms to evade immune therapies, making single-agent approaches often ineffective (36, 72). Meazza et al. confirmed the significance of complete surgical remission and noted a promising (though improvable) survival rate in this patient cohort, highlighting a potential role for immunotherapy using IL-2 and LAK/NK cell activation (73). Boye et al. conducted a phase 2 study of pembrolizumab in advanced osteosarcoma, which was well-tolerated but showed no significant antitumor activity. Future trials should explore combination strategies with immunomodulatory agents in patients selected by molecular response profiles (74). Tang et al. conducted a study showing that amrelizumab combined with adriamycin, cisplatin, methotrexate, and ifosfamide in neoadjuvant treatment for resectable osteosarcoma was safe and tolerable. While this combination may not enhance tumor necrosis rate (TNR), the long-term survival benefits require further investigation (75). Wang et al. found that co-delivering a gel with the αPD-1 checkpoint inhibitor significantly enhances effectiveness in an orthotopic osteosarcoma model. Immunophenotyping data indicate a notable increase in T-cell infiltration and improved anti-tumor immunity at the whole-animal level (76). These findings highlight the necessity for combination therapies that integrate various immunotherapeutic approaches along with surgery, chemotherapy, targeted small molecules, and other novel treatments to create optimal treatment regimens. This strategy is crucial for achieving breakthroughs in the comprehensive treatment of osteosarcoma patients. Numerous clinical trials based on this approach have yielded promising results. Additionally, challenges such as personalized immunotherapy selection, immunotherapy resistance, and drug toxicity should also be addressed (Figure 8).

Strength and limitations

This study presents a comprehensive bibliometric review of the field of immunotherapy for osteosarcoma, encompassing an

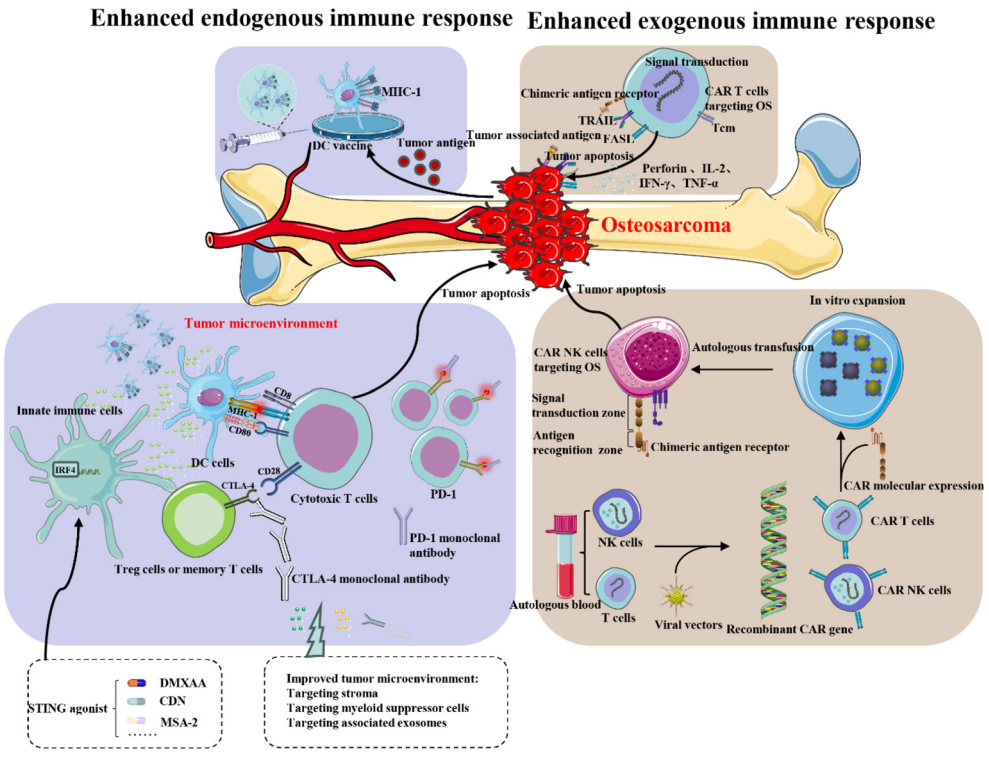

FIGURE 8
Targeted immunotherapy for osteosarcoma. The application of immunotherapy in osteosarcoma primarily involves two aspects: enhancing the patient's own immune system response to the tumor and exogenously boosting the immune function of the patient. OS, osteosarcoma; MHC-I, major histocompatibility complex; DC cells, dendrite cells; Tcm, central memory T cell.

evaluation of its overall scope, advancements, significant contributions, and emerging trends. Researchers are advised to prioritize recent and highly cited references and topics of interest. However, it is important to acknowledge certain limitations in this bibliometric analysis. Our data source relies solely on Web of Science (WOS), primarily due to the compatibility of bibliometric tools and the feasibility of data processing. We previously considered merging data from multiple databases, such as Scopus, MEDLINE, and Cochrane, to enhance literature coverage. However, we encountered several significant challenges during implementation: differences in citation data formats, the complexity of data deduplication, insufficient tool compatibility, and high resource and time costs. Still, it is worth noting that our analysis was limited to articles exclusively sourced from the WoS Core Collection, potentially limiting the breadth of our findings. Furthermore, the exclusion of recently published articles may be attributed to a temporal delay. Lastly, despite the algorithm's objective execution of the analysis, we observed an inherent subjective bias in the interpretation of the data.

Conclusion and future perspectives

The field of immunotherapy for osteosarcoma has undergone significant evolution over time, revealing a notable trend. Notably, China emerged as the leading contributor. Among institutions, Zhejiang University exhibited the highest level of productivity. The author with the highest publication output was Tsukahara, Tomohide from Japan. The article with the most citation was "DOI: 10.1200/JCO.2014.58.0225". Frontiers in Immunology emerged as the most productive journal. The most frequently occurring keywords in ITFOS research include "osteosarcoma," "immunotherapy," and "cancer." Furthermore, "sequencing," "prognostic signature,". and "immune microenvironment" have been identified as emerging research frontiers for the future. To drive notable progress in the comprehensive treatment of osteosarcoma patients, the incorporation of multifaceted therapeutic approaches is imperative. This entails the integration of combination therapies that encompass multiple immunotherapeutic modalities, alongside the inclusion of surgical interventions, chemotherapy, targeted small molecule drugs, and novel therapeutic strategies. The strategic amalgamation of these diverse treatment modalities is poised to have a pivotal impact on advancing the field of osteosarcoma treatment.

Data availability statement

The original contributions presented in the study are included in the article/supplementary material. Further inquiries can be directed to the corresponding author.

Author contributions

YH: Conceptualization, Supervision, Visualization, Writing – original draft, Writing – review & editing. RY: Investigation, Software, Supervision, Writing – original draft. SN: Methodology, Project administration, Supervision, Validation, Writing – original draft. ZS: Investigation, Resources, Writing – original draft.

Funding

The author(s) declare that no financial support was received for the research, authorship, and/or publication of this article.

Conflict of interest

The authors declare that the research was conducted in the absence of any commercial or financial relationships that could be construed as a potential conflict of interest.

Publisher's note

All claims expressed in this article are solely those of the authors and do not necessarily represent those of their affiliated organizations, or those of the publisher, the editors and the reviewers. Any product that may be evaluated in this article, or claim that may be made by its manufacturer, is not guaranteed or endorsed by the publisher.

References

1. Siegel RL, Miller KD, Jemal A. Cancer statistics, 2018. *CA Cancer J Clin*. (2018) 68:7–30. doi: 10.3322/caac.21442

2. Cersosimo F, Lonardi S, Bernardini G, Telfer B, Mandelli GE, Santucci A, et al. Tumor-associated macrophages in osteosarcoma: from mechanisms to therapy. *Int J Mol Sci*. (2020) 21:5207. doi: 10.3390/ijms21155207

3. Choi JH, Ro JY. The 2020 WHO classification of tumors of bone: an updated review. *Adv Anat Pathol*. (2021) 28:119–38. doi: 10.1097/PAP.0000000000000293

4. Jiang ZY, Liu JB, Wang XF, Ma YS, Fu D. Current status and prospects of clinical treatment of osteosarcoma. *Technol Cancer Res Treat*. (2022) 21:15330338221124696. doi: 10.1177/15330338221124696

5. Meyers PA, Healey JH, Chou AJ, Wexler LH, Merola PR, Morris CD, et al. Addition of pamidronate to chemotherapy for the treatment of osteosarcoma. *Cancer*. (2011) 117:1736–44. doi: 10.1002/cncr.v117.8

6. Patil NS, Nabet BY, Müller S, Koeppen H, Zou W, Giltnane J, et al. Intratumoral plasma cells predict outcomes to PD-L1 blockade in non-small cell lung cancer. *Cancer Cell*. (2022) 40:289–300.e284. doi: 10.1136/jitc-2022-SITC2022.0435

7. Mahoney KM, Freeman GJ, McDermott DF. The next immune-checkpoint inhibitors: PD-1/PD-L1 blockade in melanoma. *Clin Ther*. (2015) 37:764–82. doi: 10.1016/j.clinthera.2015.02.018

8. Zhang R, Yang Y, Dong W, Lin M, He J, Zhang X, et al. D-mannose facilitates immunotherapy and radiotherapy of triple-negative breast cancer via degradation of PD-L1. *Proc Natl Acad Sci U S A*. (2022) 119:e2114851119. doi: 10.1073/pnas.2114851119

9. Liu B, He X, Wang Y, Huang JW, Zheng YB, Li Y, et al. Bibliometric analysis of γδ T cells as immune regulators in cancer prognosis. *Front Immunol*. (2022) 13:874640. doi: 10.3389/fimmu.2022.874640

10. Xu Y, Jiang Z, Kuang X, Chen X, Liu H. Research trends in immune checkpoint blockade for melanoma: visualization and bibliometric analysis. *J Med Internet Res*. (2022) 24:e32728. doi: 10.2196/32728

11. Ahmed N, Brawley VS, Hegde M, Robertson C, Ghazi A, Gerken C, et al. Human epidermal growth factor receptor 2 (HER2) -specific chimeric antigen receptor-modified T cells for the immunotherapy of HER2-positive sarcoma. *J Clin Oncol*. (2015) 33:1688–96. doi: 10.1200/JCO.2014.58.0225

12. Majzner RG, Theruvath JL, Nellan A, Heitzeneder S, Cui Y, Mount CW, et al. CAR T cells targeting B7-H3, a pan-cancer antigen, demonstrate potent preclinical activity against pediatric solid tumors and brain tumors. *Clin Cancer Res*. (2019) 25:2560–74. doi: 10.1158/1078-0432.CCR-18-0432

13. Nakatsuka S, Oji Y, Horiuchi T, Kanda T, Kitagawa M, Takeuchi T, et al. Immunohistochemical detection of WT1 protein in a variety of cancer cells. *Mod Pathol*. (2006) 19:804–14. doi: 10.1038/modpathol.3800588

14. Bishop MW, Janeway KA, Gorlick R. Future directions in the treatment of osteosarcoma. *Curr Opin Pediatr*. (2016) 28:26–33. doi: 10.1097/MOP.0000000000000298

15. Koirala P, Roth ME, Gill J, Piperdi S, Chinai JM, Geller DS, et al. Immune infiltration and PD-L1 expression in the tumor microenvironment are prognostic in osteosarcoma. *Sci Rep*. (2016) 6:30093. doi: 10.1038/srep30093

16. Zhou Y, Yang D, Yang Q, Lv X, Huang W, Zhou Z, et al. Single-cell RNA landscape of intratumoral heterogeneity and immunosuppressive microenvironment in advanced osteosarcoma. *Nat Commun*. (2020) 11:6322. doi: 10.1038/s41467-020-20059-6

17. Kager L, Tamamyan G, Bielack S. Novel insights and therapeutic interventions for pediatric osteosarcoma. *Future Oncol*. (2017) 13:357–68. doi: 10.2217/fon-2016-0261

18. Lu YC, Parker LL, Lu T, Zheng Z, Toomey MA, White DE, et al. Treatment of patients with metastatic cancer using a major histocompatibility complex class II-restricted T-cell receptor targeting the cancer germline antigen MAGE-A3. *J Clin Oncol*. (2017) 35:3322–9. doi: 10.1200/JCO.2017.74.5463

19. Chen C, Xie L, Ren T, Huang Y, Xu J, Guo W. Immunotherapy for osteosarcoma: Fundamental mechanism, rationale, and recent breakthroughs. *Cancer Lett*. (2021) 500:1–10. doi: 10.1016/j.canlet.2020.12.024

20. Travis WD, Dacic S, Wistuba I, Sholl L, Adusumilli P, Bubendorf L, et al. IASLC multidisciplinary recommendations for pathologic assessment of lung cancer resection specimens after neoadjuvant therapy. *J Thorac Oncol*. (2020) 15:709–40. doi: 10.1016/j.jtho.2020.01.005

21. Corre I, Verrecchia F, Crenn V, Redini F, Trichet V. The osteosarcoma microenvironment: A complex but targetable ecosystem. *Cells*. (2020) 9:976. doi: 10.3390/cells9040976

22. Wu CC, Beird HC, Andrew Livingston J, Advani S, Mitra A, Cao S, et al. Immuno-genomic landscape of osteosarcoma. *Nat Commun*. (2020) 11:1008. doi: 10.1038/s41467-020-14646-w

23. Harrison DJ, Geller DS, Gill JD, Lewis VO, Gorlick R. Current and future therapeutic approaches for osteosarcoma. *Expert Rev Anticancer Ther*. (2018) 18:39–50. doi: 10.1080/14737140.2018.1413939

24. Coley WB. II. Contribution to the knowledge of sarcoma. *Ann Surg*. (1891) 14:199–220. doi: 10.1097/00000658-189112000-00015

25. Sutherland TE, Dyer DP, Allen JE. The extracellular matrix and the immune system: A mutually dependent relationship. *Science*. (2023) 379:eabp8964. doi: 10.1126/science.abp8964

26. Panez-Toro I, Muñoz-García J, Vargas-Franco JW, Renodon-Cornière A, Heymann MF, Lézot F, et al. Advances in osteosarcoma. *Curr Osteoporos Rep*. (2023) 21:330–43. doi: 10.1007/s11914-023-00803-9

27. Park JA, Cheung NV. Promise and challenges of T cell immunotherapy for osteosarcoma. *Int J Mol Sci*. (2023) 24:12520. doi: 10.3390/ijms241512520

28. Li H, Sui X, Wang Z, Fu H, Wang Z, Yuan M, et al. A new antisarcoma strategy: multisubtype heat shock protein/peptide immunotherapy combined with PD-L1 immunological checkpoint inhibitors. *Clin Transl Oncol*. (2021) 23:1688–704. doi: 10.1007/s12094-021-02570-4

29. Zhong C, Yang D, Zhong L, Xie W, Sun G, Jin D, et al. Single-cell and bulk RNA sequencing reveals Anoikis related genes to guide prognosis and immunotherapy in osteosarcoma. *Sci Rep*. (2023) 13:20203. doi: 10.1038/s41598-023-47367-3

30. Huang Y, Cao D, Zhang M, Yang Y, Niu G, Tang L, et al. Exploring the impact of PDGFD in osteosarcoma metastasis through single-cell sequencing analysis. *Cell Oncol (Dordr)*. (2024) 47:1715–33. doi: 10.1007/s13402-024-00949-3

31. Li Z, Xue Y, Huang X, Xiao G. Stratifying osteosarcoma patients using an epigenetic modification-related prognostic signature: implications for immunotherapy and chemotherapy selection. *Transl Cancer Res*. (2024) 13:3556–74. doi: 10.21037/tcr-23-2300

32. Chen W, Liao Y, Sun P, Tu J, Zou Y, Fang J, et al. Construction of an ER stress-related prognostic signature for predicting prognosis and screening the effective anti-tumor drug in osteosarcoma. *J Transl Med*. (2024) 22:66. doi: 10.1186/s12967-023-04794-0

33. Cillo AR, Mukherjee E, Bailey NG, Onkar S, Daley J, Salgado C, et al. Ewing sarcoma and osteosarcoma have distinct immune signatures and intercellular communication networks. *Clin Cancer Res*. (2022) 28:4968–82. doi: 10.1158/1078-0432.CCR-22-1471

34. Wu C, Gong S, Duan Y, Deng C, Kallendrusch S, Berninghausen L, et al. A tumor microenvironment-based prognostic index for osteosarcoma. *J BioMed Sci*. (2023) 30:23. doi: 10.1186/s12929-023-00917-3

35. Zhang Y, Gan W, Ru N, Xue Z, Chen W, Chen Z, et al. Comprehensive multi-omics analysis reveals m7G-related signature for evaluating prognosis and immunotherapy efficacy in osteosarcoma. *J Bone Oncol*. (2023) 40:100481. doi: 10.1016/j.jbo.2023.100481

36. Wu C, Tan J, Shen H, Deng C, Kleber C, Osterhoff G, et al. Exploring the relationship between metabolism and immune microenvironment in osteosarcoma based on metabolic pathways. *J BioMed Sci*. (2024) 31:4. doi: 10.1186/s12929-024-00999-7

37. Li W, Hao Y, Zhang X, Xu S, Pang D. Targeting RNA N(6)-methyladenosine modification: a precise weapon in overcoming tumor immune escape. *Mol Cancer*. (2022) 21:176. doi: 10.1186/s12943-022-01652-3

38. Yuan Z, Li Y, Zhang S, Wang X, Dou H, Yu X, et al. Extracellular matrix remodeling in tumor progression and immune escape: from mechanisms to treatments. *Mol Cancer*. (2023) 22:48. doi: 10.1186/s12943-023-01744-8

39. Wang R, Pan W, Jin L, Huang W, Li Y, Wu D, et al. Human papillomavirus vaccine against cervical cancer: Opportunity and challenge. *Cancer Lett*. (2020) 471:88–102. doi: 10.1016/j.canlet.2019.11.039

40. Li M, Zhao C, Zhao Y, Li J, Wei L. Immunogenicity, efficacy, and safety of human papillomavirus vaccine: Data from China. *Front Immunol*. (2023) 14:1112750. doi: 10.3389/fimmu.2023.1112750

41. Dyson KA, Stover BD, Grippin A, Mendez-Gomez HR, Lagmay J, Mitchell DA, et al. Emerging trends in immunotherapy for pediatric sarcomas. *J Hematol Oncol*. (2019) 12:78. doi: 10.1186/s13045-019-0756-z

42. Sun C, Ma X, Zhou C, Zhang Z, Guo J. Irreversible electroporation combined with dendritic cell-based vaccines for the treatment of osteosarcoma. *Anticancer Res*. (2023) 43:3389–400. doi: 10.21873/anticanres.16514

43. Cui J, Chen Y, Wang HY, Wang RF. Mechanisms and pathways of innate immune activation and regulation in health and cancer. *Hum Vaccin Immunother*. (2014) 10:3270–85. doi: 10.4161/21645515.2014.979640

44. Woo SR, Corrales L, Gajewski TF. Innate immune recognition of cancer. *Annu Rev Immunol*. (2015) 33:445–74. doi: 10.1146/annurev-immunol-032414-112043

45. Pu F, Chen F, Liu J, Zhang Z, Shao Z. Immune regulation of the cGAS-STING signaling pathway in the tumor microenvironment and its clinical application. *Onco Targets Ther*. (2021) 14:1501–16. doi: 10.2147/OTT.S298958

46. Withers SS, Moeller CE, Quick CN, Liu CC, Baham SM, Looper JS, et al. Effect of stimulator of interferon genes (STING) signaling on radiation-induced chemokine expression in human osteosarcoma cells. *PLoS One*. (2023) 18:e0284645. doi: 10.1371/journal.pone.0284645

47. Mao X, Xu J, Wang W, Liang C, Hua J, Liu J, et al. Crosstalk between cancer-associated fibroblasts and immune cells in the tumor microenvironment: new findings and future perspectives. *Mol Cancer*. (2021) 20:131. doi: 10.1186/s12943-021-01428-1

48. Lei X, Lei Y, Li JK, Du WX, Li RG, Yang J, et al. Immune cells within the tumor microenvironment: Biological functions and roles in cancer immunotherapy. *Cancer Lett*. (2020) 470:126–33. doi: 10.1016/j.canlet.2019.11.009

49. Kao KC, Vilbois S, Tsai CH, Ho PC. Metabolic communication in the tumour-immune microenvironment. *Nat Cell Biol*. (2022) 24:1574–83. doi: 10.1038/s41556-022-01002-x

50. Pu F, Chen F, Zhang Z, Liu J, Shao Z. Information transfer and biological significance of neoplastic exosomes in the tumor microenvironment of osteosarcoma. *Onco Targets Ther*. (2020) 13:8931–40. doi: 10.2147/OTT.S266835

51. Willsmore ZN, Coumbe BGT, Crescioli S, Reci S, Gupta A, Harris RJ, et al. Combined anti-PD-1 and anti-CTLA-4 checkpoint blockade: Treatment of melanoma and immune mechanisms of action. *Eur J Immunol*. (2021) 51:544–56. doi: 10.1002/eji.202048747

52. Reda M, Ngamcherdtrakul W, Nelson MA, Siriwon N, Wang R, Zaidan HY, et al. Development of a nanoparticle-based immunotherapy targeting PD-L1 and PLK1 for lung cancer treatment. *Nat Commun*. (2022) 13:4261. doi: 10.1038/s41467-022-31926-9

53. Campbell KM, Amouzgar M, Pfeiffer SM, Howes TR, Medina E, Travers M, et al. Prior anti-CTLA-4 therapy impacts molecular characteristics associated with anti-PD-1 response in advanced melanoma. *Cancer Cell*. (2023) 41:791–806.e794. doi: 10.1016/j.ccell.2023.03.010

54. Lussier DM, O'Neill L, Nieves LM, McAfee MS, Holechek SA, Collins AW, et al. Enhanced T-cell immunity to osteosarcoma through antibody blockade of PD-1/PD-L1 interactions. *J Immunother*. (2015) 38:96–106. doi: 10.1097/CJI.0000000000000065

55. Liu X, He S, Wu H, Xie H, Zhang T, Deng Z. Blocking the PD-1/PD-L1 axis enhanced cisplatin chemotherapy in osteosarcoma *in vitro* and *in vivo*. *Environ Health Prev Med*. (2019) 24:79. doi: 10.1186/s12199-019-0835-3

56. Le Cesne A, Marec-Berard P, Blay JY, Gaspar N, Bertucci F, Penel N, et al. Programmed cell death 1 (PD-1) targeting in patients with advanced osteosarcomas: results from the PEMBROSARC study. *Eur J Cancer*. (2019) 119:151–7. doi: 10.1016/j.ejca.2019.07.018

57. Kim GR, Choi JM. Current understanding of cytotoxic T lymphocyte antigen-4 (CTLA-4) signaling in T-cell biology and disease therapy. *Mol Cells*. (2022) 45:513–21. doi: 10.14348/molcells.2022.2056

58. Wolchok JD, Neyns B, Linette G, Negrier S, Lutzky J, Thomas L, et al. Ipilimumab monotherapy in patients with pretreated advanced melanoma: a randomised, double-blind, multicentre, phase 2, dose-ranging study. *Lancet Oncol*. (2010) 11:155–64. doi: 10.1016/S1470-2045(09)70334-1

59. Merchant MS, Wright M, Baird K, Wexler LH, Rodriguez-Galindo C, Bernstein D, et al. Phase I clinical trial of ipilimumab in pediatric patients with advanced solid tumors. *Clin Cancer Res*. (2016) 22:1364–70. doi: 10.1158/1078-0432.CCR-15-0491

60. Inozume T. Adoptive cell transfer therapy for melanoma. *Exp Dermatol*. (2023) 32:250–5. doi: 10.1111/exd.14707

61. Pan K, Farrukh H, Chittepu V, Xu H, Pan CX, Zhu Z. CAR race to cancer immunotherapy: from CAR T, CAR NK to CAR macrophage therapy. *J Exp Clin Cancer Res*. (2022) 41:119. doi: 10.1186/s13046-022-02327-z

62. Chohan KL, Siegler EL, Kenderian SS. CAR-T cell therapy: the efficacy and toxicity balance. *Curr Hematol Malig Rep*. (2023) 18:9–18. doi: 10.1007/s11899-023-00687-7

63. Pan J, Niu Q, Deng B, Liu S, Wu T, Gao Z, et al , et al. CD22 CAR T-cell therapy in refractory or relapsed B acute lymphoblastic leukemia. *Leukemia*. (2019) 33:2854–66. doi: 10.1038/s41375-019-0488-7

64. Zhang Q, Zhang Z, Liu G, Li D, Gu Z, Zhang L, et al. B7-H3 targeted CAR-T cells show highly efficient anti-tumor function against osteosarcoma both *in vitro* and *in vivo*. *BMC Cancer*. (2022) 22:1124. doi: 10.1186/s12885-022-10229-8

65. Quamine AE, Olsen MR, Cho MM, Capitini CM. Approaches to enhance natural killer cell-based immunotherapy for pediatric solid tumors. *Cancers (Basel)*. (2021) 13:2796. doi: 10.3390/cancers13112796

66. Lu Y, Zhang J, Chen Y, Kang Y, Liao Z, He Y, et al. Novel immunotherapies for osteosarcoma. *Front Oncol*. (2022) 12:830546. doi: 10.3389/fonc.2022.830546

67. Tawbi HA, Burgess M, Bolejack V, Van Tine BA, Schuetze SM, Hu J, et al. Pembrolizumab in advanced soft-tissue sarcoma and bone sarcoma (SARC028): a multicentre, two-cohort, single-arm, open-label, phase 2 trial. *Lancet Oncol*. (2017) 18:1493–501. doi: 10.1016/S1470-2045(17)30624-1

68. Bielack SS, Smeland S, Whelan JS, Marina N, Jovic G, Hook JM, et al. Methotrexate, doxorubicin, and cisplatin (MAP) plus maintenance pegylated interferon alfa-2b versus MAP alone in patients with resectable high-grade osteosarcoma and good histologic response to preoperative MAP: first results of the EURAMOS-1 good response randomized controlled trial. *J Clin Oncol*. (2015) 33:2279–87. doi: 10.1200/JCO.2014.60.0734

69. Blay JY, Penel N, Toulmonde M, Valentine T, Chaigneauf L, Rios M, et al. Long term survival in adult osteosarcoma patients treated with a two-drug regimen: Final results of the OSAD93 phase II study of the FSG-GETO. *Eur J Cancer*. (2024) 208:114228. doi: 10.1016/j.ejca.2024.114228

70. Xie L, Liang X, Xu J, Liu K, Sun K, Li Y, et al. Exploratory study of an anti-PD-L1/TGF-β antibody, TQB2858, in patients with refractory or recurrent osteosarcoma and alveolar soft part sarcoma: a report from Chinese sarcoma study group (TQB2858-Ib-02). *BMC Cancer*. (2023) 23:868. doi: 10.1186/s12885-023-11390-4

71. Zhou Y, Li M, Zhang B, Yang C, Wang Y, Zheng S, et al. A pilot study of multi-antigen stimulated cell therapy-I plus camrelizumab and apatinib in patients with advanced bone and soft-tissue sarcomas. *BMC Med*. (2023) 21:470. doi: 10.1186/s12916-023-03132-x

72. Zhu T, Han J, Yang L, Cai Z, Sun W, Hua Y, et al. Immune microenvironment in osteosarcoma: components, therapeutic strategies and clinical applications. *Front Immunol*. (2022) 13:907550. doi: 10.3389/fimmu.2022.907550

73. Meazza C, Cefalo G, Massimino M, Daolio P, Pastorino U, Scanagatta P, et al. Primary metastatic osteosarcoma: results of a prospective study in children given chemotherapy and interleukin-2. *Med Oncol*. (2017) 34:191. doi: 10.1007/s12032-017-1052-9

74. Boye K, Longhi A, Guren T, Lorenz S, Næss S, Pierini M, et al. Pembrolizumab in advanced osteosarcoma: results of a single-arm, open-label, phase 2 trial. *Cancer Immunol Immunother*. (2021) 70:2617–24. doi: 10.1007/s00262-021-02876-w

75. Tang Q, Zhang X, Zhu X, Xu H, Song G, Lu J, et al. Camrelizumab in combination with doxorubicin, cisplatin, ifosfamide, and methotrexate in neoadjuvant treatment of resectable osteosarcoma: A prospective, single-arm, exploratory phase II trial. *Cancer Med*. (2024) 13:e70206. doi: 10.1002/cam4.v13.18

76. Wang H, Chen Y, Wei R, Zhang J, Zhu J, Wang W, et al. Synergistic chemoimmunotherapy augmentation via sequential nanocomposite hydrogel-mediated reprogramming of cancer-associated fibroblasts in osteosarcoma. *Adv Mater*. (2024) 36:e2309591. doi: 10.1002/adma.202309591

frontiers | Frontiers in Oncology

TYPE Review
PUBLISHED 14 February 2025
DOI 10.3389/fonc.2024.1456959

OPEN ACCESS

EDITED BY
Tong-Chuan He,
University of Chicago Medicine, United States

REVIEWED BY
Yang Yang,
Affiliated Hospital of Nantong University, China
Guowei Zuo,
Chongqing Medical University, China

*CORRESPONDENCE
Qin Chen
chenq198101@163.com

RECEIVED 29 June 2024
ACCEPTED 24 December 2024
PUBLISHED 14 February 2025

CITATION
Ding Y and Chen Q (2025) Wnt/β-catenin signaling pathway: an attractive potential therapeutic target in osteosarcoma. *Front. Oncol.* 14:1456959. doi: 10.3389/fonc.2024.1456959

Wnt/β-catenin signaling pathway: an attractive potential therapeutic target in osteosarcoma

Yi Ding[1,2] and Qin Chen[1,2]*

[1]Department of Spine Surgery, Ganzhou People's Hospital, Ganzhou, China, [2]Department of Spine Surgery, Ganzhou Hospital-Nanfang Hospital, Southern Medical University, Ganzhou, China

Osteosarcoma (OS) is the most common bone malignancy in children and adolescents, and although current neoadjuvant chemotherapy has shown efficacy against OS, the long-term survival rate for patients with OS remains low, highlighting the need to find more effective treatments. In cancer cells, abnormal activation of signaling pathways can widely affect cell activity from growth and proliferation to apoptosis, invasion and metastasis. Wnt/β-catenin is a complex and unique signaling pathway that is considered to be one of the most important carcinogenic pathways in human cancer. Research have confirmed that the Wnt/β-catenin signaling pathway is an important driving factor for the occurrence and development of osteosarcoma, and abnormal activation of this pathway can promote the pathological processes of cell proliferation, invasion, migration, tumor angiogenesis and chemical resistance of osteosarcoma. However, inhibition of Wnt/β-catenin signaling pathway can effectively inhibit or reverse the above pathological processes. Therefore, manipulating the expression or function of the Wnt/β-catenin pathway may be a potential targeted pathway for the treatment of OS. In this review, we describe the characteristics of the Wnt/β-catenin signaling pathway and summarize the role and mechanism of this pathway in OS. This paper discusses the therapeutic significance of inhibiting or targeting Wnt/β-catenin pathway in OS and the shortcomings of current studies on this pathway in OS and the problems to be solved. This review helps us to understand the role of Wnt/β-catenin on OS, and provides a theoretical basis and new ideas for targeting Wnt/β-catenin pathway as a therapeutic target for OS.

KEYWORDS

osteosarcoma (OS), Wnt/β-catenin, targeted therapy, chemotherapy, mechanism

1 Introduction

Osteosarcoma (OS) is the most common aggressive malignant bone tumor in children and adolescents worldwide (1). It originates from the original transformed cells of mesenchymal origin and mainly affects the differentiation of osteoblasts and produces immature bone (2, 3). Although the exact cause of OS is not fully understood, it is clear that the development and pathogenesis of OS is associated with multiple factors, including age, sex, ethnicity, genetics, and familial factors (4). OS is characterized by locally aggressive growth and high metastatic potential (5, 6), characterized by local invasion of bone and soft tissue, loss of function of the affected limbs, and distant metastasis, most often to the lungs (7). At present, the main treatments for OS are surgery, radiotherapy, neoadjuvant chemotherapy and postoperative adjuvant chemotherapy and other multi-scientific and multi-mode treatments, but the therapeutic effect is not satisfactory. Due to the early onset of bone and lung metastasis of OS, the 5-year overall survival rate of OS patients with metastasis at diagnosis is less than 30% (8, 9). More importantly, due to the complexity of the progression mechanism of osteosarcoma, the etiology and molecular mechanism of the pathogenesis are still vague or unknown. Therefore, there is an urgent need to further understand the physiological and pathological mechanism of OS, develop more effective anti-OS agents and new therapeutic strategies to improve the symptoms of OS from the molecular pathological level, so as to improve the prognosis and quality of life of osteosarcoma patients.

Although the cause of OS has not been fully elucidated, there is a large amount of evidence that the disease is related to the dysregulation of various intracellular signaling pathways, especially the Wnt/β-catenin pathway (10). Wnt/β-catenin signaling pathway has been reported to be one of the most important carcinogenic pathways in almost all human cancers (11) and seems to be a good candidate for molecular therapies in malignant tumors (12, 13). The activation of Wnt/β-catenin signaling pathway is also associated with the occurrence, development and pathological mechanism of a variety of diseases, such as cancer, Alzheimer's disease, schizophrenia, diabetes and Parkinson's disease (14–17). It has been found that overactivation of Wnt/β-catenin signaling pathway plays a carcinogenic role in various sarcomas by driving cell cycle progression and increasing cell proliferation (18–20). It has been confirmed that Wnt/β-catenin pathway is over-activated in osteosarcoma (21), and abnormal activation of this pathway can promote pathological processes such as cell cycle, migration, invasion, angiogenesis, chemotherapy resistance and accelerate the occurrence and development of OS, while inhibition of Wnt/β-catenin pathway activity can effectively inhibit the above processes (22). Therefore, targeting Wnt/β-catenin could provide a new perspective for designing more effective drugs for the treatment of OS. In this review, we reviewed the biological characteristics of Wnt/β-catenin, the role and mechanism of Wnt/β-catenin in the pathological process of OS. This paper aims to provide evidence for the effect of Wnt/β-catenin signaling pathway activation on OS and the treatment of OS, and to emphasize the role of inhibiting Wnt/β-catenin pathway in delaying OS by clarifying the mechanism, so as to provide theoretical basis and new ideas for targeting Wnt/β-catenin pathway as therapeutic targets for OS.

2 Summary of Wnt/β-catenin signaling pathway

Wnt/β-catenin signaling is an evolutionarily conserved signal that regulates many important embryonic and somatic processes such as cell fate determination, organogenesis, tissue homeostasis, and various pathological states (23, 24). In addition, the abnormal regulation of this signal transduction is often closely related to many aspects of tumor occurrence and development, malignant transformation and recurrence (23, 25–27). Wnt signaling can be classified into classical or non-classical pathways, the classical pathway is involved in cell survival, proliferation, differentiation and migration, while the non-classical pathway regulates cell polarity and migration (28). However, most current studies on the Wnt pathway focus on the Wnt/β-catenin branch of the Wnt pathway, the disorder of which is associated with a variety of diseases (29).

2.1 Classic Wnt pathway

Classic Wnt pathway is a signal cascade mediated by β-catenin. The classical Wnt pathway is marked by the accumulation and translocation of the adherence-linked protein β-catenin in the nucleus. β-catenin is an Integral protein in the Wnt signaling pathway that regulates gene transcription and intercellular adhesion. Mutations in beta-catenin lead to amino acid substitution, resulting in inappropriate phosphorylation of the protein. Subsequently, ubiquitin ligase E3 does not correctly recognize the phosphorylated protein. Thus, dysregulation of the Wnt pathway leads to β-catenin accumulation without degradation and then transfer to the nucleus, thus activating transcription of oncogenes (30). Wnt is a secretory glycoprotein that binds to the cell surface transmembrane frizzled serpentine receptors (FZD) and low-density lipoprotein receptor-associated protein 5/6 (LRP5/6) complex, resulting in the accumulation of β-catenin in the nucleus, which leads to cell cycle activation and transcriptional regulation (31). FZD is the main binding site of Wnt (32), which mainly contains 7 transmembrane and extracellular N-terminal cysteine-rich domains (CRDS) (33, 34). However, in the absence of Wnt signaling, cytoplasmic β-catenin is degraded by β-catenin-destroying complexes such as Axin, adenomatous polyposis (APC), protein phosphatase 2A (PP2A), glycogen synthase kinase 3 (GSK3), and casein kinase 1α (CK1α). This results in the failure of the classical Wnt pathway (35, 36) (Figure 1).

2.2 Non-classical Wnt pathways

The non-classical pathway is often referred to as the beta-catenin-independent pathway, which can be further divided into the Wnt/Planar Cell polarity (PCP) pathway and the Wnt/Ca^{2+} pathway. In the

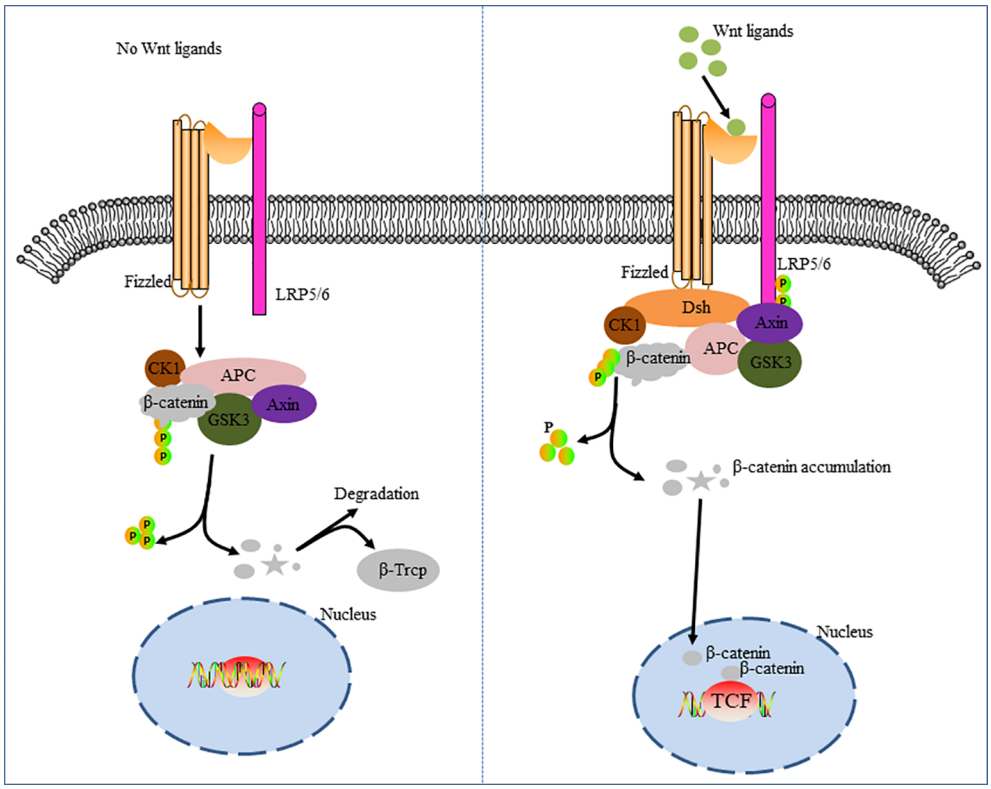

FIGURE 1
Classic Wnt/β-catenin pathway cascade diagram. The figure on the left shows the deactivation of the Wnt pathway. In the absence of Wnt signaling, β-catenin in the cytoplasm is recognized, folded, and phosphorylated by a destructive complex composed of scaffold proteins Axin, APC, GSK3β, and CK1, and targeted for degradation by a β-TRCP-mediated proteomic mechanism. The figure on the right shows activation of the Wnt pathway. The signal induces double phosphorylation of LRP6 by CK1 and GSK3-β via the Fizzled receptor and LRP5/6 co-receptor complex, which allows the axon-containing protein complex to transfer from the cytoplasm to the plasma membrane. Dsh is also recruited to the cell membrane and binds to Fizzied, and Axin binds to phosphorylated LRP5/6. The complex forms on the Fizzled/LRP5/6 membrane and induces stabilization of β-catenin by separating and/or degrading axons. β-catenin, which accumulates in the cytoplasm, translocates into the nucleus and, together with the transcription factor TCF, drives the expression of downstream target genes.

Wnt/PCP pathway, after the Wnt molecule binds to the receptor FZD, it recruits Dvl and further activates the small GTPases Rho and Rac, triggering the recruitment of downstream RHO-associated kinases (ROCK) and c-Jun N-terminal kinase (JNK), thereby allowing cytoskeletal recombination (Figure 2). In the Wnt/Ca^{2+} pathway, Dvl is activated when Wnt binds to FZD, and the activated Dvl recruits phospholipase C (PLC). PLC converts phosphatidylinositol 4, 5-diphosphate (PIP2) to diacylglycerol (DAG) and inositol 1,4, 5-triphosphate (IP3). IP3 stimulates the release of Ca^{2+} from the endoplasmic reticulum, and DAG and Ca^{2+} together activate downstream protein kinase C (PKC), calcineurin (CaN), and Ca^{2+}/calmodulin-dependent protein kinase II (CaMKII), thereby regulating intracellular calcium flux and downstream calcium-dependent cytoskeleton and/or transcriptional responses (Figure 3).

3 Expression of Wnt/β-catenin signaling pathway in OS

Research have confirmed that the Wnt/β-catenin signaling pathway is involved in the development of osteosarcoma, and the Wnt signaling pathway is abnormally activated in OS and plays a crucial role in tumorigenic and metastatic transmission (37, 38). Wnt-β-catenin pathway has been reported to be significantly higher in human OS tissues and cell lines than in normal tissues or osteoid osteomas (39, 40). In addition, the analysis of relevant patient samples found that Wnt/β-catenin level in osteosarcoma tissues was significantly higher than that in neighboring healthy tissues, and was associated with poor prognosis and lung metastasis and diffusion (41, 42). Haydon et al. found that 33 out of 47 OS samples had increased Wnt/β-catenin expression level accumulation (43).

4 Role of Wnt/beta - catenin pathway in OS

As an intracellular signaling pathway, Wnt/β-catenin pathway has been found in many types of cancer and plays an important regulatory role in the occurrence and development of tumors. Kinase analysis has identified active Wnt/β-catenin signaling in most OS cell lines (44). Wnt/β-catenin pathway is a complex signaling pathway, and its abnormal activation plays a key role in the pathogenesis of OS (45). A large amount of evidence has shown

that dysregulation of this pathway is involved in multiple pathological processes of OS, including tumor cell proliferation, invasion and metastasis, and chemical resistance (46, 47) (Figure 4).

4.1 Promote the proliferation of tumor cells

The autonomous growth of cancer cells is usually controlled by changes in the expression of growth factors or growth factor receptors, resulting in cell proliferation. Many studies have shown that abnormal activation of Wnt/β-catenin signaling pathway plays a crucial role in the occurrence and development of osteosarcoma (38, 48, 49). Cell proliferation is an important feature of tumorigenesis and development, and also an important factor leading to poor prognosis. A large number of studies have shown that abnormal activation of Wnt signaling and high expression of β-catenin in OS are associated with abnormal histological morphology and cell proliferation and differentiation of osteosarcoma, ultimately leading to the occurrence of osteosarcoma (45, 50). When the level of β-catenin in the cytoplasm reaches a certain concentration, it begins to transfer to the nucleus and bind specifically to the nuclear transcription factor TCF/LEF, resulting in the exposure of downstream target gene promoter, activation and expression of promoter, causing abnormal cell proliferation and anti-apoptosis, thus promoting the formation of tumors (51). Huang et al. found that the Wnt/β-catenin pathway was activated in tumor tissues of patients with OS, and the activated Wnt/β-catenin pathway induced cell cycle progression and promoted the proliferation of OS cells. While cinnamaldehyde can inhibit Wnt/β-catenin signaling activity by down-regulating the phosphorylation of β-catenin and GSK-β as well as downstream target proteins c-Myc and MMP7, thereby inhibiting cell proliferation and promoting tumor cell apoptosis (52). In another

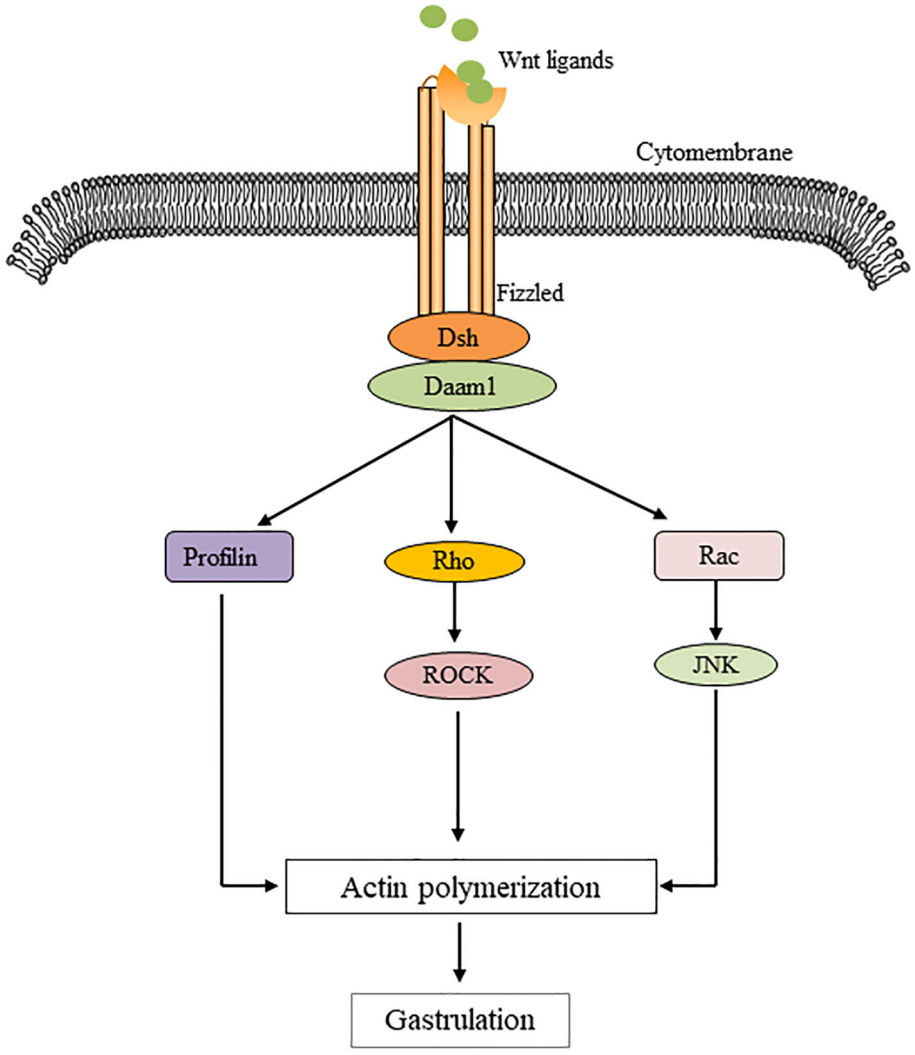

FIGURE 2
Illustration of a planar cell polarity transition cascade. Wnt signal transduction via Fizzled independent of LRP5/6 leads to Dsh activation. Dsh mediates the activation of Rho via Daam1, which activates Rho kinase (ROCK). Daam1 also mediates actin polymerization via the actin binding protein Profilin. Dsh also mediates the activation of Rac, which in turn activates JNK. Signals from Rock, JNK, and Profilin are integrated into cytoskeletal changes in cell polarization and movement during gastrum formation.

study, activation of the Wnt/β-catenin pathway accelerated the progression of osteosarcoma, while inhibition of the activity of this pathway significantly inhibited the proliferation, migration, and invasion of osteosarcoma cells (53). In addition, Chen et al. (37) demonstrated abnormal activation of Wnt/β-catenin signaling in osteosarcoma cells, involving the autocrine Wnt signaling cycle and the upregulation of specific Wnt ligands and receptors. Activation of Wnt/β-catenin signaling with Wnt3a or GSK-3β inhibitors drives proliferation of osteosarcoma cells, whereas downregulation of activated Wnt signaling with dnTCF4 or siLEF1 inhibits proliferation and induces cell cycle arrest. From these studies, it was determined that activation of the Wnt/β-catenin pathway can promote cell proliferation in OS, thereby accelerating OS progression. Inhibition of this pathway can be an effective target to inhibit the progression of OS.

4.2 Inhibit apoptosis

Apoptosis is a kind of programmed cell death, which is an important process of normal development and tissue homeostasis. In many cancers, including osteosarcoma, apoptosis is the primary mechanism by which chemotherapy and radiotherapy induce cell death. The balance between cell proliferation and apoptosis in cancer cells is disturbed and leads to excessive proliferation of cancer cells through different molecular mechanisms (e.g. resistance to apoptosis). A large number of studies have shown that Wnt/β-catenin signaling pathway plays an important role in regulating the apoptosis process of tumor cells and is a key gene mediator involved in tumor cell apoptosis (12). Anti-apoptosis is a common feature of cancer cells, which is associated with increased expression of anti-apoptotic factors such as Bcl-2 or Bcl-xL or decreased expression, inactivation or mutation of pro-apoptotic factors such as Foxo3a or p53 (54). Interestingly, Wnt/β-catenin directly regulates an effective anti-apoptotic pathway and can also activate the expression of several anti-apoptotic genes, Bcl-2, Bad and Bcl-xl (55). Activation of the Wnt/β-catenin signaling pathway during cancer progression can promote the viability of osteosarcoma cells and inhibit apoptosis, and inhibition of this signaling can reverse this phenomenon (56). The mechanism may be through inhibiting Bcl-2 and promoting the expression levels of Bad and Bax (57). Studies have shown that miR-1-3p can deactivate Wnt/β-catenin signaling activity, thereby inhibiting the proliferation and cell cycle progression of osteosarcoma cells and promoting cell apoptosis (58). In addition, studies have also found that melittin is an anti-tumor Chinese medicine with few side effects, which can inhibit the

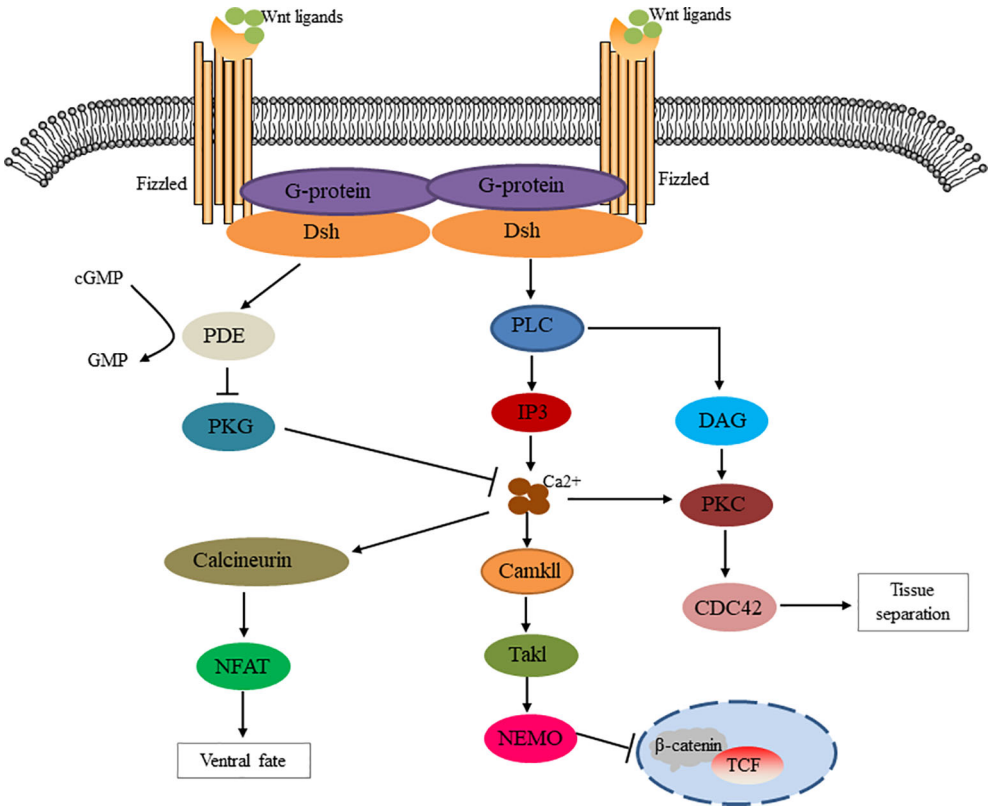

FIGURE 3
Schematic diagram of Wnt/Ca^{2+} signaling cascade. The Wnt signaling via Fizzled mediates the activation of Dsh through g protein activation. Dishevelled activates phosphodiesterase PDE, which inhibits PKG and in turn inhibits Ca^{2+} release. Dsh activates IP3 via PLC, resulting in the release of intracellular Ca^{2+}, which activates CamK11 and calcineurin. NF-AT activation by calcineurin regulates the fate of ventral cells. CamK11 activates TAK and NLK, inhibits β-catenin/TCF function and negatively regulates dorsal axis formation. DAG mediates tissue separation and cell motility during gastrulation through PKC activation of CDC42.

activity of Wnt/β-catenin signaling pathway, up-regulate the ratio of Bax/Bcl-2 in osteosarcoma cells and inhibit the expression of proliferative protein, thus inducing apoptosis and inhibiting proliferation of tumor cells (59). These studies indicate that the abnormal expression of Wnt/β-catenin pathway plays an important role in the regulation of OS, and the activation of NF-κB pathway can inhibit the apoptosis of cancer cells. This allows targeting the Wnt/β-catenin pathway to eliminate the inhibition of OS cell apoptosis, so targeting Wnt/β-catenin may be a potential means to treat OS.

4.3 Promoting epithelial mesenchymal transformation and tumor cell invasion and metastasis

Epithelial mesenchymal transformation (EMT) is a process of migration of adherent epithelial cells to mesenchymal cells under certain conditions. It gives epithelial cells the characteristics of mesenchymal cells. In malignant tumors, EMT is closely related to the invasion and metastasis of tumor cells (60, 61). Proliferation and invasion play a crucial role in the progression of malignant tumors, including OS (7). There is growing evidence that the Wnt/β-catenin pathway promotes these aggressive behaviors (62, 63). On the other hand, osteosarcoma is an interstitial tumor, and patients with high malignancy tend to have distant metastases at an early stage and have a poor prognosis, in which EMT plays an important role (64). EMT is an important mechanism of embryogenesis, wound healing, fibrosis and other physiological processes (65–67), as well as an important process of distant metastasis and migration of tumor cells (68). Studies have shown that EMT plays an important role in the metastasis and migration progression of various tumor cells, including OS (69–71). It is well known that there are multiple interactions between molecular pathways and EMT mechanisms that promote cancer cell invasion. Many studies have shown that Wnt signaling pathway increases the invasion and malignancy of tumor cells through EMT induction (72–74). Wnt-induced EMT can enhance the proliferation of cancer cells and trigger their resistance to apoptosis (75, 76). The Wnt/β-catenin pathway is activated in OS, and the activated Wnt/β-catenin pathway promotes

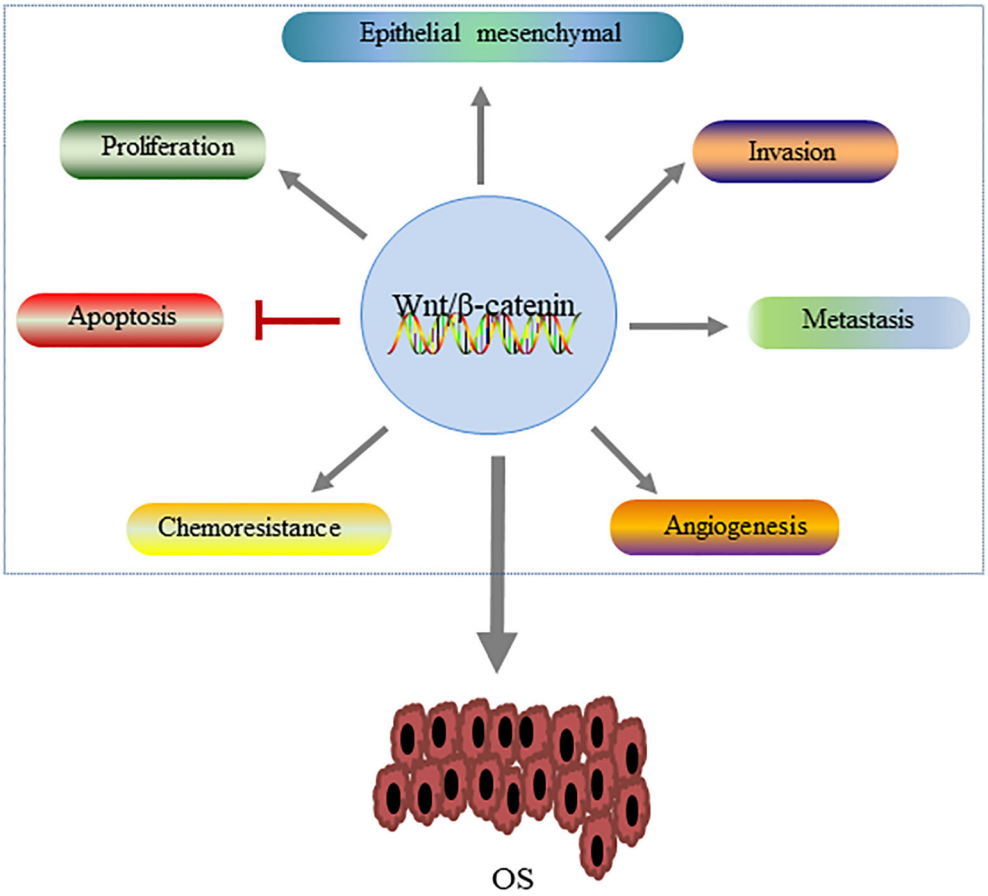

FIGURE 4
The role of the Wnt/β-catenin pathway in the development of OS. Activation of this signaling pathway regulates OS by promoting tumor cell proliferation, epithelial-mesenchymal transformation and tumor cell invasion and metastasis, angiogenesis and chemical resistance, and inhibiting apoptosis.

the migration and invasion of OS cells by enhancing the epithelial-mesenchymal transformation of OS (77). At the same time, activation of the Wnt/β-catenin pathway was associated with prognosis in patients with OS, and this study found that patients with over-activation of this pathway had significantly lower prognosis than patients with expression (78). Similar findings have been reported in another study of microRNAs on cancer occurrence and malignant progression in various tumors. This study found that inhibition of Wnt/β-catenin pathway activity could not only inhibit the EMT of OS, but also inhibit the progression and prognosis of OS (79). The invasion and metastasis of tumor cells are the main causes of death in patients with malignant tumors, and about 90% of patients with malignant tumors die from tumor metastasis (80). Studies on the prognosis of OS have found that the Wnt-β-catenin pathway can be used as a biological marker of metastasis (5). Lung metastasis is the most common site of osteosarcoma and the most common cause of death (81). Therefore, metastasis prediction is of great significance in the design of treatment strategies. Since the expression of β-catenin in the cytoplasm is significantly associated with the incidence of distant metastasis (82), β-catenin has been used as a biomarker for the potential of OS metastasis to the lung (81). β-catenin is a key component of the Wnt/β-catenin signaling pathway, relocating from the cytoplasm to the nucleus after Wnt ligand stimulation, thereby regulating gene expression (83). Wnt/β-catenin may also promote cancer cell migration and invasion by inducing the expression of transfer-related proteins such as intercellular adhesion molecule-1 (ICAM-1) and matrix metalloproteinases (MMPs) (84–88). It has been reported that inhibiting the Wnt/β-catenin pathway in OS cells MG-63 can inhibit the expression of MMP14, thus inhibiting the invasion and movement of MG-63 cells (89). In addition, Fu et al. (90) also found that the activation of Wnt/β-catenin in OS can promote the activity of MMP-9, and the enhancement of the activity of the latter can promote the invasion and metastasis of OS cells. In addition, KLF5 is a positive regulator of the Wnt/β-catenin signaling pathway, and KLF5 can increase β-catenin expression and interact directly with β-catenin to stabilize it and promote its nuclear transfer (91). ML264 is a small molecule inhibitor of KLF5, and ML264 can inhibit the activity of Wnt/β-catenin signaling pathway, thereby inducing G0/G1 cell cycle arrest and inhibiting the migration and invasion ability of osteosarcoma cells (92). Based on the above studies, it can be determined that the activation of Wnt/β-catenin can promote the invasion and migration of OS, and inhibiting the activation of Wnt/β-catenin signaling pathway may be a potential therapeutic target to prevent the deterioration of osteosarcoma.

4.4 Promote angiogenesis

Angiogenesis is a complex biological process that leads to the development of new blood vessels and plays a key role in the progression and metastasis potential of various malignant tumors (93). In the process of angiogenesis, VEGF is the most important factor of angiogenesis, which can increase capillary permeability and promote the migration of tip cells (94). MMPs accelerated the proliferation and differentiation of endothelial cells cultured on type IV and type I collagen in a dose-dependent manner (95). It has been confirmed that Wnt/β-catenin signaling pathway plays an important role in the regulation of tumor angiogenesis. Studies have shown that activation of Wnt/β-catenin pathway can promote cytoskeletal recombination and new blood vessel formation of endothelial cells, possibly through promoting the expression of VEGF and MMPs (96, 97). In addition, transcriptional regulation of VEGF by β-catenin/TCF complex involves TCF binding sites in VEGF gene promoters. Activation of Wnt/β-catenin can induce VEGF overexpression, thus promoting angiogenesis (98, 99). However, there are relatively few studies on the role of Wnt/β-catenin pathway in the angiogenesis of OS, and its mechanism has not been fully cleared. However, it can be preliminarily confirmed that the abnormal expression of NF-κB pathway can promote the angiogenesis of OS.

4.5 Chemoresistance

Neoadjuvant therapy and adjuvant chemotherapy in addition to radical surgery have been shown to significantly improve the prognosis of patients with osteosarcoma. At present, the treatment of OS patients is mainly based on radical surgical treatment with standard three-drug chemotherapy regimen (including doxorubicin, cisplatin and high-dose methotrexate) to improve the survival rate (100). However, chemotherapy can create chemotherapy resistance and even lead to disease recurrence or metastasis (101). There are several mechanisms of drug resistance in chemotherapy, including reduced intracellular drug accumulation, drug inactivation, increased DNA repair, and signal transduction pathway perturbation (102). Some studies have found that abnormal activation of the Wnt-β-catenin signaling pathway is involved in chemotherapy resistance of OS cells, especially resistance to standard three-drug chemotherapy. Doxorubicin is an anthracycline antibiotic that is widely used to treat a variety of cancers, including OS. Wnt-β-catenin signaling targeting T-cell factor represses syndecan-2, a key modulator of apoptosis and chemosensitivity in OS cells, contributing to the resistance of OS to doxorubicin (103, 104). Methotrexate (MTX) is another common component of chemotherapy regimens for osteosarcoma. MTX resistance is a problem in OS chemotherapy and one of the mechanisms underlying MTX resistance is associated with Wnt/β-catenin signaling. Ma and colleagues (105) found that knocking down β-catenin increased the sensitivity of Saos2 cells to MTX-induced cell death. Thus, Wnt/β-catenin signaling may contribute to MTX resistance. In addition, it has been found that activation of the Wnt/β-catenin pathway in human OS cells can induce cell resistance to cisplatin, and the use of Wnt/β-catenin pathway inhibitors can improve or reverse the resistance of OS cells to cisplatin (106, 107). In summary, the Wnt/β-catenin pathway is often abnormally expressed in OS and regulates the pathophysiological processes of osteosarcoma cell proliferation and apoptosis, invasion, migration, tumor angiogenesis, and chemical drug resistance.

5 The effect of crosstalk between Wnt/β-catenin and other signal pathways on OS

In addition to the abnormal expression of Wnt/β-catenin pathway, abnormal activation of other signaling pathways, such as phosphoinositol 3-kinase/protein kinase B (PI3K/AKT) and NF-κB signaling pathways, also play an important role in the pathogenesis of OS. Signaling pathways may interact, and enhancement of one signaling pathway may enhance or inhibit the other. In the process of tumor formation and development, Wnt/β-catenin signaling pathway can directly or indirectly interact with other signaling pathways to regulate the pathophysiological processes of OS. This section describes crosstalk between Wnt/β-catenin and the PI3K/Akt and NF-κB pathways in OS.

5.1 PI3K/Akt signaling pathway

Phosphatidylinositol 3-kinase/protein kinase B (PI3K/Akt) signaling pathway is an important signal transduction bridge connecting extracellular signals and cellular responses (108). Phosphatidylinositol 3-kinase (PI3K) is a large class of signaling lipases, a family of enzymes that phosphorylates the 3'-OH of phosphatidylinositol inositol rings (109). Protein kinase B (Akt), an evolutionarily conserved serine protein kinase of the serine/threonine kinase family, is a central mediator in PI3K signaling (110). The PI3K/Akt signaling pathway is a highly conserved signal transduction network in eukaryotic cells and can promote cell survival, cell growth and cell cycle progression (111, 112). It has been reported that the PI3K/Akt signaling pathway is a common activation pathway in human cancer, and it is believed that the dysfunction of this pathway will drive the occurrence and development of cancer and participate in the regulation of cancer pathological process (113–115).

The PI3K/Akt and Wnt/β-catenin signaling pathways are generally not abnormally activated in a variety of tumors, including osteosarcoma (116, 117). These two pathways play an important role in the occurrence and development of osteosarcoma by regulating cell cycle, inhibiting apoptosis, promoting angiogenesis, enhancing metastasis and inducing chemotherapy resistance (118, 119). GSK-3β is a key protein in the downstream PI3K/Akt pathway (120), and activation of PI3K/Akt pathway can significantly inhibit the expression of GSK-3β (121). GSK3-β phosphorylates serine/threonine residues in β-catenin proteins, thereby promoting ubiquitination and subsequent proteasome-mediated β-catenin degradation (41). In addition, it has been found that overexpression of Wnt5a in non-transforming Wnt family members can stimulate the migration of osteosarcoma MG63 cells by promoting the phosphorylation of PI3K and Akt (122). In addition, another transforming member of the Wnt family, Wnt7b, activates mTORC1 via PI3K-AKT signaling, thereby promoting bone formation (123). Therefore, we speculated that PI3K/Akt and Wnt/β-catenin signaling pathways in OS regulate each other, and jointly participate in the regulation of the pathological process of OS.

5.2 NF-κB signaling pathway

As an intracellular signaling pathway, NF-κB signaling pathway plays a key role in a variety of physiological and pathological processes, such as inducing immune and inflammatory responses and regulating apoptosis (124–126). The NF-κB signaling pathway has been reported to be an important carcinogenic pathway in human cancers. Dysregulation of this pathway has been found in many types of cancer, such as prostate cancer, colorectal cancer, bladder cancer, breast cancer, and osteosarcoma (127–131). It has been reported that the NF-κB pathway is over-activated in osteosarcoma, leading to excessive proliferation of tumor cells and accelerated development of OS (132). In addition, abnormal expression of this pathway is widely involved in cell processes such as proliferation, apoptosis, cycle, chemotherapy resistance, and metastasis of tumors, including osteosarcoma (133, 134).

Studies have shown that Wnt/β-catenin pathway components can regulate inflammation and immune responses through interaction with NF-κB (135). NF-κB has been shown to indirectly regulate Wnt/β-catenin by regulating target genes that affect β-catenin activity or stability (136). Several studies have shown that the NF-κB and Wnt signaling pathways collaborate at multiple levels in different physiological and pathological contexts. In breast cancer cells, beta-catenin binds to the p65-p50 complex and inhibits its nuclear translocation (137). β-TrCP1 simultaneously activates NF-κB and inhibits the Wnt pathway in vascular smooth muscle cells (138). IKKα and IKKβ are key activators of the NF-κB pathway, which regulate Wnt/β-catenin signaling activity in different ways (139). IKKα inhibitors block the expression of CCND1, a downstream Wnt gene, in mouse embryonic fibroblasts (136).

6 Targeted Wnt/β- catenin pathway treatment OS

At present, the main treatment strategies for OS are surgery, radiotherapy and chemotherapy. Although current neoadjuvant chemotherapy has shown efficacy against OS, the long-term survival rate for patients with OS remains low, highlighting the need to find new treatments. As an important pathway regulating cell growth, metabolism, survival, and chemotherapy resistance, targeting the Wnt/β-catenin pathway may be a potential therapeutic approach for patients with OS. This section focuses on the therapeutic effects of non-coding RNAs and drugs on OS by regulating the Wnt/β-catenin signaling pathway.

6.1 Non-coding RNA

Non-coding RNA plays an indispensable role in the growth and development of organisms through its influence on transcription and translation. Abnormal expression of NcRNAs has been shown to affect the development and evolution of OS disease. MiRNA s are highly conserved ncRNAs that can affect mRNA expression by binding to the 3′ untranslated region of mRNA (3′UTR) (140). It was found that multiple miRNAs were overexpressed in OS. For example, miR-21-5p (141) and miR-374a (142) are upregulated in OS cells and tissues and promote OS cell migration by activating Wnt/β-catenin signaling, while downregulation of these miRNAs can inhibit the activity of Wnt/β-catenin to inhibit the progression of osteosarcoma. In addition, some miRNAs are underexpressed in OS and participate in the regulation of the pathological process of OS by activating the Wnt/β-catenin signaling pathway. For example, decreased miR-22-3p and increased miR-22-3p in OS tissues and cells inhibit the Wnt/β-catenin pathway by targeting TCF7L2, thereby preventing the progression of osteosarcoma (143). In addition, the expression of miR-1-3p is decreased in osteosarcoma tissues and cells, and upregulation of miR-1-3p inhibits the proliferation and cell cycle process of osteosarcoma cells by targeting CDK14 and inactivating Wnt/β-catenin signaling, while promoting cell apoptosis (58). In addition to the above miRNAs, the overexpression of miR-199b-3p (144) and miR-377-3p (79) can also inhibit the progression of osteosarcoma by inhibiting the Wnt/β-catenin signaling pathway. In addition, overexpression of miR-140 may inhibit the proliferation of human OS cells and may enhance drug sensitivity by directly regulating Wnt/β-catenin signaling (145).

Circular RNAs (circRNAs) are a class of non-coding RNAs characterized by covalently closed loops that have been found in a variety of diseases, including cancer (146). It was found that the expression of various circRNAs in OS was up-regulated and involved in the regulation of its pathological process. For example, Circ_0003732 is up-regulated in osteosarcoma tissues and cells, and activates the Wnt/β-catenin signaling pathway by regulating the miR-377-3p/CPEB1 axis, promoting the proliferation, migration and invasion of osteosarcoma cells, and inhibiting apoptosis. Silencing circ_0003732 can reverse the effect on the progression of osteosarcoma cells (147). The expression of hsa_circ_0087302 is low in osteosarcoma cells, and overexpression of hsa_circ_0087302 can inhibit the proliferation, cell cycle, migration and invasion of osteosarcoma cells by inhibiting the Wnt/β-catenin signaling pathway (148). In addition, circUBAP2 expression is upregulated in osteosarcoma tissues and cells, and knock down circUBAP2 can act as a sponge of miR-506-3p to inhibit Wnt/β-catenin signaling pathway activity, thereby inhibiting cell proliferation, migration and invasion, and promoting apoptosis of cisplatin-resistant osteosarcoma cells (149).

Long non-coding RNAs (LncRNAs) are endogenous ncRNAs with a length > 200 nucleotide transcripts and do not have protein-coding capabilities (150). By acting as a miRNA molecular sponge and competitively binding to miRNA, it is involved in a variety of *in vivo* pathophysiological processes, including cancer proliferation and invasion (151, 152). UCA1 influences the invasion and migration of osteosarcoma cells by mediating the Wnt/β-catenin pathway through the miR-145/HMGA1 axis (153). lncRNA SNHG10 is overexpressed in OS and acts as a sponge of miR-182-5p to activate the Wnt/β-catenin signaling pathway, promoting the proliferation, migration and invasion of osteosarcoma cells, while downregulation of SNHG10 can inhibit the above results (154). MRPL23-AS1 competitively interacts with miR-30b to activate the Wnt/β-catenin pathway, thus promoting tumorigenesis and metastasis of OS (155). In addition, HOTAIR (156), LncRNA FLVCR1-AS1 (53), CASC15 (157), and LINC00665 (158) are all upregulated in OS cells and affect the cell cycle by activating the Wnt/β-catenin pathway, thereby promoting cell proliferation (Table 1).

6.2 Drugs

At present, it has been found that many drugs can participate in the regulation of the pathological process of OS by inhibiting the activity of Wnt/β-catenin signaling pathway. For example, Resveratrol is a natural phenol (159). It has been reported that the treatment of resveratrol can arrest the cell cycle of various malignant tumors, promote cell apoptosis and inhibit the proliferation of cancer cells (160). In addition, resveratrol inhibits cell growth and induces senescence in OS cells by altering DNA metabolism (161). Zou et al. (30) found that resveratrol could inhibit the expression of β-catenin and c-Myc protein and mRNA, thereby inhibiting the proliferation of OS cells. Another study also came to a similar conclusion that resveratrol can inhibit the activity of Wnt/β-catenin signaling pathway and down-regulate the levels of c-myc, cyclin D1, MMP-2 and MMP-9, thus promoting apoptosis and inhibiting the proliferation and invasion of OS cells (162). Curcumin is a natural compound that comes from the roots of turmeric. Its anti-cancer properties have been demonstrated in many types of cancer, including OS (163, 164). Curcumin has been reported to delay the progression of osteosarcoma by regulating the Wnt/β-catenin pathway in osteosarcoma cells (165). Leow et al. found that curcumin analogs could inhibit the activity of Wnt/β-catenin pathway and prevent the invasion of osteosarcoma cells (90). Baicalein, a flavonoid extracted from the root of scutellaria baicalensis, has been proven to play an anti-tumor role by inhibiting the metastasis of various cancers and inducing apoptosis (166, 167). Studies have shown that baicalin can delay the progression of osteosarcoma by inhibiting the Wnt/β-catenin signaling pathway (168). Melatonin is a natural derivative of tryptophan, an amino acid with various biological activities (169), which plays a key inhibitory role in the pathogenesis of various types of tumors (170, 171). Li et al. (172) found that melatonin inhibited the expression of lncRNA JPX by regulating the Wnt/β-catenin pathway, thereby inhibiting the progression of OS. In addition, Oridonin (173), dihydroartemisinin (174), polyfolin I (175) and oleandrin (176) can also inhibit cell proliferation and induce apoptosis by inhibiting the activity of Wnt/β-catenin pathway, thus inhibiting the progression of OS (Table 2). Based on the above study, it is not difficult to find that targeting the

TABLE 1 Non coding RNAs associated with Wnt/β-catenin signaling pathway in OS.

NcRNAs	Mechanisms	Reference
miRNAs		
miR-21-5p	miR-21-5p↓→ Inhibit Wnt/β-catenin pathway → Inhibit cell proliferation and migration	(141)
miR-374a	miR-374a↓ → Inhibit Wnt/β-catenin pathway → Inhibit cell proliferation and migration	(142)
miR-22-3p	miR-22-3p↑ → Target TCF7L2 → Inhibit Wnt/β-catenin pathway → Inhibit proliferation and cell cycle of osteosarcoma cells and promoted apoptosis	(143)
miR-1-3p	miR-1-3p↑ → Target CDK14→Inhibit Wnt/β-catenin pathway → Inhibit proliferation and cell cycle of osteosarcoma cells and promoted apoptosis	(58)
miR-199b-3p	miR-199b-3p↑ → Inhibit Wnt/β-catenin pathway → Inhibit proliferation and cell cycle of osteosarcoma cells and promoted apoptosis	(144)
miR-377-3p	miR-377-3p↑ → Inhibit Wnt/β-catenin pathway → Inhibit proliferation and cell cycle of osteosarcoma cells and promoted apoptosis	(79)
miR-140	miR-140↑ → Inhibit Wnt/β-catenin pathway → Enhanced drug sensitivity	(145)
circRNA		
Circ_0003732	Circ_0003732↓→Regulation of miR-377-3p/CPEB1 axis → Inhibit Wnt/β-catenin pathway → Inhibit the proliferation, migration and invasion of osteosarcoma cells, and promote cell apoptosis	(147)
Hsa_circ_0087302	hsa_circ_0087302↓ → Inhibit Wnt/β-catenin pathway → Inhibit the proliferation, cell cycle, migration and invasion of osteosarcoma cells	(148)
CircUBAP2	circUBAP2↓ → Sponges acting as miR-506-3p → inhibit Wnt/β-catenin pathway → Inhibit cell proliferation, migration and invasion, and promoted apoptosis of cisplatin-resistant osteosarcoma cells	(149)
lncRNA		
lncRNA UCA1	lncRNA UCA1↓ →inhibit Wnt/β-catenin pathway → Inhibits cell invasion and migration	(153)
lncRNA SNHG10	lncRNA SNHG10↓→Act as a sponge for miR-182-5p → inhibit Wnt/β-catenin pathway → Inhibit proliferation, migration and invasion of cancer cells	(154)
MRPL23-AS1	MRPL23-AS1↓ → MRPL23-AS1 competitively interacts with miR-30b→Inhibit Wnt/β-catenin pathway → Inhibit cell proliferation and migration	(155)
HOTAIR	HOTAIR↓ → inhibit Wnt/β-catenin pathway→ Inhibits cell cycle and cell proliferation	(156)
LncRNA FLVCR1-AS1	LncRNA FLVCR1-AS1↓→ Inhibit Wnt/β-catenin pathway→ Inhibits cell cycle and cell proliferation	(53)
CASC15	CASC15↓ → inhibit Wnt/β-catenin pathway → Inhibits cell cycle and cell proliferation	(157)
LINC00665	LINC00665↓ → inhibit Wnt/β-catenin pathway→ Inhibits cell cycle and cell proliferation	(158)

↓, Expression down; ↑, expression up.

Wnt/β-catenin pathway may be an innovative approach to treat osteosarcoma.

6.3 Combination treatment regimen

Due to the complexity of the tumor microenvironment, it is difficult to control the progression and recurrence of cancer with a single traditional treatment. Therefore, the combination treatment strategy has gradually become an inevitable trend in cancer treatment (177). Through combination therapy, Wnt/β-catenin signaling pathway inhibitors combined with other drugs can promote therapeutic efficacy and improve prognosis. Hattinger CM et al. used lithium carbonate in combination with neoadjuvant chemotherapy and 9-ING-41 in combination with doxorubicin to effectively inhibit GSK3-β, thereby enhancing the inhibitory effect on Wnt/β-catenin signaling pathway activity (178). In addition, preclinical studies by Leow et al. showed that inhibiting the Wnt/β-catenin pathway with curcumin and PKF118-310 reduced nuclear β-catenin levels, which in turn reduced intrinsic and activated β-catenin/TCF transcriptional activity and, consequently, the expression of β-catenin target genes. This resulted in the down-regulation of MMP-9, a reduction in the expression of cyclin-D, c-MYC, and survivin, and inhibition of the potential for migration. This had a suppressive effect on cell proliferation and increased cell mortality (165).

7 Discussion and future outlook

Wnt/β-catenin signaling pathway is an intracellular signaling pathway that is finely regulated, and abnormal expression of this pathway plays a crucial role in the occurrence and development of a variety of malignant tumors, including OS. Structural activation of

TABLE 2 Drugs associated with Wnt/β-catenin signaling pathway in OS.

Drugs	Mechanisms	Reference
Resveratrol	Inhibit Wnt/β-catenin pathway → Inhibit the expression of c-Myc, Cyclin D1, MMP-2 and MMP-9 → Promote OS cell apoptosis, inhibit cell proliferation and invasion	(162)
Curcumin	Inhibit Wnt/β-catenin pathway → inhibit cell proliferation and invasion	(90)
Baicalein	Inhibit Wnt/β-catenin pathway → Inhibit metastasis and induce apoptosis	(168)
Melatonin	Inhibit Wnt/β-catenin pathway→Inhibit the expression of lncRNA JPX → Inhibit OS progression	(172)
Oridonin	Inhibit Wnt/β-catenin pathway→Inhibit cell proliferation and induce apoptosis	(173)
Dihydroartemisinin	Inhibit Wnt/β-catenin pathway→Inhibit cell proliferation and induce apoptosis	(174)
Polyfolin I	Inhibit Wnt/β-catenin pathway→Inhibit cell proliferation and induce apoptosis	(175)
Oleandrin	Inhibit Wnt/β-catenin pathway→Inhibit cell proliferation and induce apoptosis	(176)

Wnt/β-catenin is a novel hallmark of various tumor types, and many *in vitro* and animal models have shown that this pathway is involved in multiple steps of cell proliferation, apoptosis, epithelial-mesenchymal transformation, tumor angiogenesis, invasion, and metastasis through complex molecular mechanisms. At present, under the multi-science and multi-mode therapy, the research work to improve the effect of chemotherapy has led to the improvement of the survival rate of patients, but the prognosis of OS is not satisfactory, so molecular targeted therapy has gradually attracted widespread attention. Combined with the role of the Wnt/β-catenin pathway in the progression of OS, it can be seen that this pathway may be a potential target for OS therapy, and targeting the Wnt/β-catenin pathway may be an innovative approach for the treatment of osteosarcoma and a potential target for cancer drug development.

7.1 Limitations of current research on the Wnt/β-catenin signaling pathway

Most existing preclinical trial reports suggest that the Wnt/β-catenin pathway plays an important role in OS. Since Wnt/β-catenin signal plays a variety of functions in the pathological process of OS, it is generally difficult to verify the specific role of this signaling pathway in OS. Current epidemiological studies on Wnt/β-catenin and OS have some limitations, including lack of depth of study design, incomplete study subjects, and traditional targeted drug delivery. At a macro level, most of the current research designs on the Wnt/β-catenin pathway in the field of OS are still at the stage of cell or rodent research, and different experimental conditions and modeling will inevitably produce different experimental results. At the same time, there is a lack of clinical research in this field. At the micro level, current studies have focused on the protein expression of the Wnt/β-catenin pathway, rather than the gene and single-cell level. The development of OS is a complex process involving multiple molecular signaling pathways, so the interaction of the Wnt/β-catenin signaling pathway with other pathways in OS is also noteworthy. In terms of drug delivery, although some drugs are already in the preclinical research stage, the route of administration largely determines the therapeutic effect, efficacy and safety of drugs (179). Due to the first-pass effect of oral administration, only a small amount of the active ingredient can reach the designated site. Multiple adverse reactions may also be induced, thus limiting clinical application (180).

7.2 Challenges in translating Wnt/β-catenin targeted therapies

Wnt/β-catenin is expressed not only in cancer cells, but also in healthy cells, which may lead to unexpected effects of treatment. Therefore, one of the major challenges facing the use of Wnt/beta-catenin inhibitors in the treatment of osteosarcoma is safety and efficacy. Blocking or disabling Wnt/β-catenin signaling may impair immunity or induce toxic reactions. In addition to the development of cancer, many other factors, such as microbial infections or physical and chemical damage, can cause damage to the body (181). Therefore, systemic administration of Wnt/β-catenin inhibitors may worsen immune function or response. The degree of toxicity depends on the dose, time, and baseline health of the patient. Strategies to mitigate these toxicities and improve safety therefore include dose optimization and the use of modified or alternative Wnt/β-catenin-targeting drugs (182). Tumor heterogeneity is also a challenge for Wnt/β-catenin targeted therapies, as some cancer cells may have different levels of Wnt/β-catenin expression, which can lead to differences in the sensitivity of different cells to Wnt/β-catenin targeted therapies. In addition, due to the presence of immunosuppressive cells such as tumor-associated macrophages and tumor-associated neutrophils, cancer cells can upregulate immune checkpoint molecules to evade immune surveillance and escape immune cell destruction, which interferes with the effectiveness of Wnt/β-catenin targeted therapy (183). At presently, some challenges remain existed in the treatment accurately targeting the Wnt/β-catenin signaling pathway. The biggest obstacle is devoid of reliable predictive biomarkers that can identify patients who will be most likely to benefit from these types of therapy.

To overcome these challenges, a variety of strategies are being developed. One approach is to combine targeted therapies with other immune checkpoint inhibitors to overcome the immune escape mechanism adopted by tumor cells (184). Another

approach is to develop bispecic antibodies that can simultaneously target Wnt/β-catenin and another immune checkpoint molecule. Finally, other advanced and efficient techniques and methods should be used to enhance the efficacy of Wnt/β-catenin targeted therapy.

7.3 Current and future research trends of Wnt/β-catenin pathway in OS

The mechanism of action of the Wnt/β-catenin pathway in OS has been widely discussed, but there is still much to be improved. First, due to the lack of large-scale multi-center clinical trials, the specific molecular mechanisms leading to the activation or inhibition of the Wnt/β-catenin signaling pathway during OS have not been cleared. Therefore, future studies should focus on large-scale clinical studies and pharmacological studies to further explore the specific mechanism of action of Wnt/β-catenin signaling pathway in OS, and strive to provide reliable medical evidence for the development of clinical treatment for patients with OS. Second, current studies targeting the Wnt/β-catenin pathway for OS treatment have been too conventional. Future studies are needed to determine how to link targeted Wnt/β-catenin with corresponding front-line therapies for OS with improved drug delivery strategies leading to internalization to achieve *in vivo* drug delivery, targeted drug release, and biological activity to enhance drug administration efficiency, improve therapeutic effectiveness, and maximize targeting and reduce resistance. It is continuously released to enhance the efficiency of drug use, improve the therapeutic effect and reduce side effects (185). In particular, mesenchymal stem cells, nanoparticles and hydrogels are used. The main limitation of nanoparticles, however, is their toxic profile. Due to the wide variety of nanoparticles, the toxicity characteristics of nanoparticles are not well characterized, and the toxicity assessment of each class of these nanoparticles requires great efforts.

8 Conclusion

As an intracellular signaling pathway, abnormal activation of Wnt/β-catenin signaling pathway can promote the proliferation of osteosarcoma cells, epithelial-mesenchymal transformation, invasion and metastasis, tumor angiogenesis, and chemical resistance of tumor cells, and inhibit the activity of Wnt/β-catenin signaling pathway can delay the progression of osteosarcoma. Based on the role of the Wnt/β-catenin pathway in the development of OS, we suggest that targeting or manipulating the expression or function of the relevant Wnt/β-catenin signaling pathway may be an innovative approach to the treatment of OS and a potential target for cancer drug development.

Author contributions

YD: Writing – original draft, Writing – review & editing. QC: Writing – original draft, Writing – review & editing.

Funding

The author(s) declare financial support was received for the research, authorship, and/or publication of this article. This work is supported by funding of Ganzhou City "Science and technology and National Regional Medical Center" joint project (No. 2022-YB1396), Ganzhou City guiding science and technology plan project (No. 20222ZDX7705) and Ganzhou Municipal Science and Technology Project (GZ2022ZSF096).

Conflict of interest

The authors declare that the research was conducted in the absence of any commercial or financial relationships that could be construed as a potential conflict of interest.

Publisher's note

References

1. Yin F, Wang Z, Jiang Y, Zhang T, Wang Z, Hua Y, et al. Reduction-responsive polypeptide nanomedicines significantly inhibit progression of orthotopic osteosarcoma. *Nanomedicine*. (2020) 23:102085. doi: 10.1016/j.nano.2019.102085

2. Luetke A, Meyers PA, Lewis I, Juergens H. Osteosarcoma treatment - where do we stand? A state of the art review. *Cancer Treat Rev*. (2014) 40:523–32. doi: 10.1016/j.ctrv.2013.11.006

3. Bielack S, Carrle D, Casali PG. Osteosarcoma: ESMO clinical recommendations for diagnosis, treatment and follow-up. *Ann Oncol*. (2009) 20 Suppl 4:137–9. doi: 10.1093/annonc/mdp154

4. Ottaviani G, Jaffe N. The etiology of osteosarcoma. *Cancer Treat Res*. (2009) 152:15–32. doi: 10.1007/978-1-4419-0284-9_2

5. Mirabello L, Troisi RJ, Savage SA. Osteosarcoma incidence and survival rates from 1973 to 2004: data from the Surveillance, Epidemiology, and End Results Program. *Cancer*. (2009) 115:1531–43. doi: 10.1002/cncr.v115:7

6. Suehara Y, Alex D, Bowman A, Middha S, Zehir A, Chakravarty D, et al. Clinical genomic sequencing of pediatric and adult osteosarcoma reveals distinct molecular subsets with potentially targetable alterations. *Clin Cancer Res*. (2019) 25:6346–56. doi: 10.1158/1078-0432.CCR-18-4032

7. Zhang J, Yu X-H, Yan Y-G, Wang C, Wang W-J. PI3K/Akt signaling in osteosarcoma. *Clin Chim Acta*. (2015) 444:182–92. doi: 10.1016/j.cca.2014.12.041

8. Panez-Toro I, Muñoz-García J, Vargas-Franco JW, Renodon-Cornière A, Heymann M-F, Lézot F, et al. Advances in osteosarcoma. *Curr osteoporosis Rep*. (2023) 21:330–43. doi: 10.1007/s11914-023-00803-9

9. Self C, Macquarrie KL, Cost CR. Osteosarcoma/ewing sarcoma. *Pediatr Rev*. (2022) 43:256–65. doi: 10.1542/pir.2021-005065

10. Fuloria S, Yadav G, Menon SV, Ali H, Pant K, Kaur M, et al. Targeting the Wnt/β-catenin cascade in osteosarcoma: The potential of ncRNAs as biomarkers and therapeutics. *Pathology Res Pract*. (2024) 259:155346. doi: 10.1016/j.prp.2024.155346

11. Liu J, Xiao Q, Xiao J, Niu C, Li Y, Zhang X, et al. Wnt/β-catenin signalling: function, biological mechanisms, and therapeutic opportunities. *Signal transduction targeted Ther*. (2022) 7:3. doi: 10.1038/s41392-021-00762-6

12. Singla A, Wang J, Yang R, Geller DS, Loeb DM, Hoang BH. Wnt signaling in osteosarcoma. *Adv Exp Med Biol*. (2020) 1258:125–39. doi: 10.1007/978-3-030-43085-6_8

13. Ji H, Kong L, Wang Y, Hou Z, Kong W, Qi J, et al. CD44 expression is correlated with osteosarcoma cell progression and immune infiltration and affects the Wnt/β-catenin signaling pathway. *J Bone Oncol*. (2023) 41:100487. doi: 10.1016/j.jbo.2023.100487

14. Nusse R, Varmus H. Three decades of Wnts: a personal perspective on how a scientific field developed. *EMBO J*. (2012) 31:2670–84. doi: 10.1038/emboj.2012.146

15. Cisternas P, Henriquez JP, Brandan E, Inestrosa NC. Wnt signaling in skeletal muscle dynamics: myogenesis, neuromuscular synapse and fibrosis. *Mol Neurobiol*. (2014) 49:574–89. doi: 10.1007/s12035-013-8540-5

16. Varela-Nallar L, Inestrosa NC. Wnt signaling in the regulation of adult hippocampal neurogenesis. *Front Cell Neurosci*. (2013) 7:100. doi: 10.3389/fncel.2013.00100

17. Ríos JA, Cisternas P, Arrese M, Barja S, Inestrosa NC. Is Alzheimer's disease related to metabolic syndrome? A Wnt signaling conundrum. *Prog Neurobiol*. (2014) 121:125–46. doi: 10.1016/j.pneurobio.2014.07.004

18. Fang F, Vancleave A, Helmuth R, Torres H, Rickel K, Wollenzien H, et al. Targeting the Wnt/β-catenin pathway in human osteosarcoma cells. *Oncotarget*. (2018) 9:36780–92. doi: 10.18632/oncotarget.26377

19. Trautmann M, Sievers E, Aretz S, Kindler D, Michels S, Friedrichs N, et al. SS18-SSX fusion protein-induced Wnt/β-catenin signaling is a therapeutic target in synovial sarcoma. *Oncogene*. (2014) 33:5006–16. doi: 10.1038/onc.2013.443

20. Vijayakumar S, Liu G, Rus IA, Yao S, Chen Y, Akiri G, et al. High-frequency canonical Wnt activation in multiple sarcoma subtypes drives proliferation through a TCF/β-catenin target gene, CDC25A. *Cancer Cell*. (2011) 19:601–12. doi: 10.1016/j.ccr.2011.03.010

21. Du Z, Li F, Wang L, Huang H, Xu S. Regulatory effects of microRNA−184 on osteosarcoma via the Wnt/β−catenin signaling pathway. *Mol Med Rep*. (2018) 18:1917–24. doi: 10.3892/mmr.2018.9184

22. Monroe DG, Mcgee-Lawrence ME, Oursler MJ, Westendorf JJ. Update on Wnt signaling in bone cell biology and bone disease. *Gene*. (2012) 492:1–18. doi: 10.1016/j.gene.2011.10.044

23. Duchartre Y, Kim YM, Kahn M. The Wnt signaling pathway in cancer. *Crit Rev oncology/hematol*. (2016) 99:141–9. doi: 10.1016/j.critrevonc.2015.12.005

24. Clevers HJC. Wnt/β-catenin signaling in development and disease. *Cell*. (2006) 127:469–80. doi: 10.1016/j.cell.2006.10.018

25. Polakis P. Wnt signaling in cancer. *Cold Spring Harb Perspect Biol*. (2012) 4:a008052. doi: 10.1101/cshperspect.a008052

26. Tai D, Wells K, Arcaroli J, Vanderbilt C, Aisner DL, Messersmith WA, et al. Targeting the WNT signaling pathway in cancer therapeutics. *Oncologist*. (2015) 20:1189–98. doi: 10.1634/theoncologist.2015-0057

27. Le PN, Keysar SB, Miller B, Eagles JR, Chimed T-S, Reisinger J, et al. Wnt signaling dynamics in head and neck squamous cell cancer tumor-stroma interactions. *Mol carcinogenesis*. (2019) 58:398–410. doi: 10.1002/mc.22937

28. Zhao H, Ming T, Tang S, Ren S, Yang H, Liu M, et al. Wnt signaling in colorectal cancer: pathogenic role and therapeutic target. *Mol Cancer*. (2022) 21:144. doi: 10.1186/s12943-022-01616-7

29. Nusse R, Clevers HJC. Wnt/β-catenin signaling, disease, and emerging therapeutic modalities. *Cell*. (2017) 169:985–99. doi: 10.1016/j.cell.2017.05.016

30. Zou Y, Yang J, Jiang D. Resveratrol inhibits canonical Wnt signaling in human MG-63 osteosarcoma cells. *Mol Med Rep*. (2015) 12:7221–6. doi: 10.3892/mmr.2015.4338

31. Komiya Y, Habas R. Wnt signal transduction pathways. *Organogenesis*. (2008) 4:68–75. doi: 10.4161/org.4.2.5851

32. Clark HF, Brentrup D, Schneitz K, Bieber A, Goodman C, Noll M. Dachsous encodes a member of the cadherin superfamily that controls imaginal disc morphogenesis in Drosophila. *Genes Dev*. (1995) 9:1530–42. doi: 10.1101/gad.9.12.1530

33. Hsieh JC, Rattner A, Smallwood PM, Nathans J. Biochemical characterization of Wnt-frizzled interactions using a soluble, biologically active vertebrate Wnt protein. *Proc Natl Acad Sci U.S.A*. (1999) 96:3546–51. doi: 10.1073/pnas.96.7.3546

34. Bhanot P, Brink M, Samos CH, Hsieh JC, Wang Y, Macke JP, et al. A new member of the frizzled family from Drosophila functions as a Wingless receptor. *Nature*. (1996) 382:225–30. doi: 10.1038/382225a0

35. He X, Semenov M, Tamai K, Zeng X. LDL receptor-related proteins 5 and 6 in Wnt/beta-catenin signaling: arrows point the way. *Development*. (2004) 131:1663–77. doi: 10.1242/dev.01117

36. Gordon MD, Nusse R. Wnt signaling: multiple pathways, multiple receptors, and multiple transcription factors. *J Biol Chem*. (2006) 281:22429–33. doi: 10.1074/jbc.R600015200

37. Chen C, Zhao M, Tian A, Zhang X, Yao Z, Ma X. Aberrant activation of Wnt/β-catenin signaling drives proliferation of bone sarcoma cells. *Oncotarget*. (2015) 6:17570–83. doi: 10.18632/oncotarget.v6i19

38. Iwaya K, Ogawa H, Kuroda M, Izumi M, Ishida T, Mukai K. Cytoplasmic and/or nuclear staining of beta-catenin is associated with lung metastasis. *Clin Exp Metastasis*. (2003) 20:525–9. doi: 10.1023/A:1025821229013

39. Zhou L, Park BH, Park JH, Jang KY, Park HS, Wagle S, et al. Overexpression of the prolyl isomerase PIN1 promotes cell growth in osteosarcoma cells. *Oncol Rep*. (2013) 29:193–8. doi: 10.3892/or.2012.2112

40. Yang JZ, Zhang XH, Liu JR, Ding Y, Gao F, Wang Y. Expression and significance of N-cadherin and β-catenin protein in osteosarcoma. *Zhonghua Zhong Liu Za Zhi*. (2010) 32:586–9.

41. Liu W, Zhao Z, Wang Y, Li W, Su Q, Jia Q, et al. Dioscin inhibits stem-cell-like properties and tumor growth of osteosarcoma through Akt/GSK3/β-catenin signaling pathway. *Cell Death Dis*. (2018) 9:343. doi: 10.1038/s41419-018-0363-x

42. Lu Y, Guan GF, Chen J, Hu B, Sun C, Ma Q, et al. Aberrant CXCR4 and β-catenin expression in osteosarcoma correlates with patient survival. *Oncol Lett*. (2015) 10:2123–9. doi: 10.3892/ol.2015.3535

43. Haydon RC, Deyrup A, Ishikawa A, Heck R, Jiang W, Zhou L, et al. Cytoplasmic and/or nuclear accumulation of the beta-catenin protein is a frequent event in human osteosarcoma. *Int J Cancer*. (2002) 102:338–42. doi: 10.1002/ijc.v102:4

44. Major MB, Roberts BS, Berndt JD, Marine S, Anastas J, Chung N, et al. New regulators of Wnt/beta-catenin signaling revealed by integrative molecular screening. *Sci Signal*. (2008) 1:ra12. doi: 10.1126/scisignal.2000037

45. Lin CH, Ji T, Chen CF, Hoang BH. Wnt signaling in osteosarcoma. *Adv Exp Med Biol*. (2014) 804:33–45. doi: 10.1007/978-3-319-04843-7_2

46. Rabbani SA, Arakelian A, Farookhi R. LRP5 knockdown: effect on prostate cancer invasion growth and skeletal metastasis *in vitro* and *in vivo*. *Cancer Med*. (2013) 2:625–35. doi: 10.1002/cam4.2013.2.issue-5

47. Chu T, Teng J, Jiang L, Zhong H, Han B. Lung cancer-derived Dickkopf1 is associated with bone metastasis and the mechanism involves the inhibition of osteoblast differentiation. *Biochem Biophys Res Commun*. (2014) 443:962–8. doi: 10.1016/j.bbrc.2013.12.076

48. Lin CH, Guo Y, Ghaffar S, McQueen P, Pourmorady J, Christ A, et al. Dkk-3, a secreted wnt antagonist, suppresses tumorigenic potential and pulmonary metastasis in osteosarcoma. *Sarcoma*. (2013) 2013:147541. doi: 10.1155/2013/147541

49. Cai Y, Cai T, Chen Y. Wnt pathway in osteosarcoma, from oncogenic to therapeutic. *J Cell Biochem*. (2014) 115:625–31. doi: 10.1002/jcb.24708

50. Di Fiore R, Guercio A, Puleio R, Di Marco P, Drago-Ferrante R, D'Anneo A, et al. Modeling human osteosarcoma in mice through 3AB-OS cancer stem cell xenografts. *J Cell Biochem*. (2012) 113:3380–92. doi: 10.1002/jcb.v113.11

51. Liu C, Li Y, Semenov M, Han C, Baeg GH, Tan Y, et al. Control of beta-catenin phosphorylation/degradation by a dual-kinase mechanism. *Cell*. (2002) 108:837–47. doi: 10.1016/S0092-8674(02)00685-2

52. Huang Y, Chen J, Yang S, et al. Cinnamaldehyde inhibits the function of osteosarcoma by suppressing the Wnt/β-catenin and PI3K/Akt signaling pathways. *Drug Des Devel Ther*. (2020) 14:4625–37. doi: 10.2147/DDDT.S277160

53. Jiang S, Kong P, Liu X, Yuan C, Peng K, Liang Y. LncRNA FLVCR1-AS1 accelerates osteosarcoma cells to proliferate, migrate and invade via activating wnt/β-catenin pathway. *J Buon: Off J Balkan Union Oncol*. (2020) 25:2078–85.

54. Chen Y, Chen S, Liang H, Yang H, Liu L, Zhou K, et al. Bcl-2 protects TK6 cells against hydroquinone-induced apoptosis through PARP-1 cytoplasm translocation and stabilizing mitochondrial membrane potential. *Environ Mol mutagenesis*. (2018) 59:49–59. doi: 10.1002/em.22126

55. Sha L, Ma D, Chen C. Exosome-mediated Hic-5 regulates proliferation and apoptosis of osteosarcoma via Wnt/β-catenin signal pathway. *Aging*. (2020) 12:23598–608. doi: 10.18632/aging.103546

56. Wei Z, Zheng D, Pi W, Qiu Y, Xia K, Guo W. Isoquercitrin restrains the proliferation and promotes apoptosis of human osteosarcoma cells by inhibiting the Wnt/β-catenin pathway. *J Bone Oncol*. (2023) 38:100468. doi: 10.1016/j.jbo.2023.100468

57. Yang C, Zhang L, Huang H, Yuan X, Zhang P, Ye C, et al. Alantolactone inhibits proliferation, metastasis and promotes apoptosis of human osteosarcoma cells by suppressing Wnt/β-catenin and MAPKs signaling pathways. *Genes Dis*. (2022) 9:466–78. doi: 10.1016/j.gendis.2020.07.014

58. Zhang G, Guan Q, Zhao Y, Wang S, Li H. miR-1-3p inhibits osteosarcoma cell proliferation and cell cycle progression while promoting cell apoptosis by targeting CDK14 to inactivate Wnt/beta-catenin signaling. *Mol Biotechnol*. (2023) 66:1704–17. doi: 10.1007/s12033-023-00811-1

59. Xie X, Li Y, Zhu H, Chen L, Chen D, Lin S, et al. Melittin Inhibits Growth of Human Osteosarcoma 143B Cells through Induction of Apoptosis via Suppressing the Wnt/β-catenin Signaling Pathway. *Anti-cancer Agents medicinal Chem*. (2022) 22:3172–81. doi: 10.2174/1871520622666220509121627

60. Dudas J, Ladanyi A, Ingruber J, Steinbichler TB, Riechelmann H. Epithelial to mesenchymal transition: A mechanism that fuels cancer radio/chemoresistance. *Cells*. (2020) 9:428. doi: 10.3390/cells9020428

61. Chong ZX, Yeap SK, Ho WY. Unraveling the roles of miRNAs in regulating epithelial-to-mesenchymal transition (EMT) in osteosarcoma. . *Pharmacol Res*. (2021) 172:105818. doi: 10.1016/j.phrs.2021.105818

62. Lu Q, Huang H, Wang X, Xia H, Zhang L, Xu J, et al. EChinatin inhibits the growth and metastasis of human osteosarcoma cells through Wnt/β-catenin and p38 signaling pathways. *Pharmacol Res*. (2023) 191:106760. doi: 10.1016/j.phrs.2023.106760

63. Ye C, Wei M, Huang H, Wang Y, Zhang L, Yang C, et al. Nitazoxanide inhibits osteosarcoma cells growth and metastasis by suppressing AKT/mTOR and Wnt/β-catenin signaling pathways. *Biol Chem*. (2022) 403:929–43. doi: 10.1515/hsz-2022-0148

64. Yu L, Liu S, Guo W, Zhang C, Zhang B, Yan H, et al. hTERT promoter activity identifies osteosarcoma cells with increased EMT characteristics. *Oncol Lett*. (2014) 7:239–44. doi: 10.3892/ol.2013.1692

65. Haensel D, Dai X. Epithelial-to-mesenchymal transition in cutaneous wound healing: Where we are and where we are heading. *Dev Dyn*. (2018) 247:473–80. doi: 10.1002/dvdy.v247.3

66. Kim DH, Xing T, Yang Z, Dudek R, Lu Q, Chen Y-H. Epithelial mesenchymal transition in embryonic development, tissue repair and cancer: A comprehensive overview. *J Clin Med*. (2017) 7:1. doi: 10.3390/jcm7010001

67. Rout-Pitt N, Farrow N, Parsons D, Donnelley M. Epithelial mesenchymal transition (EMT): a universal process in lung diseases with implications for cystic fibrosis pathophysiology. *Respir Res*. (2018) 19:136. doi: 10.1186/s12931-018-0834-8

68. Dai J, He H, Lin D, Wang C, Zhu Y, Xu D. Up-regulation of E-cadherin by saRNA inhibits the migration and invasion of renal carcinoma cells. *Int J Clin Exp Pathol*. (2018) 11:5792–800.

69. Liu W, Jiang D, Gong F, Huang Y, Luo Y, Rong Y, et al. miR-210-5p promotes epithelial-mesenchymal transition by inhibiting PIK3R5 thereby activating oncogenic autophagy in osteosarcoma cells. *Cell Death Dis*. (2020) 11:93. doi: 10.1038/s41419-020-2270-1

70. Hardy KM, Booth BW, Hendrix MJ, Salomon DS, Strizzi L. ErbB/EGF signaling and EMT in mammary development and breast cancer. *J Mammary Gland Biol Neoplasia*. (2010) 15:191–9. doi: 10.1007/s10911-010-9172-2

71. Al Moustafa AE, Achkhar A, Yasmeen A. EGF-receptor signaling and epithelial-mesenchymal transition in human carcinomas. *Front Biosci (Schol Ed)*. (2012) 4:671–84. doi: 10.2741/s292

72. Yi Z, Pu Y, Gou R, Chen Y, Ren X, Liu W, et al. Silencing of RIPK4 inhibits epithelial–mesenchymal transition by inactivating the Wnt/β–catenin signaling pathway in osteosarcoma. *Mol Med Rep*. (2020) 21:1154–62. doi: 10.3892/mmr.2020.10939

73. Lu Y, Sun W, Zhang L, Li J. Silencing of MAGI1 promotes the proliferation and inhibits apoptosis of glioma cells via the Wnt/β-catenin and PTEN/AKT signaling pathways. *Onco Targets Ther*. (2019) 12:9639–50. doi: 10.2147/OTT.S215400

74. Cheng C, Huang Z, Zhou R, An H, Cao G, Ye J, et al. Numb negatively regulates the epithelial-to-mesenchymal transition in colorectal cancer through the Wnt signaling pathway. *Am J Physiol Gastrointest Liver Physiol*. (2020) 318:G841–g53. doi: 10.1152/ajpgi.00178.2019

75. Wu W, Guo L, Liang Z, Liu Y, Yao Z. Lnc-SNHG16/miR-128 axis modulates Malignant phenotype through WNT/β-catenin pathway in cervical cancer cells. *J Cancer*. (2020) 11:2201–12. doi: 10.7150/jca.40319

76. Qiao Y, Zhou Y, Song C, Zhang X, Zou Y. MID1 and MID2 regulate cell migration and epithelial-mesenchymal transition via modulating Wnt/β-catenin signaling. *Ann Transl Med*. (2020) 8:1021. doi: 10.21037/atm-20-5583

77. Zhang Y, Sheng Z, Su C, Xia Y, Chen X, Huang X, et al. Caudatin inhibits the proliferation, invasion, and glycolysis of osteosarcoma cells via the Wnt/β- catenin pathway. *Evidence-Based complementary Altern medicine: eCAM*. (2022) 2022:4026688. doi: 10.1155/2022/4026688

78. Ding Q, Mo F, Cai X, Zhang W, Wang J, Yang S, et al. LncRNA CRNDE is activated by SP1 and promotes osteosarcoma proliferation, invasion, and epithelial-mesenchymal transition via Wnt/β-catenin signaling pathway. *J Cell Biochem*. (2020) 121:3358–71. doi: 10.1002/jcb.v121.5-6

79. Liang K, Liao L, Liu Q, Ouyang Q, Jia L, Wu G. microRNA-377-3p inhibits osteosarcoma progression by targeting CUL1 and regulating Wnt/β-catenin signaling pathway. *Clin Trans oncology: Off Publ Fed Spanish Oncol Societies Natl Cancer Institute Mexico*. (2021) 23:2350–7. doi: 10.1007/s12094-021-02633-6

80. Thiery JP, Acloque H, Huang RY, Nieto MA. Epithelial-mesenchymal transitions in development and disease. *Cell*. (2009) 139:871–90. doi: 10.1016/j.cell.2009.11.007

81. Gorlick R, Khanna C. Osteosarcoma. *J Bone Miner Res*. (2010) 25:683–91. doi: 10.1002/jbmr.77

82. Bongiovanni L, Mazzocchetti F, Malatesta D, Romanucci M, Ciccarelli A, Buracco P, et al. Immunohistochemical investigation of cell cycle and apoptosis regulators (survivin, β-catenin, p53, caspase 3) in canine appendicular osteosarcoma. *BMC Vet Res*. (2012) 8:78. doi: 10.1186/1746-6148-8-78

83. Mora-Blanco EL, Mishina Y, Tillman EJ, Cho Y-J, Thom CS, Pomeroy SL, et al. Activation of β-catenin/TCF targets following loss of the tumor suppressor SNF5. *Oncogene*. (2014) 33:933–8. doi: 10.1038/onc.2013.37

84. Ahmad A, Ahsan H. Ras-mediated activation of NF-κB and DNA damage response in carcinogenesis. *Cancer Invest*. (2020) 38:185–208. doi: 10.1080/07357907.2020.1721523

85. Iademarco MF, Mcquillan JJ, Rosen GD, Dean DC. Characterization of the promoter for vascular cell adhesion molecule-1 (VCAM-1). *J Biol Chem*. (1992) 267:16323–9. doi: 10.1016/S0021-9258(18)42004-2

86. Whelan J, Ghersa P, Hooft van Huijsduijnen R, Gray J, Chandra G, Talabot F, et al. An NF kappa B-like factor is essential but not sufficient for cytokine induction of endothelial leukocyte adhesion molecule 1 (ELAM-1) gene transcription. *Nucleic Acids Res*. (1991) 19:2645–53. doi: 10.1093/nar/19.10.2645

87. Borghaei RC, Rawlings PL Jr., Javadi M, Woloshin J. NF-kappaB binds to a polymorphic repressor element in the MMP-3 promoter. *Biochem Biophys Res Commun*. (2004) 316:182–8. doi: 10.1016/j.bbrc.2004.02.030

88. Bond M, Fabunmi RP, Baker AH, Newby AC. Synergistic upregulation of metalloproteinase-9 by growth factors and inflammatory cytokines: an absolute requirement for transcription factor NF-kappa B. *FEBS Lett*. (1998) 435:29–34. doi: 10.1016/S0014-5793(98)01034-5

89. Zhang F, Chen A, Chen J, Yu T, Guo F. SiRNA-mediated silencing of beta-catenin suppresses invasion and chemosensitivity to doxorubicin in MG-63 osteosarcoma cells. *Asian Pac J Cancer Prev*. (2011) 12:239–45.

90. Leow PC, Bahety P, Boon CP, Lee CY, Tan KL, Yang T, et al. Functionalized curcumin analogs as potent modulators of the Wnt/β-catenin signaling pathway. *Eur J Med Chem*. (2014) 71:67–80. doi: 10.1016/j.ejmech.2013.10.073

91. Mcconnell BB, Bialkowska AB, Nandan MO, Ghaleb AM, Gordon FJ, Yang VW. Haploinsufficiency of Krüppel-like factor 5 rescues the tumor-initiating effect of the Apc(Min) mutation in the intestine. *Cancer Res*. (2009) 69:4125–33. doi: 10.1158/0008-5472.CAN-08-4402

92. Huang H, Han Y, Chen Z, Pan X, Yuan P, Zhao X, et al. ML264 inhibits osteosarcoma growth and metastasis via inhibition of JAK2/STAT3 and WNT/β-catenin signalling pathways. *J Cell Mol Med*. (2020) 24:5652–64. doi: 10.1111/jcmm.v24.10

93. Olsen JJ, Pohl S, Deshmukh A, Visweswaran M, Ward NC, Arfuso F, et al. The role of wnt signalling in angiogenesis. *Clin Biochem Rev*. (2017) 38:131–42.

94. Chandolu V, Dass CR. Cell and molecular biology underpinning the effects of PEDF on cancers in general and osteosarcoma in particular. *J biomedicine Biotechnol*. (2012) 2012:740295. doi: 10.1155/2012/740295

95. Huo N, Ichikawa Y, Kamiyama M, Ishikawa T, Hamaguchi Y, Hasegawa S, et al. MMP-7 (matrilysin) accelerated growth of human umbilical vein endothelial cells. *Cancer Lett*. (2002) 177:95–100. doi: 10.1016/S0304-3835(01)00772-8

96. Dufourcq P, Leroux L, Ezan J, Descamps B, Lamazière J-MD, Costet P, et al. Regulation of endothelial cell cytoskeletal reorganization by a secreted frizzled-related protein-1 and frizzled 4- and frizzled 7-dependent pathway: role in neovessel formation. *Am J Pathol*. (2008) 172:37–49. doi: 10.2353/ajpath.2008.070130

97. Duplàa C, Jaspard B, Moreau C, D'Amore PA. Identification and cloning of a secreted protein related to the cysteine-rich domain of frizzled. *Evidence role endothelial Cell Growth control. Circ Res*. (1999) 84:1433–45. doi: 10.1161/01.RES.84.12.1433

98. Easwaran V, Lee SH, Inge L, Guo L, Goldbeck C, Garrett E, et al. beta-Catenin regulates vascular endothelial growth factor expression in colon cancer. *Cancer Res*. (2003) 63:3145–53.

99. Zhang X, Gaspard JP, Chung DC. Regulation of vascular endothelial growth factor by the Wnt and K-ras pathways in colonic neoplasia. *Cancer Res*. (2001) 61:6050–4.

100. Chou AJ, Gorlick R. Chemotherapy resistance in osteosarcoma: current challenges and future directions. *Expert Rev Anticancer Ther*. (2006) 6:1075–85. doi: 10.1586/14737140.6.7.1075

101. D'adamo DR. Appraising the current role of chemotherapy for the treatment of sarcoma. *Semin Oncol*. (2011) 38 Suppl 3:S19–29. doi: 10.1053/j.seminoncol.2011.09.004

102. He H, Ni J, Huang J. Molecular mechanisms of chemoresistance in osteosarcoma (Review). *Oncol Lett*. (2014) 7:1352–62. doi: 10.3892/ol.2014.1935

103. Dieudonné FX, Marion A, Haÿ E, Marie PJ, Modrowski D. High Wnt signaling represses the proapoptotic proteoglycan syndecan-2 in osteosarcoma cells. *Cancer Res*. (2010) 70:5399–408. doi: 10.1158/0008-5472.CAN-10-0090

104. Dieudonné FX, Marion A, Marie PJ, Modrowski D. Targeted inhibition of T-cell factor activity promotes syndecan-2 expression and sensitization to doxorubicin in osteosarcoma cells and bone tumors in mice. *J Bone mineral research: Off J Am Soc Bone Mineral Res*. (2012) 27:2118–29. doi: 10.1002/jbmr.1650

105. Ma Y, Ren Y, Han EQ, Li H, Chen D, Jacobs JJ, et al. Inhibition of the Wnt-β-catenin and Notch signaling pathways sensitizes osteosarcoma cells to chemotherapy. *Biochem Biophys Res Commun*. (2013) 431:274–9. doi: 10.1016/j.bbrc.2012.12.118

106. Li Z, Zhao L, Wang Q. Overexpression of long non-coding RNA HOTTIP increases chemoresistance of osteosarcoma cell by activating the Wnt/β-catenin pathway. *Am J Transl Res*. (2016) 8:2385–93.

107. Scholten DJ 2nd, Timmer CM, Peacock JD, Pelle DW, Williams BO, Steensma MR. Down regulation of Wnt signaling mitigates hypoxia-induced chemoresistance in human osteosarcoma cells. *PloS One*. (2014) 9:e111431. doi: 10.1371/journal.pone.0111431

108. Fukuchi M, Nakajima M, Fukai Y, Miyazaki T, Masuda N, Sohda M, et al. Increased expression of c-Ski as a co-repressor in transforming growth factor-beta signaling correlates with progression of esophageal squamous cell carcinoma. *Int J Cancer*. (2004) 108:818–24. doi: 10.1002/ijc.v108:6

109. Tang LA, Dixon BN, Maples KT, Poppiti KM, Peterson TJ. Current and investigational agents targeting the phosphoinositide 3-kinase pathway. *Pharmacotherapy*. (2018) 38:1058–67. doi: 10.1002/phar.2018.38.issue-10

110. Carmona FJ, Montemurro F, Kannan S, Rossi V, Verma C, Baselga J, et al. AKT signaling in ERBB2-amplified breast cancer. *Pharmacol Ther*. (2016) 158:63–70. doi: 10.1016/j.pharmthera.2015.11.013

111. Tian LY, Smit DJ, Jücker M. The role of PI3K/AKT/mTOR signaling in hepatocellular carcinoma metabolism. *Int J Mol Sci*. (2023) 24:2652. doi: 10.3390/ijms24032652

112. Ahmad I, Hoque M, Alam SSM, Zughaibi TA, Tabrez S. Curcumin and plumbagin synergistically target the PI3K/Akt/mTOR pathway: A prospective role in cancer treatment. *Int J Mol Sci*. (2023) 24:6651. doi: 10.3390/ijms24076651

113. Lee JH, Kim C, Um JY, Sethi G, Ahn KS. Casticin-induced inhibition of cell growth and survival are mediated through the dual modulation of Akt/mTOR signaling cascade. *Cancers*. (2019) 11:254. doi: 10.3390/cancers11020254

114. Ong PS, Wang LZ, Dai X, Tseng SH, Loo SJ, Sethi G. Judicious toggling of mTOR activity to combat insulin resistance and cancer: current evidence and perspectives. *Front Pharmacol*. (2016) 7:395. doi: 10.3389/fphar.2016.00395

115. Yuan Y, Long H, Zhou Z, Fu Y, Jiang B. PI3K-AKT-targeting breast cancer treatments: natural products and synthetic compounds. *Biomolecules*. (2023) 13:93. doi: 10.3390/biom13010093

116. Wang Y, Chen J, Huang Y, Yang S, Tan T, Wang N, et al. Schisandrin B suppresses osteosarcoma lung metastasis *in vivo* by inhibiting the activation of the Wnt/β–catenin and PI3K/Akt signaling pathways. *Oncol Rep*. (2022) 47:50. doi: 10.3892/or.2022.8261

117. Yuan X-H, Zhang P, Yu T-T, Huang H-K, Zhang L-L, Yang C-M, et al. Lycorine inhibits tumor growth of human osteosarcoma cells by blocking Wnt/β-catenin, ERK1/2/MAPK and PI3K/AKT signaling pathway. *Am J Trans Res*. (2020) 12:5381–98.

118. Keremu A, Maimaiti X, Aimaiti A, Yushan M, Alike Y, Yilihamu Y, et al. NRSN2 promotes osteosarcoma cell proliferation and growth through PI3K/Akt/MTOR and Wnt/β-catenin signaling. *Am J Cancer Res*. (2017) 7:565–73.

119. Huang H, Lu Q, Yuan X, Zhang P, Ye C, Wei M, et al. Andrographolide inhibits the growth of human osteosarcoma cells by suppressing Wnt/β-catenin, PI3K/AKT and NF-κB signaling pathways. *Chemico-biological Interact*. (2022) 365:110068. doi: 10.1016/j.cbi.2022.110068

120. Kim DE, Kim B, Shin HS, Kwon HJ, Park E-S. The protective effect of hispidin against hydrogen peroxide-induced apoptosis in H9c2 cardiomyoblast cells through Akt/GSK-3β and ERK1/2 signaling pathway. *Exp Cell Res*. (2014) 327:264–75. doi: 10.1016/j.yexcr.2014.07.037

121. Bai X, Guo X, Zhang F, Zheng L, Ding W, Yang S. Resveratrol combined with 17β-estradiol prevents IL-1β Induced apoptosis in human nucleus pulposus via the PI3K/AKT/Mtor and PI3K/AKT/GSK-3β Pathway. *J Invest surgery: Off J Acad Surg Res*. (2021) 34:904–11. doi: 10.1080/08941939.2019.1705941

122. Zhang A, He S, Sun X, Ding L, Bao X, Wang N. Wnt5a promotes migration of human osteosarcoma cells by triggering a phosphatidylinositol-3 kinase/Akt signals. *Cancer Cell Int*. (2014) 14:15. doi: 10.1186/1475-2867-14-15

123. Chen J, Tu X, Esen E, Joeng KS, Lin C, Arbeit JM, et al. WNT7B promotes bone formation in part through mTORC1. *PLoS Genet*. (2014) 10:e1004145. doi: 10.1371/journal.pgen.1004145

124. Barnes PJ, Karin M. Nuclear factor-kappaB: a pivotal transcription factor in chronic inflammatory diseases. *N Engl J Med*. (1997) 336:1066–71. doi: 10.1056/NEJM199704103361506

125. Foo SY, Nolan GP. NF-kappaB to the rescue: RELs, apoptosis and cellular transformation. *Trends Genet*. (1999) 15:229–35. doi: 10.1016/s0168-9525(99)01719-9

126. Bakkar N, Guttridge DC. NF-kappaB signaling: a tale of two pathways in skeletal myogenesis. *Physiol Rev*. (2010) 90:495–511. doi: 10.1152/physrev.00040.2009

127. Chang M, Zhu D, Chen Y, Zhang W, Liu X, Li X-L, et al. Total flavonoids of litchi seed attenuate prostate cancer progression via inhibiting AKT/mTOR and NF-kB signaling pathways. *Front Pharmacol*. (2021) 12:758219. doi: 10.3389/fphar.2021.758219

128. Othman MS, Al-Bagawi AH, Obeidat ST, Fareid MA, Habotta OA, Moneim AEA. Antitumor activity of zinc nanoparticles synthesized with berberine on human epithelial colorectal adenocarcinoma (Caco-2) cells through acting on Cox-2/NF-kB and p53 pathways. *Anticancer Agents Med Chem*. (2021) 22:2002–10. doi: 10.2174/1871520621666211004115839

129. Tao H, Liao Y, Yan Y, He Z, Zhou J, Wang X, et al. BRCC3 promotes tumorigenesis of bladder cancer by activating the NF-κB signaling pathway through targeting TRAF2. *Front Cell Dev Biol*. (2021) 9:720349. doi: 10.3389/fcell.2021.720349

130. Ren C, Han X, Lu C, Yang T, Qiao P, Sun Y, et al. Ubiquitination of NF-κB p65 by FBXW2 suppresses breast cancer stemness, tumorigenesis, and paclitaxel resistance. *Cell Death Differ*. (2022) 29:381–92. doi: 10.1038/s41418-021-00862-4

131. Chou C-H, Lu K-H, Yang J-S, Hsieh Y-H, Lin C-W, Yang S-F. Dihydromyricetin suppresses cell metastasis in human osteosarcoma through SP-1- and NF-κB-modulated urokinase plasminogen activator inhibition. *Phytomedicine*. (2021) 90:153642. doi: 10.1016/j.phymed.2021.153642

132. Dong S, Liu P-M, Du X-Y, Li F-Y, Cao Y, Lin D-Y, et al. Glycyrrhetinic acid inhibits proliferation of osteosarcoma cell line MG63 by inhibiting NF-κB signaling pathway. *Zhongguo Ying Yong Sheng Li Xue Za Zhi*. (2020) 36:399–401. doi: 10.12047/j.cjap.5966.2020.085

133. Javaid N, Choi S. Toll-like receptors from the perspective of cancer treatment. *Cancers (Basel)*. (2020) 12:297. doi: 10.3390/cancers12020297

134. Zhou J, Liu Q, Qian R, Liu S, Hu W, Liu Z. Paeonol antagonizes oncogenesis of osteosarcoma by inhibiting the function of TLR4/MAPK/NF-κB pathway. *Acta histochemica*. (2020) 122:151455. doi: 10.1016/j.acthis.2019.151455

135. Nejak-Bowen K, Kikuchi A, Monga SP. Beta-catenin-NF-κB interactions in murine hepatocytes: a complex to die for. *Hepatol (Baltimore Md)*. (2013) 57:763–74. doi: 10.1002/hep.26042

136. Albanese C, Wu K, D'amico M, Jarrett C, Joyce D, Hughes J, et al. IKKalpha regulates mitogenic signaling through transcriptional induction of cyclin D1 via Tcf. *Mol Biol Cell*. (2003) 14:585–99. doi: 10.1091/mbc.02-06-0101

137. Deng J, Miller SA, Wang HY, Xia W, Wen Y, Zhou BP, et al. beta-catenin interacts with and inhibits NF-kappa B in human colon and breast cancer. *Cancer Cell*. (2002) 2:323–34. doi: 10.1016/S1535-6108(02)00154-X

138. Wang CY, Mayo MW, Korneluk RG, Goeddel DV, Baldwin AS. NF-kappaB antiapoptosis: induction of TRAF1 and TRAF2 and c-IAP1 and c-IAP2 to suppress caspase-8 activation. *Sci (New York NY)*. (1998) 281:1680–3. doi: 10.1126/science.281.5383.1680

139. Lamberti C, Lin KM, Yamamoto Y, Verma U, Verma IM, Byers S, et al. Regulation of beta-catenin function by the IkappaB kinases. *J Biol Chem*. (2001) 276:42276–86. doi: 10.1074/jbc.M104227200

140. Bartel DP. MicroRNAs: genomics, biogenesis, mechanism, and function. *Cell*. (2004) 116:281–97. doi: 10.1016/S0092-8674(04)00045-5

141. Wu Z, Zhou Z, Zhang W, Yu Y. MiR-21-5p inhibition attenuates Warburg effect and stemness maintenance in osteosarcoma cells via inactivation of Wnt/β-catenin signaling. *Acta Biochim Polonica*. (2021) 68:725–32. doi: 10.18388/abp.2020_5631

142. Li W, Meng Z, Zou T, Wang G, Su Y, Yao S, et al. MiR-374a activates Wnt/β-catenin signaling to promote osteosarcoma cell migration by targeting WIF-1. *Pathol Oncol research: POR*. (2020) 26:533–9. doi: 10.1007/s12253-018-0556-8

143. Xue Y, Guo Y, Liu N, Meng X. MicroRNA-22-3p targeted regulating transcription factor 7-like 2 (TCF7L2) constrains the Wnt/β-catenin pathway and Malignant behavior in osteosarcoma. *Bioengineered*. (2022) 13:9135–47. doi: 10.1080/21655979.2021.2003942

144. Zhu D, Qi H, Zhu H. hsa-miR-199b-3p suppresses osteosarcoma progression by targeting CCDC88A, inhibiting epithelial-to-mesenchymal transition, and Wnt/beta-catenin signaling pathway. *Sci Rep*. (2023) 13:12544. doi: 10.1038/s41598-023-39537-0

145. Zhi W, Feng Q, Mingzhu Z. MiR-140 targets Wnt1 to inhibit the proliferation and enhance drug sensitivity in osteosarcoma cells. *Cell Mol Biol (Noisy-le-Grand France)*. (2022) 68:140–6. doi: 10.14715/cmb/2022.68.1.18

146. Kristensen LS, Andersen MS, Stagsted LVW, Ebbesen KK, Hansen TB, Kjems J. The biogenesis, biology and characterization of circular RNAs. *Nat Rev Genet*. (2019) 20:675–91. doi: 10.1038/s41576-019-0158-7

147. Zhou Z, Liu T, Li Z, Wang L. Circ_0003732 promotes osteosarcoma progression through regulating miR-377-3p/CPEB1 axis and Wnt/β-catenin signaling pathway. *Anti-cancer Drugs*. (2022) 33:e299–310. doi: 10.1097/CAD.0000000000001206

148. Peng L, Liu Q, Wu T, Li P, Cai Y, Wei X, et al. Hsa_circ_0087302, a circular RNA, affects the progression of osteosarcoma via the Wnt/β-catenin signaling pathway. *Int J Med Sci*. (2022) 19:1377–87. doi: 10.7150/ijms.69501

149. Dong L, Qu F. CircUBAP2 promotes SEMA6D expression to enhance the cisplatin resistance in osteosarcoma through sponging miR-506-3p by activating Wnt/β-catenin signaling pathway. *J Mol Histol*. (2020) 51:329–40. doi: 10.1007/s10735-020-09883-8

150. Spizzo R, Almeida MI, Colombatti A, Calin GA. Long non-coding RNAs and cancer: a new frontier of translational research? *Oncogene*. (2012) 31:4577–87. doi: 10.1038/onc.2011.621

151. Paraskevopoulou MD, Hatzigeorgiou AG. Analyzing MiRNA-LncRNA interactions. *Methods Mol Biol (Clifton NJ)*. (2016) 1402:271–86. doi: 10.1007/978-1-4939-3378-5_21

152. Li J, Li Z, Zheng W, Li X, Wang Z, Cui Y, et al. LncRNA-ATB: An indispensable cancer-related long noncoding RNA. *Cell proliferation*. (2017) 50:e12381. doi: 10.1111/cpr.2017.50.issue-6

153. Guan J, He J, Liao S, Wu Z, Lin X, Liu B, et al. LncRNA UCA1 accelerates osteosarcoma progression via miR-145 and Wnt/β-catenin pathway. *Am J Trans Res*. (2022) 14:6029–42.

154. Zhu S, Liu Y, Wang X, Wang J, Xi G. lncRNA SNHG10 promotes the proliferation and invasion of osteosarcoma via Wnt/β-catenin signaling. *Mol Ther Nucleic Acids*. (2020) 22:957–70. doi: 10.1016/j.omtn.2020.10.010

155. Zhang H, Liu S, Tang L, Ge J, Lu X. Long non-coding RNA (LncRNA) MRPL23-AS1 promotes tumor progression and carcinogenesis in osteosarcoma by

activating Wnt/β-catenin signaling via inhibiting microRNA miR-30b and upregulating myosin heavy chain 9 (MYH9). *Bioengineered*. (2021) 12:162–71. doi: 10.1080/21655979.2020.1863014

156. Li H, Fu S, Wang W. Long non-coding RNA HOTAIR promotes human osteosarcoma proliferation, migration through activation of the Wnt/b-catenin signaling pathway. *J Oncol*. (2023) 2023:9667920. doi: 10.1155/2023/9667920

157. Wang H, Zhang P. lncRNA–CASC15 promotes osteosarcoma proliferation and metastasis by regulating epithelial–mesenchymal transition via the Wnt/β–catenin signaling pathway. *Oncol Rep*. (2021) 45:76. doi: 10.3892/or.2021.8027

158. Bai J, Zhang X, Jiang F, Shan H, Gao X, Bo L, et al. A feedback loop of LINC00665 and the Wnt signaling pathway expedites osteosarcoma cell proliferation, invasion, and epithelial-mesenchymal transition. *Orthopaedic Surg*. (2023) 15:286–300. doi: 10.1111/os.13532

159. Ferrucci V, Boffa I, de Masi G, Zollo M. Natural compounds for pediatric cancer treatment. *Naunyn Schmiedebergs Arch Pharmacol*. (2016) 389:131–49. doi: 10.1007/s00210-015-1191-5

160. Varoni EM, Lo Faro AF, Sharifi-rad J, Sharifi-Rad J, Iriti M. Anticancer molecular mechanisms of resveratrol. *Front Nutr*. (2016) 3:8. doi: 10.3389/fnut.2016.00008

161. Rusin M, Zajkowicz A, Butkiewicz D. Resveratrol induces senescence-like growth inhibition of U-2 OS cells associated with the instability of telomeric DNA and upregulation of BRCA1. *Mech Ageing Dev*. (2009) 130:528–37. doi: 10.1016/j.mad.2009.06.005

162. Xie D, Zheng GZ, Xie P, Zhang Q-H, Lin F-X, Chang B, et al. Antitumor activity of resveratrol against human osteosarcoma cells: a key role of Cx43 and Wnt/β-catenin signaling pathway. *Oncotarget*. (2017) 8:111419–32. doi: 10.18632/oncotarget.22810

163. Aggarwal BB, Sundaram C, Malani N, Ichikawa H. Curcumin: the Indian solid gold. *Adv Exp Med Biol*. (2007) 595:1–75. doi: 10.1007/978-0-387-46401-5

164. Chang R, Sun L, Webster TJ. Short communication: selective cytotoxicity of curcumin on osteosarcoma cells compared to healthy osteoblasts. *Int J Nanomedicine*. (2014) 9:461–5. doi: 10.2147/IJN.S55505

165. Leow P-C, Tian Q, Ong Z-Y, Yang Z, Ee P-LR. Antitumor activity of natural compounds, curcumin and PKF118-310, as Wnt/β-catenin antagonists against human osteosarcoma cells. *Invest New Drugs*. (2010) 28:766–82. doi: 10.1007/s10637-009-9311-z

166. Ye F, Wang H, Zhang L, Zou Y, Han H, Huang J. Baicalein induces human osteosarcoma cell line MG-63 apoptosis via ROS-induced BNIP3 expression. *Tumour biology: J Int Soc Oncodevelopmental Biol Med*. (2015) 36:4731–40. doi: 10.1007/s13277-015-3122-y

167. Guo Z, Hu X, Xing Z, Xing R, Lv R, Cheng X, et al. Baicalein inhibits prostate cancer cell growth and metastasis via the caveolin-1/AKT/mTOR pathway. *Mol Cell Biochem*. (2015) 406:111–9. doi: 10.1007/s11010-015-2429-8

168. Örenlili Yaylagül E, Ülger C. The effect of baicalein on Wnt/β-catenin pathway and miR-25 expression in Saos-2 osteosarcoma cell line. *Turkish J Med Sci*. (2020) 50:1168–79. doi: 10.3906/sag-2001-161

169. Lin P-H, Tung Y-T, Chen H-Y, Chiang Y-F, Hong H-C, Huang K-C, et al. Melatonin activates cell death programs for the suppression of uterine leiomyoma cell proliferation. *J Pineal Res*. (2020) 68:e12620. doi: 10.1111/jpi.12620

170. Gil-Martín E, Egea J, Reiter RJ, Romero A. The emergence of melatonin in oncology: Focus on colorectal cancer. *Medicinal Res Rev*. (2019) 39:2239–85. doi: 10.1002/med.21582

171. Proietti S, Cucina A, Minini M, Bizzarri M. Melatonin, mitochondria, and the cancer cell. *Cell Mol Life sciences: CMLS*. (2017) 74:4015–25. doi: 10.1007/s00018-017-2612-z

172. Li Y, Zou J, Li B, Du J. Anticancer effects of melatonin via regulating lncRNA JPX-Wnt/β-catenin signalling pathway in human osteosarcoma cells. *J Cell Mol Med*. (2021) 25:9543–56. doi: 10.1111/jcmm.v25.20

173. Liu Y, Liu Y-Z, Zhang R-X, Wang X, Meng Z-J, Huang J, et al. Oridonin inhibits the proliferation of human osteosarcoma cells by suppressing Wnt/β-catenin signaling. *Int J Oncol*. (2014) 45:795–803. doi: 10.3892/ijo.2014.2456

174. Liu Y, Wang W, Xu J, Li L, Dong Q, Shi Q, et al. Dihydroartemisinin inhibits tumor growth of human osteosarcoma cells by suppressing Wnt/β-catenin signaling. *Oncol Rep*. (2013) 30:1723–30. doi: 10.3892/or.2013.2658

175. Chang J, Li Y, Wang X, Hu S, Wang H, Shi Q, et al. Polyphyllin I suppresses human osteosarcoma growth by inactivation of Wnt/β-catenin pathway *in vitro* and *in vivo*. *Sci Rep*. (2017) 7:7605. doi: 10.1038/s41598-017-07194-9

176. Ma Y, Zhu B, Liu X, Yu H, Yong L, Liu X, et al. Inhibition of oleandrin on the proliferation show and invasion of osteosarcoma cells *in vitro* by suppressing Wnt/β-catenin signaling pathway. *J Exp Clin Cancer research: CR*. (2015) 34:115. doi: 10.1186/s13046-015-0232-8

177. He Y, Sun MM, Zhang GG, Yang J, Chen KS, Xu WW, et al. Targeting PI3K/Akt signal transduction for cancer therapy. *Signal transduction targeted Ther*. (2021) 6:425. doi: 10.1038/s41392-021-00828-5

178. Hattinger CM, Patrizio MP, Magagnoli F, Luppi S, Serra M. An update on emerging drugs in osteosarcoma: towards tailored therapies? *Expert Opin Emerg Drugs*. (2019) 24:153–71. doi: 10.1080/14728214.2019.1654455

179. Fleischmann RM, Bliddal H, Blanco FJ, Schnitzer TJ, Peterfy C, Chen S, et al. A phase II trial of lutikizumab, an anti-interleukin-1α/β Dual variable domain immunoglobulin, in knee osteoarthritis patients with synovitis. *Arthritis Rheumatol (Hoboken NJ)*. (2019) 71:1056–69. doi: 10.1002/art.2019.71.issue-7

180. He Z, Wang B, Hu C, Zhao J. An overview of hydrogel-based intra-articular drug delivery for the treatment of osteoarthritis. *Colloids surfaces B Biointerfaces*. (2017) 154:33–9. doi: 10.1016/j.colsurfb.2017.03.003

181. Vallabhapurapu S, Karin M. Regulation and function of NF-kappaB transcription factors in the immune system. *Annu Rev Immunol*. (2009) 27:693–733. doi: 10.1146/annurev.immunol.021908.132641

182. Baud V, Karin M. Is NF-kappaB a good target for cancer therapy? Hopes and pitfalls. *Nat Rev Drug Discovery*. (2009) 8:33–40. doi: 10.1038/nrd2781

183. Dutta S, Ganguly A, Chatterjee K, Spada S, Mukherjee S. Targets of immune escape mechanisms in cancer: basis for development and evolution of cancer immune checkpoint inhibitors. *Nat Rev Drug Discov*. (2023) 12:218. doi: 10.3390/biology12020218

184. Bian Y, Lin T, Jakos T, Xiao X, Zhu J. The generation of dual-targeting fusion protein Pd-L1/CD47 for the inhibition of triple-negative breast cancer. *Biology*. (2022) 10:1843. doi: 10.3390/biomedicines10081843

185. Sheng S, Wang X, Liu X, Hu X, Shao Y, Wang G, et al. The role of resveratrol on rheumatoid arthritis: From bench to bedside. *Front Pharmacol*. (2022) 13:829677. doi: 10.3389/fphar.2022.829677

frontiers | Frontiers in Oncology

TYPE Case Report
PUBLISHED 17 February 2025
DOI 10.3389/fonc.2025.1469072

OPEN ACCESS

EDITED BY
Yang Wang,
Sichuan Academy of Medical Sciences and Sichuan Provincial People's Hospital, China

REVIEWED BY
Paulo Roberto Lacerda Leal,
Federal University of Ceara, Brazil
Ying Chen,
Peking Union Medical College Hospital (CAMS), China
Ahmed Guiga,
Centre Hôpital Universitaire Farhat Hached, Tunisia

*CORRESPONDENCE
Jiangtao Pu
drjiangtaop@163.com

†These authors share first authorship

RECEIVED 23 July 2024
ACCEPTED 30 January 2025
PUBLISHED 17 February 2025

CITATION
Yang Z, Wang K and Pu J (2025) Costal chondrosarcoma in a woman with hereditary multiple exostoses - a case report.
Front. Oncol. 15:1469072.
doi: 10.3389/fonc.2025.1469072

Costal chondrosarcoma in a woman with hereditary multiple exostoses - a case report

Ze Yang†, Kaiqiang Wang† and Jiangtao Pu*

Department of Thoracic Surgery, Affiliated Hospital of Southwest Medical University, Luzhou, China

In this report, we present a case of a 32-year-old female previously diagnosed with hereditary multiple exostoses(HME) who was incidentally found to have an asymptomatic anterior mediastinal mass during a routine examination. Computed tomography imaging revealed a well-defined mass measuring approximately 2.3 cm x 4.0 cm x 4.7 cm in the anterior mediastinum with multiple nodular areas of high density within. The mass caused compression and narrowing of the right ventricle. The patient subsequently underwent intralesional resection of the tumor, and histopathological examination confirmed a diagnosis of well-differentiated chondrosarcoma. Given the patient's medical history, the chondrosarcoma was suspected to have originated from malignant transformation of a rib osteochondroma. The patient received adjuvant radiotherapy postoperatively and has been followed up for one year with no evidence of recurrence. This case reports a highly rare costal chondrosarcoma secondary to hereditary multiple exostoses, located in the anterior mediastinum and compressing the right ventricle. To our knowledge, this is the first reported case of costal chondrosarcoma secondary to HME occurring in the anterior mediastinum, which requires differentiation from other common anterior mediastinal tumors.

KEYWORDS

hereditary multiple exostoses, malignant conversion, costal chondrosarcoma, mediastinal tumor, treatment

Introduction

Chondrosarcoma is a relatively common malignant bone tumor originating from cartilage, accounting for approximately 20-30% of all primary malignant bone tumors in the United States, with an annual incidence of 1 to 4 cases per million population, depending on geographic and population differences (1, 2). A subset of chondrosarcomas arises from pre-existing benign conditions, such as hereditary multiple exostoses (HME), and is referred to as secondary chondrosarcoma. HME, an autosomal dominant genetic disorder, is characterized by the formation of multiple osteochondromas throughout the skeleton. These osteochondromas predominantly affect the metaphyses of long bones, the scapulae, and the pelvis, while rib involvement is comparatively rare (3). The cause of HME

is linked to mutations in the EXT1 and EXT2 genes. These mutations disrupt the synthesis and elongation of heparan sulfate (HS), a glycosaminoglycan essential for regulating growth factor signaling pathways such as Indian hedgehog (IHH), fibroblast growth factors (FGFs), and bone morphogenetic proteins (BMPs). The impaired HS biosynthesis affects chondrocyte differentiation and proliferation, leading to the formation of osteochondromas (4–6). The most serious complication of HME is malignant transformation into chondrosarcoma, with previous studies estimating the incidence of malignant transformation to be approximately 1-5% (7, 8). This transformation is more commonly observed in osteochondromas located in the pelvis and proximal femur, and less frequently in the ribs (9). Costal chondrosarcoma caused by HME is very rare, with only a few reports available. For example, Acharya et al. reported a large chondrosarcoma in the anterior chest wall from a rib osteochondroma, and Liu et al. described a similar case in the posterior chest wall (10, 11). To our knowledge, there are no prior reports of costal chondrosarcoma secondary to HME occurring in the anterior mediastinum, which presents significant diagnostic challenges due to its rarity and the need to differentiate it from more common mediastinal tumors. In this study, we present an extremely rare case of costal chondrosarcoma located in the anterior mediastinum secondary to HME.

Case presentation

The case involves a 32-year-old female patient who presented to our hospital in July 2023 after a routine health checkup revealed an anterior mediastinal mass. Despite the presence of the mass, she did not exhibit any symptoms typically associated with such findings, such as chest pain, cough, fever, or shortness of breath. A contrast-enhanced computed tomography (CT) scan of her chest demonstrated a well-defined mass measuring approximately 2.3 cm x 4.0 cm x 4.7 cm in the anterior mediastinum, causing compression of the right ventricle. The mass had multiple nodular high-density areas within it (Figures 1A, B). Bone abnormalities were observed, including a bony prominence on the right scapula, a bony prominence on the proximal left fibula, and localized bone expansion of the right fifth anterior rib, which were all considered to be potential osteochondromas (Figures 1C, D). Cardiac assessments, including electrocardiogram and echocardiogram, showed T-wave changes and mild tricuspid valve regurgitation, respectively. A whole-body bone scan ruled out distant bone metastasis, and laboratory tests including complete blood count, alkaline phosphatase (ALP), and lactate dehydrogenase (LDH) levels were unremarkable. Physical examination and abdominal ultrasound did not reveal any significant abnormalities.

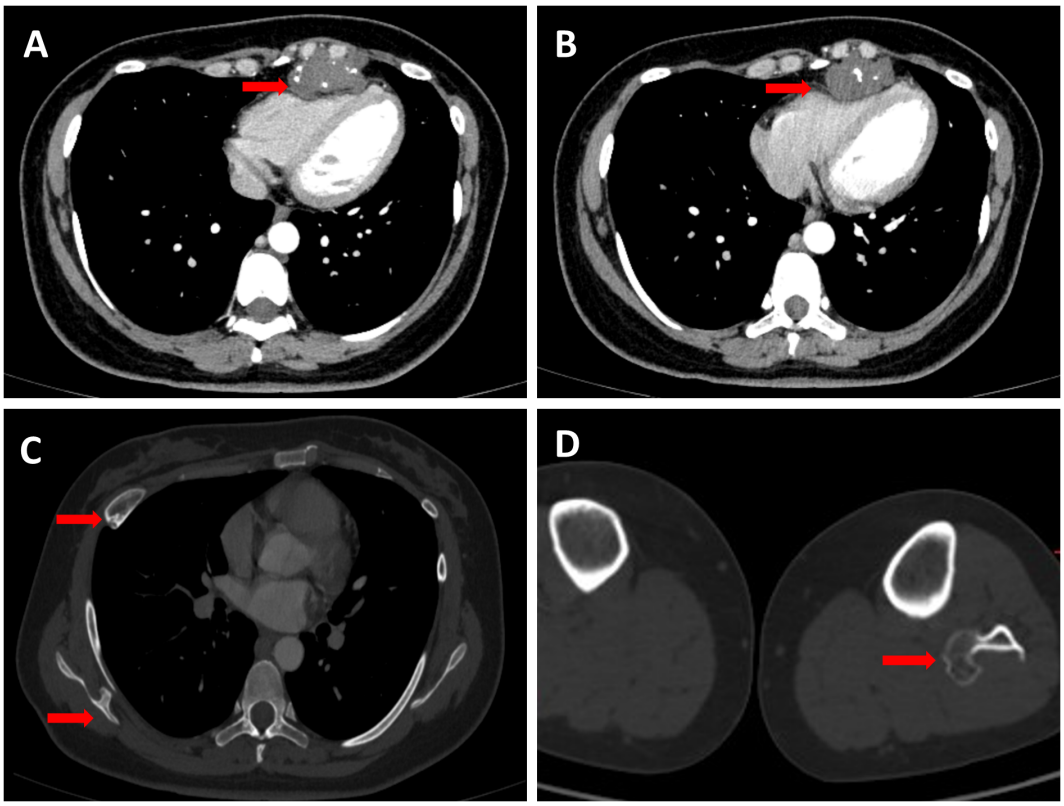

FIGURE 1
(A,B) Red arrows indicate the tumor in the anterior mediastinum with visible calcifications and clear edges. The tumor is pressing on the right ventricle, making it smaller. **(C)** Two red arrows highlight significant findings: one indicates a focal bony expansion on the right fifth anterior rib, suggesting a potential osteochondroma; the other points to a typical osteochondroma located on the right scapula. **(D)** The red arrow highlights an osteochondroma situated at the proximal end of the left fibula.

The patient had a significant surgical history. Four years prior, she presented to our orthopedic department with bilateral knee pain. X-rays of the knee joints revealed bone protrusions at the distal femur, right proximal tibia, consistent with osteochondromas. The lesions caused significant knee pain, which led to the decision to surgically excise them. Histopathological examination of the excised tissue confirmed the diagnosis of osteochondroma (Figures 2A, B). The patient's father had hereditary multiple exostoses, suggesting a genetic predisposition. The diagnosis of HME is typically based on clinical, radiological, and histological findings. Although genetic testing was not performed at that time, the patient was diagnosed with HME given her family history, imaging results, and postoperative pathological findings, which provided sufficient evidence for the diagnosis (4, 7).

To remove the tumor and relieve its compression on the heart, the patient underwent resection of the mediastinal tumor after obtaining informed consent: a left subxiphoid incision was made, with a 4 cm incision along the rib arch, assisted by thoracoscopy. The tumor was excised without extensive resection, preserving adjacent ribs and sternum. Intraoperatively, a hard, popcorn-like mass was observed in the left anterior mediastinum, with unclear demarcation from the rib cartilage and anterior chest wall but relatively clear relation to the pericardium and surrounding structures, suggesting that the tumor likely originated from the rib rather than from the mediastinum itself (Figure 3A). Postoperative histopathological examination suggested a diagnosis of well-differentiated chondrosarcoma, this was consistent with the tumor features we observed during surgery. (Figures 3B, C). The patient recovered and was discharged on the third postoperative day. One month after the surgery, the patient consulted the oncology department at our hospital for a follow-up and to determine the next steps for treatment. A PET-CT scan was performed to assess for potential distant metastases, and fortunately, it revealed no evidence of distant metastasis (Figure 3D). There was visible soft tissue swelling and increased glucose metabolism in the surgical area, with a standardized uptake value (SUV) of 8.8, indicative of postoperative changes (Figure 3E). Follow-up echocardiography and electrocardiogram showed no evidence of tricuspid valve regurgitation or T-wave changes, possibly due to relief of right ventricular compression post-surgery (12). CT scans confirmed that the tumor had been successfully removed, with visible improvement in right ventricular compression (Figure 3F). According to the NCCN guidelines, for low-grade chondrosarcomas, either wide resection or intralesional resection followed by adjuvant radiotherapy is recommended (13). Therefore, the patient received adjuvant intensity-modulated radiotherapy at our hospital. Currently, the patient has been regularly followed up for one year without evidence of tumor recurrence.

Discussion

Chondrosarcoma is a relatively common malignant bone tumor originating from cartilage and is the second most common primary malignant bone tumor after osteosarcoma (2). Chondrosarcomas can be classified into conventional chondrosarcoma and special subtypes, with the conventional type comprising approximately 85% of all cases. Conventional chondrosarcoma can be further divided into primary chondrosarcoma and secondary chondrosarcoma, which arises from benign conditions such as hereditary multiple exostoses, Ollier disease (multiple enchondromatosis), and Maffucci syndrome.

Hereditary multiple exostoses (HME), also known as hereditary multiple osteochondromas (HMO), is a rare autosomal dominant genetic disorder with an incidence of approximately 1 in 50,000 among Caucasians (14). Current research indicates that mutations in the EXT1 and EXT2 tumor suppressor genes from the EXT gene family are responsible for both sporadic and syndromic osteochondromas, including hereditary multiple exostoses (HME) (5, 15–17). The condition is characterized by multiple benign bone outgrowths covered with cartilage caps, primarily affecting the metaphyses of long bones in the limbs, as well as the scapula and pelvis, with relatively rare involvement of the ribs.

HME can lead to various complications, with the most serious being malignant transformation into chondrosarcoma. Previous studies have estimated the malignant transformation rate of HME to

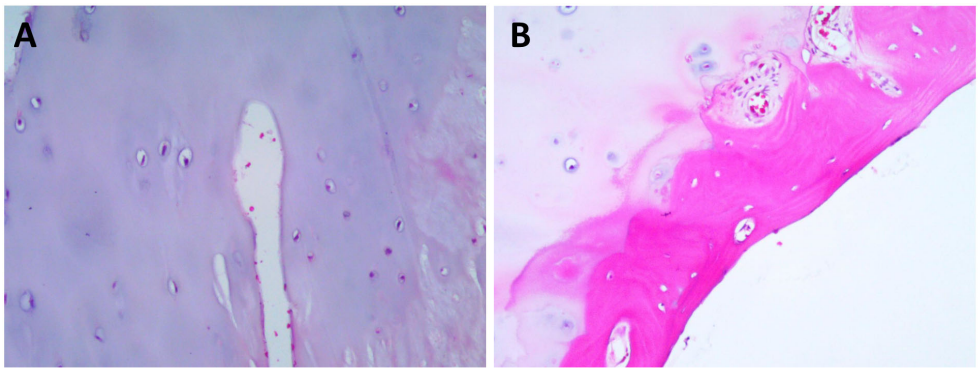

FIGURE 2
Hematoxylin and Eosin (HEx200) staining results. **(A)** HE Staining reveals the characteristic cartilage cap. **(B)** HE Staining delineates the cartilaginous cap and the adjacent fibrous layer, highlighting the distinct histological attributes of the tumor.

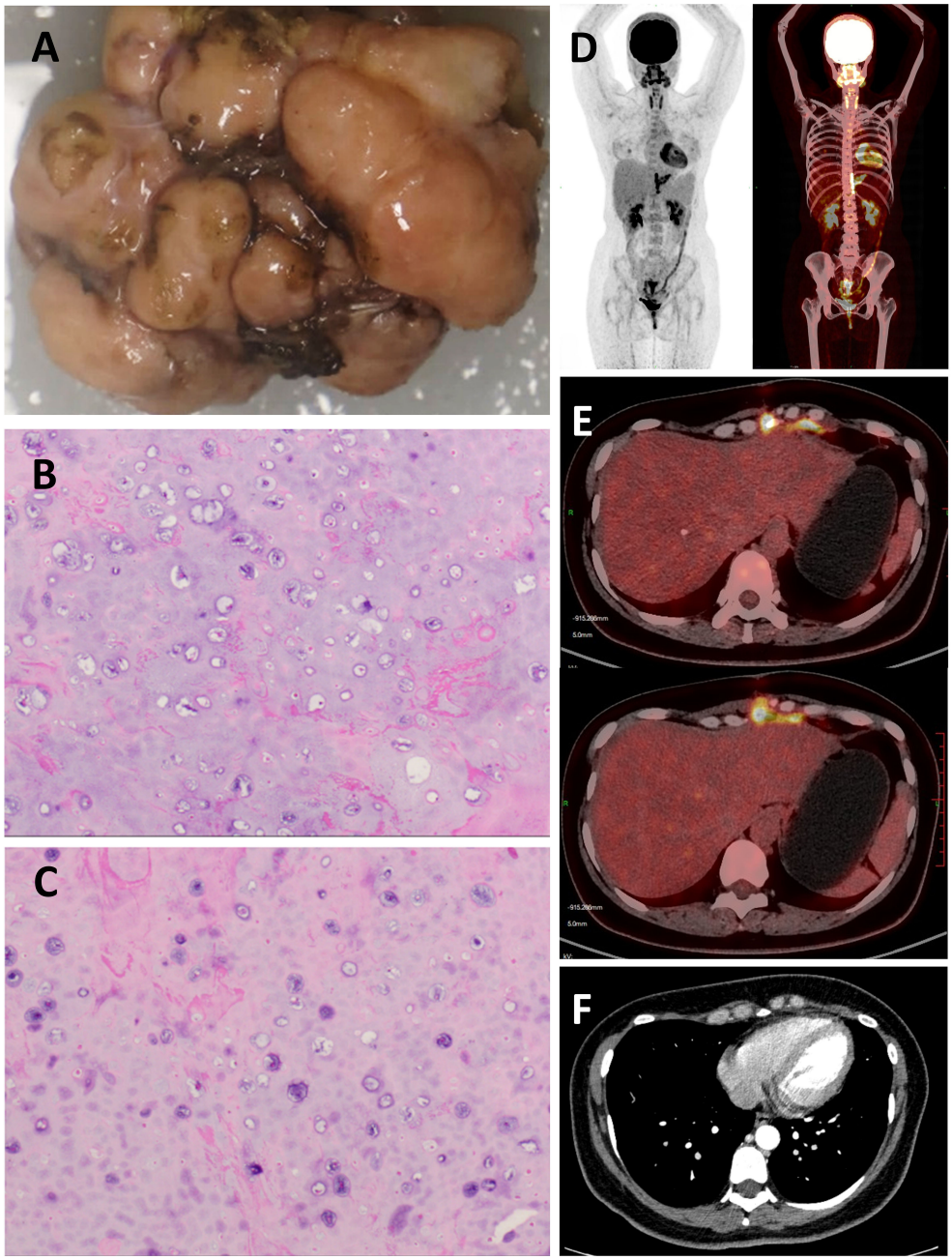

FIGURE 3
(A) Macroscopic Examination: The excised tumor, exhibiting a multinodular surface and a hard consistency, measured 2.3 cm × 4.0 cm × 4.7cm. **(B, C)** Histopathological Examination (Hematoxylin and Eosin Stain): Micrographs at high magnification revealed chondrocyte hyperplasia within the cartilaginous matrix, indicative of a malignant process. **(D)** No distant metastatic lesions were identified upon PET-CT examination. **(E)** Increased glucose metabolism was observed in the surgical site on PET-CT imaging, consistent with postoperative changes. **(F)** Contrast-enhanced chest CT during postoperative follow-up.

be approximately 1-5%. However, the timing of symptom development can vary depending on the tumor's location. Early signs of malignant transformation of HME can be detected through imaging techniques such as CT and MRI (18, 19). Fortunately, secondary chondrosarcomas are generally low-grade and have a lower rate of metastasis, which aligns with the condition of the patient we report here (20, 21). The risk of malignant transformation is related to the location of the osteochondromas; those located in the pelvis and proximal femur are more prone to malignant transformation, while malignant transformation of rib osteochondromas into chondrosarcoma is exceedingly rare, with only a few cases reported in the literature. Malignant transformation is often initially detected by clinical symptoms, such as growth and pain occurring after puberty. However, the timing of symptom development can vary depending on the tumor's location. Metesh Acharya et al. reported a case of a large chondrosarcoma primarily located in the anterior chest wall originating

from a rib (10). Similarly, Wenliang Liu et al. reported a case of a large chondrosarcoma primarily located in the posterior chest wall, both believed to have arisen from malignant transformation of HME (11). In contrast, our patient benefited from early detection, with a relatively small tumor size. However, the growth pattern of the tumor in this case extended into the thoracic cavity, directly compressing the heart and significantly narrowing the right ventricle. Additionally, due to the tumor's location in the anterior mediastinum, the diagnosis was challenging as it needed to be differentiated from other common anterior mediastinal tumors. These include teratomas, lymphomas, and other cartilage-origin tumors such as chondroblastomas (22).

The treatment strategy for chondrosarcoma depends on the tumor's histological grade and location. Well-differentiated (low-grade) chondrosarcomas typically grow slowly and have a relatively low recurrence rate. Due to the rarity of costal chondrosarcoma, there is no standardized treatment protocol for this condition. According to the NCCN guidelines, the preferred approach for low-grade chondrosarcomas is either wide resection or intralesional resection followed by adjuvant therapy to minimize recurrence risk. However, wide resection often requires extensive removal of adjacent chest wall structures, such as the sternum and rib cartilage, which necessitates complex reconstruction. In this case, intralesional resection was chosen to preserve the structural integrity of the chest wall, as wide resection would have caused substantial disruption to surrounding structures. Recognizing the increased risk of local recurrence with intralesional resection, the patient underwent adjuvant intensity-modulated radiotherapy (IMRT). While chondrosarcomas are traditionally considered radioresistant, recent advancements in radiotherapy, including IMRT, have shown improved potential for local control (23, 24).

In summary, we report a highly rare case of costal chondrosarcoma secondary to HME, located in the anterior mediastinum and causing compression of the right ventricle, which required differentiation from other common anterior mediastinal tumors. This case underscores the importance of routine imaging follow-up for patients with HME to enable early detection of malignant transformation. It also highlights the critical role of a multidisciplinary team, including surgeons, oncologists, radiologists, and pathologists, in improving diagnostic accuracy, surgical planning, and postoperative management (3, 25). To our knowledge, this is the first reported case of costal chondrosarcoma secondary to HME occurring in the anterior mediastinum. Our experience highlights the need to suspect secondary chondrosarcoma in HME patients when a mediastinal mass with calcified foci is detected, especially if the mass is in close proximity to the chest wall.

Data availability statement

The raw data supporting the conclusions of this article will be made available by the authors, without undue reservation.

Ethics statement

The studies involving humans were approved by Ethics Committee of the Affiliated Hospital of Southwest Medical University. The studies were conducted in accordance with the local legislation and institutional requirements. The participants provided their written informed consent to participate in this study. Written informed consent was obtained from the individual(s) for the publication of any potentially identifiable images or data included in this article.

Author contributions

ZY: Conceptualization, Data curation, Formal analysis, Investigation, Methodology, Software, Validation, Writing – original draft, Writing – review & editing. KW: Data curation, Formal analysis, Investigation, Methodology, Writing – original draft, Writing – review & editing. JP: Conceptualization, Formal analysis, Funding acquisition, Methodology, Resources, Supervision, Validation, Writing – original draft, Writing – review & editing.

Funding

The author(s) declare that no financial support was received for the research, authorship, and/or publication of this article.

Acknowledgments

We would like to express our gratitude to the patient who provided written informed consent for publication and to the research personnel involved in this study.

Conflict of interest

The authors declare that the research was conducted in the absence of any commercial or financial relationships that could be construed as a potential conflict of interest.

Publisher's note

References

1. Thorkildsen J, Myklebust T. The national incidence of chondrosarcoma of bone; a review. *Acta Oncol (Stockholm Sweden)*. (2023) 62:110–7. doi: 10.1080/0284186x.2023.2177975

2. Gazendam A, Popovic S, Parasu N, Ghert M. Chondrosarcoma: A clinical review. *J Clin Med*. (2023) 12. doi: 10.3390/jcm12072506

3. D'Arienzo A, Andreani L, Sacchetti F, Colangeli S, Capanna R. Hereditary multiple exostoses: current insights. *Orthop Res Rev*. (2019) 11:199–211. doi: 10.2147/ORR.S183979

4. Bukowska-Olech E, Trzebiatowska W, Czech W, Drzymała O, Frąk P, Klarowski F, et al. Hereditary multiple exostoses-A review of the molecular background, diagnostics, and potential therapeutic strategies. *Front Genet*. (2021) 12:759129. doi: 10.3389/fgene.2021.759129

5. Al-Zayed Z, Al-Rijjal RA, Al-Ghofaili L, BinEssa HA, Pant R, Alrabiah A, et al. Mutation spectrum of EXT1 and EXT2 in the Saudi patients with hereditary multiple exostoses. *Orphanet J Rare Dis*. (2021) 16:100. doi: 10.1186/s13023-021-01738-z

6. Wang Y, Zhong L, Xu Y, Ding L, Ji Y, Schutz S, et al. EXT1 and EXT2 variants in 22 chinese families with multiple osteochondromas: seven new variants and potentiation of preimplantation genetic testing and prenatal diagnosis. *Front Genet*. (2020) 11:607838. doi: 10.3389/fgene.2020.607838

7. Pierz KA, Stieber JR, Kusumi K, Dormans JP. Hereditary multiple exostoses: one center's experience and review of etiology. *Clin Orthopaedics Related Res*. (2002) 401:49–59. doi: 10.1097/00003086-200208000-00008

8. Fei L, Ngoh C, Porter DE. Chondrosarcoma transformation in hereditary multiple exostoses: A systematic review and clinical and cost-effectiveness of a proposed screening model. *J Bone Oncol*. (2018) 13:114–22. doi: 10.1016/j.jbo.2018.09.011

9. Gnoli M, Gambarotti M, Righi A, Staals EL, Evangelista A, Tremosini M, et al. Secondary peripheral chondrosarcoma in multiple osteochondromas: a retrospective single-institution case series. *Orphanet J Rare Dis*. (2024) 19:63. doi: 10.1186/s13023-023-03006-8

10. Acharya M, Jamali A, Rao J. Giant costal chondrosarcoma in a patient with hereditary multiple exostoses. *Ann Thorac Surgery*. (2014) 98:1848. doi: 10.1016/j.athoracsur.2014.06.081

11. Liu W, Kong D, Tang J, Yu F. Giant costal osteochondroma in a man with multiple exostoses. *Ann Thorac Surgery*. (2013) 96:675–7. doi: 10.1016/j.athoracsur.2012.12.007

12. Kozaki T, Fuchigami T, Nagata N. Tricuspid regurgitation caused by right ventricle compression by pectus excavatum. *Asian Cardiovasc Thorac Ann*. (2018) 26:582–3. doi: 10.1177/0218492318799928

13. Biermann JS, Chow W, Reed DR, Lucas D, Adkins DR, Agulnik M, et al. NCCN guidelines insights: bone cancer, version 2.2017. *J Natl Compr Cancer Network: JNCCN*. (2017) 15:155–67. doi: 10.6004/jnccn.2017.0017

14. Schmale GA, Conrad EU III, Raskind WH. The natural history of hereditary multiple exostoses. *J Bone Joint Surg Am*. (1994) 76(7):986–92. doi: 10.2106/00004623-199407000-00005

15. Fusco C, Nardella G, Fischetto R, Copetti M, Petracca A, Annunziata F, et al. Mutational spectrum and clinical signatures in 114 families with hereditary multiple osteochondromas: insights into molecular properties of selected exostosin variants. *Hum Mol Genet*. (2019) 28:2133–42. doi: 10.1093/hmg/ddz046

16. Pacifici M. The pathogenic roles of heparan sulfate deficiency in hereditary multiple exostoses. *Matrix Biol*. (2018) 71-72:28–39. doi: 10.1016/j.matbio.2017.12.011

17. Sinha S, Mundy C, Bechtold T, Sgariglia F, Ibrahim MM, Billings PC, et al. Unsuspected osteochondroma-like outgrowths in the cranial base of Hereditary Multiple Exostoses patients and modeling and treatment with a BMP antagonist in mice. *PloS Genet*. (2017) 13:e1006742. doi: 10.1371/journal.pgen.1006742

18. Verdegaal SH, Bovée JV, Pansuriya TC, Grimer RJ, Ozger H, Jutte PC, et al. Incidence, predictive factors, and prognosis of chondrosarcoma in patients with Ollier disease and Maffucci syndrome: an international multicenter study of 161 patients. *Oncol*. (2011) 16:1771–9. doi: 10.1634/theoncologist.2011-0200

19. Kwee RM, Fayad LM, Fishman EK, Fritz J. Multidetector computed tomography in the evaluation of hereditary multiple exostoses. *Eur J Radiol*. (2016) 85:383–91. doi: 10.1016/j.ejrad.2015.11.034

20. Ahmed AR, Tan TS, Unni KK, Collins MS, Wenger DE, Sim FH. Secondary chondrosarcoma in osteochondroma: report of 107 patients. *Clin Orthopaedics Related Res*. (2003) 411:193–206. doi: 10.1097/01.blo.0000069888.31220.2b

21. Tsuda Y, Gregory JJ, Fujiwara T, Abudu S. Secondary chondrosarcoma arising from osteochondroma: outcomes and prognostic factors. *Bone Joint J*. (2019) 101-B:1313–20. doi: 10.1302/0301-620X.101B9.BJJ-2019-0190.R1

22. Nakazono T, Yamaguchi K, Egashira R, Mizuguchi M, Irie H. Anterior mediastinal lesions: CT and MRI features and differential diagnosis. *Jpn J Radiol*. (2021) 39:101–17. doi: 10.1007/s11604-020-01031-2

23. Sahgal A, Chan MW, Atenafu EG, Masson-Cote L, Bahl G, Yu E, et al. Image-guided, intensity-modulated radiation therapy (IG-IMRT) for skull base chordoma and chondrosarcoma: preliminary outcomes. *Neuro-oncology*. (2015) 17:889–94. doi: 10.1093/neuonc/nou347

24. Gilbert A, Tudor M, Montanari J, Commenchail K, Savu DI, Lesueur P, et al. Chondrosarcoma resistance to radiation therapy: origins and potential therapeutic solutions. *Cancers (Basel)*. (2023) 15. doi: 10.3390/cancers15071962

25. Phan AQ, Pacifici M, Esko JD. Advances in the pathogenesis and possible treatments for multiple hereditary exostoses from the 2016 international MHE conference. *Connect Tissue Res*. (2018) 59:85–98. doi: 10.1080/03008207.2017.1394295

Frontiers in
Molecular Biosciences

Explores biological processes in living organisms on a molecular scale

Focuses on the molecular mechanisms underpinning and regulating biological processes in organisms across all branches of life.

Discover the latest Research Topics

See more →

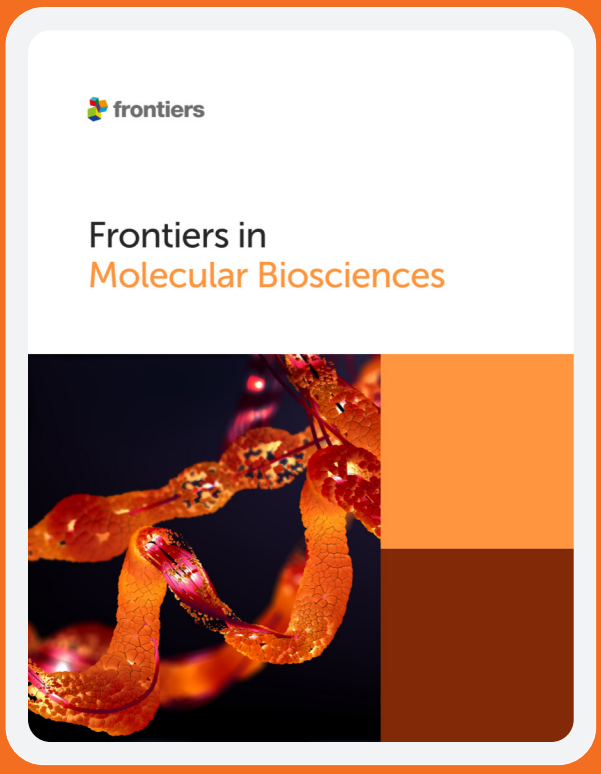

Frontiers

Avenue du Tribunal-Fédéral 34
1005 Lausanne, Switzerland
frontiersin.org

Contact us

+41 (0)21 510 17 00
frontiersin.org/about/contact